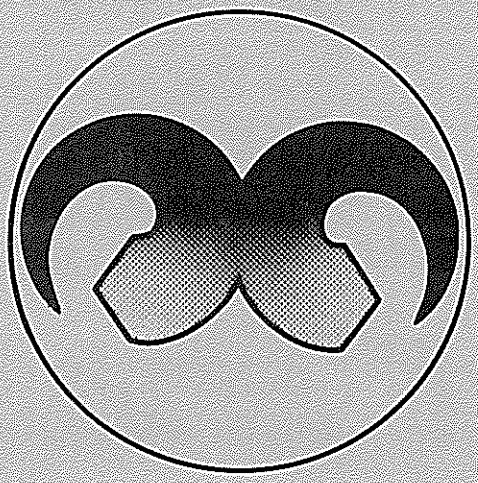
J. VLACHOPOULOS

FOURTH ANNUAL MEETING
HYATT-ORLANDO HOTEL
ORLANDO, FLORIDA, USA
MAY, 8-11, 1988

PROGRAM AND ABSTRACTS



POLYMER PROCESSING SOCIETY

INTERNATIONAL

Organized by

CENTER FOR MACROMOLECULAR SCIENCE AND ENGINEERING
DIVISION OF SPONSORED RESEARCH
UNIVERSITY OF FLORIDA
GAINESVILLE, FLORIDA 32611
USA

PLENARY SPEAKER

Professor Dr. G. Schenkel
Institut fur Kunststofftechnologie
der Universitat Stuttgart
Stuttgart, West Germany

CONFERENCE COMMITTEE

General Chairman:	C.L. Beatty, U. Florida
Program Chairman:	A.L. Fricke, U. Florida
Program Co-Chairman:	G.A. Campbell, Clarkson U.
Treasurer:	C.L. Beatty, U. Florida
Publicity Chairman:	J.H. Southern, Monsanto Corp.
Exhibit Chairman:	G.A. Campbell, Clarkson U.
Coordinators:	S. Habbaba, Uniglobe
	E. Edwards, Uniglobe
Secretaries:	J. Jacobs, U. Florida
	P. Howell, U. Florida
	C. Zimmerman, U. Florida

PPS EXECUTIVE COMMITTEE

President:	L.A. Utracki
President-Elect:	H.G. Fritz
Secretary:	J.A. Biesenberger
Treasurer:	J.F. Stevenson
Member-at-Large:	J.F. Agassant
Member-at-Large:	Y. Oyanagi

PPS INTERNATIONAL REPRESENTATIVES

Europe, Middle East and Africa:	H. Herrmann
	Z. Tadmor
East Asia and Australia:	K.U. Kim
	T. Masuda
North and South America:	M.R. Kamal
	G. Vassilatos

SYMPOSIA ORGANIZERS

1. Injection and Compression Molding
   C.L. Tucker, H. Takahasi, J.F. Agassant
2. Blow Molding
   H.G. Fritz, P.M. Subramanian
3. Fibers and Films
   G. Perez, S. Kase, J.F. Fellers
4. Extrusion
   P.J. Carreau, H. Potente
5. Polymerization and Reactive Processing
   J.T. Lindt, S. Omi
6. Mixing, Compounding and Blending
   J.L. White, J.W.M. Noordermeer
7. Rubber and Thermoplastics Elastomer Processing
   N. Nakajima
8. Structure Development in Processing
   J.E. Spruiell, K.I. Katayama
9. Polymer Alloys and Blends
   A.P. Plochocki, X. Xu
10. Innovative Technologies
    H.R. Thomas, Y. Oyanagi
11. Rheology and Rheometry
    L.A. Goettler, D.V. Boger, D. Acierno
12. Long Fiber Composites
    R. Bailey, J.F. Stevenson
13. Devolatilization and Foams
    R.J. Nichols, K.U. Kim, H.D. Zettler
14. Die Extrusion
    D.H. Sebastian
15. Processing in Microelectronics and Other Emerging Technologies
    D. Soane, W.F. van den Bogert, N. Kinjo
16. General
    J.P. Harmon

GENERAL INFORMATION

INTRODUCTION

The program of the forthcoming Fourth Annual IPPS Meeting again shows the Society's wide thematic scope as well as its international character. The present state of research and technical innovation in Polymer Processing is comprehensively documented. The conference committee members wish to express their gratitude to the numerous co-organizers all over the world which enable us to present such an impressive collection of highly valuable papers and posters.

THE INTERNATIONAL POLYMER PROCESSING SOCIETY (IPPS)

The IPPS was founded on March 28-29, 1985 at Akron, Ohio (USA). The audience at the Founding Meeting was composed of more than 200 internationally recognized experts from academic and industrial organizations; these experts enthusiastically approved of the objectives of the new society, and the society has grown at a rapid rate. The Third Annual Meeting of the IPPS was held in Stuttgart, West Germany during April 7-10, 1987, and attracted over 400 participants.

The goal of the IPPS, as embodied in its constitution, is to foster scientific understanding and technical innovation in polymer processing by providing a discussion forum for the worldwide community of engineers and scientists in this field. The thematic range of the IPPS encompasses all formulation, conversion and shaping operations applied to polymeric systems in the transformation from their monomeric forms to commercial products.

In addition to the annual international conference, the IPPS activities include the arrangement of regional and local meetings, publication of a journal, and sponsorship of educational seminars.

Membership in the IPPS is open to all research workers in the field, and to all individuals who feel the activities of the society advance their professional development.

Sponsorship of Student Chapters at universities has been initiated the past year with establishment of an IPPS Student Chapter at the University of Florida.

FUTURE INTERNATIONAL MEETINGS

May 1989:	Kyoto, Japan
Spring 1990:	Sophia Antiopolis (Nice), France
Spring 1991:	Toronto, Canada

CONFERENCE REGISTRATION AND FEES

Attendees can pre-register for the conference by completing the attached registration form and returning the form with required fees before April 15, 1988. Attendees can register at the conference on May 8, 3:00 - 10:00 PM, and on May 9, 7:30 - 11:30 AM.

Registration includes admission to all symposia sessions, one copy of the book of abstracts for technical and scientific papers, one ticket to the banquet, one ticket for each reception, and six refreshment coupons. Issue 1 of Volume III of International Polymer Processing is included in the registration fee. Guest tickets for the banquet can be purchased for $40 on or before Sunday evening, May 8, and guest tickets for each reception can be purchased on or before May 8 for $20 each. Pre-registration requests must be received before Friday,, April 15, 1988.

		US$
1.	1988 IPPS dues and conference registration	230/280
2.	Conference registration for non-members. (Each non-member registrant will receive a complimentary membership for the period from April 1 to December 31, 1988).	260/310
3.	Graduate students presenting papers or posters.	115/140
4.	Extra tickets	
	a. Reception, Sunday, May 8	20
	b. Reception, Tuesday, May 10	20
	c. Banquet, Tuesday, May 10	40
5.	Extra book of abstracts	50

MEMBERSHIP TERM

IPPS membership, as indicated by Dr. James F. Stevenson, IPPS Treasurer, expires March 21, 1988. Thus, the cost for registration is $230, which includes the dues for 1988. Henceforth, the membership will be based on the calendar year. Non-members are encouraged to join the society and take advantage of the special member registration rate.

ACCOMMODATION, RESERVATIONS AND LOCAL TRANSPORTATION

Reservations for air travel, auto rental and discounted hotel accommodations can be made through:

UNIGLOBE UCT Travel
1131 West University Avenue
Gainesville, Florida 32601 USA

In Florida, call:	(800)345-9313
USA (outside FL):	(800)527-9783
Outside the USA:	(904)377-4226
Or by Telex:	#810-007-0189

NOTE: Most major credit cards can be accepted for air transport, hotel and rental cars.

PPS MEETING REGISTRATION DESK

The registration area will be located in the TAMIAMI LOUNGE (entrance foyer of the Convention Hall). Registration and welcome information packets will be available at the registration desk during the following hours:

Sunday, May 8: 3:00 PM - 10:00 PM
Monday, May 9: 7:00 AM - 11:30 AM

BUS TOUR TO UNIVERSITY OF FLORIDA POLYMER LABORATORIES

A bus for to the University of Florida at Gainesville, Florida (approximately 160 kms. from Orlando) is planned for Thursday, May 12, 1988. Departure is to be at 8:00 AM from the conference hotel with return to the conference hotel at 6:00 PM or before. Reservations for the tour must be made on or before May 8, 1988. The cost for the tour is $40. Should less than 30 attendees place reservations for the tour, the tour will be cancelled and reservation fees refunded.

SPECIAL EVENTS

Sunday, May 9, 1988

THE POLYMER PROCESSING SOCIETY REGISTRATION RECEPTION

RECEPTION: 6:00 TO 8:00 PM
EXHIBIT HALL FOYER

Admission by badge. Cash bar.

Tuesday, May 10, 1988

THE POLYMER PROCESSING SOCIETY RECEPTION AND BANQUET

RECEPTION: 6:30 PM
TAMIAMI LOUNGE

Join your friends and associates for cocktails before the banquet. Your favorite standards will be available, or try a refreshing tropical punch.

Admission by badge. Cash bar.

BANQUET: 7:30 PM
CYPRESS BALLROOM

Tuesday evening has been reserved for the Polymer Processing Society's 4th Annual International Meeting Banquet. Dinner will begin at 7:30 PM, after the reception.

The banquet is included in the registration fee. Extra tickets are $40 per person.

FLORIDA INFORMATION AND TRAVEL TIPS

CLIMATE

Almost everywhere, people talk about the weather. Here in Central Florida, we just enjoy it.

Florida enjoys abundant sunshine with warm and pleasant temperatures. In early May, daytime high temperatures are in the mid 80's (oF). Evening temperatures are in the mid 60's. Summer usually arrives in late May.

Dress in Florida is more casual than most places, and light clothing is recommended. Business dress or dining out does include coat and tie, though not required. Air conditioning is common, and a light jacket or sweater is suggested for cooler late evenings.

Shorts and playwear are best for the children, and Tee shirts are very much "the in" attire. Don't forget swimsuits and shorts for sunbathing, but do be cautious of sunburn. Florida sun does cause sunburn much faster than most visitors expect. Be sure to use sunscreen lotions and common sense.

Lots of sunshine, but spring showers do occur. Average monthly rainfall in May is 4.0 inches. The summer rains normally don't start until late May. Unfortunately, the absence of rain can't be guaranteed, but early May is usually more dry than wet.

DINING, ATTRACTIONS, SHOPPING

Orlando offers dining for nearly every taste and budget. You will receive a copy of the Official Visitors Guide in your Welcome Package, with an extensive list of area restaurants ranging in price from "inexpensive" (under $9.00)) to "expensive" ($20.00 or more).

Area attractions are also listed in the Visitors Guide, as are many unique shopping "experiences" conviently near the Hyatt-Orlando, as well as Sporting Activities for every taste.

DRIVING IN FLORIDA

Florida has an excellent road network. City traffic can be congested during the morning and afternoon rush hours. The speed limit is posted: 65 mph on the Interstate Highways (except 55 mph in city areas) and it is enforced. Use of seatbelts is mandatory and a safety seat is required for children up to 4 years of age (available at nominal charge with car rental).

RESERVATIONS SERVICE DESK

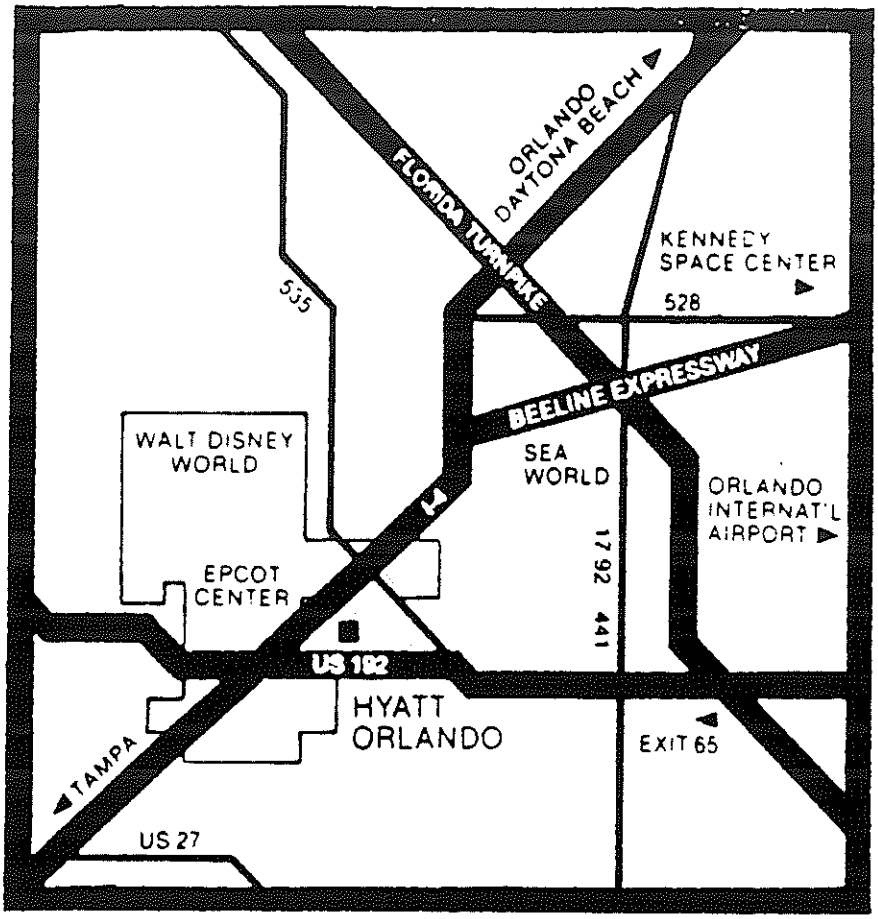
UNIGLOBE UCT Travel will operate a Service Desk in the registration area to assist attendees who may need to change reservations or make other travel arrangements. Our Travel Service Desk will be equipped with a computer terminal for confirming airline and other reservations on the spot, to handle emergencies that arise. Tickets for Special Events that aren't sold out will be available here also.

We'll provide information on area attractions in your welcome packet, and we'll be there to help you with directions and suggestions or answer your questions. Stop by to say "Hello" and let us know how we can help make your visit to Florida more enjoyable.

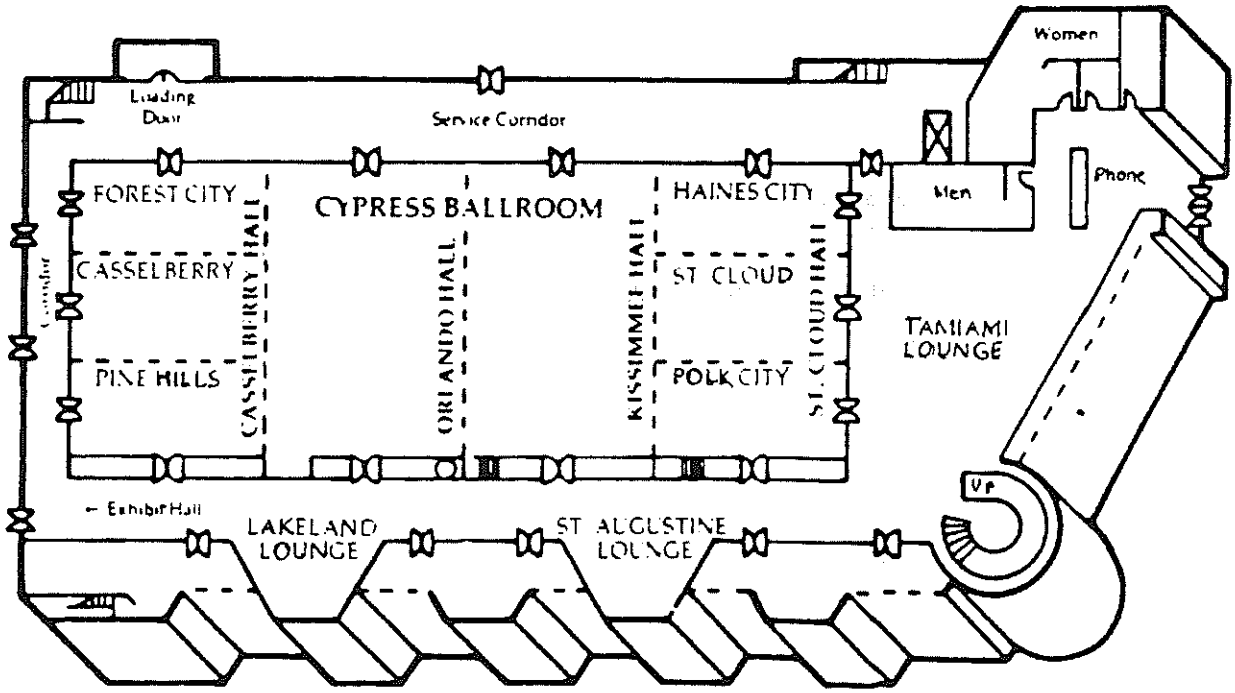
Daily, 9 AM to 5 PM, Sunday - Thursday

ORLANDO IS THE WORLD VACATION CAPITAL

There is so much to do in Central Florida that many organizations do not schedule special events. However, we think those attending the meeting will enjoy the Special Events that have been arranged exclusively for the enjoyment of PPS members and their families. All Special Events must be paid for in cash and are subject to cancellation if there is not suficient response. Tickets sold for events that must be cancelled will be fully refunded.


ORLANDO DAYTONA BEACH
FLORIDA TURNPIKE
KENNEDY SPACE CENTER
528
535
BEELINE EXPRESSWAY
WALT DISNEY WORLD
SEA WORLD
ORLANDO INTERNAT'L AIRPORT
4
EPCOT CENTER
1792
441
US 192
HYATT ORLANDO
EXIT 65
TAMPA
US 27

FIRST FLOOR


Women
Loading Dock
Service Corridor
Men
Phone
FOREST CITY
CYPRESS BALLROOM
HAINES CITY
CASSELBERRY
PINE HILLS
CASSELBERRY HALL
ORLANDO HALL
KISSIMMEE HALL
ST CLOUD
POLK CITY
ST. CLOUD HALL
TAMIAMI LOUNGE
VP
Exhibit Hall
LAKELAND LOUNGE
ST AUGUSTINE LOUNGE

PROGRAM AT A GLANCE

DATE	EVENT	TIME	LOCATION
May 8	Registration	3:00 - 10:00 PM	Tamiami Lounge
	Reception	6:00 - 8:00 PM	Exhibit Hall Foyer
May 9	Registration	7:30 - 11:30 AM	Tamiami Lounge
	Plenary Session, Business Meeting	8:30 AM	Cypress Ballroom
	Morning Session	10:00 AM - 12:30 PM	See Symposia Schedule
	Lunch, Poster A Display	12:30 - 2:00 PM	Exhibit Hall
	Afternoon Session	2:00 - 5:30 PM	See Symposia Schedule
	Poster A Discussion	5:30 - 7:00 PM	Exhibit Hall
May 10	Morning Session	8:30 AM - 12:30 PM	See Symposia Schedule
	Lunch, Poster B Display	12:30 - 2:00 PM	Exhibit Hall
	Afternoon Session	2:00 - 5:00 PM	See Symposia Schedule
	Poster B Discussion	5:00 - 6:30 PM	Exhibit Hall
	Reception	6:30 - 7:30 PM	Tamiami Lounge
	Banquet	7:30 PM	Cypress Ballroom
May 11	Morning Session	8:30 AM - 12:30 PM	See Symposia Schedule
	Lunch	12:30 - 2:00 PM	
	Afternoon Session	2:00 - 5:00 PM	See Symposia Schedule

SYMPOSIA SCHEDULE

LOCATION/DATE		MAY 9	MAY 10	MAY 11
Orlando,	AM	1	1	1
	PM	1	2	16
Kissimmee,	AM	3	3	14
	PM	3	3	13
Forest City,	AM	7	5	6
	PM	7	5	6
Pine Hills,	AM	10	15	11
	PM	10	15	11
Haines City,	AM	12	8	8
	PM	12	12	8
Polk City,	AM	9	9	4
	PM	9	4	4
EXHIBIT HALL		POSTER A	POSTER B	

SYMPOSIA:

NO.	TITLE
1	Injection and Compression Molding
2	Blow Molding
3	Fibers and Films
4	Extrusion
5	Polymerization and Reactive Proc
6	Mixing, Compounding and Blending
7	Rubber and Thermoplastic Elastomer Proc.
8	Structure Development in Proc.
9	Polymer Alloys and Blends
10.	Innovative Technologies
11.	Rheology and Rheometry
12.	Long Fiber Composites
13.	Devolatilization and Foams
14.	Die Extrusion
15.	Processing in Microelectronics
16.	General

Poster A - Posters for No. 1,2,7,9.10,12

Poster B - Posters for No. 3,4,5,6,8,11, 13,14,15

MAY 10, TUESDAY AFTERNOON SESSION

ORLANDO

SYMPOSIUM 2 - Blow Molding

Chairman: H.G. Fritz, Universitaet Stuttgart, Stuttgart, West Germany

Co-Chairman: P.M. Subramanian, E.I. DuPont de Nemours and Co., Inc., Wilimington, DE

2:00 K 2/1 "ACTUAL AUTOMATION STEPS IN BLOW MOLDING TECHNOLOGY," R. Hegele, Battenfield-Fischer, Lohmar, West Germany

2:30 2/2 "DYNAMICS OF THE BLOW MOLDING PROCESS AND PROPERTIES OF BLOW MOLDED ARTICLES," D.H. Kalyon, Stevens Institute of Technology, Hoboken, NJ

3:00 2/3 "ANALYSIS AND COMPUTATION OF FLUID FLOW IN BLOW MOLDING DIES," D.J. Coyle, General Electric Co., Schenectady, NY

3:30 2/4 "INJECTION STRETCH BLOW MOLDING - PROCESS SIMULATION," S. Jabarin and L.S. Chang, University of Toledo, Toledo, OH

4:00 2/5 "BLOW MOLDING TECHNOLOGY FOR MICROSCOPIC REPLICATION OF MOLDED SURFACES," R. Marin and M. Cho, E.I. DuPont de Nemours and Co., Inc., Wilmington, DE

4:30 2/6 "FUNDAMENTALS OF COEXTRUSION BLOW MOLDING," W.L. Strum, E.I. DuPont de Nemours and Co., Inc., Wilmington, De

5:00 2/7 "NEW DEVELOPMENTS IN COEXTRUSION-BLOW MOLDING TECHNOLOGY," W. Neubauer, Bekum Maschinen-fabriken, Berlin, West Germany

5:00 - 6:30 - POSTER SESSION B IN EXHIBIT HALL

MAY 10, TUESDAY AFTERNOON SESSION

KISSIMMEE

SYMPOSIUM 3 - Fibers and Films

Chairman: G. Perez, Centre de Research Saint-Fons, Saint-Fons, France

Co-Chairmen: S. Kase, Kyoto Institute of Technology, Kyoto, Japan and J.F. Fellers, The University of Tennessee, Knoxville, TN

2:00 3/21 "A MORPHOLOGICAL AND PHYSICO-CHEMICAL STUDY OF OZONIZED POLYPROPYLENE POWDER AND FIBERS," B. Catoire, R. Hagege and M. Sotton, Institut Textile de France, Cedex, France

2:30 3/22 "HOT TUBE SPINNING OF POLYESTER FIBERS," H. Brody and N.W. Hayman, ICI Fibres, North Yorkshire, England

3:00 3/23 "EFFECT OF THERMAL HISTORY ON ORIENTED FIBERS," J.M. Schultz, University of Delaware, Newark, DE

3:30 3/24 "PROGRESS TOWARDS MAKING ULTRA-HIGH PERFORMANCE FIBERS FROM MESOPHASES IN THE CELLULOSE/AMMONIA/AMMONIUM THIOCYANATE SYSTEM," J.A. Cuculo, M.H. Theil and K.S. Yang, North Carolina State University, Raleigh, NC

4:00 3/25 "CRIMPING BEHAVIOR: A FUNCTION OF PROCESS CONDITIONS AND FIBER GEOMETRY FOR NYLON 66 FIBERS," R.W. Miller, A. Beningfield, J.F. Dizor and J.H. Southern, Monsanto Chemical Co., Pensacola, FL and C.L. Beatty, University of Florida, Gainesville, FL

4:30 3/26 "RELATIONSHIP BETWEEN NYLON 6 FIBER STRUCTURE AND DYE TRANSPORT ANISOTROPY," H.D. Weigmann, R.A.F. Moore, S. Ruetsch and D.R. Salen, Textile Research Institute, Princeton, NJ

5:00 - 6:30 - POSTER SESSION B IN EXHIBIT HALL

MAY 10, TUESDAY MORNING SESSION

HAINES CITY

SYMPOSIUM 8 -Structure Development in Processing

Chairman: J.E. Spruiell, Univ. of Tennessee, Knoxville, TN

Co-Chairman: K.I. Katayama, Kyoto University, Uji, Japan

8:30 K 8/1 "SOL-GEL TRANSITION IN POLYMER SOLUTIONS AND DEVELOPMENT OF POROUS STRUCTURE BY COAGULATION," T. Inoue, Tokyo Institute of Technology, Tokyo, Japan

9:00 8/2 "FIBROUS MATERIALS FROM THE PHASE DECOMPOSITION OF LCP SOLUTIONS," M.A. Alonso, C.L. Jackson and M.T. Shaw, Univ. of Connecticut, Storrs, CN

9:30 8/3 "A CONSTITUTIVE EQUATION INCLUDING COMPRESSIBLE EFFECTS: APPLICATION TO RAPIDLY COOLED, CONSTRAINED SAMPLES," D.C. Bogue and W.C. Ko, Univ. of Tennessee, Knoxville, TN

0:00 8/4 "OPTIMAL COOLING FOR MINIMUM RESIDUAL THERMAL STRESSES," M.J. Liou, Ohio State Univ., Columbus, OH and N.P. Suh, Massachusetts Institute of Technology, Cambridge, MA

0:30 8/5 "HEAT TRANSFER DRIVEN STRESS BUILD-UP AND RELAXATION IN A POST-FORMING STAGE OF THERMOPLASTIC MATERIALS," A. Cohen and M.G. Dibbs, Dow Chemical, Midland, MI

1:00 8/6 "THE EFFECT OF MODIFYING THREAD LINE DYNAMICS IN THE HIGH SPEED SPINNING PROCESS," J.A. Cuculo, P.A. Tucker, G. Chen and C.Y. Lin, North Carolina State Univ., Raleigh, NC

1:30 8/7 "DEFORMATION STUDIES OF LIQUID CRYSTALLINE POLYMERS," A.E. Zachairades, IBM Almaden Research Center, San Jose, CA

12:30 - 2:00 - LUNCH

MAY 10, TUESDAY MORNING SESSION

POLK CITY

SYMPOSIUM 9 - Polymer Alloys and Blends

Chairman: A.P. Plochocki, Stevens Institute of Technology, Hoboken, NJ

Co-Chairman: X. Xu, Chengdu Univ. of Science and Technology, Chengdu, Sichuan, China

8:30 K 9/13 "FUTURE OF POLYMER BLENDS: EXPECTATIONS BASED ON TECHNICAL AND PATENT LITERATURE," L.A. Utracki, National Research Council of Canada, Boucherville, Quebec, Canada

9:00 9/14 "RHEOLOGICAL ASPECTS OF PHASE SEPARATION KINETICS IN PS/PVME BLENDS," A. Ajji, L. Choplin and R.E. Prud'homme, Laval Univ., Quebec, Canada

9:30 9/15 "MELT RHEOLOGY OF LLDPE/PP BLENDS: DYNAMIC BEHAVIOR," M.M. Dumoulin, DuPont Canada Research Centre, Kingston, Ontario, Canada; L.A. Utracki, National Research Council of Canada, Boucherville, Quebec, Canada; and, P.T. Carreau, Ecole Polytechnique, Montreal, Canada

10:00 9/16 "RHEOLOGICAL BEHAVIOR AND IMPACT STRENGTH OF POLY(VINYL CHLORIDE) BLENDS WITH POLY (ETHYLENE-CO-VINYL ACETATE)," X. Xu, H. Li, Q. Wang and S. Guo, Univ. of Science and Technology, Chengdu, Sichuan, China

10:30 9/17 "BIREFRINGENCE IN INJECTION-MOLDED DISK OF TWO-COMPONENT POLYMER SYSTEMS: PC/PS BLEND, PC/PS GRAFT POLYMER AND PPE/PS BLEND," Y. Kimima and T. Kawaki, Mitsubishi Gas Chemical Co., Inc., Tokyo, Japan and T. Inoue, Tokyo Institute of Technology, Tokyo, Japan

11:00 9/18 "CONTRIBUTION TO THE STUDY OF EPOXY-LIGNIN POLYBLENDS," D. Feldman and M. Khoury, Concordia Univ., Montreal, Quebec, Canada

11:30 9/19 "FORMATION OF MICROSTRUCTURE IN POLYBLENDS," D. Heikens, Eindhoven Technological University, Eindhoven, The Netherlands

12:30 - 2:00 - LUNCH

MAY 10, TUESDAY MORNING SESSION

FOREST CITY

SYMPOSIUM 5 - Polymerization and Reactive Processing

Chairman: J.T. Lindt, Univ. of Pittsburgh, Pittsburgh, PA

Co-Chairman: S. Omi, Tokyo Univ. of Agriculture and Technology, Tokyo, Japan

8:30 K 5/1 "STRUCTURE FORMATION IN THE CURE OF UNSATURATED POLYESTER RESINS," L.J. Lee and Y.S. Yang, Ohio State Univ., Columbus, OH

9:00 5/2 "REACTION-INDUCED CRYSTALLIZATION DURING THE RIM PROCESS OF NYLON 6," K.H. Lee and S.C. Kim, Korea Advanced Institute of Scientific Technology, Seoul, Korea

9:30 5/3 "FABRICATION OF MICROSTRUCTURES WITH EXTREME STRUCTURAL HEIGHTS BY REACTION INJECTION MOLDING," P. Hagmann and W. Ehrfeld, Institut fur Kernverfahrenstechnik, Karlsruhe, West Germany

10:00 5/4 "PROBLEMS OF SIMULATING THE PROCESSING OF THERMOSET POLYMERS," S.F. Shen, U. Gonzalez and C. Cohen, Cornell Univ., Ithaca, NY

10:30 5/5 "MIXING OF NATURAL RUBBER WITH CARBON BLACK IN A HIGHLY INSTRUMENTED INTERNAL MIXER," J.L. den Otter, TNO Plastics and Rubber Institute, Delft, Holland

11:00 5/6 "EFFECT OF STOICHIOMETRIC RATIO ON REACTION RATE KINETICS AND PROPERTIES OF A DGEBA/ MIXED AMINE EPOXY VIA DYNAMIC MECHANICAL SPECTROSCOPY," D. Wingard and C.L. Beatty, Univ. of Florida, Gainesville, FL

11:30 5/7 "A FUNDAMENTAL STUDY ON THE KINETICS OF STYRENE-BASED COPOLYMERS," S. Omni, I. Iwata, K. Inubuse and M. Iso, Tokyo University of Agriculture and Technology, Tokyo, Japan and M. Suka, Nippon Plant Co., Ltd., Tokyo Japan

12:00 5/8 "RHEOLOGICAL PROPERTIES OF CROSS-LINKED POLYETHYLENES," S. Venkatraman and L. Kliner, Raychem, Menlo Park, CA.

12:30 - 2:00 -LUNCH

MAY 10, TUESDAY MORNING SESSION

PINE HILLS

SYMPOSIUM 15 - Processing Microelectronics and Other Emerging Technologies

Chairman: D. Soane, Univ. of California, Berkeley, CA

Co-Chairmen: W.F. van den Bogert, Signetics Corporation, Sunnyvale, CA and N. Kinjo, Hitachi, Ltd., Ibaraki-ken, Japan

8:30 15/1 "POLYMERS IN MICROELECTRONICS: AN OVERVIEW," D.S. Soane and Z. Martynenko, Univ. of California, Berkeley, CA

9:00 15/2 "LITHOGRAPHIC PERFORMANCE OF SELECTED SILICON - CONTAINING RESISTS," M.J. Jurek, A.E. Novembre, R.G. Tarascon, I.P. Heyward, A. Shugard and E. Reichmanis, AT & T Bell Laboratories, Murray Hill, NJ

9:30 15/3 "NEW HIGH TEMPERATURE STABLE PHOTORESISTS BASED ON SOLUBLE POLYIMIDES AND POLYAMIDES CONTAINING THE HEXAFLUOROISOPROPYLIDENE LINKING GROUP," W.H. Mueller and D.N. Khanna, Hoechst Celanese Corp., Coventry, RI

10:00 15/4 "REACTIVE ION ETCHING OF POLYMER FILMS," B.C. Dems, F. Rodriguez, C.M. Solbrig, Y.M. Namaste and S.K. Obendorf, Cornell Univ., Ithaca, NY

10:30 K 15/5 "PROCESSING ULTRATHIN POLYMER FILMS," J.B. Lando and S.E. Rickert, Case Western Reserve Univ., Cleveland, OH

11:00 K 15/6 "FUNDAMENTAL STUDIES IN PLASTIC PACKAGING OF MICROELECTRONIC DEVICES," L.T. Mangione, AT & T Bell Laboratories, Murray Hill, NJ

11:30 15/7 "STABLE BROMINATED EPOXIES FOR MICROELECTRONICS ENCAPSULATION," C.W. Wang, and D.B. Fritz, Dow Chemical Co., Freeport, TX

12:30 - 2:00 - LUNCH

MAY 10, TUESDAY MORNING SESSION

ORLANDO

SYMPOSIUM 1 - Injection and Compression Molding

Chairman: C.L. Tucker, Univ. of Illinois, Urbana, IL

Co-Chairmen: H. Takahashi, Toyota Central Research and Development Labs, Inc., Aichi, Japan and J.F. Agassant, Ecole Nationale Superieure des Mines de Paris, Valbonne, France

8:30 1/13 "COMPUTER AIDED PREDICTIONS OF MOLECULAR ORIENTATION IN INJECTION MOLDING," J. Vlachopoulos, H. Mavridis and A.N. Hrymak, McMaster Univ., Hamilton, Ontario, Canada

9:00 1/14 "THE APPLICATION OF MULTI LIVE-FEED MOLDING FOR THE MECHANICAL PROPERTY ENHANCEMENT OF POLYETHYLENE MOLDINGS," P.S. Allan, M.J. Bevis, C. Ogbonna and H. Thapar, Brunel Univ., Uxbride, Middlesex, England

9:30 1/15 "CHARACTERIZATION OF THE ORIENTATION DEVELOPMENT IN THE INJECTION MOLDING OF A MAPHTHALENIC-BASED LC COPOLYESTER," E. Suokas and P. Tormala, Tampere Univ. of Technology, Tampere, Finland

10:00 1/16 "EFFECT OF PROCESS CONDITIONS ON THE FRACTURE PROPERTIES OF INJECTED MOLDED HIPS," G.A. Campbell and S.R. Settlemire, Clarkson University, Potsdam, NY and D. Small, D. Bennett, A. Fricke and C.L. Beatty, University of Florida, Gainesville, FL

10:30 1/17 "TRANSIENT COMPRESSIBLE FLOW IN INJECTION MOLDING RUBBER - EXPERIMENTAL DATA AND SIMPLIFIED ANALYSIS," M. Amon, American National Can Company, Barrington, IL

11:00 1/18 "CALCULATION OF FIBER ORIENTATION IN INJECTION MOLDED PARTS," H.H. de Frahan and M.J. Crochet, Univ. Catholique de Louvain, Louvain-la-Neuve, Belgium

11:30 1/19 "A NUMERICAL MODEL FOR PREDICTING FIBER ORIENTATION IN INJECTION MOLDING," A. Barbe, Ecole des Mines de Paris, Valbonne, France and M. Vincent, J.L. Cottalorda, J.L. Wybo and J.F. Agassant, Cdf-Chimie, Vernevil en Abatte, France

12:00 1/20 "MOLD FILLING AND CURING OF SHEET MOLDING COMPOUNDS," J.D. Fan, J. Kim, Y.J. Im and L.J. Lee, Ohio State University, Columbus, OH

12:30 -2:00 - LUNCH

MAY 10, TUESDAY MORNING SESSION

KISSIMMEE

SYMPOSIUM 3 -Fibers and Films

Chairman: G. Perez, Centre de Research Saint-Fons, Saint-Fons, France

Co-Chairmen: S. Kase, Kyoto Institute of Technology, Kyoto, Japan and J.F. Fellers, The University of Tennessee, Knoxville, TN

8:30 3/13 "TRENDS AND NEW DEVELOPMENTS IN FIBER AND FILM EXTRUSION," F. Hensen, Barmag AG, Remscheid, West Germany

9:00 3/14 "COMPUTER SIMULATION OF MULTIFILAMENT AIR JET MELT SPINNING," H. Ishihara, S. Hayashi, H. Yasuda and H. Ikeuchi, Toyobo Co., Ltd., Shiga, Japan

9:30 3/15 "DISTURBANCE PROPAGATION IN MELT SPINNING," D. Young and M. Denn, Univ. of California, Berkeley, CA

10:00 3/16 "USE OF MELT SPINNING SIMULATION IN PROCESS CONTROL," E. Jung, Rhone-Poulenc Fibres, Lyon, France

10:30 3/17 "TRAVELLING NECK AS A SHOCK WAVE, PART II," S. Kase, Kyoto Institute of Technology, Kyoto, Japan

11:00 3/18 "DEFORMATION MECHANISM OF HIGH SPEED SPINNING OF PET," Y. Maeda, K. Oka and M. Mineo, Toray Industries, Inc. Shizuoka-ken, Japan

11:30 3/19 "EFFECT OF SPINLINE QUENCHING ON STRUCTURE DEVELOPMENT IN HIGH SPEED MELT SPINNING OF SPINNING OF POLY(ETHYLENETEREPHTHALATE)," T. Kikutani, H. Morinaga, A. Takaku and J. Shimizu, Tokyo Institute of Technology, Tokyo, Japan

12:00 3/20 "INFLUENCE OF FORMING CONDITIONS ON MECHANICAL PROPERTIES OF MODIFIED PET FIBERS," J. Militky, Jvanicek Research Institute for Textile Finishing, Nedleho, Czechoslovakia

12:30 - 2:00 - LUNCH

MAY 9, MONDAY AFTERNOON SESSION

HAINES CITY

SYMPOSIUM 12 - Long Fiber Composites

Chairman: R. Bailey, ICI PLC, Cleveland, England

Co-Chairman: J.F. Stevenson, GenCorp, Akron, OH

2:00 K 12/6 "REFRACTION EFFECTS AND METAMORPHOSIS IN HARD ELASTIC POLYPROPYLENE (HEPP) DURING STRETCHING," R. Hosemann and I. Schulze, Bundesanstalt fur Materialforschung (BAM), Berlin, West Germany

2:30 12/7 "CONTINUOUS FIBRE REINFORCED THERMOPLASTICS," G. Cuff and R.M. Turner, ICI PLC, Cleveland, England

3:00 12/8 "HEAT TRANSFER ANALYSIS OF THERMOPLASTIC-CARBON FIBER COMPOSITES," M. Adams and G.A. Campbell, Clarkson University, Potsdam, NY

3:30 12/9 "LONG FIBER REINFORCED THERMOPLASTIC MATRIX COMPOSITES BY SLURRY DEPOSITION," D.M. Bigg and D.F. Hiscock, Battelle Columbus Labs., Columbus, OH

4:00 2/10 "FIBER ORIENTATION MECHANISMS IN LONG FIBER REINFORCED MOLDINGS," B. Rzepka and R. Bailey, ICI PLC, Cleveland, England

4:30 2/11 "THE EFFECT OF FIBER LENGTH ON THE MECHANICAL PROPERTY PERFORMANCE OF REINFORCED THERMOPLASTIC COMPOSITES," S. Ward, J. Crosby and P. Mokay, LNP Engineering and Plastics Corp., Malvern, PA

5:00 2/12 "THE INFLUENCE OF MACHINE AND TOOL PARAMETERS ON LONG GLASS FIBER REINFORCED POLYAMIDE," M. Akay and D. Barkley, University of Ulster at Jordanstown, Antrim, Northern Ireland

5:30 - 7:00 - POSTER SESSION A IN EXHIBIT HALL

MAY 9, MONDAY AFTERNOON SESSION

POLK CITY

SYMPOSIUM 9 - Polymer Alloys and Blends

Chairman: A.P. Plochocki, Stevens Institute of Technology, Hoboken, NJ

Co-Chairman: X. Xu, Chengdu University of Science and Technology, Chengdu, China

2:00 9/6 "THE EFFECT OF PROCESSING PARAMETERS ON THE FORMATION OF THE DISPERSED PHASE IN AN IMMISCIBLE BINARY BLEND," B.D. Favis and J.P. Chalifous, National Research Council of Canada, Boucherville, Quebec, Canada

2:30 9/7 "MODIFICATION OF THE CRYSTALLIZATION BEHAVIOR OF THERMOPLASTIC POLYESTERS BY BLENDING WITH AMORPHOUS NYLON," V.M. Nadkarni, V.L. Shingankuli andd J.P. Jog, National Chemical Laboratory, Pune, India

3:00 9/8 "PROCESSING OF STARCH BASED BIODEGRADABLE PLASTICS," R.P. Wool, University of Illinois, Urbana, IL

3:30 9/9 "STUDY ON NAPHTHALENE-RING-CONTAINING THERMOTROPIC COPOLYESTER AND ITS BLEND WITH POLYETHYLENE TEREPHTHALATE," Z. Zhou, X. Wu and M. Yu, China Textile University, Shanghai, China

4:00 9/10 "PERMANENCE OF PVC BASED POLYMER BLENDS INTENDED FOR BIOMEDICAL APPLICATIONS," S.N. Pal and A.V. Ramani, Sree Chitra Tirunal Institute for Medical Sciences and Technology, Poojapura, India; and N. Subramanian, IIT, Madras, India

4:00 9/11 "RHEOLOGY OF LIQUID CRYSTALLINE POLYMERIC BLENDS," T.M. Malik, P. Carreau, N. Chapleau and M. Yu, China Textile University, Shanghai, China

5:00 9/12 "STRUCTURE FORMATION IN CRYSTALLIZING BLENDS," A.J. McHugh and D.A. Tree, University of Illinois, Urbana, IL

5:30 - 7:00 - POSTER SESSION A IN EXHIBIT HALL

MAY 9, MONDAY AFTERNOON SESSION

FOREST CITY

SYMPOSIUM 7 - Rubber and Thermoplastic Processing

Chairman: N. Nakajima, University of Akron, Akron, OH

2:00 7/6 **"THE RHEOLOGICAL CHARACTERIZATION OF ELASTOMERS USING THE BICONICAL SHEAR RHEOMETER,"** H. Tang, Z.J. Lobos, Polysar Limited, Sarnia, Ontario, Canada and P.K. Freakley, University of Loughborough, England

2:30 7/7 **"INFLUENCE OF CARBON BLACK ON THE RHEOLOGICAL PROPERTIES OF RUBBER-CARBON BLACK COMPOUNDS,"** S. Montes, J.L. White and N. Nakajima, The University of Akron, Akron, OH

3:00 7/8 **"RHEOLOGICAL DETERMINATION OF MW AND MWD FOR BUTYL ELASTOMERS,"** Z.J. Lobos and H. Tang, Polysar Limited, Sarnia, Ontario, Canada

3:30 7/9 **"STUDY ON VULCANIZATION OF RUBBER COMPOUNDS FILLED WITH SAC BLACK,"** Z. Yanhao, Z. Suhe, L. Donghong, W. Fagang and L. Chengxiang, Beijing Institute of Chemical Technology, Beijing, China

4:00 7/10 **"STUDIES ON A NEW BINARY ACCELERATOR SYSTEM IN RUBBER VULCANIZATION,"** A.P. Kuriakose and G. Mathew, University of Cochin, Cochin, India

4:30 7/11 **"MIXER CONTROL THE BASIS FOR A MORE EFFICIENT RUBBER INDUSTRY,"** H.D. Griffin, Francis Shaw & Co., Ltd., Manchester, United Kingdom

5:00 7/12 **"RELATIONSHIP BETWEEN THE CROSSOVER MODULUS AND THE MOLECULAR WEIGHT DISTRIBUTION USING THE DOI-EDWARDS THEORY OF REPTATION AND THE ROUSE THEORY,"** R. R. Rahalkar and H. Tang, Polysar Limited, Sarnia, Ontario, Canada

5:30 - 7:00 - POSTER SESSION A IN EXHIBIT HALL

MAY 9, MONDAY AFTERNOON SESSION

PINE HILLS

SYMPOSIUM 10 - Innovative Technologies

Chairman: H.R. Thomas, Polar Materials, Inc., Martins Creek, PA

Co-Chairman: Y. Oyanagi, Kogakuin University, Tokyo, Japan

2:00 10/6 **"PREPARATION AND RHEOLOGICAL BEHAVIOR OF POLYIMIDE/SILICONE INTERPENETRATING POLYMER NETWORKS,"** X. Xu and M. Hao, Chengdu University of Science and Technology, Chendu, China

2:30 10/7 **"NUCLEAR MAGNETIC RESONANCE IMAGING OF DYNAMIC POLYMER-SOLVENT SYSTEMS,"** T.H. Mareci, M.D. Cockman and A. Rigamonti, University of Florida, Gainesville, FL

3:00 10/8 **"VIBRO-THERMOJOINING OF PLASTICS BASED ON REPEATED DEFORMATION,"** H. Yokoi and H. Arakawa, University of Tokyo, Tokyo, Japan

3:30 10/9 **"INTERRELATIONSHIP/SYNERGY OF THE DIFFERENT FORMS OF INTELLECTUAL PROPERTY,"** J. Faro, Faro and Associates, Boca Raton, FL

4:00 10/10 **"ROLES OF THE INTERFACE AND MORPHOLOGY IN FRACTURE PERFORMANCE OF THERMOPLASTIC COMPOSITES,"** J. Denault and T. Vukhanh, National Research Council of Canada, Boucherville, Quebec, Canada

4:30 10/11 **"PLASTICS-RUBBER COMPOSITES,"** H. Jadamus and K.P. Richter, Huels AG, Marl, West Germany

5:00 10/12 **"RAPID CURING OF EPOXY/GLASS BRAID COMPOSITES VIA ELECTRIC HEATING,"** D. Wingard and C.L. Beatty, University of Florida, Gainesville, FL

5:30 - 7:00 - POSTER SESSION A IN EXHIBIT HALL

MAY 9, MONDAY AFTERNOON SESSION

ORLANDO

SYMPOSIUM 1 - Injection and Compression Molding

Chairman: C.L. Tucker, University of Illinois, Urbana, IL

Co-Chairmen: H. Takahashi, Toyota Central Research and Development Labs., Inc., Aichi, Japan and J.F. Agassant, Ecole Nationale Superieure des Mines de Paris, Valbonne, France

2:00 1/6 "AN UNDERSTANDING OF THE FLUID MOTION AND DENSITY BUILD-UP DURING INJECTION PACKING STAGE," T.S. Chung, Hoechst Celanese Research Co., Summit, NJ

2:30 1/7 "EFFECT OF PROCESSING ON MICRO-STRUCTURE," M.R. Kamal, McGill University, Montreal, Quebec, Canada

3:00 1/8 "EXPERIMENTAL AND THEORETICAL STUDY OF THERMAL STRESSES IN THERMOELASTIC MOLDED PARTS," O. Denizart, M. Vincent and J.F. Agassant, Ecole des Mines de Paris, Valbonne, France

3:30 1/9 "PREDICTION OF BIREFRINGENCE DISTRIBUTION FOR PC OPTICAL MEMORY DISK," T. Kanai, Y. Uryu and K. Shimizu, Chiba, Japan

4:00 1/10 "MELT TEMPERATURE HOMOGENEITY IN INJECTION MOLDING," G.C. Peischl and I. Bruker, General Electric Company, Schenectady, NY

4:30 1/11 "THE J-INTEGRAL AS A FRACTURE CRITERION FOR INJECTION MOLDED POLYCARBONATE PARTS," B.H. Kim and H.Y. Oh, University of Massachusetts, Amherst, MA

5:00 1/12 "IMAGE ANALYSIS - A TOOL IN POLYMER PROCESSING," G. Fischer, B. Schmid and P. Schwarz, Universitat Stuttgart, Stuttgart, West Germany

5:30 - 7:00 - POSTER SESSION A IN EXHIBIT HALL

MAY 9, MONDAY AFTERNOON SESSION

KISSIMMEE

SYMPOSIUM 3 - Fibers and Films

Chairman: G. Perez, Centre de Research Saint-Fons, Saint-Fons, France

Co-Chairmen: S. Kase, Kyoto University, Kyoto, Japan and J.F. Fellers, The University of Tennessee, Knoxville, TN

2:00 3/6 "DRAW RESONANCE IN FILM CASTING OF POLYMERIC MELTS," A. Co and C.M. Lin, University of Maine, Orono, ME

2:30 3/7 "PREPARATION OF HIGH-MODULUS PLASTIC FILMS ZONE-ANNEALING METHOD," T. Kunugi, Yamanashi University, Kofu, Japan

3:00 3/8 "ELECTROTHERMOMECHANICAL FILM (ETMF) AND ITS PROCESSING," A. Savolainen and K. Kirjavainen, Tampere University of Technology, Tampere, Finland

3:30 3/9 "ANALYSIS OF DRAWING IN THE FLAT PET FILM PROCESS," G. Le Bourvellec, Rhone-Poulenc Recherches, Saint Fons, France

4:00 3/10 "INSTABILITY PHENOMENA IN FILM CASTING PROCESS: EXPERIMENTAL AND NUMERICAL APPROACHES," P.H. Barq, J.M. Haudin and J.F. Agassant, Ecole Nationale Superieure des Mines de Paris, Valbonne, France; and H. Roth and P. Bourgin, Rhone-Poulenc Films, Cedex. France

4:30 3/11 "HIGH PERFORMANCE STRUCTURES BASED ON COMMODITY PLASTICS," P.J. Lemstra, Eindhoven University of Technology, Eindhoven, The Netherlands

5:00 3/12 "APPLICATION OF IR SPECTROSCOPY TO OPTIMIZATION OF MULTICOMPONENT POLYMER FILMS," W. Vidrine, Measurex Corp., Cupertino, CA

5:30 - 7:00 - POSTER SESSION A IN EXHIBIT HALL

MAY 9, MONDAY MORNING SESSION

HAINES CITY

SYMPOSIUM 12 - Long Fiber Composites

Chairman: R. Bailey, ICI PLC, Middlesbrough, Cleveland, England

Co-Chairman: J.F. Stevenson, GenCorp, Akron, OH

8:00 WELCOME: DR. L.A. UTRACKI AND PROF. C.L. BEATTY

INTRODUCTORY REMARKS: DR. D.R. PRICE, VICE PRESIDENT, RESEARCH, UNIVERSITY OF FLORIDA

8:10 PLENARY LECTURE: PROF. DR. GERHARD P.M. SCHENKEL, INSTITUT FUR KUNSTSTOFFTECHNOLOGIE, (IKT) DER UNIVERSITAT, STUTTGART, WEST GERMANY

9:10 BUSINESS MEETING

9:40 BREAK

10:00 K 12/1 "SIMULATION OF THE AUTOCLAVE CURING PROCESS FOR CONTINUOUS FIBER/THERMOSETTING RESIN COMPOSITES," J.L. Kardos, R. Dave and M.P. Dudukovic, Washington Univ., St. Louis, MO

10:30 12/2 "AN EXPERT SYSTEM FOR AUTOCLAVE CURE," F.L. Abrams, AFWAL/MLBC, Wright Patterson AFB, OH and C.W. Lee, University of Dayton, Dayton, OH

11:00 12/3 "MECHANICAL PROPERTIES OF EPOXY/GLASS BRAID COMPOSITES," D. Wingard and C.L. Beatty, Univ. of Florida, Gainesville, FL

11:30 12/4 "INNOVATIVE FIBER AND FABRIC REINFORCEMENTS FOR ADVANCED COMPOSITES," J.M. Margolis, Margolis Marketing and Research Co., New York, NY

12:00 12/5 "AN ACCURATE AND CONVENIENT MODEL FOR THE DIE ENTRY FLOW OF POLYMER MELTS," S.P. Corscaden, A.G. Gibson and A.N. McClelland, Univ. of Liverpool, Liverpool, England

12:30 - 2:00 - LUNCH

MAY 9, MONDAY MORNING SESSION

POLK CITY

SYMPOSIUM 9 - Polymer Alloys and Blends

Chairman: A.P. Plochocki, Stevens Institute of Technology, Hoboken, NJ

Co-Chairman: X. Xu, Chengdu Univ. of Science and Technology, Chengdu, Sichuan, China

8:00 WELCOME: DR. L.A. UTRACKI AND PROF. C.L. BEATTY

INTRODUCTORY REMARKS: DR. D.R. PRICE, VICE PRESIDENT, RESEARCH, UNIVERSITY OF FLORIDA

8:10 PLENARY LECTURE: PROF. DR. GERHARD P.M. SCHENKEL, INSTITUT FUR KUNSTSTOFFTECHNOLOGIE, (IKT) DER UNIVERSITAT, STUTTGART, WEST GERMANY

9:10 BUSINESS MEETING

9:40 BREAK

10:00 K 9/1 "FACTORS AFFECTING POLYMER BLEND MISCIBILITY," I.C. Sanchez, Alcoa Laboratories, Alcoa Center, PA

10:30 9/2 "FLOW-INDUCED MIXING AND DEMIXING IN POLYMER BLENDS," M.F. Malone and H.H. Winter, Univ. of Massachusetts, Amherst, MA

11:00 9/3 "TOUGHNESS ENHANCEMENT IN PC/PMMA BLENDS VIA POLYMER PHASE SEPARATION," T. Kyu, J.M. Saldanha and M.J. Kiesel, Univ. of Akron, Akron, OH

11:30 9/4 "PHYSIOCHEMICAL INVESTIGATION OF THE COMPATIBILIZATION OF POLYAMIDE/POLYOLEFIN BLENDS: MORPHOLOGY, SPECIFIC INTERACTIONS AND THERMAL ANALYSIS," J.M. Willis, V. Caldas and B.D. Favis, National Research Council of Canada, Boucherville, Quebec, Canada

12:00 9/5 "ORIENTATION AND MECHANICAL PROPERTIES OF PC/LLDPE BLENDS," A. Ajji and R.E. Prud'homme, Laval University, Quebec, Canada

12:30 - 2:00 LUNCH

MAY 9, MONDAY MORNING SESSION

FOREST CITY

SYMPOSIUM 7 - Rubber and Thermoplastics Elastomer Processing

Chairman: N. Nakajima, Univ. of Akron, Akron, OH

8:00 WELCOME: DR. L.A. UTRACKI AND PROF. C.L. BEATTY

INTRODUCTORY REMARKS: DR. D.R. PRICE, VICE PRESIDENT, RESEARCH, UNIVERSITY OF FLORIDA

8:10 PLENARY LECTURE: PROF. DR. GERHARD P.M. SCHENKEL, INSTITUT FUR KUNSTSTOFFTECHNOLOGIE, (IKT) DER UNIVERSITAT, STUTTGART, WEST GERMANY

9:10 BUSINESS MEETING

9:40 BREAK

0:00 K 7/1 "RHEOLOGY AND PROCESSING OF THERMOPLASTIC ELASTOMERS," L.A. Goettler and J.R. Richwine, Monsanto Chemical Co., Akron, OH

0:30 7/2 IMPROVING THE PROCESSING OF THERMOPLASTIC ELASTOMERS," J. Vander Kooi, B.C. Howard and D.C. Hall, Struktol Company of America, Stow, OH

1:00 7/3 "SCANNING ELECTRON MICROSCOPIC STUDIES OF GELATION AND FUSION OF PVC PLASTISOLS WITH PLASTICIZER OF VARYING SOLVENT POWER," N. Nakajima and M.R. Sadeghi, University of Akron, Akron, OH

1:30 7/4 "EXPERIMENTAL AND THEORETICAL STUDIES OF THE BEHAVIOR OF RUBBER COMPOUNDS IN A PIN BARREL SCREW EXTRUDER," Y. Yabushita, R. Brzoskowski, J.L. White and N. Nakajima, University of Akron, Akron, OH

2:00 7/5 "NUMERICAL SIMULATION OF TIRE CURING PROCESS," B. Chung, J.P. Chang and M.S. James, General Tire, Inc., Akron, OH 44329

12:30 - 2:00 - LUNCH

MAY 9, MONDAY MORNING SESSION

PINE HILLS

SYMPOSIUM 10 - Innovative Technologies

Chairman: H.R. Thomas, Polar Materials, Inc., Martins Creek, PA

Co-Chairman: Y. Oyanagi, Kogakuin University, Tokyo, Japan

8:00 WELCOME: DR. L.A. UTRACKI AND PROF. C.L. BEATTY

INTRODUCTORY REMARKS. DR. D.R. PRICE, VICE PRESIDENT, RESEARCH, UNIVERSITY OF FLORIDA

8:10 PLENARY LECTURE: PROF. DR. GERHARD P.M. SCHENKEL, INSTITUT FUR KUNSTSTOFFTECHNOLOGIE, (IKT) DER UNIVERSITAT, STUTTGART, WEST GERMANY

9:10 BUSINESS MEETING

9:40 BREAK

10:00 K 10/1 "MICROWAVE PROCESSING OF POLYMERS," T.C. Ward, J.D. Graybeal, J.F. Wolfe, J.E. McGrath, G.L. Wilkes and D.A. Lewis, Virginia Polytechnic Institute and State Univ., Blacksburg, VA

10:30 10/2 "RADIO-FREQUENCY HEATING OF REINFORCED UHMWPE," R. Gauvin and C. Ouellet, Ecole Polytechnique de Montreal, Montreal, Quebec, Canada

11:00 10/3 "VIBRO-THERMOFORMING OF THERMOPLASTIC SHEETS WITH POOR FORMABILITY," H. Yokoi, Univ. of Tokyo, Japan; H. Arakawa, Nachi-Fujikoshi Corp., Toyama, Japan; and, N. Kobayashi, Shin-Etsu Polymer Co., Ltd., Ohmiya, Japan

11:30 10/4 "VIBRO-PUNCHING OF PLASTIC COMPOSITES AND THERMOPLASTIC SHEETS WITH POOR PUNCHABILITY," H. Yokoi and T. Nakagawa, Univ. of Waterloo, Waterloo, Ontario, Canada

12:00 10/5 "NEW PROCESS FOR ULTRADRAWN STRUCTURES," W.J. Tchir, Dow Chemical, Ft. Saskatchewan, Canada; H.P. Schreiber, Ecole Polytechnic, Montreal, Canada and A. Rudin, University of Waterloo, Waterloo, Canada.

12:30 - 2:00 - LUNCH

MAY 9, MONDAY MORNING SESSION

ORLANDO

SYMPOSIUM 1 - Injection and Compression Molding

Chairman: C.L. Tucker, Univ. of Illinois, Urbana, IL

Co-Chairmen: H. Takahashi, Toyota Central Research & Development Labs, Inc., Aichi, Japan and J.F. Agassant, Ecole National Superieure des Mines de Paris, Valbonne, France

8:00 WELCOME: DR. L.A. UTRACKI AND PROF. C.L. BEATTY

INTRODUCTORY REMARKS: DR. D.R. PRICE, VICE PRESIDENT, RESEARCH, UNIVERSITY OF FLORIDA

8:10 PLENARY LECTURE: PROF. DR. GERHARD P.M. SCHENKEL, INSTITUT FUR KUNSTSTOFFTECHNOLOGIE (IKT) DER UNIVERSITAT, STUTTGART, WEST GERMANY

9:10 BUSINESS MEETING

9:40 BREAK

10:00 K 1/1 "TOWARD A UNIFIED MODELLING OF THE INJECTION MOLDING PROCESS", K. Wang and C.A. Hieber, Cornell Univ., Ithaca, NY

10:30 1/2 "THE SOLIDIFICATION PROCESSING OF POLYMERS IN INJECTION MOLDING PROCESSES", N. Narazaki, Mitsubishi Gas Chemical Co., Inc., Osaka, Japan; H. Hamada, Kyoto Institute of Technology, Kyoto, Japan; and, K. Tomari, Osaka, Japan

11:00 1/3 "ROLE OF EXPERIMENTS IN USING CAE INJECTION MOLD DESIGN SOFTWARES", K. Palit and I. Chen, David Sarnoff Research Center, Princeton, NJ

11:30 1/4 "ADVANCES IN RHEOLOGICAL ANALYSIS: A NEW MODEL FOR THE SOLUTION OF MOVING BOUNDARY PROBLEMS", E.C. Bernhardt, G. Bertacchi and A. Moroni, Plastics and Computer, Inc., Montclair, NJ

12:00 1/5 "A STAGGERED SCHEME FOR FINITE ELEMENT MOLD-FILLING SIMULATION," H.P. Wang and H.S. Lee, General Electric Co., Schenectady, NY

12:30 - 2:00 - LUNCH

MAY 9, MONDAY MORNING SESSION

KISSIMMEE

SYMPOSIUM 3 - Fibers and Films

Chairman: G. Perez, Centre de Research Saint-Fons, Saint-Fons, France

Co-Chairman: S. Kase, Kyoto Institute of Technology, Kyoto, Japan and J.F. Fellers, The Univ. of Tennessee, Knoxville, TN

8:00 WELCOME: DR. L.A. UTRACKI AND PROF. C.L. BEATTY

INTRODUCTORY REMARKS: DR. D.R. PRICE, VICE PRESIDENT, RESEARCH, UNIVERSITY OF FLORIDA

8:10 PLENARY LECTURE: PROF. DR. GERHARD P.M. SCHENKEL, INSTITUT FUR KUNSTSTOFFTECHNOLOGIE (IKT) DER UNIVERSITAT, STUTTGART, WEST GERMANY

9:10 BUSINESS MEETING

9:40 BREAK

10:00 K 3/1 "BLOWN FILM PROCESSES - SOME NEW AND ALTERNATIVE CONSIDERATIONS LEADING TO BETTER PREDICTION OF BUBBLE SHAPE AND HEAT TRANSFER DYNAMICS," G.A. Campbell, Clarkson Univ., Potsdam, NY

10:30 3/2 "PECULIARITIES CONNECTED WITH MEASUREMENT AND INTERPRETATION OF THE TEXTURE IN BIAXIALLY DRAWN PETP FILMS," B.J. Jungnickel, Deutsches Kunststoff-Institut, Darmstadt, West Germany

11:00 K 3/3 "DOUBLE BUBBLE TUBULAR FILM PROCESS FOR MAKING BIAXIALLY ORIENTED POLYETHYLENE TEREPHTHALATE FILM," H.J. Kang, M. Cakmak and J.L. White, Univ. of Akron, Akron, OH

11:30 3/4 "THEORETICAL ANALYSIS OF FILM EXTRUSION AND ITS APPLICATIONS," T. Kanai, Idemitsu Petrochemical Co., Ltd., Chiba, Japan

12:00 3/5 "CAST FILM EXTRUSION THERMOMECHANICAL AND PHYSICAL ASPECTS," J.M. Haudin, Ecole Nationale Superieure des Mines de Paris, Valbonne, France

12:30 - 2:00 - LUNCH

PLENARY LECTURE

TRENDS AND HIGHLIGHTS IN POLYMER PROCESSING 1938/1988

Gerhard P.M. Schenkel, Institut für Kunststofftechnologie
(IKT) der Universität Stuttgart
Böblinger Str. 70, D-7000 Stuttgart, FRG

An attempt is made to give a survey of polymer processing during the past 50 years, with a backward glance to earlier periods and the roots of development in related branches of industrial production. Selected topics are treated in some detail, with comments and comparisons, showing typical trends and forecasting possible progress in the near future: Extrusion, injection molding, blow molding, calendering and sundries. A separate chapter deals with the role of theory and experiment in polymer processing. Generally, it may be stated that in the main fields development is changing from a practical art to applied science. - For rounding-off, the paper is closed with some anecdotes and stories about pioneers in the front line of plastics progress.

Specification of the extended paper as published in IPP:

1 Introduction
2 The Starting Phase
3 Extrusion
  3.1 Periods of Development
  3.2 Historical Comments
  3.3 Scaling-Up
  3.4 Non-Conventional Screws
  3.5 Extruders with Grooved Feed-Zones
  3.6 Process Control
4 Injection Molding
  4.1 Periods of Development
  4.2 Movable-Screw Units
  4.3 Some Innovations
5 Blow Molding
  5.1 Periods of Development
  5.2 Some Innovations
6 Calendering
  6.1 Roots of Development
  6.2 Progress since 1950
7 The Role of Theory and Experiment in Polymer Processing
  7.1 Fundamentals
  7.2 Extrusion
  7.3 Calendering
8 Sundries
9 Anecdotes and Curiosities

THE POLYMER PROCESSING SOCIETY

FOURTH ANNUAL MEETING
ORLANDO, FLORIDA, USA
MAY 8-11, 1988

ABSTRACTS

P39. **Sorption of Liquids into Foams and Subsequent Changes in Mechanical Properties of the Foams**
J.P. Harmon, D. Wingard, D. Bennett, J. Dixon, W. Williams and C.L. Beatty, Univ. of Florida, Gainesville, FL

P40. **Modelling and Visualization of the Flow of Miscible and Immiscible Polyethylene Blends Through Capillaries and Slits**
B. Tremblay and L.A. Utracki, Industrial Materials Research Inst., Boucherville, Quebec, Canada

P41. **Application of a Lumped Parameter Method on Control Volumes for Flow Simulation Inside Extrusion Dies**
J. Vlcek and V. Kral, Rubber and Plastic Research Inst., Gottwaldov, Czechoslovakia; J. Perdikoulias, Brampton Eng., Inc., Brampton, Ontario, Canada; J. Vlachopoulos, McMaster Univ., Hamilton, Ontario, Canada

P42. **Flow Visualization of Chopped Fibers in Polymers via Magnetic Resonance Imaging**
T. Mareci, J. Harmon, L. Goettler* and C.L. Beatty, Univ. of Florida, Gainesville, FL; and *Monsanto, Akron, Ohio

P43. **Patterned Ceramic Coatings by CO_2 Laser Pyrolysis**
M. Johnson, C. Watson, J. Eyler and C.L. Beatty, Univ. of Florida, Gainesville, FL

P44. **Determination of Bulk Properties from Dynamic Mechanical Thermal Analysis of Glass Supported PMMA**
K. Wolking, J. Pujol, J.P. Harmon, T. Hogen-Esch and C.L. Beatty, Univ. of Florida, Gainesville, FL

P45. **Screw Design in Injection Moulding**
H.E.H. Meijer, Eindhoven Univ. of Tech., Eindhoven; C.P.J.M. Verbraak, DSM-Research, Geleen, Netherlands

P46. **Using Mold Opening to Relate the Molding Process to Molded Products**
F.J. Buja, Kodak Co., Rochester, NY

P47. **A Procedure for Measurement of Mixing in Complex Geometrics for Creeping Flow: Case Study: Counter-Rotating Twin Screw Extruder**
D. Bigio and S. Zerafati, Univ. of Maryland, College Park, MD

P49. **Effects of Spacing Fibers in Epoxy Composite Systems Using Copper or Tungsten Wires**
J.M. Yarboro and C.L. Beatty, Univ. of Florida, Gainevilde, FL

P50. **A Study on Dynamically Co-Vulcanized Poly(vinyl chloride)/Nitrile Rubber 40 Blends**
L. Ning, Northwest Institute, Xianyang, and Z. Yinxi, Research Institute of MCI, Xianyang, China

P51. **Structured Blends**
H.E.H. Meijer, P.J. Lemstra and P.H.M. Elemens, Eindhoven Univ., Eindhoven, Netherlands

TUESDAY DISCUSSION 5:00 - 6:30 PM
POSTER SESSION B - EXHIBIT HALL FOYER

P24. **The Study on Extended Chain Crystals of Gel Spinning PE Fibers**
Z. Wu, A. Zhang, K. Chen, P. Lin and B. Qian, China Textile Univ., Shanghai, P.R.O.C.

P25. **Anionic Polymerization and Copolymerization of Phenyl Vinyl Sulfoxide and Thermal Degradation Studies of Poly(phenyl vinyl sulfoxide)**
R. Kanga, M. Buese and T.E. Hogen-Esch, Univ. of Florida, Gainesville, FL

P26. **Relaxational Properties of PET Fibers**
H. Sristov and J.M. Schultz, Univ. of Delaware, Newark, DE

P27. **Computer Aided Design of Single Screw Extruders**
P.G. Lafleur and K. Amellal, Ecole Polytechnique, Montreal, Quebec - Canada

P28. **DSC Analysis of Reaction Rate Kinetics of a DGEBA/Mixed Amine Epoxy**
M. Stoy, A. Fricke, D. Wingard and C.L. Beatty, Univ. of Florida, Gainesville, FL

P29. **Use of Dynamic Mechanical Spectroscopy for Polyurethane Reaction Rate Studies**
K. Chehab, G. Campbell* and C.L. Beatty, Univ. of Florida, Gainesville, FL; and Clarkson Univ., Potsdam, NY

P30. **Effect of Mixing on Bead Size and Sequence Distribution in Styrene/n-Butyl Methacrylate Co-polymers**
S. Canova, T. Anderson and C.L. Beatty, Univ. of Florida, Gainesville, FL

P31. **Flexural Endurance of Biaxially Oriented Polycarbonate Film as a Function of Orientation and Tensile Stress**
J. Pujol, L. Rivera and C.L. Beatty, Univ. of Florida, Gainesville, FL

P32. **Polyolefin-Wood Fiber Composites**
R.G. Raj, B.V. Kokta and C. Daneault, Univ. of Quebec at Three Rivieres, Three Rivieres, Quebec, Canada

P33. **Reactive Polymer Compounding of Modified EVA and Oligomeric Polyamides**
S. Lorek, M. Lambla and S. Nawrot, Inst. Charles Sadron, Strasbourg, Attochem, Serquigny, France

P34. **Crystallization of Polymer Processing**
K. Katayama, M. Tsuji, S. Murakami and R.J. Ihm, Kyoto Univ., Japan

P35. **Study of Filler Orientation in Injection Molded Pieces by Mechanical and Thermoanalytical Methods**
G. Banhegyi and S. Naderi, Research Inst. for Plastics, Budapest, Hungary

P36. **Incremental Drawing of Polyethylene Terephthalate**
A. Misra, B. Dutta and A.K. Mukhopadhyay, Indian Inst. of Tech., New Delhi, India

P37. **Recent Techniques for Yield Stress Measurement**
D. DeKee, Univ. of Windsor, Windsor, Ontario, Canada

P38. **Effect of Sorbed Water on the Dynamic Mechanical Properties of an Ionic Polyurethane**
W. Williams and C.L. Beatty, Univ. of Florida, Gainesville, FL

P15. **Quantitative Characterization of Impact Fracture of Polymers**
T. Vu-Khanh, National Research Council of Canada, Boucherville, Quebec, Canada

P16. **Rapid Fusing of PVC Plastisol by RF and Microwave Dielectric Heating**
W. Daher, J. Harmon and C.L. Beatty, Univ. of Florida, Gainesville, FL

P17. **Fatigue Resistant Anti-Corrosion Coatings**
J.P. Harmon, S. Singleton and C.L. Beatty, Univ. of Florida, Gainesville, FL

P18. **Microwave Processing and Measurement of Properties for Various Fiber/Epoxy Ratios**
M.C. Hawley, J. Jow, C. Schwalm, S. Singer and J. DeLong, Michigan State Univ., East Lansing, MI

P19. **Polymers in Ceramics Processing**
K. Venkataswamy, Ceramics Process Systems, Cambridge, MA

P20. **Stress-Strain Behavior of Polyolefine Filled with Plasma Treated Mica**
X. Gong and X. Xu, Chengdu Univ., and X. Liu, Changchun Inst., China

P21. **Dynamic Mechanical Properties of Glass Particle Reinforced Ionic Polyurethane**
W. Williams and C.L. Beatty, Univ. of Florida, Gainesville, FL

P22. **Stress-Strain Behavior of Glass Reinforced Dry Ionic Polyurethane**
W. Williams and C.L. Beatty, Univ. of Florida, Gainesville, FL

P23. **Effect of Coupling Agents on Lap Shear Strength of Glass Ionic Polyurethane Joints**
W. Williams and C.L. Beatty, Univ. of Florida, Gainesville, FL

MONDAY DISCUSSION 5:30 - 7:00 PM
POSTER SESSION A - EXHIBIT HALL FOYER

P1. **Direct Observation of Mold Flow Under High Injection Pressure and Speed**
H. Yokoi, T. Hayashi and Y. Murata, Univ. of Tokyo, Tokyo, Japan

P2. **Two Layer Flexible Printed Circuits Using Low Thermal Expansion Polyimides**
J. Imaizumi, K. Nagao, H. Nomura, E. Satoh, and M. Kato, Hitachi Chemical Co., Shimodate, Japan and S. Numate and N. Kinjo, Hitachi, Hitachi-shi, Japan

P3. **Properties of Weld Line in Injection Molding Parts**
H. Hamada and Z. Maekawa, Kyoto Inst. of Tech., Kyoto, Japan

P4. **Studies on Fiber Degradation During Compounding and Injection Molding of Carbon, Metal and Glass Fiber Filled Thermoplastics**
B. Franzen, Carl Klason and J. Kubat, Chalmers Univ. of Tech., Gothenburg, Sweden

P5. **Plastics Machinery Control PMC-1000**
E. Gemdjian, Pyrometer Instrument Co., Inc., Northvale, NJ

P6. **Effect of Aging Studies on the Mechanical Properties of Wood Fibers Filled Polystyrene Composites**
D. Maldas and B.V. Kokta, Univ. of Quebec at Three Rivieres, Three Rivieres, Quebec, Canada

P7. **Orientation Effects on the Dynamic Mechanical Properties of Polyurethane Thermoplastic Elastomer**
D. Bennett, K, Chehab and C.L. Beatty, Univ. of Florida, Gainesville, FL

P8. **Dynamic Mechanical Properties and Stress-Strain Behavior of Polyurethane Mica Composites**
K. Chehab and C.L. Beatty, Univ. of Florida, Gainesville, FL

P9. **Mica Flake Orientation Effects on Dynamic Mechanical Properties of Polyurethane Mica Composites**
A. Hoelzer, K. Chehab, S.R. Bates and C.L. Beatty, Univ. of Florida, Gainesville, FL

P10. **Impact Strength and Phase Separation in PC/PBT Alloys**
H. Bertilsson, B. Franzen and J. Kubat, Chalmers Univ. of Tech., Gothenburg, Sweden

P11. **Blends of Copolymers with Their Homopolymers**
K. Fujioka, Y. Baba, A. Kagemoto, N. Malone* and C.L. Beatty**, *Dept. of Chem., *Osaka Inst. of Tech., Osaka, Japan; **Univ. of Florida, Gainesville, FL

P12. **Synthesis, Characterization and Properties of Nylon-g-Poly(Ethylene glycol) Copolymers**
C.S. Ha, N.G. Yun and W.J. Cho, Pusan National Univ., Pusan, Korea

P13. **Effect of Blending Polyolefins on the Rheology and Properties of Nylon 6**
Y.P. Singh, B.V. Ankleshwaria, M.D. Daxini and M.H. Mehta, Gujarat Fertilizers State Co., Ltd., Gujarat, India

P14. **Plasma Polymerization as a Coating Process for Plastic and Metallic Parts**
P. Plein and G. Menges, Inst. fur Kunststoffverarbeitung, Aachen, West Germany

MAY 11, WEDNESDAY AFTERNOON SESSION

HAINES CITY

SYMPOSIUM 8 - Structure Development in Processing

Chairman: J.E. Spruiell, University of Tennessee, Knoxville, TN

Co-Chairman: K.I. Katayama, Kyoto University, Uji, Japan

2:00 K 8/16 "NEWER METHODS OF CHARACTERIZING STRUCTURE IN PROCESSED POLYMERS," R.J. Samuels, Georgia Institute of Technology, Atlanta, GA

2:30 8/17 "TIME-RESOLVED SAXS AND WAXS STUDIES OF ORIENTED CRYSTALLIZATION OF POLYMERS," K. Saijo and T. Hashimoto, Kyoto University, Kyoto, Japan

3:00 8/18 "STUDIES OF POLYETHYLENE TEREPHTHALATE POLYCARBONATE AND POLYPROPYLENE," A. Misra, B. Deopura and R. Haldar, Indian Institute of Technology, New Delhi, India

3:30 8/19 "STRUCTURE DEVELOPMENT IN MELT SPINNING NYLON 11 AND 12," Y. Shi and J.L. White, University of Akron, Akron, OH

4:00 8/20 "THE GROWTH AND DECAY OF STRUCTURE IN POLYMER LIQUID CRYSTALS VIA RHEO-OPTICAL MEASUREMENTS," G.W. Farell and J.F. Fellers, University of Tennessee, Knoxville, TN

4:30 8/21 "STRUCTURE DEVELOPMENT IN THERMOTROPIC LIQUID CRYSTALLINE POLYMERS," K.G. Blizard, T.S. Wilson and D.G. Baird, Virginia Polytechnic Institute, Blacksburg, VA

MAY 11, WEDNESDAY AFTERNOON SESSION

POLK CITY

SYMPOSIUM 4 - Extrusion

Chairman: P.J. Carreau, Ecole Polytechnique of Montreal, Montreal, Quebec, Canada

Co-Chairman: H. Potente, Universitat Paderborn, Paderborn, West Germany

2:00 4/15 "DIES FOR PIPE EXTRUSION WHICH COMPENSATE FOR GRAVITY FLOW," A.J. Giacomin and T. Habinak, Texas A&M University, College Station, TX

2:30 4/16 "IMPROVEMENT IN CONTROL METHODS FOR GAS PIPE EXTRUSION," D. Saint-Royre, Applied Science and Technology Research Center, France

3:00 4/17 "INFLUENCE OF FILLERS AND FLOW ADDITIVES ON FLOW DISCONTINUITIES IN LLDPE PROCESSING," B.V. Johnson and T.J. Blong, 3M Corp., St. Paul, MN; and H.P. Schreiber, Ecole Polytechnique, Montreal, Quebec, Canada

3:30 4/18 "COEXTRUSION TECHNOLOGY DEVELOPED IN GREECE: BARRIER CONTAINERS FOR AGROCHEMICALS," A. Stassinopoulos, Argo S.A., Koropi, Greece

4:00 4/19 "CHARACTERIZATION OF THE SHARKSKIN DEFECT AND ITS DEVELOPMENT WITH THE FLOW CONDITIONS," P. Beaufils, B. Vergnes and J.F. Agassant, Ecole des Mines de Paris, Valbonne, France

MAY 11, WEDNESDAY AFTERNOON SESSION

FOREST CITY

SYMPOSIUM 6 - Mixing, Compounding and Blending

Chairman: J.L. White, University of Akron, Akron, OH

Co-Chairman: J.W.M. Noordemeer, DSM Kunstoffen BV, Geleen, Netherlands

2:00 K 6/9 "COMPOUNDING FROM A TWIN SCREW VIEWPOINT," D.B. Todd, APV Chemical Machinery, Inc., South Plainfield, NJ

2:30 6/10 "A NUMERICAL PROCEDURE FOR EVALUATING THE EFFECT OF THE NIP REGION GEOMETRY ON THE MIXING PERFORMANCE OF A NON-INTERMESHING COUNTER-ROTATING TWIN SCREW EXTRUDER," D. Bigio and S. Zerafati, University of Maryland, College Park, MD

3:00 6/11 "NON-NEWTONIAN FLOW MODELLING OF A MODULAR INTERMESHING CO-ROTATING TWIN SCREW EXTRUDER," W. Szydlowski and J.L. White, University of Akron, Akron, OH

3:30 6/12 "EXPERIMENTAL COMPARISON BETWEEN INTERMESHED COUNTER AND CO-ROTATION TWIN SCREW EXTRUDER ON INORGANIC FILLER COMPOUNDING CHARACTERISTICS," T. Sakai, Japan Steel Works, Hiroshima, Japan

4:00 6/13 "EXPERIMENTAL STUDIES OF FLOW VISUALIZATION AND PERFORMANCE OF A NON-INTERMESHING COUNTER-ROTATING TWIN SCREW EXTRUDER," K. Min, M.H. Kim and J.L. White, University of Akron, Akron, OH

4:30 6/14 "FILLING AND RESIDENCE TIME DISTRIBUTIONS IN MIXER REGIONS OF CO-ROTATING TWIN SCREW EXTRUDER," K.L. Nichols, K. Jayaraman and E.G. Grulke, Michigan State University, East Lansing, MI

MAY 11, WEDNESDAY AFTERNOON SESSION

PINE HILLS

SYMPOSIUM 11 - Rheology and Rheometry

Chairman: L.A. Goettler, Monsanto Chemical Co., Akron, OH

Co-Chairmen: D.V. Boger, University of Melbourne, Parkville, Victoria, Australia and D. Acierno, Universita de Salerno, Salerno, Italy

2:00 K 11/9 "MOLECULAR ORIENTATION PROCESS IN PLASTICS INJECTION MOLDING," M. Fujiyama, Tokuyama Soda Company, Ltd., Yamaguchi-ken, Japan

2:30 11/10 "THE IMPORTANCE OF EXTENSIONAL VISCOSITY TO THE EXTRUSION OF POLYMER MELTS," D.G. Baird, D.S. Done and R. Ramanathan, Virginia Polytechnic Institute, Blacksburg, VA

3:00 11/11 "RHEOLOGY AND MORPHOLOGY OF PC/LLDPE BLENDS," D. Acierno, G. Demma, F.P. LaMantia, E. Martuscelli, V. Romano and A. Valenza, University of Salerno and Palermo, Salerno, Italy

3:30 11/12 "PREDICTION OF FIBER ORIENTATION DISTRIBUTION AND RHEOLOGICAL PROPERTIES OF FIBER REINFORCED MELTS IN SIMPLE FLOWS," A.T. Mutel and M.R. Kamal, McGill University, Montreal, Quebec, Canada

4:00 11/13 "MECHANICAL AND PHYSICAL PROPERTIES OF PEARLITE FILLED STYRENE-BUTADIENE RUBBER," T. Tincer and N. Ulkem, METU, Ankara, Turkey

4:30 11/14 "RHEOLOGICAL CHARACTERISTICS OF A SHORT CELLULOSE FIBER FILLED ELASTOMER," Z.Yanhao and J.L. White, Beijing Institute of Chemical Technology, Beijing, China and N. Nakajima, K. Min and F.C. Weissert, University of Akron, Akron, OH

MAY 11, WEDNESDAY AFTERNOON SESSION

ORLANDO

SYMPOSIUM 16 - General

Chairman: J.P. Harmon, University of Florida, Gainesville, FL

2:00 16/1 "PREDICTION OF PARISON SWELL IN THE BLOW MOLDING PROCESS," H. Kaiser, Universitat Stuttgart, West Germany

2:30 16/2 "PROCESSING CHARACTERISTICS OF PET IN THE THERMOELASTIC REGION: APPLICATION TO BLOW MOULDED AND THERMOFORMED CONTAINERS," B. Haworth, F.H. Axtell and A.O. Ola, University of Technology, Loughborough, UK

3:00 16/3 "FINITE ELEMENT SIMULATION OF INJECTION MOLDING," M.J. Crochet and F. Dupret, Universite Catholique de Louvain, Louvain, Belgium

3:30 16/4 "MECHANICAL STABILITY OF GAS/LIQUID FOAMS," H. Meinecke and M.H. Pahl, Universitat (GH) Paderhorn, West Germany

4:00 K 16/5 "NUMERICALLY STABLE FINITE ELEMENT TECHNIQUES FOR VISCOELASTIC CALCULATIONS IN SMOOTH AND SINGULAR GEOMETRIES," R.C. King, M.R. Apelian, R.A. Brown and R.C. Armstrong, Massachusetts Institute of Technology, Cambridge, MA

4:30 16/6 "TG MOLD: A COMPUTATIONAL APPROACH FOR MODELLING THE NON-ISOTHERMAL FLOW DURING INJECTION MOLDING," S. Subbiah and S.I. Guceri, University of Delaware, Newark, DE

MAY 11, WEDNESDAY AFTERNOON SESSION

KISSIMMEE

SYMPOSIUM 13 - Devolatilization and Foams

Chairman: R.J. Nichols, Welding Engineers, Inc., Blue Bell, PA

Co-Chairman: K.U. Kim, KAIST, Seoul, South Korea and H.D. Zettler, BASF Aktiengessellschaft, Ludwigshafen, West Germany

2:00 K 13/1 "ISOLATION OF POLYMERS FROM LIQUID SOLUTIONS," T.. Lindt, University of Pittsburgh, Pittsburgh, PA

2:30 13/2 "MODELLING OF POLYMER MELT DEVOLATILIZATION ENHANCED BY FOAMING," J.R. Bric and R.L. Laurence, University of Massachusetts, Amherst, MA

3:00 13/3 "STRUCTURE-PROPERTY RELATIONSHIPS IN INJECTION MOLDED THERMOSET AND THERMOPLASTICS STRUCTURAL FOAMS," A. Ahmadi, M.J. Brenner and P.R. Hornsby, Brunel University, Uxbridge, Middlesex, England

3:30 13/4 "INTERPRETATION OF POLYMER SWELLING/DRYING ON A MOLECULAR BASIS," L.A. Errede, 3M Company, St. Paul, MN

4:00 13/5 "RHEOLOGICAL MEASUREMENT OF RIGID FOAM EXTRUSION OF POLYVINYLCHLORIDE," K.U. Kim, B.C. Kim, S.M. Hong, and S.K. Park, Korea Advanced Institute of Science and Technology, Seoul, Korea

4:30 13/6 "LIQUID TRANSPORT IN ANELASTICALLY DEFORMED GLASSY POLYMERS," J.P. Harmon, S. Lee and J.C.M. Li, University of Rochester, Rochester, NY

MAY 11, WEDNESDAY MORNING SESSION

HAINES CITY

SYMPOSIUM 8 - Structure Development in Processing

Chairman: J.E. Spruiell, University of Tennessee, Knoxville, TN

Co-Chairman: K.I. Katayama, Kyoto University, Uji, Japan

8:30 8/8 "ANALYSIS OF DRAWINGS IN FLAT PET FILM PROCESS," G. Le Bourvellec and J. Beautemps, Rhone-Poulenc Recherches CRC, Saint Fons, Cedex, France; and J.P. Jarry, Rhone-Poulenc Recherches CRA, Aubervilliers, France

9:00 8/9 "MECHANICAL PROPERTIES AND MORPHOLOGY OF POLYPROPYLENE-POLYETHYLENE BLENDS," P. Jaaskelainen and T. Aalto, Neste Oy, Kulloo, Finland

9:30 8/10 "PROPERTIES OF ROLLED MULTILAYER POLYMER SHEETS," K. Nakayama, A. Kaito and M. Kato, Research Institute for Polymers and Textiles, Ibaraki, Japan and S. Takahashi, S. Nakayma and Y. Sekiguchi, Fujikura Ltd., Japan

10:00 8/11 "STUDIES ON THE BLENDS OF POLYETHYLENE TEREPHTHALATE POLYCARBONATE AND POLYPROPYLENE," A. Misra, B.L. Deopura and R.S. Haldar, Indian Institute of Technology, New Delhi, India

10:30 8/12 "STRUCTURE DEVELOPMENT IN SEQUENTIAL SIDE STRETCHING OF FILMS," J.P. Wu, M. Cakmak and J.L. White, University of Akron, Akron, OH

11:00 8/13 "EFFECT OF BIAXIAL STRETCHING ON SURFACE ROUGHNESS OF THIN METAL FILM COATED PET, PPS, AND PEEK FILMS," M. Cakmak, Y.D. Wang and K. Iwakura, University of Akron, Akron, OH

11:30 8/14 "STRUCTURE OF PE FIBER PRODUCED BY ZONE DRAWING SYSTEM," T. Takahiro, T. Takaheshi, N. Okui and T. Sakai, Tokyo Institute of Technology, Tokyo, Japan

12:00 8/15 "STUDIES OF STRUCTURAL DEVELOPMENT IN PROCESSED POLYMERS BY SMALL ANGLE SCATTERING TECHNIQUES," J.S. Lin, Oak Ridge National Laboratories, Oak Ridge, TN

12:30 - 2:00 - LUNCH

MAY 11, WEDNESDAY MORNING SESSION

POLK CITY

SYMPOSIUM 4 - Extrusion

Chairman: P.J. Carreau, Ecole Polytechnique of Montreal, Montreal, Quebec, Canada

Co-Chairman: H. Potente, Universitat Paderborn, Paderborn, West Germany

8:30 4/7 "TEMPERATURE EFFECTS IN SCREW EXTRUSION," C. Rauwendaal, Raychem Corp., Menlo Park, CA

9:00 4/8 "TEMPERATURE DEVELOPMENT IN SINGLE SCREW EXTRUDERS," H. Potente and M. Koch, Universitat Paderborn, Paderborn, West Germany

9:30 4/9 "NEW ASPECTS IN THE DESIGN OF EXTRUDERS WITH A FORCED FEEDING SECTION" H. Potente and M. Koch, Universitat Paderborn, Paderborn, West Germany

10:00 4/10 "EXTRUSION OF THERMALLY SENSITIVE THERMO-PLASTIC RESINS," K.S. Hyun, S.R. Jenkins and R.J. Streu, Dow Chemical Co., Midland, MI

10:30 4/11 "A STUDY ON FLOW FRACTURE BEHAVIOR OF MELTS AT DIE INLET," Y. Oyanagi, K. Kubota and K. Ohji, Kogakuin University, Tokyo, Japan

11:00 4/12 "DEGASSING OF PLASTICS UNDER ECONOMIC ASPECTS: SINGLE-SCREW OR CO-ROTATING TWIN-SCREW EXTRUDERS?" H. Wobbe, Hermann Berstoff Maschinenbau GmbH, Hannover, West Germany

11:30 4/13 "EXTRUSION OF POLYETHYLENES WITH A CHILLED DIE," A. Rudin, D. Cook and R. Cooke, University of Waterloo, Waterloo, Ontario, Canada

12:00 4/14 "VOID FORMATION IN EXTRUSION: CAUSES OF PROBLEM AND ITS ELIMINATION," I. Klein, Scientific Process and Research, Inc., Somerset, NJ

12:30 - 2:00 - LUNCH

MAY 11, WEDNESDAY MORNING SESSION

FOREST CITY

SYMPOSIUM 6 - Mixing, Compounding and Blending
Chairman: J.L. White, University of Akron, Akron, OH

Co-Chairman: J.W.M. Noordermeer, DSM Kunstoffen BV, Geleen, Netherlands

8:30 K 6/1 "MIXING: THEORY AND PRACTICE AS RELATED TO POLYMERS," P. Hold, Milford, CT

9:00 6/2 "ANALYSIS OF AGGLOMERATE RUPTURE IN LINEAR FLOW FIELDS," I. Manas-Zloczower and D.L. Feke, Case Western Reserve University, Cleveland, OH

9:30 6/3 "PIGMENT DISPERSION IN POLAR AND NON-POLAR POLYMERS," H.P. Schreiber and Y.M. Boluk, Ecole Polytechnique, Montreal, Quebec, Canada

10:00 6/4 "CHANGE-CAN MIXING TECHNOLOGY," B. Lagman, Charles Ross and Son Co., Inc., Hauppauge, NY

10:30 6/5 "CONTROL OF RUBBER MIXERS," P. O'Neill, Measurex Corp., Cupertino, CA

1:00 6/6 "A NOVEL COLOR CHANGING SYSTEM USING A MOTIONLESS MIXER IN THE WIRE COATING EXTRUSION," C. Kwag, J. Lee, J. Kim, K. Lee and S. Pyun, Gold Star Cable Co., Ltd., Anyang, Korea

1:30 6/7 "MILL-BEHAVIOR OF EPDM-RUBBERS WITH DIFFERENT MOLECULAR STRUCTURES IN RELATIONSHIP TO THEIR MIXING IN DIFFERENT MIXERS," J.W.M. Noordemeer and M. Wilms, DSM Kunstoffen BV, Geleen, Netherlands

2:00 6/8 "DETERMINATION OF THE DEGREE OF GELATION OF PVC WITH DSC," H. Potente and P. Michel, Universitat Paderborn, Paderborn, West Germany and S.M. Schultheis, Alpine AG, Ausburg, West Germany

12:30 - 2:00 - LUNCH

MAY 11, WEDNESDAY MORNING SESSION

PINE HILLS

SYMPOSIUM 11 - Rheology and Rheometry
Chairman: L.A. Goettler, Monsanto Chemical Co., Akron, OH

Co-Chairmen: D.V. Boger, University of Melbourne, Parkville, Victoria, Australia and D. Acierno, Universita di Salerno, Salerno, Italy

8:30 K 11/1 "THE RHEOMETRICAL BEHAVIOR OF POLYMER MELTS," K. Walters, D.M. Binding and T.A. Hadithi, University College of Wales, Aberystwyth, United Kingdom

9:00 11/2 "THE EFFECT OF PARTICLE SIZE AND CONCENTRATION ON THE MELT RHEOLOGY OF POLYSTYRENE - $CaCO_3$ COMPOSITES," J.D. Small and A. Fricke, University of Florida, Gainesville, FL

9:30 11/3 "PREDICTION OF THE NON-NEWTONIAN VISCOSITY AND SHEAR STABILITY OF POLYMERIC LIQUIDS," W.M. Kulicke and M. Bouldin, Universitat Hamburg, Hamburg, West Germany

10:00 11/4 "LDV MEASUREMENTS OF FLOW OF VISCOELASTIC FLUID THROUGH ABRUPT CONTRACTIONS," R.C. Armstrong, W.P. Raiford, L.M. Quinzani and R.A. Brown, Massachusetts Institute of Technology, Cambridge, MA

10:30 11/5 "RHEOLOGICAL MEASUREMENT OF SOLVENT EFFECTS ON VISCOELASTIC PROPERTIES IN THE SEMI-DILUTE REGIME," W.J. Shuely and B.S. Ince, Department of the Army, Aberdeen Proving Ground, MD

11:00 11/6 "ANOMALOUS GAP DEPENDENCE OF MEASURED RHEOLOGICAL PROPERTIES OF POLYOLEFINS," D.S. Kalika and M.M. Denn, University of California, Berkeley, CA

11:30 11/7 "RHEOLOGICAL PROPERTIES OF POLYCARBONATE/ LIQUID CRYSTALLINE POLYESTER BLENDS," D. Acierno, E. Amendola, C. Carfagna, L. Nicolais and R. Nobile, University of Salerno and Naples, Salerno, Italy

12:00 11/8 "RHEOLOGY AND ENTRY FLOW OF SHORT GLASS FIBER SUSPENSIONS," D.V. Boger and D.V. Hur, University of Melbourne, Parkville, Victoria, Australia

12:30 - 2:00 - LUNCH

MAY 11, WEDNESDAY MORNING SESSION

ORLANDO

SYMPOSIUM 1 - Injection and Compression Molding

Chairman: C.L. Tucker, University of Illinois, Urbana, IL

Co-Chairmen: H. Takahashi, Toyota Central Research and Development Labs., Inc., Aichi, Japan and J.F. Agassant, Ecole Nationale Superieure des Mines de Paris, Valbonne, France

8:30 1/21 "INJECTION MOLDING OF THERMOTROPIC POLYMERS," B. Ernst and P. Navard, Ecole des Mines de Paris, Valbonne, France

9:00 1/22 "SIMULATION OF BALANCED FILLING IN A MULTI-CAVITY MOLD FOR ENCAPSULATION," J. Saeki and A. Kaneda, Hitachi, Ltd., Yokohama, Japan

9:30 1/23 "COMPUTER SIMULATION FOR THE INJECTION MOLDING OF HIGHLY LOADED LONG FIBER REINFORCED THERMOPLASTICS," K.T. O'Brien, Hoechst Celanese Engineering Resins, Chatham, NJ

0:00 1/24 "FIBER AND MATRIX ORIENTATIONS IN INJECTION MOLDED FIBER REINFORCED LIQUID CRYSTALLINE POLYMER," F. Baba, H. Horibe, S. Etoh and A. Fukami, Mitsubishi Electric Corp., Hyougo, Japan

0:30 1/25 "CHARACTER AND PROPERTIES OF POLYMERIC COMPOUNDS OBTAINED BY EXTREMELY HIGH SHEAR RATE PROCESSING," H. Takahashi, T. Matsuoka, T. Ohta, K. Fukumori, T. Kurauchi and O. Kamigaito, Toyota Central Research and Development Labs., Inc., Aichi, Japan

1:00 1/26 "THE PRODUCTION OF MICROCELLULAR FOAMS IN AMORPHOUS AND SEMI-CRYSTALLINE THERMOPLASTICS," J.S. Colton, Georgia Institute of Technology, Atlanta, GA

.1:30 1/27 "FIBER ORIENTATION IN INJECTION MOLDING: OBSERVATIONS AND PREDICTIONS," S.G. Advani, University of Delaware, Newark, DE and R.B. Davis and C.L. Tucker, University of Illinois, Urbana, IL

12:00 1/28 "NEW SOFTWARE DEVELOPMENTS IN PART DESIGN AND PROCESS SIMULATION IN INJECTION MOLDING," P. Filz and G. Menges, Institut fuer Kunststoffverarbeitung, Aachen, West Germany

12:30 - 2:00 - LUNCH

MAY 11, WEDNESDAY MORNING SESSION

KISSIMMEE

SYMPOSIUM 14 - Die Extrusion

Chairman: D.H. Sebastian, Stevens Institute of Technology, Hoboken, NJ

8:30 14/1 "RECENT DEVELOPMENTS IN EXTRUSION STABILITY OF OF POLYMERS," R. Ramanathan, R. Moynahan and D.G. Baird, Virginia Polytechnique Institute, Blacksburg, VA

9:00 14/2 "DIE DESIGN FOR DUAL WIRE INSULATION," E. Mitsoulis and F.L. Heng, University of Ottawa, Ottawa, Ontario, Canada

9:30 14/3 "IMPROVED DESIGN OF A FISHTAIL SHEET DIE: 1-D AND 2-D THEORETICAL APPROACHES," J.M. Charrier and R.V. Ciplijauskas, McGill University, Montreal, Quebec, Canada; and B. Vergnes and J.F. Agassant, Ecole des Mines de Paris, Valbonne, France

10:00 14/4 "3-D EFFECTS IN COEXTRUSION," A. Karagiannis, J. Vlachopoulos and A. Hrymak, McMaster University, Hamilton, Ontario, Canada

10:30 14/5 "DIMENSIONAL VARIATION IN EXTRUSION OF POLYMERS: EXPERIMENT AND THEORY," S.E. Bechtel, K.J. Lin and J.D. Chang, Ohio State University, Columbus, OH

11:00 14/6 "ANALYSIS OF DIE DESIGN STRATEGY BY SIMULATION AND EXPERIMENT," C.C. Lee and J.F. Stevenson, GenCorp Research, Akron, OH

11:30 14/7 "OPTIMAL DESIGN OF PROFILE EXTRUSION DIES: A FULL THREE DIMENSIONAL FINITE ELEMENT SOLUTION TECHNIQUE," R.R. Rakos, A. Kiani and D.H. Sebastian, Stevens Institute of Technology, Hoboken, NJ

12:00 14/8 "FLOW OF POLYMERS THROUGH A DIE WITH OSCILLATING BOUNDARIES: MODELLING AND EXPERIMENT," A.I. Isayev, V. Wong and X. Zeng, University of Akron, Akron, OH

12:30 - 2:00 - LUNCH

MAY 10, TUESDAY AFTERNOON SESSION

HAINES CITY

SYMPOSIUM 12 -Long Fiber Composites
Chairman: R. Bailey, ICI PLC, Cleveland, England

Co-Chairman: J.F. Stevenson, GenCorp, Akron, OH

2:00 2/13 **"NEW RESULTS FOR INJECTION MOLDING OF LONG FIBER POLYAMIDE,"** E. Doering, Deutsche ICI Automotive Plastics, Frankfurt, West Germany

2:30 2/14 **"POSITION OF NEUTRAL PLANE DURING HOLLOW DISK COMPRESSION MOLDING OF LONG FIBER-REINFORCED THERMOPLASTICS,"** H. Hojo, E.G. Kim, T. Onodera, H. Yaguchi, S.H. Kim and M. Koshimoto, Tohoku University, Sendai, Japan

3:00 2/15 **"FRACTURE BEHAVIOR OF LONGER GLASS FIBER REINFORCED POLYPROPYLENE,"** D.E. Spahr and J.M. Schultz, University of Delaware, Newark, DE; K. Friedrich, Technical University Hamburg, Hamburg, West Germany; and G. Nutting, Imperial Chemical Industries, Cleveland, United Kingdom

3:30 2/16 **"THE INFLUENCE OF INJECTION MOLDING PARAMETERS ON THE FRACTURE STRENGTH OF LONG GLASS FIBER REINFORCED POLYAMIDE,"** M. Davies, R. Bailey and D.R. Moore, ICI Advanced Materials, Cleveland, Middlesbrough, England

4:00 2/17 **"A THEORETICAL STUDY OF HOT MELT IMPREGNATION OF FIBER BUNDLES,"** C. Chmielewski, K. Jayaraman and C.A. Petty, Michigan State University, Lansing, MI

4:30 2/18 **"A CENTRIPETAL PUMP FOR HOT MELT IMPREGNATION OF FIBER BUNDLES WITH VISCOELASTIC FLUIDS,"** N. Losure, K. Jayaraman and C.A. Petty, Michigan State University, East Lansing, MI

5:00 - 6:30 - POSTER SESSION B IN EXHIBIT HALL

MAY 10, TUESDAY AFTERNOON SESSION

POLK CITY

SYMPOSIUM 4 - Extrusion
Chairman: P.J. Carreau, Ecole Polytechnique of Montreal, Montreal, Quebec, Canada

Co-Chairman: H. Potente, Universitat Paderborn, Paderborn, West Germany

2:00 4/1 **"PREDICTION OF PRODUCT PROPERTIES IN EXTRUSION AND INJECTION MOLDING,"** W. Michaeli, Institut fur Kunststoffverarbeitung, Aachen, West Germany

2:30 4/2 **"A 3-D FINITE ELEMENT SIMULATION OF POLYMERIC FLUID FLOW THROUGH DIES,"** P.A. Tanguy, F.E. Bertrand and M. Gadbois, Laval University, Quebec, Canada

3:00 4/3 **"A COMPARISON OF NUMERICAL SIMULATIONS OF MELTING MECHANISMS IN THE PLASTICATING EXTRUDER,"** C. Miaw, General Electric Company, Schenectady, NY and D. Lange, Georgia Institute of Technology, Atlanta, GA

3:30 4/4 **"MODELLING OF SINGLE-SCREW EXTRUDERS,"** C. Guerrero, A. Vincellete and P.J. Carreau, Ecole Polytechnique, Montreal, Quebec, Canada

4:00 4/5 **"RESIDENCE TIME DISTRIBUTION IN COUNTER-ROTATING TWIN SCREW EXTRUDERS (CALCULATIONS AND EXPERIMENT),"** H. Potente, and P. Michel, Universitat Paderborn, Paderborn, West Germany and S.M. Schultheis, Alpine AG, Ausburg, West Germany

4:30 4/6 **"THE EFFECT OF SCREW STAGGER ON MIXING IN A TANGENTIAL COUNTER-ROTATING TWIN SCREW EXTRUDER,"** D. Bigio, University of Maryland, College Park, MD

5:00 - 6:30 - POSTER SESSION B IN EXHIBIT HALL

MAY 10, TUESDAY AFTERNOON SESSION

FOREST CITY

SYMPOSIUM 5 - Polymerization and Reactive Processing

Chairman: J.T. Lindt, University of Pitttsburgh, Pittsburgh, PA

Co-Chairman: S. Omi, Tokyo University of Agriculture and Technology, Tokyo, Japan

2:00 5/9 "THE REACTIVE EXTRUSION OF POLYSTYRENE/POLYPROPYLENE BLENDS," P. Cheung and S.T. Balke, University of Toronto, Toronto, Ontario, Canada

2:30 5/10 "REACTIVE EXTRUSION OF POLYPROPYLENE," C. Tzoganakis, J. Vlachopoulos and A.E. Hamielec, McMaster University, Hamilton, Ontario, Canada

3:00 5/11 "REACTIVE BLENDING OF POLYAMIDE AND CARBOXYLATED NITRILE RUBBER," W. Baker and M. Saleem, Queen's University, Kingston, Ontario, Canada

3:30 5/12 "OPTIMAL CONTROL OF RIM IMPINGEMENT MIXHEADS," P.D. Coates and A.F. Johnson, University of Bradford, Bradford, UK

4:00 5/13 "GRAFT COPOLYMERIZATION OF BUTYL ACRYLATE ONTO POLY(VINYL CHLORIDE)," H. Shaojun and L. Jianxiong, South China Institute of Technology, Guangzhou, China

4:30 5/14 "EFFECT OF THE CORRELATION BETWEEN PRE-COPOLYMERIZATION INGREDIENTS AND REACTION VOLUME ON IMPACT POLYSTYRENE MORPHOLOGY AND PROPERTIES," D.D. Kechajov, Petroleum Research Institute, Bourgas, Bulgaria

5:00 - 6:30 - POSTER SESSION B IN EXHIBIT HALL

MAY 10, TUESDAY AFTERNOON SESSION

PINE HILLS

SYMPOSIUM 15 - Processing in Microelectronics and Other Emerging Technologies

Chairman: D. Soane, University of California, Berkeley, CA

Co-Chairmen: W.F. van den Bogert, Signetics Corporation, Sunnyvale, CA and N. Kinjo, Hitachi, Ltd., Ibaraki-ken, Japan

2:00 15/8 "STRESS CHARACTERIZATION OF EPOXY MOLDING COMPOUNDS," W.F. van den Bogert, M. Molter and D.J. Belton, Signetics Corp., Sunnyvale, CA

2:30 15/9 "THE BIREFRINGENCE PROBLEM IN OPTICAL DISK SUBSTRATES: A MODELING APPROACH," J. Greener, Eastman Kodak Co., Rochester, NY

3:00 K 15/10 "THERMOPLASTICS WITH NOVEL PROPERTIES AND THEIR IMPACT ON ELECTRONICS," H. Munstedt, BASF Aktiengesellschaft, Ludwigshafen, West Germany

3:30 15/11 "NEW MATERIALS FOR MULTILAYER MICROELECTRONIC APPLICATIONS: POLYMERIZATION AND PROPERTIES OF BISBENZOCYCLOBUTENE BASED POLYMERS," S.F. Hahn, P.H. Townsend, J.A. Gilpin and D.C. Burdeaux, Dow Chemical, Midland, MI

4:00 15/12 "SPIN-ON GLASS AS A PLANARIZING INTERLAYER DIELECTRIC FOR VLSI," T. Rucker, H.Y. Lin, P.L. Pai and C.H. Ting, Intel Corp., Santa Clara, CA

4:30 15/13 "NEW EPOXY ENCAPSULANTS WITH CONTROLLED THERMAL EXPANSION COEFFICIENTS FOR PACKAGING," N. Kingo and M. Ogata, Hitachi Ltd., Kuji-Cho, Japan

5:00 - 6:30 - POSTER SESSION B IN EXHIBIT HALL

TOWARD A UNIFIED MODELLING OF THE INJECTION-MOLDING PROCESS

K.K. Wang and C.A. Hieber, Cornell University, Ithaca, NY 14853-7501

Based upon a purely viscous modelling combined with compressibility in order to handle the post-filling stage, the injection-molding flow dynamics in a thin cavity of arbitrary planar geometry can be described by

$$G(x,y,t)\,\frac{\partial p}{\partial t} - \frac{\partial}{\partial x}\left(S\,\frac{\partial p}{\partial x}\right) - \frac{\partial}{\partial y}\left(S\,\frac{\partial p}{\partial y}\right) = -\,F(x,y,t)$$

where

$$S \equiv \int_0^h \frac{z^2}{\eta}\,dz$$

in which z is the gapwise coordinate, h is the half-gap thickness and $\eta(\dot{\gamma},T,p)$ the shear viscosity with

$$G(x,y,t) \equiv \left(\frac{1}{p + \hat{p}}\right) \int_0^h \left(1 - \frac{\rho}{\hat{\rho}}\right) dz$$

$$F(x,y,t) \equiv \int_0^h \left(1 - \frac{\rho}{\hat{\rho}}\right)\left(-\frac{\partial \ln T}{\partial t}\right) dz$$

where $\rho(T,p)$ is here based upon the Spencer-Gilmore equation of state:

$$(p + \hat{p})\left(\frac{1}{\rho} - \frac{1}{\hat{\rho}}\right) = \hat{R}\,T$$

During the filling stage, the terms involving G and F are of smaller order and one recovers the usual field equations for an incompressible fluid. At the instant of fill, however, when the inlet pressure gets abruptly changed to the preset packing pressure and the condition along the melt front gets switched to an impermeability condition ($\partial p/\partial n = 0$), the term involving G first becomes important. In fact, the typical diffusion time for this first phase of the post-filling stage is on the order of .1 sec or less, such that the pressure field rapidly approaches a uniform value with the temperature field remaining essentially unchanged during this short period. Thereafter, the F term becomes important as substantial cooling eventually occurs (with a characteristic cooling time on the order of ≈ 10 seconds). During this latter phase, F is the driving term; in particular, the increased density due to decreasing T requires additional flow into the cavity which, from the dynamic force balance, requires a pressure gradient to balance the viscous resistance. Accordingly, during this cooling phase, the pressure in the cavity begins to fall. Hence, whereas the cavity pressure traces will be characterized by a monotonic approach to the imposed holding pressure under isothermal conditions, in the actual non-isothermal situation the pressure traces will be characterized by a peak value followed by decay during the cooling-dominated phase.

The above behavior will be substantiated by experimental results for filling a simple strip mold with polystyrene. In order to accurately predict the cavity pressure traces during the cooling phase, it is found essential that the temperature and pressure sensitivities of η be based upon a WLF-type functional form instead of the more customary Arrhenius-type form, even though both models are essentially equivalent during the filling and early post-filling stage. It is further demonstrated that the power-law limit is accurate even during the cooling-dominated phase. That is, although the flow rates may be low, the associated stress levels are high due to the very large viscosities at the low temperatures. In turn, it is the stress level which determines the shear-thinning behavior of the viscosity.

The Solidification Proceeding of Polymer in Injection Molding Process

N. Narazaki -- Mitsubishi Gas Chemical Company,Inc.,Osaka,JPN
H. Hamada -- Kyoto Institute of Technology,Kyoto,JPN
K. Tomari -- Osaka Municipal Technical Research Institute, Osaka,JPN

Recently,it has been recognized a very effective method on designing mold by using computer to simulate flow of melt polymer in the mold.
But, simulation is fairly difficult, because melt flow behavier is dependent on the temperature, pressure of melt polymer and temperature of cavity wall. Particularly the Solidification Proceeding of Polymer on the neighborhood of cavity wall is complicated. For simulating the Solidification Proceeding of Polymer in Injection Molding, it may be needed to solve the equations of momentum, continium and energy.
To solve all these governing equations, computer require time may be very large. Then, we propose next solution procedure.

Procedure:
(1)To solve the equations of momentum and continium.
(2)To predict the cavity thickness (flow gap) from the experimental data(pressure-time in cavity and screw displacement-time), in stead of solving energy equation.
These data(pressure-time in cavity and displacement-time of screw) were gathered by using computer from the seven pressure sensors mounted to spiral flow mold cavity wall and displacement monitor equipped to injection machine.

In this presentation firstly describe experimental method to obtain pressure-time data and prediction method to obtain Solidification Proceeding Rate of Polymer on the neighborhood of cavity wall.
And next the verification between Prediction of Solidification Proceeding Rate by using experimental data and simulation of that by FEM. On the simulation, the viscosity data(viscosity - shear rate) by capillary rheometer and specific heat capacity (Cp-temp) by Differential Scanning Caloriemeter were used.
Using FEM codes are MARC and FREMKIT developed by MARC Analysis Research Corpration.

1/3

ROLE OF EXPERIMENTS IN USING CAE INJECTION MOLD DESIGN SOFTWARES

K. Palit and I. Chen, David Sarnoff Research Center, Princeton, New Jersey 08543-5300, U.S.A.

A number of CAE mold design softwares are now commercially available and used as aids by the plastics engineers to design injection molds. Most of these softwares are based on the mathematical modeling of plastics melt flow during injection. In order to reduce the degree of complexities in solving the governing partial differential equations of conservation of mass, momentum and energy, a number of simplifying assumptions including the melt being inelastic and incompressible are used in the mathematical modeling. The results obtained from CAE mold design softwares need to be assessed carefully for materials, molds and molding conditions of interests. For accuracy each CAE software should be validated through experiments. This paper describes how experiments can play an important role in the use of CAE injection mold design softwares.

In order to assess the quality and accuracy of CAE results, experiments were performed on a 360 ton Battenfeld injection molding machine at a wide range of injection speeds using a test mold of variable thickness including forty eight different ribs, tapers and bosses. A flame retardant high impact polystyrene was used as a typical material for injection molding applications. The ram position and melt pressures at the sprue, gate and several locations in the cavity during filling were monitored for slow, medium and fast injection speeds to help determine the start and end of filling of the sprue, runner and cavity system, variable flowrate during the course of filling and point of switch-over from filling to packing and holding. For each injection speed the airshot melt temperature at the tip of the injection nozzle was measured.

The airshot melt temperature, coolant temperature as the mold temperature, fill time and variable volume flowrate as determined from the experiments were used as the input data for molding conditions in a finite element cum finite difference based mold filling analysis software. The rheological coefficients of Cross model based on the true viscosities of the material at the temperature range of 200 to 260°C and the thermal properties such as the specific heat, melt density and thermal conductivity at the process temperature of the material were used in the software as the input data for the material properties. The finite element mesh consisting of 830 elements and 536 nodes was used in the software to represent the flow geometry of the sprue, runner and cavity.

The CAE results are compared with experiments in terms of the pressure vs. time history during filling as well as the sprue and gate pressure at the end of filling for the selected slow, medium and fast injection speeds. It is shown that experiments can be used to help determine the accuracy of the CAE predictions over a wide range of process conditions.

ADVANCES IN RHEOLOGICAL ANALYSIS
A New Model for the Solution of Moving Boundary Problems

Ernest C. Bernhardt, Giorgio Bertacchi, Antonino Moroni
Plastics & Computer Inc., Montclair, NJ 07043

This paper describes a new finite element flow analysis model (**faBest**).

BASIC APPROACHES TO DESCRIBE THE CAVITY TO BE ANALYZED

Most commonly, the geometry of the cavity to be filled is described by a two dimensional 'layflat' representation of the part. In this technique the analyst applies his judgement to predict the major flow paths, and we refer to it as the 'USER-DEFINED FLOW PATH' method.

The alternate method to describe the cavity is through the use of a FINITE ELEMENT MODEL. An appropriate finite element model would require only the description of the part configuration and would obviate the need for any fluid dynamic considerations, e.g. flow direction. Additional advantages of a finite element model are a more detailed picture of the flow conditions at any point, the possibility to change the gating without redescribing the entire cavity and the potential for integration with CAD/CAM systems.

Schematically, the models may be classified into two groups:

* Qualitative solutions * Quantitative solutions

In the first category, to reduce the complexity of the problem, isothermal and newtonian assumptions are used to predict the flow front position. However, even for this 'simple' condition, a special calculation strategy must be developed. Non-linearity is introduced through non-newtonian viscosity, and the problem reaches a very high level of complexity. Not only is a time step solution required, but a dynamic analysis must be used to predict the position of the advancing flow front.

Industry needs quantitative solutions. It is natural to first consider the use of one of the existing models for finite element structural analysis. However, since flow computations are quite different from linear stress/strain calculations, it becomes necessary to introduce 'user defined correction factors' to account for all the special circumstances encountered, and the technique becomes of questionable value.

TECHNICAL CHALLENGE AND THE faBest SOLUTION

Finite element models for plastics flow in a cold cavity must deal with:

* non-linear material properties * moving boundary conditions.

Traditional finite element techniques which employ linear equations to calculate the nodal value of field variables cannot handle material non-linearity. This limitation can be overcome through appropriate iteration techniques. One begins with a constant value of material property (viscosity) at an initial (assumed) shear rate, and solves the system of equations. Then a new calculation must be made with the new viscosity as a function of the shear rate determined in the preceding solution, etc. until the desired convergence is obtained.

Moving boundaries, coupled with the problem of non-linear material properties, pose a much more difficult challenge. Finite element techniques, to determine the unknowns, need information on the boundaries to which the relationships between nodal variables apply. In mold filling, however, the boundary of the flow front is not known, and its location is the desired output of the program. There is no steady state flow, because a flow can speed up or slow down at any given time, due to a change in resistance encountered by another flow at a different location. Only a dynamic analysis can provide a solution to this problem.

The solution lies in making a starting assumption of a possible location for the flow front at a given time, and verifying whether the starting hypothesis is coherent with the boundary conditions of the flow front. The pressure drop must be the same from the melt inlet to every point along the front. If this is not the case, the starting assumption must be corrected, and the calculation repeated, until convergence is achieved. It is not sufficient to verify the starting assumptions and the relevant iterations only at the end of filling. They must be repeated and all elements must be re-computed at short time intervals throughout the filling process.

As in any finite element model, the cavity geometry must be meshed with elements, each corner of the element being a node. In each element, the flow can enter at any corner or side, and exit from the opposite sides or corners.

From a starting assumption of flow rate distribution at the flow front, we calculate the pressure drops to fill each flow front element in time steps equal to the shortest time to reach the end of one of the front elements. If all pressure drops are not equal at a given interval, the flow rate distribution is changed, until convergence is achieved. At that point, a new flow front is created by including the elements connected to the filled elements of the preceding time step calculation, and so on until the entire cavity is filled.

In our development we have also addressed two other common problems encountered in finite element analyses: The model should be able to use elements of nonuniform size and the quality of the results should be sufficiently independent of mesh density. The objective was met completely through the use of quadrilateral elements with 8 nodes and through the automatic generation of first order sub-elements, to smooth possible element geometrical distortion, coupled to a second order sub-elements fragmentation, a function of the Local Dynamic Resistivity. With **faBest**, the element density can be changed according to the requirements for precision in various sections of the part. In this way, the calculation times can be minimized. The overall quality of results is almost independent of the mesh density. Another advantage is that a flow can move in any direction of space, and there is no limitation to describing ribs, etc. Annular runners can be combined with the cavity description, so that, in the case of hot runner systems, the mold can be analyzed integrally.

A STAGGERED SCHEME FOR FINITE ELEMENT MOLD-FILLING SIMULATION

H.P. Wang and H.S. Lee
General Electric Company
Schenectady, New York 12345

FEMAP, a Finite Element Mold-filling Analysis Program, has recently been developed at GE Corporate Research and Development. It is a finite element based mold-filling analysis software using a staggered node/element scheme.

The staggered node/element scheme developed in FEMAP specifying the pressure at nodes and the temperature and the velocity at element centroids is a variation of the well-known staggered grid finite difference approach, long recognized for its better accuracy. The benefits of this staggered node/element scheme in modeling the plastics mold filling are profound and include: precise calculations of velocity and flow rate at element centroids based on the FEM theory and consistency of velocity and temperature nodes. This latter condition eliminates the excessive averaging processes required for calculating velocity, shear rate, nodal thickness, material properties and viscous heating in a traditional nodal based system. Averaging is needed only for the temperature gradient in the convective term.

In addition, this scheme is compatible with the front tracking algorithm in FEMAP which uses the fractional volume of fluid technique to define free surfaces. The computational domain of fluid elements has to be updated at every filling step. For minimizing the storage requirement and the computing time, the momentum and the energy equations are coupled through iteration. A multiple time step algorithm for solving the momentum and the energy equations is utilized for allowing different time steps for the pressure and the temperature fields. The embedded stability criteria of the temperature field are generally more stringent than those of the pressure field necessitating smaller time increments.

Extensive validation tests using many different plastics molds ranging from simple 2-D to complex 3-D geometries under various process conditions have been conducted for investigating the accuracy and the efficiency of this code. Figure 1 shows the typical validation results of a complex mold. The pressure history plots between the measurements and the predictions are in excellent agreement. Many short-shot experiments on real parts have also proved the accuracy of the front tracking algorithm.

In order to avoid the use of a no-flow temperature in the input, the velocity and the temperature fields are modeled in a very precise manner using a multi-layered structure. Because the available viscosity data is usually in a limited range of temperature and shear rate, some extrapolation of the viscosity data near the mold surface, a cold region, is inevitable. The degree of deviations in the pressure predictions due to the extrapolation depends on the viscosity model used in the code; some are more sensitive than others. The ideal viscosity model should be able to cover a wide range of temperature and shear-rate representing the true process conditions.

FEMAP has been routinely used in the field for over one year; and many examples of real part applications from TV housings to automobile bumpers will be shown to illustrate the many unique features of this advanced CAE tooling analysis software.

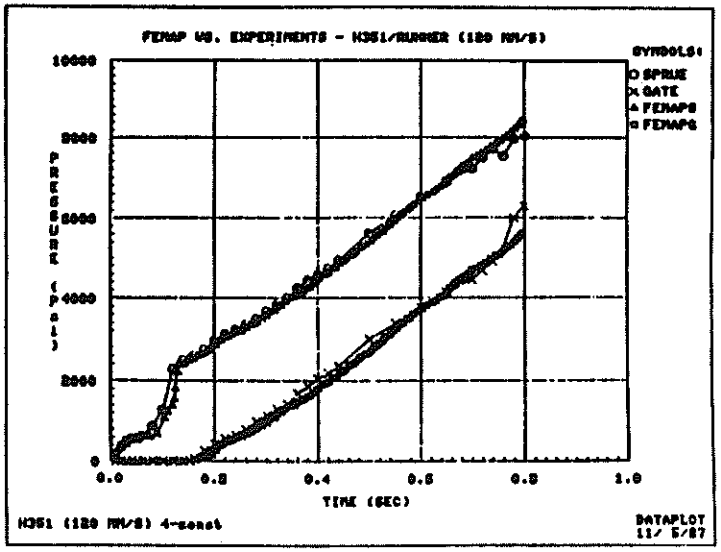


Figure 1 Pressure History Plots at the sprue and the gate.

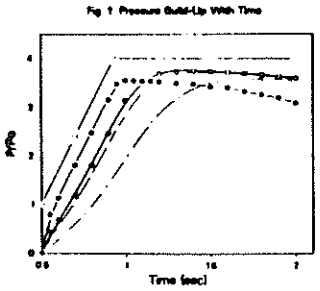
1/6

AN UNDERSTANDING OF THE FLUID MOTION AND PRESSURE BUILD-UP IN A NON-ISOTHERMAL INJECTION MOLD PACKING STAGE

Tai-Shung Chung
Hoechst Celanese Research Division
86 Morris Avenue
Summit, New Jersey 07901

Recent experimental data on the gapwise-density variation across a mold thickness have shown that most of the previous mathematic models for packing have severe deficiencies and limitations. The purpose of this work is to review and re-examine the non-isothermal fluid motion within a mold cavity during this stage. The non-isothermal governing equations for the pressure and density built-up within a cavity for a generalized Newtonian fluid are derived. The equation of state for polymeric melts is assumed to obey either the Spencer-Gilmore or the Tait equation. The tranitional pressure change in an injection mold cavity is manipulated by two opposite factors; namely, solidification and flow. The former tends to reduce local pressure, while the latter tries to increase the pressure within a cavity and to make it more uniform. The effects of melt compressibility, molding conditions, and the cavity boundary on the fluid motion are determined.

For example, Figure 1 describes the transitional pressure build-up at the end of a cavity for polyethylenes with various melt compressibilities. Their compressibilities follow this order: dot line > triangle > circle > solid circle. The square denotes the injection pressure profile at gate. This result shows that the higher the melt compressibility, the slower the pressure build-up. Figure 2 presents the calculated gap-wise density variation. The densities are calculated at 400°K, and the number in each set of parentheses indicates the time when that layer is almost solidified (400°K). Fifty percent down from the surface denotes one-half of the thickness. The calculated density increases with an increase in the distance away from the mold surface and the density near the gate is greater than that near the end. These phenomena are in agreement with experimental results published by Kamal and his coworkers.



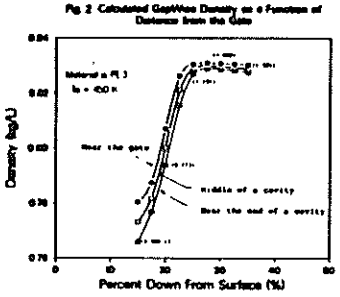
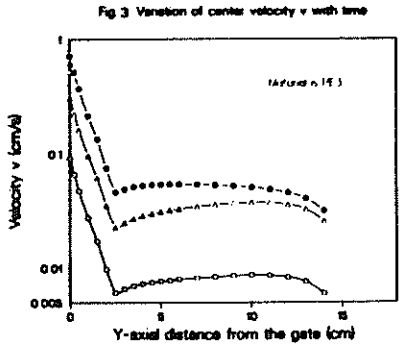
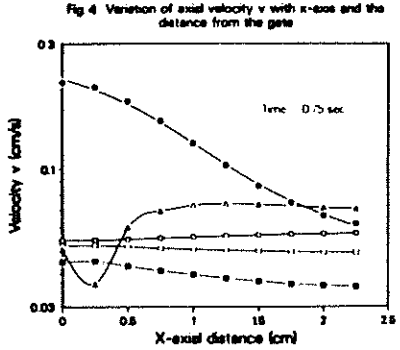


Figure 3 shows the calculated velocity in the machine direction. The three curves present three transitional velocities in the packing; namely, after onset (top curve), middle, and near the end (bottom curve). There are two interesting phenomena in this figure; one is the existing of a V shape with the minimum point at x approximately equal to the half width of a mold cavity, and the other is the very nearly equal velocity gradients (about 0.45-0.5) near the gate for these curves. The former may be explained based on the boundary flow, while the latter stems from the radial flow mechanism.

Figure 4 gives the velocity in the machine direction as a function of x (transverse direction) at various distances from the gate. Near the gate, the magnitude of v is highest at the center line of the cavity and rapidly decreases in the x-direction to the cavity wall. When the axial distance is almost equal to the width of the cavity, melt near the wall moves faster than that near the center line of the cavity. This interesting phenomenon is attributed to the transition of flow patterns and the influence of the cavity corner and wall. In other words, flow changes from a radial to an axial flow around x = b (mold width), and, since we imposed the boundary conditions that no melt is allowed to flow across the walls, the compressed polymeric melt in the corner has to move in the machine direction in order to dissipate pressure. This phenomenon disappears at a distance away from the corner, and the axial velocity in the machine direction becomes uniform across the width of the cavity.





I/7

EFFECT OF PROCESSING ON MICROSTRUCTURE

Musa R. Kamal, Department of Chemical Engineering
McGill University, Montreal, Canada H3A 2A7

Many of the important commercial plastics products involve polymer blends and composites, which tend to exhibit obvious anisotropic characteristics. Even when only one, unfilled or reinforced polymer is employed in the composition, the plastics product usually exhibits a microstructure which is not uniform throughout the system. Typically, the product shows skin-core structure, a range of morphological zones, variations in crystallinity, molecular orientation and frozen stresses, in addition to complex patterns of concentration, particle size, shape, and orientation distributions in the case of blends and filled or reinforced systems. In all plastics applications, the above characteristics (normally referred to as microstructure) have a profound impact on the properties and utility of the product. In fact, microstructure control through the manipulation of composition and/or processing conditions, represents one of the most important challenges of polymer scientists and engineers.

Microstructure is determined by the thermo-mechanical history experienced by the plastic composition during processing. The thermo-mechanical history, in turn, represents the interaction between the material (as reflected by its thermodynamic and transport properties) and the design and operating parameters of the processing system. Thus, mathematical modeling or computer simulation should provide an approach, complex as it may be, to the understanding, prediction, and control of microstructure development in plastics parts.

Some interesting manifestations of microstructure in unfilled plastics, fiber-reinforced polymers, and blends will be illustrated. Subsequently, some of the important issues relating to the application of computer simulation to microstructure prediction will be discussed. Finally, examples of the use of computer simulation for microstructure prediction will be shown. Emphasis will be placed on injection molding.

"EXPERIMENTAL AND THEORETICAL STUDY OF THERMAL STRESSES IN THERMOPLASTIC MOULDED PARTS"

O. DENIZART, M. VINCENT, J.F. AGASSANT

Centre de Mise en Forme des Matériaux
UA CNRS n° 852
Ecole des Mines de Paris
Sophia Antipolis
06560 VALBONNE FRANCE

The knowledge of the residual stresses (RS) level is of great interest for the dimensional stability of moulded articles. Each stage of the injection cycle contributes to the development of the RS. Filling in a cold mould induces high thermal gradients in the part's thickness. Then, packing counteracts the thermal shrinkage and leads to a large molecular orientation which is frozen-in during inhomogeneous solidification. Finally, unmoulding is possible when the core has reached a sufficient low temperature. Cooling to room temperature follows.
This work deals with the experimental determination and the computation of the thermal residual stresses.

Experimental measurement of the thermal stresses.

Polystyrene disks were injected under a wide spectrum of moulding conditions, including melt and mould temperature, injection rate and packing pressure. Two methods were used to measure RS. The first one is the layer removal method. Thin layers of 0.2mm thickness were removed from rectangular samples (length: 50mm, width: 10 mm, thickness: 3mm) parallel and perpendicular to the flow direction. Then the resultant curvature was measured with a three-dimensional "roughness-calibrator". The internal stresses were then deduced with the stress-strain relationship of Treuting and Read based on an isotropic elastic and pure bending behavior of the material. The mould temperature was found to have a great influence to the stress development in the skin area: a decrease in mould temperature (70°C to 20°C) leads to an increase in compressive stresses (-3MPa to -10MPa).
Another method was developped to measure the residual strains due to a dissymmetrical cooling (mould walls are regulated at different temperatures). After unmoulding, the warpage which balances the dissymmetrical stress profile is measured.

Computation of the residual stresses

Several models are considered on the base of the following hypothesis.

- The thermal stresses computation is initiated at the beginning of the packing stage. It stops when the part reaches an homogeneous room temperature. A thermoelastic behavior is implemented for both the melt and the solid material with thermal dependence of the Young's modulus E(T), of the Poisson ratio $\nu(T)$, the thermal dilatation coefficient $\alpha(T)$, and the thermal diffusivity a(T).

- During its residence time in the mould, the part is supposed to remain in contact with the mould (thermal conduction). After unmoulding we assume a heat transfert coefficient and a zero stress along the boundaries of the part.
- The anisotropy of the elastic modulus E and the thermal dilatation coefficient due to simple orientation effects is neglected.
- During the packing stage, the flow of molten polymer between the frozen-in layers is not taken into account.
- The melt is supposed to be purely viscous and submitted to an uniform hydrostatic pressure.

The initial temperature field is computed using a mould filling code developped in our laboratory.
An incremental computation of the residual stresses has been developped. At each time step the temperature field is actualized and the stress field is computed using two different methods which will be presented bellow.
The first model may be applied to simple geometries. The classical assumption of an homogeneous strain throughout the part thickness is made. The heat equation is solved by a finite difference method and the incremental stresses are then computed using a slab method. The residual stresses distributions were computed for several injection conditions. They are in close agreement with the experimental study.
The second model is more general and may be applied to more complex geometries or boundary conditions. A bidimensional temperature distribution is considered and the incremental stresses are computed using a finite element method. This model has been applied to compute the warpage developpment of a dissymmetrically cooled part. Results are in good agreement with the experiments.

PREDICTION OF BIREFRINGENCE FOR PC OPTICAL MEMORY DISK

Toshitaka Kanai , Keijiro Shimizu
Idemitsu Petrochemical Co., Ltd.
1-1 Anesaki-Kaigan, Ichihara, Chiba 299-01 Japan

Polycarbonate(PC) is considered to be a proper resin for optical memory disk, however PC resin show high birefringence. It is very important to reduce birefringence of PC optical disk. This research is to obtain the relation between birefringence and the process conditions and to get the optimum condition for the production of low birefringence substrate of PC optical disk.

The birefringence distribution of PC optical disk was theoretically predicted by the calculations of both the stress distribution caused by molecular orientation during the filling stage and the thermal stress (residual stress) caused by temperature difference during the cooling stage.

1. Birefringence caused by molecular orientation

The stress distribution during the filling, cooling and relaxation process was calculated by using theoretical equations of momentum equation, energy equation and Leonov type constitutive eq.(4) described blow.

$$\frac{\partial \tau_{12}}{\partial y} - \frac{\partial p}{\partial x} = 0 \qquad (1) \qquad \frac{\partial T}{\partial t} = \alpha \frac{\partial^2 T}{\partial y^2} \qquad (2)$$

$$2\pi \int_{-b}^{b} u r \, dz = Q \qquad (3)$$

Leonov model

$$\tau(t) = \sum_{k=1}^{M} \eta_k \left(\begin{pmatrix} C_{11,k}(t) & C_{12,k}(t) & 0 \\ C_{12,k}(t) & C_{22,k}(t) & 0 \\ 0 & 0 & 1 \end{pmatrix} \cdot 2\nu \, s(t) \, e_1(T) \begin{pmatrix} 0 & 1 & 0 \\ 1 & 0 & 0 \\ 0 & 0 & 0 \end{pmatrix} \right) \qquad (4)$$

where

$$\eta = \eta(\dot{\gamma}) \cdot \eta_0 = \eta_0(T)_{\dot{\gamma}=0} = \eta_0(T)_1 \quad \eta_0 = \sum_{k=1}^{M} \eta_k/(1-s) \qquad (5)$$

Storage Modulus G' and Loss Modulus G''

$$G'(\omega) = \sum_{k=1}^{M} \frac{\eta_k \theta_k \omega^2}{1+\theta_k^2 \omega^2} \qquad G''(\omega) = \eta_0 s \omega + \sum_{k=1}^{M} \frac{\eta_k \omega}{1+\theta_k^2 \omega^2} \qquad (6)$$

Birefringence Δn_{13}

$$\Delta n_{13} = n_{11}(r,t) - n_{33}(r,t) = C(T) \cdot 2 \sum_{k=1}^{M} w_k \left(C_{11,k}(r,t) - 1 \right) \qquad (7)$$

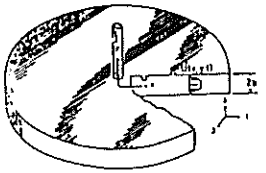


Figure 1. Schematic view of disk flow

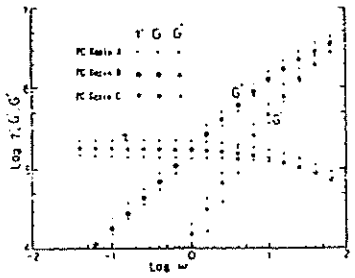


Figure 2. Rheological data of PC disk grade

Rheological behaviors of typical PC disk grades are shown in Figure 1.

2. Residual stress

Residual stress was obtained by temperature distribution which 3 dimensional unsteady state FEM analysis predicts. Birefringence of substrate was obtained from the thermal stress.

$$\Delta n_{13} = C_{opt} \cdot \Delta \sigma = C_{opt} \cdot (\sigma_r - \sigma_\theta)$$

where C_{opt} is stress-optical coefficient.

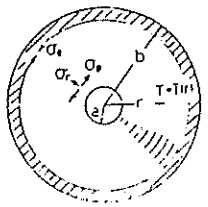


Figure 3. Thermal stress

3. Results and discussion

The following results are obtained by theoretical analysis.

Figure 4 shows the birefringence has the maximum value at the instant of filling, and then decreases until the freeze of the disk which means the relaxation terminated. PC disk has high value of birefringence at the surface region and very low value at the center region (Figure 5).

The birefringence near the gate shows high value and decreases with increasing the distance from the gate. PC having low viscosity and short relaxation time shows low birefringence.

Figure 6 shows isothermal lines in a mold which were predicted by thermal analysis of 3 dimensional unsteady state. The set temperature and positions of cooling cavities and chillers influence the temperature distribution of substrate.

Surface temperature of substrate at the cooling time of 12 sec. is shown in Figure 7.

Relationship between the birefringence distribution and the process conditions such as rheological properties of PC, injection temperature, mold temperature, chiller location and annealing condition is possible to be predicted theoretically by calculating shear stress during the injection process and thermal stress during the cooling process. The birefringence distribution is influenced by those process conditions. As an example, predictions of birefringence for three different PC resins are shown in Figure 8. This shows retardation Δn_{13} due to thermal stress is in a same level as Δn_{13} due to shear flow.

Those results qualitatetively agree with the experimental ones.

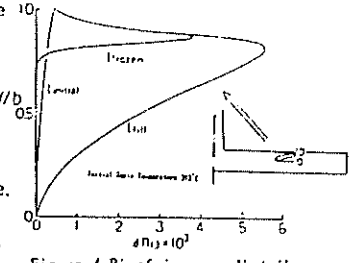


Figure 4. Birefringence distribution along thickness direction

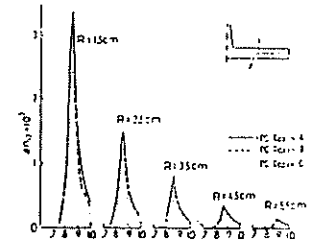


Figure 5. Birefringence distribution along radial direction and thickness direction

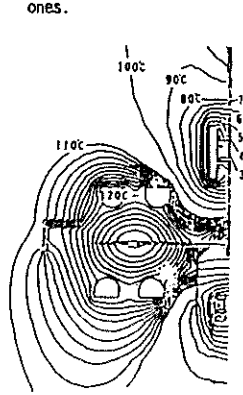


Figure 6. Thermal analysis for the disk mold

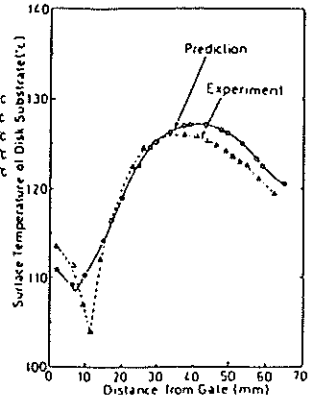


Figure 7. Temperature distribution of substrate (cooling time 12sec)

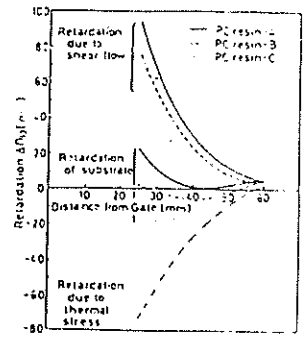


Figure 8. Retardation of three PC substrates

<Acknowledgement> The authers wish to thank Dr.C.A.Hieber and Dr.K.K.Wang (Cornell University) for their grateful help and valuable discusion in the prediction of birefringence due to the filling process.

MELT TEMPERATURE HOMOGENEITY IN INJECTION MOLDING

C.C. Pelschl and I. Bruker
General Electric Corporate R and D Center
P.O. Box 8 - CEB/221
Schenectady, New York 12309

Engineering thermoplastic materials are increasingly finding large part applications in consumer markets, in particular in the automotive markets. There is a strong tendency to mold these large parts in relatively small injection units (small screw channel volume to shot volume ratio) to reduce resin residence time in the barrel. However, this procedure has been shown to lead to incomplete melting, mold filling difficulties and variations in impact properties and morphology within a given part. Presumably, all of these problems could be related to the thermal history and temperature variations within a shot, necessitating means of predicting and measuring melt temperatures in injection molding.

This need to determine melt temperature of a shot prior to injection has prompted the development of a thermocouple "ring-bar" device and a graphical shot "history" analysis of injection molding extrusion. This device, and the accompanying analysis technique have been used to determine the thermal homogeneity, axial and radial, of a shot as a function of screw channel volume to shot size ratio, barrel temperature profile, screw speed and back pressure.

The ring-bar device was used to measure the melt temperatures between the screw-tip and the nozzle. As the polymer melt flowed through the ring and perpendicular to the bar to which thermocouples were placed, radial temperature profiles could be measured at short time intervals (every 2-3 seconds) during the injection portion of successive air shot cycles, providing full temperature contours of the shot.

The experiments were carried on a 275 ton machine equipped with a 45mm 20:1 L/D barrel. The single flighted, conventional screw was designed for use with engineering plastics and had a compression ratio of 2.3. The data acquisition system was based on a LSI 11/23 microprocessor.

The results indicate the shot volume to screw channel volume to be the dominant factor in determining the axial thermal homogeneity. The distribution of the shot on the screw during the last "soak", the duration of "soak time" relative to screw rotation time and the numbers of "soaks" are shown to be factors contributing to the thermal state of the shot. Back pressure, screw speed and barrel temperature profile are shown to have secondary effects. The radial temperature profile is seen to be affected by the shear rate in the metering section of the screw due to viscous heating. Its development can be estimated with the Graetz number.

These results suggest the use of pins for increasing radial thermal homogeneity and the use of slots on the flights for increasing axial thermal homogeneity.

THE J-INTEGRAL AS A FRACTURE CRITERION FOR INJECTION MOLDED POLYCARBONATE PARTS

B. H. KIM and H. Y. OH
University of Massachusetts, Amherst, MA 01003

Fracture property of the injection molded polycarbonate is influenced by the residual stress within the molded part. The residual stress alters the stress and strain field at the crack tip region and therefore it causes a change in the fracture property. In the injection molding process, the residual stress is developed due to the molecular orientation and thermal quenching. Since the molding process itself generates residual stress in the molded part, the fracture property is sensitive to the process parameters. In particular, the effect of the polymer melt temperature on the fracure property is investigated.

The J-integral [1] is chosen as a parameter which characterizes the onset of crack propagation since it is a valid criterion for both linear and nonlinear elastic materials. In fact, the critical J-integral is equal to the critical linear elastic strain energy release rate in the case of linear elastic material. Although development of the J-integral is based on the nonlinear elastic fracture mechanics, it can be applied to nonelastic material with some restrictions.[2]

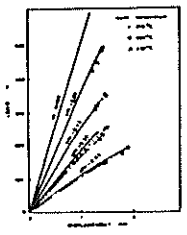


Fig 1

Fig.1 shows load-displacement curves for the injection molded polycarbonate (CD-2000 from Mobay Chemical Corporation) with three different melt (barrel) temperatures (230 °C, 250°C, and 270°C). The residual stresses are determined from the measurement of the curvature of the part after a succesive layer removal. The curvature is measured by an optical amplification using a laboratory laser. The residual stress distribution in the half the thickness of the injection molded parts for the three different melt temperatures is shown in Fig.2. The residual stress at the surface and the center of the part is about

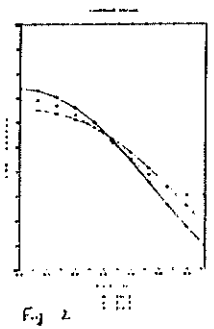


Fig 2

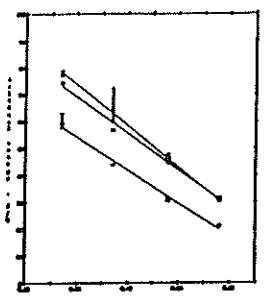


Fig.3

be in compression and tension, respectively. Fig.3 shows the critical energy calculated from load-displacement curves in Fig.1 by using locus of fracture initiation points[3]. Jc at the onset of crack propagation is the slope of the least square fitted line.(Jc = 7.1, 8.0, and 6.4 KJ/m² for 270, 250, and 230 °C, respectively). Jc at 250 °C is higher than the others while surface compressive stress of 250 °C is lower than that at 230 °C. But, tensile residual stress alone cannot account for the increase in J_c because the injection molded part is normally tougher than the annealed one(no residual stress).

This indicates that the fracture toughness in presence of residual stress can not be explained simply by surface compressive stress nor tensile stress in the center. Three-dimensional analysis is attempted to relate residual stress to fracture toughness. First, stress intensity factor(Kr) due to residual stress is calculated by using the weight function method[4]. Second, stress intensity fator(K) at the crack tip is obtained by superposing Kr on applied stress intensity(Ka). That is, K= Kr + Ka. Here, K is a function of position through the thickness. A new fracture criterion is applied to calculate Kc instead of applying K=Kc as in a two-dimensional problem since the crack does not normally propagate at K=Kc due to compressive stress at the surface. Finally, the applied critical stress intensity factor, (Ka)c, is calculated and converted to Jc (Jc = Gc in this case). The calculated Jc is compared with experimental results. Because the load-displacement curves of the injection molded Polycarbonate (PC) of 5.2 mm thickness is almost linear, G_c or K can also be used. The relation of J_c and the residual stress is expected to be quite complex for thinner PC (plane stress) exhibiting nonlinear property.

REFERENCES

[1] J.R. Rice, J. of Applied Mechanics, 35 (1968) 379-386
[2] D. Broek, Elementary Engineering Fracture Mechanics, 3rd Ed, Sijthoff & Noordhoff (1982)
[3] B.H. Kim and C.R. Joe, Int. J. of Fracture 34 (1987) R 57-60
[4] M. Oore, D.J.Burns, J. of Pressure Vessel Technology, 102, (May 1980) 202-211

IMAGE ANALYSIS - A TOOL IN POLYMER PROCESSING

G.FISCHER, IKP B.SCHMID, IKT P.SCHWARZ, IKP
UNIVERSITÄT STUTTGART, D-7000 STUTTGART

Increasing use of long fibers in reinforced thermoplastics requires new methods in controlling morphological parameters like mean fiber length and local fiber orientation. Knowledge of these parameters gives a quantitative information about processing machinery and design of the cavity. The good mechanical performance of long fiber compared to short fiber reinforced materials results in

- higher elastic moduli (stiffness)
- higher strength
- higher impact resistance
- smaller thermal expansion coefficient
- better dimension stability
- better surface quality.

If non-optimized processing parameters are applied, a decay in mean fiber length and badly orientated fibers in areas of high stress may result and by that, the above mentioned properties diminish.
It is a well-known fact, that injection-processing of fiber reinforced materials causes a more or less decrease in fiber length and a broad fiber length distribution, *Fig.* 1. This effect may be reduced by a morphology-based optimization of processing parameters, using image analysis. Recent progresses in image processing instrumentation and automated measuring software give new tools in developing better fiber reinforced parts, optimizing processing parameters and in daily quality control.
Using microradiography methods, fiber orientation may be optimized in regions of high stress in a rather qualitative way. A newer method /1/, based on image analysis of polished cross-sections, gives quite more quantitative information on spatial fiber orientation. If magnitude or symmetry - see *Fig.* 2 - of fiber orientation are insufficient or out of tolerance, a stepwise change of process parameters may be applied to improve properties by morphology. Some applications are shown.

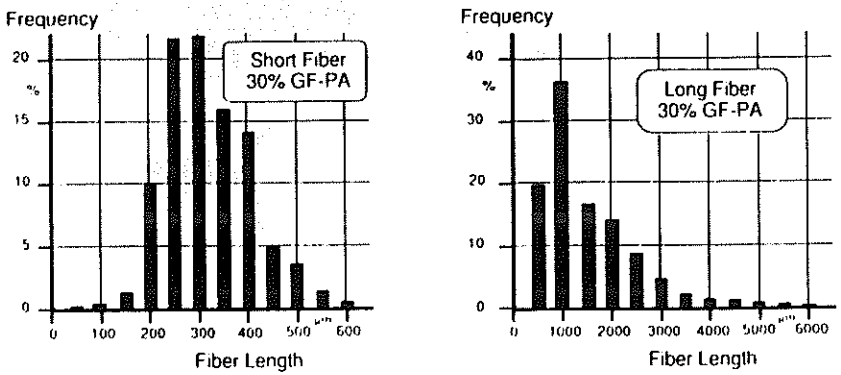


*Fig.*1 : Fiber length distribution of short fiber and long fiber reinforced PA after processing

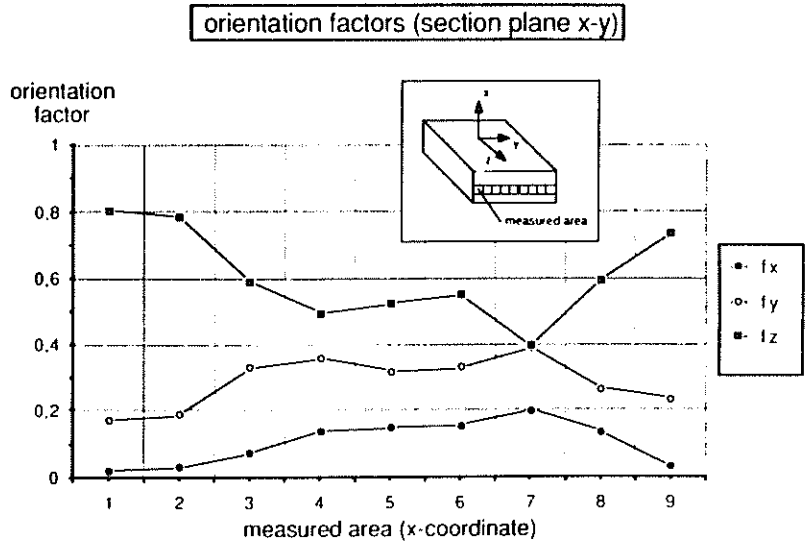


Fig. 2: Spatial distribution of fiber orientation in the cross-section of an injection molded bar, exhibiting an asymmetrical orientation in y-direction (measured areas: 0.3x0.3 mm^2, mold flow in z-direction)

/1/ Fischer, G. : Quantitative determination of the orientation of short fibres by image analysis. German Plastics 77 (1987) 5

1/13

COMPUTER-AIDED PREDICTION OF MOLECULAR ORIENTATION IN INJECTION MOLDING

H.Mavridis, A.N.Hrymak and J.Vlachopoulos
Department of Chemical Engineering, McMaster University
Hamilton, Ontario, Canada, L8S4L7

A complex molecular orientation distribution is observed in the injection molding of amorphous polymers. A major contribution is due to the flow-induced deformation of the polymer molecules during mold filling and incomplete relaxation during cooling, after cessation of flow. In this work a numerical study was undertaken in an effort to resolve the impact of the fluid mechanics of mold filling on the molecular orientation of the final part as reflected in available birefringence measurements.

A special feature of mold filling is the flow rearrangement behind the advancing front, known as "fountain flow". This flow field was simulated with a Galerkin/Finite Element Method and the Leonov viscoelastic model. Numerical studies indicated that the viscoelastic computations converge with mesh refinement provided a slip boundary condition is employed to alleviate the stress singularities. Tracking of material elements illustrated the flow-induced deformation experienced by the fluid, which results in a highly oriented surface layer (Figure 1).

Using the calculated stress field and the theory of Isayev & Hieber (Rheol. Acta,19,168,(1980)), frozen-in birefringence profiles were predicted for a commercial polystyrene and compared to available experiments (Figure 2). Predictions agree reasonably well with experiments.

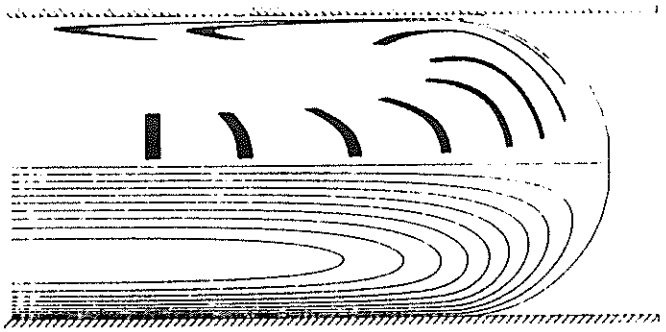


Figure 1. Streamlines and deformation of a fluid element behind the flow front

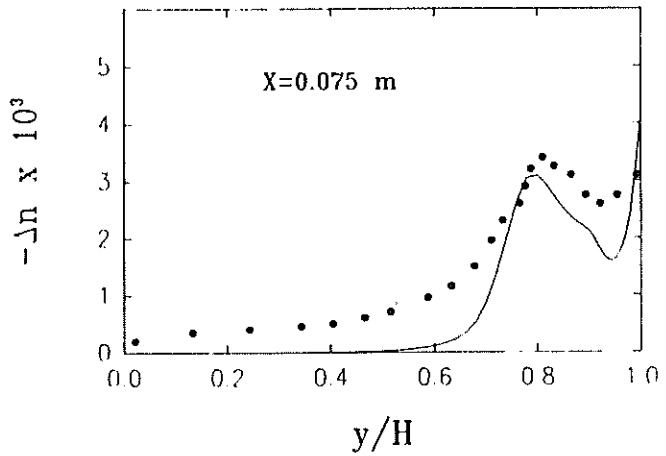


Figure 2. Comparison of predicted birefringence profile with the experiments of Kamal & Tan, Polym. Eng. Sci.,19,558 (1979)

The Application of Multi Live-Feed Moulding for the Mechanical Property Enhancement of Polyethylene Mouldings.

P.S. Allan, M.J. Bevis, C. Ogbonna and H. Thapar.

Brunel University,
UXBRIDGE, Middlesex UB8 3PH, England.

The preparation of polyethylene artefacts with exceptionally high modulus by tensile drawing, solution spinning, solid state extrusion, drawing of gel spun fibres is well documented. Several investigations (1,2) have related to the enhancement of tensile modulus in injection moulded artefacts, although there is appreciably less understanding of the processes required to achieve high modulus in thick-sectioned complex shaped parts by melt processing.

Multi live-feed moulding (3) MLFM has been developed to provide a facility for the production of complex shaped artefacts whilst maintaining control over the preferred orientation of matrix material and reinforcing fibres. The process has been applied to a range of polyethylenes which were moulded into 6 x 6mm cross section mouldings. These in turn were characterised using WAXS, DSC, light microscopy of microtomed sections, microhardness profiles, TEM of replicas taken from sections etched using a solution of $KMnO_4$ in a specified mixture of suplhuric and orthophosphoric acids, and tensile testing to give quoted Youngs modulus at 1 per cent strain.

Fitting a barrel end-cap attachment to a conventional injection moulding machine, as illustrated, is one embodiment of the MLFM process.

The appropriate sequencing of the activation of the injection pistons can cause shearing of the melt - 180° out of phase operation, or compression and decompression of the melt - in phase operation. The solidifying melt in the mould cavity can be made to undergo a profile of processing parameters, typically in twenty stages during the packing cycle, thereby providing for optimium control over micromorphology and properties. The attachment also provides for much higher mould cavity pressures to be used than in conventional injection moulding.

The effect of MLFM on the microstructure and mechanical properties of mouldings, produced at normal injection pressures will be presented. For example, injection mouldings of BP Chemicals Rigidex 50 were prepared using three modes of operation to give Youngs Modulus values:

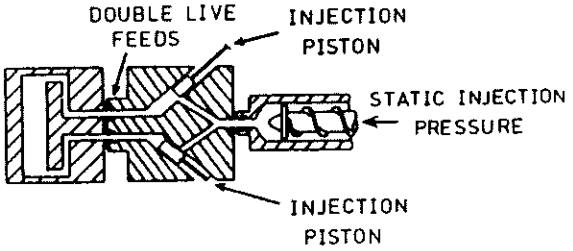
conventional moulding	1.62GPa
compression/decompression	1.84GPa
multi live feed-shear	3.76GPa

In all three mouldings the distribution and nature of micromorphologies was shown to vary through the thickness. The higher modulus mouldings that result from MLFM are attributed to the presence of substantial bands of shish debab micromorphology. Youngs modulus in these bands exceeds 5 GPa.

The presentation will amplify the results presented above and their extension to a selection of polyethylene grades, processed using a wide range of MLFM process parameters. This will illustrate the potential of MLFM for the control and optimisation of the micromorphology and physical properties of injection moulded thermoplastics.

References

1. J. Kubat and J.A. Manson, Polymer Engineering and Science 23 (1983) 869-876
2. G.W. Ehrenstein and Cl. Maertin, Kunstoffe 75 (1985) 105-110.
3. P.S. Allan and M.J. Bevis, Plastics and Rubber Processing and Applications 7 (1987) 3-10. UK Patent Application 85-31374.



CHARACTERIZATION OF THE ORIENTATION DEVELOPMENT IN THE INJECTION MOLDING OF A NAPHTHALENIC-BASED LC COPOLYESTER

E. Suokas and P. Törmälä, Tampere University of Technology,
P.O. Box 527, SF-33101 Tampere, Finland

The commercial liquid crystalline polymer (VECTRA A900, Celanese) was injection molded into test samples. The shape and dimensions of the mold gate and cavity, the holding pressure, the nozzle and mold temperature were varied in the injection molding. Polarized light micrographs were taken from the test bars cut in the machine direction. In addition, capillary flow and small amplitude oscillatory shear measurements were performed.

The viscosity of the used LC copolyester based on a naphthalene derivative and hydroxybenzoic acid was highly temperature and shear dependent. A plate-and-plate rheometer revealed that the storage modulus G', i.e. the elasticity, decreased abruptly in the temperature range of 300°C to 320°C. Moreover, G' was greater than G" at 300°C. The situation became reversed as the temperature was increased by 20°C.

In the injection molding of the LCP the development of molecular orientation can be divided into two states. At the first stage in the cavity filling process without holding pressure the free flow of the LC melt resulted in a microstructure composed of 4 distinct layers[1]). The geometric or dimensional factors of the mold gate and cavity had a significant effect on the formation of these strata. By proceeding from the skin to the center of the cross-section of a 3 mm thick bar the 1st and 3rd layers should represent transition flow, probably elongational, and the 2nd and 4th layers shear.

The thicknesses of the two transition zones were temperature dependent. Raising the mold temperature decreased the thickness of the 1st layer but increased the thickness of the 3rd layer. At a constant mold temperature an elevated nozzle temperature reduced the 3rd layer, which was most pronounced near the LC-glass transition[1]).

At the second stage holding pressure expanded the 2nd layer at the expense of the 1st and the 4th at the expense of the 3rd, and equalized the difference in molecular orientation. So the thicknesses of the transition zones, especially of the 3rd layer, were pressure dependent.

Because of the elastic constants and the viscosity coefficients, which are mainly unknown, the flow behaviour of LCP's is very complex[2]). The molecular orientation of the 2nd and 4th layers was arc-like. Between them existed a transition zone, the 3rd layer, where the molecular orientation should be discontinuous. At a constant mold temperature a reduction in the nozzle temperature expanded the 3rd layer. This was probably due to the supercooling effect[3]) of the LC melt, which increased elasticity and die swell[3]). In the case of a monodomain flow the rise in the elasticity and perhaps also viscosity could offer one explanation for the rapid change in the molecular orientation of the 3rd layer. This second transition zone may thus represent a flow separation for the director field[4]). The first transition zone (the 1st layer) should be related to the viscous boundary layer.

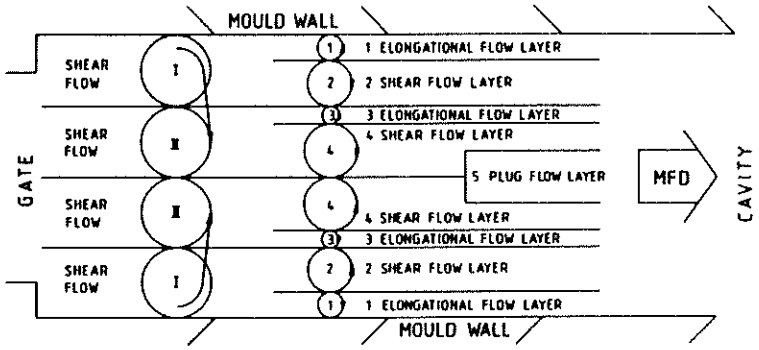


Fig. 1 A free flow model of a LC melt for the mold cavity filling process resulting in a microstructure composed of 4 distinct layers.

There are indications that nematic polydomain melts should be of tumbling type in a shear field[2]). On these grounds a rotary flow model of a LC melt has been proposed in Figure 1[1]). The rotational shear, heat conduction, viscous heat generation, a time parameter, mass temperature, the thickness and length of a cavity, the shape of the gate and the mold wall temperature have an effect on the velocity gradient. The low mold wall temperature decelerates the motion of the liquid crystalline melt in the cavity. The heat conduction reduces the rotational velocity of domain I in relation to domain II. The cold mold wall tears a small part tumbling in the reverse direction, i.e. the 1st layer, from domain I, whose propagation velocity slows down. Because the domains II and 2 with free shafts have a tendency to rotate in the reverse direction, domain II also divides into two sections due to the heat conduction and the velocity profile. This results in the 3rd layer, i.e. the second transition zone.

References

1) E. Suokas et al., "Molecular Crystals and Liquid Crystals," H. Gasparoux and F. Hardouin, Eds., Gordon and Breach, in press
2) G. Marrucci, Pure & Appl Chem, 57, 1545 (1985)
3) D. Done et al., Polym Eng and Sci, 27, 816 (1987)
4) W.B. Vanderheyden et al., J Non-Newt Fluid Mech, 23, 383 (1987)

Effect of Process Conditions on the Fracture Properties of Injection Molded HIPS

G.A. Campbell and S.R. Settlemire
Clarkson University, Potsdam, New York 13676
D. Small and C.L. Beatty
University of Florida, Gainesville, Florida 32611

This investigation was undertaken to determine the influence of injection molding process parameters, melt temperature, melt viscosity, mold temperature, injection rate, and injection time on the physical properties of high impact styrene. During this investigation we have molded a polystyrene which has about 0.8 micron rubber particles. The results presented today will compare the physical properties of the styrene under different molding conditions to the physical properties of the same styrene that has been molded using typical laboratory compression molding techniques. The polymers were molded on a 50 ton state-of-the-art injection molding machine over a wide range of melt temperatures and injection times. The mold was temperature controlled using a hot water temperature control unit and the mold face was maintained between approximately 30 C and 80 C. The wide range in temperature in the mold necessitated a fairly wide range in cycle time due to the extended cooling necessary when the mold temperature was at a maximum.

The molded samples which consist of impact disks, tensile bars and heat deflection bars were tested using standard procedures for tensile, flex, and impact strengths. The impact strength was measured using an instrumented falling dart drop device. Each of the samples from the different operating conditions was also monitored for the percent of recoverable strain that could be detected by immersion in hot silicone oil.

The results of this investigation indicate that molding conditions have a very strong influence on the physical properties of the molded high impact styrene parts. We have found that there is a correlation between impact strength and the mold cycle time, mold temperature, and polymer melt temperature. The tensile modulus and flexural modulus were found to be less influenced by these molding parameters, however the elongation was found to be a function of the processing condition. We have also developed a correlation between the physical properties of these molded materials and the recoverable strain as measured by the hot oil test.

TRANSIENT COMPRESSIBLE FLOW IN INJECTION MOLDING RUNNER

Moris Amon, American National Can Co., Barrington, Il

Most analyses of the mold filling stage of injection molding assume negligible melt compressibility. However, when the runner pressure drop, runner volume, or injection speed is high, this is a poor assumption. With a significantly compressible melt, the flow out of the nozzle does not respond instantaneously to ram motions. In fact, the response lag may be comparable to the total fill time, and predictions of mold fill rate as a function of time based on incompressibility may be in serious error. As a result, predictions of cycle time, temperature and velocity distributions, and, for co-injection molding, layer configuration may also be incorrect. This paper presents experimental data on and a simplified mathematical model of nozzle flow rate in response to constant-speed ram injection in a highly compressible industrial system.

The system used is schematically depicted in Figure 1. The experiments were performed on an injection molding machine with a hot runner manifold, servo-controlled ram, and nozzle shutoff valve. Initially, the valve was closed, the ram stationary, and the melt uniformly precompressed to pressure p_0. At time t=0, the valve opened, and the ram started moving at a constant volumetric displacement rate Q_{ram}. The mass flow rate at the nozzle, $\dot{m}(t)$, was then monitored by a technique to be described in the full paper.

The experimental data are schematically summarized by Figure 2. The following features are noteworthy:

1. A finite initial mass flow rate $\dot{m}_0$ depending on p_0, but not Q_{ram}.
2. At low Q_{ram} or high p_0, constant or falling $\dot{m}$ at early t.
3. A final equilibrium $\dot{m}$ linearly proportional to Q_{ram} and independent of p_0.
4. At high p_0 or Q_{ram}, an overshoot of $\dot{m}$ preceding the equilibrium.

For the analysis, the following principal assumptions were made:

1. Negligible pressure drop in ram.
2. Newtonian fluid with high viscosity μ.
3. Constant bulk viscosity $K \gg \mu$ (based on literature data.)
4. Constant compressibility β.
5. Constant tube diameter.

The actual runner system consisted of a series of channels with different cross-sectional geometries. It will be shown that the last assumption by itself precludes good quantitative agreement between predictions and data. However, all of the qualitative features of the data were successfully reproduced by the model. This is remarkable considering that the large melt elasticity was ignored.

Four governing dimensionless parameters were derived from the analysis. Their effects will be discussed in the full paper. These parameters make design scale-up and the generalization of experimental data possible.

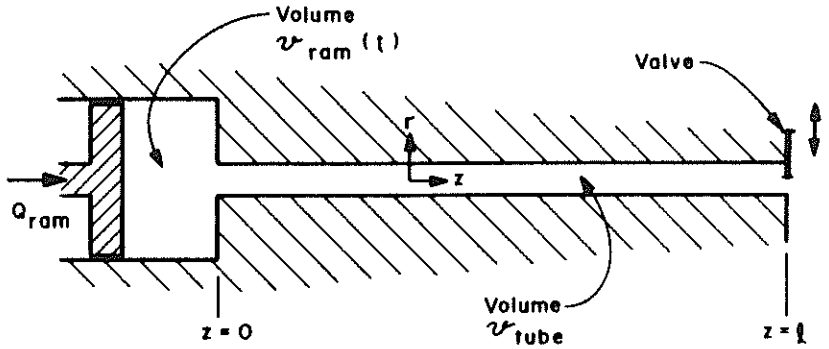


FIG. 1

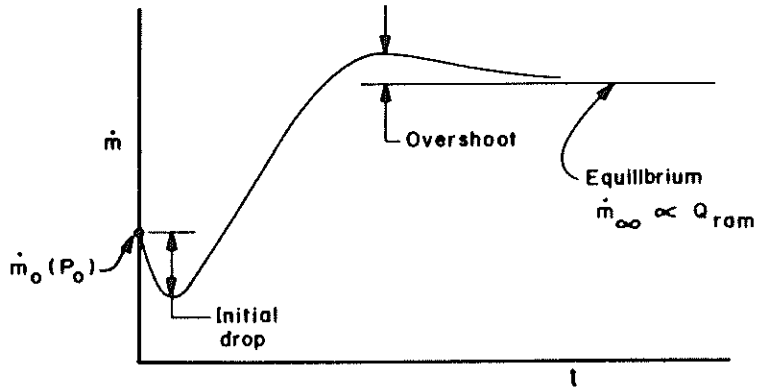


FIG. 2

CALCULATION OF FIBER ORIENTATION IN INJECTION MOLDED PARTS

H. Henry de Frahan, M.J. Crochet

Unité de Mécanique Appliquée
Université Catholique de Louvain
2, Place du Levant
1348 Louvain-la-Neuve, Belgium.

A numerical procedure recently developed by the Unité de Mécanique Appliquée allows us to calculate with great accuracy the time dependent velocity and temperature fields during injection molding of thin parts. Briefly, the advancing flow front defines at each time step a flow region which is automatically covered by a finite element mesh on which the calculation can proceed.

For short fiber thermoset composites, the power-law index of the fluid is low. As a consequence, we simplify the model by only considering a plug flow between the walls of the cavity. We also assume that fiber orientation in the mid-surface directions is fully characterized by the velocity field averaged across the thickness of the mold. A good qualitative prediction of fiber orientation is therefore obtained by solving Jeffery's equation.

Spatial discretization is performed using the Finite Element Method. The successive meshes covering the flow domain are generated by the remeshing algorithm of the injection molding program. Results are improved by applying the streamline upwinding Petrov-Galerkin (SUPG) technique, which is particularly convenient for pure advection problems. The solution is accurate, since 2 x 2 bilinear sub-elements are used.

Time integration of the resulting system of ordinary differential equations is performed by means of the classical fourth-order Runge-Kutta scheme. Note that only single-step methods were available, since the mesh is changing at every time step. A suitable control of the time step allows the error to be kept under a prescribed tolerance.

As the orientation field is integrated with respect to time using the initial mesh at the present time interval, a suitable extarpolation of the result to the corresponding final mesh is performed. The least square approximation method is used.

Several examples have been investigated in detail, including filling of planar molds with obstacles and box-like thin objects.

A NUMERICAL MODEL FOR PREDICTING FIBER ORIENTATION IN INJECTION MOLDING

A. BARBE*- M. VINCENT**- J.L. COTTALORDA** - J.L. WYBO** - J.F. AGASSANT**

* CdF-Chimie - CERCHAR B.P. 2
60550 VERNEUIL EN ALATTE

** Centre de Mise en Forme des Matériaux
UA CNRS nº 852
Ecole des Mines de Paris
Sophia Antipolis
06560 VALBONNE

In injection molding of reinforced plastics, the reinforcement (essentially glass fiber) get oriented during the mold filling by the stresses resulting from the flow. The prediction of this orientation is very important because the mechanical properties of the part are directly related to it. The aim of this work is to connect a flow calculation during mold filling to a calculation of particle orientation. An expert system corrects the calculation by applying knowledge from experiments, which makes the program usefull for a large variety of geometries and materials, including glass fiber reinforced thermoplastic (average length 0.4 mm) and reinforced thermosets (average fiber length 2 cm).

The mold filling program is a bi-dimensional modelisation. A complex mold is described as an assembling of three kinds of elementary geometries. In each one, the unsteady mechanical and thermal equations are solved at each time step using an implicit finite difference discretization. It gives the shear and elongational rates distributions.

The orientation calculation is based on Jeffery's theory on particle motion in dilute suspensions. Despite strong hypothesis, this calculation gives good qualitative results. The knowledge of the shear and elongational rates in the neighborhood of the particule during its displacement, of the fiber dimension, and of its initial orientation, permits to compute its motion, and so its orientation at the end of the mold filling.

The computation results are usually in good agreement with experimental observations but some discreapancies appear which may be related to the model assumptions (for example flow discontinuities at the connection between certain elementary geometries, neglecting of fiber-fiber interactions). It is the reason why the orientation computation has been coupled to the expert system PEGASE which has been developed in our laboratory. The expert system manage the orientation computation by examination and modifications of intermediate results according to a rule based system. These rules are obtained from experimental situations where the orientation computation fail (gates, strongly diverging flows, connection between elementary geometries...). The rules can be modified very easily to include new observed behaviour for new materials or new geometries for instance. The theoretical results are then very close to the experimental measurements.

Mold Filling and Curing of Sheet Molding Compounds

J. D. Fan, Junil Kim, Yong-Taek Im, and L. James Lee
(Engineering Research Center for Net Shape Manufacturing,
The Ohio State University, Columbus, Ohio, U.S.A.)

Compression molding of sheet molding compound (SMC) can be delineated as a two-stage process; namely, mold filling and curing. In the mold filling stage, flow begins when the mold contacts the top of the charge, and continues until the mold is filled. During this period, heat conduction from mold surface to the charge may result in a non-isothermal flow which in turn induces inconsistent physical properties across the workpiece. Once the mold is filled, a constant force is maintained on the mold, and the curing reaction occurs. Due to its fast and highly exothermic nature, there is a great interaction between heat transfer and reaction kinetics (1).

The flow mechanism during mold filling has been studied theoretically and experimentally. A two-dimensional finite element code ALPID (Analysis of Large Plastic Incremental Deformation) is applied for theoretical analysis. By coding the measured physical properties of SMC into the program, the detailed information about the local flow can be obtained, which includes temperature, stress, strain, and strain rate profiles across the workpiece. The predicted results compare well with the experimental data.

For the relatively short mold filling time, the interaction between flow and curing is comparatively small and the curing can be neglected during the mold filling stage (2,3). Therefore, the final results at the end of this stage may be applied as the initial condition of curing stage. To analyze the process, the curing kinetics of SMC must be studied first. A kinetic model is developed for high temperature curing reaction of SMC. When cured at high temperature, the initiator dissociates very fast and tends to exhaust before the completion of the cure reaction. At the same time, the vinyl group of styrene also starts to dissociate due to the thermal-initiation mechanism and offers the free radical source to continue the curing process. The kinetic model is then formulated by considering both initiation mechanisms. The parameters of the kinetic model was measured with SMC systems w/ and w/o initiator.

The kinetic model is then applied to compression molding to predict the reaction conversion, temperature, and pressure profiles. The simulation results are compared with the experimental data.

REFERENCES

1. L. J. Lee, Polym. Eng. and Sci., 21, 483, 1981.
2. C. C. Lee, F. Folgar and C. L. Tucker III, Trans. ASME, J. Engr. for Ind., 106, 114, 1984.
3. M. R. Barone and D. A. Caulk, Trans. ASME, J. Appl. Mech., 53, 361, 1986.

INJECTION MOULDING OF THERMOTROPIC POLYMERS

B. ERNST and P. NAVARD
Ecole Nationale Supérieure des Mines de Paris
Centre de Mise en Forme des Matériaux
Sophia-Antipolis, 06565 VALBONNE CEDEX - FRANCE

Injection moulding of a thermotropic copolyester polymer was performed varying mould temperature, mould geometry and injection time. The aim was to understand the relation between the flow conditions in the mould and the orientation of the solidified injected parts.

The first result was the recognition that this orientation could be much more easily unsderstood than in conventional flexible polymers, due to the small molecular relaxation. The prediction of the orientation during flow is enough, as a first approximation, to know the orientation in the part. A comparison between standard injection programs and measured orientation has been done.

The second result is the evaluation of the efficiency of shear and elongation for orienting a LC Polymer. This was studied using a centered gated disk. Shear and elongation can easily orient the polymer, elongation being more efficient. This has to be contrasted to many reported results in which shear is given as not capable of inducing orientation. A theoretical approach is given using a comparison with a modified Doi theory, which shows the orienting effect of shear for a concentrated rod-like polymer solution. Nematic polymers need a very large shear deformation to attain a structurally-stable oriented state. This is shown by studying the rheo-optical properties of nematic rod-like polymer solutions.

The last result concerns the orientation of the surface layer of injected parts, shown by X-ray pole figures to be different from the other regions (skin and core).

"SIMULATION OF BALANCED FILLING IN A MULTI-CAVITY MOLD FOR ENCAPSULATION OF SEMICONDUCTOR DEVICES"

J.Saeki and A.Kaneda
Hitachi Ltd.
Production Engineering Research Laboratory
292, Yoshida-cho, Totsuka-ku, Yokohama, 244 Japan

Abstract

With the aim of eliminating trial and error in mold design and increasing the quality of resin encapsulated semiconductor devices, computer simulation systems for predicting mold filling behaviour of thermosetting molding compounds have been developed.

First, a practical method for analyzing mold filling dynamics through a channel of circular cross section has been developed. Shear viscosity has been examined in the absence of any chemical reaction that would cause a viscosity rise by using silica-filled trial epoxy resin systems having neither a curing agent nor a catalyst. Viscosity was found to be dominated by temperature rather than by shear rate. On the basis of this result, a simple and practical constitutive equation model (as a function of time and temperature) for commercial molding compounds was derived. This model was used for predicting actual nonisothermal viscosity changes. The simultaneous equations, including the conservation equations of total mass, momentum and energy that represent the mold filling in a circular channel, and the constitutive equation model were solved with the aid of a finite difference method. This program computes viscosity, temperature and velocity distribution, apparent mean viscosity, pressure drop and flow length at each time interval during the mold filling process up until the cessation of flow, due to gelation.

Secondly, for quick and accurate evaluation of rheological properties of commercial molding compounds, an automatic data measuring and analyzing apparatus consisting of a transfer molding press, test molds, transducers, and data processing and display units has been developed. Values such as pressure drop, flow rate, flow length, and apparent mean viscosity during the filling process in a channel of circular cross section can be obtained at pre-set time intervals up until the cessation of flow, due to gelation. Characteristics of an epoxy molding compound for encapsulation of semiconductor devices were examined by using three different channel radii and several mold temperatures. The nonisothermal viscosity change data of the compound were used to estimate values of coefficients in the constitutive equation model. Final values of these coefficients were determined by using a combination of the simulation method described earlier and a curve fitting technique. The calculated profiles of apparent mean viscosity with time of the compound corresponded well with the experimental data. The developed apparatus and procedure enable the characterization of rheological properties inherent to the commercial molding compounds, which allows the precise prediction of viscosity changes.

Finally, a method of flow channel design for achieving balanced filling in a multi-cavity mold has been developed. This program computes runner and gate dimensions such that the pressure drop during filling from the pot to each cavity is the same in order to obtain equal flow rate in each cavity. To save computer time and cost, the complex phenomena of actual mold filling in the manufacturing process were simplified by the following procedure: (1) Flow channels were divided into appropriate sections. (2) In each section, flow resistance caused by channel shape and dimensions was calculated by using general solutions of Newtonian flow. (3) Viscosity, temperature and velocity distribution, and apparent mean viscosity in each section were estimated by replacing the actual shape with a circular channel having equivalent volume, and by using the aforementioned simulation model. (4) Pressure drop in each section was calculated as the product of flow resistance, apparent mean viscosity and flow rate. Cumulative pressure drops from the first section connected to the pot down to the furthest cavity were determined successively by repeating this procedure for each section.

By using this design program together with the properties of the molding compound including coefficients of the constitutive equation model, flow channels of the actual mold used for encapsulation of LSI devices were designed. As a result, well balanced filling was achieved in the configuration of a convergent runner together with convergent gates having successively increasing angles in the direction away from the pot. The behaviour of balanced filling was found to yield a great reduction in defects such as wire sweep and void formation in molded devices compared with those produced by a conventional mold.

COMPUTER SIMULATION FOR THE INJECTION MOLDING OF HIGHLY-LOADED LONG FIBER-REINFORCED THERMOPLASTICS

Keith T. O'Brien,
Engineering Plastics Division,
Hoechst Celanese Corporation

Long strand fiber-reinforced thermoplastics have entered commercial use during the past several years. These materials are highly filled, up to 60% by weight, containing fibers up to 1 1/2 inches in length, and are injection moldable on existing equipment. Although these materials will flow into mold cavities without great difficulty, they do present some challenges to those wishing to simulate their flow by computer. Not least of these challenges is how to measure their flow characteristics, or rheology.

Conventional capillary rheometry is impossible with materials so heavily loaded with fibers, and with materials containing fibers of lengths similar to the capillary. So the rheology of these materials was obtained using strand dies of extruders, and by comparing spiral flow lengths to other materials whose rheology is known. Neither technique is exact, but provides an approximate way to make flow predictions.

With the input data so obtained, computer simulations were made, using spiral flow molds geometries. These were compared to the exact spiral flow lengths obtained under the same operating conditions on an injection molding machine. The rheological constants were then adjusted to provide a better fit of the simulation to the actual molding results. From this point, simulations were made using mold cavity geometries which were available for comparative testing, and/or which had been used for alternative materials whose rheology was well defined. These included molds with simple single cavities (2-D), complex single cavities (3-D), and simple multi cavities.

The long strand fiber-reinforced materials utilized in the simulations included polypropylene, thermoplastic polyurethane, nylon 6/6, polybutylene terephthalate, polyethylene terephthalate, and acetal copolymer. The glass loadings by weight varied from 30% to 60%, and initial glass length was held constant at 1/2 inch.

The results indicated that although the scientific base for the work was questionable, the engineering data obtainable was very useful. Mold filling patterns, short shots, weld line locations, and meld line locations were predictable. Molding parameters such as injection molding pressure, fill time, and isotherms were also predictable. The simulations also provided input on how to avoid high stress regions likely to attenuate the long glass fibers.

So basically the simulation of mold filling for highly loaded long strand fiber-reinforced thermoplastics was brought to the same understanding level as other thermoplastics. So mold designers can now have the same confidence in molds designed for long strand fiber-reinforced thermoplastics as they currently have with other thermoplastics.

FIBER AND MATRIX ORIENTATIONS IN INJECTION MOLDED FIBER REINFORCED LIQUID CRYSTALLINE POLYMERS

F. Baba, H. Horibe, S. Etoh and A. Fukami

Materials and Electronic Devices Laboratory
Mitsubishi Electric Corporation
8-1-1 Tsukaguchi-honmachi, Amagasaki, Hyogo 661, JAPAN

There has been an increasing interest in the development of thermotropic liquid crystalline polymers as specialty high performance materials for molded articles. Thermotropic polymers are composed of stiff, rod-like molecules which have the ability to orient themselves in the melt. The flow behavior of thermotropic polymers is both qualitatively and quantitatively different from that of isotropic polymers[1-5]. Thermotropic polymers show very low melt viscosities and long relaxation times in the melt. The fiber and matrix orientations were investigated in injection molded carbon-fiber reinforced thermotropic polymers.

Two thermotropic polymers, from aromatic polyesters, with 15 weight percent carbon fiber were used to study the fiber and polymer orientations. Three molds were used in this work. One was three cavity bar mold , with film gates of bar thickness, dimensions which were 5mm x 50mm x 0.2, 0.3 and 0.5mm ,respectively. This was chosen to understand the flow behavior in a simple geometry. The other molds were cone molds with cavity thickness of 0.2mm and 0.4mm, respectively. These are for loudspeaker diaphragm of mid-range unit and low-range unit. A 5-oz. injection molding machine with hydraulic accumulator was used in this work. Examinations of individual fiber orientation was performed using surfaces prepared by the metallographic polishing technique. The fracture surfaces of specimens were viewed in the scanning electron microscope(SEM).

SEM micrographs of the fracture surfaces and the visual appearance of polished surfaces revealed the presence of a complex hierarchical organization. Five distinct macrolayers were observed in all specimens. They were composed of two skin layers, a core layer and two mid layers between the skin and the core. This skin-core morphorogy is clearly demonstrated in Figure 1.

The skin layers of both cone specimens and bar specimens contain fibers with a fairly random orientation. Mid layers of cone specimens contain fibers highly aligned in the flow direction. The core layer of cone specimens contain fibers mainly aligned transversely to the flow direction. On the other hand, random fiber orientations are observed in both mid layers and core layers of bar specimens. The difference of fiber orientation mechanism, between the cone and the bar, is explained using the flow pattern in a cavity. In the cone mold, the melt front is assumed to be a spreading radial flow which causes orientation in the transverse to the flow direction.

As regards polymer orientation, highly oriented mid-layers observed in the cone and the bar specimens may be represented by an elongation effect caused by fountain flow in the melt front region. These thicknesses of the cones were greater than those of the bar specimens. In particular for the cone molds, highly oriented mid-layers in both the mid-range unit and the low-range unit have nearly thickness. It seems that the polymer orientation of the thermotropic polymers in the cone mold is very dependent on the mold temperature. It has been reported that the fibers did not appear to have any direct effect on the polymer orientation inn the low-range of fiber concentrations[5]. However, the polymer orientation was strongly dominated by the orientation of the fibers in injection molding of thermotropic liquid crystalline polymers.

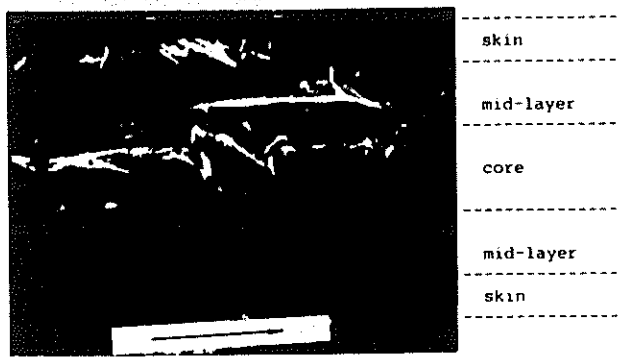


Figure 1 Scannning electron micrograph of a typical fracture surface of a cone specimen. The draw direction is normal to the plane of the picture. The flow direction is indicated by the arrow.

[1] D. G. Baird, Polym. Sci. Technology,28(1986)119
[2] W. B. Vanderheyden and G. Ryskin, J. Non-Newtonian Fluid Mech., 23(1987)383
[3] T. Weng, A. Hiltner and E. Baer, J. Mater. Sci.,21(1986)744
[4] S. K. Garg and S. Kenig in "HIGH MODULUS POLYMERS",(A. E. Zachariades and R. S. Porter, ed), Dekker, New York, 1988
[5] M. J. Folles and D. A. M. Russell, Polymer,21(1980)1252

1/25

CHARACTER AND PROPERTIES OF POLYMERIC COMPOUNDS OBTAINED BY EXTREMELY HIGH SHEAR RATE PROCESSING

H. Takahashi, T. Matsuoka, T. Ohta, K. Fukumori
T. Kurauchi and O. Kamigaito
Toyota Central Research & Development Labs., Inc.
Nagakute-cho, Aichi-gun, Aichi-ken, 480-11, Japan

Extremely high shear rate processing was applied to polymeric compound systems. The viscosity was measured against the shear rate up to 10^7 s^{-1}.[1] 1st non-Newtonian region, 2nd Newtonian region and 2nd non-Newtonian region were observed in the compound system of SAN and PC (Fig.1)[2]. The occurrence of these regions are very similar to those in the parents polymers. For the calculation of the viscosity-shear rate curve, a concentric multi-layer model was proposed. $\eta - \dot{\gamma}$ curve was expressed by approximating Rabinovitsch-corrected curve by power-laws with different constants against the three kinds of regions on $\eta - \dot{\gamma}$ curve. The model gives good agreement between the calculated value and the measured one (Fig.2). A new mechanism for the occurrence of the 2nd Newtonian and 2nd non-Newtonian region was proposed. Nuclear spin-spin relaxation time measurements on SAN exposed to the high shear proved the proposed explanation.[3]

In the compound system of semi-crystalline polymers, it was found that the morphology development such as coarsely dispersed phase, fibrillation of the dispersed phase and finely dispersed phase was able to be controlled at a certain range of stock temperature by extremely high shear rate processing. The relationship between such morphologies and properties of those compound systems is also discussed in this paper.

References
1. H.Takahashi et.al., J.Applied Polym.Sci.,30,4669(1985)
2. H.Takahashi et.al., J.Applied Polym.Sci., in press
3. H.Takahashi et.al., J.Applied Polym.Sci., to be submitted

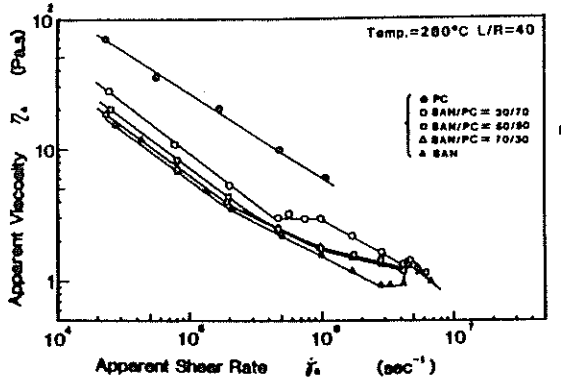


Fig.1 Plot of apparent viscosity vs. apparent shear rate for SAN/PC

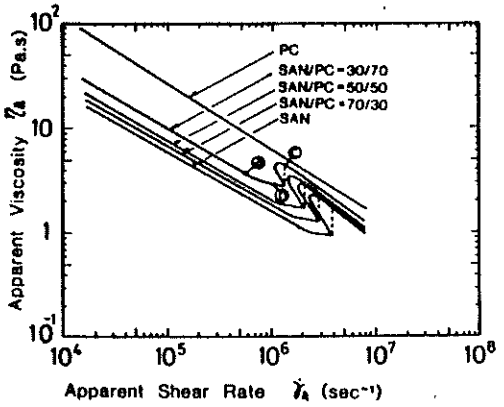


Fig.2 Apparent viscosity vs. apparent shear rate curves calculated by using concentric multi-layer model

THE PRODUCTION OF MICROCELLULAR FOAMS IN AMORPHOUS AND SEMI-CRYSTALLINE THERMOPLASTICS

Prof. Jonathan S. Colton
Georgia Institute of Technology
George W. Woodruff School of Mechanical Engineering
Atlanta, GA 30332-0405

Microcellular foam is a polymeric foam with bubble sizes of 10 microns or less that is produced by saturating a polymer with gas and then utilizing the thermodynamic instabilities that result when the polymer is heated and the pressure reduced to nucleate the cells. A model for the nucleation of microcellular foam in amorphous and semi-crystalline thermoplastic polymers has been developed. The nucleation process depends heavily on the solubility, concentration, and interfacial energy of any additives present. At very low levels, additives in solution act to increase the free volume of the polymer, resulting in homogeneous nucleation within the free volume. Well above the solubility limit, heterogeneous nucleation dominates, as it lowers the activation energy to levels below that for homogeneous nucleation. In the vicinity of the solubility limit of the additive, these two nucleation mechanisms compete.

Microcellular foams have been found to have superior impact and insulation properties, as compared to solid structures of the same linear dimensions. Because of the small cell size, very thin parts can be foamed, leading to large material savings and improved material properties.

Experiments were performed to validate the model in amorphous and semi-crystalline thermoplastic polymers. Polystyrene, polypropylene, and polypropylene copolymers were chosen as the experimental models. Additives used in the polystyrene included zinc stearate, stearic acid, carbon black and polytetrafluoroethylene. Additives in the polypropylene included sodium benzoate and ethylene to produce the copolymer. The blowing gases used were nitrogen and carbon dioxide.

Microcellular foams are produced in amorphous polymers by saturating them with gas at either room or elevated temperatures and then heating them to their glass transition temperatures. The pressure is then released to nucleate the bubbles. The temperature is dropped to stop the bubble growth process at the desired level. For the polystyrene, it was found that an amount of zinc stearate just slightly below its solubility limit (0.3% by weight) produced the greatest number of small, uniform cells ($\approx 10^{11}/cm^3$). Stearic acid also produced a microcellular structure, but not in as great numbers ($\approx 10^{9}/cm^3$). Nitrogen was found to have the correct combination of solubility and diffusivity to repeatedly produce microcellular structures. Carbon dioxide's solubility was too high and diffusivity too low to produce microcellular foams. Increasing the gas saturation pressure also increased the bubble density. Molecular weight was found to have no effect on cell nucleation.

Microcellular foams are produced in semi-crystalline polymers by first melting out the crystal phase, thereby creating an amorphous structure. The crystalline phase greatly reduces the solubility of gas in the polymer, thereby preventing microcellular foam nucleation. After melting, the polymer is saturated with gas. The pressure is then released and the temperature reduced to form a microcellular structure. It was found that microcellular foams can easily be formed in polypropylene nucleated with sodium benzoate and polypropylene-ethylene copolymers. Cell densities were on the order of $10^{10}/cm^3$. Again, nitrogen was found to produce good foam structures.

The agreement between theoretical predictions and experimental results is reasonably good. The theory allows for the prediction of the effect of processing parameters on cell nucleation. This allows the design of processing techniques to produce commercial quantities of microcellular foam parts. Injection molding and extrusion have been used successfully to produce microcellular foams in amorphous thermoplastics. Extruded, foamed sheets can be further processed into finished parts by thermoforming or stamping. Processes are under development to similarly foam semi-crystalline materials.

FIBER ORIENTATION IN INJECTION MOLDING: OBSERVATIONS AND PREDICTIONS

S. G. Advani
University of Delaware, Newark DE 19716

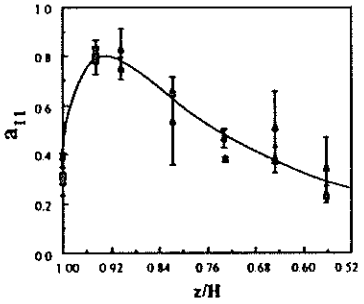
R. B. Davis, and C. L. Tucker
University of Illinois, Urbana IL 61801

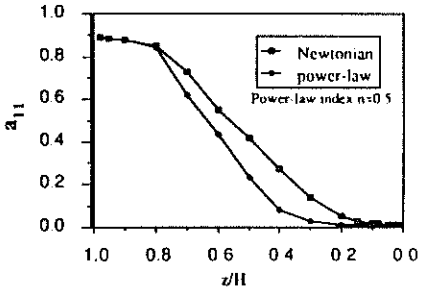
The mechanical properties of parts made from short fiber reinforced thermoplastic materials are determined by the fiber orientation pattern created during processing. Predictions of the final fiber orientation in an injection molded part from the processing parameters would be of great value for designers. The processing parameters affect the fiber orientation by changing the velocity and temperature profiles experienced by the polymer melt during mold filling.

Preliminary experimental results [1] show three orientation layers through the part: a center layer aligned transverse to the flow and outer shells aligned predominately in the flow direction (Fig. 1). (The orientation is nearly random in the plane of the part and a_{11} represents the amount of orientation in the flow direction; values greater than 0.5 are more aligned along the flow direction and values less than 0.5 are more aligned across the flow direction). There is also a thin skin on the surface of the part which has random fiber orientation. A preliminary theoretical predicition was performed [2], using the isothermal velocity distribution for a center-gated disk and a second-order tensor representation for fiber orientation [2,3]. The results, shown in Fig. 2, are qualitatively in agreement with the experiments except that they do not show the randomly-oriented surface skin. A more in-depth study was performed to consider the effect of temperature on the velocity profile (and thus on orientation).

Experiments and calculations were performed for two simple part geometries: a center-gated disk, and a long strip with a film gate at one end. Parts were made from a nylon resin with four different glass fiber concentrations (DuPont Zytel 70Gxx). Processing conditions were selected to provide a wide variety of the dimensionless parameters that govern temperature and flow of the melt during filling. Pressures and temperatures within the mold and machine readings were monitored during the experiments. Rheological data was obtained with a capillary rheometer. Three-dimensional fiber orientation states in the parts were measured by analyzing polished sections [1].

Temperature and velocity fields within the cavity were modeled with the finite element package FIDAP, using the full equations of motion and energy, an inelastic rheological model and assuming a completely filled geometry and steady state. The resulting velocity profiles were used as input for the fiber orientation predictions. These utilized a tensor representation of the three-dimensional orientation state and a particle tracing scheme. The predictions were compared to the experimental data to study the effect of the temperature-induced velocity profile on fiber orientation.





Figures 1 and 2: Experimental and predicted fiber orientation data.

References

1. T. S. Konicek, "A Method to Determine Three-Dimensional Fiber Orientation in Fiber Reinforced Polymers," *M. S. Thesis*, University of Illinois, Urbana, IL (1987).
2. S. G. Advani, "Prediction of Fiber Orientation During Processing of Short Fiber Composites," *Ph. D. Thesis*, University of Illinois, Urbana, IL (1987).
3. S. G. Advani and C. L. Tucker, "The Use of Tensors to Describe and Predict Fiber Orientation in Short Fiber Composites," *J. Rheol.*, *31*, 751-784 (1987).

NEW SOFTWARE DEVELOPMENTS FOR PART DESIGN AND PROCESS-SIMULATION IN INJECTION MOULDING

P. Filz, G. Menges, Institut für Kunststoffverarbeitung, Pontstraße 49, D-5100 Aachen, West Germany

The fundamental things for the quality of injection moulded parts are:

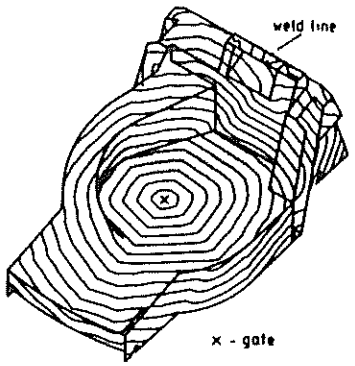
- part and mould geometry
- used raw material
- and process conditions during injection moulding

During the last ten years IKV has developed software to support part- and mould designers as well as mould makers and injection moulders.

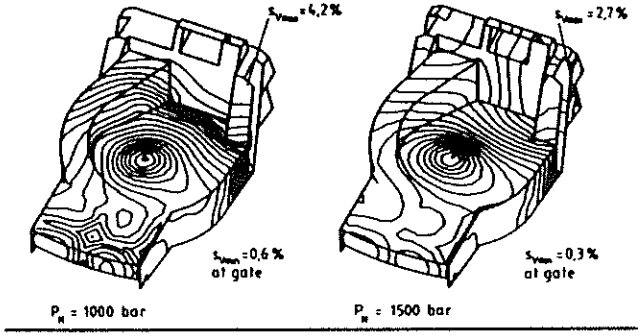
Part design:
A complex data base can give aids to the user in finding a suitable raw material. During construction of a moulding with a CAD-System it is possible to link Macros to certain points in the drawing. With a design controller the part can automatically be examined for details which are not a good plastic design.

Process simulation:
For process simulation it is essential to make a 3D-flow analysis of the filling phase for the part and the runner system and to predict pressure to fill, temperatures, shear stress and shear rate at every point in the part.

Further it is useful to make an analysis of the holding pressure phase and to try to predict linear shrinkage. For the mould designer it is a good information to know what loadings will be on certain parts of the moulding during filling and holding pressure phase. This paper explains the methods standing behind the above mentioned programs and shows their usage at a practical part. Additional it comments the possibility to use the generated geometry and the calculated data to cut the mould and to set up the injection moulding machine.



Filling pattern of a lawn mower housing fig 2



Lines of equal Volume shrinkage fig 6

ACTUAL AUTOMATION STEPS IN BLOWMOLDING TECHNOLOGY

Dr. R. Hegele
Battenfeld-Fischer
Lohmar, West Germany

In the blowmolding industry a distinct gap in automatic handling can be noticed, whereas in injection molding considerable automation steps, such as handling devices, automatic mold changes, and even fully automatic manufacturing plants have been established for years.

Even though the blowmolding process has complex processing parameters and the initial set-up can be rather difficult and time-consuming until the final optimization is concluded, the near future will definitely bring about automation steps in the bottle production as well as in the blowmolding of technical and large industrial parts in order to reduce costs.

By employing micro-processor control machine manufacturers have taken initial steps to simplify the machine set-up for mold changes. A number of additional set-up parameters, e. g. vertical distance between die and blowmold, positioning of the die-head towards the mold parting line and the cutter position, must be digitized for simplified machine set-up. However, the processing parameters, such as melt shearing in the die-gap, are more important. Today the ejection speed of the polymer piston in the accumulator head machines can follow a given profile, and the micro-processor technology will very soon make it possible to combine die-gap variations with ejection speed.

The result will be a parison which is in its total length ejected at a constant shearing rate.

A connected master computer enables the input of the new machine parameters before the current production process will be finished. Predeterminations on the swell factor of the parison can already be made by various mathematical models. This enables even less experienced technicians to determine the correct wallthickness profile.

Simplified mold changes and easy installation of blow pin and auxiliary equipment are the first steps towards an automatic production plant. In order to reduce down time, it is essential to use specific handling equipment when changing large molds, dies and the corresponding spreading and parison welding devices.

By analyzing today's production process for large blowmolded articles it becomes evident that a reduction of manufacturing costs can only be achieved by a fully automatic downstream transportation of the molded parts to the individual post-processing steps.
One of the most important tasks of future manufacturing plants will be the linking of post-operations, such as deflashing, weight control, machining and drilling as well as automatic quality control and the possible inserting of parts into the mold.

Apart from neck calibration by horizontal wheel machines which is nowadays stand of technology, the leak test, the automatic wallthickness test in the blowmold, the automatic sorting, bundling and packing in shrink foil will be utilized by bottle producers who are using high output-rate machines.

As in injection molding, machine manufacturers are presently defining how quality criteria of blowmolded articles can be linked to the blowmolding process. Apart from dimensional parameters (e. g. thread diameter, neck ovality, bottle height) other geometric criteria (e. g. surface convexing) and wallthickness controls have to be considered. The solution of these difficult tasks will result in a self-optimizing blowmolding process.

Dynamics of the Blow Molding Process and Properties of Blow Molded Articles

Dilhan M. Kalyon Stevens Institute of Technology
Chemistry and Chemical Engineering Castle Point,
Hoboken, N.J. 07030

Various properties of blow molded articles are intimately related to the thermo-mechanical history that the resin is exposed to during various stages of the blow molding process. These stages include:

1) The formation of the parison, whether by injection, extrusion or co-extrusion.
2) The deformation of the parison by clamping and inflation or by stretching and inflation.
3) The cooling of the article with or without internal intensive cooling.

A rigorous analysis of the blow molding process can generate a detailed understanding of the dynamics of the process and the properties of the blow molded article. In this paper, various components of such an analysis will be reviewed utilizing the extrusion blow molding process as a case study.

In the extrusion blow molding process, mixing of various ingredients and plastication of the melt in the single or twin screw extruder and the flow through the blow molding die is straightforward. However, the extrusion of the parison out of the die and the free standing formation of the parison under swell and sag effects is quite complicated (1) and defies a rigorous treatment. Despite some very recent and extremely encouraging analyses, which involve the successful coupling of finite element method with viscoelastic constitutive equations (2), only experimental methods are currently available for determining the parison shape as a function of temperature, shear rate, residence time in the die and outside the die (3). With a proper experimental set-up and selection of relevant conditions, the time dependent dimensions of a parison can be predicted on the basis of experiments carried-out with a capillary rheometer, high speed cinematography and isothermal, oil filled chamber.

The inflation of the parison is relatively a fast process where the response of the melt can be considered to be nonlinearly elastic with a negligible viscous response (4-6). The stress distribution prevailing in the shaped article at the end of the inflation stage is altered upon the thermal history in the cooling stage to give rise to maximum anisotropy (and minimum density for semi-crystalline resins) at locations close to the mold cavity surface, where the cooling rates are maximum. The orientation distribution is modified considerably in processes involving intensive internal cooling.

The thickness distribution of the blow molded article (8) can reasonably be predicted on the basis of the parison dimensions and mold geometry (4,9). Thickness variations in the article give rise to variations in crystallinity/density and orientation distributions, on the basis of the variations in thermal history (7,8).

Various ultimate properties of blow molded articles depend primarily on the distributions of density and orientation. Furthermore, some locations, including the parting lines, exhibit significantly lower properties (10). Basically, various phenomena including internal flows during the cooling stage are responsible for reduced strength, by providing morphological features which act as stress concentration points.

References

1. Dilhan M. Kalyon, M. Kamal and V. Tan, "The Dynamics of Parison Development in Blow Molding", Polymer Engineering and Science, 20, 773-777 (1980)
2. R. Brown, " Numerical Calculation of Complex Viscoelastic Flow", AIChE Conference on Emerging Technologies in Materials, Minneapolis, August 18, 1987
3. D. Kalyon and M. Kamal, "An Experimental Investigation of Capillary Extrudate Swell in Relation to Parison Swell Behavior in Blow Molding", Polymer Engineering and Science, 26, 7, 504-512 (1986)
4. C.J. Petrie and K. Ito, Plast. Rubber: Processing, 68-72 (1980)
5. M. Kamal, Dilhan M. Kalyon and V. Tan, "Melt Deformation during Parison Formation and Inflation in Extrusion Blow Molding", in Rheology - Volume 3 : Applications, edited by G. Astarita, G. Marrucci and L. Nicolais, Plenum Press, New York (1980)
6. D. Kalyon and J. Yu, Unpublished Results (1987)
7. M. Kamal and Dilhan Kalyon, "Heat Transfer and Microstructure in Extrusion blow Molding", Polymer Engineering and Science, 23, 9, 503-509 (1983)
8. M. Kamal, D. Kalyon and V. Tan, "Anisotropy and Dimensions of Blow Molded Polyethylene Bottles", Polymer Engineering and Science, 22, 287-291 (1982)
9. M. Kamal, V. Tan and D. Kalyon, "Measurement and Calculation of Parison Dimensions and Bottle Thickness Distribution during Blow Molding", Polymer Engineering and Science, 21, 331-338 (1981)
10. M. Kamal and D. Kalyon, "Microstructure and Ultimate Properties of Extrusion Blow Molded Polyethylene Bottles" in Interrelations between Processing, Structure and Properties of Polymeric Materials, edited by J. Seferis and P. Theocaris, Elsevier Science Publishers, Amsterdam (1984)

2/3

ANALYSIS AND COMPUTATION OF FLUID FLOW IN BLOW MOLDING DIES

D.J. Coyle
General Electric Company
Corporate Research and Development
Schenectady, NY 12301

ABSTRACT

In the processes of blow molding, film-blowing, and sheet extrusion, a polymer melt stream is shaped into the desired profile by flow through a die. The primary objective in the design of such dies is to find the proper geometry which will result in a uniform melt profile - the so-called flow distribution problem. A common die geometry is the coathanger, which consists of a large cross-section manifold which spreads the melt to its full width, followed by a thin slit which controls the sheet (or tubular parison) thickness. The precise taper of the manifold and its curvature downstream, which determines the slit length, together determine the relative uniformity of the sheet. Another common geometry is the spiral mandrel die most often used in film-blowing. Here there are several manifolds which wrap around the mandrel in a helical fashion.

Such dies are usually designed by use of one-dimensional flow models which assume that the flows in the manifold and slit are coupled only by the mass balance so that the flow in each is decribed by a 1D pressure drop - flow rate relationship. These assumptions may be good for some die shapes but always break down near the ends of the manifold where manifold and slit are of similar dimensions.

A particularly interesting case is where the manifold is a large aspect ratio slit, which has been analysed by Winter and Fritz (Polym. Eng. Sci.,26, 543 (1986)). They developed 1D models and performed experiments on two types of coathanger manifolds: 1) constant width but varying depth, and 2) constant aspect ratio. The key feature was that according to the model the predicted geometry for uniform flow was independent of power law exponent. This type of analysis is extended to spiral manifold dies in general, where there are M manifols, each of which wraps around the mandrel N times. The analysis allows one to predict the geometry necessary to obtain uniform flow by numerical integration of a first order ordinary differential equation.

In order to more closely evaluate these simple flow models, full three- dimensional flow computations are carried out using FIDAP, a commercially-available fluid flow computation package. Newtonian isothermal calculations had up to 20,000 degrees of freedom, used 100 megabytes of storage, and took 8 minutes on a Cray-2 supercomputer, while calculations for a shear-thinning viscosity took four times as long. The geometries examined include the constant width and constant aspect ratio dies of Winter and Fritz, shown in Figure 1, along with simple spiral mandrel dies such as is shown in Figure 2. The calculated flow non-uniformity for the blow-molding dies is about 5-10% of the total flow rate, which is close to the experimental data.

These computations establish the accuracy and range of applicability of the simple 1D models of die flow. The effects of non-Newtonian viscosity and nonisothermal flow are also examined. The practical aspects of using such computational tools in die design is also discussed.

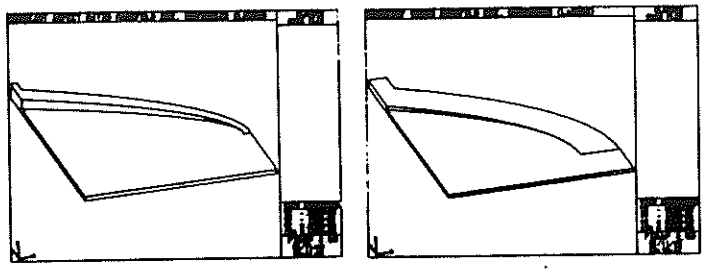


Figure 1. Models of blow molding dies of Winter and Fritz, (a) constant width manifold, and (b) constant aspect ratio manifold.

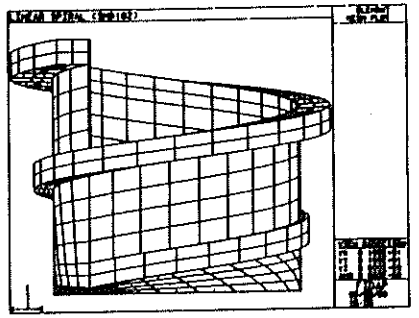


Figure 2. Finite element mesh of three-dimensional brick elements describing a simple spiral mandrel die having one manifold which makes two wraps around mandrel.

2/4

INJECTION STRETCH BLOW MOLDING - PROCESS SIMULATION

S. A. Jabarin and L. F. Chang
Polymer Institute
The University of Toledo
Toledo, Ohio 43606-3390

It is known that both the mechanical and gas barrier properties of polyethylene terephthalate (PET) may be dramatically improved through orientation. Typically, the mechanical strength, in terms of elastic modulus, can be tripled, whereas the gas barrier can be nearly doubled with proper biaxial orientation. In practice, the required orientation for beverage bottles can be achieved by stretching approximately four times in the circumferential direction, and at least two and one-half times in the axial direction at the orientation temperature of PET. The stretching conditions in the circumferential direction approximately coincide with the natural stretch ratio, at which strain hardening of the material occurs.

The fabrication of oriented PET containers with a high degree of efficiency requires that parisons and containers be designed in order to achieve the maximum balance among material distribution, degree of orientation and property improvement.

At the blow molding step of the bottle-making process, the parison temperature must be in the range leading to the molecular orientation of PET, which is generally in the region between 90-120°C. In addition, the temperature profile in the axial direction usually must be adjusted to obtain a proper material distribution in this direction, according to the specific needs of the package.

In the reheat and blow process, the parison is normally heated with an infra-red (IR) heating system to take advantage of the deep penetrating capability of the IR heat source in the short wave length region. With this type of IR heating system, the desirable temperature profile can be achieved in a short time, with properly adjusted power inputs to each heating element. In addition, the parison can be designed to supplement the heating system.

In the case of the injection stretch and blow molding process, the desirable temperature pattern of the preform just prior to blow molding can only be obtained through careful parison design which takes into account the effects of the injection process variables on the parison temperature distribution. While the parison mold is being filled during the injection molding process, the melt flow inside the channel takes the well known form of a fountain shape. The melt in the middle of the channel reaches the flow front with increasing velocity, while the flow near both sides of the wall slows down steadily due to the constant loss of heat into the coolant through the mold wall. This means that in the mold filling stage there is a constant supply of heat from the fresh melt near the gate. In addition the flow front constantly receives melted polymer passing through the middle of the channel. Consequently, at the end of the filling stage for a parison with a uniform wall thickness temperatures near the gate and near the downstream end of the mold are relatively high, compared to the temperature in the region in between. Zone cooling of parison molds has been utilized to correct the situation with only limited success.

Another possibility for obtaining a desirable parison temperature distribution in the injection and blow process is to provide a temperature conditioning step in the production system. However, from the point of view of the productivity of the system, it is impractical to substantially modify the temperature pattern in the conditioning stage of a typical injection stretch and blow system, such as the Nissei ASB machine.

One practical and effective method of achieving a good parison temperature distribution pattern at the time of blow molding is to adjust the parison wall thickness distribution in the design stage to account for the process variables, and to use the conditioning stage for further optimization.

The models for the parison mold filling process described above and the subsequent heat transfer problems involved in the parison cooling process inside the mold have been formulated. The respective computer simulation programs have also been developed. These programs can be used to design parisons for injection, stretch, and blow molding processes for ASB machines. The same programs have also been used on a trial basis to design parisons for conventional injection blow molding in which the container is blown above the orientation temperature of PET.

In this presentation, the basic properties of PET including the rheological, orientation, melting and crystallization behavior will be discussed in relation to the general principles governing the parison design and characteristics of oriented PET containers. In addition some results of the modeling and simulation of the injection molding of PET parison will be discussed. Emphasis will be given to consideration of the effects of various design parameters and process variables on the parison temperature distribution patterns at the blow molding time. A scheme which is used for the estimation of the bottle wall thickness distribution from the parison wall thickness, the parison temperature profile, and the container geometry will also be discussed. Finally, the system's approach to the oriented PET bottle is considered by integrating each of the above steps.

BLOW MOLDING TECHNOLOGY FOR MICROSCOPIC REPLICATION OF MOLDED SURFACES

Robert A. Marin, Engineering Department, Marcia J. Cho, Automotive Products Department, E. I. du Pont de Nemours & Co., Inc.

INTRODUCTION

A new blow molding process has been developed which yields Class "A" paintable surfaces on Bexloy® exterior body panels directly out of the mold. The process is the result of three years of research and involves a thermo-cycling technique which maintains the surface of the part at a temperature above the plastic flow point. This enables the material to exactly replicate the mold surface, thus eliminating surface defects such as die lines, pits, and waviness. This technology offers reduced finishing costs and greater design freedom for the use of Bexloy® thermoplastics in large Class "A" exterior body panels. Within the last three years, expanded adoption of thermoplastics for Class "A" exterior body panels has been seen primarily through injection molded or compression techniques. These processes are well suited for high volume parts where expensive tooling costs can be amortized over long runs. These high tooling costs have prohibited the adoption of large size thermoplastic parts for low volume applications. Blow molding offers low tooling costs, and is presently being used to produce Class "A" spoilers, but requires extensive sanding and finishing to provide a true Class "A" paintable surface. These sanding and finishing costs, required to provide an acceptable Class "A" surface, usually account for about 50% of the total part cost.

SURFACE DEFECTS - CAUSE AND ELIMINATION

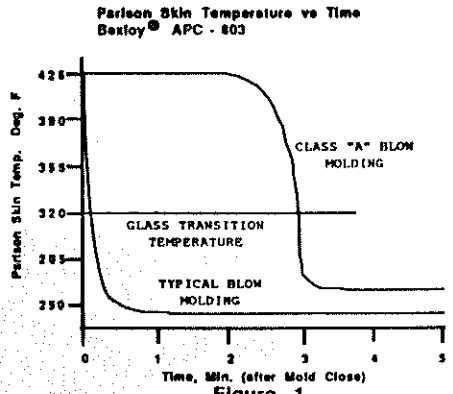


Figure 1

The defects caused by the current blow molding process are the result of too low of a flow at the part surface to enable the relatively low blow pressures to replicate the mold surface. Within tenths of a second after the mold closes, the parison surface temperature drops below the glass transition point thus preventing the plastic from flowing at the mold surface. During the Class "A" blow molding process, the skin temperature remains above its glass transition point for a sufficient time to permit prolonged flow of the parison surface, thus replicating the mold. Figure 1 illustrates this.

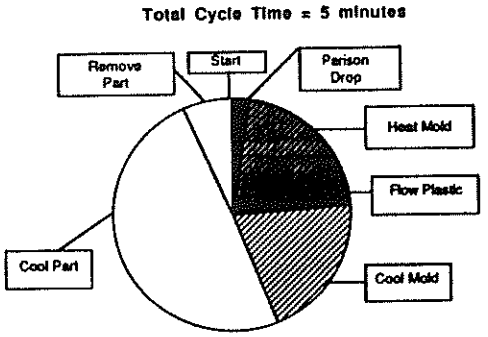


Figure 2

PROCESS DEVELOPMENT

To achieve sufficient flow at the part and mold interface, it was necessary to thermocycle the mold to a temperature high enough to permit flow and low enough to permit part removal without deformation. Two key technical challenges needed to be solved. The process would require a very low thermal mass mold and a very high heat transfer thermocycling system. The computer designed, aluminum mold incorporated large internal fluid channels and minimum structural support to optimize the heat transfer to the mold surface. Mold mass reduction of the large one by five foot spoiler required a critical finite element analysis to prevent collapse during the thermal cycling and application of the 90 psig blow pressure. The thermocycling system alternately cycles hot and cold, low pressure, non-toxic heat transfer fluid to a series of common mold channels at a high flow rate. The fluid cycling is computer controlled to minimize mixing and to ensure consistent and accurate mold temperature control. Oil was chosen for its better utility and safety aspects.

PROCESS CYCLE

Figure 2 shows the overall steps in the typical Class "A" blow molding cycle. The actual time requirements for each of these segments depend on the specific application. In the spoiler application, approximately one minute was added to the overall cycle. However, the Class "A" process reduced the reject/recycle rate from 30% to almost zero. In addition, a low scrap rate combined with the elimination of the sanding and finishing resulted in a final part cost reduction of more than 50%.

FUTURE APPLICATIONS

The availability of the new Class "A" Blow Molding technology will open the door for the wider use of thermoplastics in low volume Class "A" applications in automotive, furniture, appliance, and industrial markets.

William L. Strum, E. I. Du Pont De Nemours & Co., Inc.
Polymer Products Department - Packaging Products Division
Wilmington, Delaware, U.S.A.

The success of the plastic squeeze bottle for ketchup has heightened interest in coextrusion blow molded containers for many other food and non-food applications. The ketchup bottles are usually somewhat symmetrical in construction and are on the order of, in to out; 35%PP/5% adhesive/5% EVOH/ 5% adhesive/35% Regrind/15% PP. The food producers are concerned about "plastic" odors, absorption of flavors by plastics and higher levels of oxygen barrier to protect sensitive products. In the non-food applications, there is concern about chemical resistance, environmental stress cracking, solvent and odor barrier and impact strength. The "ketchup bottle" construction is not suited for every application so new constructions must be developed to answer the concerns listed above. These new constructions will probably be highly unsymmetrical, use a thin inside surface layer and may contain at least one polymer requiring a higher processing temperature, all of which present new challenges for the industry.

Two examples of non-symmetrical containers for liquids are: 1) orange juice and 2) agricultural chemicals. (In to Out)

1. 5% EVOH/3% Adhesive/58% Regrind/3% Adh/3% EVOH/3% Adh/25% HDPE

2. 5% PA/3% ADH/40% Regrind/52% HDPE

In the first example, the 5% EVOH inner layer provides a contact surface which has a relatively low solubility parameter and therefore does not absorb the natural flavors. This polymer must also be free of extractables and volatiles which would impart an undesirable taste or smell to the product. The oxygen barrier property of the inner layer is relatively unimportant and in the case of EVOH is essentially sacrificed due to H_2O saturation. The O_2 barrier is derived from the 3% EVOH layer which is protected by the 58% regrind layer and the two 3% adhesive layers. This container presents several technical problems for the molder. First, a seven layer coextrusion head is required, extruders must be sized and screws selected for the various layers and resins. The mold must be designed with an appropriate bottom weld and flashed area pinch pocket in order to provide adequate impact strength with the thin inside EVOH layer. The adhesive bond at the EVOH/regrind interface is critical to the impact performance of this container.

In the second example, only a four layer head is needed to produce this container. The solution may be to run all extruders using HDPE in the outer four layers. Some head designs require polymer in all layers while other may allow removal or addition of layer modules. Mold design and deflashing considerations are similar in both cases.

Our laboratory work with a five layer, five extruder continuous extrusion blow molding machine has confirmed a number of factors which should be considered when setting up a coextrusion blow molding line or when designing containers which are radically different from the "ketchup bottle". The most important factors are:

- Extruder size and type
- Screw design
- Coextrusion head design
- Number/thickness of layers
- Number of resins
- Bottom weld or pinch-off design
- Regrind use

These are the fundamental issues of coextrusion blow molding.

NEW DEVELOPMENTS IN COEXTRUSION-BLOW MOLDING TECHNOLOGY

W. Neubauer -- BEKUM Maschinenfabriken GmbH, Berlin 42, West Germany

Contrary to the blow molding process of single layer hollow containers the coextrusion-process for the production of multilayer containers has got an intensive development only the last 10 years and it has reached now a very high standard both with regard to process technology and concerning the machninery. The market has expanded and the increasing application of coextruded containers as well as the developments of industry on these equipments are showing the importance of these products for the packing industry.

The conextrusion blowing process makes use of the specific properties of idfferent materials for the production of high-tech multilayer containers. The main factors for the coextrusion, respectively their application is:

- increasing responsability for environmental matters (packing of chemicals and detergents)
- increased shelf live of foodstuffs
- extended storage possibility of cosmetics
- optical surface creation.

Besides these requisites the economical production of packings is one of the main topics and claims to the coextruded article. The decisive step for compliance to this requirement was the development of the multilayer extrusion head, which allows to produce a multilayer parison with thin wallthickness by keeping a constant and perfect coaxial wallthickness distribution. This multilayer head, in conjunction with extruders and screws adopted to their corresponding jobs, take care of smooth plastification of resins and good homogeneity, being the core of a coex-plant.

The calculation of the flow channels and the design in consideration of process technology is of utmost importance for the quality of the production process and of the produced article.

For the rheological conception of the flow channels, that means its calculation, there are available today different programs and other means, which serve specially to bring the coex-head into best production conditions. The purpose of this lecture is to go into details of a calculations procedure.

New developments on the coextrusion field:

Considering the great number of modifications and changes we concentrate on three items:

- coextrusion-head with spiral distributor
- coextrusion element head as per mandrel process (heart curve)
- PVC-coextrusion-head as per ring torpedo system.

Decisive and important for the consideration of quality is the finished article respectively the parison. Of utmist influence is the multilayer haed with and the way it handles the process melt plastification. But also the handling within the blowing machine which forms the parison to the finished article is very important and in this connection the technology of the coextrusion-twin head is explained.

The economical production of coextruded articles depends to a high degree on the obtainable thickness of layers for the barrier and for the tie. These two materials are very expensive. They are required only in very thin layer configuration for their function (barrier for preventing permeation, tie for assuring a reliable connection between different plastic layers). For that reason the barrier complies with its function within a layer range between 20 and 30 µm. For that reason a production process which allows the blowing of thin layer in equal thickness and without failures such as the doubling effect, has many advantages in comparison to equipment which is producing with thick layers. Even the saving in material offers compensation of higher investment. Today the desired layer thickness of 20 - 30 µm can be obtained with the modern multilayer twin heads.

3/1

Blown Film Processes - Some New and Alterative Considerations Leading to Better Prediction of Bubble Shape and Heat Transfer Dynamics

G.A. Campbell
Clarkson University, Potsdam, New York 13676

Commercial blown film processes are controlled by film speed and blow-up ratio. These two parameters are used to develop the gauge of the film. In addition, control of these two parameters also leads to the important physical properties of impact strength and machine and transverse direction tear strength. The simulations that have been previously proposed in the literature do not address the important issue of film velocity. Results will be presented in this lecture which lead to a simulation that does have the proper bubble shape and has been shown to have a very good correlation with the film velocity as reported by literature experimental data.

A new concept has been developed by adapting observations in the literature that polyethylene and other polymers exhibit a yield at or near the transition temperature. By incorporating this yield phenomena in the rheological description used in the simulation we have been able to develop models that produce the appropriate bubble shape and the correct velocity profile for the film. It is important to recognize that most of the models that have been previously used are only qualitatively valid up to the so-called freeze line. At this point both the bubble shape and the velocity of the film as predicted by the models differ dramatically from the experimentally reported data in the literature. By incorporating a yield phenomena we have been able to develop the proper bubble shape and velocity for both crystalline and amorphous polymers.

The new models that were developed fit the data quite well in the region near the freeze line, however they were found to be deficient in the manner in which they fit the experimental data close to the die. Therefore, the work was extended to investigate the influence of the air flow from the air ring. The local pressure profile on the film was determined as a function of position from the die. We have developed experimental techniques and theoretical analysis which are in quite good agreement considering the assumptions that are used in developing the pressure, position, and curvature relationship. Our theoretical analysis agrees very well with the experimentally predicted results. These results indicate that there is a pressure on the outside of the bubble which opposes the internal pressure for a concave curvature and which adds to the pressure for a convex curvature. The relationship that has been developed for the effective pressure drop as a function of position has only one parameter for which the laboratory data that we have currently analyzed can be fixed at 0.6. Thus, the expression that we have developed gives us the ability to look at the simultaneous interaction of the polymer viscosity and the air flow rate and on the actual hoop stress to which the polymeric fluid is subjected. Utilizing this relationship we have been able to predict the straight stock type of behavior that has been reported in the literature for both polystyrene and polyethylene.

The combination of the appropriate models allows us to predict bubble velocity as a function of position through the freeze line and up into the constant diameter portion of the bubble. The ability to predict the interaction of bubble shape with air flow from the air ring now allows us to look at the effect of the air and film speed on the heat transfer. It is, of course, well known that the heat transfer coefficient in a flowing system is a function of the relative velocities of the polymer interface and the air velocity. We now have the necessary theoretical tools to characterize the heat transfer coefficient as it changes due to the decrease it the velocity of the air and the increase in the velocity of the film. This should lead to improved analysis of the blown film process such that we can predict crystallization dynamics and the vitreous transition from a deformable fluid to a solid glass. It is these two transitions which cause the polymer to have frozen in strains and thus the improved physical properties that we see when we convert polymers to biaxially oriented blown film materials.

PECULIARITIES CONNECTED WITH MEASUREMENT AND INTERPRETATION OF THE TEXTURE IN BIAXIALLY DRAWN PETP FILMS

B.-J. Jungnickel, Deutsches Kunststoff-Institut, 6100 Darmstadt, West Germany

The main aim of the present paper is to show that a lot of peculiarities are to consider with the interpretation of birefringence and anisotropic X-ray scattering measurements for films of biaxially drawn poly (ethylene terephthalate), PETP. Some of them are occasionally neglected in the literature so far, this sometimes leading to misinterpretations or wrong results.

The evaluation of orientation by birefringence measurements after having corrected them for stress and form birefringence is based on the equation

$$n_k - n_l = \Delta n_{kl} = c \sum_{i,j} (p_i - p_j) f_{klij}(\underline{\Omega}) = \sum_{i,j} n^o_{ij} f_{klij}(\underline{\Omega})$$

In this equation, the n_k are the refractive indices, c is a constant, the p_i are the polarizabilities of the monomer unit, the Δn^o_{ij} are the "intrinsic birefringences" and the $f_{klij}(\underline{\Omega})$ are "orientation factors". These factors are averages of trigonometric functions of the orientation angles $(\vartheta, \varphi, \psi) = \underline{\Omega}$ of the monomer units (ϑ, φ, ψ: Eulerian angles) and, therefore, contain the information on the orientation. Generally, there are eight different orientation factors, the estimation of all of which through the only two birefringence values is impossible. Moreover, the intrinsic birefringences have to be known and to be orientation independent. The latter condition means that the conformation of the monomer units must not change during deformation of the sample. In the present paper it will be shown that both conditions are not fullfilled for biaxially drawn films of PETP because of their specific texture and of deformation induced crystallization and stretching of the chains in the amorphous regions.

Because of the particular polarizability values of the PETP monomer unit, the birefringence in the film plane increases with decreasing orientation in contrast to the usual rule. Since the type of the texture can not be evaluated by birefringence measurements, one generally is not able to decide changes in which of the different texture components are responsible for observed changes in birefringence: different orientations (different both with respect to the type of the texture and to the completeness of it) can cause identical birefringences. Moreover, there is no clear rule connecting the direction of change in birefringence (increase or decrease) with the direction of change in the completeness of orientation. These complicated connections between molecular conformation, orientation and birefringence will be analysed in detail and illustrated by experiments.

For the X-ray measurements there is the basic problem to conclude on the orientation distribution of important structural directions like the chain direction or the benzene plane normal from those of measurable net planes. It is well known that the distribution of the $(\bar{1}05)$ net plane and the chain direction distribution can be identified in a sufficient approximation. In the present paper it is shown that a similar connection holds between the benzene plane and the $(2\bar{1}1)$ net plane. The orientation distribution of the latter can be registrated at $2\Theta = 52.2^o$ for $\lambda = 1.54$ Å. With this one finds that in oriented films crystallized with fixed ends the benzene plane orients in the film plane whereas the (100) planes and the crystalline b-axes assume this orientation after a loose end crystallization. These conclusions are illustrated by suitable experimental results.

For an interpretation of the connections between deformation and chain orientation one has to consider that the reorientation, the accompanying changes in structure and the crystallization of PETP differ from that of other polymers in many respects. This is caused by the two facts that, on the one hand, PETP is usually drawn in the amorphous state and, on the other hand, that a lot of secondary valences are created during a thermal or mechanical treatment in this material. By this, mesomorphous structures are created the character of which covers the whole structural spectrum between the amorphous and the crystalline state. After normalizing it to one, the number and the completeness of arrangement of these secondary valences c_d can be thought to be an order parameter in the terminology of thermodynamics. Then, all values c_d between c_o (starting material) and one (crystal) can be created by deformation. Moreover, a thermally induced phase transition from c_d to one ("crystallization") can occur. For an oriented material that is crystallized with fixed ends, this phase transition is characterized by two essentials:

- the chain folding and the spherulithic crystal growth are suppressed; the crystals have micellar surfaces;
- the mesomorphous regions and the crystals created from them have the same average orientation.

REFERENCE
Jungnickel, B.-J.: Polymer Eng. Sci. 27 (1987) 1021-1034

3/3

DOUBLE BUBBLE TUBULAR FILM PROCESS FOR MAKING BIAXIALLY ORIENTED POLYETHYLENE TEREPHTHALATE FILM

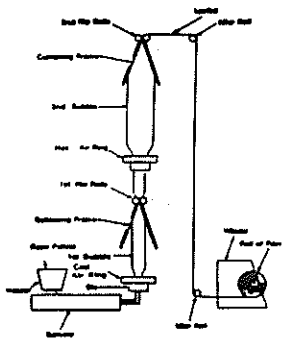
by

H-J. Kang, M. Cakmak and J. L. White
Polymer Engineering Center
The University of Akron
Akron, Ohio 44325 U.S.A.

Double bubble tubular film processes have a long history (1,2). There have, however, been no published basic studies.

A double bubble processing techology for producing biaxially oriented polyethylene terephthalate film has been developed in our laboratory. These are two stage tubular film extrusion. Polyethylene terephthalate tubular films are prepared with a screw extruder using an annular die. The bubble is collapsed and re-inflated in a hot air ring as shown in the figure. In the second stage, the films which are amorphous are stretched and then crystallized by the imposed stress of trapping air in the second bubble. Consequently, biaxial orientation was developed. Selected samples were clamped and annealed at 150°C for 10 minutes.

The stability of tubular film extrusion was observed for both single and double bubbles considering the influence of process conditions. Following Kanai and White (3), we sought to find the operating windows both single and double bubbles. This is based on the processing parameters; draw down ratio (DR), blowup ration (BUR), the frost height (FLH) for the first bubble; double bubble draw down ratio (DDR), double bubble blowup ratio (DBUR) for the second bubble. For low DBUR, the second bubble is stable. Increasing DBUR results in an axisymmetric periodic instability especially at low DDR.



The crystallinity of the double bubble film increases with increasing DBUR and DDR.

The glass transition temperature decreases with increasing DDR in constant DBUR samples. Low DBUR samples with high DDR exhibit an increase of transition temperature. The crystallization peak temperature decreases with increasing DDR. DBUR also influences the crystallization temperature.

Analysis of WAXS flat film patterns show that films produced by the first bubble remains in the glassy state while the second bubble film shows crystalline characteristics. Molecular orientation was characterized by means of WAXS pole figures. The 100 and -105 planes determine c-axis and phenyl ring orientation.

Results indicated that the chain axes align along the machine direction with increasing DDR and along the transverse direction with increasing DBUR. The phenyl ring plane are increasingly oriented parallel to the film surface both at increasing DDR and DBUR. This is similar to the characteristics of cast and biaxially stretched film (5).

White-Spruiell (4) biaxial orientation factors were determined and plotted in an orientation triangle. Increasing DBUR produces equal biaxial orientation factors and biaxiality. High double draw down ratio samples, on the other hand, approach uniaxial behavior with respect to the machine direction.

References

1. K. E. Gerber — U.S. Patent 2,862,234 (1958); U.S. Patent 2,916,764 (1959)
2. E. J. Moore — U.S. Patent 3,311,679 (1967)
3. T. Kanai and J. L. White — Polym. Eng. Sci. 24, 1185 (1984)
4. J. L. White and J. E. Spruiell — Polym. Eng. Sci. 21, 859 (1981)
5. M. Cakmak, J. L. White and J. E. Spruiell — J. Polym. Eng. 6, 291 (1986)

THEORETICAL ANALYSIS OF FILM EXTRUSION AND ITS APPLICATIONS

Toshitaka Kanai
Polymer Research Laboratory
Idemitsu Petrochemical Co.,Ltd.
1 1 Anesaki Kaigan, Ichihara, Chiba, Japan 299 01

As the film processability during the film extrusion and the physical properties of film are much influenced by the resin quality and process conditions, it is very important to obtain the relationship between rheological behavior of the resin, process conditions, deformation behavior and physical properties of films.

The results of tubular film extrusion and T-die film extrusion are studied.

1. Rheological behaviors of PEs

In the case of film extrusion, elongational deformation occurs between the die exit and the take-up roll. The elongational viscosity should be of most interest to evaluate the deformation behavior during the film extrusion.

Figure 1 shows elongational viscosities of representative PE grades for tubular film extrusion.

Elongational viscosity of narrow molecular weight distribution LLDPE shows about $3\eta_0$. HDPE having broad molecular weight distribution exhibits a strong elastic behavior and doesn't possess constant elongational viscosity.

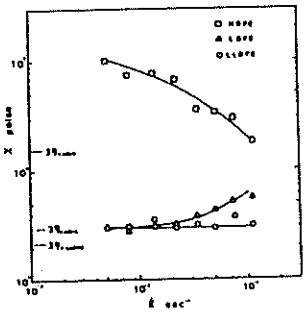


Figure 1. Steady-state elongational viscosity χ for LDPE and LLDPE melts and χ_{max} for HDPE as a function of elongational rate

2. Analysis of elongational deformation during tubular film extrusion

Figure 2 shows local velocities, bubble temperature as well as bubble shape. It may be seen that V_z increases monotonically, most rapidly in the region of most rapid bubble inflation and plateauing beyond the frost line. HDPE is a typical resin showing the sharp deformation in the narrow region. This may be due to the low activation energy and deformation rate softening of HDPE.

Cooling condition of tubular film extrusion influences the physical properties and processability. Eq. 1 is the energy balance equation including the terms of heat transfer, heat radiation and crystallization heat.

$$\rho C_p Q\cos\theta\frac{dT}{dz}=-2\pi R[U(T-T_{air})+\varepsilon\lambda(T^4-T^4_{room})]+Q\Delta H_f\cos\theta\frac{dX}{dz}\quad(1)$$

$$\frac{UL_m}{K_{air}}=0.043\left(\frac{L_m V_{air}\rho_{air}}{\eta_{air}}\right)^{0.75}\quad(2)$$

T:film temperature, T_{air} :cooling air temperature, T_{room}: room temperature, U:local heat transfer coefficient, λ:the Stefan Boltzmann constant, C_p:specific heat, ΔH_f :the heat of fusion, X:crystallinity, ρ:density, ε:emissivity, θ:angle between bubble axis and bubble surface, K_{air} :thermal conductivity, V_{air} :local maximum air velocity, ρ_{air} :density, U:local heat transfer coefficient

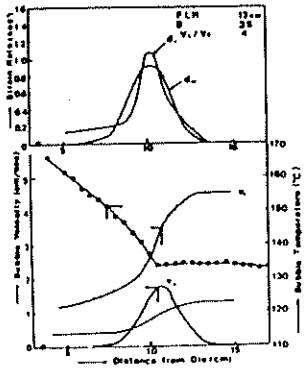


Figure 2. Local velocities V_r, V_z, deformation rate d_{11}, d_{22} and temperature along the length of bubble for HDPE (V_L/V_0=4, R_L/R_0 3.5, Z_f 12cm)

The crystallization rate calculatud from the Eq.1, heat transfer data and temperature distribution obtained from experiment is shown in Figure 3.

The force balance on the tubular film bubble is most readily develped from membrane theory.

$$F_L=2\pi RH\sigma_{11}\cos\theta+\pi(R^2_L-R^2)\cdot\Delta P\quad(3)$$

$$\frac{H\sigma_{11}}{R_1}+\frac{H\sigma_{22}}{R}=\Delta P\quad(4)$$

$$\eta(\Pi_d,T,X)=A\exp(E/RT+GX)\Pi_d^{(n-1)/2}\quad(5)$$

$$A=\eta_0\exp(-E/RT_0)\quad(6)$$

F_L :bubble tension, ΔP:bubble inside pressure, X:crystallinity, R_L :bubble radius at frost line, η:viscosity, R:the gas constant, E:activation energy, G:viscosity constant, Π_d : second invariant

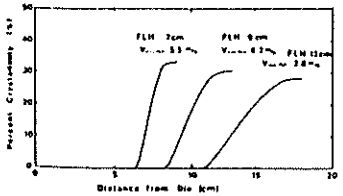


Figure 3. Crystallinity of a function of distance from die for LLDPE at various frost line heights

Combining eqs. (1) (6) with the data of resin properties and process conditions the melt behavior during the tubular film process can be predicted. The bubble shape is much influenced by activation energy E and power law index n. The resin having small value of n and low activation energy gives wine glass shape which is shown in Figure 4.

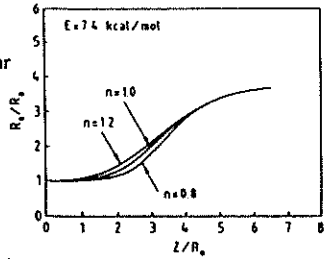


Figure 4. Predicted bubble shapes for different values of power law index n (R_L/R_0=3.7, V_L/V_0=3.4, Z/R_0=6.5)

The maximum stresses σ_{11max} and σ_{22max} which are closely related to the physical properties of film decrease with increasing frost line height (Figure 5).

Maximum stresses at the frost line height were used to set up the scale-up rule. We should consider process conditions which make the stretch stresses constant both in machine direction and in transverse direction. At the frost line height, bubble diameter is equal to final bubble diameter.

$$\sigma_{11}=\frac{F_L}{2\pi R_L H_L}\qquad \sigma_{22}=\frac{\Delta P\cdot R_L}{H_L}\quad(7)$$

By using the analysis of dimensionless terms, stresses σ_{11max} and σ_{22max} are represented by equation (8).

$$\sigma_{11}=G_1\frac{Q\eta_0}{R_0R_LH_L}\qquad \sigma_{22}=G_2\frac{Q\eta_0R_L}{R_0^2H_L}\quad(8)$$

G_1,G_2 are constants under the condition of constant blow up ratio, draw down ratio and frost line height. Figure 6 shows film impact strength as a function of film thickness and width.

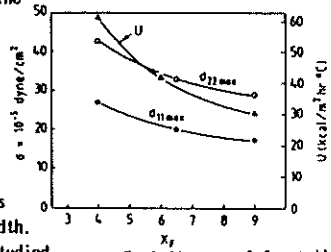


Figure 5. Influence of frost line height on tension σ_{11} and σ_{22} and heat transfer coefficient U (R_L/R_0=3.5, V_L/V_0=3.8)

Theoretical analysis of T-die film extrusion also is studied. It was found that stability is dependent on draw ratio and dimensionless deformation rate represented by equation (9).

$$\varepsilon=(L/V_L)(\partial V/\partial Z)_L\quad L:\text{air gap},\ V_L:\text{take-up speed}\quad(9)$$

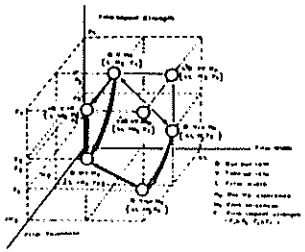


Figure 6. Film impact strength as a function of film thickness and film width

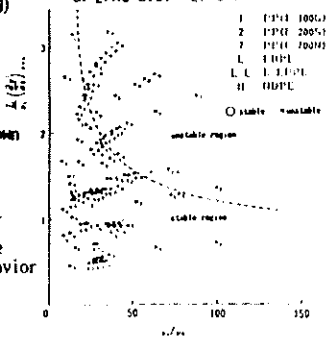


Figure 7. Draw down ratio (V_L/V_0) dimensionless deformation rate $(L/V_L)(\partial V/\partial Z)_L$ plot showing regions of stable and unstable behavior

CAST FILM EXTRUSION. THERMOMECHANICAL AND PHYSICAL ASPECTS

J.M. HAUDIN
Centre de Mise en Forme des Matériaux, UA CNRS n° 852
Ecole Nationale Supérieure des Mines de Paris
Sophia-Antipolis, 06560 VALBONNE (FRANCE)

Cast film extrusion is one of the important processes to manufacture plates, sheets and films of polymer. In this process, the polymer melt is extruded through a slit die, slightly stretched in air and cooled on a chill roll. The present work is divided into two parts : first the development of thermomechanical models, which can be applied either to polypropylene or to polyethylene terephtalate, and second the structural analysis of extruded polypropylene films, in order to deduce interrelations between processing conditions and microstructures.

THERMOMECHANICAL MODELS

The models developed in our laboratory for a complete thermomechanical description of the whole process consist of a thermomechanical analysis of stretching in air and of a purely thermal model of cooling on the roll. The equations are solved using finite difference methods.

Stretching in air

In all the models the chosen velocity field implies that the film section remains rectangular. The polymer is assumed to be Newtonian and the process is stationary.

In a first approach, Sergent [1] proposed an isothermal Newtonian model neglecting gravity and inertia forces. This model calculates the film geometry (width and thickness), the velocity and the stretching stress during the path in air. Thermal effects were then introduced by Cotto [2], but to a first approximation, the heat transfer coefficients were considered as constants.

A more sophisticated model is now developed by Barq et al. [3]. Gravity and inertia forces are taken into account, which makes it possible to predict the film profile when the gravity forces induce a curvature of the film. Furthermore, the temperature field is calculated using a local heat transfer coefficient.

Cooling on the roll

Two different methods have been used to take into account the heat of crystallization. In the first one [2], the energy equation is first solved without taking crystallization into account. Crystallization effects are then introduced as local perturbations of the calculated temperature profiles. A second approach [4] is based on the combination of Ozawa's kinetic law and of a formulation of the energy equation integrating the heat liberated by the crystallization. This latter approach allows to determine the transformed volume fraction in the film thickness.

STRUCTURAL ANALYSIS

Results given by the models associated with microstructural observations make it possible to describe the respective effects of stretching in air and cooling on the roll on the final microstructure of extruded polypropylene films.

The main effects of stretching in air are to increase the number of crystalline nuclei and to favour an anisotropic spherulite growth.

Dissymmetrical cooling on the chill roll induces an inhomogeneous microstructure within the films. The formation of a transcrystalline region is attributed to intense surface nucleation at the roll surface. The presence of a zone with a finer microstructure near the roll is correlated with the cooling rates and thermal gradients calculated by the model.

References

[1] J.Ph. SERGENT, Thesis, Université Louis Pasteur, Strasbourg (1977)
[2] D. COTTO, Thesis, Ecole des Mines de Paris (1984)
[3] Ph. BARQ, J.F. AGASSANT and J.M. HAUDIN, Third Annual PPS Meeting, Stuggart (1987)
[4] N. BILLON, Thesis, Ecole des Mines de Paris (1987)

DRAW RESONANCE IN FILM CASTING OF POLYMERIC MELTS

Albert Co and Chung-Ming Lin
Department of Chemical Engineering
University of Maine, Orono, ME 04469

As the molten polymer film is extruded from the slit die, it is stretched uniaxially and is drawn down in cross-sectional area before being quenched and solidified by the chill roll. The ratio of the cross-sectional area of the film leaving the die to the cross-sectional area of the film at the chill roll is defined as the draw ratio. For incompressible fluids, this is equal to the ratio of the take-up velocity to the extrusion velocity.

At certain draw ratios, sustained oscillations of distinct period and amplitude in the film thickness are observed. This type of flow instability, which occurs in spite of constant extrusion speed and constant take-up velocity, is referred to as draw resonance.

In order to understand the role of viscoelasticity on draw resonance in the film casting process, we have undertaken both theoretical and experimental investigations of the phenomenon. This paper presents part of our experimental studies.

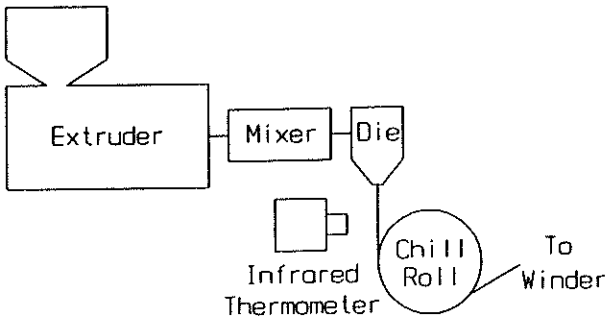


Fig. 1. The film casting experiments.

The film casting experiments are conducted using a 1-1/2 in. single-screw extruder with an L/D ratio of 24. The adjustable gap opening of the 10 in. wide slit die is set at about 30 mils in the current experiments. In order to obtain a more uniform melt temperature, a static mixer is installed between the extruder and the die. The 12 in. wide double-shell spiral-baffled chill roll can be located at 2 to 6 in. below the slit die. The temperature profile of the film between the die and the chill roll is measured with an infrared thermometer operating around the wavelength of 3.43 micron. The thickness profile of the solidified film is measured off-line using an electronic micrometer with a resolution of 0.01 mil.

The resins currently investigated are Union Carbide G-Resin 7042 and 7047 linear low-density polyethylenes. Rheological characterizations of these resins are conducted with a Rheometrics mechanical spectrometer.

For a given extrusion speed, the ratio of the maximum thickness to the minimum thickness, as indicated by the measured thickness profile, is plotted against the corresponding draw ratio. The draw ratio at which the thickness ratio changes from unity (stable flow) to a value greater than one (unstable flow) is identified as the critical draw ratio. The dependence of the critical draw ratio on the extrusion speed, the distance between the die and the chill roll, the operating temperature, and the resin rheological properties are investigated.

3/7

PREPARATION OF HIGH-MODULUS PLASTIC FILMS BY ZONE-ANNEALING METHOD

Toshio Kunugi, Department of Applied Chemistry, Faculty of Engineering, Yamanashi University, Takeda-4, Kofu 400 Japan

The zone-annealing method was proposed by us[1] in 1979. The method has so far been applied to prepare high-modulus and high-strength fibers. The resulting fibers have exhibited excellent mechanical properties and dimensional stability at elevated temperatures. This method can also be applied to plastic films solely by the use of a slit-shaped heater instead of a ring-shaped one in the case of fibers. The mechanical properties of films or tapes have been much more improved by the method. Table 1 shows the main results obtained so far.

The characteristic of this method is that the drawing and annealing processes are achieved by shifting a narrow heating zone (2-3mm) at a constant speed producing a suitable tension in the films. So the films are drawn homogeneously and smoothly, and are annealed successively and regularly from one end of the film. The original films are consequently transformed into homogeneous structure with a high molecular orientation and a high crystallinity. Usually, the procedure is divided into two stages, zone-drawing and zone-annealing, and further each stage is repeated gradually increasing tension and/or temperature to avoid a rapid change in the structure.

This method possesses the following advantages;

(1) The heat quantity required for drawing and annealing is remarkably smaller compared with other conventional oven- or bath-processes, because the films are heated only narrow linear zone.

(2) Thermal degradation or heat-treatment effects induced prior to drawing or annealing can be prevented, because the film enters the controled heating zone as a first experience.

(3) The decrease in width becomes small with broadening of the film and/or decreasing of the vertical width of the heating zone. Deformation of the film is attained mainly in support of decrease in thickness of the film.

(4) This method can be easily applied to heat-resistant polymers with a high glass transition temperature or a high crystallization temperature, because heating zone is very narrow.

In general, the zone-drawing temperatures were selected from temperatures above Tg and below Tc (crystallization temperature) of the polymer under consideration. For example, those for PET and PEEK were 90°C and 140°C, respectively. However, it was recently found that the remarkably high temperature near or above Tm (melting temperature) was very effective for 1st zone-drawing of crystalline polymers. The method was named by us the high-temperature necking zone-drawing. For single crystal mats of ultra-high molecular weight PE and it-PP films, 125-135°C and 150°C were used as 1st zone-drawing temperatures, respectively. At such temperatures, the crystals became fully soft and were effectively unfolded with sutable tension. By the subsequent zone-drawing and zone-annealing, the moduli were strikingly increased as seen in Table 1.

Further, we have developed a novel method "Vertical two-step zone-drawing". This method consists of transverse drawing and longitudinal zone-drawing. The principle is as follows. By 1st drawing, the lamellae in the film are oriented and a stacked lamella structure is formed. Next, by longitudinal zone-drawing, the molecular chains of lamellae are unfolded in a manner similar to zone-drawing of single crystal mats. The drawn films are further zone-drawn and zone-annealed under more strict conditions. The tapes thus obtained have much higher modulus than those obtained by the conventional zone-drawing/zone-annealing method. We have succeeded in the improvement of mechanical properties for nylon 6 and it-PP tapes.

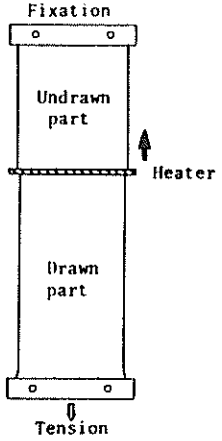


Fig. 1 Zone-drawing of film

Table 1 The main results obtained for plastic films

Polymer	Maximum Modulus (GPa)	Maximum Strength (GPa)	Ref.
PET	14.5	0.85	2)
UHMW PE	232	6	3)
it-PP	27	1.1	4)
Nylon 6	8	0.87	5)
PEEK	13.3	1.1	6)
Kanton H	22	1.1	7)

The modulus values in Table 1 are indicated by the dynamic moduli with high reproducibility.

References

1) T. Kunugi et al., Polym. Prepr., Am. Chem. Soc. Div. Polym. Chem., 20, 778 (1979).
2) T. Kunugi et al., J. Appl. Polym. Sci., 26, 213 (1981).
3) T. Kunugi et al., Polymer, in press.
4) T. Kunugi et al., Polym. Prepr., Japan 36, 1115 (1987).
5) T. Kunugi et al., ibid., 34, 1093 (1985).
6) T. Kunugi et al., Polym. Commun., 27, 175 (1986).
7) T. Kunugi, 2nd SPSJ International Polymer Conference, Japan 1A22 (1986).

ELECTROTHERMOMECHANICAL FILM (ETMF) AND ITS PROCESSING

A. Savolainen, K. Kirjavainen,
Institute of Plastics Technology
Tampere University of Technology,
P.O. Box 527, SF-33101 Tampere, Finland

Electrothermomechanical film (ETMF) [1] is a cellular, biaxially oriented plastic film which is coated with electrically conductive layers. It connects electrical, mechanical and thermal energies as well as parameters together. ETMF is an elastic impedance, (Fig.1). The film can be applied in measuring techniques, in acoustics, in ultrasonics, in motion elements, in energy transformation etc.

(Fig.2) shows schematically a bubble method for manufacturing of ETMF. Because of the diffusion of gases from cellular film (base matrix will be PP., PA6 etc.) the three layer system with barrier polymers is inevitable [2]. Therefore the processing method is a coextrusion with two extruders, first one for cellular matrix and second one for barrier polymers.

The film grade PP and barrier polymers are extruded to a tube with a wall thickness of about 400-500µm. Gas bubbles of about 10µm diameter with 10µm spacing have been formed immediately after die exit. The three layer tube has been drawn over cooling mandrel into oven where it is reheated to a temperature level suitable for biaxial stretching. After stretching the three layer film has been preheated again to minimize the shrinkage phenomenon. Finally, the film is sputtered by copper or aluminium with a layer thickness of about 200-300 Ångströms.

The main detail in ETMF processing is the functioning of the die. For preparing a homogenous cellular (with closed cells) PP tube an extrusion head with inner rotating mixing disks has been developed, (Fig. 3)[3]. It is well known that the melt has a flow memory and at least partly this memory causes distortions such like stripes and joints etc. into the extruded article. In addition an unsteady flow often characterized with a changing velocity gradient introduces a changing thickness profile in blown film manufacturing. The head developed during ETMF project bases on an idea of rotating mixing disks which destroy the flow memory so that in each layer of the product the properties are uniform and homogenous.

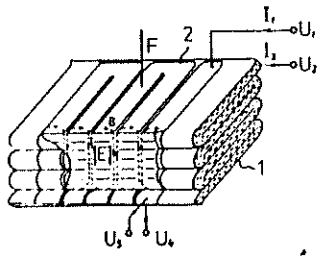


Fig.1. Multilayer structure of ETMF which is capacitive and inductive.
1; Individual foamed film matrix and
2; A patterned metal layer through the folded film element to form a magnetic circuit.

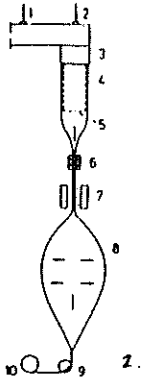


Fig.2. Biaxial orientation of PP schematically. Extruder (1), Air feeding (2), Die (3), Tube (4), Cooling mandrel (5), Caterpillar (6), Heating (7), Bubble forming (8), Nip roll (9), Reel (10).

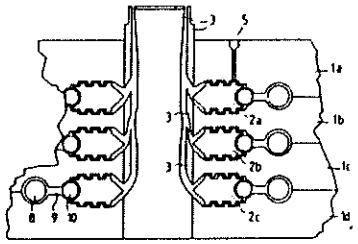


Fig.3. Cross section of three layer extrusion die; Rotating disks (2a-2c), Die matrice (3), Inlet for colours etc. (5).

1. PAT. US 4654546, K. Kirjavainen
2. A. Savolainen, K. Kirjavainen, J. Polym. Sci. Chem. in press.
3. PAT. PCT/FI 87/00047, A. Savolainen, K. Kirjavainen, J. Suomi

ANALYSIS OF DRAWINGS IN THE FLAT PET FILM PROCESS

G. LE BOURVELLEC, J. BEAUTEMPS Rhône-Poulenc Recherches - CRC - 85, Av. des Frères Perret - 69190 St Fons - FRANCE

J.P. JARRY Rhône-Poulenc Recherches - CRA - 14, R. des Gardinoux - 93308 Aubervilliers - FRANCE

One of the main uses of poly ethylene terephthalate is the film processing for applications in the field of magnetic tapes, packaging, capacitors, etc. The PET films can be made by a flat process (Figure 1), in which the film is biaxially oriented as it is successively stretched in two directions, the machine direction (MD) and the transverse direction (TD).

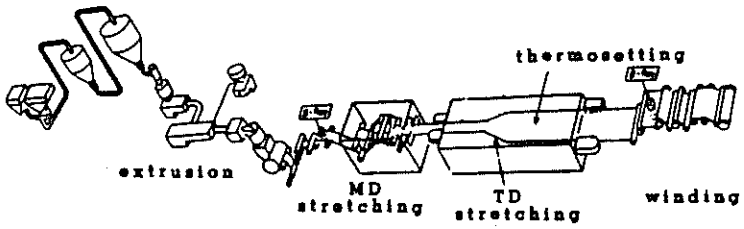


Figure 1 : Example of a flat film process.

However, according to the flat process, the first drawing can be either MD stretching or TD stretching. As the drawability in the second direction depends on the structure generated by the first stretching, it is important to know the evolution of the structure during the first drawing.

In this work, we performed laboratory simulations of MD and TD stretchings involved in a flat process.

The TD stretching, performed in a stenter, can be simulated by a drawing at constant speed of elongation. The MD stretching, performed between rolls, is equivalent to a drawing under constant load

The kinetics of deformation are described for each stretching. It is shown that the strain rates involved in a drawing under constant load can reach very high values (20 to 30 s^{-1} at 97°C) compared to the case of stretching at constant speed of elongation (less than 1 s^{-1}). We also found specific features for the stretching at constant force (Figure 2) :

* All the curves end by a plateau.
* There is a minimum plateau deformation (natural draw ratio)
* Under low tension, the plateau deformation increases when the force F decreases.
* Under high tension, the plateau deformation increases with F.
* In all cases, the kinetics increases with the tension.

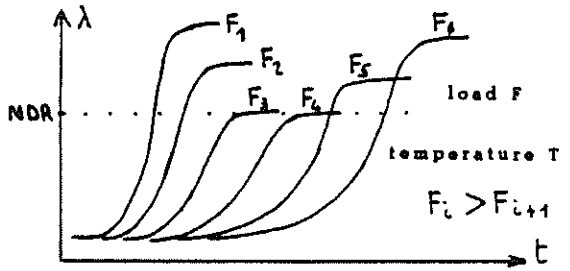


Figure 2 : Typical deformation curves of stretching under constant load

A structural analysis has been done for both stretchings in terms of orientations and crystallinity.

For TD stretching, we found that the crystallinity is almost independent of the drawing temperature because of the balance between mobility and chains orientation.

For MD stretching, the main results are the following:
* For a given temperature and a given draw ratio, the structural properties increase with the stretching force.
* The plateau is equivalent to an annealing at constant length.
* At the beginning of a plateau, for a given draw ratio, the crystallinity is independent of the temperature of drawing
* The temperature is the main parameter which controls the chains orientation, whatever the strain rates spectrum.

Finally, a comparison between MD and TD stretchings showed that :
* at low strain rates (less than 1 s^{-1}), the crystallinity depends only on the chains orientation and the temperature.
* at higher strain rates, the induced crystallization is limited by a kinetic effect (industrial case).

INSTABILITY PHENOMENA IN FILM CASTING PROCESS EXPERIMENTAL AND NUMERICAL APPROACHES

Ph.BARQ - J.M.HAUDIN - J.F.AGASSANT *
H.ROTH - P.BOURGIN **

* Centre de Mise en Forme des Materiaux
U. A. CNRS n° 852
Ecole Nationale Supérieure des Mines de Paris
Sophia - Antipolis 06560 Valbonne - France

** Rhône - Poulenc - Films
Saint - Maurice de Beynost
B.P. 140
01701 Miribel Cedex - France

Flat thin polyester sheets are obtained by extrusion through a slit die and then by stretching in the longitudinal and transversal directions. For the films produced for audio or video equipment, it is well known that the thickness regularity is of prime importance, and depends greatly on the stability of the first stretching operation between the die and the roll.

We have studied these phenomena both experimentally and theoretically.

The experimental measurements have been conducted on a casting plant at the Rhône - Poulenc - Film company. The primary film thickness is measured continuously with a captor. Several polyester compounds and processing conditions have been tested.

Isothermal models have been developed. Mass, inertia, friction with air and surface tension are neglected. The polymer is supposed to be incompressible. Newtonian and Maxwell constitutive equations have been considered. The sheet is supposed to be vertical and the lateral necking is not taken into account. The partial differential equations have been solved along the stretching path in air at each time step using a finite difference scheme. The same kind of approach has already been developed by ISHIHARA for the melt spinning.

RESULTS

Three kinds of perturbationsof the roll velocity have been studied and the computation results have been compared to experimental measurements.

- In a first time, successive increases of the roll velocity are exerted and the resulting film thickness regularity is measured. For low draw ratios, the thickness variation vanishes with time and the polyester film becomes progressively regular. For high draw ratios, the thickness perturbation becomes periodic. This points out the existence of a critical draw ratio which discriminates stable and unstable stretching conditions. A diagram of the thickness versus the derivation of the thickness may be computed. For low draw ratios, the derivative of the thickness vanishes with time as for high draw ratios a limit cycle may be observed which points out the appearance of the "draw - resonance" phenomenon.

- In a second time, a sinusoidal variation of the roll velocity has been imposed. A good agreement is observed between the computed thickness variations and the experiments.

- Finally, the roll velocity is varying aleatory between a minimal and a maximal value, and the resulting film thickness is computed. The "draw - resonance" phenomenon is observed for high draw ratios, which corresponds to the experiments.

PERSPECTIVES

Further developments are in progress taking into account the width variation of the film between the die and the roll and the gravity forces influence.

3/11

HIGH-PERFORMANCE STRUCTURES BASED ON COMMODITY PLASTICS

P.J. Lemstra, Department of Polymer Technology, Eindhoven University of Technology, P.O. Box 513, 5600 MB Eindhoven, The Netherlands

Commodity polymers such as polyethylene, polypropylene and polystyrene are usually not considered to be interesting materials for engineering purposes. Recently however, various routes have been found to produce chain-extended polyethylene and polypropylene structures possessing excellent mechanical properties in comparison with their isotropic counterparts. In order to obtain these high-performance materials a precursor is generated, via spinning/casting from solution or direct polymerization, possessing a low entanglement-density followed by ultra-drawing to induce chain-extension. The importance of entanglements during solid-state deformation of semi-crystalline as well as glassy polymers has been discussed extensively in the recent literature. Properties such as drawability and maximum draw ratio in the case of semi-crystalline [1] and crazing in amorphous glassy polymers [2] have been related to the presence of an entanglement network and the molecular weight between physical crosslinks/entanglements. Via solution-spinning and blending, the entanglement-density can be influenced resulting in minor or dramatic changes in the mechanical and physical properties in the solid-state depending on the experimental conditions and materials. The prime example is the production of high-strength/high-modulus polyethylene fibres/tapes via solution-spinning/ultra-drawing of UHMW-PE.

In order to obtain 3-D structures, these fibres have to be embedded in suitable matrices. Several problems are encountered related to the relative low melting point and surface inertness of the fibres with respect to adhesion. The melting behaviour of chain-extended polyolefins is rather complex. Melting can be retarded or completely presented when fibres are properly embedded in suitable matrices. For example solution-spun/drawn polypropylene fibres, embedded in epoxy, can be heated at 200°C without a noticable loss in fibre properties. Chain-extended polyethylene is an exception however due to a solid-solid phase transition at 155°C from the orthorombic to hexagonal crystal structure. Above 155°C the chains are relatively mobile and relaxation occurs. Selective crosslinking prevents relaxation and results will be presented to show the effect of crosslinking upon thermal behavior of embedded polyethylene fibres.

Another important parameter is the fibre-matrix adhesion which is rather poor in the case of oriented polyolefin structures. Various methods have been found to improve the adhesion of the matrix to for example polyethylene fibres. Presently perfect adhesion can be obtained using both chemical and physical (radiation) methods. Some results will be presented concerning the advantages and limitations of chain-extended polyolefin structures in composite applications taking into account the maximum use temperature, adhesion, crosslinking and intrinsic fibre properties.

1. P.J. Lemstra, R. Kirschbaum, T. Ohta, H. Yasuda, Developments in Oriented Polymers, Ed. Ward, Elsevier, London (1987) p. 39-79
2. E.J. Kramer, Advances in Polymer Science 52/53, Springer-Verlag (1983), p. 1-57

New Development in Fiber- and Filmextrusion

F. Hensen, Barmag AG, Remscheid FRG and
IKV, Techn. University of Aachen FRG

The demands of the Fiber- and Film producers, the result of scientific polymer studies and the ideas and research work of the machine manufacturers and the trends and developments in Fiber- and Filmextrusion.

The main goal is the improvement of the Fiber- and Film-product-quality and of the process efficiency.

The most significant new developments in the Fiber- and Film-extrusion are

- Polymercleaning by melt filtration
- Polymer blends by dynamic Polymer mixing
- Coextrusion of different Polymers
- Product specific orientation
- Precision in melt metering
- High Speed spinning resp. high speed film extrusion
- Inline processes with automatic process control

Especially for low denier fibers and thin films and orientation at high draw ratios and high speed it is obvious that not only solid particles but also melt particles with higher degrees of polymerisation like specks and gels must be separated out of the polymer melt.

This can only be reached by using filtration media with very low porosity, big capillary winding and big thickness of the filter medium.
These filtration properties can be achieved by filtration medium out of multilayer screen cloth, sintered metal powder or sintered metal filaments with extremely large filtration area.

In fiber- and film extrusion filters are used with up to 45 m^2 medium area installed in a housing with short residence time, mesh width of less than 10 µm and a porosity of 0,3 - 0.5.
Due to newly developed dynamic melt mixers specific fiber or film characteristics can be improved by blends or matrix polymers with different other polymers.

Blends	to improve:	blends	to improve:
PP/LDPE	thermobonding	LDPE/LLDPE	weldability
PP/LDPE	spinning speed	PP/EVA	weldability
PP/PETP	tensile strength	LDPE/HDPE	tensile strength
PP/LLDPE	softness	PA6/PA6-Cop	Oxigene barrier
PETP/PP	crimp stability	PETP/LDPE	crystallisation

Coextrusion of different polymers with low compatibility like PA6, PP or PETP at fiber spinning offers

-crimping by different shrinkage or
-splitting into fibers with ultrafine deniers

With polymers of good compatibility like PP and PE can be achieved

-good binding of fibers at thermoforming or
-more softness of fibers

In the film production specific properties of different polymers are combined to improve the machinability and the enduse-properties of the film like

-sealability, stiffness
-gas barrier, moisture barrier, tenacity, grease resistance, heat resistance, flex-crack resistance and coloration
-cost-reduction by raw materail saving due to thinner layers.

At the present time for packaging of food coextrusion of 5 layers is already state of the art and coextrusion of 7 layers is in development.

Since fibers are spun by pushing and pulling polymer melt through small orifices physical properties like tenacity, elongation at break, shrinkage, bulk and softness are not only depending on the raw material but also on orientation and cristallisation at processing.

For PP it can be shown that with intensive cooling of the fibers direct after the spinnerette instead of crystalline morphology smectic morphology with excellent drawability for much higher tenacity will be reached.

Non-uniform cooling of the fibers causes different crystallinity in the cross section of the fibers and by this a latent potential for better crimping and good bulk.

The uniformaty of melt metering has been improved by extrusion systems consisting of differnet melting-, filtering-, metering aggregates in cascade formation.

The economics of the manufacturing processes are steadily improved by increase of the spinning- resp. winding-speed due to better performance of the machines and improved process parameters and by combining process steps into inline processes.

These processes are controlled by sophisticated micro processor systems.

COMPUTER SIMULATION OF MULTIFILAMENT AIR JET MELT SPINNING

H. Ishihara, S. Hayashi, H. Yasuda, and H. Ikeuchi
Katata Research Center, Toyobo Company, Ltd.
Katata 2-1-1, Otsu, Shiga 520-02, Japan

Air jet melt spinning for multifilament system was studied both theoretically and experimentally. Air jet melt spinning is a process for obtaining spunbonded nonwovens. Spinline tension during this process is generated by air drag in an air jet apparatus which is settled downward fro a spinneret point. Because of nonexistence of a take-up winder, final spinline velocity is a kind of output quantities which is determined by processing conditions. This may be a main different point compared with conventional melt spinning. Therefore, numerical computation of the basic equations for air jet melt spinning might be rather complicated.

Basic equations describing the multifilament system of air jet melt spinning may be divided into three parts : 1. Same equations as conventional melt spinning, i.e. continuity, motion, energy and rheology, 2. Equations for ambient conditions of interfilaments, 3. Equation of air drag force in an air jet apparatus.

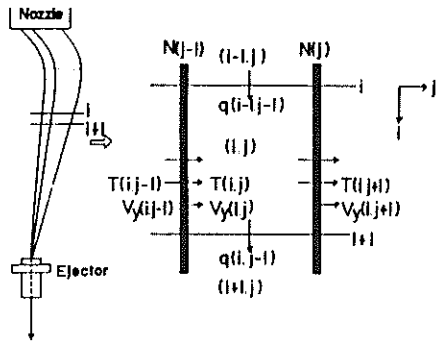


Fig. 1 Schematic diagram of Multifilament System of Air jet Melt Spinning
N:Spinline, T:Air temperature
Vy:Air velocity, q:Entrained air volume

Schematic diagram of multifilament air jet melt spinning is shown in Fig. 1. A small element of (i,j) cell is used to decide cooling air conditions such as ambient air temperature and velocity surrounding the individual spinlines. Entrained air volume q can be estimated using the boundary layer theory by Sakiadis[1] to which the effect of spinline velocity is added by us. On the other hand, equation of air drag force in an ejector was estimated as functions of the perameters such as air pressure of ejector and so on.

Fig. 2 shows an example of computation results of the final spinline velocity and the spinline temperature at the entrance position of the ejector. As shown by this figure, the spinline velocity becomes decreasing with increase of throughput, while the spinline temperature becomes increasing. The distance from the spinneret point to the position of ejector influences the absolute values of spinline velocity and temperature, respectively.

In addition, many useful informations about the spinning behaviors and the fiber properties such as birefringence can be obtained by using this simulation program.

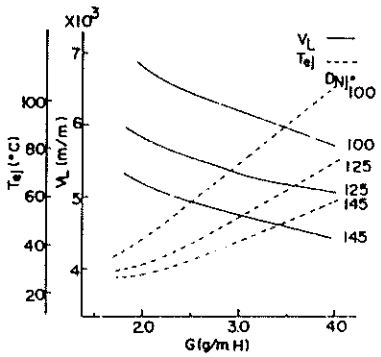


Fig. 2 An example of computation results
V_L:Spinline velocity,
Tej:Spinline Temperature
G:throughput, D_{NJ}:Distance

reference :
B.C. Sakiadis, A.I.ch. E. Jounal 7(No. 3), 467(1961)

3/15

DISTURBANCE PROPAGATION IN MELT SPINNING

David G. Young and Morton M. Denn, Department of Chemical Engineering,
University of California at Berkeley, Berkeley, CA 94720 USA

We report on an experimental study of the process sensitivity of the final fiber diameter in melt spinning to local disturbances in the quench air system. Experiments have been conducted to measure the frequency response characteristics and to investigate the influence of changes in operating variables, polymer properties, and lateral displacement of the fiber. The quench air disturbances were measured using a hot wire anemometer, and the fiber diameter fluctuations were measured using an on-line laser micrometer. The input-output relationship between the two was analyzed in the frequency domain using spectral techniques.

A variation in the quench air velocity produces both a change in the rate of heat transfer and a mechanical deflection of the spinline. Experiments have been conducted to examine the relative influence of these two mechanisms on the fiber diameter fluctuations. Figure 1 shows the final fiber area variation as a function of the temperature of the air jet disturbance for a PET monofilament. Manipulating the driving force for heat transfer changes the area fluctuation by an order of magnitude. As shown in Figure 2, the area fluctuation decreases dramatically due to a reduction in the heat transfer as the disturbance is moved away from the die, in spite of the greater lateral motion of the spinline. These observations indicate that heat transfer is the dominant mechanism for air disturbances to produce fluctuations in the fiber diameter.

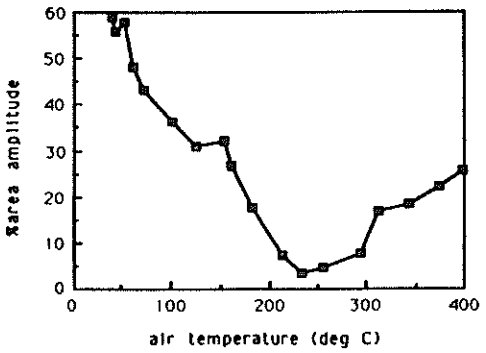


Figure 1

The frequency response of the melt spinning process was measured using a square wave frequency sweep; a typical result using PET is shown in Figure 3. The frequency response contains several peaks. The spinline possesses a natural frequency which is governed by the residence time of the molten polymer. The multiple peak structure is a consequence of the hyperbolic nature of the system; the reflecting boundaries of the spinline create an oscillatory gain in the transform domain. These resonant peaks in the frequency response are the regions of the greatest sensitivity to quench air disturbances, and are predicted by simple spinline models.

This research was supported by the National Science Foundation under grant #MSM-82 16381.

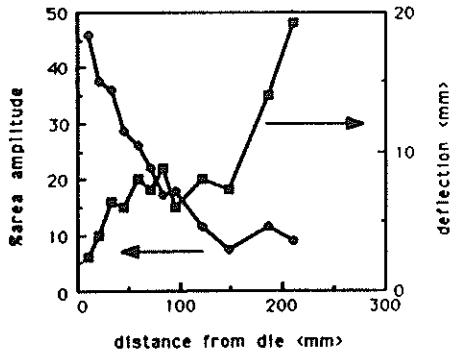


Figure 2

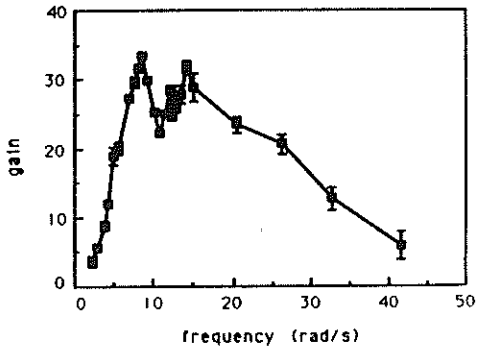


Figure 3

USE OF MELT SPINNING SIMULATION IN PROCESS CONTROL

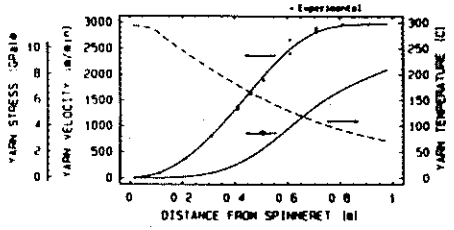
E.JUNG
RHONE-POULENC FIBRES
Centre Technique de Vénissieux
BP 8241
69355 LYON CEDEX 08

The thermomechanical simulation of PET melt spinning process has been largely studied in the last 20 years, specially in improving the validity of the equations. The thermal stationary problem was solved by KASE and MATSUO (1), and one of the first contributions to the viscoelastic problem is due to FISHER and DENN (2).Later came some interesting works on the dynamics of the process, and on the multifilament spinning problem.

As the fundamental equations of melt spinning can be now considered well known, we tried in this work to use them in a comprehensive approach of process control. Some molecular aspects are discussed, and a model of process control is suggested.

Experimental and simulation

We study the melt spinning process of PET yarns at intermediate speeds (POY), where no cristalline structure occurs in the spinline. Velocity profile of the yarn is measured with an LDA velocimeter, temperature profile with an infrared analyser. The stress of the solidified yarn is measured with a quasi-contactless sensor.

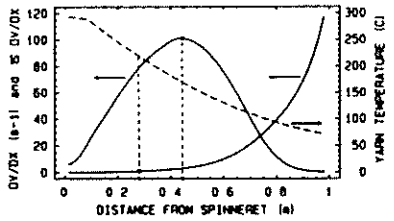


The simulation is developed according to (2) , using a Maxwell type polymer behaviour.An exemple of results is shown in Fig.1. The agreement with experimental results is considered good enough to allow the following theoretical work.

Fig.1 : PET MELT SPINNING PROCESS - 3000 m/min
Experimental (points) and simulation results

Molecular discussion

We know that the rheological behaviour of a molten polymer in an elongational flow can be described by the antagonist effects of flow induced orientation and thermal relaxation of the entangled molecules. If we simplify this concept, it leads to consider not only the stress but also the thermal and deformation parameters calculated from spinning simulation responsible for the orientation and therefore of the mechanical properties of the yarn. Two particular points in the spinline seem to be of major interest.



The first one is when the elongation rate reaches a maximum, the second one, when its product with relaxation time equals 1. The corresponding values of stress, temperature, relaxation time and elongation rate have been selected as main spinline parameters, as shown in Fig.2.

Fig.2 : Major spinline parameters

Polynomial simulation

In order to build a model of melt spinning process control for textile yarns, it is convenient to get a polynomial model of the response of the main spinline parameters, as a function of the process parameters. Since a good representation of experimental results is given by simulation, we defined, by use of the technics of experimental design, an optimal set of numerical trials that permit to calculate a second order polynomial model. It is possible in this way to calculate the quasi-stationary perturbance due to the slow deviation of some process parameters.
It can be shown that major spinline parameters can be divided into three groups that explain 99% of the variability of the model. This is useful for the selection of a reduced number of polynomial models that describe the spinning process.

Process control

To study process control, we use the polynomial model of simulated responses as a model of the real process itself. A non-linear algorithm is used to find the optimal set of process parameters that keep the selected major spinline parameters as close as possible of their initial value. The resulting mechanical properties of the yarn are thus theoretically kept quasi-constant. Since most of online measurements of selected main spineline parameters are generally not available, the experimental work was done by reducing their number. We lose the accuracy of numerical calculation but the improvement of the regularity of the yarn is still attractive.

All this work is made for polymers that do not cristallize in the spinline. It should be of great interest to know how cristallization affects the rheological behaviour of cristallizable polymers, and therefore which major spinline parameters are significant for process control.

(1) KASE and MATSUO, J.Polymer Sci., 3 p.2541 (1965) and 11 p.251 (1967)
(2) FISHER and DENN, AIChe Journal, 23 p.23 (1977)

3/17

Travelling Neck as a Shock Wave, Part II

Dr. Susumu Kase
Kyoto Institute of Technology, Sakyoku Matsugasaki, Kyoto 606 Japan.

The ultimate purpose of this study is to explain the necking , or the travelling neck, known to occur in the melt spinning of PET at take up speeds approximately above 5500 m/min in terms of dynamics and rheology.

As a first step, however, the present work is limited to an attempt to model the necking that occurs in the cold drawing of solid polymer filament rather than the one in PET melt spinning since the former necking is much longer known, more basic, believed by the author to be almost identical to the latter necking and yet still lacks rational explanation of its mechanism of formation. Results of the author's analysis up to the present are as follows:

i) Travelling neck observed in the cold drawing of solid polymer filament was assumed to be a stepwise discontinuity in filament cross-sectional area that moves along the Lagrangian space coordinate λ as the filament is extended and the constitutive model of the solid polymer is assumed to be expressible by a tensile force η versus elongational deformation X curve.

ii) When inertia is neglected the neck so defined was found to occur only when the solid constitutive model $\eta(X)$ curve possesses an exactly horizontal plateau but otherwise monotonically increasing with respect to X. Statistically speaking the probability of the formation of such a plateau is practically zero to suggest very strongly that a specific mechanism must exist behind the plateau formation.

iii) The specific mechanism is found when inertia is taken into consideration. Then a more general constitutive $\eta(X)$ curve having a maxima and a minima as shown in Fig. 1 give rise to a governing equation of the form

$$\frac{\partial^2 \eta(X)}{\partial \lambda^2} = C_1 \frac{\partial^2 X}{\partial \tau^2} \qquad (1)$$

where λ is the Lagrangian space coordinate. Equation (1) is called the nonlinear wave equation and has been in frequent use for about 40 years in the field of dynamic plasticity which deals with the plastic deformation of metals by means of explosive charges. Equation (1) can also be shown to approximately govern the atmospheric shock wave. When the problem is set up as a one-shot transient stretching of solid polymer filament having the constitutive model of Fig. 1 then eq. (1) produces a travelling neck type solution shown in Fig. 2 provided the pulling force is greater than the yield tensile force η_B and the $\eta(X)$ curve is accompanied by the usual hysterisis feature of the type of ABEFHGCD shown in Fig. 1.

iv) Travellinvg speed $V=d\lambda/d\tau$ of the neck solution of eq. (1) shown in Fig. 2 is an increasing function of the pulling force η as shown in Fig. 3 and V becomes equal to zero when the tensile force lowers to the yield value η_B. The zero V is consistent with the extremely slow travelling neck observed in the cold drawing of polymer filament.

v) The neck shown in Fig. 2 can also be shown to obey the Rankine-Hugoniot conditions which a shock wave must satisfy. The neck, therefore, is a shock wave mathematically.

vi) The neck in Fig. 2 is long known to be the simulation of the plastic wave which propagates within an aluminum rod after hit by a rifle bullet on one end as Figure 4 shows. After the impact part A of the rod is unstressed, part B is in elastic compression and part C is in plastic compression. The plastic wave is the border between parts B and C.

vii) Though conclusive proof is not yet found it is suspected very strongly that the neck solution in Fig. 2 is the correct simulation of the travelling neck observed in the cold drawing of solid polymer filaments in view of the similarity of the computed neck to experimental observations.

viii) In the tensile testing of mild steel shown in Fig. 5 yield of the material occurs locally as in Part C in Fig. 5 rather than uniformly over the whole specimen. As further extension proceeds over the yield plateau AB on the load-elongation diagram the yield front E moves downward until the yielded part covers the whole specimen. The author strongly suspects that the front E too is very close in nature to the travelling neck in the polymer filament extension.

ix) Next step in explaining the mechanism of travelling neck formation probably is a two dimensional simulation of neck form assuming the constitutive model of an yielding solid.

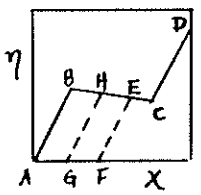


Fig. 1

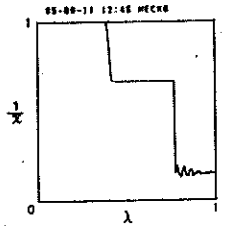


Fig. 2

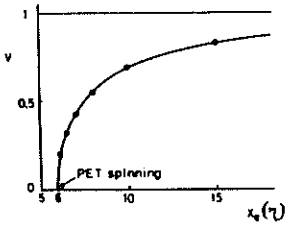


Fig. 3

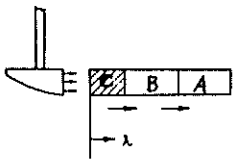


Fig. 4

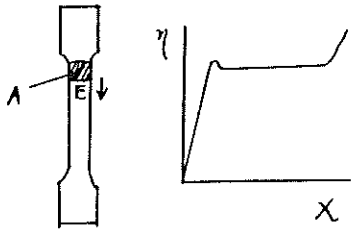


Fig. 5

3/18

Deformation Mechanism of High Speed Spinning of PET

Yuuhei Maeda, Ken-ichiro Oka and Masatoshi Mineo
Fibers and Textiles Research Laboratories Toray Industries Inc.
4845 Mishima-shi, Shizuoka, Japan

Introduction

Development of fiber structure during high speed spinning has become clear, since intensive researches on that process have done for the past several years. For example, the structure and the properties of these yarns are different from conventional two step process yarns. The amorphous orientation of high speed spun yarn is lower, the crystallinity is higher and such characteristic structure contributes to the properties: lower tenacity, greater elongation, higher dyeability, more rapid reduction in alkaline solutions, less shrinkage and higher melting point. On the other hand, a neck-like deformation is recognized in the spin line of high speed spinning with on-line measurement. It is very important to analize the relation between process conditions, deformation and structure formation.

On-line Measurement

Measurement of velocity profiles in the spin line is suitable for considering deformation mechanism. Laser Doppler Velocimeter (LDV) and digital correlater were used on perfect no-touch method. The measured spot, where two He-Ne laser beams intersects, is ϕ 0.3 x 20 mm. All of the velocities of the filaments running at the spot are integrated between experiment duration by the correlater method.

Experiment

Poly (ethylene terephthalate) IV 0.64, TiO_2 0.5% was extruded at the temperature of 300℃, from spinneret of ϕ 0.23mm x 24H, throughput of 1.33g/min hole, and quenched by cross flow air, then taken up at the spinning speed of 4000 - 7000 m/min.

Results

At the spinnng speed of 6000 m/min, the double peak was shown in the velocity distribution curve at the distance of 49.3 - 50.8 cm from spinneret. The double peak means the neck-like deformation (NLD), and the necking ratio is 2.4. The curve, that each peak is sharp, means the length of NLD is very short, less than about 1 mm, that is the NLD is similar to the neck deformation of undrawn yarn.

We show the effect of spinning speed, quenching air velocity and filament denier.

Discussions

We calculated the stress just before and after the location of NLD from the profile, assuming F_{frict}, F_{surf}, F_{grav} = 0. The stress just before the NLD is 0.037, 0.021, 0.014 g/d at the spinning speed of 5000, 6000, 7000 m/min, respectively, and the stress just after the NLD is nearly equal to the inertia stress ρVs^2 , because the air resistance force is small in the range from spinneret to NLD.

Because of the form of NLD and the deformation development at certain stress, NLD on high speed spinning seems to occur the same mechanism as the necking of undrawn yarn. In such case, yield stress is dominated by molecular orientation f, and f shows as follows:

$$\frac{df}{dt} = A \cdot \frac{dV}{dx} - \frac{f}{\tau}$$

The temperature at NLD is presumed to be much higher than Tg, and τ is small. Then the extremely high dV/dx causes the NLD on high speed spinning.

We estimated the temperaure at NLD from the temperature vs extension viscosity equaton. The viscosity is 45000 poise and the estimated temperature was about 210℃ at spinning speed of 6000 m/min. Though 210℃ is only an estimated value and it is necessary to measure the spin line temperature, it is clear that the large crystal size and low amorphous orientaion which are the charactristic structure on high speed spun yarn are formed at such higher temperature circumstances.

EFFECT OF SPINLINE QUENCHING ON STRUCTURE DEVELOPMENT IN HIGH-SPEED MELT SPINNING OF POLY(ETHYLENE TEREPHTHALATE)

T. Kikutani, H. Morinaga, A. Takaku and J. Shimizu
Department of Organic and Polymeric Materials
Tokyo Institute of Technology
Ookayama, Meguro-ku, Tokyo 152, JAPAN

[Introduction]

Poly(ethylene terephthalate) (PET) fibers melt spun at high-speed have a high degree of crystallinity and low degree of amorphous orientation. Consequently, those fibers have the characteristics of lower Young's Modulus and larger elongation than conventional fully oriented fibers. On the other hand, it is widely known that orientation-induced crystallization in high-speed spinning process is accompanied by neck-like deformation. The mechanical and structural characteristics of high-speed spun fibers may closely related to the thinning profile of polymer fluid in the spinline. However, because of the difficulty of on-line measurements, details of the fiber structure formation in melt spinning process is still not completely understood.

In this study, spinline was quenched with a water-bath. A change in diameter profile and suppression of crystallization caused by spinline quenching may give us some information on the nature of neck-like deformation and mechanism of structure development.

[Experiments]

PET fibers were spun at melt temperature of 293 ℃ and mass out flow rate of 5.5 g/min. Take-up velocity was changed from 1 to 6 km/min. A water-bath was mounted in the spinline. The depth of water was 10 cm, and position of the water-surface was varied from 80 to 220 cm down from the spinneret. Spinnability was fairly good at any given spinning conditions.

[Results]

Diameter and birefringence of fibers spun at 3-4 km/min showed considerable irregularity along the fiber axis. The period of irregularity was several hundreds of microns, and the irregularity seemed to become greater when the water-bath was moved closer to the spinneret. However, fibers spun at 6 km/min had uniform thickness regardless of water-bath position.

When take-up velocity was higher than 5 km/min, density of fibers spun with the water-bath was lower than that of standard fibers which were prepared without the water-bath, whereas birefringence of quenched fibers was higher than standard fibers. Highest birefringence of 0.16 was obtained for the fibers spun at take-up velocity of 6 km/min and water-bath position of 170 cm.

All of the WAXS patterns of quenched fibers showed diffused halos, and no crystalline reflections were observed. It should be noted that the neck-like deformation can be observed at ca. 150 cm down from the spinneret if PET is spun at 6 km/min without the water-bath and the standard fibers have highly crystalline structure. However, even if the water-bath was located at 220cm, the WAXS pattern of quenched fibers spun at 6 km/min showed a diffused halo.

These results suggest that the water-bath acts not only as a quenching medium but also as a medium which applies considerable frictional force on the surface of the running filament, and the filament may deform to a certain extent in the water.

Influence of Forming Conditions on Mechanical Properties of Modified PET Fibres

Jiří Militký, Research Institute for Textile Finishing, 544 28 Dvůr Králové nad Labem, Czechoslovakia
Jiří Vaníček, Silon Combine, Planá nad Lužnicí, Czechoslovakia

The mechanical properties will outstanding influence both the processability and the practical applicability of synthetic fibres.

It is well known that ultimate strength of polymeric fibres has a statistical nature and can be characterized by suitable distribution function /1/. The simple structural model of the semicrystalline polymer breaking was published by Peterlin /2/. Basing on this model, the breaking stress σ_B will be dependent on defect area properties only. In our paper /3/ it was proved that it is possible to express the stress at break by a formal relation

$$\sigma_B = f_B \cdot \rho \cdot \lambda (1 - S_R) \cdot \left[T_{d_0} (1 - 2\nu \cdot \varepsilon_B) \right]^{-1} \qquad (1)$$

where f_B is breaking strength, ρ is the specific weight of a fibre, λ is the drawing ratio, S_R is the relative shrinkage, T_{d_0} is the finess of an undrawn fibre /dtex/, ε_B is the strain at break and ν is the Poisson ratio.

From eqn (1) it may be concluded that stress at break σ_B is mostly influenced by the structue of undrawn fibres (by their geometrical properties, preorientation and chemical composition).

On the other hand the shrinkage properties of semicrystalline polymers is highly dependent on forming conditions /4/.

Based on our experiments in a laboratory scale, it will be concluded that :

1. for modified PET fibres (with isophtalic, sulfoisophtalic and adipic acid or polyetylene glycole) prepared under comparable conditions the σ_B is dependent on chemical constitution selectively.
2. for the one starting undrawn PET fibre (combined modification with isophtalic and sulfoisophtalic acid) the thermal and mechanical conditions of fibre forming affects the structural parameters and shrinkage properties but not the stress at break σ_B .
3. under suitable forming conditions (drawing and annealing) it is possible to variate in broad range the shrinkage properties of fibres formed from the same undrawn one.
4. distribution of stress at break is strongly unimodal and can be described by Weibull model.

References :

/1/ Kausch H.H. (1971), The role of network orientation and microstructure in fracture initiation, Polym. Sci Symp. No 3, p 1

/2/ Peterlin A. (1978), Fracture of fibrous polymers, Polym. Engn. Sci 18 p. 1062

/3/ Vaníček J., Militký J., Jansa J. (1980) Ultimate strength of PET Fibres and its relation to thermal and mechanical history, VIII-th Int Congress on Rheology, Plenum Press vol II. p 361

/4/ Militký J. et. all (1984) Modified PET Fibress, SNTL Press Praque p 37, 77

3/21

A MORPHOLOGICAL AND PHYSICO-CHEMICAL STUDY OF OZONIZED POLYPROPYLENE POWDER AND FIBERS .

B. CATOIRE, R. HAGEGE, M. SOTTON
Institut Textile de France
V. VERNEY, A. MICHEL
Centre National de la Recherche Scientifique - LMO

Because of its efficiency and its easyness to carry out ozonization is a usefull way to create peroxides in the bulk of polypropylene material (1,2,3) .

Optimization of grafting reactions closely depends on such parameters as temperature, peroxide thermal decomposition kinetics, nature of generated radicals, monomer diffusion into the bulk of ozonized matrix . In order to follow the thermal decomposition of peroxidic species at different temperatures we used the Spin - Trapping technique because the generated radicals are generally too short-lived species at temperatures of experiences (4,5) .

R°	+	ST	===>	SA°
Radical to be trapped		Spin-Trap		Spin Adduct

The diffusion of monomers into the bulk of the material was followed in ESR with the help of Spin-Probes technique . For this purpose two types of nitroxides molecules with different chemical structures were used (6,7) .

Morphological Probes technique in Transmission Electron Microscopy (TEM) (unsaturated organic molecules such as polyisoprene OsO4-stained) were used to study the modifications of the structure after different conditions of ozonization (8,9) .

The ESR data show that :

- Spin-Trapping technique permits to follow " in-situ " the thermal decomposition of hydroperoxidic and peroxidic structures on ozonized polypropylene . Thermal decomposition isotherms of reactive species at different temperatures (75, 83, 95 and 115 °C) were obtained with ozonized polypropylene including two different spin-traps (N-ter-butyl-α-phenyl-nitrone and N-ter-butyl-4α-pyridil-1 oxide) . Whatever the nitrone molecule used identical phenomena are observed . No significant response in ESR was observed at temperatures lower than 70 °C .

- The Spin-Probe technique results indicate that the diffusion of a monomer into the polymer bulk strongly depends on its chemical structure . A molecule with a lipophilic fraction deeply penetrates into the accessible zones of polypropylene microstructure and is statistically distributed . This situation is suitable for a close contact between the monomer and reactive sites .

ESR and TEM data clearly show that ozone treatment in addition to hydroperoxide and peroxide formation permits a better diffusion of molecules into the polypropylene structure ; such modification would be due to chains breakdown .

A peripheric zone (skin) of different electron density was observed on ozonized samples (treated at 70 °C during 300 min with O3) ; In that skin the degree of oxidation is probably higher than in the bulk of polypropylene granules . The same type of behavior was observed with polypropylene fibers although with more intense skin - core effect . The influence of the solvant on the morphology was also examined .

REFERENCES :

1- A. A. POPOV and al.
J. POL. Sci. Phys. Ed. , 21, 1017, (1983)
2- G. SMETS, G. WEINAND, S. DEGUCHI
J. POL. Sci. Chem. Ed. , 16, 3077, (1978)
3- A. MICHEL, C. MONNET
Eur. Pol. J. , 17,1145, (1981)
4- T. S. DUM and al
J. POL. Sci. Chem. Ed. , 20, 1599, (1982)
5- B. CATOIRE, C. TASSIN, R. OUESLATI, C. PROST, V. VERNEY , A. MICHEL
Pol. Proc. Engng , 4, 271, (1986)
6- R. RANBY, J. F. RABEK
ESR spectroscopy in polymer
Research Polymers / properties and application
Springer Verlag (1977)
7- B. CATOIRE, P. BOURIOT, R. HAGEGE
Bull. Scient. ITF 5, 21, (1977)
8- B. CATOIRE, R. HAGEGE, D. NEIMOUN
Bull. Scient. ITF 23, 521, (1969)
9- R. HAGEGE, P. KASSENBECK, D. NEIMOUN, A. PARISOT
Text. Res. J. , 39, 1015, (1969)

3/22

HOT TUBE SPINNING OF POLYESTER FIBRES

H Brody

ICI Fibres, United Kingdom

As the WUS (wind-up speed) increases, the tensile properties of spun PET (polyethylene terephthalate) correspondingly increase, but for processes running at 4000 mpm it is still necessary to draw the POY (partially oriented yarn) in a later stage in a draw twist operation in order to obtain desirable tensile properties. However, it has been found that if a hot tube is placed in the spinning threadline at a carefully selected position, the spun tensile properties at this WUS are almost as good as drawn POY. The hot tube offers all the obvious advantages of economy provided by a single stage integrated process. But, in addition to high productivity and minimum machine modification, the dye uptake variability of fabric made from the direct spun fibre is an order of magnitude better than from drawn POY.

At high temperatures so-called flow drawing occurs, a reduction of diameter which does not orient molecules and is therefore ineffective in increasing tensile properties. In the spinning threadline at WUS of about 4000 mpm most of the diameter reduction does take place at higher temperatures. The hot tube is placed where the air drag rises steeply and reheats the fibre here, so that the combination of tensile force plus temperature is analogous to the situation in a separate drawing step, and a drawing stage occurs. At higher WUS than 4000 mpm the air drag tension is greater, and this might be expected to give an even higher draw ratio in the tube. However, in practice there is an increase in orientation of the fibre entering the tube, which of course reduces the draw ratio possible, and this increase occurs faster than the increase in tension. The result is that the draw ratio actually falls with WUS until at about 5500 mpm there is a single stage only.

The most valuable bonus of using a hot tube, a central feature of its operation, which leads to a very low position-to-position dye uptake variability, is its ability to self-compensate for process changes in IV, extrusion temperature, quench flow, etc. This is because the air drag force at the entry to the tube does not stay constant if the draw ratio changes. If the draw ratio increases, the velocity entering is lower, with a corresponding lower air drag, and vice versa. This change in air drag then affects the subsequent draw in the tube, operating in such a way as to oppose the original change.

To quantify this more precisely, the amount that a fibre could be drawn under a given stress if it had a given orientation was determined separately in an independent experiment. Fibre having different orientations from being spun at different WUS was drawn between cold rolls over a hot plate. Enough is known about the effect of the various operating variables, such as draw ratio and orientation, on the properties of PET to be able to predict the effect of such changes. These predictions for tenacity and dye uptake will be exemplified, and the results of actual measurements given. An operating curve can be constructed by using the results of drawing the fibres with different orientations, discussed above, the orientation now referring to fibre entering the tube. Such an operating curve can be constructed for any product. The effect of various process variables, such as IV, extrusion temperature and quench flow on the orientation in the spinning threadline, and hence on the operating point, will be shown. In the actual results from practical operation the critical variable of extrusion temperature has been varied over a large range. The variable of IV has also been included and plotted on the same temperature base by correcting the extrusion temperature, using an experimental correlation between a change in IV and the extrusion temperature.

As in all feedback control loops, hunting and resonance are possible, and some degree of dye uptake variability may result. For instance there is a time delay between a change of process condition in the tube and the response by the yarn entering the tube. However, we know how to minimise this condition in terms of the operating variables of distance of hot tube from the spinneret, WUS, hot air tube conditions, etc.

3/23

EFFECT OF THERMAL HISTORY ON ORIENTED FIBERS

J. M. Schultz, University of Delaware, Newark, DE 19711, USA

Reported are the results of investigations on the development of microstructure during the post-spinning isothermal heat-treatment of poly(ethylene terephthalate) (PET) fibers. Two types of measurements are reported: (a) various property measurements made on fibers quenched to room temperature after heat-treatment for specified times and (b) length changes recorded at temperature.

In the case of heated and quenched fibers, the time at temperature was controlled through the speed at which the fiber passes over a heated block with constant contact length. The initial fibers, spun at 3300/min, are oriented but amorphous. Measurements made on quenched fibers include length changes, optical birefringence, small- and wide-angle x-ray scattering (SAXS and WAXS), and density. Figure 1 shows the density and opical birefringence versus heat-treatment time for four different temperatures and a low threadline stress (21.2 kg/cm$_2$). At the earliest stage, the fiber shrinks and becomes less oriented. At a later stage, the fiber elongates and simultaneously orients. WAXS shows that the latter stage is coincident with the development of crystallinity. These results reflect a competition between shrinkage of the noncrystalline phase and crystallization. At higher stress (53 kg/cm^2) and temperature, the shrinkage stage is absent. SAXS and WAXS line-broadening results, combined, indicate that the earliest transformation product is highly defective, fine, fibrillar crystals. This result is in line with the theoretical prediction of Tiller and Schultz [J. Polymer Sci., Polym. Phys. Ed., 22, 143 (1984)] The imperfect fibrils gradually transform to a state in which relatively perfect regions and amorregions alternate along the fiber axis

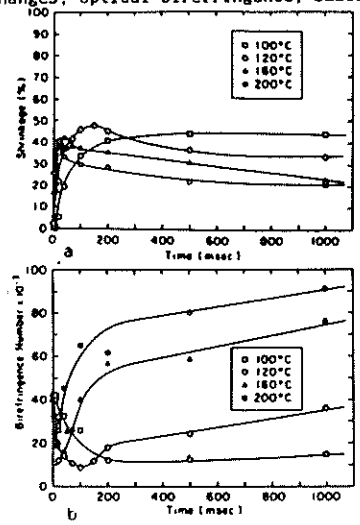
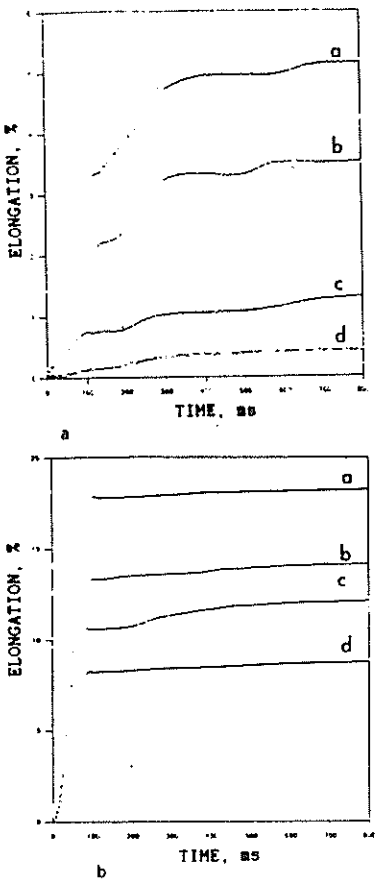


Fig 1. Shrinkage (a) and optical birefringence (b) versus treatment time under 21 kg/cm^2 and the temperatures indicated



In the at-temperature length-change measurements, the fiber was brought to the specified treatment temperature in 10-15 msec. In these measurements, higher stress levels (72 - 170 kg/cm^2) were employed than were possible in the treat-and-quench experiments. In no case was shrinkage observed. Figure 2 shows length-change versus treatment time data at (a) 72 kg/cm^2 and (b) 170 kg/cm^2 stress levels. Four treatment temperatures (A = 230C, B = 200C, C = 170C, D = 140C) were used. Upon reaching temperature, the fiber elongates immediately. At the lower stress level, three stages of transformation are observed; at the higher level, these merge into one. WAXS results suggest that the first stage at the lower stress level coincides with the creation of defective crystals, that the second stage coincides with increased perfection of the crystals and that the third stage may be the crystallization of previously undisturbed material. Experiments with fibers of different lengths shows that the transformation rate is equivalent to the rate of growth of crystals over the heated length of fiber. From this result, a growth velocity of 75 ± 5 cm/s at 200C is found, for the single stage process at high stress or the first stage at the lowest stress

Fig. 2. Fiber length change (%) versus treatment time at two different stress levels: (a) 72 kg/cm^2 and (b) 170 kg/cm^2. Temperatures described in the text

3/24

PROGRESS TOWARDS MAKING ULTRA-HIGH PERFORMANCE FIBERS FROM MESOPHASES IN THE CELLULOSE/AMMONIA/AMMONIUM THIOCYANATE SYSTEM

J. A. Cuculo, M. H. Theil and K. S. Yang
Department of Textile Chemistry, North Carolina State University
Raleigh, North Carolina 27695-8302

The vast majority of materials made from polymers are much less stiff and strong than are traditional materials such as glass, ceramics, and metals. However, if the covalent bonds of polymeric chains were co-aligned within a polymeric material, that material would have exceptional stiffness and strength within the chain direction. The ultimate properties of polymers can be estimated from consideration of bonding forces between appropriate atoms in the molecules. From these studies, it is clear that neither natural nor man made cellulose fibers have achieved properties that approach what is theoretically possible. The primary objective of this research is to produce fibers and films having properties that approach the theoretical limits.

Cellulose, which consists of semirigid polymer chains, can be dissolved in an (ammonia/ammonium thiocyanate) NH_3/NH_4SCN solvent system over a solvent composition range 70-80% (w/w) NH_4SCN (1). There is a cellulose concentration for each solvent composition studied beyond which the solution is no longer isotropic but has begun to form an anisotropic mesophase, i.e., a lyotropic liquid crystalline system. In a solvent containing 70% NH_4SCN, cellulose having a degree of polymerization of 210 forms mesophases at concentrations of 3.5 g/100 mL, which is considerably lower than that found in other solvent systems. The threshold cellulose concentration at which mesophases are observed passes through a maximum at a NH_4SCN content 75.5%. Most compositions of the liquid crystalline solutions of this chiral polymer displayed patterns under the polarizing microscope that are characteristic of a cholesteric system. A cholesteric mesophase has unidirectional orientation within layers, but successive layers are twisted with respect to one another in a helicoidal arrangement. The pitch of the cholesteric helix is observed to grow larger as cellulose concentration is diminished and as the solvent composition is changed up to 75.5% NH_4SCN. At cellulose concentrations of 8-16% (w/v) and in a solvent containing 75.5% NH_4SCN, the cholesteric phase has apparently untwisted and the solution has become nematic or totally unidirectional within a domain. The optical rotatory power of these solutions increases with time, but does so more slowly and to a lesser extent as the solvent composition approaches 75.5% NH_4SCN. The nematic phase appears to form under conditions in which the inter-chain interactions of the chiral cellulose molecules are suppressed as the solvent shields these centers or compensates for their interactions. Because of the uniaxial co-alignment of its constituent molecules, the nematic phase intuitively appears to be the preferred medium from which to extrude high performance fibers.

In order to obtain optimum fiber spinning solutions and film casting solutions, the phase relationships of these systems must be thoroughly understood. Studies are now in progress in which information leading to the construction of phase diagrams is being obtained. Preliminary results, in which the solvent composition has been determined in the separate phases of biphasic solutions, indicate that the solvent composition does not vary appreciably between coexisting phases. Thus, the polymer/solvent system may be regarded as pseudobinary. A pseudobinary phase diagram in which solvent composition is plotted against polymer concentration has been partially delineated, and the composition range for biphasic coexistence is being established for solvent compositions containing less than 75.5% of NH_4SCN.

These liquid crystalline solutions are quite viscous and do not show characteristic maxima in viscosity as a function of polymer concentration such as is found for poly(p-phenylene terephthalamide). This is an impediment in our quest to spin ultra-high performance fibers.

Nevertheless, early fiber and film formation experiments have shown promise. Scanning electron microscopy reveals that fibers spun from the nematic phase appear to have a more fibrillar microstructure than fibers spun from from the cholesteric phase. Microscopy with polarized light reveals that the cellulose molecules in the fibers spun from the nematic solution are the more highly oriented. The nematic phase yielded fibers that were stiffer and stronger than those spun from a cholesteric solution. The moduli of the former fibers approached that of Fortisan(R) which is widely regarded as a stiff, strong regenerated cellulose fiber.

REFERENCE

1. S. M. Hudson and J. A. Cuculo, J. Polymer Sci., Polym. Chem. Ed., 18, 3469 (1980).

3/25

CRIMPING BEHAVIOR: A FUNCTION OF PROCESS CONDITIONS AND FIBER GEOMETRY FOR NYLON 66 FIBERS

Richard W. Miller, Alec Beningfield, John F. Dizor, and John H. Southern, Monsanto Chemical Company, Pensacola, Florida 32575,

Charles L. Beatty, University of Florida, Gainesville, Florida 32611.

Streaks in tufted carpets do occasionally occur within all fiber types: the polyesters, the polypropylenes, and the acrylics, as well as the nylons 6 and 66. They occur in both staple and continuous filament yarns (BCF), and, unquestionably, their occurrence is costly to the carpet manufacturer when, in the extreme case, he has to downgrade his production to seconds. By far the most misunderstood, hence troublesome, streak is that not related to dye-on-fiber variation -- the "optical" streak. Since fiber crimp variation between carpet tuftlines is the most troublesome, non dye-on-fiber streak contributor, understanding crimp has become a focus in our investigations.

My intention here is to, first, review the carpet process, establishing the link between streak level and developed crimp, then, concentrate on the mechanism responsible for light reflectance from a crimped fiber surface and the general evolution of that crimped surface through the carpet process.

Figure 1 shows the relationship between carpet streak level and preheatset crimp level. Clearly, high crimp (more fiber buckling) leads to more severe, light carpet streaks. Figure 2 outlines the crimp development evolution, showing the effect of both tensile and thermal stress.

Crimp development and degree of crimp permanence, as measured by the crimped fiber's resistance to tensile stress, increase with fiber size, drawn fiber orientation level, quality of crimp setting, and lower crimp development temperatures. This work discusses the analytical techniques used to characterize crimp, from the single filament to the intact carpet tuft, and the quality of that technique with regard to carpet property relationships. Further, crimp development is discussed in terms of morphology development.

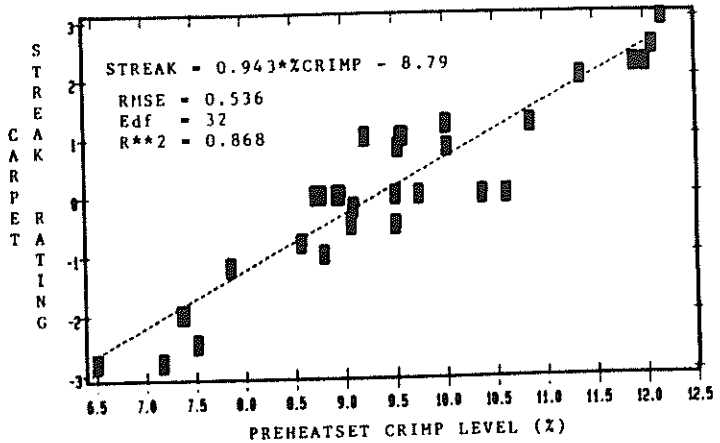


Figure 1: Carpet Streak Intensity is a function of the preheatset fiber crimp level.

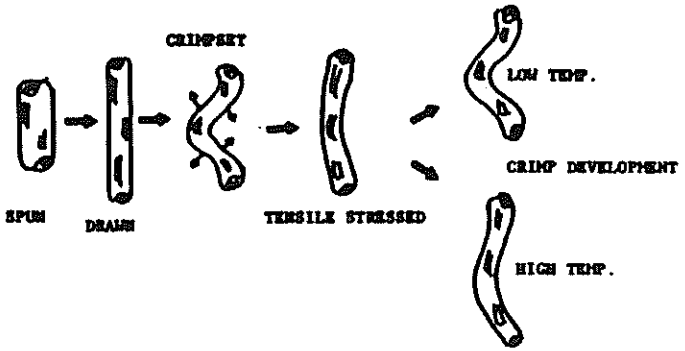


Figure 2: Fiber crimp evolves through the carpet process.

3/26

RELATIONSHIP BETWEEN NYLON 6 FIBER STRUCTURE AND DYE TRANSPORT ANISOTROPY

H.-D. Weigmann, R. A. F. Moore, S. Ruetsch, and D. R. Salem
Textile Research Institute
Princeton, New Jersey 08542

Dye transport behavior in textile fibers is strongly dependent on the properties and structure of the substrate. In particular, the nature and the properties of the noncrystalline domains have to be considered since this is where dye transport occurs. Unfortunately the structural parameters of these domains are difficult to obtain and it becomes necessary to carefully characterize the crystalline structure of the fiber in order to deduce information about the noncrystalline domains. This has been done for a series of high speed spun nylon 6 yarns using x-ray diffraction, density, birefringence, and sonic modulus. It was found that the dimensions of the crystalline unit cell of the α and the γ forms are affected by winding speed resulting in different crystalline densities. These effects have to be taken into consideration in order to get accurate data on volume fraction crystallinity and with it information on volume fraction and orientation of the noncrystalline domains.

The virtually exclusive direction of transport of dyestuffs into fibers is in the radial direction. However, in efforts to understand the effect of fiber structure on dye transport it becomes of interest to explore the relationship of dye diffusion parallel and perpendicular to the filament axis. Methods have been developed to measure dye concentration profiles in the fiber cross section as well as in the longitudinal or axial direction of the fiber. Dye diffusion coefficients have been determined and activation energies of diffusion have been calculated from the temperature dependence of diffusion into the 2 principal directions. Dye diffusion anisotropy, i.e., the ratio of diffusion coefficients in the radial and axial direction, has been determined and the effect of spinning speed on this anisotropy parameter has been determined. Comparisons are made between the effects produced by structural changes due to differences in spinning speed on the one hand, and effects produced by structure development during drawing of nylon 6 monofilaments. Attempts are made to interpret the dye diffusion behavior in terms of dye diffusion mechanisms and structural parameters.

PREDICTION OF PRODUCT PROPERTIES IN EXTRUSION AND INJECTION MOLDING

W. Michaeli (Institut für Kunststoffverarbeitung - IKV - D-5100 Aachen, West Germany)

IKV has been and will be heavily involved in finding correlations between process-influenced material structure (morphology, orientation, crystallinity, internal stresses) and the achievable product properties. If the properties of a polymer material are to be used to the full whilst still assuring a high level of quality, the many correlations between production parameters and component properties require a systematic classification of all processes during production. Once it has been seen now the process affects product quality, it becomes possible to influence and improve quality selectively through distinct process adjustment.

This paper describes for the two main production processes of thermoplastic parts - extrusion and injection molding - the present research work at IKV.

For the field of extrusion the emphasis is on illustrating the influence of melt stressing during processing on product properties including the internal structure of the extrudate.

For impact-modified polystyrene tensile impact tests showed, for example, that thoughness is affected very largely by the duration of thermal and mechanical stressing in the extruder. The morphology of the butadiene phase emerged here as a decisive parameter.

Liquid-crystal polymers and with short-fiber reinforced thermoplastic materials are used whereever advanced mechanical properties and light weight are asked for. With these materials the frozen orientations of injection-molded components lead to distinct non-isotropic material behaviour. Deliberate exploitation of this anisotropic behaviour for weight reduction is only possible if there is a way to calculate these orientations and the resulting component characteristics.

The starting point for such a calculation in injection molding is a simulation of the filling process of the mold cavity. A suitable technique here is the control volume method.

Once flow is known the orientations in the molding can be calculated taking into account a laminar layer structure.

Different principal orientations are obtained for the core and surface zones of the part. An interface to the commercially available finite element calculation programme ABAQUS makes it possible to design the anisotropic component, i.e. to calculate its load carrying capacity.

The paper finalizes with the discussion of calculating volume shrinkage during the pressure holding phase in injection molding.

4/2

A 3-D Finite Element Model of Flows Through Dies

P.A. Tanguy, F. Bertrand and M. Gadbois
CERSIM and Dep. de génie chimique
Université Laval, Québec
Canada

In a continuous effort to improve the finite element methodology for the simulation of polymer melt flows in processing equipment, the present study aims to present the progress made by our group for the solution of three dimensional, non isothermal, flow problems of shear-thinning fluids and Bingham fluids in complex geometry.

Finite element simulations of three-dimensional thermal fluid flow problems are at present performed quite exclusively on large mainframes or supercomputers. Indeed, the current practice (a very bad one!) consists of bringing into three dimensional use the algorithms developed for two dimensional problems (direct solver, skyline storage and bandwidth optimization). This standard approach is inefficient and very costly: the memory requirements are very huge due to the sparsity of the matrix which demands unreasonable CPU time to get the solution.

To specifically address such a problem, we have been developing a new finite element methodology which combines the advantages of augmented Lagangian formulations for the treatment of non linearities, reliable discretizations and iterative solvers. We just recall here that the augmented lagrangian method, already described in [1], consists of introducing in the equations of change a dummy tensor in lieu of the rate-of-strain tensor and then imposing the equality constraint by a Lagrange multiplier technique. This enables to decouple the computation of the velocity and the non-linearities introduced by the rheological model, which makes the algorithm very efficient. The choice of adequate elements for three dimensional fluid flow problems is still an open question. It is well known that to obtain reliable velocity and pressure results, the discretization of these two variables must satisfy the Brezzi-Babuska compatibility condition at the element level. This condition gives rise to a series of so-called enriched elements [2] whose accuracy was tested in [3]. These elements (brick-shaped) are based on the cheapest available brick element, the Q_1-P_0, on which additional degrees of freedom (normal velocity at each mid-face) were added in order to verify the compatibility condition. The pressure is approximated with discontinuous polynomials so as to ensure elementary mass conservation. Although these elements are satisfactory from a theoretical point of view, they are not very convenient to use for practical calculations due the treatment of the normal velocity degree of freedom in the matrix assembling process. Moreover, the accuracy is only o(h) though the interpolation basis contains quadratic terms. In the present work, we have decided to use full quadratic elements in the computation in order to increase the accuracy of the simulation. We selected the three dimensional version of the famous Q_2-P_1 element (quadratic velocity, discontinuous linear pressure) which contains 85 degrees of freedom (81 velocities and 4 pressure terms). In practical calculations, 6 of the 7 d.o.f. associated with the internal node (located at the center of gravity) can be eliminated by static condensation which yields 79 d.o.f. per element. The direct solution of a three dimensional flow problem involving a large number of quadratic elements is nearly out of reach even on supercomputers because of the huge memory requirements and CPU time. It is now accepted that alternate methods such as iterative or spectral methods must be selected. In this study, we make use of an algorithm that was developed in [4] for large constrained systems such as the one arising in fluid flow problems. This algorithm is an extension of the Uzawa algorithm [5] and uses an incomplete Choleski preconditionner. The performance of this algorithm is outstanding. Indeed for a problem having 10^6 equations, the memory requirements and the CPU time are respectively 80 times less and one order of magnitude smaller than with the standard approach. In general, the CPU time needed for the solution of a system of N equations varies as $N^{1.6}$, which compares very favorably to the figures given by direct solvers ($N^{2.33}$).

We used the above methodolgy to model the flow of a polymer melt (the fluid elasticity is neglected) around an obstacle located inside an extrusion die such as the 'spider leg' used in pipe or tube dies. We were interested in studying how the perturbation induced by this insert dampens downflow in the die so as to prevent the appearance of seam lines at the surface of the extrudate. The following results will be presented: streaklines, pressure profile, temperature and stress fields. Conclusions will be drawn on the practical use of advanced finite element techniques in a context of CAD/CAE technology in plastics processing.

[1] P. Tanguy, M. Fortin and L. Choplin, Int. J. Num. Meth. Fluids 4:459 (1984).

[2] M. Fortin, Int. J. Num. Meth. Fluids 1:347 (1981)

[3] M. Robichaud and P. Tanguy, Comm. Appl. Num. Meth. 3:223 (1987)

[4] M. Robichaud, M. Fortin et P.A. Tanguy, 8th Int. Conf. Comp. Meth. in Appl. Sc. and Eng., INRIA (1987), Paris, Vol. I, 273.

[5] M. Fortin and R. Glowinski, Méthodes de lagrangien augmenté, Dunod, 1982.

A COMPARISON OF NUMERICAL SIMULATIONS OF MELTING MECHANISMS IN THE PLASTICATING EXTRUDER

by

Chibao Miaw and David Lange*

General Electric Company
Corporate Research and Development
Polymer Physics and Engineering Branch
Schenectady, New York

ABSTRACT

The numerical simulation of the melting of thermoplastics in single screw extruders is a useful aid in the design and operation of extruder systems. If different materials, operating conditions and screw geometries could be simulated on a computer with reliable accuracy, then the design of extruder screws could be achieved without costly trial and error experimental work.

There are three distinct regions in extrusion to be considered and their results combined to derive the overall picture. The first region is the conveying of particulate solids from the feed hopper to the start of melting. The melting region is the next section and it depends upon the solids conveying section for its initial conditions. In the melting region the melting rate of the solid bed is related to the amount of heat input by conduction and viscous dissipation in the system. The start of the melting section is determined by the point at which a distinguishable melt film is formed. The end of the melting section is determined by the point at which the solid bed shrinks too small to allow the calculations to converge. Results from the melting section simulation are used to determine the starting point and initial conditions of the melt conveying section. In the melt conveying section, melted polymer is pumped through the end of the extruder. The rotation of the screw is used to induce drag flow and pressurization of the polymer through the extruder.

In this study only the melting section was simulated. At present there are two well-known techniques for the theoretical analysis of the melting process. Tadmor developed the first analysis of melting in a single screw extruder based on assumptions leading to a "rigid" solid bed behavior. His analysis assumes that melting only occurs between the solid bed and barrel surface and that the solid bed moves at a constant velocity. The other analysis technique was developed by Fenner. His assumptions allow the solid bed to deform during melting and is considered a "freely-deformable" solid bed analysis. Fenner also accounted for the melt films between the solid bed and screw surfaces observed with most systems. This analysis allows the bed to deform and accelerate (or deaccelerate) under geometric and operating conditions.

The results of experimental work found in the literature were used for comparison between Tadmor and Fenner's melting models. Discrepancies between experimental data and modeling results were discussed. Further work is recommended to reduce the effects of assumptions in the modeling process and to analyze other factors on the melting of the solid bed.

---

* Current Address: Dept. of Chemical Engineering, Georgia Institute of Technology, Atlanta, Georgia

MODELLING OF SINGLE-SCREW EXTRUDERS

C. Guerrero, A. Vincelette and P.J. Carreau,
Ecole Polytechnique, Department of Chemical Engineering,
Montreal, Quebec, H3C 3A7, Canada

A computer program of rapid execution on P.C. is proposed for the modelling of single-screw extruders. It simulates all the phenomena occurring in plasticating extruders with main objectives of optimizing screw designs and operating conditions, as well as to examine the influence of the polymer properties. The model allows for the prediction of the solid bed profile, the pressure and polymer temperature profiles in the screw channel. The rheological behavior of the polymer can be represented by a temperature dependent power-law or Munsted polynomial model.

Five subsections are included in this model which represents modifications and improvements of previous work (Tadmor and Gogos, 1979). In the solid conveying zone, the pressure profile is determined by solving a force balance. A modified Tadmor melting model for the plastication of the polymer solid bed is employed. It includes a simultaneous solution of the momentum and heat transfer equations in the melt film. A power-law fluid, locally isothermal, flow model is used for the prediction of the pressure profile; correction factors for flight walls, channel slope and curvature are included. A finite difference (Crank - Nicholson method) is used to compute the polymer temperature profile. Finally, an isothermal non-Newtonian flow model permits the analysis of the polymer flow through the circular cross-section adapter which connects the die to the extruder barrel.

The computer program offers the option of by-passing the solid conveying zone, and/or the plasticating zone for studying the effects of specific parameters on the pumping of the melt flow. Other options include the calculation of the flow rate to obtain a required pressure at the die inlet and the computation of the solid bed acceleration parameter to verify experimental conditions. This is the only adjustable parameter.

The model has been tested with experimental data for three different extruders and five polymers (two high density polyethylenes, a low density polyethylene, a polystyrene and a polypropylene. The results of the simulations are in good agreement with the experiments. The rheological parameters have been obtained from Instron capillary or cone-plate (Rheometrics) data.

<u>Reference</u>

Tadmor, Z., and Gogos, C.G., "Principles of Polymer Processing", Wiley, 1979.

4/5

RESIDENCE TIME DISTRIBUTION IN COUNTER-ROTATING TWIN SCREW EXTRUDERS (CALCULATIONS AND EXPERIMENT)

H. Potente, P. Michel (University of Paderborn, West Germany)
S. M. Schultheis (Alpine AG, 8900 Augsburg, West Germany)

A description of the longitudinal mixing behaviour in extruders can result from the variance of the residence time distribution behaviour. The residence time behaviour of a fluid in the screw channel is therefore an important criterion for laying out screw machines.

The residence time behaviour of plastics in counter-rotating plastifier twin-screw extruders is determined with the aid of a correlation equation, whereby the residence time behaviour can only be calculated in relation to the mean und the minimal residence time.

The qualitative course of the residence time distribution functions in counter-rotating plastifier twin-screw extruders can be described by a double Weybull distribution (equation 1).

$$F(\theta)=[1-\exp(-C_1(\frac{\theta-\theta_1}{1-\theta_1})^{C_2})][1-\exp(-C_3(\frac{\theta-\theta_1}{1-\theta_1})^{C_4})]$$

θ is the quotient from actual to mean residence time and the minimal dimensionless residence time, θ_1 is the quotient from the shortest to the mean residence time. The mean residence time results from the division of screw channel masses through the mass throughput.

The parameter C_1 - C_4 have to satisfy the following demands:

- calculated and determined residence time distribution functions must correspond well
- the minimal dimensionless residence time θ_1 can only accept values between 0 and 1
- the mean dimensionless residence time has a value of 1
- the borderline cases of the pure blocking currents and of the ideal agitator vessels must be reflected

- the variance of the residence time distribution function given by equation (2)

$$\sigma^2=\int_{\theta_1}^{\infty}(\theta-1)^2 f(\theta)d\theta$$

monotically decreases and has the value 0 for θ_1 = 1,

whereby the parameters C_1 - C_4 are only a function of the minimal dimensionless residence time θ_1.

The newly developed measuring method to determine the residence time behaviour fulfills the following demands:

- On or In-line measuring
- simpler, more cost-effective test set-up
- insensitivity to external influences
- high resolution of the test readings
- high reproducibility, and
- measured data evaluation with a PC.

The process bases on the optical transmission of the melts into a special die. A molecular-soluble pigment is added to the material, which absorbs the incoming light in relation to the concentration during transmission of the melt. The remaining residue light is measured by a photocell. The filtered digitalised values are logged into a PC for further processing. The entered course is shown on the screen. Due to the high scan frequency and resolution, the minimal and the mean residence time can be calculated from the entered values.

4/6

THE EFFECT OF SCREW STAGGER ON MIXING IN A TANGENTIAL, COUNTER-ROTATING TWIN SCREW EXTRUDER

David Bigio

University of Maryland
Department of Mechanical Engineering
College Park, MD 20742

The Counter-Rotating, Tangential Twin Screw Extruder (CRTSE) is a polymer processing device which has been in industrial use for dozens of years. Over this period of time, many of the design parameters have been studied for their effect on processing issues that are related to a particular application. Recent studies [1,2] have shown that the CRTSE is a greater-than-linear mixer and that is due primarily to the flow in the nip region. In this study, the optimization of the design parameters of the nip region are considered against the presented mixing theory [2].

Some of the important design parameters that could be addressed include apex dimensions, channel depth and aspect ratio, screw velocities, and screw stagger. Screw stagger refers to the matching/mismatching of the screw flights. Of these parameters, the screw stagger parameter proved to be an important one to examine. First, there has already been data showing its importance in effecting mixing [3,4]. These studies only tested a few stagger settings and concluded the optimum mixing occurred at a stagger of 50/50, i.e. perfectly mismatched. Secondly, screw stagger can be controlled on current production extruders, regardless of the type of polymer which must be processed. An industrial user needs to know whether a close tolerance of the amount of stagger is required (which is difficult over the length of a machine), or whether there is some stagger range over which the effect on mixing is small. Finally, although screw velocities seem promising on their effect on mixing rates, implementation of design changes require large financial and hardware commitments.

This study seeks to determine the relationship between mixing rates and percent of screw stagger. Using a flow visualization technique [3], experiments were conducted varying the stagger setting every 10%. the fluid mixtures pumped through the extuder were: 1) corn syrup mixed with acetic acid and 2) corn syrup mixed with potassium hydroxide and phenolthalien. The latter mixture had a deep red color which disappeared with mixing. In this experiment the total mixing length was used as the measure of mixing. Data was taken at the time of the experiment and the process was videotaped for later review and data evaluation. The technique provides both qualitative and quantitative information.

The results from the experiments indicate that, as reported before, the optimum mixing occurs at 50/50 stagger and the worst occurs at perfectly matched screws. The difference in the experimental mixing length results was nearly a factor of two. More importantly, it was found that changing the stagger setting from perfectly matched to 80/20 stagger (or 20/80) produced a large improvement in mixing rate. In the region between 80/20 to 20/80 stagger, the change in mixing length was slight, with 50/50 stagger being the shortest length. One implication of this result is that control of the stagger settings over the entire length of the extruder is not a critical factor.

An interpretation of the data suggests that the important factor for causing reorientation in the nip region is the interaction of an essentially 2-dimensional flow in the channel before entering the nip region and the machine direction component in the nip. At perfectly matched (0% stagger) this component is at minimum. Just changing the stagger to 80/20% is sufficient to make the machine direction component large enough to cause the reorientation.

References
---

1) Howland, C. & L. Erwin, SPE Antec, 1983.

2) Bigio, D. & L. Erwin, SPE Antec, 164, 1987.

3) M. Conners, MIT BS Thesis, 1985.

4) Bigio, D. & D. Penn, SPE Antec, 1988.

TEMPERATURE EFFECTS IN SCREW EXTRUSION

Keynote address by Chris Rauwendaal, Raychem Corporation

Two key polymer properties play an important role in the thermal phenomena taking place in the screw extrusion process; these are the thermal conductivity and the melt viscosity. Polymers have low thermal conductivity; as a result, heat transfer by pure conduction is very slow, particularly when the heat transfer distance is large. This is a problem in the extrusion apparatus where the polymer stock temperature has to be raised from the inlet feed temperature to the required process temperature; a typical temperature rise is 200 to 300 degrees C. A similar problem occurs downstream of the extruder where the polymer stock temperature has to be reduced to room temperature. Both the heating and the cooling processes are limited in rate by the low thermal conductivities of polymer melts. Polymers have a high melt viscosity; as a result, significant viscous heat generation takes place in the extrusion process. When excessive viscous heat generation occurs, the polymer may degrade.

The viscous heat generation per unit mass $\hat{E}$ in screw extruders increases with screw speed N. When the polymer melt is less shear thinning (higher value of power law index n), $\hat{E}$ increases more strongly with N. The specific energy required by the polymer is primarily determined by the enthalpy rise $\hat{H}$ in the extrusion process. At low screw speeds $\hat{E} < \hat{H}$ and additional energy has to be added to the polymer, typically by the action of external barrel heaters. As the screw speed increases, $\hat{E}$ increases and external heating can be reduced. When $\hat{E} = \hat{H}$, the autogenous operating point is reached with corresponding screw speed N_a. When the screw speed is increased beyond N_a, the result is $\hat{E} > \hat{H}$. In this case, energy has to be taken away from the polymer by barrel cooling and/or screw cooling. When the cooling capacity is insufficient, the melt temperature can no longer be controlled and melt temperature override, MTO, will occur.

Low melt index, MI, polymers with relatively high power law index values will have a low autogenous screw speed, N_a. In order to allow reasonable extrusion rates, the extruder screw should be designed to give the highest N_a value. This is done by determining the screw geometry that will give the minimum specific energy consumption, SEC. The most important variables can be determined from a simple analysis; they are channel depth, flight clearance, flight width, and helix angle. Optimum values for these variables can be determined from extrusion theory. If the power consumption is Z and the mass flow rate $\dot{M}$, the optimum helix angle ϕ can be found from:

$$\frac{\partial \dot{M}}{\partial \phi}\, Z = \frac{\partial Z}{\partial \phi}\, \dot{M}$$

Similar expressions can be used to determine the optimum channel depth, flight clearance, and flight width. It is found that the optimum clearance for polymers with a high power law index can be considerably larger than the value typically used in the extruder industry, which is δ=0.001D, where δ is the radial flight clearance and D the screw diameter. A similar situation prevails for the optimum helix angle for polymers with a high power law index. The SEC can be reduced by reducing the flight width. The minimum flight width is determined primarily by the mechanical strength of the flight. Experimental results of the effects of certain screw design changes will be presented.

In order to analyze the effect of viscous heat generation on extrusion, drag flow of a temperature dependent power law fluid will be considered. Analytical solutions will be presented for the temperature profiles, velocity profiles and flow rate for different thermal boundary conditions. These solutions can be used in an improved analytical description of the melting process. They can further be used to accurately analyze the effect the viscous heat generation and thermal boundary conditions on the melt conveying process.

In the analysis of the melting process where the melt viscosity has an exponential dependence on temperature, it can be shown that the melting rate reduces with increasing barrel temperature when the Brinkman number is high. At low Brinkman numbers, the melting rate increases with increasing barrel temperature. A practical consequence of this characteristic is that high barrel temperatures in the melting zone are appropriate for good melting when the screw speed is low. However, at high screw speeds, low barrel temperatures may be more appropriate for good melting efficiency. Conventional analytical melting models for temperature independent materials do not allow an analysis of this important effect.

The effect of the temperature dependance of melt viscosity is to reduce the stock temperatures relative to those of a temperature independent fluid. At positive pressure gradients, the temperature sensitivity of the flow rate increases when the pressure gradient increases. However, at positive pressure gradients, the temperature sensitivity reduces when the screw temperature increases relative to the barrel temperature. The temperature sensitivity of the flow rate also increases with reducing power law index, i.e. for more strongly non-Newtonian fluids. With shear thinning fluids, increased plate separation increases the stock temperatures, even though the shear rates in the fluid will be reduced. The increased temperatures are due to longer heat transfer distances; the viscous heat generated is less easily conducted away to the walls.

It can be shown that the pumping rate is increased when the screw temperature is higher than the barrel temperature. In this case, the stability of the pumping process is also improved. This indicates that considerable process improvements can potentially be obtained by using screw heating. As the screw speed is increased, the shear stress first increases, then reaches a maximum, and then reduces. Thus, the specific energy consumption initially increases with screw speed; however, it is possible that the SEC actually reduces at high screw speeds.

TEMPERATURE DEVELOPMENT IN SINGLE SCREW EXTRUDERS

H.Potente, M.Koch (University of Paderborn, West Germany)

A decisive intention of the single screw extruder process is to reach and keep the required melt temperature in front of the screw tip. Highly experience oriented studies and large effort calculations characterize the state of the art.

Here a new method will be presented, which allows to estimate the melt temperature profile along the screw channel including material-, geometry- and process data /1,2/.

Starting with a differential energy balance an analytical solution is obtained giving the principal physical conditions depending on simplifying boundary conditions. Solving the differential equation with the boundary conditions

- isothermal barrel wall with infinite heat transfer
- adiabatic screw
- initial temperature = barrel temperatur

the solution never can represent the real process but gives an idea of the principal thermodynamic state of the system. The main step to adapt the equation to the single screw extruder flow is the invention of a correlation equation allowing to calculate the initial temperature at the place in the screw channel where the melt pool forms, which indicates the beginning of the melting process. Starting the calculation of the melt temperature profile at this point being calculated by the equations given in /3/ the profile leads to the stock temperature in front of the screw tip. Comparing measured and calculated data for an extruder with a forced feeding section good agreement (+/- 8%) is obtained.

The presented equation mainly gives the temperature rise in the screw channel in dependence on the dimensionless Graetz- and Brinkman numbers. These have to be calculated for each section of the screw corresponding to each segment of the barrel with the actual barrel temperature. A schematic procedure is shown in fig. 1 for a three section screw where each section simplifying refers to one significant barrel temperature. Each segment of the three graphs are added to obtain the complete melt temperature profile along the screw channel starting with the mean melt pool temperature und leading to the average stock temperature in front of the screw tip.

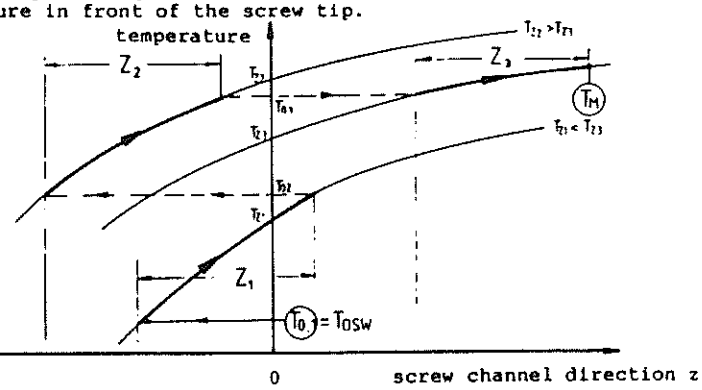


Fig.1 Procedure for the calculation of the melt temperature profile along the screw channel

As the melt temperature rise only depends on the local barrel temperature and the two dimensionless numbers Graetz and Brinkman the application of nomgrams makes sense as a mean of practicable estimation. Using the procedure as described and shown in fig.1 each Produkt βT_z (power law temperature coefficient barrel temperature) requires one nomogram.

Altogether, the presented procedure is a short time estimation method to get knownledge of the melt temperature profile in single screw extruders without high calculation expenditure.

References

/1/ Potente,H. Unpublished Paper
Universität-GH-Paderborn 1986

/2/ Koch,M. Berechnung und Auslegung von Nutbuchsenextrudern
Ph.D.thesis, Universität-GH-Paderborn 1987

/3/ Potente,H. et.al. Verfahrenstechnische Auslegung von Plastifizier- und Schmelzeaggregaten
1.Kunststofftechnisches Seminar, Paderborn'86

4/9

NEW ASPECTS IN THE DESIGN OF EXTRUDERS WITH A FORCED FEEDING SECTION

H.Potente, M.Koch (University of Paderborn, West Germany)

The design of single screw extruders with a forced feeding section, as they are in use for the processing of bulk plastics in europe, mainly aims at the experience oriented realization of the processing advantages known in high throughput rates and a good energetic efficiency. The advantages are faced with the disadvantages of wear problems, high screw torque, poor mixing efficiency without special aids and additional constructive requirements.

New studies of the process behaviour in the grooved feed section and its mathematical formulation /1,2/ base on the examination, which prove high energy consumption at the grooved barrel surface. This high energy consumption had been recognized by shearing of granules and formation of a partly melt film friction. Both effects resulted from high pressure at the end of the grooves and high screw speeds. Recent understanding of the forced feeding section extruder depends on the idea of building up a maximized pressure at the grooves end. This high pressure is unterstood to lead to forced conveyance with negative pressure gradients in channel direction following the feeding section and therefore giving only poor mixing results. The throughput rate is called mainly back-pressure independent in a wide range. This situation is only assured as long as solid state friction is kept up by intensive cooling of the grooves so that the expected throughput rate is guarenteed. These conditions are only assured up to a characteristic screw speed which can be called a limiting screw speed and this is, in most of the industrial application, not satisfying. If process runs with a higher than the limiting screw speed, melt film friction occurs by high energy consumption as a result of high pressure and high circumferential velocity. This way process runs out of energetic control. The specific output rate ($\dot{m}/n_0$) decreases rapidly as exceeding the limiting screw speed.

Aim of a better screw design should therefore be a reduction of the pressure at the grooves end. Furtheron the grooved feed section must be understood as a pressure reducing section, which decreases (vice versa to conveying direction) the pressure at the grooves end caused by the pressure profile along the rest of the screw and the die pressure. The grooved section should be able to do so by less than the grooves length to keep up a back-pressure independent throughput rate.

The reduction of the pressure at the grooves end and by the way a constant specific throughput rate ($\dot{m}/n_0$) can be achieved by an optimization of the pressure profile in the melting, melt conveying and mixing section. This optimization can be realized by changing the helix angle or the channel depth. Theoretical and experimental studies /1,2/ proved, that an increase of the helix angle in the melt conveying sections could lead to a reduction of factor 2-3 concerning the pressure at the grooves end. With this aid a neutral pressure profile or even a pressure build up along the screw can be achieved in a forced feeding section extruder.

In total, screw speed independent specific throughput rates ($\dot{m}/n_0$), less screw torque and a mentionable reduction of wear in the feeding section are realizable. Better mixing effects are the consequence of a drop in dimensional throughput (total flow rate/ drag flow rate) keeping the specific throughput rate constant. As a helpful device special melting aids must be pointed out to plasticize the conveyed solid bed. This leads to improvements using barrier sections or other melting active shear elements.

Altogether, these facts point out a possible optimization of the screw design for grooved barrel extruders avoiding the known disadvantages and giving place to a further revaluation in regard to economic processing.

References

/1/ Potente,H. Der Nutbuchsenextruder muß umgedacht werden appears in Kunststoffe/ German Plastics '88

/2/ Koch,M. Berechnung und Auslegung von Nutbuchsenextrudern Ph.D.thesis Universität-GH- Paderborn 1987

4/10

Extrusion of Thermally Sensitive Thermoplastic Resins

Kun S. Hyun, Steven R. Jenkins, Robert J. Streu
Barrier Resins & Fabrication Laboratory
Dow Chemical U.S.A.
Midland, Michigan 48674

Abstract

One of the thermally sensitive thermoplastic resins in commercial use today is Saran* PVDC copolymer which is used as a premier barrier material in the food packaging area. Monolayer barrier film has been produced for over 30 years. Recently, the use of PVDC copolymer as a barrier layer in multilayer food containers, became reality. Therefore, better understanding of the extrusion behavior of PVDC copolymers in coextrusion systems is very important.

Long-term continuous extrusion of PVDC copolymers without carbon specks or contamination in the extrudate is desired, in addition to meeting rate requirements of the sheet or film production.

In this paper, we will discuss the constraints imposed on the extrusion of PVDC copolymer in multilayer coextrusion. The effects of process variables, materials of construction, screw temperature control and screw design on the processability of PVDC are to be discussed.

Experiments were carried out with two highly instrumented extruders, one 2-1/2 inch (21 L/D) and another 3-1/2 inch (24 L/D) extruder. Several screws of different types, barrier screws as well as conventional screws, were evaluated. An encapsulation die was used to prevent direct contact of PVDC melt to the die wall to avoid carbon formation in the die. In this way, any carbon in the extrudate can be attributed to the screw.

The objective was to study several key parameters to achieve extrusion without carbon showers and air voids for at least 48 hours. The parameters are: (1) compression rate or taper, (2) compression ratio, (3) straight vs. tapered feed section, (4) feed section barrel temperature, (5) screw temperature, (6) pressure profiles along the barrel, and (7) length of the metering section.

Extrusion rate can be predicted simply by using the generalized Newtonian formula (1), because PVDC copolymer melt has high viscosity making the pressure flow term relatively small compared to the drag flow term.

Experimental observations will be discussed in light of thermal and physical properties of PVDC copolymers, such as heat capacity, crystallinity, annealing, bulk density, melting points, melt viscosity, melt adhesion, and friction characteristics.

We have found the compression rate is a better index to represent the degree of deformation taking place within the solid bed of PVDC copolymer than the compression ratio. One can achieve various compression rates with the same compression ratio depending on the screw design. In terms of carbon build-up on the screw, the lower the compression rate, the less carbon on the screw. However, too low compression rate could cause air bubbles or voids in the extrudate, due to slower melting rate. Therefore, it requires balancing the solid conveying rate and the pressure build-up in the transition which affects the melting rate.

Carbon was detected at the beginning of melting, at the interfacial line between the solids bed and melt pool over two or three flights before the line disappeared. This might have been related to the screw temperature at the beginning of melting being at the very temperature at which PVDC copolymer becomes sticky. A proper formulation can reduce the melt adhesion, thus eliminating carbon in a conventional screw. For a barrier screw, a perfect match of solid channel and melt channel would eliminate any carbon formation in the solid channel especially at the beginning of melting. The melt 'spill-over' in the solid channel after screw temperature reached the 'normal' melt temperature did not cause the carbon.

One of the major concerns in the extrusion of PVDC copolymer as a barrier layer in the coextrusion system is whether the PVDC layer will survive the thermal history with the skin layer. The melt temperature of the PVDC layer has to be kept to a minimum as much as possible, and this requirement limits the rate ranges a screw can provide.

*Trademark of The Dow Chemical Company

Reference

1. K. S Hyun, W. A. Trumbull, S. R. Jenkins, and C. I. Chung, "Extrusion of Saran* Resins," 43rd Annual Tech. Conf. Proceedings, Society of Plastics Engineers, April 29 - May 2, 1985, pp 38-41.

4/11

A Study on Flow Fracture Behavior of Melts at Die Inlet

Yasushi Oyanagi, Kazuhisa Kubota
and
Kazuya Ohji
Kogakuin University, 1-24-2 Nishishinjuku,Shinjuku-ku
Tokyo 160
Japan

Abstract

When polymer melts are extruded from a die or a slite at some point above limiting shear stress,the extrudates generally show spiralling,pulsating and intermittent phenomena[1]. These phenomena are called "Unstable Flow" or "Melt Fracture "[1-3],and some of the pertinent problems associated with rheological properties and thus the fabrication process,such as high speed extrusion,injection and blow molding of their materials, especially the jetting phenomena in the injection process is affected strongly by the fracture flow behavior.

Some efforts have already been made to resolve these problems by many researcher throughout world,and several suggestions as to the causes of these phenomena have been proposed. There are,however, still remain some elusive points concerning its mechnism for initiations[4-8].

One of the researchers of this study presented some experimental results and a hypothesis on mechanism for initiation of high density polyethylene[9].

This study represented continuously on the flow fracture behaviors of several polymer melts at or near die inlet by using a new experimental methods, frquency analyzer. The apparatus consists of INSTRON CAPILLARY RHEOMETER with extended transparent glass reservoir ,polarized light unit and VTR system involved frequency analyzer.

The tested materials are polycarbonate(PC),polystyrene(PS) and high density polyethylene(HDPE),respectively,as shown in Table 1.

Table 1. The tested Materials and Test Conditions

Material	Grade No.	Test Conditions	
		Temperature	Shear stress
Polycarbonate	Teijin Panlite,	250, 270 °C	0.5-20 Kgf/cm^2
Polystyrene	Asahi Chem. Styron 666	170, 190 °C	0.25-26.67 Kg/cm^2
High density polyethylene	Mitsui Chem. Hizex 7000	170, 190 °C	0.42-12.17Kg/cm^2

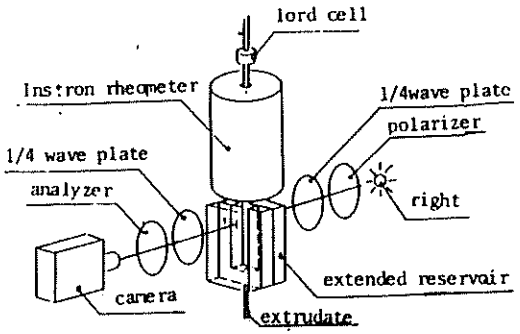


Fig.1 Schematic view of apparatus

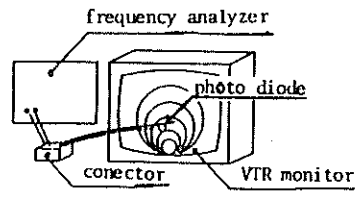


Fig.2 Frequency analysis method



Fig. 3 A polarized fringe pattern of stable flow for PS at 170°C, $\dot{\gamma}$=72s^{-1}, L/D=2.0

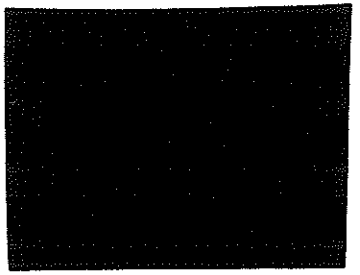


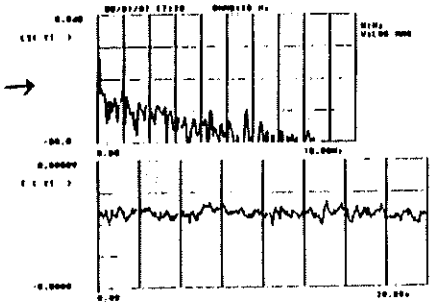
Fig.4 A polarized fringe pattern of unstable flow for PS at 170°C, $\dot{\gamma}$=720s^{-1}, L/D=2.0

Fig.5 A resuls of frequency analysis at the critical point under instable flow region for PS

170°C , $\dot{\gamma}$=720 s^{-1}, L/D=2.0

upper:frequency distribution

lower:time dependency



References
[1] J.P.Tordella,J.Appl. Phys.,27,454(1956)
[2] Y.Tomita, Trans. Jap. Soc. Mech. Eng.,32,242(1966)
[3] Y.Mori and J.Ue,Kobunshi Kagaku,21,231,385(1964)
[4] F.E.Westover and B.Maxwell,S. P. E. J., 13,27(1957)
[5] T.F.Ballenger and J.L.White,J. Appl. Polym. Sci.,15,1949(1971)
[6] J.P.Tordella,Trans. Soc. Rhel., 202(1957)
[7] R.S.Lenk, Plastics Rheology,Wiley,New York,1968)
[8] J.A.Brydson, Flow Properties of Polymer Melts,Iliffe,London,1970,ch.5
[9] Y.Oyanagi,Appl. Polym. Symp ., 20,123-136(1973)

DEGASSING OF PLASTICS UNDER ECONOMIC ASPECTS: SINGLE-SCREW OR CO-ROTATING TWIN-SCREW EXTRUDERS?

Dr. Haus Wobbe
Hermann Berrtorff Machihenbau GmbH
Hanover, West Germany

Due to considerations concerning environmental standards and increased economic efficiency, an effective degassing nowadays represents a fundamental prerequisite for the degassing process. The criteria of an effective degassing are elaborated in order to compare on this basis single-screw and twin-screw extruders by means of the screw geometry. This comparison shows clearly that - as far as the degassing capacity is concerned - single-screw extruders can undoubtedly compete with twin-screw extruders.

The paper ends with examples taken from the practice.

Extrusion of Polyethylenes with a Chilled Die

Alfred Rudin, David Cook and Ronald Cooke
Guelph-Waterloo Centre for Graduate Work in Chemistry
Department of Chemistry
University of Waterloo
Waterloo, Ontario, Canada N2L 3G1

At low flow rates polymer melts produce regularly-shaped extrudates with smooth surfaces. The extrudate often develops an unacceptable irregular shape or surface at higher rates, however. The severity and sometimes the type of extrusion defect increases with higher extrusion rates. The processing of LLDPE's and HDPE's is limited by the onset of surface defects, the most common of which is "sharkskin" surface in tubular film extrusion.

Various expedients may be used to extend the extrusion range of these polymers. These include operation with higher melt or die lip temperatures, use of wider die gaps and the employment of fluorocarbon elastomer processing aids.

In general, one observes an increase in the severity of processing defects and an increase in extrudate swell with lower melt or die temperatures. This report explores the observation that the processing range of LLDPE's and HDPE's can be extended to higher rates by operating at normal or warm melt temperatures with a cold die. The die temperature is preferably below 150°C for current film grade LLDPE's and HDPE's.

Examples will be given of the effects of die temperature on the flow regimes that are seen in the extrusion of these polyolefins.

TABLE 1

Extrusion of LLDPE A at 24 rpm and 160°C

Melt Temperature: Effects of Die Temperature

Die Temperature (°C)	Pressure (psi)	Extrudate Appearance
154	1850	Gross distortion
152	1900	Cyclic melt fracture
150	1900	Cyclic melt fracture
148	1900	Cyclic melt fracture
146	1905	Sharkskin or matte
144	1905	Smooth
142	1905	Smooth
140	1905	Smooth
138	1950	Smooth
136	2060	Smooth, increasing dieswell

TABLE 2

Extrusion of LLDPE A at 24 rpm and Various Melt

Temperatures: Effects of Die Wall Temperature

(a) Melt Temperature 185°C

Die Temperature (°C)	Pressure (psi)	Extrudate
174	1540	Gross distortion
158	1645	Gross distortion
156	1750	Gross distortion
154	1850	Matte
150	1850	Matte
148	1850	Smooth
146	1850	Smooth

(b) Melt Temperature 205°C

Die Temperature (°C)	Pressure (psi)	Extrudate
197	975	Gross distortion
193	1340	Gross distortion
190	1390	Gross distortion
184	1440	Gross distortion
170	1540	Gross distortion
164	1700	Sharkskin
154	1700	Sharkskin
146	1700	Smooth

ABSTRACT

Void Formation in Extrusion:
Causes of Problem and its Elimination

by:

Imrich Klein
Scientific Process & Research, Inc.

The formation of bubbles or voids in extruded products plagues extrusion processing operations. The problem can manifest itself in almost every extruded product but is particularly troublesome in the extrusion of low viscosity melts such as polypropylene, nylon, polyesters, and in the extrusion of PVC dry blends.

The cause of this problem was found to be associated with solids conveying, a generally neglected functional zone of the extruder. It was found that in all cases tested, the presence of voids in the extrudate was caused by poor solids conveying and all traces of voids could be eliminated by finding operating conditions in the solids conveying zone of the extruder that prevent a drop in pressure along the solids conveying zone and insure a pressure rise along the zone. An additional solution to this problem is by selecting screws particularly designed to optimize solids conveying and thereby achieve higher levels of solids compaction.

Solids conveying occurs in the vicinity of the hopper and is restricted to the extremely short distance of unheated and often intensively cooled barrel immediately following the hopper. The conveying of solids can be enhanced by increasing the coefficient of friction between the resin pellets and the barrel surface and by lowering its value on the screw surface. A friction tester capable of measuring the coefficient of friction on these metal surfaces at very low pressures, at various surface temperatures and surface velocities is necessary for finding the proper operating conditions in the extruder and the optimum screw design.

Finding optimum operating conditions for the solids conveying zone not only eliminates voids but was found to increase the production rate of the extruder by 30%. Screws designed for optimal solids conveying were found to increase production rate, often by over 50%, as well. Optimum solids conveying zone geometry represents a particular channel depth and screw lead. Designing a screw with an optimum solids conveying zone includes the evaluation of flights having variable lead since optimum screw lead for solids conveying is often different from the screw lead needed for melt pumping. A smooth transition between the two screw leads necessitates a variable lead screw.

The paper will explore the mathematical relationship between resin properties, screw geometry and operating conditions and the effect of these variables on void formation in the extruded product. Criteria for the elimination of the void formation problem will also be presented.

DIES FOR PIPE EXTRUSION WHICH COMPENSATE FOR GRAVITY FLOW

A.J. Giacomin, T. Habinak
Mechanical Engineering Department
Texas A&M University, College Station, TX 77843

and

S.R. Doshi
Department of Chemical Engineering
McGill University, Montreal, Canada*

Plastic pipe is conventionally extruded from an annular die with a circular mandrel of adjustable eccentricity. A recent numerical scheme permits the effect of gravity flow on pipe wall thickness distribution to be computed.[1] Hence, wall thickness distribution can be optimized with mandrel eccentricity when process rates, temperatures and melt viscosity data are known.[1] Furthermore, using this scheme the mandrel shape required to compensate for gravity flow can be computed.

Sophisticated schemes accounting for melt viscoelasticity have been developed to predict extrudate shape[2,3,4] and heat transfer[3,4] in the post-die region. Since these models assume axial symmetry, they do not account for the effect of self-weight flow on wall thickness distribution. This axial asymmetry has been numerically modelled using a cascade of interconnected inclined plates.[1]

The maximum hoop stress in a pressurized pipe with a nonuniform wall occurs where the wall is thinnest. Thus, pipe material used to exceed the minimum thickness, t_*, is wasted. For instance, for a circular pipe with an eccentric circular bore, the fraction of waste material is:

$$W = \frac{(2 + e/r_*)\, e/r_*}{1 - (r_i/r_*)^2}$$

where r_i is the bore radius, r_* is the outer radius and e is the bore eccentricity. Hence, even for thick walled pipe, where r_i/r_* is as low as .80, a 3% value of e/r_* causes 16% waste.

For a noncircular bore the average wall thickness, t_*, can be computed from the wall thickness distribution:

$$t_* = \frac{1}{2\pi}\int t(\theta)\, d\theta.$$

The cross-sectional area of a nearly tubular extrudate is approximately $\pi t_*(2r_*-t_*)$ and its required area is simply $\pi t_*(2r_*-t_*)$. Thus,

$$W \approx \frac{t_*(2r_*-t_*)}{t_*(2r_*-t_*)} - 1$$

For Figures 1-2, the initial diameter of the extrudate bore is .4 m, the cooling time is 400 s and the temperature of the pipe inner surface was 200°C. Property values for high density polyethylene were used[1] with a time step of $t_*/100$ and an angular step size of $\pi/50$.

Figure 1 shows the effect of eccentricity for a circular mandrel on fractional waste. A sharp optimum mandrel eccentricity of 1.75 cm is predicted. By running the model in the negative time direction, one can design the mandrel shape required for a perfect tube. Figure 2 compares the desired mandrel shape (M) with the perfect tube (T).

1. Giacomin, A.J. and S.R. Doshi, S.P.E. Tech. Papers, XXXIV, Proc. 46th Annual Tech. Conf. & Exhib., Atlanta (April, 1988).
2. Ryan, M.E. and A. Dutta, Proc. 2nd World Congr. Chem. Eng., Montreal, VI, 277 (1981).
3. Crochet, M.J. and R. Keunings, Proc. 2nd World Congr. Chem. Eng., VI, 285 (1981).
4. Crochet, M.J. and R. Keunings, J. Non-Newt. Fluid Mech., 7, 199-212 (1980).
5. Spivey, J.J. and N. Barona, A.S.M.E. Paper #80-HT-104 (A) D115 (1980).
6. Kamp, W. and H.-D. Kurz, German Plastics, translated from Kunststoffe, 70(5), 257-263 (1980).

FIGURE 1: OPTIMIZING ECCENTRICITY

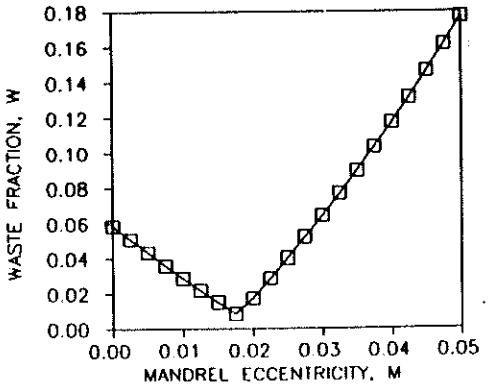
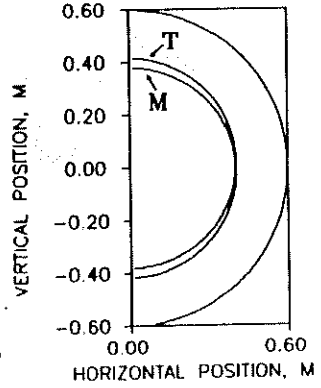


FIGURE 2: DESIRED MANDREL SHAPE



*Current address: DuPont Canada, Inc., Kingston, Canada.

IMPROVEMENT IN CONTROL METHODS FOR GAS PIPE EXTRUSION

D. SAINT-ROYRE

GAZ DE FRANCE - RESEARCH AND DEVELOPMENT DIVISION
APPLIED SCIENCE AND TECHNOLOGY RESEARCH CENTER
361 avenue du Président Wilson - B.P. 33
93211 LA PLAINE-SAINT-DENIS CEDEX - FRANCE

More than 90 % of the pipes laid for gas distribution in FRANCE are now made of polyethylene and they currently constitute 20 % of the network. Their operating pressure is generally 4 bar.

In the field of pipe fabrication, original studies are being conducted to devise methods for ensuring pipe quality based on the control of extrusion conditions.

For a given extrusion sequence, using a raw material with a set commercial reference, the final properties of the pipes produced are influenced by various physical extrusion parameters such as flow rate, temperature of the material at different points in the sequence, pressure, distribution of unmelted material along the screw etc. These physical parameters are liable to fluctuate around their ordinary values with different adjustments of the machine (speed of rotation of the screw, regulation temperature, etc) and with small variations in the properties of the different batches of raw material.

It is very useful to understand the physical parameters of extrusion if we wish to study and hence predict the influence of fabrication conditions on pipe quality.

The methods envisaged for ensuring pipe quality involve monitoring physical parameters of pipe extrusion by equipping the production line with measuring instruments, and controlling the properties of raw materials.

To implement such methods, it is necessary to know :

1) the relations between the properties of the raw material and both the sequence adjustments and the physical extrusion parameters (flow rate, temperatures, pressures...),

2) the relations between the physical extrusion parameters and the quality of the pipes produced.

This paper presents the work carried out on the first point. The objective was to select a limited number of fabrication conditions, corresponding to physical extrusion parameters which are significantly different, in order to facilitate an effective study of the second point.

The study concerned an industrial pipe production line equipped with instruments to monitor and analyse production conditions. The measurement and associated computing systems are presented.

The physical parameters recorded for several production shifts are compared.

INFLUENCE OF FILLERS AND FLOW ADDITIVES ON FLOW DISCONTINUITIES IN LINEAR LOW DENSITY POLYETHYLENE PROCESSING

B. V. Johnson and T. J. Blong, 3M Corporation, St. Paul, MN
H. P. Schreiber, Ecole Polytechnique, Montreal, Canada

The effectiveness of fluorocarbon elastomer polymer process aids (PPA's) in rutile-filled polyethylene resins was considered within the context of the surface coating of the filler. Five common commercial samples of titanium dioxide were prepared in 30% masterbatches and let down by melt blending with a 2% masterbatch of PPA in linear low density polyethylene. Final concentrations were 10% TiO2 and 500 ppm PPA. Apparent viscosity and the shear rate for the onset of flow discontinuity were evaluated by capillary rheometry and found to differ significantly for the five samples (Table I). The compounding sequence was then altered by melt blending a combined masterbatch of 58/40/2 LLDPE/TiO2/PPA and subsequently diluting this blend to the same level of 10% TiO2 and 500 ppm PPA. As a result of this mixing procedure, differences between the five samples increased considerably (Table I).

The two rutile samples producing the largest difference in PPA effectiveness were selected for further comparison, at the same relative concentrations, under blown film extrusion conditions. In the presence of sample C the process aid was unable to eliminate film surface defects after two hours of extrusion at an apparent shear rate of 300 s-1. In contrast, the combination of sample A with the PPA was effective in removing surface defects within 40 minutes.

Rheological results and the influence of compounding sequence may also be considered in light of rutile dispersibility and acid-base characteristics. The influence of surface coating on these parameters has been demonstrated previously. Estimates of pigment agglomerate cohesive strength, obtained by measurement of inherent agglomeration indexes (C) suggest pigment sample C to be the least dispersible (Table II). The acid-base character of the rutiles, measured by inverse gas chromatography, rates sample B to be moderately basic while C and D are essentially neutral (Table II). These results allow qualitative rationalization to be made of the observed rheological effects but the precise mechanism by which rutile dispersibility and acid-base character influences the effectiveness of fluorocarbon elastomer process aids remains a matter for further study.

TABLE I
CAPILLARY RHEOMETRY RESULTS FOR TiO2/PPA COMBINATIONS

SEPARATE MASTERBATCHES

TiO2	Apparent Viscosity at 600 s-1 (Poise)	Shear Rate for Onset of Melt Fracture (s-1)
A	3950	1600
B	4600	1000
C	4250	600
D	4050	1400
E	4600	1400
None	3400	1400

COMBINED MASTERBATCH

TiO2	Apparent Viscosity at 400 s-1 (Poise)	Shear Rate for Onset of Melt Fracture (s-1)
A	6300	1600 (ripple)
B	8050	200 (sharkskin) 600 (cyclic)
C	9000	200 (sharkskin) 600 (cyclic)
D	7450	400 (sharkskin) 800 (cyclic)
E	7240	900 (cyclic)

TABLE II
INHERENT AGGLOMERATION INDEXES (C) AND ACID BASE INTERACTION POTENTIALS (Ω) OF TITANIUM DIOXIDE SAMPLES

TiO2	Ω @ 30°C	(C)
A	0.67	110
B	1.26	160
C	0.18	440
D	-0.06	240
E	0.90	210

COEXTRUSION TECHNOLOGY DEVELOPED IN GREECE. BARRIER CONTAINERS FOR AGROCHEMICALS

Alexis Stassinopoulos
Argo S.A. 194 00 Koropi, Greece

Early developments of coex technology were related to multilayer film and sheet production. Patents on multilayer hollow bodies production started appearing in 1980 [1] although there was some work reported in this area early in 1977 [2]. R & D on multilayer containers was, and is, performed by equipment manufacturers, raw material manufacturers and, in some cases, manufacturers of plastic containers [3].

Our R & D effort in this area was initiated in 1979 as a customer problem solving project. The problem was how to substitute glass and aluminum containers with plastic containers resistent , compatible and impermeable to agrochemical formulations in organic solvents. Glass bottles were not safe for transportation of dangerous and toxic materials. Aluminum containers were in limited availability and non compatible with certain formulations. Bottles from commodity plastics were either permeable (HDPE, PP) or not resistent (PVC).

We have tried three approaches to the problem :

(a) HPDE internally coated with PVDC.
(b) Monolayer bottles made of resistent and impermeable polymers.
(c) Multilayer coex constructions.

A theoretical performance to cost analysis indicated that the third approach was the most promising. Laboratory trials and theoretical calculationsled to a three layer construction, PA/ bonding layer/HDPE, or, a HDPE/PVAL/HDPE combination.

As no commercial coex blow molding equipment was available at the time we were forced to develop our own. We designed a three layer extrusion head which, together with extra extruders, feeding lines and control equipment was retrofitted on standard monolayer twin station machines.

In this presentantion we describe the methodology we followed for the evaluation of various types of containers and barrier materials, and the disigning of production equipment and testing methods.

Our three layer bottles were introduced early in 1981 under the trade name Argo - Coex. However, the addition of a succesfull product to our production line was not the only result of this development project. It was equally important that we acquired expertise in the following areas :

a. Development of three, and lately, five layer extrusion heads.
b. Development of a set of in-house laboratory methods for testing of bottle properties and product-container compatibility.
c. Know how in improving rheological and permeation properties of barrier and bonding materials.

Our current project in the line of packaging of agrochemicals concerns the development of a two piece monolayer container. The two parts of this novel container are produced by injection molding of a polyester barrier material and, then, sealed together. The main advantage of this container will be the low transportation cost. The two pieces can be transported separately and joined together at the point of use. In this way the transportation volume is reduced by 80%. The joining of the two parts will be performed by a special low cost HF sealing equipment which we are in the process of developing.

References :

(1) Martin Fleit, Patent status of Barrier Materials for Food Packaging. Foodplas Conference 85/86.
(2) VDI - Gesellschaft Kunststofftechnik. Technologien des Blasformens, VDI - Verlag 1977, pp 111 - 130.
(3) Most of the interesting developments in coextrusion have been reported in Schotland Conferences, COEX 82-87.

CHARACTERIZATION OF THE SHARKSKIN DEFECT AND ITS DEVELOPMENT WITH THE FLOW CONDITIONS

P. BEAUFILS, B. VERGNES, J.F. AGASSANT
(CEMEF - Ecole des Mines de Paris
Sophia-Antipolis - 06560 VALBONNE - FRANCE)

The sharkskin defect encountered in LLDPE extrusion was studied using two complementary experimental methods :

- roughness measurements on extruded samples permits to precisely characterize the defect : amplitude, possible periodicity, three-dimensional picture...
- flow birefringence experiments through a flat die with transparent glass walls permits to define the development of the stresses and the molecular orientation.

The influences of experimental conditions (flow rate, temperature) and die geometry (land length, entry angle) were studied.

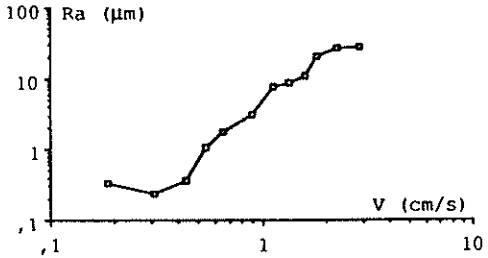


Figure 1: Average roughness Ra as function of average extrusion velocity V.

It was shown that the amplitude of the surface irregularities increases continuously with the flow rate, from less than 0.1 µm to about 50 µm (see figure 1).
This behaviour is strongly dependent on the temperature and quasi-independent on the die geometry.

The birefringence on the flow axis reaches a maximum at the die entry, decreases as the polymer relaxes along the land and increases again just before the exit (see figure 2).
The maximum birefringence increases with the flow rate in the same way as the amplitude of the defect. It seems possible to establish relationship between the defect observed at the die exit and flow parameters as local birefringence.

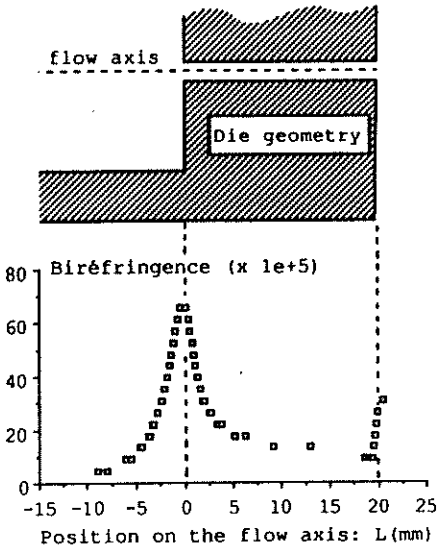


Figure 2: Evolution of birefringence on the flow axis

STRUCTURE FORMATION IN THE CURE OF UNSATURATED POLYESTER RESINS

Y. S. Yang and L. James Lee (Department of Chemical Engineering, The Ohio State University,) Columbus, Ohio USA)

The most widely used thermoset resins are polyesters. Thermoset polyesters, while relatively inexpensive, offer such advantages as light weight, high strength, and excellent mechanical properties. With the aid of fillers, reinforcements and additives, they are usually available in the form of compounds for compression molding (e.g., sheet molding compound, SMC), injection (e.g., bulk molding compound, BMC), resin transfer molding and pultrusion.

The reaction of unsaturated polyester resin is a free radical chain growth copolymerization between the styrene monomer and the unsaturated polyester molecule. Polyester molecules form the backbone of the polymer network, while styrene monomers serve as a crosslinking agent to link the adjacent polyester molecules. In the styrene (ST)-unsaturated polyester (PES) crosslinking copolymerization, there are three possible reactions: styrene to styrene, styrene to PES C=C bond, and PES C=C bond to PES C=C bond. These reactions can be further classified into four types. They are (I) inter-molecular crosslinking with or without linking through styrene monomers; (II) intra-molecular crosslinking with or without linking through styrene monomers: (III) branching on the polyester molecule by styrene; and (IV) free styrene homopolymerization. Among the four, reaction (I) results in a macroscopic network formation through the connection of adjacent polyester molecules; reaction (II) increases the crosslinking density and reduces the size of polyester coil, but does not contribute to the macroscopic network formation; reaction (III) consumes crosslinking units and may slightly increase the polymer coil size, but has little effect on network formation; reaction (IV) forms a soluable polymer segment which does not participate in the polymer network. Although all the reactions affect the curing kinetics, only the first two contribute to the network formation.

During the ST/PES copolymerization, the initiator decomposes and creates free radicals in the system. The free radicals grow and form long chain molecules through connecting styrene monomers and polyester molecules by both inter- and intra-molecular reactions. These long chain molecules tend to form spherical type of structures or "microgel particles" due to the intra-molecular crosslinking among the pendant C=C bonds of polyester molecules. At high styrene concentrations, i.e., low concentration of microgels, the individual microgel particle can be easily observed and the microgel size is large due to the styrene swelling effect. The particles are externally connected by styrene chains to form a "dumbbell" shape with particles at the ends and styrene chains in the middle. The overall network built up by the dumbbell shape is a "tree-like" or "coral-like" structure. The formation of microstructure is a key feature of the styrene-unsaturated polyester copolymerization. It affects not only the reaction kinetics and rheological changes of the molding compounds but also the physical properties of the molded products.

Several well-characterized unsaturated polyester resins were used in this study. The reaction kinetics of styrene monomer and polyester vinyl groups were measured by an FTIR spectrometer (Nicolet 20DX) with a resolution of 4 cm^{-1} in the transmission mode. The monomer conversion of each resin was measured by following the changes of its characteristic peaks. The morphology of molded samples was analyzed using a Hitachi S-510 scanning electron microscope at various magnifications.

5/2

REACTION-INDUCED CRYSTALLIZATION DURING THE RIM PROCESS OF NYLON 6

KWANG HEE LEE and SUNG CHUL KIM

Department of Chemical Engineering

Korea Advanced Institute of Science and Technology

P.O. Box 131, Cheongryang, Seoul, Korea

The anionic polymerization of ε caprolactam to nylon 6 is carried out somewhat below the melting point of the polymerized product, and thus nonisothermal crystallization occurs as the reaction proceeds[1]. Because the polymerization and crystallization occur at the same time, it is quite difficult to analyze the crystallization kinetics during polymerization. One must understand the nonisothermal crystallization behavior during polymerization in order to simulate the RIM process of nylon 6 [2].

The kinetics of crystallization during anionic polymerization of ε caprolactam was studied by the adiabatic temperature rise method. A new kinetic model for the nonisothermal crystallization was derived and the possibility of its application was investigated. The experimental and predicted temperature rise showed pretty good agreement, which indicated that the model equation was applicable to describe the reaction-induced crystallization kinetics of nylon 6. By evaluating the model's diffusion and nucleation parameters for the given system, the crystallization behavior during polymerization was analyzed. At low conversion the reaction mixture was less viscous, a condition which made transport to the liquid-crystal interface easier, and thus the activation energy for transfer decreased. On the other hand, the increasing mobility retarded the formation of the stable nucleus and the free energy of formation of a nucleus increased (Fig. 1).

A computer simulation model was developed to analyze the nylon 6 RIM. Balance equations calculating the temperature, conversion, and crystallinity change in a disc type mold were solved simultaneously with the aid of a computer. As an attempt to optimize the RIM process, the effects of molding parameters such as the feed temeprature, the wall temperature, and the overall reaction constant on the process criteria of the eject time were analyzed.

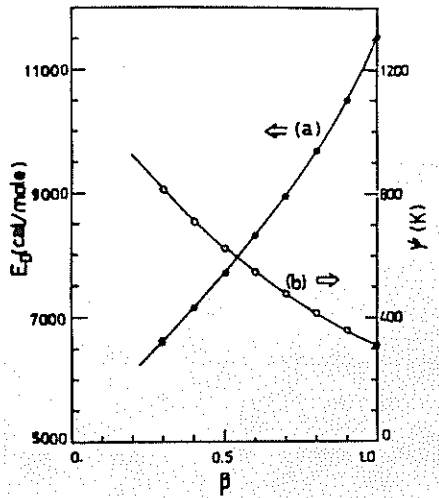


Fig. 1. E_D and ψ vs. conversion : E_D is the activation energy for diffusion and ψ is a constant related to the free energy of nucleus formation.

Reference

1. O. Wichterle, J. Tomka, and T. Sebenda, Collet. Tech. Chem. Commun., 29, 610 (1964).

2. S.A. Iobst, Poly. Eng. Sci., 25, 425 (1985).

5/3

FABRICATION OF MICROSTRUCTURES WITH EXTREME STRUCTURAL HEIGHTS BY REACTION INJECTION MOLDING

P. Hagmann, W. Ehrfeld, Kernforschungszentrum Karlsruhe GmbH,
Institut für Kernverfahrenstechnik, Postfach 3640,
7500 Karlsruhe 1, Federal Republic of Germany

For fabricating microstructures with extreme structural heights a new microfabrication technique has been developed by the Karlsruhe Nuclear Research Center in Cooperation with the industrial companies Steag AG, Essen, and Degussa AG, Frankfurt. The so-called LIGA method is based on a combination of deep-etch X-ray lithography, electroforming and molding processes (in German: Lithographie, Galvanoformung, Abformung) [1]. The minimum lateral dimensions of the microstructures which can be fabricated from metals and plastics without any restrictions in the cross-sectional shape, are in the micrometer range and the structural heights are some hundred micrometers. A large number of innovative microstructure products may be produced in the field of sensors, compound materials, filtration, fluid dynamics, microoptics, synthetic fibers, communication techniques and microelectronics. Various concepts of such products, e. g. microfiltration modules, spinneret plates, electrical microconnectors, optical multiplexers, micronozzles, and various sensors, have been worked out [2].

In nearly all applications, low cost mass fabrication is a stringent requirement. It has been shown that this requirement can be favorably met by the micromolding process step of the LIGA method. In this step, metallic microstructures produced by X-ray lithography and electroforming are reproduced many times by plastic molding and, if required, an additional electroforming process.

The current development work on the micromolding process includes the evaluation of fabrication methods for mold inserts, the optimization of molding and demolding conditions, thermo-mechanical measurements, and electroforming of metallic microstructures using templates generated by micromolding with casting resins [3].

For the various microstructure products several process schemes are being developed, depending on the geometrical configuration of the microstructures. If, for example, the actual microstructures are connected to relatively large openings the mold insert is covered with an electrically conductive gate plate provided with injection holes which match with the large openings. The mold material is introduced into the mold cavities through the holes of the gate plate. This plate which has a formlocking connection with the plastic microstructures after hardening of the resin serves as an electrode in an electroforming process for generating metallic microstructures. It has been demonstrated by many experiments that, in spite of an aspect ratio of about 100 and minimum lateral dimensions of only some micrometers, a yield of approximately 100 % can be obtained in the micromolding process using methacrylate base resins with an internal mold release agent. Work has been started with RIM nylon and also to produce microstructures by injection molding.

If the final product is not a metallic but a plastic structure, the process scheme may be simplified considerably. The mold material is poured onto the mold insert as a sufficiently thick layer in a vacuum vessel and then forced to fill the gaps between the metallic mirostructures by subjecting the liquid or pasty material to high pressure. By a double-layer process involving electrically insulating and conductive mold materials, the sequence of the process can be extended to generating templates with a plating base for electroforming of metallic microstructures.

The feasibility of this new microfabrication method has been sucessfully demonstrated by laboratory experiments. It is to be expected that this method will be superior to other processes if specific requirements are imposed on the spatial resolution, the aspect ratio, the structural height, the parallelism of the structure walls and, in particular, if an unrestricted design of the cross-sectional shape and an optimum selection of the material required for each microstructure product has to be ensured.

References

1) E.W. Becker, W. Ehrfeld, P. Hagmann, A. Maner, D. Münchmeyer, Microelectronic Engineering 4 (1986) 35-56.
2) W. Ehrfeld, P. Bley, F. Götz, P. Hagmann, A. Maner, J. Mohr, H.O. Moser, D. Münchmeyer, W. Schelb, D. Schmidt, E.W. Becker, Micro Robots and Teleoperators Workshop, November 9-11, 1987, Hyannis, Cape Cod, MA, USA. Proc. IEEE, K.J. Gabriel, W.S.N. Trimmer, eds., IEEE Catalog Number 87TH0204-8 (1987).
3) H. Vollmer, W. Ehrfeld, P. Hagmann, KfK-Bericht 4267, Kernforschungszentrum Karlsruhe, 1987.

PROBLEMS OF SIMULATING THE PROCESSING OF THERMOSET POLYMERS

U. Gonzalez, S. F. Shen and C. Cohen
Cornell University

Thermosetting polymers undergo exothermic chemical changes during processing operations. While problems dealing with reactive materials occur in many fields, the modelling of thermoset processes is particulary complicated by the polymeric nature of thermosets and by the highly complex system geometries and operating conditions encountered in molding practices. The simulation of such processes requires the simultaneous consideration of not only the flow and thermal aspects, as in the case of thermoplastic processing, but also of the chemical reactions and the consequent property changes. Thus, to provide useful answers to processing problems, adequate mathematical modelling and proper solution techniques are even more challenging than what has been achieved for thermoplastics.

We have chosen to work with the epoxy-amine system previously studied by Kamal [1], who proposed to model its chemical kinetics, under isothermal conditions, with the rate equation:

$$\frac{d\alpha}{dt} = (K_1 + K_2\alpha^m)(1 - \alpha)^n \qquad (1)$$

where α is the cure level, varying between 0 and 1, K_1 and K_2 are constants of Arrhenius type temperature dependence, and m and n are exponents independent of temperature. The cure level is related to the heat released during the reaction by,

$$\alpha = \frac{\int_0^t \dot{Q}\, dt}{Q_H} \qquad (2)$$

where $\dot{Q}$ is the instantaneous rate of heat release, and Q_H is the total heat released at the completion of the reaction. We performed experiments in a differential scanning calorimeter (DSC), paying particular attention to the constancy of the prevailing temperature during the reaction, to verify the adequacy of Eq. (1) and to determine the various constants in the temperature range expected to be of interest for injection molding. The procedure and results will be described.

To represent the rheology of the material at different cure levels, we first determined the glass-transition temperature, T_G, again using the DSC. Our results show that, if we postulate Eq. (1), T_G is in essence a function only of the cure level. The viscosity of the partially cured material was measured with a parallel-plate rheometer in the oscillatory mode. The dependence of viscosity on both temperature T and cure level α was fitted to the WLF equation, as suggested in [2],

$$\ln \frac{\eta_0}{\eta_{0,\,ref.}} = \frac{-C_1 (T - T_G(\alpha))}{C_2 + T - T_G(\alpha)} + \frac{C_1 (T_{ref.} - T_{G,\,ref.})}{C_2 + T_{ref.} - T_{G,\,ref.}} \qquad (3)$$

At different oscillating frequencies, however, the data showed an apparent anomaly, Fig. 1, which could indicate a shear-rate dependence of the reaction constants of Eq. (1). Further investigation of this question is in progress.

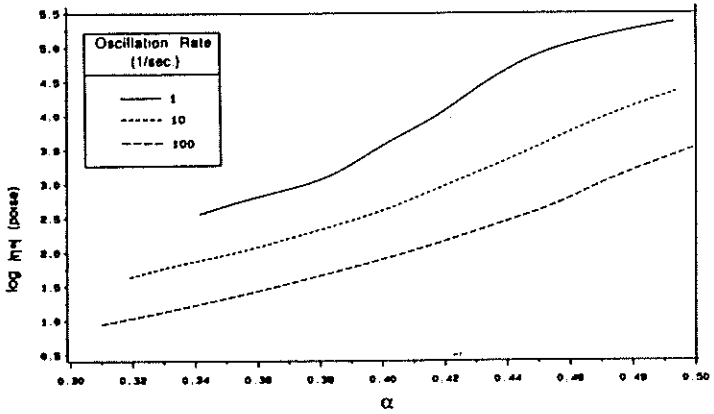


FIGURE 1 Complex viscosity versus cure level for experiments performed at 105°C, but at different oscillation rates.

The flow simulation incorporates the above with new features beyond those, now fairly well established, for thermoplastic materials. In particular, the chemical reaction tends to effectively make all problems basically time-dependent. For instance, the distribution of the cure level at the end of the cavity-filling stage in injection molding must be deduced from Eq. (1), which is Lagrangian by definition.

References

1 Kamal, M.,M. Ryan, Polymer Engineering and Science, 20, 859 (1980)
2 Apicella, A.,P. Masi and L. Nicolais, Rheologica Acta, 23, 291 (1984)

5/5

Mixing of natural rubber with carbon black in a highly instrumented internal mixer

Author: Dr. J.L. den Otter,
TNO Plastics and Rubber Research Institute TNO,
Delft, Holland

A tire tread formulation containing only natural rubber (NR) and three industrial compounds containing large amounts of NR were mixed in a laboratory internal mixer and in three industrial mixers, all of the Banbury type.

Most experiments were performed in the small (1,8 l) laboratory mixer, in which process conditions can be changed easily and cheaply over a large range.

The laboratory mixer is highly automated. A selection of important process variables, e.g. the torques on the two rotors, speed of rotation, rubber temperature, two wall temperatures, two pressures at the wall, flow rates and temperature changes of cooling liquid, ram position and ram pressure are continuously sampled by a small computer at frequencies from 1/min to 20/s or 600/s (wall pressures only).

The mixer is equipped with interchangeable inner linings. This enables us to change the roughness of the wall surface and the size of the gaps between rotor tip and wall without changing the rotors. The rotors are made of stainless steel on a computer programmed milling machine. Bij changing the parameters of the computer program the rotor geometry can be changed systematically, enabling us in future to test the influence of rotor geometry on mixer efficiency.

The degree of mixing was characterized by physical methods such as the size of sub-micron carbon black conglomerates and rheological measurements. In addition, industrial methods such as Cabot rating and Mooney viscosity were used. On vulcanized samples a number of industrial quality tests were performed, such as modulus, hardness, tensile strength and fatigue. For the simulated NR tire tread formulation we found that large changes in mixing conditions gave large structural changes, but little effect on the industrial quality tests, with the exception of fatigue. The rating in fatigue properties correlated not at all with Cabot rating or electrical conductivity, but quite well with the microstructure of carbon black (conglomerates from 0.1 to 5 μm).

The mixing process is strongly influenced by the friction properties of the compound. Friction properties were measured in a lateral friction tester as a function of temperature, pressure, velocity and roughness of the wall. All compounds investigated showed a stick-slip transition temperature. This transition temperature was found to depend strongly on the degree of mixing.

The results of the systematic investigation of the influence of process conditions in the laboratory mixers was used to increase the efficiency of two industrial mixers. The proposed changes resulted in a decrease in energy use of 5 - 10% and a decrease in mixing time of also about 5 - 10%.

5/6

EFFECT OF STOICHIOMETRIC RATIO ON REACTION RATE KINETICS AND PROPERTIES OF A DGEBA/MIXED AMINE EPOXY VIA DYNAMIC MECHANICAL SPECTROSCOPY

D. Wingard and C.L. Beatty, Univ. of Florida, Gainesville, FL

Introduction. Accurate determination of epoxy to curing agent for a crosslinked system is important because a variation of more than ±2 wt.% of the stoichiometric ratio of epoxy to curing agent can have a significant effect on the final mechanical properties of the cured resin. This work focuses on the use of dynamic mechanical spectroscopy to characterize the curing behavior of an epoxy-amine system analogous to previous dynamic mechanical studies of epoxy crosslinking (1,2). For this work, the epoxy/amine ratio was varied and the dynamic mechanical response was determined for: 1) Conversion of the mixed system to the B-stage cure condition to yield isothermal cure kinetics; and 2) A C-stage cure of the neat resin and glass braid composite as a function of temperature and frequency.

Experimental. The dynamic mechanical properties were studied via a Polymer Laboratories Dynamic Mechanical Thermal Analyzer (DMTA). Samples were run in both the flexural and shear modes.

For the cure kinetics, samples were run in both flexure and shear at isothermal temperatures from 80-150°C, and at a single frequency, primarily 30 Hz. In the flexural mode, the mixed resin was mounted between two pieces of stainless steel shimstock as the neat resin and as a glass cloth composite. For shear measurements, only the neat resin was analyzed.

For temperature scanning of the cured resin, samples were C-stage cured in an aluminum mold, and were then analyzed from -100 to 200°C at a heating rate of 3°C/min. and at five frequencies (0.33-30 Hz).

The epoxy system used was a DGEBA-type resin with a mixed aromatic amine curing agent. The recommended stoichiometric ratio of epoxy to amine was 81 wt.% to 19 wt.%. Studies were conducted by varying the concentration of epoxy by ±2, ±5 and ±10 wt% from the stoichiometric value of 81 wt.%.

Results and Discussion. The cure kinetics of the mixed resin was determined by using the time to gelation corresponding to the loss peak maximum of tan delta as a measure of the rate of reaction at each temperature and frequency. The slope of a plot of $\ln(t_{gel})$ vs. 1/T was then used to determine the activation energy of cure. For samples run in flexure, the activation energy of cure passed through a maximum at the stoichiometric ratio. For samples run in shear, a minimum was observed. In shear, overall rate constants were also determined by assuming the change in modulus with time to be directly proportional to the crosslink density after the gel point of the epoxy system (3).

Samples that were C-stage cured were scanned in temperature on the DMTA. For the ultimately cured resin, the molecular weight between crosslinks (M_c) passed through a minimum and the glass transition temperature (T_g) passed through a maximum at the stoichiometric ratio (Fig. 1). The "sub-T_g", a secondary transition near -40 to -30°C, also passed through a maximum near the stoichiometric ratio. The activation energy of the ultimately cured resin also passed through a maximum at the stoichiometric ratio for both the T_g and sub-T_g. In addition, the effect of glass braid filler on the molecular weight between crosslinks was estimated from the linear rule of mixtures.

References.

1. Murayama, T.; Bell, J.P. J. Polym. Sci.: Part A-2 1970, 8, 437.
2. Senich, G.; MacKnight, W.J.; Schneider, N.S. Polym. Eng. Sci. 1979, 19(4), 313.
3. Babayevsky, P.G.; Gillham, J.K. J. Appl. Polym. Sci. 1973, 17, 2067.

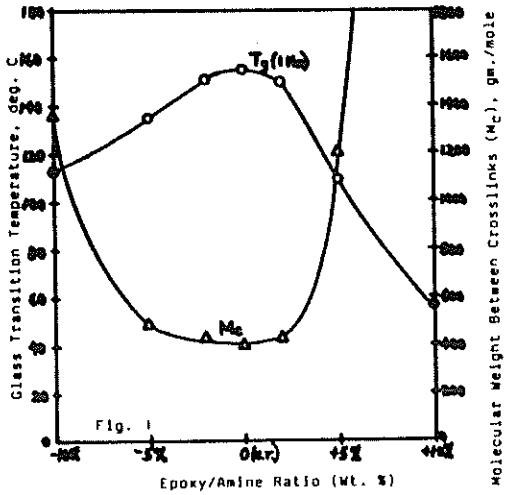


Fig. 1

5/7

A FUNDAMENTAL STUDY ON THE KINETICS OF STYRENE-BASED COPOLYMERS

Shinzo Omi, Ineo Iwata, Kiyoshi Inubuse, Mamoru Iso, Shoji Urushiyama (Tokyo University of Agriculture and Technology) and Motoshi Suka (Nippon Plant Co. Ltd.)

The authors have been working with a particular pilot plant system to produce pure polymers by thermally-initiated bulk polymerizations. As the feasibility of the reactor system has been successfully demonstrated with the polymerization of styrene (ST), technically more troublesome systems, such as MMA and acrylonitrile (AN) containing copolymers, have emerged as a next objective because of their increasing viscosity during the polymerization. Successful productions of these copolymers with extra purity and high molecular weight (MW) will be unquestionably desired.

Kinetic studies of chemically-initiated bulk copolymerizations of MMA-ST and ST-AN have been reported so far, however those with thermal initiation are very scarce.

As a preliminary investigation before operating the pilot system, fundamental kinetic data are being collected by the authors changing the reaction temperature and composition of comonomer. Glass ampoules containing measured amount of comonomer were sealed after the conventional freeze-and-thaw cycles to eliminate the dissolved air. Dimension of the glass ampoule is 10 mm ID, 12 mm OD and 100 mm in length. A constant temperature oil bath equipped with an agitator and a controlled heater was used to immerse ampoules. Monomers were distilled under the reduced pressure and stored in a refrigerator prior to use.

Total conversion of comonomer was measured gravimetrically, MW by GPC using THF as a solvent, and average composition of monomer in copolymer and average chain length were determined from H-NMR analysis.

Total monomer conversion vs. reaction time curve of MMA-ST observed at 373K was shown in Figure 1 with varied composition of comonomer. Enhanced gel effect is clearly observed as the ratio of MMA in comonomer increases. Strickler et al reported that MMA polymerized quite slowly in the thermally-initiated system at 403K, however, as shown in the figure MMA homopolymerized very rapidly. Initiating species may have been formed during the distillation though the temperature atop was maintained as low as 313K. On the other hand, Strickler et al eliminated inhibitor in MMA by washing.

Average mole fraction of ST in copolymer vs. total monomer conversion curve was shown in Figure 2. Broken lines in the figure were calculated by assuming the reactivity ratios as rST = 0.87 and rMMA = 0.47 obtained from the Fineman-Ross plot. rST seems to be unusually high compared with the reported values.

Though not shown in the figure, average MW became higher as the content of MMA in comonomer increased, and dramatically increased as the reaction approaches to the limiting conversion of monomer. For example with the monomer ratio MMA/ST = 8/2, weight average MW was approximately one million, stayed nearly constant up to 80% conversion, and then increased to around 1.5 millions. Dispersion index was around 2.0, indicating pretty narrow MWD.

Total monomer conversion vs. reaction time curve of ST-AN observed at 393K was shown in Figure 3. For the chemically initiated system, Garcia-Rubio et al reported that the rate of polymerization was higher with increasing amount of AN in comonomer. In the thermal initiation, no appreciable change of reaction rate was observed except the run that ST/AN = 9/1 in comonomer. Similar behaviours were also observed in the MMA-ST system at 393K.

These peculiar behaviours may be reduced to the mechanism of the thermal initiation between two monomers.

Analytical and simulative investigations will be conducted to understand the overall mechanism quantitatively.

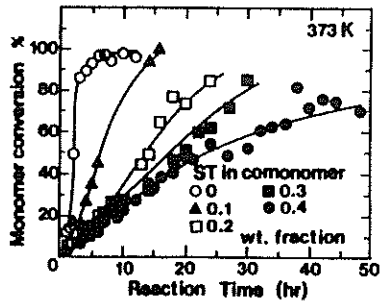


Figure 1. Profiles of monomer conversion (MMA-ST at 373K).

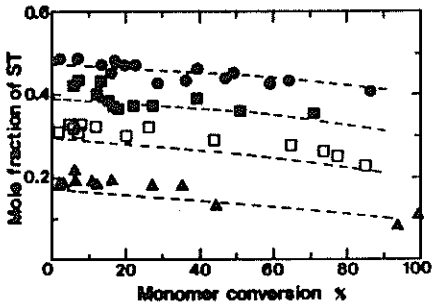


Figure 2. Mole fraction of ST in copolymer (MMA-ST at 373K).

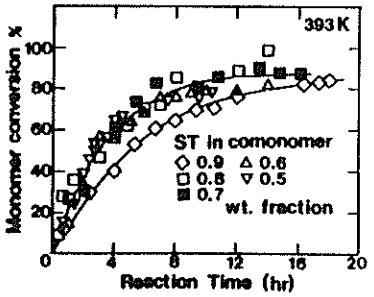


Figure 3. Profiles of monomer conversion (ST-AN at 393K).

RHEOLOGICAL PROPERTIES OF CROSS-LINKED POLYETHYLENES

S.Venkatraman and L.Kleiner, Raychem Corporation,
300 Constitution Drive, Menlo Park, CA 94025.

Traditionally, cross-linking of polyethylenes has been carried out mostly by three possible routes:
(a) Radiation-induced, (b)Chemical(peroxide-initiated), and
(c) Moisture-initiated curing of grafted polyethylenes.
Although each of these methods involves cross-linking via free-radical intermediates, the resulting rheological and thermo-mechanical properties may be different for each system (1,2).

Radiation-induced cross-linking takes place in the solid-state. High-energy radiation (electrons, gamma-rays) generates free-radicals, mainly in the amorphous regions. Reactive sites on adjacent molecules then couple to form a cross-link.

Chemical- or peroxide-initiated cross-linking is carried out at or above the melting point of polyethylene. Molecular mobility in the molten state aids in randomizing the location of cross-link sites.

The moisture-initiated cross-linking occurs as a result of three steps. First, vinyl-silane molecules (such as vinyl trimethoxy silane) are grafted onto the polyethylene at random locations along the backbone, the reaction being carried out in the melt. Next, exposure of this grafted polyethylene to moisture leads to hydrolysis of the silane groups. This is followed by a condensation between hydrolyzed silanes on adjacent molecules, leading to the formation of a cross-link. Although the silane groups are likely to be randomly distributed along the chain, the cross-linking process, carried out in the solid-state, may be restricted to the amorphous regions. Thus, the three methods are expected to yield materials with different network structures.

In this work, a high-density polyethylene (with a specific gravity of 0.96 and a melt-flow-index of 1.0) was cross-linked via the three routes mentioned above. The resulting materials had macroscopic properties (such as ultimate mechanical properties, modulus etc.) that depended on molecular parameters (such as the average molecular weight between crosslinks, Mc) differently for each mode of crosslinking. Comparisons were made at similar gel-contents. These differences are traceable to the different network structures that are formed in the three cases.

Other properties, such as degree of crystallinity and melting points, were also examined. The dependence of these properties on variables such as dosage, peroxide concentration,etc. will be discussed in relation to previous work on radiation- and peroxide-crosslinked polyethylenes(1).

References:
(1): M.Narkis et.al.,
J.Macromol.Sci.-Phys., B26(1), pp37-58,1987.
(2): C.Beveridge et. al.,
Materials and Design, 3(5), Sept/Oct 1987.

THE REACTIVE EXTRUSION OF POLYSTYRENE/POLYPROPYLENE BLENDS

P. Cheung, S.T. Balke, Department of Chemical Engineering and Applied Chemistry, University of Toronto, Toronto, Ontario, M5S 1A4.

In this reactive extrusion process, free radical initiator is injected into polystyrene and polypropylene as they are blended in an extruder. The objective is to see if block or graft copolymers can be obtained. Small quantities of such copolymers would be expected to compatibilize the blends. Larger quantities would be useful specialty products. There have been some published successes with similar processes in forming compatible blends of polypropylene/polyethylene copolymers with polyethylene. Also, copolymers have been formed from polyethylene/polystyrene blends. However, this type of process is often considered to not result in a predictable or well-controlled product. Here, the polymers are very incompatible, polypropylene readily degrades, polystyrene resists degradation and the free radicals formed may not be sufficiently cross-reactive. However, the possibility of upgraded products in recycle of these commodity polymers is a strong motivator. Furthermore, recent success in modeling polypropylene degradation (1,2), the demonstrated effectiveness of a static mixer for dispersion of this polymer blend (3) and advances in interpreting data from size exclusion chromatography (SEC) (4) provide the elements for a new approach.

In the initial work reported here, polystyrene (PS 201, Polysar) and polypropylene (a development resin from Himont) alone and together as a 50:50 by wt. blend were added to a single screw extruder (1.5" diameter, 24:1 L/D) equipped with a static mixer (Thermogenizer, Kenics). Initiator (Lupersol 101, Lucidol) was simultaneously injected at the feed port. At 190°C and at 220°C, feed concentrations of initiator were 0., 0.1, 0.2 and 0.3 wt. %. At 190°C, 0.9 wt. % was also used. Determination of both homopolymer degradation and copolymer formation was attempted using high temperature SEC using the same conditions as before (1,2,4) but with new columns (development columns from Polymer Labs). Figures 1 and 2 show the results at 220°C. Molecular weight distributions all consistently showed lower molecular weights with higher initiator concentrations. At 190°C results were similar but of lesser magnitude except with the 0.9 wt. % initiator concentration level which resulted in significantly more degradation to both polymers present.

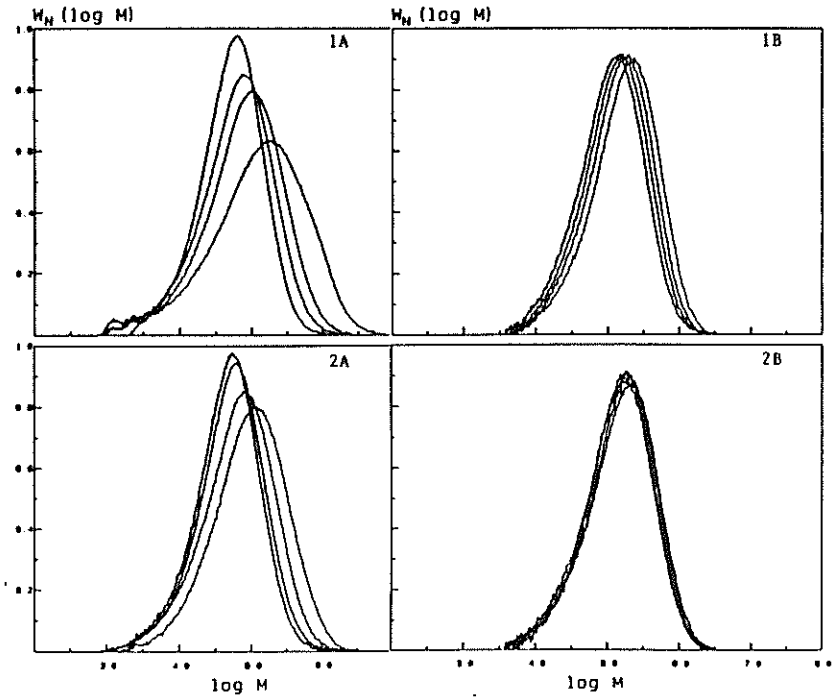
Our conclusions to date are: both polystyrene and polypropylene can be readily degraded by the initiator; in the blend, the polypropylene is likely preferentially degraded, even at zero initiator concentration; no copolymer is so far evident. Current work is aimed at better utilization of the static mixer to increase the surface area between the polymers during reaction. Also, application of our previously developed degradation kinetic model for polypropylene, as well as microscopy and mechanical property testing are in progress.

References

1. S.T. Balke, D. Suwanda and R. Lew, J.Polym.Sci., C, 25, 313(1987).
2. D. Suwanda, R.Lew and S.T. Balke, "The Reactive Extrusion of Polypropylene I and II", J. Appl. Polym. Sci., in press 1988.
3. C.D. Han, Y.W. Kim, S.J. Chen, J. Appl. Polym. Sci., 19, 2831(1975).
4. R.Lew, P. Cheung, D. Suwanda and S.T. Balke, "Quantitative Analysis of Polypropylene II", J. Appl. Polym. Sci, in press 1988.

Figures 1A and 1B: Polypropylene (A) and polystyrene (B) after extrusion at 220°C with 0., 0.1, 0.2 and 0.3 wt. % initiator.

Figures 2A and 2B: Polypropylene rich phase (A) and polystyrene rich phase (B) after extrusion in blend with 0., 0.1, 0.2 and 0.3 wt. % initiator.



5/10

REACTIVE EXTRUSION OF POLYPROPYLENE

C.Tzoganakis,J.Vlachopoulos and A.E.Hamielec
Department of Chemical Engineering, McMaster University,
Hamilton , Ontario, CANADA

Specialty polypropylene (PP) resins with narrow molecular weight distributions can be produced by chemical modification of cheap commodity resins. A fully-predictive mathematical model has been developed for the peroxide promoted degradation of PP in a plasticating single-screw extruder. The model is based on a free radical kinetic mechanism for the degradation reaction and on conventional plasticating extrusion theory. Solids conveying, melting, melt pumping and reaction phenomena have been combined and the interactions between flow pattern, mass and heat transfer fields via residence time distribution and the chemorheology of the reactive melt have been considered.

The effects of shear rate, temperature and molecular weight on the viscosity of the melt have been included and the conservation equations of mass, momentum, energy and species in the melt phase are solved by means of a finite difference scheme. Given the geometrical configuration of the screw, the operating conditions and the physical properties of the starting polymer, the model predicts : flow rate, pressure, temperature and molecular weight profiles in the extruder channel and in the die, extrudate swell at the die exit and the residence time distribution in the system.

Model predictions are compared with experimental data from runs on a 38 mm , 24:1 L/D single-screw extruder using various peroxide concentrations and rotational screw speeds.

Results from experimental studies of the grafting of polypropylene and maleic anhydride are also presented. Maleic anhydride was grafted on polypropylene in the melt phase in the same plasticating extruder. Experimental runs with varying amounts of maleic anhydride and peroxide were carried out and the degree of grafting was determined by NMR measurements. Correlations between degree of grafting and rheological properties of the materials produced have been developed while the adhesive and mechanical properties of the grafted resins are currently being evaluated. Finally, a simple kinetic model for the grafting reaction is being developed.

5/11

REACTIVE BLENDING OF POLYAMIDE AND CARBOXYLATED NITRILE RUBBER.

W.E. Baker and M. Saleem
Department of Chemistry, Queen's University, Kingston, Ontario
Canada K7L 3N6.

Blends of a low melting point polyamide (PA) and a nitrile rubber having carboxylic acid groups (XNBR), were prepared in a Haake mixer Model 600. The mixing was carried out for 10 minutes at a temperature of 180°C and a speed of 100 RPM. For comparison, blends of PA and nitrile rubber without acid functionality (NBR) but similar molecular weight and composition were also prepared under the same conditions. Morphology and mechanical properties of these two sets of blends were investigated and compared. The scanning electron micrographs (SEM) of the fractured and solvent itched surfaces show that in PA-XNBR (80/20) blend the average rubber particle size is about 0.5 μm compared to 3 μm for PA-NBR blend of the same proportion. Also, the rubber rich blends of PA-XNBR (20/80) have finer morphology than their PA-NBR counterpart. Tensile measurements were made on injection molded samples and it was found that the addition of rubber increases the tensile strength of both sets of blends reaching a maximum value in about 20% rubber blends. Moreover, in this region the tensile strength of the reactive PA-XNBR blends is about 6 Mpa (~15%) higher than the unreactive PA-NBR blends.

The impact strength of these blends were determined using a Dynatup instrumented impact tester on 5 cm injection molded discs. The peak load and total energy at break were measured. All failures were ductile. The incorporation of the XNBR or NBR into the otherwise tough terpolymer (6,6.6,6.10) polyamide resulted in a drop in the total energy at break but in all cases the XNBR blend displayed higher total energy than the comparable NBR blend. The unexpected drop in the impact strength with the addition of rubber may be a result of not having optimized these blends for percent rubber, viscosity ratio and interfacial adhesion or the high intrinsic impact strength of the polyamide.

The improvement in both tensile and impact strength of the PA-XNBR blend over the PA-NBR is consistent with previous work (1-2) on a reactive polystyrene/polyethylene system. In that work a similar improvement in properties for potentially reactive blends was observed and through DSC and FTIR studies the improvements were correlated to interpolymer reaction during melt blending. A parallel study on reactive polystyrene - XNBR shows the same trend (3). These observations indicate that the fine morphology and improvement in tensile and impact properties of the PA-XNBR blends over the PA-NBR blends is likely the result of a chemical reaction between the carboxylic acid in the rubber and terminal amine groups of the polyamide.

REFERENCES

1) W.E. Baker and M. Saleem, Polymer 28, 2057, 1987.

2) W.E. Baker and M. Saleem, accepted by Polym. Eng. and Sci for early 1988.

3) W.E. Baker and M. Fowler, presented at Polyblends '88, April 1988, IMRI-NRCC, Boncherville, Quebec.

Optimal Control of RIM Impingement Mixheads

P D Coates and A F Johnson,
Polymer Research Unit,
University of Bradford,
Bradford BD7 1DP, UK

Abstract

High pressure impingement is the dominant method for rapid mixing in reaction injection moulding (RIM). Experimental studies on polyurethane RIM have identified

(i) requirements for optimal control of both major modes of mixhead operation (high flow rate recirculation and static pre-pressurisation modes), to avoid off-ratio mixing at the start of injection, and

(ii) design constraints on mixhead orifices.

Modelling of reactant compressible flows extends understanding of the control requirements to minimise errors in the *actual* dispense ratio of reactants, particularly at the start of injection.

The results are applicable to any RIM chemical system, but have particular relevance to those demanding very close control of ratio (for example PUs, polyureas and interpenetrating polymer networks or alloys containing either of these), or where production repeatability is important to quality control.

5/13

Graft Copolymerization of Butyl Acrylate onto Poly(vinyl Chloride)

ShaoJun Huang & Jianxiong Li
Materials Science Research Institute,
South China Institute of Technology
Guangzhou, P. R. of China

This paper concerns the synthesis, characterization and properties of Poly(Vinyl Chloride-g-Butyl Acrylate).

The desired amounts of PVC, monomer and initiator were mixed and swollen at 25 °C for 10 hr. The mixture was placed into a glass tube under a stream of nitrogen then sealed under reduced pressure. The graft reaction was carried out in a constant temperature bath. After polymerization for a given time, the tube was opened, the products (added 1 % terminator) was dried at 25 °C under vacuum and weighed, then extracted with cyclohexane.

The products, before and after extraction, was analysed by using Gel Permeation Chromatography. In GPC graph their molecular weight distribition curvers are all bimodal, one hump is similar to PVC, the other has higher molecular weight than that of PVC. These can indicated that PVC was partly grafted with PBA, formed PVC-g-BA graft copolymer.

Drying the products for differental reaction period in vacuum oven, the dynamic curvers were obtained. The curvers show that the polymerization rate of BA swollen into PVC is rather rapid and conversions can be above 95 % usually. From the curvers, reaction order of BA has been determined. The dynamic equation at 90 °C is:

$$Vp = 5.10 * 10^{-2} (M)^{1.27} (I)^{0.688}$$

The products on various reactions were extracted. The grafting efficiency of PBA increases with increasing BA conversion. At hight conversion, the average rate of grafting is quicker than that of polymerization. These may show that the growing PBA chain have long life, attak PVC chains, form graft copolymer.

The products reaching same conversion at various initiator concentration, but same starting monomer concentration and reaction temperature, have almost equal grafting efficiency. This show that the initiator concentration does not inflence on the graft efficiecy. The main factors of inflence on grafting efficiency are the reaction temperature and monomer concentration. The efficiency changes from 40 % to 80 %, increases with increasing the concentration and decreasing the temperature. The higher the concentration and the lower the temperature, the more marked the inflence. The inflence of reaction temperature and starting monomer concentration on the grafting efficiency can be well described by following regression equation:

$$G.E = 68.956 + 10.417X - 11.333Y - 65.583X^2 - 5.333Y^2 - 2.475XY$$

$$X = \frac{(M) - 40}{20} \qquad Y = \frac{T - 80}{10}$$

DSC was used for indication the glass transition of the products. The multi-transitions of products can be seen in DSC graph. The glass transition temperature of PVC shifts from 91 °C to 70 °C, the glass temperature of PBA shifts from -47 °C to -40 °C. These confirmed that the reaction took place through over the PVC particles.

DTA was used for evaluating the thermal stability of the product. The onset of decomposition of PVC occurs at 235 °C and the peak decomposition is 287 °C. The onset of decomposition of products occurs at 255 °C and the peak at 298 °C. Moreover, for PVC, DTA curver shows a weak endothermic peak at 246 °C, whereas the graft products does not show. These may indicate that grafting removes the active chloride of PVC and improves the thermal stability of PVC.

Table 1. Average Rate of Polymerization & Graft

(M)=60 g/100 g PVC			(M)=30 g/100 g PVC		
conversion	Vp	Vg	conversion	Vp	Vg
%	BA/100PVC min.		%	BA/100PVC min.	
76.5-90.4	1.670	3.600	37.2-71.6	1.030	2.840
90.4-95.0	0.550	1.530	71.6-82.4	0.648	0.760
95.0-97.0	0.012	.0172	82.4-92.4	0.300	0.440
97.0-98.7	.00227	.00264	92.4-95.0	0.026	0.113

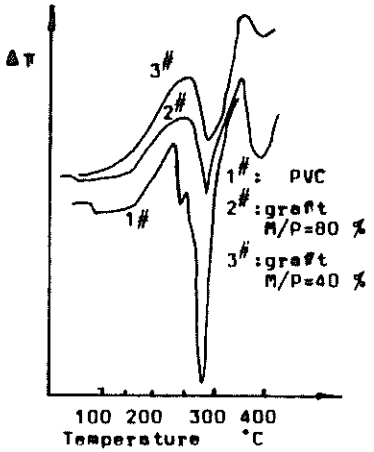
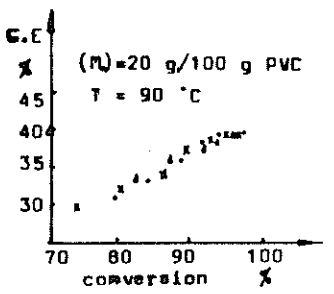


Fig.1 DTA graph



● (I)=2.0g/100g PVC
× (I)=1.5g/100g PVC
▲ (I)=1.0g/100g PVC

Fig.2 Inflence of conversion on graft efficiency

5/14

EFFECT OF THE CORRELATION BETWEEN PRE-COPOLYMERIZATION INGREDIENTS AND REACTION VOLUME ON THE IMPACT POLYSTYRENE MORPHOLOGY AND PROPERTIES

D.D.Kechajov - Petroleum Research Institute,Neftochim, Bourgas 8104,Bulgaria

It is well-known that the Impact Polystyrene(IPS) morphology and properties are closely interrelated and dependent on co - polymerization conditions-e.g.on the type and concentration of: the rubber,the initiator,the molecular mass regulator; on the pre-copolymerization temperature etc./1,2/.

This paper reviews the correlation " pre-copolymerization ingredients and Reaction Volume-IPS morphology and physicomechanical properties".IPS is obtained by block-suspension copolymerization of polybutadiene rubber (6% solution) pre-dissolved in styrene/3/.What characterizes this particular case is the fact that the pre-copolymerization is carried out at a specific combination(and variation) of 4 factors: 3 ingredients and the Reaction Volume(RV) of the copolymerization mixture.The first ingredient is the molecular mass regulator-e.g. n-Lauroyl Mer - captan(LM); the second one is a graft-active initiator - e.g. Benzoyl Peroxide(BP);and the third is a graft-inactive initiator e.g.Lauroyl Peroxide(LP).The ingredients are subjects to dosing in the reactor before the start of pre-copolymerization or during the first 1-6% conversion; it is then that the RV is being fixed up either by means of the monomer quantity change or by means of water dosage in the reactor.During the pre-copolymerization the RV makes 35 - 75% of the reactor total volume; rubber content and agitation intensity are constant.

The LM/BP/LP/RV ratio variation(during pre-copolymerization) makes it possible to purposefully effect and control the IPS morphology and properties.

This is illustrated by the data in the table below:

Number	Factors ratio at pre-copolymerization. Product morphology and properties.	SAMPLES 1	2	3
1.	LM/BP/LP/RV	1/2/0,33/50	2,66/3,33/ 1/65	4,17/10/ 1/40
2.	Rubber particles:			
	- interval of diameters, μm	0,8-26,2	1,0-50,4	0,5-3,2
	- prevailing diameters, μm	1,0-18,0	2,0-24,0	0,5-2,4
3.	Izod impact strength,notched at 23°C J/m	72	78	81
4.	Elongation at break,%	47	59	37
5.	Flexural strength, MPa	55	49	65

NOTE: The physicomechanical properties are determined according to Bulgarian National Standard 12603-85.

The method,described herein,is also a way of sensitively influencing the molecular mass distribution of the plastomeric phase in the IPS.This is indirectly manifested by the table data,especially having in mind the results,described in /4/.

REFERENCES:

1.A.Echte,Angew.Makromol.Chem.,58/59,175(1977).

2.D.D.Kechajov,Eur.Polym.J.,22,No.8,675 (1986) .

3.D.D.Kechajov,Bulgarian invention No.31864,Cl.C08F279/02, publ.April 15th.,1982.

4.M.Natov,D.Kechajov and M.Michailova,Angew.Makromol.Chem., 102, 175 (1982).

6/1

Mixing: Theory and Practice as Related to Polymers.

Peter Hold, Polymer Processing Institute at Stevens Institute of Technology.

A systematic treatment of polymer processing is greatly facilitated by dividing it into 5 elementary processing steps. Mixing represents a very important one because almost all polymeric materials have to be mixed with additives, fillers,and other components prior to transformation into a final product.

The first industrial mixing devices used for processing of polymers, the two-roll mill and the internal mixer were developed purely based upon experience in other mixing applications and intuition. Serious efforts to develop scientific methods to describe the process of mixing and to predict its outcome date back to the fifties. Owing to the enormously large number of ultimate particles involved in the process of mixing, the relative spatial position of which has to be followed, to describe that process, the development of a theory of mixing presents a difficult problem. The temperature dependant viscoelastic behavior of polymers and in many cases the necessity to break up agglomerates of solids further contribute to its complexity.

Depending upon the state, solid or liquid, and the size of the solid ultimate particles we differentiate between 4 different mixing cases which require different processing strategies.

A basic method to rank the efficiency of the mixing operation based upon the morphology of samples had to be developed to be able to follow the progress of the process. Mixing can be considered a process which increases the degree of disorder and thus the entropy of the components involved. a statistical defintion for the "perfect" mixture can be defined. It describes however a large number of equally perfect arrangements which leaves the question open whether they would all result in the same practical performance of the mixture. The various practical methods to characterize a mixture at different scales of examination are based upon a statistical definition of the state of the mix.

Laminar convection by the application of strain results in extensive mixing capable of improving gross uniformity texture and local structure. But by the application of stress laminar convection can perform intensive mixing improving texture and local structure. Random bulk or plug convection moving blobs of material randomly is an essential mechanism to achieve gross uniformity and to change the relative direction of the shear. Laminar extensive mixing has been extensively investigated and depending upon the type of laminar flow the progress of mixing can be expressed as a function of the strain imparted. A reliable model of intensive mixing, break up of agglomerates, is so far not available. Also mathematical modeling of the random phase of mixing which is important to break the streamlines up is still in its infancy.

Differences in viscosity across the mixture due to differences in viscosity of the components or non-isothermal conditions can have serious effects on the process.

With the introduction of viscoelasticity the system becomes capable of storing and releasing energy and as a result time enters the model as an additional variable. The effect of viscoelasticity depends upon the ratio of the relaxation time and the time characteristic of the process or some phase of it.

The residence time distribution the history of the elements of the system which can be computed provided the flow pattern in the system can be determined, renders important informations about the performance of a continous mixer.

Looking into the future of modeling of the mixing process, in order to overcome the problems caused by the complex rheology of the materials methods will have be developed which model the operation in repetitive steps starting with simplified assumptions and introducing more complex conditions during the following steps.

During the review of the mixing process certain features conducive to efficient mixing have been established. Using these characteristics the operation and performance of the most important commercial mixers the two roll mill, the single screw extruder and the twin rotor mixers are discussed.

6/2

ANALYSIS OF AGGLOMERATE RUPTURE IN LINEAR FLOW FIELDS

Ica Manas-Zloczower[1] and Donald L. Feke[2], Departments of Macromolecular Science[1] and Chemical Engineering[2], Case Western Reserve University, Cleveland, Ohio

A dispersive mixing model in which rupture of agglomerates primarily determines the dynamics of the mixing process was developed. Agglomerate rupture occurs when hydrodynamic forces exerted on the solids exceed the cohesive forces within the agglomerate. Agglomerates are modeled as clusters of particles bound by van der Waals forces. The magnitude and orientation of the rupturing force depends on the local stress field in the fluid.

Assuming that cleavage of the agglomerate occurs at the mid-plane, where the effects of hydrodynamic tension is the largest, the kinetics of the rupture process is found to be independent of cluster size. This results because the strength of cohesion within the agglomerate and the net hydrodynamic force acting to rupture the cluster are both proportional to the square of the agglomerate size. The effective outcome of this analysis is that the dispersion process is dominated by flow dynamics, i.e., a minimum value of flow strength, which depends on the geometry of the bulk flow field, is required for rupture of the cluster.

The dispersion process was investigated in four flow geometries: simple shear; pure elongation; uniaxial extension; and biaxial extension. Fig. 1 shows an example of predicted agglomerate lifetimes as a function of flow strength in simple shear flow. The dynamics of particle size distribution, which can be obtained using a population balance model, is demonstrated in Fig. 2. The efficiency of each flow geometry can be compared on the basis of power and time requirements (see Fig. 3). This analysis provide useful guidelines for the design of mixing equipment.

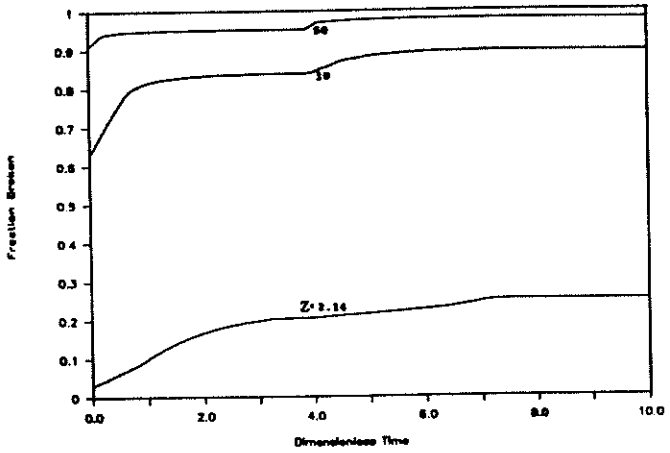


Figure 1: Fraction of agglomerates ruptured as a function of relative flow strength. Here Z is the ratio of flow strength to the strength of agglomerate cohesion.

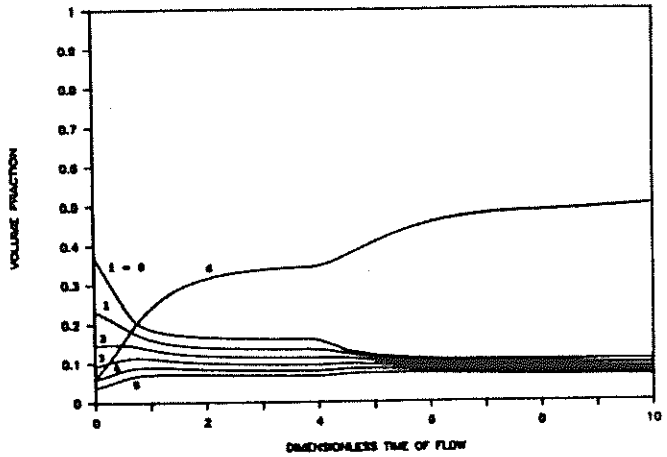


Figure 2: Evolution of population distribution in simple shear flow.

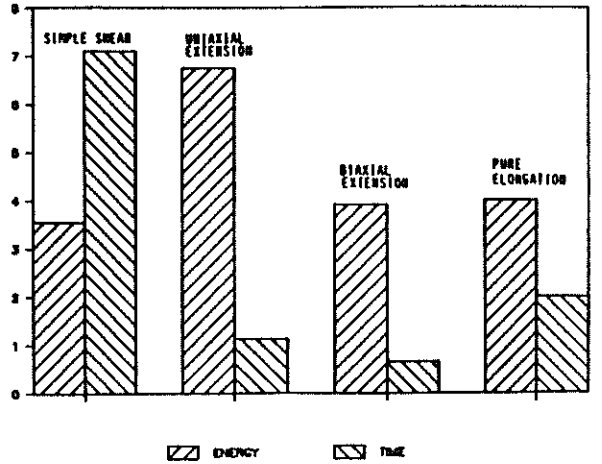


Figure 3: Comparison of the four flow geometries in terms of the power and time requirements to achieve a given degree of dispersive mixing.

6/3

PIGMENT DISPERSION IN POLAR AND NON-POLAR POLYMERS.

H.P. Schreiber and Y.M. Boluk *
Department of Chemical Engineering, Ecole Polytechnique
PO Box 6079,Stn.A. Montreal, Que. Canada,H3C 3A7.

Particulates, such as rutile TiO_2, are frequently surface coated to promote dispersion in polymer hosts. In this work, variously coated rutiles were dispersed in melts of polar and non-polar matrixes, in order to relate dispersion performance with conditions at the pigment/polymer interface. The rutiles, all with surface areas at 8 1 m^2/g,were characterized as to their acid/base interaction potential,Ω, following inverse gas chromatographic (IGC) procedures described earlier[1]. Also determined was an inherent agglomeration index, C . This applied the principles of powder rheology by milling the dry powders in a Brabender mixing chamber under controlled, variable loads. The torque generated was found to be a linear function of the applied load, allowing for an extrapolation to zero load, and thus the definition of the C parameter. The parameters are tabled and show a range of interaction potentials from strong bases (Ω>0), to acids (Ω<0); further the specimens range from strong agglomeration (C> 300) to non-agglomerated states as C tends to 0. Evidently the surface properties of rutile are dramatically affected by surface coating routines.

TABLE I: INTERACTION,AGGLOMERATION INDEXES FOR TiO_2.

Rutile:	A	B	C	D	E	F	G
Ω,30°C:	0.06	1.27	5.25	0.02	1.69	-0.42	-0.50
C (arb.u.)	790	590	280	110	75	170	5

A low density polyethylene (PE) and a chlorinated polyethylene (CPE) were hosts to rutiles added in 0.5 vol.% concentrations. The PE was found to be non-polar (Ω = 0), the CPE a strong acid (Ω = -1.7). A standard dispersion procedure was followed, employing the Brabender at fixed melt temperature,and at controlled motor speed,volume loading and mixing time. Contact X-ray micrographs of microtome sections were the source of visual and statistical analyses of dispersion quality.

The dispersion processes followed very different routes in the two host polymers. In the non-polar PE, dispersion quality correlated strongly with the inherent agglomeration of the particles, but not at all with the acid/base characteristics of polymer and pigments. Very fine dispersions were obtained for rutiles with C values below about 250, the incidence of larger particle agglomerates and clusters rising with increasing C values. A correlation coefficient of >0.94 applied to the relationship. The reverse was found to be true for dispersions in the acidic CPE matrix. Here dispersion quality was only weakly dependent on the C index, but varied appreciably with the Ω values in the set. Fine dispersions were obtained for basic pigments and increasingly coarse ones as the surface interaction potential of particulates entered the acidic range.

It follows from these experiments that dispersing particles in the size range of the rutiles,i.e. ~0.2μm, is a process dependent both on particle-particle and particle-matrix interactions. When the matrix is able to interact with particles through dispersion forces alone (PE), interparticle forces play a leading part in determining dispersion quality, at least in procedures using relatively mild shearing forces. Interactions due to non-dispersive forces, here characterized by acid/base parameters, play increasingly dominant roles in the dispersion procedures,as acid/base potentials increase. Considerable benefits in dispersion time and energy requirement may be derived from an exploitation of favorable acid/base interactions at the pigment /matrix interface. Clearly, an awareness on the part of the polymer processor is called for,of the wide variations which can exist in the surface states of commonly used particulates. Analogously, particle surface treatments tailored for performance optimization in specified host polymers appear to represent a worthwhile challenge to suppliers of particulates for polymer systems.

1. Y.M.Boluk and H.P. Schreiber,Polym.Comp.7,295 (1986).

* Present address: Pulp and Paper Research Institute of Canada, St.John's Blvd., Pointe Claire, Que. Canada.

CHANGE-CAN MIXING TECHNOLOGY

Bogard Lagman
Charles Ross and Son Company
710 Old Willets Path
Hauppauge, New York 11788
Phone: 516-234-0500

ABSTRACT

Mixing equipment may be classified in terms of its shear intensity (low or high shear) and in terms of its general design configuration (fixed-tank or change-can).

Fixed-tank mixers such as sigma blade mixers, turbine, cone screw and ribbon mixers were developed many years ago. Change-can mixing equipment such as planetary dispersers and multi-shaft mixers, however, have surfaced only in recent years.

Change-can mixers have a number of advantages over fixed-tank mixing equipment. These advantages include ease of cleaning and low possibility of batch contamination due to the absence of seals or stuffing boxes in the mixing zone. Another advantage is higher productivity because the change-can concept allows the mixer to do its job while additional cans are being loaded or unloaded. Fixed-tank mixers are unproductive while the tanks are being loaded or unloaded.

The decision to use fixed-tank or change-can mixing equipment for a given application can be reached quite easily. Deeper evaluation, however, is required to select the most suitable among the many mixer blade designs. In an effort to assist processors in the evaluation, an analysis of various types of modern change-can mixers is presented.

Today, change-can mixing systems are available with up to three different mixers to handle formulations having viscosities up to several million centipoise. These systems incorporate low and high shear and low and high speed mixers that are independently driven and controlled. This permits processors to fine-tune the equipment for single or multiple tasks including emulsification, particle size reduction, dispersion and suspension.

Because of the high viscosity mixing capability of modern change-can mixers, a Follower Plate Discharge System has been specially designed. This discharge system pushes the viscous mixture out of the can into product cartridges, moulds or hoppers of packaging machinery.

The development of new mixing and discharging systems and their integration open fresh opportunities to streamline processing operations and substantially lower production costs.

CONTROL OF RUBBER MIXERS

Pat O'Neill
Measurex Corporation, Cupertino, CA

Abstract

An effective approach to rubber mixing is essential to meeting today's high quality standards in the rubber industry. Rubber customers require more uniform mixes. Auto manufacturers demand more uniform tires. Tire production departments all require uniform components and materials in order to make on-spec products. Because rubber mixing has traditionally been a black art, the mixer operator was delegated the task of controlling the batch without the tools to evaluate materials coming to the mixer, monitor the process in the mixer, or predict the quality of current and future batches being mixed. Today, control systems cannot only bring rubber mixing out of the black art stage, but also provide the necessary tools to measure and control the mixing process in order to meet quality standards. This paper will cover control for rubber mixing.

The need for uniform rubber mixing is driven by economics. Increasing raw material and operating costs have dictated that compounds be correctly mixed the first time and evaluated as they are produced, thereby reducing scrap and off-spec product. Batch recipes need to be repeated in order to increase the mixer's throughput of compounds with identical quality and consistency characteristics. A control system for rubber mixing can achieve these goals through improved process visibility, consistency, and control.

Process visibility is loosely defined as the ability to display process parameters. Improvement in process visibility is achieved by: selection of parameters critical to the control of the process; accurate sensor measurements; and, displays which can be easily changed to represent the current process requirements. Process consistency is defined as the ability to set-up the controllable process features, in identical properties and sequence, in order to produce the same product characteristics each time a batch is processed. Process consistency requires: storage and automatic retrieval of control parameters; consistent proportioning and sequencing of raw materials; and, the mechanical stability and efficiency of mixing equipment. Process control is defined as the real time measurement and system availability to the process. It requires: verification of raw material presence and proportion; temperature stability of raw materials; accurate measurement of process parameters; and, system duplication of operator inputs.

More consistent mixing uniformity can be obtained as a result of a three phase approach. In the first phase, improved process visibility is used to increase the performance of the current manual operation. The key in ergonomic presentation of process data is that the data should be presented in forms which may be easily understood by operators such as graphic displays which use color changes to indicate unusual or out-of-limits conditions, and presentation of current data to allow simple comparison with standard, historical, or previous best run data including the use of alarms to alert the operator to large deviations from standard. Charting of process values in standard SQC formats would form part of this phase.

In the second phase greater consistency is developed both from batch to batch and from run to run, by replacing manual with automatic operation wherever practical. This would include not only automatic sequencing of the mixer unit but also stricter enforcement of recipe ingredient additions by prompting and checking operator actions thereby reducing or eliminating errors from this source.

The third phase which builds on the more stable operation resulting from phases one and two is optimization through a constant process of improvement. The key is the comparison of current operation with historical data to continually raise the baseline of mixing quality. This can include the use of a model with inputs such as time, mix temperature, work input per unit mass and so on, to predict the optimum drop time.

Today control systems offer an effective approach to uniform polymer mixing. Through process visibility, consistency, and control it will enable the rubber mixing industry to remain competitive and respond to the quality standards of its customers.

6/6

A novel color changing system using a motionless mixer in the wire coating extrusion

Choongyong Kwag, Jhong-Ho Lee, June Sun Kim, Kyu Jung Lee and Sun Ho Pyun
Gold Star Cable Co., Ltd., Anyang 171 Korea

In the wire coating extrusion, where wires of various kind of colors are to be produced, the changing of colors is time-consuming and uneconomic if dyestuff/masterbatch is supplied through the extruder hopper. For the purpose of the improvement of such a process, a novel method of the changing of colors is described in this paper.

At the exit of an extruder, extrudates are devided into two streams, i.e. one of which constitutes the inner layer of the wire insulation and the other stream is mixed with suitable pigments and used as the outer colored skin layer. The liquid pigment is injected uniformely by a gear pump according to predetermined pigment/extrudate ratios at the extruder exit. Then the extrudate of base resin is mixed with the liquid pigment through a motionless mixer and reached the cross head where the wire conductor is covered with double layers.

As Schott et al (Chem. Eng. Prog., Vol. 71, p54-58, 1975) have reviewed, the motionless mixer contributes to mix the polymer melt(LDPE, soft PVC etc) and the liquid pigment which have much different viscosities. However, the longer the length of the motionless mixer, more pressure drop is caused. Therefore, an additional equipment is indispensible for the compensation of the pressure drop and the effectiveness of the motionless mixer is reduced. In this study, an adjunct mixing head is designed for the premixing of constituents prior to the mixing by the motionless mixer and this attributes not only to shortening the length of the motionless mixer (L/D - ca. 9) but also makes it unnecessary to use an additional equipment for the pressure drop compensation.

For the analysis of the machine performance of the novel system, both qualitative and quantitive evaluations of the mixing performance is tried. The influence of operating conditions upon the mixing performance is also investigated to identify optimum conditions for mixing. Power consumptions of the system under various operating conditions are examined for the evaluation of mixing energy efficiencies. The novel system is applied for the production of 10 different colored wires in a 60mm single screw extruder. Data on the quality of colored extrudates including physical and electrical properties are compared with those of the intensively mixed blends using a roll mixer. The performance characteristics of the system proves the expected improvement of processibility through cost savings by reduced consumption of polymers, lower reject rates and shortening of changing time of colors in comparison with those of the conventional dyestuff/masterbatch system.

Finally, the mixing performance with various additives other than the liquid pigment and the automation of the system is now under study.

MILL-BEHAVIOUR OF EPDM-RUBBERS WITH DIFFERENT MOLECULAR STRUCTURES IN RELATIONSHIP TO THEIR MIXING IN INTERNAL MIXERS

Jacobus W.M. Noordermeer and Mathias Wilms
DSM Kunststoffen B.V.
Applied Research & Technical Service Elastomers
PO Box 604, 6160 AP Geleen, The Netherlands.

The mixing behaviour of various EPDM-rubbers with different molecular weight distributions and long chain branching, has been studied in a 3-liter internal mixer. An average EPDM-compound recipe with 70 phr FEF-black, 40 phr SRF-black and 70 phr naphthenic oil was used. Electrical resistivity measurements were used to quantify the quality of the carbon black dispersion.

For EPDM-types with a narrow molecular weight distribution and little long chain branching a conspicuous plateau in carbon black dispersion is observed as a function of mixing energy and batch-temperature.
These products pass through a period in the mixing-process, in which the energy supplied to the compound is primarily converted into a temperature-rise of the mix and further transferred to the cooling-system, instead of being used for an improvement of the carbon black dispersion. Only when the temperature of the compound has reached a sufficiently high level the carbon black distribution starts to improve again. For EPDM-types with a broad molecular weight distribution such a plateau-behaviour is not observed.

In literature (N. Tokita and J.L. White, J. Appl.Polymer Sci., 10, 1011-1026 (1966)) it is discribed, that the behaviour of pure rubber on a two-roll open mill can be divided into four distinctive regimes depending upon the mill dimensions, roll speeds and operating temperature. In Regime 1 the highly elastic rubber will not move without difficulty into the mill nip. In Regime 2 a good elastic band is obtained on one of the rolls. In Regime 3 the elastomer crumbles and cannot be massed. In Regime 4 a melt fluid coats on one of the rolls.

Progressive transitions from one regime to a higher one can be brought about, among others, by raising the temperature. These regimes differ with respect to the mixing efficiency, which can be achieved while the rubber passes through those regimes, due to greatly different shear forces which can be generated.

Characterising the pure rubbers in terms of above mentioned regimes is for practical reasons not possible in an internal mixer. To obtain an impression on how the EPDM-rubbers, used for this study, behave in terms of these regimes as a function of temperature, they have also been investigated on an open mill.

While during the normal rubber mixing cycle oil is being mixed in and this oil will influence the rheological behaviour of the pure rubber, the influence of oil extension on the mill-behaviour was also studied.

The difference in mill-behaviour between a narrow molecular weight distribution EPDM-rubber and a broad one can clearly be observed. The narrow distributed polymer shows a predominantly regime 3-behaviour, except for very narrow nip-widths at low temperatures, and shows a transition to fluid behaviour, regime 4, at 100 to 125°C. The broad distributed polymer shows a predominantly regime 2 behaviour, a narrow band regime 3 and only for large nip widths and at high temperatures a regime 4 behaviour.

The influence of oil-extension is, that the regimes 2 and 4 grow at the expense of regime 3. For the broad molecular weight distribution rubber the regime 3-behaviour completely disappears.

The transition from regime 2 to 3 is linked to the internal failure characteristics of the pure rubber, as a function of temperature, resulting in internal crazing or crumbling before high enough stresses are built up to break carbon black agglomerates. This phenomenon can be related to the green elongation of pure EPDM-rubber as a function of its Ethylene/Propylene ratio and its dependence on temperature.

The transition from regime 3 to 4 is related to an increase of the viscous behaviour of the rubber relative to the elastic behaviour. The broad molecular weight distribution polymer has a strongly enhanced elastic behaviour relative to the narrow distributed rubber, which enhances regime 2 behaviour, directly changing in regime 4 behaviour without showing a regime 3.

On the basis of these regimes in the behaviour of the pure rubber, the phenomena observed during mixing in the internal mixer can be interpreted as an intricate balance between distributive and dispersive mixing.
Distributive mixing taking place mainly in regime 3, but without an improvement of the carbon black dispersion.
Dispersive mixing taking place when the rubber is in regime 2 or 4, with an improvement of the carbon black dispersion.

6/8

DETERMINATION OF THE DEGREE OF GELATION OF PVC WITH DCS

H. Potente, P. Michel (University of Paderborn, West Germany)
S. M. Schultheis (Alpine AG, 8900 Augsburg, West Germany)

It is shown that the degree of gelation of PVC blends can be precisely determined with the DSC analytical method. Measurement and subsequent evaluation are performed computer-controlled. In this way the influence of the operating personnel is eliminated.

Besides the determination of the degree of gelation of PVC, the accurate determination of the processing temperature with the DSC method is of paramount importance. Due to the required low sample amounts (about 10 mg for every measurement) it is possible to study the processed PVC as regards temperature inhomogeneities and thus to evaluate the processing aggregate and the selected operating point.

After polymerization PVC is obtained as a powder. The grain is an agglomerate of primary particles. These primary particles are called globulites. They exhibit a fine structure, the so-called fibrils. This structure is the same with all PVC grades with the exception of S-PVC which, as regards manufacture (suspension polymerization), in addition possesses a protective colloid skin which bulk and E-PVC (emulsion PVC) do not have.

Processing of plasticized PVC consists of two steps, compounding and gelation. A distinction is made between precompounding and final compounding. Precompounding, which is performed in a mixer, involves homogeneous mixing of the components of the PVC blend (PVC, plasticizer and additive). Liquid components diffuse into the powder grains whereas solid components are distributed homogeneously. The dry blend thus obtained is susceptible to flotation but still cannot be subjected to melting.

Final compounding is effected by shearing at 130 to 150 °C, i. e. below the gelation temperature. In this process the powder grains are destroyed, and the structure of the blends is now dependent on the globulites. At the prevailing temperatures the low molecular additives are low-viscous liquids which homogeneously coat the surface of the globulites. The globulites are still not fused. Compounding has now been terminated.

Completely compounded PVC can be fused by simple heating. For this process the term "gelation" has come into use which simply means melting of globulites.

The degree of gelation G is a structural characteristic parameter which varies between 0 and 100 %. It gives the percentage of the maximum degree of melting reached during processing. The parameter G is thus suitable for the quantitative characterization of different melting stages of PVC. Thus, G = 0 % designates a completely unfused material; G = 100 % characterizes a completely fused material.

With the DSC analysis the following characteristic values can be determined:

- glass transition temperatur T_G,
- final processing temperatur T_M,
- decomposition temperatur T_Z,
- gelation during the processing,
- post-gelation.

For each of these parameters the reproducibility error is ca. 1%.

The studies were performed with a control and evaluation system (model TA 3000, manufacturer Mettler, Gießen).

The degree of gelation C is obtained form the relation

$$G = \frac{H(a)}{H(a) + H(b)} \quad 100\ \%$$

where H(a) refers to the enthalpy of a region called 'a'and H(b) to the enthalpy of a region called 'b'. The enthalpies H(a) and H(b) are obtained from the DSC evaluation programme "Peak Integration". The degree of gelation can therefore directly be calculated so that a standardization (MFI) is no longer required.

As test material a commercial HI-PVC, compounded in a heating mixer at 100 °C, was employed. Weighed samples of 120 g each were processed to a rolled sheet on a laboratory roll mill. The roll temperatures were thereby, under otherwise equal conditions, raised from 160 to 220 °C in steps of 10 K. The degree of gelation of the resulting seven rolled sheets was determined by the following quantitative methods:

- MFI determination
- DSC determination of the degree of gelation

The results obtained

- MFI determination

- DSC determination of the degree of gelation

The results obtained with both methods (DSC, MFI) are compiled.
The two curves are in good agreement.

COMPOUNDING FROM A TWIN SCREW VIEWPOINT

David B. Todd
APV Chemical Machinery, Inc.
(Baker Perkins/Sterling Extruder)
South Plainfield, New Jersey 07080

The tasks involved in compounding generally involve melting the polymer, mixing in and uniformly distributing the additives, breaking up agglomerates, perhaps venting, and developing pressure for forming or pelletizing. With twin screw extruders, the processing behavior in feeding, venting, and pressure generation is quite similar to that of single screw extruders, but with some specific differences which may warrant a different processing approach. For example, most twin screws can be starve-fed, and rate control reverts to the upstream feeder(s) rather than extruder screw speed.

It is the kneading paddle portions of twin screw extruders which most set them apart from single screw extruders, and which provide basically different mechanisms for the melting, dispersing, and distributing tasks. Within the twin screw catagories even these mechanims differ significantly between corotating and counterrotating and between tangential and fully intermeshing selfwiping variants.

The kneading paddle sections of self-wiping corotating twin screw compounders provide mixing action by three mechanisms. First is the dispersive action of the face of the paddle itself, against its opposing paddle as well as against the wall. This action contributes to rapid input of energy for breakup of agglomerates as well as melting of polymer.

The second mechanism is a compression-expansion kneading action as a consequence of the changing volumes between rotor and barrel across every section, creating unique combinations of extensional and shear flow. This kneading action is strongly dependent upon the degree of fill of the cross section, so control of degree of fill provides control over mixing intensity and energy input.

The third mechanism is reorientation of the polymer not only peripherally as it passes from one barrel to the other, but also axially as flow from the paddle on one rotor interacts (like scissors) with the next upstream and downstream paddles on the opposite rotor.

All three mechanisms are dependent upon the width of the paddles and the relative orientation of the next upstream and downstream members. Staggering the paddles in a forwarding array provides some of the conveying capacity (drag flow) of regular feed screws. The peripheral gaps between successive paddles have a strong influence on the leakage or pressure flow characteristics. The Erector-set approach to rotor design enables twin screw compounders to be constructed to meet a very broad range and sequence of process applications.

6/10

"A NUMERICAL PROCEDURE FOR EVALUATING THE EFFECT OF THE NIP REGION GEOMETRY ON THE MIXING PERFORMANCE OF A NON-INTERMESHING COUNTER-ROTATING TWIN SCREW EXTRUDER"

by

David Bigio

Saeid Zerafati

University of Maryland
Department of Mechanical
College Park, MD 20742

Twin screw extruders in general, and non-intermeshing, counter-rotating twin screw extruder (CRTSE), in specific, are being called upon to perform intricate mixing tasks, in which, maintaining the properties of the polymers to very close tolerances is critical for product quality. The use of blending, fillers, and multiple fluid systems are being used to satisfy various application requirements.

Recent studies have shown that the degree of mixing achieved by the CRTSE, strongly depends on the flow field induced in the region of intersection between the two screws. This region where fluid flow in the downchannel direction of the screws intersects with the flow in the machine direction, is called nip region of the extruder. Moreover, the nip region geometry may be a major factor in causing the greater-than-linear mixing performance in this extruder.

Until now, many of the studies on mixing processes has been carried out experimentally (mainly providing bulk information about the performance of the extruder). Experimental results give little insight to the mixing and, moreover, in this method, change of geometry needs a great deal of effort and is expensive and time consuming.

A numerical approach which accounts for mixing is needed to distinguish the effects of different parts of the region and the effect of the geometry of the nip on mixing. In the first attempt to provide these information, a 2-D model of the nip region of a CRTSE with appropriate boundary conditions was chosen. Solving this complicated flow problem using analytical methods seemed to be impossible therefore, a FEM code, called FIDAP, was used for finding the solution to the fluid dynamic equations. This software was available to us on CRAY X-MP at the San Diego Supercomputer Center.

A critical part of the solution was the determination of a measure for mixing. Line and area growth as a function of total average strain have long been accepted as measure of mixing in creeping flow. Therefore, we developed a software called LINE for tracking an arbitrary interface in the nip region. In this program the velocity and position outputs from FIDAP are used as input. Each interface is represented by a number of segments comprised of a finite number of points. The code determines the location of the points (and hence the position of the interface) at each time step, finds the velocity at that point by bilinear interpolation and uses second order Runge-Kutta method to determine the next location of the point after each time step. At the end of each step, to insure the linear assumption, the segment is sub-divided into two smaller segments, wherever a given length value is exceeded. The output of this program is the length of the interface at each time step and the rate of growth of the line as it travels through the region.

Orientation of the interface relative to the rate-of-strain tensor was measured by the intersected angle. The change of the angle for the interface relative to the local velocity field as it proceeded through the nip region is a direct measure of changes in the rate of mixing. It was found that changes in the rate-of-strain tensor affect the orientation of the interface, increasing mixing rates.

Several interfaces are inserted into different parts of the region determining their growth as a function of and total growth upon leaving the region are determined.

The effect of different parameters of the nip region (like depth of the channel, apex opening, velocity of screws, etc.) on the mixing, can be easily determined by running FIDAP, LINE and the measurement algorithm, for each configuration. The orientation angle yields added insight as to the causes of increased mixing rates. Conclusions are drawn as to which parameters more strongly affect mixing.

In order to be able to do the above tasks and relate different programs, a job control program was developed on CRAY. This program can be modified, to optimize the nip geometry in order to get the best mixing, automatically.

NON-NEWTONIAN FLOW MODELLING OF A MODULAR INTERMESHING COROTATING TWIN SCREW EXTRUDER

by

W. Szydlowski and J. L. White
Polymer Engineering Center
The University of Akron
Akron, OH 44325 U.S.A.

The authors have undertaken an extensive investigation of flow in modular intemeshing corotating twin screw extruders. (For a recent review of twin screw extrusion technology, see our paper (1).) The screws have not only right handed forward pumping screw elements, but backward pumping screws and kneading discs. The latter are mixing elements. Earlier research by the authors have used hydrodynamic lubrication theory to simulate the flow of Newtonian fluids in both screw (2) and kneading disc (3,4) elements.

More recently a composite model has been developed which combines the responses in individual screw and kneading disc modules to represent system performance.

Experimental studies using a clam shell barrel unit on a Werner and Pfleiderer ZSK-30 twin screw extruder have been carried out in our laboratories. These researches indicated that while kneading disc regions were primarily filled with polymer, right handed screw elements were largely starved, except in front of the die.

We report here modelling of flow in an intermeshing corotating twin screw extruder using a power law fluid. Hydrodynamic lubrication theory and modified FAN methods are used. Emphasis is placed on the kneading disc region of the machine. The influence of non-Newtonian shear viscosity on the pressure field and fluid fluxes in the kneading disc region is considered. Different approximate methods of representing power law shear viscosity in the modified FAN method are used and contrasted.

References

1. J. L. White, W. Szydlowski, K. Min and M. Kim
Adv. Polym. Techn. 7, 295 (1987)

2. W. Szydlowski and J. L. White
Adv. Polym. Techn. 7, 177 (1987)

3. W. Szydlowski, R. Brzoskowski and J. L. White
Int. Polym. Proc. 1, 107 (1987)

4. W. Szydlowski and J. L. White
Int. Polym. Proc. 2, 000 (1988)

5. J. L. White and W. Szydlowski
Adv. Polym. Techn. 7, 419 (1987)

EXPERIMENTAL COMPARISON BETWEEN INTERMESHED COUNTER- AND CO-ROTATION TWIN SCREW EXTRUDER ON INORGANIC FILLER COMPOUNDING CHARACTERISTICS

Tadamoto Sakai, Japan Steel Works
Funakoshiminami 1-6, Aki-ku, Hiroshima, Japan

The device which is possible to study the melting zone of twin screw extruder independent of the molten polymer mixing zone has been manufactured, and the influence of intermeshing type and screw rotational direction has been investigated using same twin screw geometries. In this report, the relationship between the melting behavior and inorganic filler dispersion of the extrudates obtained from the exit of the melting region has been described.

Raw materials used in this study is Polypropylene- $CaCO_3$ compound fed separately from two hopper. Filler dispersion has been evaluated from the agglomerate size at the exit of the melting zone. The $CaCO_3$ concentration of 30% and 50% was used respectively.

[EXPERIMENTALS]

The experimental results concerning dispersion and melting behavior are as follows;

polymer material: pellet feeding ($CaCO_3$ 50% addition)

twin type (meshing)	speed (rpm)	output (kg/h)	Tp (°C)	Esp (kg/hkw)	Mix.grade	remark
Intermesh.	350	35	208	0.124	8.9	adiab.
co-rotatn.	350	53	198	0.100	9.2	"
twin	500	36	228	0.135	6.9	
screw	500	72	203	-	9.3	
Intermesh.	500	36	228	0.119	5.5	adiab.
counter-	500	52	219	0.108	7.4	
rotation	500	70	197	0.104	8.5	
twin	350	36	216	0.101	6.4	
screw	350	54	203	0.086	8.6	
non-inter.	350	32	236	0.137	7.8	adiab.
counter-	500	19	265	0.161	3.3	
rotation	500	32	248	0.147	6.5	

Esp: specific energy at mixing zone
Tp : polymer temperature

(1) $CaCO_3$ dispersion was improved as ouput was decreased at same screw speed.

(2) The dispersion was improved as screw speed was increased at same output rate operation.

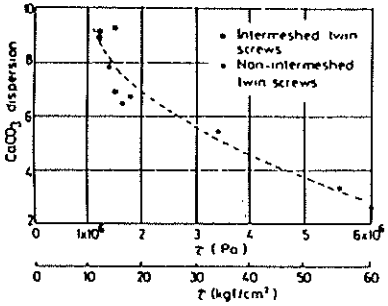
(3) When compared with the counter-rotation and co-rotation, the dispersion obtained from counter-rotation twin screws was better than that of the co-rotation.

(4) When compared with powder and pellet as polymer material, the former dispersion was better.

(5) Cooling of the screw and cylinder had no improvement effect for $CaCO_3$ dispersion.

(6) It was very important to decrease the agglomerate size at the melting zone as much as possible, even if the dipersion was much improved at the molten polymer zone.

[DISCUSSION]



The relationship between the shearing stresses theoretically calculated at the melting zone and the dispersion of the extrudates obtained experimentally was studied. As a result, there was a close tendency that shear stress at the melting zone had the influence on the dispersion at the exit of the melting region. This result showed that screw geometry should be designed properly so as to fit for the pysical or rheological properties of compound.

[APPLICATION]

Using the twin screw extruder having the change lever to operate both of the counter- and co-rotation was used for the practical compounding operation. Some interesting compounding aspects have been obtained.

[REFERENCE]

1) T.Sakai, Japan Soc. of Mecha. Eng. 47(420) p 156,('81)
2) T.Sakai, Japan Soc. of Mecha. Eng. 48(431) p1306,('82)
3) T.Sakai, Japan Soc. of Mecha. Eng. 48(446) p2078,('82)
4) T.Sakai,et al SPE ANTEC '87 (Los Angeles) p 146,('87)

EXPERIMENTAL STUDIES OF FLOW VISUALIZATION AND PERFORMANCE OF A NON-INTERMESHING COUNTER ROTATING TWIN SCREW EXTRUDER

BY

K.Min, M.H.Kim and J.L.White

Polymer Engineering Center
The university of Akron
Akron, Ohio 44325 U.S.A.

A laboratory counter rotating non-intermeshing twin screw extruder with various modular elements and tangential/transverse apex glass windows was designed and built in our laboratory. It allows us to visualize dynamic flow behavior of materials in the twin screw extruder

A systematic, experimental study was coducted on the flow behavior and performance of the twin screw extruder including the pressure profile along the length of the screw channel. A comparison among the various assemblies of modular elements including forward pumping and backward pumping screw elements was carried out. Comparisons were also made of configurations with matched and staggered screw flights.

The matched configurations exhibited a higher throughput and pressure rise than the staggered configurations. For right-handed screws, the pressure rises monotonically. Left-handed screw elements produce regions of decreasing pressure. The magnitude of the difference of Q between matched and staggered configurations increase for both pumping forward and pumping backward screw arrangements with increasing pressure as shown in Figure 1. A correlation between the pumping characteristics and the geometries of modular elements was developed using composite model[1].

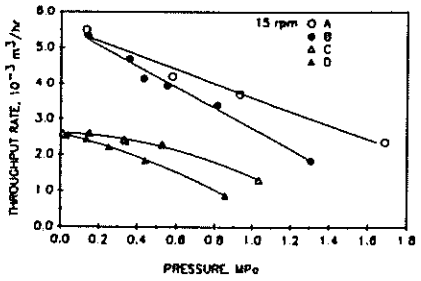


Figure 1. Screw characteristic curves Q-Δp for various configurations A,B,C and D at fixed screw speed, N.

Flow patterns in the various configuration have been observed through the lower tangential and apex transverse glass windows. In most of cases, tracer particles indicated that there was no interscrew migration except a configuration including staggered backward screw elements. For a staggered flight configuration with left-handed screw elements transfer flow in the apex area was viewed.

The melting mechanism was observed through tangential apex area glass windows. The melting transition occured in the second chamber. Our results were different from those of previous reseachers[2-5], largely for tangential counter-rotating twin screw extruders. We observed that the melting pool could develop on the advancing flight and move towards the center of the screw channel as one moves along the channel. Eventually the melt pool seemed to move to the opposite flight. The solid bed seemed to hold together without breaking up.

REFERENCES

1. J. L. White and W. Szydlowski; Adv. Polym. Tech., 7, 419 (1987)
2. A. Kaplan and Z. Tadmor; Polym. Eng. Sci., 19, 58 (1974)
3. T. Sakai; Nippon Kikai Gakkai Ronbunshu B47, 420 (1981)
4. T. Sakai; Gosei Jushi, 29, 7 (1978)
5. R. J. Nichols and F. Kheradi; Mod. Plastics 61(2), 71 (1984)

Filling and Residence Time Distributions in Mixing Regions of Co-rotating Twin Screw Extruder

Kevin L. Nichols, Krishnamurthy Jayaraman, and Eric A. Grulke,
Michigan State University, East Lansing, Michigan 48824-1326

The objective of this work was to investigate the degree of filling in mixing regions of a co-rotating intermeshing twin screw extruder over a range of operating conditions and mixer configurations. The degree of filling was determined from mean residence time measurements at different axial locations along the extruder, and also examined visually by opening up the clam-shell type barrel of the twin screw extruder. The operating variables were feedrate of polymer (10-40 g/min), screw rotation rate (100, 250, 500 rpm), barrel valve position (fully opened or fully closed), and flow characteristic of the polymer (viscosity vs. shear rate). The "twin screws" in this work consisted of two distinct mixing sections separated by screw sections. The mixing sections were made up of six consecutive slip-on kneading paddles followed by orifice plugs. Orifice plugs in conjunction with a barrel valve are used to control the cross sectional area available for flow. In the experiments performed here the solid to melt transition was completed in the first mixing zone. The density change upon melting in the first mixing zone makes it difficult to determine the volumetric hold-up of polymer in this zone. However, the volumetric hold-up of polymer melt in the second mixing zone can be estimated quite accurately from the mean residence time.

A novel aspect of the residence time experiments done here is that the tracer was chemically identical to the extruded polymer. This was accomplished by selecting polymers containing chlorine, such as polyvinyl chloride (PVC) and chlorinated polyethylene (CPE), to extrude where the tracer was a radioactive chip of the polymer (the chlorine was neutron activated). It is possible to obtain chlorinated polymers with a wide range of physical properties. In this study, one PVC and one CPE compound were used. The CPE compound and PVC compound had similar viscosities at low shear rates, but the CPE compound was more shear thinning and more elastic than the PVC as shear rate increased. The residence time experiments were performed by injecting a radioactive chip into the feed port of the extruder, after steady state was achieved at a given set of operating conditions. Then the intensity of gamma radiation through the wall of the extruder at one of three axial positions(after 1st or 2nd mixing zone or at the end of the screw) was monitored as a function of time.

Visual examination of the screws in several runs revealed that the restriction at the orifice plugs as well as the amount of forwarding in the paddles upstream of the orfice plug are key to the degree of filling. During any experiment in which the screws contained two mixing zones (with paddles and orifice plugs) there was little polymer in the screw type segments and most of the polymer was contained in the mixing zones or in the die attachment after the end of the screw, but even the mixing zones were not completely full. The polymer appeared to travel axially between the different hold-up regions by breaking off from around the orfice plugs in small chunks, and then being forwarded quickly by the screw type segments. When the extruder was operated without orifice plugs or with the paddles replaced by continuous screw sections, the entire screw appeared starved.

For the first mixing zone which contains the solid to melt transition region, the mean residence time of PVC decreased with feedrate at a constant screw rotation rate, where the magnitude of the decrease was much greater for 100 rpm than for 250 or 500 rpm. The mean residence time also decreased with increasing screw rotation rate, where this effect was much greater at low feedrates than at high feedrates. At the same mass feedrate and screw rotation rate the mean residence time of CPE compound was always less than half that of the PVC compound in the first mixing zone. The standard deviation in residence time about the mean is a measure of axial dispersion. This measure for the first mixing zone, in most runs, was close to that for the entire extruder, indicating that axial dispersion occurs mostly in the first mixing zone. The effect of changing barrel valve position from completely closed to completely open, on the mean residence time in the first mixing zone, was quite sensitive to operating conditions as well as polymer type.

In the second mixing zone which contained all melt, the mean residence time decreased with increasing feedrate of PVC or CPE, but the hold-up increased with increasing feedrate. An increase in screw rotation rate caused a decrease in holdup of PVC in the second mixing zone but had little effect on the hold-up of CPE. At the same screw rotation rate, the hold-up of CPE in the second mixing zone was one half to one third that of PVC at low feedrates, however at high feedrates the volumetric hold-up of PVC and CPE in the second mixing zone was about the same. A more forwarding arrangement of kneading paddles in the second mixing zone resulted in a lower hold-up of polymer under similar operating conditions. In all cases, opening the barrel valve caused the hold-up of PVC in the second mixing zone to increase, while opening the barrel valve had little effect on the hold-up of CPE in the second mixing zone.

In conclusion, trends in the degree of filling and residence times for the mixing zones are quite sensitive to the paddle configuration, the restriction at the orfice plug, and polymer properties. The spread in residence time distributions within the extruder is mostly a result of the mixing process in the first mixing zone where the solid to melt transition is completed.

7/1

RHEOLOGY AND PROCESSING OF THERMOPLASTIC ELASTOMERS

L. A. Goettler and J. R. Richwine, Monsanto Chemical Company,
260 Springside Dr., Akron, OH 44313

Thermoplastic elastomers are rubbery polymers that combine the performance properties of thermoset rubbers with the efficient fabrication characteristics of conventional thermoplastics. Their applications in the common processing methods of extrusion, injection molding, and blow molding, along with some specialty operations like foaming and hose or wire and cable covering, will be reviewed in this paper. Also included will be the development of pertinent relationships to the melt rheology, by which fabricability can be predicted.

The major classifications of thermoplastic elastomers include: styrenic block copolymers, rubber-polyolefin blends, elastomeric alloys, thermoplastic polyesters, thermoplastic polyurethanes, and thermoplastic polyamides. These permit a wide variety of commercial products (about 40), each with its own characteristic rheology, that provides a spectrum of processing performance and design flexibility.

While the rubber industry may better understand the mechanical performance, design and marketing of thermoplastic elastomers, their distinct advantage in simpler and more economical processing routes is most familiar to the thermoplastics processor. These include the virtual elimination of the need for compounding or blending, which introduces much variability into conventional rubber stocks, faster thermoplastic fabrication, in which final properties can be developed simply by cooling of the fabricated part below its melting point, and the ability to reuse scrap, simply by grinding it and reforming at temperatures above its melting point. In addition to simplicity, the thermoplastic processing route is also more energy efficient, which adds to processing economics.

The broad range in rheological characteristics of thermoplastic elastomers is very similar to that found in conventional plastic materials. Thus they enjoy the same latitude of processing capabilities, such as the ability to fill out injection molds, to produce extrusions at high rates with smooth surfaces, and to provide high draw ratios that are necessary for good performance in stretching operations like blow molding and thermoforming.

Metal or high melting plastic inserts can be over-molded with a thermoplastic elastomer to add a rubbery functionality to a rigid substrate. Bonding can be achieved either through the use of an adhesive layer preapplied to the insert, or by direct fusion bonding when the plastic insert composition is compatible wih the TPE melt. This technology has been applied in the direct injection molding of caster wheel treads around a polypropylene hub, for example.

In the extrusion area, the processing attributes of thermoplastic elastomers can be exploited in the efficient production of complex solid or foamed profiles, including coextrusions, along wih hose and wire and cable coverings. Their unique rheological properties permit the production of high precision components without the need for special forming or sizing equipment in the takeoff train.

The blow molding process is not common in rubber fabrication. Rubber molders have been limited to relatively small hollow parts that incorporate thick wall sections to facilitate removal from the hot mold without tearing. These restrictions are removed with thermoplastic elastomers, which open up the process window to conventional practice.

Thermoplastic elastomers thus offer the processing ease common to plastics. As part of the thermoplastic class of polymers, they can take advantage of the high productivity, low scrap, and good dimensional tolerance capabilities of thermoplastic processing to produce economical alternatives for thermoset rubber components. In addition, a range of materials is available, and new products are being developed and introduced to the marketplace at a rapid rate to serve special applications. All of these attributes are offered along with favorable economics to make thermoplastic elastomers a strong contender to conventional materials in the rubber industry.

7/2

IMPROVING THE PROCESSING OF THERMOPLASTIC ELASTOMERS

J. P. Vander Kooi, B. C. Howard, D. R. Hall
Struktol Company, Stow, Ohio 44224

A relatively new family of compounded materials are the thermoplastic elastomers; these TPE's have physical properties which exhibit typical rubbery behavior but when processed behave as filled plastics. Since they typically process with some degree of difficulty, attempts to improve the process characteristics of some TPE's has led to the evaluation of process modifiers in a variety of rubbery thermoplastics.

It has long been recognized that chemical additives can improve flow characteristics through various forms of plastication. In the rubber and plastics industry, petroleum products and fatty acid derivatives have been a valuable component of compound recipes (1,2). In this study, a representative material in each class has been examined as an additive in commercial TPE's. Struktol TR 060 is a mixture of light colored aliphatic resins with a molecular weight less than 2000. Struktol TR 016 is a blend of metal fatty acid salt and amide with sites available for hydrogen bonding. The materials were incorporated into the TPE's in normal polymer processing equipment and evaluated for effect in mixing, processing, and physical properties.

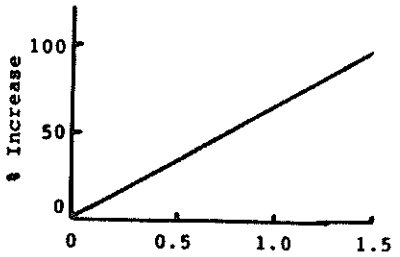
The processing agents showed many positive qualitative and quantitative results in TPE. Improved uniformity and efficiency are noted in mixing and processing. The processing improvements have been achieved without detrimental effects to cost and finished good properties.

References

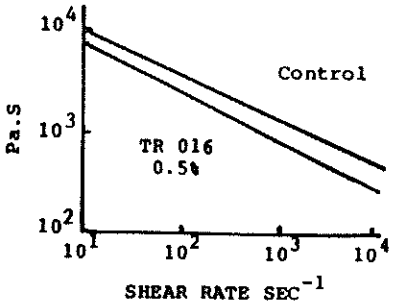
1. Blue Book, published by Rubber World Magazine, Lippincott & Peto, OH, (1987).

2. E. W. Flick, "Plastics Additives, An Industrial Guide," Noyes Publishing, NJ, (1986).

CAPILLARY FLOW RATE
BLOCK COPOLYMER



APPARENT VISCOSITY
PP/EPDM



PROPERTIES
OLEFINIC TPV

	Control	TR 016	TR 060
Level	--	0.75 Phr	0.75 Phr
Mold Release	Good	Very Good	Good
Flow	Good	Excellent	Excellent
Bloom, 30 Days	None	None	None
Injection Molded			
Tensile, psi	590	610	580
300% Modulus	500	590	570
Elongation %	310	320	310
Hardness	56	56	55
Knit Flow	100%	100%	100%
Extrusion			
Die Swell %	+4.69%	+3.95%	+4.76%
Spiral Flow			
% Change	--	+9.8%	+16.9%

BENEFITS

Mixing:
- Improves filler incorporation and mixing efficiency.

Molding:
- Improves flow during injection molding.
- Improves mold release, especially filled systems.
- Increases parison hot strength for blow molding.
- Surface appearance improved.
- Non-blooming at low levels.

Extrusion:
- Improves extrusion uniformity.
- Reduced die swell.
- Improves surface appearance.

Properties:
- Maintained or improved.

7/3

SCANNING ELECTRON MICROSCOPIC STUDIES OF GELATIONS OF FUSION OF PVC PLASTISOLS WITH PLASTICIZERS OF VARYING SOLVENT POWER

by

N. Nakajima and M. R. Sadeghi
Polymer Engineering Center
The University of Akron
Akron, Ohio 44325 U.S.A.

PVC plastisol is a well-established commercial material (1,2). It is a paste consisting of a mixture of plasticizer and fine particles of PVC. The plastisol is processed through various techniques such as dip-coating, slush molding, rotational molding and knife-edge coating. In these processes common features are to spread plastisol on a substrate and to heat it in an oven to make a finished product through gelations and fusion. In the gelation step the plasticizer becomes absorbed in PVC particles, changing the system from a liquid suspension to a solid of low cohesive strength. Only after heating at a higher temperature, e.g., 190°C the material becomes completely uniform, achieving the inherent strength. This process is called fusion.

In the previous works viscoelastic measurements were used to follow the progress of gelation and fusion. A characteristic change of moduli were recorded, providing a unique finger-print for each resin-plasticizer system (3). The resin variables included in the finger-printing were molecular weight (3), extractable additives (emulsifiers), (3) agglomerates and fine particles (4) and size of primary particles (5).

With selected samples of plastisol, morphological changes during the gelation and fusion were followed with a scanning electron microscopy, (SEM). The retention of the particulate structure, swelling of particles and gradual disappearance of the particle boundaries were observed at various stages of gelation and fusion (4) (6). These structural changes were contrasted with and used to interpret the changes in viscoelastic behavior. A plasticizer used in these studies was di-2-ethyl hexyl phthalate (DOP). The present work is an extension of the above work to include several plasticizers, having varying solvent power; they were dioctyl phthalate, dioctyl sebacate, dibutyl sebacate and tricresyl phosphate.

The scanning electron micrographs indicated complex variations of solvent power of plasticizers with respect to its temperature and concentration dependence. Although this information is only relative and not quantitative, such information has not been obtained from quantitative measures of viscoelastic properties during gelation and fusion. Therefore, SEM offers unique information which is not obtainable otherwise.

References

1. "Plastisols", Encyclopedia of Chemical Technology, 3rd ed., Wiley, New York, 1983, vol. 23, p. 922.

2. "Plastisols", Encyclopedia of Polymer Science and Technology, Wiley, New York, 1971, vol. 14, p. 370.

3. N. Nakajima and D. W. Ward, J. Appl. Polym. Sci. 28, 807 (1983).

4. N. Nakajima, J. D. Isner and E. R. Harrell, Polym. J. 13, 955 (1981).

5. N. Nakajima and E. R. Harrell, Adv. Polym. Technol. 6, 409 (1986).

6. N. Nakajima J. D. Isner and E. R. Harrell, J. Macromol. Sci. - Phys. B20, 349 (1981).

7/4

EXPERIMENTAL AND THEORETICAL STUDIES OF THE BEHAVIOR OF RUBBER COMPOUNDS IN A PIN BARREL SCREW EXTRUDER

by

Y. Yabushita, R. Brzoskowski, J. L. White and N. Nakajima
Polymer Engineering Center
The University of Akron
Akron, OH 44325 U.S.A.

An experimental and theoretical study of the mechanism of flow of rubber compounds in a pin barrel extruder (1,2) is presented. Special attention is given to evaluate the role of pins and grooves in the mixing process and to compare mixing and pressure generation capabilities of the pin barrel extruder and an equivalent cold feed rubber screw extruder.

Two types of experiments were carried out. First, we obtained extrusion rate Q - pressure development Δp data for the pin barrel section and equivalent screw section. Next, using 'screw pushing' (3) experiments, the flow pattern of the rubber compound in the pin barrel section was investigated. For "flow pattern" experiments, the extruder was fed simultaneously with two black and white strips of the rubber compounds. After steady state extrusion had been achieved, the rubber was cured and the screw removed. A butadiene-styrene copolymer-polybutadiene carbon black compound called PTT, was used in all of our experiments (3).

The flow of rubber compounds in the pin barrel extruder was also described with the help of two methods (4). (i) The flow analysis network method, which gives two-dimensional simulation of the flows, and (ii) an analytical method. In both cases, the flow was considered as laminar and isothermal, entrance and exit effects and gravity were neglected. The rubber compound was assumed to be incompressible and to exhibit Newtonian behavior.

Both the theoretical and experimental results demonstrate that the pin barrel section is a poorer pump than the normal screw section. It means that grooves in the flight reduce pressure generating capabilities and extruder output. The pin barrel extruder gives however, much better mixing. The reorientation and stretching of the rubber by the moving pins are the key factors in the mixing process. Another mechanism of mixing develops in the high shear zone; it is in the region where the pins pass through the grooves in the screw flights. Repeated passage through these zones aid the dispersion.

References

1. G. Menges and E. Harms Z. Kautschuk Gummi u Kunststoffe 25, 469 (1972)

2. G. Menges and E. Harms, Ibid 27, 187 (1974)

3. R. Brzoskowski, K. Kubota, K. Chung, J. L. White, F. C. Weissert, N. Nakajima and K. Min
Int. Polym. Proc. 1, 130 (1987)

4. R. Brzoskowski, J. L. White, W. Szydlowski, N. Nakajima and K. Min, Int. Polym. Proc. (in press).

7/5

NUMERICAL SIMULATION OF TIRE CURING PROCESS

B. Chung, J. P. Chang, and M. S. James
General Tire, Inc.
Akron, OH 44329

ABSTRACT

Tire curing is an important and time-consuming step in the tire manufacturing process. The green tire (tire before cured), initially at ambient temperature, is cured in the curing press at high temperature environment provided externally by the steam-heated mold and internally by high temperature medium, e.g., high pressure steam or high-temperature nitrogen. The tire performance, for example, rolling resistance, can be significantly affected by the curing time, temperature, and history. Since rubber is a poor heat conductor, a typical curing time in the mold varies from 10 - 16 minutes (for passenger tires) to 60 minutes (for medium truck tires). How to cut down the curing time in the mold to boost the productivity without hurting the tire performance is the major concern in the tire industry. However, this is not an easy task due to the nonuniform curing history throughout the tire, resulting from the complex geometry and structure of the tire and complicated curing reactions.

The numerical simulation can be a useful tool for studying the effects of process parameters on the curing history of the tire. It can help us obtain a better understanding of the curing process in order to optimize the tire performance (for given criteria) under economic curing cycle. A computation program using finite element method was applied to simulate the tire curing process, which is a process coupled with heat transfer and chemical reactions. The heat of reaction was taken into account through the source term in the energy equation; it can be temperature and time dependent. Any kind of cure kinetics can be incorporated into the program. In this study, the Kamal model was adopted to fit the kinetic data obtained from DSC measurements. The degree of cure and temperature at nodal points were calculated. The equivalent minutes which have been widely used in the rubber industry were also calculated based on the nodal temperature. The program has the capability to simulate the complete curing cycle by automatically switching from in-mold curing simulation to post curing simulation, which have different boundary conditions, based on the predetermined degree of cure or equivalent minutes.

A parametric study of the rubber slab was carried out first to illustrate the effects of slab thickness, mold temperature, and initial rubber temperature on the degree of cure (or equivalent minutes), and time-temperature curing history. More extensive 2-D simulations were applied to the complicated tire curing system which included heated mold, tire body, rubber bladder, and internal heating medium. Both in-mold and post tire curing were simulated to obtain the complete curing history of the tire in order to optimize the curing cycle and still meet the required minimum degree of cure throughout the tire.

THE RHEOLOGICAL CHARACTERIZATION OF ELASTOMERS USING THE BICONICAL SHEAR RHEOMETER

H.Tang and Z.J.Lobos, Polysar Limited, Sarnia, Canada N7T 7M2
and P.K.Freakley, University of Loughborough, Loughborough, England.

The objective of this study is to evaluate the potential of the biconical shear rheometer for studying the rheological behavior of elastomers with different structural parameters. These results are compared with those obtained by the Mooney viscometer, which is a standard in the rubber industry.

The biconical shear rheometer is a variable speed machine which permits a relationship to be established between shear stress and shear rate (1). Its geometry enables the results to be expressed in fundamental units without any prior assumptions about the flow behavior of the material being tested. The cone angle of the biconical rotor employed in this study is six degrees. This is sufficiently small to provide a uniform shear rate throughout the sample. Transfer molding is used to ensure that the small clearance between rotor and cavity surfaces is accurately set prior to each test run. This is required to provide a reproducible shear rate. All these features are absent in a Mooney viscometer, which is a single-speed machine.

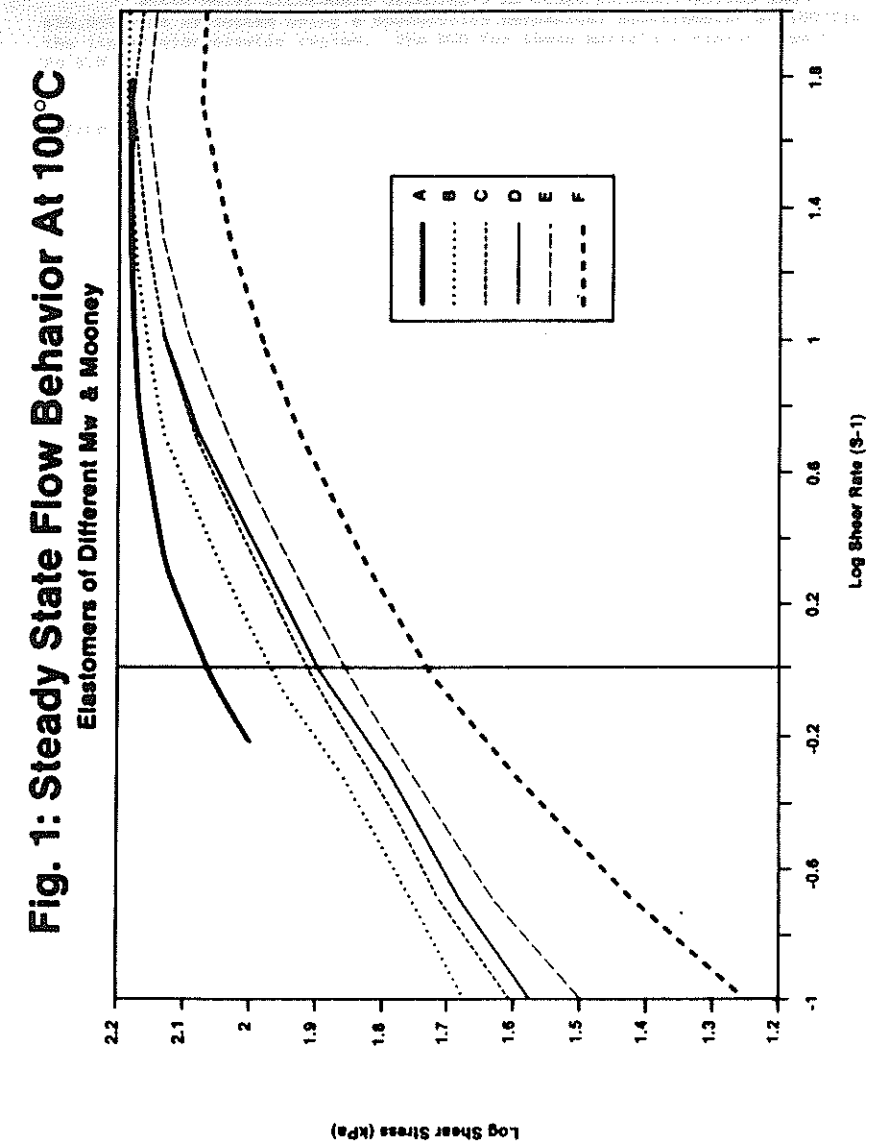
The flow behavior of a series of modified butyl elastomers (Figure 1), which span a large range of molecular weights and Mooney values, was characterized utilizing the TMS Rheometer, a biconical shear rheometer manufactured by Negretti Limited.

There exists a correlation between Mooney values and biconical shear rheometer flow curves for modified butyl elastomers. The correlation is very good for the low shear rate region, but deteriorates in the high shear rate region. Correlations exist between molecular weight and (a) Mooney measurements, and (b) biconical shear stress values in the low shear rate region. However, these correlations deteriorate in the high shear rate region. Shear stress measurements are more sensitive to molecular architecture at low testing temperatures.

The biconical shear rheometer provides highly reproducible measurements for commercial butyl elastomers. For these polymers, the rheometer flow curves crossover, indicating that elastomers with similar Mooney values can exhibit different behavior at low and high shear rates. The biconical rheometer can also be utilized to characterize the feedthrough rheological behavior of elastomers (raw polymer to compound).

<u>References</u>

1. P.K. Freakley, Rubber Processing and Production Organization, Plenum Press (1985).



7/7

INFLUENCE OF CARBON BLACK ON THE RHEOLOGICAL PROPERTIES OF RUBBER-CARBON BLACK COMPOUNDS

by

S. Montes, J. L. White and N. Nakajima
Polymer Engineering Center
The University of Akron
Akron, OH 44325 U.S.A.

There have been few studies of the influence of carbon black on the rheological properties of rubber compounds (1-4).

The rheological properties of carbon black rubber compounds have been studied in shear flow using a sandwich viscometer, a pressurized multispeed Mooney viscometer and a capillary rheometer. Stress relaxation, transient and steady shear flow, sequential flow history, stress relaxation after steady flow, and hysterisis and storage effects are studied for rubber carbon black compounds based on a natural rubber and a styrene butadiene copolymer at carbon black loadings of 10, 20 and 30 percent by volume.

At low carbon black concentrations, or high concentrations of very large particle size carbon black, the rheological response is similar in character to that of unfilled elastomers. For carbon black concentrations of 20 percent and above, compounds containing small particles exhibit yield values in steady state shear steady flow. Compare (2-4). Stresses in stress relaxation experiments decay to non-zero values. Compare (2). These yield values and stress relaxation asymptotes increase with carbon black concentration and decreasing particle size. The stress relaxation asymptotic value of the shear modulus decreases with increasing shear strain.

The highly thixotropic character of these materials manifests itself in hysteresis loops and storage effects. Hysteresis increases with increasing carbon black concentration and decreasing particle size. For the 20 and 30 percent compounds the magnitude of the viscosity overshoot in a start up of flow experiment depends on the storage time after insertion of a sample in a Mooney rheometer. It also depends on the rest period after a steady flow has been achieved on a two step steady deformation program. It increases and then levels off with time. The steady state values, however, are the same. These effects are more pronounced with increasing carbon black concentration and decreasing particle size.

The overall response of the highly loaded compounds is very similar to that observed in previously reported thixotropic systems such as dispersions of carbon black in oils. This study shows that carbon black compounds show three different types of rheological response; thixotropic, plastic and viscoelastic. These results are analyzed in terms of rheological models.

The influence of applied pressure on the flow of rubber compounds is also investigated. It is shown that at low pressures, slippage occurs.

Reference

1. L. Mullins and R. W. Whorlow — Trans. IRI 27, 55 (1951)

2. V. M. Lobe and J. L. White — Polym. Eng. Sci. 19, 617 (1979)

3. S. Montes and J. L. White — Rubber Chem. Technol. 55, 1354 (1982)

4. J. L. White, Y. Wang, A. I. Isayev, N. Nakajima, F. C. Weissert and K. Min — Rubber Chem. Technol. 66, 337 (1987)

RHEOLOGICAL DETERMINATION OF MW AND MWD FOR BUTYL ELASTOMERS.

Z.J.Lobos and H.Tang, Polysar Limited, Sarnia, Ontario, Canada N7T 7H2

Currently in the rubber industry, the Mooney rheometer is utilized to establish product specification. However, with the current emphasis on improved quality, there is a desire to obtain more fundamental information on molecular parameters which influence the processability of elastomers. Size can provide a quantitative measure of molecular weight and its distribution for linear elastomers. Nevertheless, GPC has its limitation as a quality control tool.

Dynamic mechanical testing is proposed as an alternative approach for the rapid and reliable determination of Mw and MWD for butyl elastomers. Utilizing a Rheometrics Mechanical Spectrometer, a correlation has been obtained between structural parameters (Mw and MWD) and the cross-over point in the terminal region of the dynamic mechanical spectrum. This technique could potentially be implemented in a QC environment.

A dynamic mechanical spectrum for a linear polymer can in general be divided into four zones on the frequency scale. These include (in the order of increasing frequency) the terminal zone, the plateau zone, the transition zone and the glassy zone. Each of these zones can be associated with a distinctive type of molecular motion[1]. As far as the dynamic spectrum - structural parameter relationship is concerned, all the relevant information is contained in the first two zones (Figure 1). Extension into the other zones provides no additional information other than the effect of chemical structure on the glass transition phenomenon.

At the high frequency end of the terminal region (or the low frequency end of the plateau region) lies the cross-over point at which the storage modulus G' equals the loss modulus G". The frequency corresponding to the cross-over point has been found to be closely related to a characteristic relaxation time (the terminal relaxation time in this case). According to various researchers [2,3], the terminal relaxation time is approximately equal to the inverse of the cross-over frequency. Also, there appears to be a linear relationship between the longest relaxation time and molecular weight (for monodisperse samples) when both parameters are plotted on a logarithmic scale [3].

The modulus which corresponds to the cross-over point is here termed the cross-over modulus. Patel[4] defined a polydispersity index (PI) in terms of the cross-over modulus Gc (PI = constant/Gc) and obtained a linear relationship between Log PI and Log MWD for polypropylene. MWD is the molecular weight distribution as determined by SEC or GPC.

Eight butyl elastomers spanning a Mw range between 450,000 and 650,000 were evaluated using a Rheometrics Mechanical Spectrometer at 100°C in the linear viscoelastic region. The MWD for these materials ranged from 3.0 to 6.0.

References

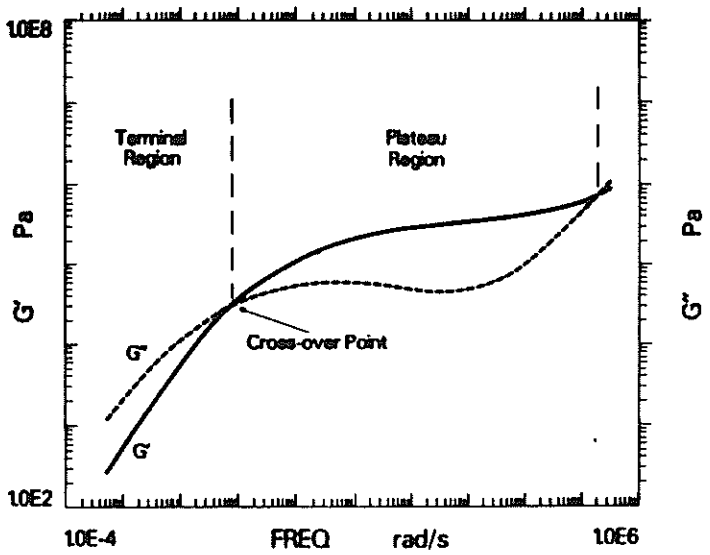
1. J.D. Ferry, Viscoelastic Properties of Polymers, John Wiley and Sons, New York, 1979.

2. F.R. Eirich (ed.), Science and Technology of Rubber, Academic Press, New York, 1978, pp. 199.

3. J. Roovers, Polymer Journal, 18, No. 2: 153 (1986).

4. G.R. Zeichner and P.D. Patel, Proceedings of the 2nd World Congress on Chemical Engineering 6:333, Montreal (1981).

Fig. 1. — Master Curve for Butyl Rubber at 100°C

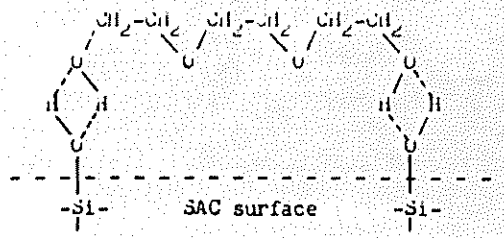


STUDY ON VULCANIZATION OF RUBBER COMPOUNDS FILLED WITH SAC BLACK

Zhou Yanhao, Zhao Suhe, Li Donghong, Zhang Jiajang, Li Chengxiang
(Department of Polymer Science, Beijing Institute of Chemical Technology, Beijing, China)

Silica-Alumina Carbon Black (abbr.: SAC) is made from gangue through mechanical disintegration, grinding and roasting etc. SAC is a new cheap extended reinforcing agent, it can partially replace SRF black(1). The main compositions and phisco-chemical properties of SAC are: Silica(40%), alumina(20%), and carbon black-like substance (35) etc, average particle diameter 0.40 nm, specific surface 24.2 m^2/g, DBP value 0.341 cm^3/g, DRC value 5%, pH value 9. The researching results of structure and reinforcement of SAC(2), rheological and mechanical properties of SAC compounds(3,4), and its applications in rubber and plastics products(5) have been reported. However, it has to be noted that SAC delays vulcanization. For this reason we have studied the vulcanization of rubber compounds filled with SAC black. It has been found that the remained wastes (Tar Oil, abbr.: T.O.) in vacuum rectifying still of glycol possess activation of sulfur vulcanization of SAC rubber compounds besides the good softening-plastication(3). T.O. consists of glycol (0.01%), diglycol (0.05%), triglycol (72.84%) and polyglycol (26.10%). It is shown that the optimum cure time (t_{90}) of NR, SR, NBR, SBR/BR filled with SAC is greatly decreased by T.O. (for ex.: SBR/BR=70/30, decreasing to 14 min. from 56 min.) except for sulfurless vulcanizing CR. T.O. also has an obvious activation effect on compounds filled with silica-gel and clay. In accelerator blend system of CZ/TMTD or DM/D, T.O. can replace TMTD or D and decrease the level of CZ or DM (about 1/3) (Tab.1) and shorten t_{90} but does not reduce the mechanical properties of the vulcanizates, of course, the cost of compounds will decrease.

The research on activation of model chemical compounds to vulcanization of SAC filled rubber compounds has shown that the activation vulcanization possessed by T.O. attributes to two hydroxyl groups in its components and not to ether bond (Tab.2). On the surface of SAC there are a few hydroxyl groups, which have been proved by infrared spectrum(2), which can easily adsorb accelerator substances carried non-paired electron, so that the delayed vulcanization will occur. However, if there is T.O. in the compounds then T.O. will be strongly adsorbed by SAC prior to accelerators and form:



protecting accelerator from adsorption of SAC. To sum up, the combination of preventing SAC from delayed vulcanization and giving play to characteristics of T.O.(partial basicity, Pd=6-9) leads to activation vulcanization.

After measuring the vulcanization curves of SBR compounds added different blend levels of accelerator and T.O. with vulcameter, determining the max. torque(M_∞) at various temperatures(140°-170°C), and the torque(M) at different times(t) in the same temperature and $\frac{dM}{dt}$, and then ploting $\lg(\frac{1}{M_\infty}\frac{dM}{dt})$ against $\lg(\frac{M_\infty - M}{M})$ the reaction order (n) will be given from the slope of the line, n is about 1. We can get the apparent activation energy of vulcanization(E) from the slope of the plot of $\ln t_{90}$ against 1/T, (where T is absolute temperature) (Tab.3). It will be seen from Tab.3 that the (E) is decreased by T.O.. It is concluded that T.O. can wholly replace secondary accelerator and partially replace primary accelerator.

REFERENCES

(1) Xi Yunxia, Patent of China, CN 3K 86100840, Announce date: May 20, 1987.
(2) Zhou Yanhao, Li Donghong, Zhao Suhe, to be published.
(3) Zhao Suhe, Zhou Yanhao, Zhang Jianzhen, "The influence of glycol Tar Oil on the rheological properties of SAC black filled SBR compounds and valuation for its softening effectiveness", presented at "The Second National Congress on Rheology"(Chengdu, Sichuan Prov., China, Nov. 15-19, 1987).
(4) Li Donghong, Zhou Yanhao, China Rubber Industry, (10), 21 (1987).
(5) Xi Yunxia, China Carbon Black Industry, (1), 15 (1985).

Tab.1 Effect of T.O. on t_{90} of CZ/TMTD and DM/D Systems (pphr)

CZ/ TMTD/T.O.	1.1/0.2/0	1.1/0.1/5	1.1/0/7	0.6/0/9	0/0/3
t_{90}, min.	45	10	15	16	51
DM/D/T.O.	1.5/0.7/0	1.5/0.7/3	1.5/0.35/5	1.5/0/7	0/0/9
t_{90}, min.	59	15	9.5	9.5	15

Basic recipe: SBR 100; Sulfur 2.2; Stearic acid 2.0; ZnO 5.0; SAC 100.

Tab.2 Effect of Model Chemical Compounds on t_{90}

	glycol	diglycol	triglycol	n-butanol	dioxane
t_{90}, min.	13	11	9	25	41
	isopropyl ether	vinyl isobutyl ether	T.O.	control	
t_{90}, min.	42	48	10	46	

Basic recipe: the same Tab.1, but CZ 1.1; TMTD 0.1; Model Chemical Compounds 5.0.

Tab.3 Activation Energy of Vulcanization (E) in different levels of TMTD/T.O. System

TMTD/T.O.	0.4/0	0.2/4	0/4
E, KJ/mol.	93.1	82.4	78.3

Basic recipe: the same Tab.1, but CZ 1.5.

Studies on a New Binary Accelerator System in Rubber Vulcanization - Part II

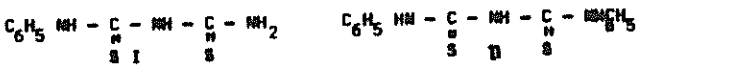
A.P. Kuriakose and George Mathew
Department of Polymer Science & Rubber Technology
Cochin University of Science & Technology Cochin - 682 022. India.

In the rubber vulcanization reaction no accelerator can be considered ideal, i.e. one that is absolutely safe at processing temperature and also cures fast. Use of suitable mixed accelerator systems has been found to approach this ideal behaviour to a great extent. Thiourea and its various derivatives are finding much use in mixed accelerator systems in rubber vulcanization. Derivatives of thiourea are more popular in neoprene and natural rubber latex systems. These derivatives ensure fast vulcanization at comparitively lower temperatures. The danger of scorching can be reduced in the presence of other suitable accelerators. The exact mechanism of their reaction is not fully understood even now. It has been proved that accelerators in which sulphur is combined as S - S, C - S - C or S - N are virtually inactive at temperatures below 100°C because of the high thermal stability of their S - bonds. It has also been shown that sulphur containing nucleophiles enable such accelerators to operate at lower vulcanization temperatures. The cleavage of the S - S bond by the nucleophile may be represented as;

$$R - S - S - R^1 + Y^- \longrightarrow R - S - Y + R^1 - S^-$$

In his studies on different nucleophiles, philpot has shown that thiourea showed high reactivity in the vulcanization studies on natural rubber latex with TMTD. Similar reactivity was also observed in accelerators containing S - C linkage (monosulphidic) and sulphonamide type accelerators containing S - N linkage.

If the above postulates are correct, we thought that dithiobiurets, which are also derivatives of thiourea should show more accelerator activity than simple thiourea derivatives because of their higher nucleophilic nature. It should also provide the necessary proof to the above mechanism of vulcanization in the binary system containing a nucleophile. There is no mention in literature, whatsoever on the study of accelerator activity of a dithiobiuret or its derivatives. 1- Phenyl 2, 4 - dithiobiuret and 1, 5 diphenyl 2, 4 dithiobiuret (I and II) were synthesised in our laboratory; and



the present work forms a systematic study of their accelerator activity in the sulphur vulcanization of natural rubber along with tetramethyl thiuram disulphide (TMTD). The results obtained were compared with those obtained from a reference mix containing TMTD and thiourea. 9 Different mixes were prepared for each biuret derivative, (composition of the mixes to be represented as table 1, 2 and 3 in the paper) and an attempt was made to find out the optimum concentration of the dithiobiurets in the vulcanization reaction under standard conditions. The cure time for the various mixes were evaluated at 150°C and 120°C using a Monsanto rheometer (rheographs to be represented as Fig.1, 2 and 3 in the paper). The physical properties like tensile strength, modulus, elongation at break, tear strength, hardness compression set, abrasion loss, heat build up, flex cracking and resilience of the various vulcanizates were also evaluated (the values are represented in table 4, 5 and 6 in the paper).

In our studies we have found that the two dithiobiurets we have used in these experiments showed superior accelerator activity in the binary systems along with TMTD. When the mix containing 1 - phenyl 2, 4 - dithiobiuret (0.5 phr) and TMTD (1.5 phr) showed an optimum cure time of 7 min. at 150°C; the one containing 1, 5 diphenyl 2, 4 dithiobiuret under identical conditions showed an optimum cure time of 7.5 min.; while the reference mix containing thiourea (0.5 phr) showed an optimum cure time of 9.5 min. At 120°C, the optimum cure time for the above mixes were 27, 48 and 46.5 min. respectively. From these results it may clearly be inferred that the dithiobiuret derivatives facilitated the S - cleavage in TMTD more effectively. The more nucleophilic the reagent is, more is the accelerator activity observed in the systems under review. The vulcanizates were evaluated for their tensile properties viz. modulus (300%), tensile strength and elongation at break and definite increase in these properties was observed in the mixes containing the dithiobiuret derivatives. These mixes showed better retention of these properties after ageing also. As regards the other physical properties estimated; flex cracking resistance was superior while abrasion resistance, resilience, compression set, hardness etc. showed no significant changes. It was also observed that when higher concentrations of the dithiobiurets were used, the mixes showed slightly higher heat build up. This also makes them slightly scorchy. But this is observed only when higher concentrations of the dithiobiurets than what is necessary is employed. We have been able to conclude that in view of the significant reduction in cure time with definite increase in tensile properties of the vulcanizates containing the thiobiuret derivatives; these binary systems will be of definite practical advantage. The optimum level of the dithiobiuret derivative in each system is also derived at.

.....

7/11

MIXER CONTROL

THE BASIS FOR A MORE EFFICIENT RUBBER INDUSTRY

H.D.Giffin, B.Sc., A.C.G.I., F.I.E.E., F.I.Mech.E.

Managing Director

Francis Shaw & Company (Manchester) Limited

Traditional methods of mixer control have not ensured that compound leaving the millroom has consistent characteristics. Batch Condition Control is a real-time system by which a computer ensures that the mixing process for every batch of material is modified in such a manner that compound produced always has the same viscosity, dispersion and heat history. Application of Batch Condition Control ensures that the mixing process is carried out with maximum efficiency, but of significantly greater importance, it allows all the downstream equipment to be operated in a consistent manner from day to day, thus increasing efficiency and reducing rejects throughout the whole factory.

The system was developed jointly by Francis Shaw and Loughborough University in England. The method is based on a closed-loop real-time control of the mixing process using viscosity to determine the degree of mix at intervals during the process. Based on the viscosity measurement the controllable variables are modified so that every time a given formulation is mixed the compound will have the same viscosity and heat history; these factors are, of course, the ones which particularly affect downstream processing characteristics.

The viscosity can be calculated from the motor torque which is readily measured but must be corrected for compound temperature, the rate of shear, fill factor and drive train losses. Appropriate corrective equations have been determined and the constants applicable in these equations for each formulation can be determined automatically by the BCC computer during the processing of 4 or 5 set-up batches.

Based on the viscosity readings obtained, the control computer calculates optimum operating conditions of speed and ram pressure to complete each stage of mixing (i.e. obtain the correct viscosity) in minimum time without exceeding the critical temperature or overloading the motor. The minimum time criterion ensures minimum heat loss to the cooling water and so maximises the energy which is applied to the compounding process and so optimises efficiency. For certain polymers (e.g. EPDM) energy will not be the controlling feature in achieving the correct viscosity. In such cases, it is possible to arrange for the computer to initiate the addition of chemical softeners at appropriate stages; obviously the amount of such additions must be limited so that side effects do not alter the properties of the finished product.

Examples are given of test results, comparing the quality of compound produced with and without BCC. The advantages of using the system are summarized and the possibility of using computer controlled evolutionary process optimisation on new formulae is discussed.

RELATIONSHIP BETWEEN THE CROSSOVER MODULUS AND THE MOLECULAR WEIGHT DISTRIBUTION USING THE DOI-EDWARDS THEORY OF REPTATION AND THE ROUSE THEORY

R.R.Rahalkar, Polysar Limited, Sarnia, Ontario, Canada N7T 7M2

In recent years, there has been some interest in relating the crossover modulus (G_{cr}) in the dynamic mechanical spectrum with the molecular weight distribution (MWD) [1]. Such a relationship may be used to monitor the MWD on line during the processing of polymers (by measuring the crossover modulus on line), thereby providing a tool for quality control. In this paper, G_{cr} has been linked with the MWD curve (and not just with $\bar{M}w/\bar{M}n$) for several polymers covering a wide range of polydispersity ($\bar{M}w/\bar{M}n \sim 1$-6).

Several polymers were studied: an anionically polymerized polybutadiene ($\bar{M}w/\bar{M}n = 1.2$); a high vinyl polybutadiene ($\bar{M}w/\bar{M}n = 1.4$); a polystyrene sample ($\bar{M}w/\bar{M}n = 2.6$) and four commercial butyl rubbers ($\bar{M}w/\bar{M}n = 3$-6). The molecular weight distribution was measured by GPC. The dynamic mechanical spectra were measured using a Rheometrics mechanical spectrometer RMS 800.

Figure 1 shows the comparison between the experimentally measured G_{cr} [2] and predictions of the theory. For the monosperse and narrow MWD polymers, Doi-Edwards theory was able to predict the crossover modulus with reasonable accuracy. Doi-Edwards theory predicts that G_{cr} depends only upon the MWD and the plateau modulus (G_N^0) and is independent of molecular weight and temperature.

The butyl rubbers studied were polydisperse, with $\bar{M}w/\bar{M}n$ values of three to six. According to the Doi-Edwards theory, G_{cr}/G_N^0 is independent of MWD in this region, having a value of $\sim$ .18. In practice, G_{cr}/G_N^0 for the butyls studied ranged from 0.13 to 0.06. Thus, the Doi-Edwards theory was totally unable to predict the G_{cr} behavior for the polydisperse butyls. Rough calculations indicate that of the total crossover modulus, $<3\%$ is due to pure reptation and hence, can be accounted for by the Doi-Edwards theory.

The motion of long chains in a polydisperse polymer is not hindered to any appreciable extent by the entanglements, since the entanglements are of much shorter duration compared to the longest relaxation time of the chain. If the long chains are assumed to be unentangled (or very lightly entangled), the flow behavior of long chains may be described by a Rouse type mechanism, since the Rouse theory is supposed to be applicable to unentangled polymers.

Using the Doi-Edwards theory for shorter chains and a Rouse type mechanism for longer chains, G_{cr} values for the butyls could be predicted with reasonable accuracy (Fig.1). Comparison with the experimental data for butyls also indicates that the longer chains are roughly three times as lightly entangled as the shorter chains. Using this entanglement value for the longer chains, G_{cr} for the polystyrene sample was calculated, leading to a reasonable agreement with the experimental value.

References

1. G.R.Zeichner and P.D.Patel, Proc. 2nd World Congress on Chem. Eng., 6,333 (1981).

2. The crossover modulus values are based on the work by Z.J.Lobos and H.Tang (to be presented separately at the Conference).

3. M.J.Struglinski, Ph.D. thesis, 'Viscoelastic Effects of Polydispersity Studied with Mixtures of Different Chain Architectures', North Western University, Illinois, 1984.

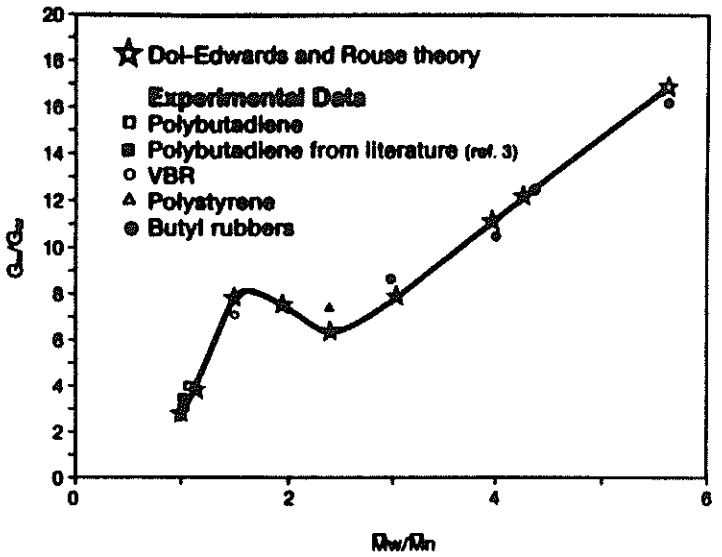


Fig. 1. — Comparison between the experimentally obtained crossover modulus (plotted as plateau modulus, G_N^0, divided by the crossover modulus, G_{cr}) and theoretically calculated values $\bar{M}w$ — weight average molecular weight, $\bar{M}n$ — number average molecular weight

8/1

SOL-GEL TRANSITION IN POLYMER SOLUTIONS AND DEVELOPMENT OF POROUS STRUCTURE BY COAGULATION

K. Kawanishi, Y. Takeda, and T. Inoue
Department of Organic & Polymeric Materials
Tokyo Institute of Technology
Ookayama, Meguro-ku, Tokyo 152, Japan

Recent light scattering studies on the thermoreversible sol-gel transition in polymer solutions, such as poly(vinyl alcohol)/water and poly(vinyl chloride)/ γ-butyrolactone systems (1,2), have revealed that spinodal curve and sol-gel transition curve divide phase diagram into four regions (Fig. 1). This situation can be well described by combining the familiar Flory-Huggins theory and a modern theory of gelation as a result of the site-bond correlated percolation problem (3).

The structure development in the solution at the region (iii) in Fig. 1 is of primary interest in relation to the formation of porous structure by coagulation. When the homogeneous solution in region (i) undergoes a rapid temperature-drop to the region (iii), the liquid-liquid phase separation takes place by spinodal decomposition. The spinodal decomposition is expected to result in the development of a regularly interconnected strucure of polymer-rich and polymer-poor regions; i.e., modulated structure (Fig. 2). This is a fast process. Then gelation in the polymer-rich region follows (probably in a way similar to that in region (iv), i.e., first by hydrogen bonding association, then by crystallization)(3). Now, immersing the phase-separated and gelled solution into a bath of non-solvent, the framework of modulated structure is expected to persist and be transformed to a skelton in the coagulated system.

Figure 3 shows a SEM of polyacrylonitrile membrane coagulated from a thin layer of the phase-separated and gelled solution, indicating the regular porous structure consisting of skelton and through-pores. The periodic distance in the membrane (ca. 300 nm) is close to the wavelength of the concentration fluctuation ($2\pi/qm$) at the highest rate of phase separation, R(qm), estimated from its dynamical analysis by light scattering. There exists an optimum time (t^*) of the phase separation prior to coagulation. When the time of phase separation is shorter and also longer than t^*, an irregular porous structure develops. A nice correlation between t^* and the relaxation time of phase decomposition, $1/R(qm)$, as shown in Fig. 4, supporting the above scenario on the transformation of modulated structure in solution to the skelton of porous membrane.

All of the polymers in our study (PVA, PAN, PVC) are gel-forming polymers. However, we found a dramatic difference in the structure development by coagulation. We believe that it originates from a difference in the attainable stage of phase-decomposition which depends on the gelation character in the polymer-rich region: "servomechanism" characteristic to the polymer species.

1) M. Komatsu, T. Inoue, K. Miyasaka; J. Polym. Sci., Phys. Ed., 24, 303 (1986)
2) K. Kawanishi, Y. Takeda, T. Inoue; Polymer J., 18, 411 (1986)
3) K. Kawanishi, M. Komatsu, T. Inoue; Polymer, 28, 980 (1987)

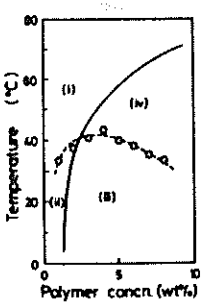


Fig. 1



Fig. 2

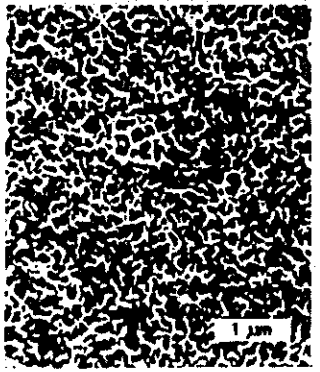


Fig. 3

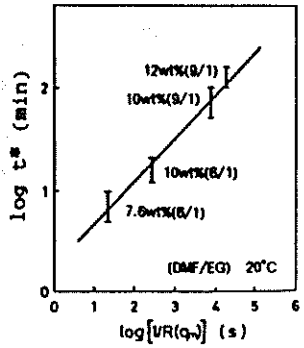


Fig. 4

Fig. 1. Sol-gel transition curve (solid line) and spinodal curve (broken line) in the δ-butyrolactone solution of PVC (Pn=3,200). Region (i) homogeneous sol. (ii) Liquid-liquid phase separation takes place by spinodal decomposition but the solution does not change to a gel. (iii) Both spinodal decomposition and gelation occur. (iv) Gelation takes place without liquid-liquid phase separation.

Fig. 2. Schematic illustration of the unit cell of modulated structure.

Fig. 3 SEM of a porous PAN membrane prepared by immersing into water after the phase-separation at 20°C for 65 min.

Fig. 4. Otpimum time of phase separation in advance of coagulation vs. relaxation time of phase separation in PAN solutions.

8/2

FIBROUS MATERIALS FROM THE PHASE DECOMPOSITION OF LCP SOLUTIONS

M.A. Alonso, C.L. Jackson and M.T. Shaw, University of Connecticut, Storrs, CT 06268

Conventional composites are either reinforced with chopped fiber or with continuous fiber. In the former case, the filled resin may be molded into complex shapes, with the orientation of the fibers generally in the direction of flow. With continuous fibers, the fiber orientation can be controlled, leading to a more efficient use of the reinforcement. However, for some applications with dynamic, multiaxial loading, it may be advantageous to have a completely isotropic distribution of the reinforcing fibers. The purpose of this paper is to describe a route by which isotropic, three-dimensional fibers may be made.

One route to three-dimensional fibers takes advantage of the dynamics of phase separation in liquid crystal polymer solutions. Figure 1 shows the expected phase behavior of a solution of rigid rods in a solvent which freezes. It can be seen that quenching an isotropic solution from point A to point B will place the solution into a unstable region with eventual equilibrium compositions consisting of concentrated liquid crystalline solution and frozen (pure) solvent. The solution will experience long-range concentration fluctuations which will predispose the geometry to one exhibiting high interconnectivity; this will be frozen in by the solvent.

Polybenzyl glutamate (PBLG) of 190,000 molecular weight was used as a model, semi-rigid rod polymer; it is convenient because of its high solubility in common organic solvents. For making serious composites, however, more rigid systems are needed. We thus selected poly(1,4-benzamide) (PBA) and poly(p-phenyleneterephthalamide) (PPTA, also known by the DuPont tradename Kevlar®) as examples. These polyamides are soluble only in strong acids (e.g. sulphuric acid, trifluoromethyl sulfonic acid) or in LiCl/DMAC mixtures.

With the PBLG, a series of experiments were run to discover the influence of the solution behavior and cooling rate on the structure of the resulting reinforcement. From published results on random-coil polymers, the difference between the critical temperature of the polymer/solvent mixture and the freezing point of the solvent is considered to be a key system variable (1). Cooling rate is the process variable of importance because of its control of the mode and rate of phase separation. The chosen solvent system was a mixture of water and dioxane, both of which are easily sublimable. The ratio of water to dioxane controls the critical temperature.

With the polyamides, mixtures of water and sulfuric acid were used. Sulfuric acid does not sublime easily; therefore extraction with methanol mixtures was used to remove the frozen solvent.

The optimum solvent system for PBLG was found to be 93/7 dioxane/water. This mixture places the critical point about 20°C above the freezing point. With moderate quench rates (~0.2°C/sec), the structure shown in Figure 2 was found after subliming the solvent. By gently stretching this structure, the struts can be aligned; a WAXS pattern on this was consistent with the molecular axes aligned along the struts.

With PPTA, homogeneous fibrous structures were more difficult to make. As can be seen in Figure 3, the structure is bimodal: a coarse irregular grid intermixed with a fine fibrous material. This suggests two mechanisms, which could be concurrent in our ternary system, but are probably sequential. The influence of quench rate in this system remains to be investigated.

With lyotropic LCP system, the distinction between structures resulting from spinodal decomposition and from nucleation and growth may not be clear — both may result in structures similar to that found in Figures 2 and 3. Because the diffusion of rods should be primarily axial (2), any nucleus will have a tendency to grow with a dendritic habit; not because of local depletion, but because of the combination of an orientation dependent chemical potential difference and the higher mobility of rods which happen to be aligned with the director of the liquid crystal.

References

1) J. H. Aubert and R. L. Clough, Polymer 26, 2047 (1985)
2) Y. Cohen and E. L. Thomas, Polym. Eng. Sci., 25, 1093 (1985)

Acknowledgments

Financial assistance for the PBLG studies is from Sandia National Laboratories and the Army Research Office, while that for the polyamides is through the DARPA-supported Liquid Crystal Polymer Research Center, University of Connecticut.

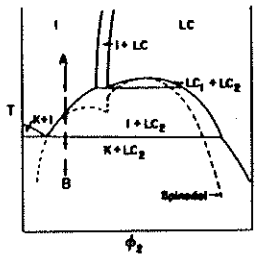


Fig. 1. Phase diagram for LCP solutions

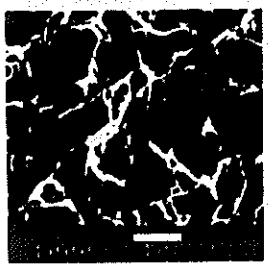


Fig. 2. PBLG structure from 93/7 dioxane/H_2O

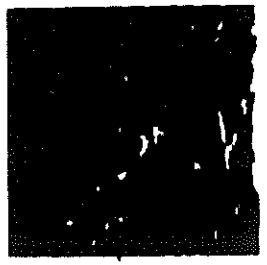


Fig. 3. PPTA structure from 96/4 H_2SO_4/H_2O

A CONSTITUTIVE EQUATION INCLUDING COMPRESSIBILITY EFFECTS: APPLICATION TO RAPIDLY COOLED, CONSTRAINED SAMPLES

D. C. Bogue and W.-C. Ko, Department of Materials Science and Engineering, University of Tennessee, Knxoville, TN 37996 USA

While there have been rapid advances in the modelling of many polymer processes, the problem of volume changes (compressibility effects) has hardly been touched. As a molded part cools, prior (flow-induced) molecular orientation and also part of the volume changes are "frozen-in" -- and seldom uniformaly through the part -- causing complicated interactions to occur. The processes are highly coupled: in a constrained sample, volume contraction (and also orientation contraction) can cause stresses; and the stresses in turn can affect the volume changes. In fact all of the variables σ_{ij} (including P), V and T can affect each other.

In 1984 Snow and Bogue (1) set down a generalized constitutive equation which includes these various effects. The integral statement there is quite complicated, however, and is difficult to execute except in the simplest deformations. Recently the present authors recast the prior equation in a more tractable and slightly modified form (Ko and Bogue (2)). Briefly summarized the new formulation consists of solving simultaneously two constitutive equations: the first, for the PVT effects, and the second, for the anisotropic stress:

$$\frac{d(\theta + \phi_f)}{dt} = \frac{-\Delta\theta}{\tau_\lambda} \qquad (1)$$

The function ϕ_f has to do with creating free volume. The quantity θ, a variable characterizing the PVT state, is defined by

$$\theta(t) = \mathcal{P}(t)/\lambda^*(t) + V(t)/V_o - \alpha(t)T(t)$$

where $\lambda^*(t)$ is the bulk modulus, $\alpha(t)$ is the thermal coefficient of expansion, and $\mathcal{P}(t)$ is a negative scalar stress.

Also,

$$\sigma_{ij} = -\mathcal{P}\delta_{ij} + \int_{-\infty}^{t} \frac{G(t')}{\tau_G(t')} \exp\left[-\int_{t'}^{t} \frac{dt''}{\tau_G(t'')}\right] c^{-1*}_{ij}\, dt' \qquad (2)$$

where $\sigma_{ij}(t)$ is the total stress, $c^{-1*}_{ij}(t,t')$ is a normalized relative Finger strain tensor. There is, in addition, a constraint imposed by the kinematics (not shown here): that is, the square root of the determinant of the Finger strain tensor is related to the volume changes. In the appropriate limits our formulation reduces to a rate equation for volume-temperature effects, to an equilibrium PVT equation, to linear elasticity theory, and to the usual (incompressible) constitutive equation for the rubbery melt state. The key to the formulation is the scalar stress $\mathcal{P}$, which is the hydrostatic pressure in isotropic deformations but has a more general meaning in anisotropic loadings.

In the present paper the behavior of the above equations will be discussed, particularly in regrad to such problems as flow-induced orientation and volume-induced residual stresses.

In the experimental part of the paper, the analysis of three experiments (using polystyrene) will be presented:

(1) The change of volume with temperature at various cooling rates, using the literature data of Greiner and Schwarzl (3).

(2) The build-up of tensile stress, due to volume contraction during rapid cooling, in a uniaxially constrained fiber (held between stationary Instron clamps).

(3) The build-up of tensile stress due to cooling-induced volume changes and also due to pulling of the sample (the sample being held now between moving Instron clamps while the rapid cooling is imposed).

The second and third of these experiments are part of the MS research and Ph.D. research, respectively, of the second author (Ko (4, 5)). Volume parameters obtained from the Greiner and Schwarzl data plus elastic moduli from the literature provide most of the parameters for the analysis of the second and third experiments; the anisotropic time constant and its shift factor can be estimated from the literature but these are "adjustable" to a considerable extent. Satisfactory fits to the three experiments noted, over a range of cooling rates, are finally achieved.

The implications, and limitations, of these results for more complex geometries and for highly stressed samples will be discussed.

(1) B. D. Snow and D. C. Bogue, J. Rheol., 28, 533 (1984).
(2) W.-C. Ko and D. C. Bogue, J. Rheol., 31, 425 (1987).
(3) R. Greiner and F. R. Schwarzl, Rheol. Acta, 23, 378 (1984).
(4) W.-C. Ko, MS thesis, University of Tennessee, Knoxville, June 1987.
(5) W.-C. Ko, Ph.D. dissertation, University of Tennessee, Knoxville (in progress)

OPTIMAL COOLING FOR MINIMUM THERMAL STRESSES

Ming J. Liou, Dept. of Mechanical Engineering, The Ohio State University
Nam P. Suh, Dept. of Mechanical Engineering, Massachusetts Institute of Technology

During the cooling of a viscoelastic part, thermal strains develop inside the part. Thermal stresses are then produced and relaxed simultaneously due to the viscoelastic nature of the part. The temperature gradient inside the part also leads to differential thermal contraction and stress relaxation. In order to reduce the thermal stresses, the cooling process must be very slow to have maximum stress relaxation. Not only is energy wasted during such a long operation, but also productivity is reduced. The goal of this study is to find an optimal thermal history within a specified time period for minimum thermal stresses in viscoelastic parts. The development of the thermal stresses in viscoelastic materials during the cooling was first studied. The analysis took into account the temperature dependent properties. A material model termed "thermorheologically simple" was used to calculate the thermal stresses in a bounded plate cooled symmetrically from both surfaces. This model exhibits a pure shift in relaxation function plotted against the logarithm of time when there is a temperature change. The resulting thermal stresses distribution across the thickness of the plate can be expressed as [1]

$$\sigma(z,t_f) = -3\,\alpha_o \int_0^{t_f} R(\xi(z,t))\,\frac{\partial}{\partial t}\,\theta(z,t)\,dt, \quad \text{where } \xi(z,t) = \int_t^{t_f} \phi(\theta(z,t))\,d\lambda.$$

The entire thermal stress field across the thickness is then minimized through optimization of the thermal history of the process. The surface temperature of the plate is chosen as the control variable while the thermal field in the plate represents the state variables. Euler-Lagrange equations are solved with first gradient algorithm [2] to iterate the optimal solution. Fig. 1 shows the final thermal stress distribution across half of the plate resulting from quenching, linear and optimal coolings. The corresponding surface temperature profiles are given in Fig. 2. Quenching gives the highest stresses while the optimal cooling leads to minimum stresses. The optimal cooling profile of the surface presents an initial rapid temperature jump followed by a slower cooling for most of the cooling period. Since the temperature across the thickness of the plate should reach the final temperature at the end of the cooling, the surface temperature should be cooled to the final temperature well before the end of the cooling. Although the final temperature jump would produce surface stress that cannot relax, the optimal cooling still results in minimum stresses.

Physical insights of the optimal cooling path is explained as follows. Since the initial and final temperatures are fixed, the total thermal strain resulting from the cooling of a bounded plate is constant. Producing more strain and therefore more stress in the very early stage would allow more time for stress relaxation due to the fixed period of cooling. A temperature jump in the very beginning is, therefore, desired.

The degree of the temperature jump in the beginning also affects the stress relaxation because the relaxation time constant increases with decreasing temperature. Although a larger temperature jump in the beginning will produce more stresses and leave a longer period for stress relaxation, only a small amount of stresses will relax because of the low temperature. On the other hand, the stresses resulting from a smaller temperature jump would relax quickly due to the high temperature. However, the stresses resulting from the large final temperature jump would not have time to relax. The trade-off between the thermal strain and the temperature has led to the optimal cooling profile for maximum stress relaxation.

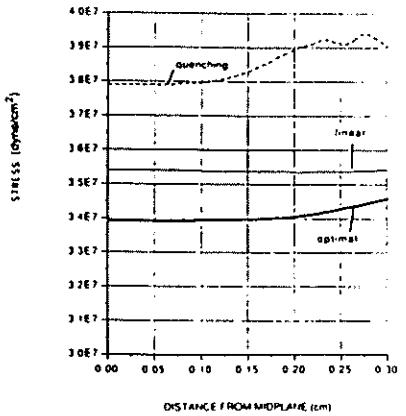


Fig. 1: Final Thermal Stress Distribution from Quenching, Linear and Optimal Coolings.

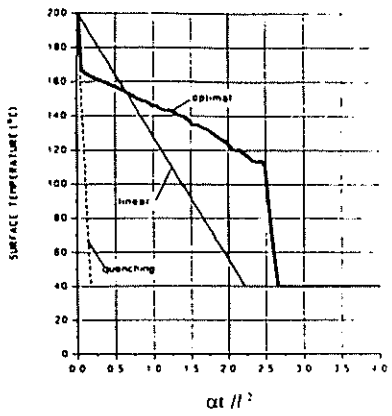


Fig. 2: Temperature Profiles of Quenching, Linear and Optimal Coolings.

References

1. Muki, R. and Sternberg, E., "On Transient Thermal Stresses in Voscoelastic Materials with Temperature Dependent Properties," Journal of Applied Mechanics, Vol. 28, p. 193, 1961.
2. Bryson, A. E. and Denham, W. F., "A Steepest-Ascent Method for Solving Optimum Programming Problems," Journal of Applied Mechanics, pp. 247-257, June, 1962.

Heat Transfer Driven Stress Build-Up and Relaxation in a Post-Forming Stage of Thermoplastic Materials.

A. Cohen and M.G. Dibbs, The Dow Chemical Company, Central Research, Polymeric Materials Research Center, 1702 Bldg Midland, Michigan 48674

An interaction between heat transfer, shrinkage and stress relaxation during post-forming cooling was studied. In order to arrive to a treatable mathematical formulation, the one-dimensional case was analyzed. The model can be visualized as a narrow strip of material held in the adiabatic mechanical grips with one long side open and exposed to the outside environment with a constant temperature T_1.

The combination of the processes leads to the equation for the stress

$$\sigma = E\,\alpha\,(T_o - T) - \int_T^{T_o} \sigma/\lambda_r \, dT/T',$$

where E is the elastic modulus, α is the coefficient of thermal expansion, and T' is the rate of cooling. Temperature T_o was selected as a value, under the glass transition temperature T_g, at which the elastic modulus E, and the coefficient of the thermal expansion α, can be approximately treated as constants. The stress relaxation time λ_r is expressed as

$$\lambda_r = \lambda_o \exp(y\,(T_o - T)),$$

where λ_o is the relaxation time at the temperature T_o.

Under certain linearizing assumptions, the solution $\sigma(T)$ is expressed as

$$\sigma(T) = \sigma^* / [\,y(T_o-T_1)^*(1+\beta)\,]\;\{\,[1 + y(T_o-T)]^{-\beta} - [1 + y(T_o-T)]\,\},$$

where the relaxation parameter $\beta = \lambda_t/\lambda_o\,/[y(T_o-T_1)]$, with λ_t - the temperature relaxation time, depending upon the diffusivity of the material, the film coefficient, and the length scale parameter, i.e. the width of the strip, [1]. The scaling stress $\sigma^* = E\alpha\,(T_o-T_1)$ is equal to the stress value due to the cooling without relaxation.

Changes of the relaxation parameter β, achieved by a variation of cooling conditions or by changes in a material composition, are very important for the post-forming behavior as can be seen in Fig. 2 where the maximal values of σ/σ^* are plotted for identical temperatures, i.e. T_o and T_1, and material parameters, i.e. σ^* .

Due to the lack of experimental data for stress relaxation of thermoplastics below T_g, parameters y and λ_o were obtained for a number of materials. A model for the 2-dimensional post-forming cooling, based upon the described material mechanisms, compared very favorably with experimental observations, [2].

References

1) J. Crank, "The Mathematics of Diffusion", Clarendon Press, Oxford
2) A. Cohen, M.G. Dibbs, 43rd ACS Fall Sci Meeting, Midland, MI Oct 87

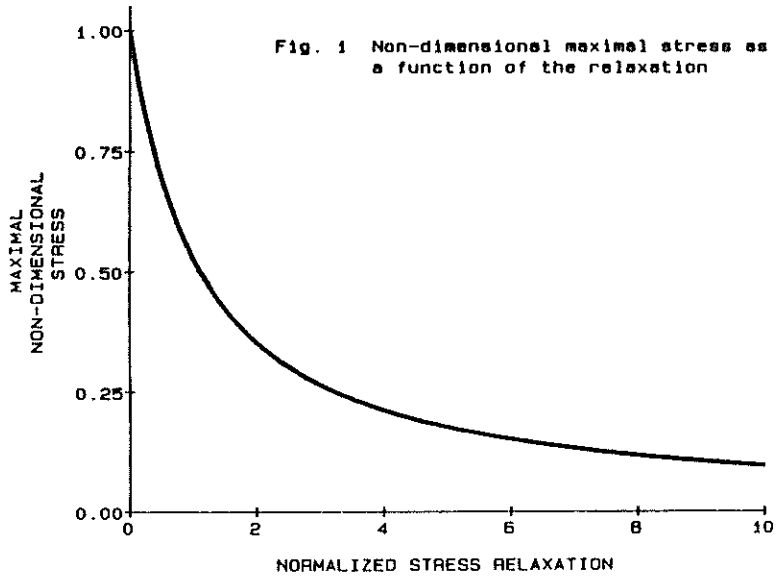


Fig. 1 Non-dimensional maximal stress as a function of the relaxation

EFFECT OF MODIFYING THREADLINE DYNAMICS IN THE HIGH SPEED SPINNING PROCESS

J. A. Cuculo, P. A. Tucker, G. Y. Chen and C. Y. Lin
School of Textiles, North Carolina State University, Raleigh, NC 27695

Commercial polyethylene terephthalate (PET) (0.57 IV) was spun into fiber at 3000 to 7000 m/min. Threadline dynamics was modified by altering threadline temperature profile. This was achieved by using a combination of controlled cooling and heating of the threadline. The key element in our approach was the appropriate heating of the threadline, termed "on-line zone heating". Our objective was to improve properties and structure of high speed spun fibers.

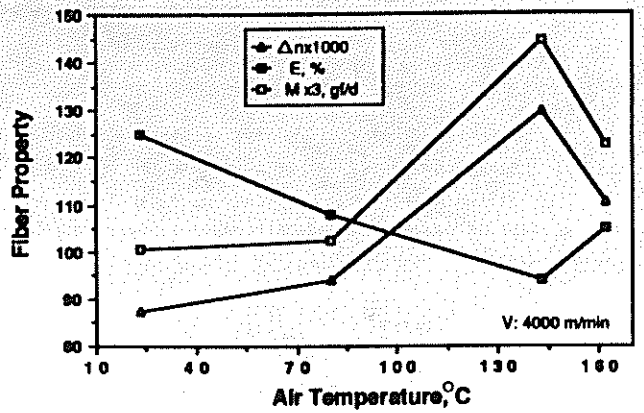


Figure 1. Fiber Property vs Air Temperature.

Figure 1 shows how the properties of a PET fiber spun at 4000 m/min are influenced by the on-line zone heating temperature (T). Apparently, birefringence (Δn) and modulus (M) increase remarkably as T exceeds 80°C. These properties appear to be maximized whereas the elongation (E) at break is minimized at 140°C. Optimum T depends on take-up speed. Higher temperatures are needed for higher take-up speeds. The position and the length of the on-line zone heating are also critical to the development of fiber structure. In general, optimum distance decreases with increasing take-up speed. These parameters are also associated with other factors such as polymer characteristics, flow of cooling air, filament denier, etc..

Figure 2 compares the birefringence data obtained in this study with those in the literature[1] Significant increase in birefringence has been obtained via the approach of on-line zone heating. Further characterization results, e.g., DSC, radial structure analysis and x-ray diffraction will be presented. On-line measurement of threadline temperature, diameter and birefringence will also be reported.

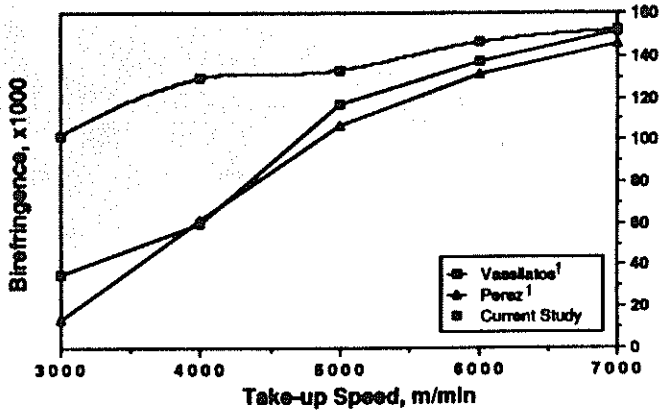


Figure 2. Birefringence vs. Take-up Speed.

REFERENCE

1. A. Ziabicki and H. Kawai (Eds.), High Speed Fiber Spinning, Wiley Interscience, New York, 1985.

8/7

DEFORMATION STUDIES OF LIQUID CRYSTALLINE POLYMERS

Anagnostis E. Zachariades, IBM Research Division, Almaden Research Center, 650 Harry Road, San Jose, CA 95120, USA

Patrick Navard, Ecole Nationale Superieure des Mines de Paris, CNRS 852, Sophia Antipolis, 06565 Valbonne Cedex, France.

Polymer liquid crystals, when subjected to shear flow, exhibit a characteristic optical effect which appears as a banded pattern of bright and dark bands perpendicular to the flow direction. This optical effect has been observed with main-chain polymer liquid crystals such as aromatic copolyesters, polypeptides, polyisocyanates, aromatic polyamides and cellulose derivatives and it appears to associate with with the characteristic molecular organization and orientation which is induced during the flow process.

Various attempts have been made to describe the origin of the banded texture, most of them in studies with nematic liquid crystalline polymers and focusing on the evaluation of the residual molecular orientation after shearing (1,2). Optical and electron microscopy studies indicate that the trajectory of the molecules is not planar but that there is some periodic rotational correlation between the molecules, in phase with the periodicity of the trajectory (3-5). Also, since the band texture phenomenon is not observed with small molecule liquid crystals and associates with some relaxation process (6), it becomes obvious that it is related to the elastic properties of the polymer chain. Thus, a cooperative relaxation motion of the molecules is believed to occur requiring that a) the relaxation occurs in the same direction, and b) there is a lateral correlation between the molecules. One way to model this phenomenon is to imagine the polymer chains gathered into long fibrils of elongated and oriented domains in the same direction. Upon relaxation, these domains buckle, leading to the optical pattern of the band texture.

In this presentation, we shall discuss the optical anisotropy of the band textures in trifluoroacetoxypropyl-cellulose (7), a thermotropic cellulose derivative, addressing in particular the issue of the molecular trajectory, an important parameter for understanding the origin of band patterns in liquid crystalline polymers.

References

1. C.E. Chaffey and R.S. Porter, J. Rheol., 29,281 (1985).
2. G. Marrucci, Pure and Appl Chem., 57,1537 (1985).
3. A.M. Donald, C. Viney, and A.H. Windle, Polymer, 24,155 (1983).
4. C. Viney, A.M. Donald, and A.H. Windle, J. Mat. Sci., 18, 1136 (1983).
5. A.M. Donald and A.H. Windle, J. Mat. Sci., 18, 1143 (1983).
6. A.E. Zachariades, P. Navard, and J.A. Logan, Mol.Crys.Liq. Cryst., 110, 93 (1984).
7. S.M. Aharoni, Macromolecules, 12, 94 (1979).

ANALYSIS OF DRAWINGS IN THE FLAT PET FILM PROCESS

G. LE BOURVELLEC, J. BEAUTEMPS Rhône-Poulenc Recherches - CRC - 85, Av. des Frères Perret - 69190 St Fons - FRANCE

J.P. JARRY Rhône-Poulenc Recherches - CRA - 14, R. des Gardinoux - 93308 Aubervilliers - FRANCE

One of the main uses of poly ethylene terephthalate is the film processing for applications in the field of magnetic tapes, packaging, capacitors, etc. The PET films can be made by a flat process (Figure 1), in which the film is biaxially oriented as it is successively stretched in two directions, the machine direction (MD) and the transverse direction (TD).

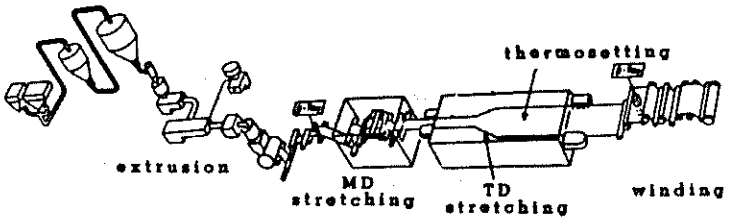


Figure 1 : Example of a flat film process.

However, according to the flat process, the first drawing can be either MD stretching or TD stretching. As the drawability in the second direction depends on the structure generated by the first stretching, it is important to know the evolution of the structure during the first drawing.

In this work, we performed laboratory simulations of MD and TD stretchings involved in a flat process.

The TD stretching, performed in a stenter, can be simulated by a drawing at constant speed of elongation. The MD stretching, performed between rolls, is equivalent to a drawing under constant load.

The kinetics of deformation are described for each stretching. It is shown that the strain rates involved in a drawing under constant load can reach very high values (20 to 30 s^{-1} at 97°C) compared to the case of stretching at constant speed of elongation (less than 1 s^{-1}). We also found specific features for the stretching at constant force (Figure 2)

* All the curves end by a plateau.
* There is a minimum plateau deformation (natural draw ratio).
* Under low tension, the plateau deformation increases when the force F decreases.
* Under high tension, the plateau deformation increases with F.
* In all cases, the kinetics increases with the tension.

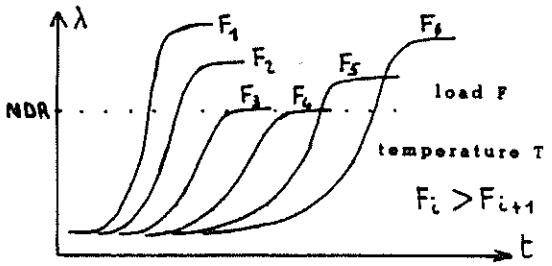


Figure 2 : Typical deformation curves of stretching under constant load

A structural analysis has been done for both stretchings in terms of orientations and crystallinity

For TD stretching, we found that the crystallinity is almost independent of the drawing temperature because of the balance between mobility and chains orientation.

For MD stretching, the main results are the following:
* For a given temperature and a given draw ratio, the structural properties increase with the stretching force.
* The plateau is equivalent to an annealing at constant length.
* At the beginning of a plateau, for a given draw ratio, the crystallinity is independent of the temperature of drawing.
* The temperature is the main parameter which controls the chains orientation, whatever the strain rates spectrum.

Finally, a comparison between MD and TD stretchings showed that:
* at low strain rates (less than 1 s^{-1}), the crystallinity depends only on the chains orientation and the temperature.
* at higher strain rates, the induced crystallization is limited by a kinetic effect (industrial case).

8/9

MECHANICAL PROPERTIES AND MORPHOLOGY OF POLYPROPYLENE-POLYETHYLENE BLENDS

P. Jääskeläinen and T. Aalto
Neste Oy, Corporate R & D, SF-06850 Kulloo, Finland

Blends of polyolefins have become commercially important where certain properties of the blends are shown to be better than the neat polymers.

Our study was primarily aimed to evaluate the mechanical properties such as toughness and elongation at break of polypropylene block copolymer.

Systematic research work on the mechanical properties and the morphology of blends made from polypropylene and speciality polyethylene grades. Two different polypropylene block copolymers and ten different very low density polyethylenes, containing 1-butene, 1-hexene and propene as a comonomer, were used. All blends contained 10 to 20 % polyethylene. Mechanical tests including tensile tests, flexural properties, impact resistance at -20 °C and analytical tests such as SEM, DSC, DMTA, TWA were conducted to compare the effect of the polyethylene type on the performance of the blend.

1) Morphological studies showed clearly the two phase structure of these blends.

2) The type of the comonomer had a significant effect on the size of dispergated phase. Polyethylene containing propene as a comonomer had the best dispersion and polyethylene containing 1-hexene had the weakest dispersion.

3) The best improvement on the impact strength and flexural modulus can be achieved by polyethylene grades containing propene as a comonomer.

4) The elongation at break of the blends increased significantly compared to the neat polypropylene block copolymer.

5) Many strong statistical correlations were found between the composition and the mechanical properties in the blends. Dynamic modulus correlated with the flexural modulus, Young's modulus, elongation at yield and stress at yield. The height of tan maxima correlates with the amount of polyethylene and impact properties.

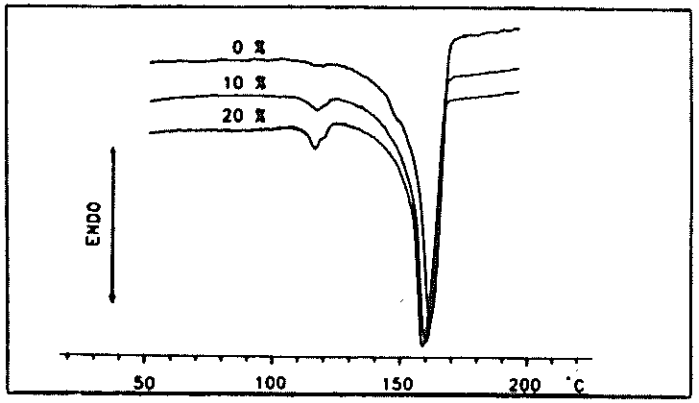


Fig. 1. Melting behavior of polypropylene-polyethylene blends containing 0, 10 and 20 % VLDPE.

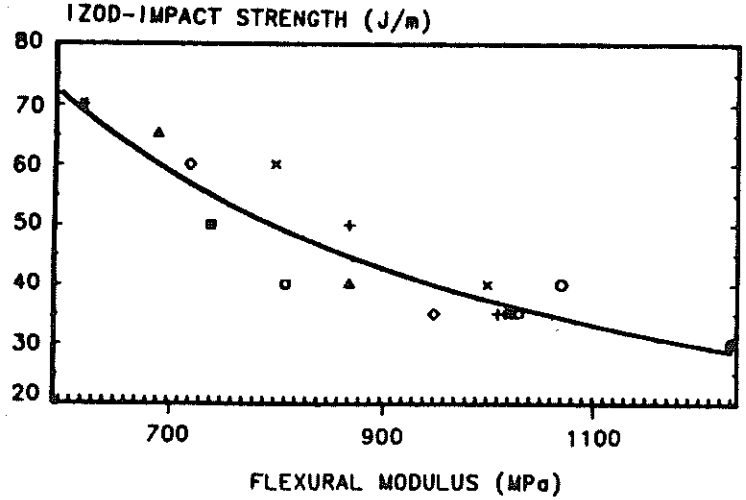


Fig. 2. Izod impact strength at -20 °C as a function of flexural modulus at ambient temperature for different polypropylene/VLDPE blends.

PROPERTIES OF ROLLED MULTILAYER POLYMER SHEETS.

K. Nakayama*, A. Kaito*, M. Kato*, S. Takahashi**,
S. Nakayama**, Y. Sekiguchi**, and Y. Oyanagi***
* Research Institute for Polymers and Textiles,
1-1-4 Higashi, Tsukuba, Ibaraki Pref. 305 (Japan)
** Fujikura Ltd., 1-5-1 Kiba, Koto-ku, Tokyo, 135 (Japan)
*** Kogakuin University, 1-24-2 Nishishinjuku, Shinjuku-ku,
Tokyo, 160 (Japan)

The rolling of polymer sheets is one of the helpful methods to improve mechanical and physical properties. The rolling has advantage of being applicable to thick sheets of semicrystalline polymer. The molecular orientation and the tensile strength of polymers in rolling direction increase by drawing.

In this study, the hot rolling of polypropylene (PP) sheets in multilayers has been successfully applied for drawing thin PP films. The sheet composed of three thin PP films were rolled together through a pair of rollers heated at temperature under the melting point of PP (Fig. 1). The PP sheets 0.08 - 0.46 mm thick were cut into strips 100 mm wide, which were used for the experiment. The rolling was conducted under the following conditions:

1. Diameter of work roll : ϕ 100 mm
2. Rolling temperature : 70 - 110 °C
3. Turning speed of roll : 1 m / min

It is difficult to roll thin film in conventional process. The use of sheet in multilayer is advantageous in rolling (Fig. 2). The rolled sheets had smooth surface. Those with high thickness reduction were highly transparent.

The main points of the results were summarized as follows:

1. The wide angle X-ray photographs and the pole figures of the rolled specimens exhibit typical c-axis orientation.
2. The density changes remarkably with thickness reduction (Fig. 3).
3. The tensile strength of rolled specimens increases with increasing thickness reduction (Fig. 4).
4. The dielectric strength of specimen is higher compared with starting material.

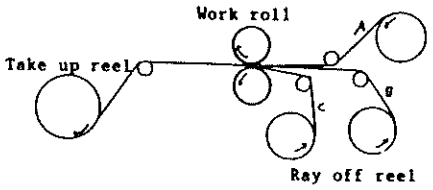


Figure 1. Schematic diagram of multilayer rolling.

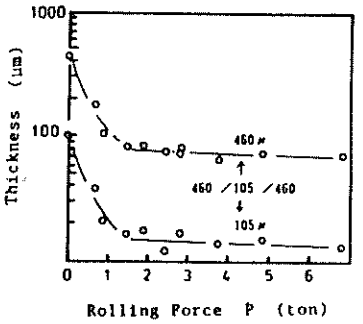


Figure 2. Relationships between rolling force and thickness of rolled multilayer sheets (460μm/105μm/460μm).

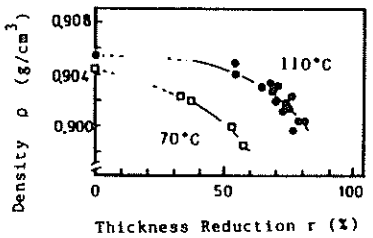


Figure 3. Relationships between thickness reduction and density.

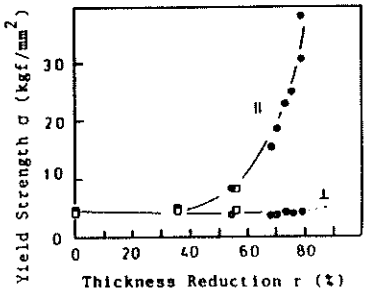


Figure 4. Relationships between thickness reduction and yield strength.

8/11

STUDIES ON THE BLENDS OF POLYETHYLENE TEREPHTHALATE POLYCARBONATE AND POLYPROPYLENE

A Misra, B L Deopura and R S Haldar
Centre for Materials Science & Technology
Indian Institute of Technology
New Delhi-110016, India

ABSTRACT

Polyethylene terephthalate (PET) possesses a number of excellent properties such as high tensile strength, dimensional stability, hardness, creep resistance, rigidity, gloss, clarity, scratch resistance, good chemical resistance, electrical insulation properties and excellent printability. On the other hand, it also has a number of shortcomings which make its molding very difficult in normal processing conditions. These are mostly its high glass transition temperature, low melt viscosity, slow rate of crystallization, low impact strength, sensitivity to processing temperature and considerably high moisture absorption (1). Although the molding of PET is uneconomical it would be a desirable molding material if the shortcomings of this polymer are overcome. From a preparative point of view, the most direct economic and versatile method of PET modifiction is its physical blending with other suitable polymer/polymers. In this study blends of polycarbonate (PC) and polypropylene (PP) with PET have been considered. PC possesses a very high melt viscosity and is a well known tough material with extremely high impact strength amongst the common thermoplastics. Furthermore, PC has a solubility parameter value very close to that of PET. In addition PP has been chosen as the third component because of its excellent moldability and low cost.

At first binary blends of PET and PC were studied with the amount of PC varying from 10 to 50% by weight. These blends were found to be compatible as has been earlier reported (2). For ternary blends the ratio of PET to PC was kept constant and different amounts of PP were added to form ternary blend systems. The level of PP in the blends was varied from 10 to 50% by weight. Moldability and mechanical properties of PET under normal molding conditions were found to improve significantly when it was blended with PC and PP to form ternary polymer blends. DSC results of these blends revealed that the PET and PC components formed a miscible phase (2) while PP being incompatible with them, formed a separate phase (3). PP was also found to form a sleeve around the PET-PC miscible phase and thereby showed a skin-core type of morphology (4) as revealed by selective solvent extraction and scanning electron microscopy. Variations of mechanical properties with increasing amounts of PP in the ternary blends was measured with the ratio of PET and PC constant. Tensile and flexural properties of the blends decreased with increasing amounts of PP. Notched impact strength increased upto a certain level of PP and then decreased, while the unnotched values decreased gradually. The effect of annealing on the mechanical properties of these blends have been discussed on the basis of the increased crystallinity of the crystallizable components. The crystallizable components get favourable conditions for crystallization on annealing and in addition the presence of PP spherulites, which form at much lower temperatures, may act as nucleating sites to enhance the crystallization of PET (5).

Some work along similar lines has been done with ternary blends of polybutylene terephthalate (PBT), PC and PP. It has been clearly shown that a judicial choice of polymers for blending can produce unique ternary blend systems. Ternary blend systems of the type discussed can be used to enhance desired mechanical properties and also make them economically more viable. Such systems give another dimension to the development of polymer blends with desired properties for their use in engineering applications.

REFERENCES

1. J.A. Brydson, "Plastic Materials", Newnes - Butterworth, London (1975).
2. T.R. Nassar, D.R. Paul and J.W. Barlow, J. Appl. Polym. Sci., 23, 85 (1979).
3. S. Krause, J. Macromol. Sci., Rev. Macromol. Chem., C7, 251(1972).
4. Heinz Herlinger and Peter Hirtandverner Koch, Lenzinger Berichte, 43, 24 (1977).
5. R.S. Haldar, Ph.D. Thesis, IIT, Delhi (1987).

8/12

STRUCTURE DEVELOPMENT IN SEQUENTIAL SKEW STRETCHING OF FILMS

by

J. P. Wu, M. Cakmak and J. L. White
Polymer Engineering Center
The University of Akron
Akron, OH 44325 U.S.A.

Analytical representations of orientation contain implicit assumptions that axes of symmetry are known. However, in many polymer products such as films produced with skew stretched or injection molded parts, the directions of the symmetry axes are unknown. This creates a different type of problem in defining orientations. One must first determine the location of the symmetry axes. At this point one determines the state of orientation relative to these axes. This view was developed earlier by two of us (1).

As a model study to characterize the products with complex orientation states, sequential skew stretched polyethylene terephthalate (PET) films were anlayzed. The symmetry axes of the skew stretched films were determined by refractive index, infrared absorptivity, and wide angle x-ray diffraction. The refractive index ellipsoid of film was obtained by the Abbe refractometer. The infrared absorption intensity ellipsoid was determined by the FTIR with polarizer. The symmetry axes were determined by the least square curve fitting of the general equation of ellipsoid. Wide angle x-ray diffraction pole figures of various planes were obtained on their films. This pole figure also yields the skewed symmetry axis with respect to the reference stretching direction. The location of symmetry axes determined by the refractive index measurement and by the infrared absorptivity measurement is well matched. Figure 1 shows the tendency to move symmetry axes toward the second stretching direction with the increasing second stretching ratio. Biaxial orientation factors (2,3) were determined with respect to these major and minor symmetry axes by infrared dichroism 975 cm^{-1} band. These are displayed in Figure 2 in an isosceles orientation triangle (2,3).

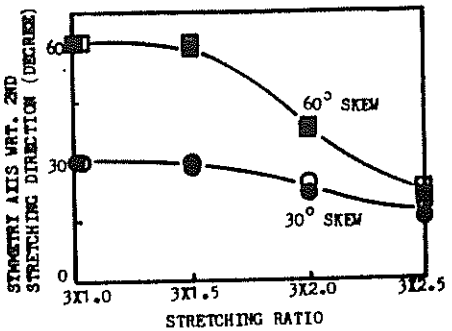


Figure 1. The Variation of Symmetry Axes on the Stretching Ratio

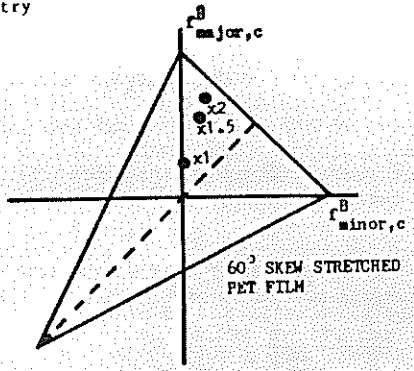


Figure 2. The Biaxial Orientation Factors of Skew Stretched PET Films Relative to the Symmetry Axis

References

1. J. L. White and M. Cakmak, Int. Polym. Proc. 2, 48 (1987)

2. J. L. White and J. E. Spruiell, Polym. Eng. Sci. 21, 859 (1981)

3. J. L . White and M. Cakmak, "Orientation" in Encyclopedia of Polymer Science and Engineering", edited by H. Mark, N. Bikales, C. Overberger and G. Menges, 2nd ed. Vol 10, pg. 595 Wiley, N.Y. (1987)

8/13

EFFECT OF BIAXIAL STRETCHING ON SURFACE ROUGHNESS OF THIN METAL FILM COATED PET, PPS PEEK FILMS

M.Cakmak, Y.D. Wang, K. Iwakura
Polymer Engineering Center
University of Akron
Akron, OH 44325

In recent years, there has been a great proliferation of the use of metal coated thin polymer film membranes in applications such as heliostats for solar collectors (1,2) , optoelectronic devices such as Ruticons (3) and compact disks (CD)(4). The surface quality in these polymer-metal composite membranes directly affect their performance in the devices they are being used.

In this study, surface roughness and thickness distribution of thin polymeric membranes have been investigated as a function of biaxial stretching conditions. In addition, the effect of metal deposition on the latter properties were investigated. It has been found that the dominant factor influencing the surface quality (roughness, thickness distribution) in the polymer films is their ability to stress harden during the stretching operation. Of the three materials investigated only PPS (Poly P-Phenylene Sulfide) did not exhibit the stress hardening behavior. This resulted in the poor surface quality and thickness variations in the final products. Initially amorphous PET (Poly ethylene terephthalate) and PEEK (Poly Ether Ether Ketone) films exhibit stress hardening due to crystallization during the stretching operation. This caused an improved surface quality and thickness distributions. This behavior is illustrated in Figure 1 where standard deviation of thickness profile is plotted as a function of biaxial stretch ratio . The difference between MD (extrusion) and TD directions in cast films are due to shrinkage marks occurred during fast quenching from the melt. At 3x3 equal biaxial condition the difference between the two directions disappears. A similar behavior was observed in micro level surface roughness of PET and PEEK films measured by a high precision surface profiler . A typical graph for standard deviation of surface profile versus stretch ratio for PEEK films is shown in Figure 2 .

Metal silver vapor deposition process was also found to have a significant effect on the surface quality of the composite films produced. The films coated with a thin layer of Silver metal (short coating time) show surfaces rougher than the precursor polymer film surface. This behavior reverses above a critical coating thickness of about 2000 A. Further increase in the silver thickness causes a reduction in the surface roughness and ultimately at about 2500 A thickness the surface quality becomes better than the surface of the original substrate surface (Figure 3). This behavior is attributed to joining of silver islands to form a smooth silver surface at higher coating times (thicknesses).

REFERENCES
1. B.A. Benson, Energy, 12, 203 (1987)
2. P. Schissel, H.H. Neidlinger and A. W. Czanderna, Energy, 12.197 (1987)
3. A. I. Lakatos, J. Appl. Phys., 45.4858 (1974)
4. Plastics Technol., 33.No.12.13 (1987)

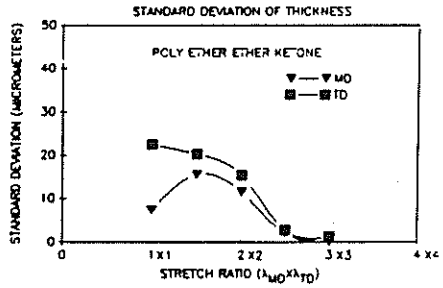


Figure 1.

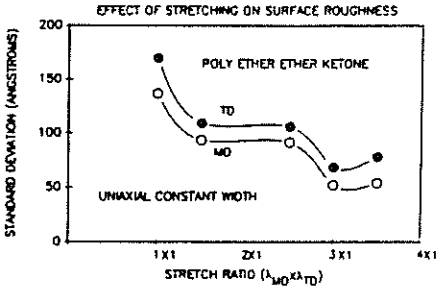


Figure 2.

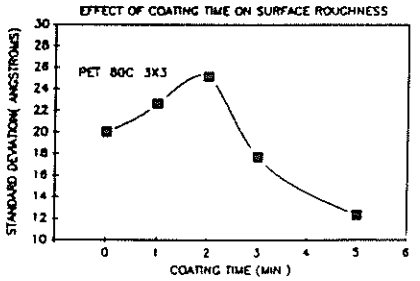


Figure 3.

STRUCTURE OF PE FIBER PRODUCED BY ZONE DRAWING SYSTEM

M.Takahiro,T.Takahashi,N.Okui,T.Sakai(Dept. of Organic Materials,Tokyo Inst. of Tech.,Meguro-ku,Tokyo,Japan)

We produced PE(Polyethylen) fiber by using a constant load type or constant rate type zone drawing system with various drawing temperaturs and draw ratios. It was shown that the reverse of Young's modulus of fiber produced by a constant load type zone drawing was linearly rational to the reverse of square of draw ratio, irrespective of a variety of drawing condition. While, the birefringence of fiber Δn was measured and the birefringence of amorphous part Δn_a was calculated by using the assumption that the fiber is composed of three parts, 1) highly oriented amorphous part, 2) randomly oriented amorphous part, 3) highly oriented crystalline part. Then it was found that the reverse of Δn_a also showed a linear relation to the reverse of square of draw ratio. From this relation, the intrinsic birefringence for amorphous PE Δn_a^* was estimated as around 0.210, if β and f_β are assumed to be unity at infinite draw ratio. β is a volume fraction of highly oriented amorphous part against total one and f_β is an orientation function of highly oriented one. Comparing these facts suggests that Young's modulus of fiber could be described with a series model consisting of crystalline and amorphous parts, and the drawing procedure might increase Young's modulus of amorphous part. Dividing Δn_a by Δn_a^* leads to $f_\beta \cdot \beta$. The orientation function f_β is connected with Young's modulus of the oriented amorphous region E_β. Further, let assume a parallel model of highly oriented amorphous part and completely random amorphous part, then Young's modulus of amorphous part is determined . Under some approximations, rearranging these equations generats an expression for the relation between Young's modulus of fiber and birefringence of amorphous part.

$$E \simeq E_a^* / [(1-X_c)\cdot(1-f_\beta)\cdot f_\beta] \cdot \Delta n_a / \Delta n_a^*$$

E_a^* is Young's modulus of random amorphous region. X_c is the volume fraction of crystalline part. Thus it is shown that Young's modulus of fiber increases with increase of draw ratio in the same way as increase of birefringence of amorphous part. In the case of constant load drawing, f_β is estimated as around 0.983. Applying the set of equations on results for the constant rate drawing, f_β was obtained. It is of interest to note that f_β was very close to the orientation function of crystalline for each of drawing conditions. Small X-ray scattering showed an existance of long period which might coincide with the series model of crystalline and amorphous parts. Here, the problem is why the highly oriented amorphous part is even sustained at a room temperature which is higher than glass transition point of amorphous PE. According to experiments , it was observed that the thermal stress of drawn fiber appeared above the crystalline dispersion temperature . The fact means the posibility of structural picture as depicted in fig.1,where some crystals block the relaxation of oriented molecular in the amorphous part. However the next question is if the structure given in fig.1 could act as a series model when extended. We tried to simulate the structural feature of given model in fig.1 with a model described in fig.2, where blocked amorphous parts are replaced by ellipsoidal bodies. And we derived Young's modulus of the new model with parameters of aspect ratio and of volume fraction of amorphous region by using modifyed Eshelby theory. The most interesting result was that aspect ratio 8 gave a Young's modulus almost the same to that of series model. This may suggest a structure as shown in fig.3 for the PE fiber made by zone drawing.

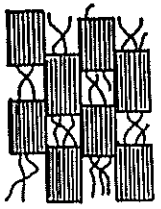


fig.1

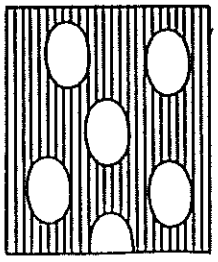


fig.2

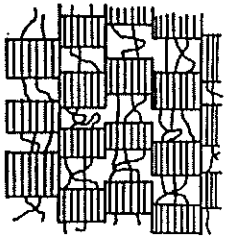


fig.3

8/15

STUDIES OF STRUCTURAL DEVELOPMENT IN PROCESSED POLYMERS BY SMALL-ANGLE SCATTERING TECHNIQUES*

J. S. Lin, Solid State Division, Oak Ridge National Laboratory, Oak Ridge, Tennessee 37831

Polymer processing in industrial applications often creates or initiates morphological changes which in turn affect the chemical, physical, and mechanical properties of polymeric products. Morphological and structural changes are usually associated with the change in electron density contrast and thus would readily be studied by the small-angle x-ray scattering (SAXS) techniques. For even more subtle change of polymer chains in the polymer processing, the deuterium labelling of polymer portion of interest has been uniquely and advantageously employed in the small-angle neutron scattering (SANS) technique.

Polymer processings, such as spinning, rolling, extrusion, molding, annealing, and many other forms of deformation have been widely used in the production of engineering plastics or quality polymers. The structural development and morphology can be followed in situ or studied for the processed polymer. SAXS studies were performed with the ORNL 10-m SAXS system which features a 12-kW rotating-anode x-ray generator and a 20 x 20 cm two-dimensional position-sensitive area detector, while SANS studies were performed with the ORNL 30-m SANS system in which thermal neutrons of 2.35 A or 4.75 A were monochromatically selected by graphite crystals from neutrons generated by a 100-megawatt steady state high-flux reactor (HFIR) at Oak Ridge. A ^{3}He-filled two-dimensional position-sensitive detector of 65 x 65 cm size provides 64 x 64 simultaneous data array acquisition. Such digitalized detection of scattering patterns offers a means to follow the structural development of processed polymers for both isotropic and anisotropic scattering behavior.

Some typical results from processed polyolefins, ionomers, and polymer blends will be discussed and to illustrate the uniqueness and applicabilities of the SAS techniques for the study of morphologies in polymer processing.

---

*Research sponsored by the Division of Materials Science and the National Science Foundation under grant DMR-8616912, with the U.S. Department of Energy under contract DE-AC05840R21400 with Martin Marietta Energy Systems, Inc.

"The submitted manuscript has been authored by a contractor of the U.S. Government under contract No. DE-AC05-84OR21400. Accordingly, the U.S. Government retains a nonexclusive, royalty-free license to publish or reproduce the published form of this contribution, or allow others to do so, for U.S. Government purposes."

NEW METHODS OF CHARACTERIZING STRUCTURE IN PROCESSED POLYMERS

Robert J. Samuels
School of Chemical Engineering
Georgia Institute of Technology
Atlanta, Georgia 30332-0100

The attraction of structural analysis to the polymer process industry is that it provides a logical link between process engineering on the one hand and commercially interesting properties on the other. For this link to be practical however it must be rapid enough to contribute to a project directly, yield information of sufficient complexity to match the complexity of the fabricated samples and if possible, do minimum damage to the sample.

Where structural information about molecular orientation and crystallinity are concerned the degree of complexity of the sample frequently dictates the practicality of a technique. Thus numerous techniques are available for the study of thin films (1) that are impractical where thicker fabricated parts are concerned. The increasing number of process - structure - property studies of thin film systems is a direct consequence of the availability of these techniques.

Studies on thin films and fibers (1) have shown that the mechanical properties and deformation behavior of a crystalline polymer frequently depends on the orientation state of one of the phases. Thus identification of the average orientation of both phases together is not a sufficient measure of the structural state of the polymer. To properly characterize the structure of the polymer it is necessary to determine the crystallinity and both the crystalline and the noncrystalline orientation separately. Once these structural parameters are known, it becomes possible to identify quantitative correlations between these parameters and mechanical properties; which then allows prediction of future performance (2,3,4,5).

On the other hand, the connection between the fabrication conditions, the resulting structure and the properties of thick crystalline polymer sheets, multilayer films, injection molded parts, etc. is poorly understood. There are several reasons for this lack of understanding, prominent among which is the complexity of the structures developed as a consequence of the thermal and flow gradients present in the thick samples during processing. These gradients can produce layered structures through the specimen which vary in orientation, crystallinity and axiality depending on the fabrication process used. Further, since the polymer will have both crystalline and noncrystalline phases, the individual orientation and axiality of each phase can be different within a given layer. Such complexity is difficult, expensive and time consuming to characterize and presently impossible to predict. One consequence of these practical problems is that comprehensive research on this industrially important subject has been limited.

Recent polarized optical and spectroscopic techniques being examined and developed in our laboratory suggest that nondestructive characterization of thick samples is possible in a rapid enough time frame to make structural evaluation of ongoing processes practical. This includes rapid quantitative identification of the orientation of each phase individually, averaged through the sample thickness. This measurement is nondestructive and fast enough, for example, for routine structural analysis of fabricated test samples, such as tensile bars or impact plaques, to be made before mechanical testing of the same samples. Several nondestructive techniques for surface structure characterization have also been introduced which make acquisition of this information more accessible. Further, new microbeam techniques offer more practical solutions to the evaluation of the layer structure through the thickness of the sample.

The purpose of this paper is to identify these techniques, give examples of their practical application and discuss their present advantages and limitations. The paper is organized in a structurally hierarchical fashion. That is, first averaged phase orientation through the thickness is discussed, then surface structure analysis and finally layer structure characterization. Isotactic polypropylene films, sheets, and moldings are used for all examples.

REFERENCES

1. R. J. Samuels, Structured Polymer Properties,Wiley- Interscience, New York, 1974.
2. J. C. Seferis and R. J. Samuels, Polym. Eng. and Sci., 19, 975 (1979).

3. J. C. Seferis, R. L. McCollough and R. J. Samuels, J. Macromol. Sci.-Phys., B13 (3), 357 (1977).
4. B. E. Linder and R. J. Samuels, Polym. Eng. and Sci., 25, 875 (1985).

5. R. J. Samuels, Polym. Eng. and Sci., 19, 66 (1979).

8/17

TIME-RESOLVED SAXS AND WAXS STUDIES OF ORIENTED CRYSTALLIZATION OF POLYMERS

Kenji Saijo and Takeji Hashimoto
Department of Polymer Chemistry, Faculty of Engineering, Kyoto University, Kyoto 606, Japan

Oriented crystallization of polymers is one of the very important problem in polymer processing and has been a subject of many theoretical and experimental investigations for a long period of time. The studies involve a fundamental physical problem concerning the effect of molecular orientation (i.e., a reduction of conformational entropy of the long-chain molecules) on liquid-solid phase transition, i.e., a problem inherent and unique to the long-chain molecular systems.

Objectives of our studies are to pursue real-time and in-situ analyses of the microscopic observables which are directly related to structure rather than the macroscopic observables such as volume, heat content and etc. during the isothermal crystallization in order to clarify mechanism and dynamics of the ordering processes of the systems. As for the microscopic observables the following quantities were investigated; the long spacing L, crystallite size D, integrated scattering intensity Q_r as measured by time-resolved small-angle X-ray scattering (SAXS) and crystallinity X_c as measured by time-resolved wide-angle X-ray scattering (WAXS), and as for one of the macroscopic observables the stress relaxation was observed.

As a moldel system to study oriented crystallization we have chosen crosslinked polybutadiene rubber(PB). PB have 99% cis-1,4-linkage and number average molecular weight 1.2×10^5 in the uncross-linked state. The polymers were cross-linked by using Sulfasan R (4,4'-dithio morpholine), having a cross-link density 1×10^{-4} mol/cc and a number average molecular weight between cross-linkes of 9000. The rubber network was first stretched uniaxially to a given draw ratio λ (λ = 1 to 5) and then crystallized isothermally at T_c (T_c = -50 to 10°C) under the constant external draw ratio.

The isothermal crystallization processes may be divided into three different regimes for the sake of convenience : Regime I for crystallization under no orientation, Regime II for crystallization under weak-to-moderate orientation, and Regime III for crystallization under relatively high orientation. λ's and T_c's covered in each regime are as follows; λ = 1 and T_c = -50 to -20°C (Regime I), λ = 2 to 3.5 and T_c = -30 to -10°C (Regime II), and λ > 4.5 and T_c = -30 to 10°C (Regime III). It should be noted that the unoriented cross-linked rubber has melting temperature of 0°C and maximum crystallization rate at -40 °C. Figure 1 schematically illustrates the time-evolution behavior of the microscopic variables in each regime at a given crystallization temperature, e.g., T_c = -30 °C. In the Regime I, the time-evolution of X_c occurs almost simultaneously with that of Q_r, and L tends to decrease slightly with time t. The crystallite thickness D is invariant with t. In the Regime II, L tends to decrease dramatically with t while D is kept constant. The time-evolution of Q_r occurs much in advance of that of X_c. In the Regime III, L does not change in the time scale covered in this experiment. The time difference between the evolution of Q_r and that of X_c further increases, and X_c gradually and slowly increases in the time scale where there is no change of L and a little change of Q_r.

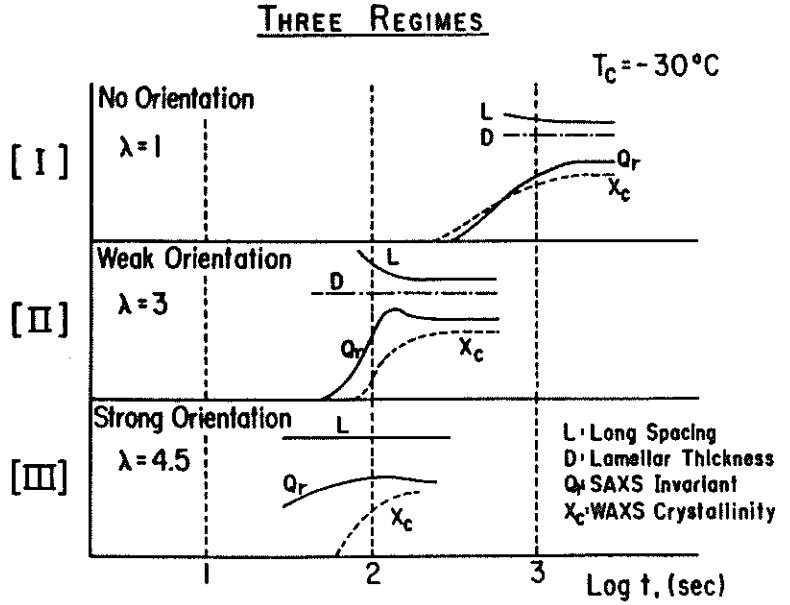


Fig.1 Schematic diagram showing time-evolution of the microscopic observables during the isothermal crysatllization in three different regimes.

STUDIES ON THE BLENDS OF POLYETHYLENE TEREPHTHALATE POLYCARBONATE AND POLYPROPYLENE

A Misra, B L. Deopura and R S Haldar
Centre for Materials Science & Technology
Indian Institute of Technology
New Delhi-110016, India

ABSTRACT

Polyethylene terephthalate (PET) possesses a number of excellent properties such as high tensile strength, dimensional stability, hardness, creep resistance, rigidity, gloss, clarity, scratch resistance, good chemical resistance, electrical insulation properties and excellent printability. On the other hand, it also has a number of shortcomings which make its molding very difficult in normal processing conditions. These are mostly its high glass transition temperature, low melt viscosity, slow rate of crystallization, low impact strength, sensitivity to processing temperature and considerably high moisture absorption (1). Although the molding of PET is uneconomical it would be a desirable molding material if the shortcomings of this polymer are overcome. From a preparative point of view, the most direct economic and versatile method of PET modifiction is its physical blending with other suitable polymer/polymers. In this study blends of polycarbonate (PC) and polypropylene (PP) with PET have been considered. PC possesses a very high melt viscosity and is a well known tough material with extremely high impact strength amongst the common thermoplastics. Furthermore, PC has a solubility parameter value very close to that of PET. In addition PP has been chosen as the third component because of its excellent moldability and low cost.

At first binary blends of PET and PC were studied with the amount of PC varying from 10 to 50% by weight. These blends were found to be compatible as has been earlier reported (2). For ternary blends the ratio of PET to PC was kept constant and different amounts of PP were added to form ternary blend systems. The level of PP in the blends was varied from 10 to 50% by weight. Moldability and mechanical properties of PET under normal molding conditions were found to improve significantly when it was blended with PC and PP to form ternary polymer blends. DSC results of these blends revealed that the PET and PC components formed a miscible phase (2) while PP being incompatible with them, formed a separate phase (3). PP was also found to form a sleeve around the PET-PC miscible phase and thereby showed a skin-core type of morphology (4) as revealed by selective solvent extraction and scanning electron microscopy. Variations of mechanical properties with increasing amounts of PP in the ternary blends was measured with the ratio of PET and PC constant. Tensile and flexural properties of the blends decreased with increasing amounts of PP. Notched impact strength increased upto a certain level of PP and then decreased, while the unnotched values decreased gradually. The effect of annealing on the mechanical properties of these blends have been discussed on the basis of the increased crystallinity of the crystallizable components. The crystallizable components get favourable conditions for crystallization on annealing and in addition the presence of PP spherulites, which form at much lower temperatures, may act as nucleating sites to enhance the crystallization of PET (5)

Some work along similar lines has been done with ternary blends of polybutylene terephthalate (PBT), PC and PP. It has been clearly shown that a judicial choice of polymers for blending can produce unique ternary blend systems. Ternary blend systems of the type discussed can be used to enhance desired mechanical properties and also make them economically more viable. Such systems give another dimension to the development of polymer blends with desired properties for their use in engineering applications.

REFERENCES

1. J.A. Brydson, "Plastic Materials", Newnes - Butterworth, London (1975).
2. T.R. Nassar, D.R. Paul and J.W. Barlow, J. Appl. Polym. Sci., 23, 85 (1979).
3. S. Krause, J. Macromol. Sci., Rev. Macromol. Chem., C7, 251(1972)
4. Heinz Harlinger and Peter Hirtandverner Koch, Lenzinger Berichte, 43, 24 (1977).
5. R.S. Haldar, Ph.D. Thesis, IIT, Delhi (1987).

STRUCTURE DEVELOPMENT IN MELT SPINNING NYLON 11 AND NYLON 12

by

Y. Shi and J. L. White
Polymer Engineering Center
The University of Akron
Akron, OH 44325 U.S.A.

Nylon 11 and nylon 12 are two of the important commercial polyamides. Though nylon 11 and 12 fibers have been mentioned in the literature, no detailed investigation of their spinning has appeared. As in the case of other nylons, one of the most striking and interesting characteristics on nylon 11 and 12 is the polymorphic structures and their variation as a function of processing conditions.

Vacuum dried pellets were melt spun from a capillary rheometer under different spinning conditions. The melt spun fibers were stretched and/or annealed. The crystal structures of the various fibers were investigated using x-ray flat film photographs and diffractometer scans, combined with differential scanning (DSC) calorimeter traces. We found:

1. The crystallinity of nylon 11 spun-fibers as estimated from the DSC melting peaks ranged from 22% - 28% under our experimental conditions. At higher extrusion temperatures or the higher drawn-down ratios, the spun fibers had a tendency toward higher crystallinity. For nylon 11 spun fibers, the general appearance of the x-ray photographs suggested a triclinic α structure, but with very broad equatorial reflections. This tendency to form a triclinic α structure is a characteristic of the even-even and odd nylons (2,3).

2. A γ structure was developed during melt spinning of nylon 12. Stretching (at room temperature or at about 120°C) and annealing only produced γ -structures. Compared to nylon 6 spun fibers (1) the structures of nylon 12 are much more stable. Even after treatment with 90% formic acid, the γ structure remained unchanged. Only with drawing at temperatures near the melting point did x-ray diffraction indicate an α structure pattern. The crystallinity levels of nylon 12 spun fibers could not be evaluated, because we do not know the heat of fusion. If the heat of fusion of the two nylons can be considered as nearly the same, the DSC measurement would indicate that the nylon 12 spun fibers had a similar level of crystallinity with that of nylon 11 spun fibers.

3. The birefringence and crystalline orientation factors of the fibers were measured using a polarized light optical microscope and an x-ray diffractometer, respectively. Both birefringence and crystalline orientation factors for both nylon 11 and nylon 12 spun fibers are monotonic increasing functions of spinline stress. At low drawn-down ratios and low spinline stresses, nylon 11 spun fibers showed a lower birefringence than nylon 12. At high spinline stresses, they approached a similar level of 0.02 within the range of our experiment conditions. The birefringence for drawn fibers were also measured and values as high as 0.05 were obtained.

References

1. V. G. Bankar, J. E. Spruiell and J. L. White, J. Appl. Polym. Sci., 21, 2341 (1977)

2. Y. Kinoshita, Macromol. Chem., 33, 1 (1959)

3. M. D. Danford, J. E. Spruiell and J. L. White, J. Appl. Polym. Sci., 22, 3351 (1978).

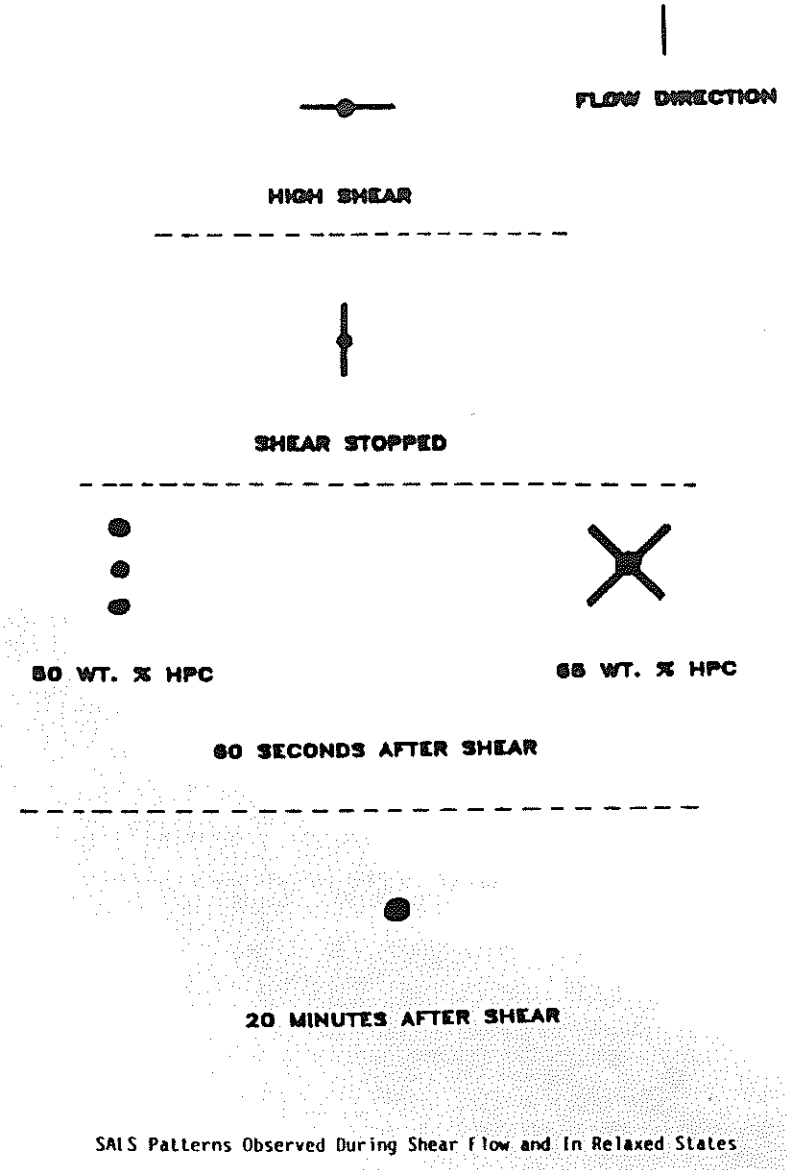
THE GROWTH AND DECAY OF STRUCTURE IN POLYMER LIQUID CRYSTALS VIA RHEO-OPTICAL MEASUREMENTS

G. W. Farell and J. F. Fellers, Materials Science and Engineering, The University of Tennessee, Knoxville, TN 37996-2200

The objective of this study is to obtain a better understanding of the generation and relaxation of molecular orientation developed in shear flow and the resulting superstructure in liquid crystalline polymers. To that end, a parallel quartz plate shear flow device with sample thicknesses of 0.003, 0.011, or 0.050 inches is fitted with two optical ports and allows transmitted intensity, light scattering, optical retardation and microscopy measurements to be made. The sample chamber is constructed so that solution and bulk samples can be observed from room temperature to 400°C. A sophisticated motor enables shear rates ranging from 0.45 sec^{-1} to 600 sec^{-1} and a broad range of transient shear conditions to be imposed on the sample. The equipment is interfaced with an IBM PC for data acquisition, management of the experiments and subsequent analysis.

Extensive experiments with hydroxpropyl cellulose (HPC) in water at 65 and 50 wt.% HPC have yielded the following phenomenological observations. The growth rate of birefringence increases as shear rate increases or sample thickness decreases. The decay rates are simple exponentials for the low shear rate case but follow Williams-Watts-Kohlrausch behavior in the higher shear rate region. In no case does the birefringence decay to the original 'at rest' value it started from. At 65 wt.% a surface orientation event is implied from the long term residual retardations observed. An estimate of the thickness being equal to 25 microns is made by using the maximum intrinsic birefringence and its relationship to the retardation. The light scattering behavior is peculiar and interesting. At high shear rates a horizontal streak is seen between crossed polars while shearing occurs. Upon the cessation of shear, a vertical streak appears and then relaxes which is then followed by sharp streaks that cross at about 45°. The behavior does depend on the shear rate at which the deformation occurs and is most dramatic at high shear rates.

The light scattering behavior of the 50 wt.% HPC solution is somewhat different than that of the 65 wt.% solution. As with the 65 wt.% solution, a sharp horizontal streak is observed at high shear rates. Upon cessation of shear the vertical streak also appears. However in the 50 wt.% solution this streak evolves into discreet spots.



SALS Patterns Observed During Shear Flow and In Relaxed States

8/21

STRUCTURE DEVELOPMENT IN THERMOTROPIC LIQUID CRYSTALLINE POLYMERS

K. G. Blizard, T. S. Wilson and D. G. Baird (Polymer Materials & Interfaces Laboratory and Department of Chemical Engineering) Virginia Polytechnic Institute & State University, Blacksburg, VA 24061-6496

The successful use of thermotropic liquid crystalline polymers (LCP's) rests primarily on finding novel ways to process these unique materials. It is known that one can make high modulus/strength fibers from LCP's. However, on injection molding these materials one may obtain a high flexural modulus in the flow direction but it is highly dependent on the mold thickness. The morphology and orientation which are generated during processing appear to be a function of thermal and flow history. Because a number of LCP's exhibit super-cooling we have been able to process them in various ways in which different deformation histories are possible. In extrusion it is possible to set the die temperature as low as 50°C below the melt temperature and still extrude the product. This, however, depends on the crystallization kinetics for the LCP and the die length. A significant increase in the modulus of an as-extruded material can be obtained in extrusion if the material is extruded below the melting point, Tm. In fact moduli of 0.5 to 1.0 x 10^6 psi are possible. However, wide angle x-ray diffraction show that it is only the outer layers which are oriented and the inner core is unoriented.

Because of the increase in elasticity observed in the super-cooled state it is possible to blow mold LCP's. The structure which is generated depends on the melt and die temperatures. For example, if the melt temperature for a 60/40 PHB/PET copolyester is set at 260°C or 275°C and the die at 190°C, then the outer and inner wall of the bottle have mostly axial orientation. However, if this polymer is extruded with a melt temperature of 220°C and a die temperature of 200°C, it is possible to obtain orientation along the circumfertial direction of the bottle. By freely blowing the parison no orientation was observed but exceptional uniform physical properties were obtained (the tensile modulus was over 1 x 10^6 psi).

Uniaxial drawing of flat films lead to the best properties with moduli of over 2 x 10^6 psi possible. The success of this progress rested on extruding the LCP's through a die set at temperatures well below Tm again. The extrudate was rubbery and had good melt strength. The morphology of the films was highly fibrous and wide angle x-ray diffraction patterns exhibit a high degree of molecular orientation.

Attempts to biaxial orient several LCP's were also carried out using three different techniques: film blowing, solid state forming, biaxial mechanical stretching. In the process of film blowing it was not possible to completely disrupt the axial orientation generated by extrusion through the film die. However, as the blow up ratio increased the modulus in the transverse direction did increase significantly while it decreased slightly in the machine direction. Tensile moduli as high as 2.0 x 10^6 psi were possible in the machine direction with values of about 0.4 x 10^6 psi in the transverse direction. Each of these methods seemed promising as potential ways to generate biaxial properties in LCP's.

FACTORS AFFECTING POLYMER BLEND MISCIBILITY

Isaac C. Sanchez, Alcoa Laboratories, Alcoa Center, PA 15069

As is well known, binary mixtures of polymers are generally immiscible and it is now becoming increasing clear what factors affect polymer blend miscibility. When two polymers are found to be miscible, phase separation can often be induced thermally by increasing temperature. The latter is an example of a system that exhibits lower critical solution temperature (LCST) behavior. The origins of LCST behavior are twofold: specific interactions and the mixture's finite compressibility. If the LCST is below the glass or crystallization temperature of the binary blend, the homogeneous or one-phase part of the phase diagram becomes effectively inaccessible. This has implications for processing because it is usually desirable to melt blend polymers in the one-phase liquid region of the phase diagram.

Another characteristic of a miscible polymer pair is a negative heat of mixing. The question of polymer blend miscibility is tantamount to the question: Will the polymer pair exhibit a negative heat of mixing? Until relatively recently it was generally believed that a specific interaction, such as a hydrogen bond, was required before a negative heat of mixing could be achieved. Now it is known that negative heats of mixing can be obtained in the absence of specific interactions providing that more than one interaction parameter is required to describe the binary system.[1-3] A good example of such a situation is the AB + C polymer pair where the AB polymer is a copolymer of A + B monomer units. Three interaction parameters, χ_{AB}, χ_{AC}, and χ_{BC}, are required to describe this system. Even when the interaction parameters are all positive, if

$$\chi_{AB}^{1/2} > \chi_{AC}^{1/2} + \chi_{BC}^{1/2}$$

a negative heat of mixing will be obtained. In an AB copolymer melt the non-bonded A and B comonomer units are forced into intimate contact. If the A-B interaction is energetically unfavorable, this yields a high potential energy system. When the high energy AB copolymer is mixed with homopolymer C, a negative heat of mixing can result because the unfavorable A-B interactions are diluted. Thus, even when all three types of monomer-monomer interactions are energetically unfavorable, a negative heat of mixing can be obtained when the above inequality holds.

In copolymers, there is experimental evidence that the comonomer sequence distribution can play an important role in determining miscibility. Block, alternating, and random AB copolymers of the same composition can exhibit different apparent interaction parameters with homopolymer C. The effect of sequence distribution can be accounted for by allowing A-C interactions (B-C and A-B interactions as well) to depend on the monomer units that are directly bonded to A; i.e., the A-C interaction could involve any of the three triplets AAA, BAB, or BAA. The idea is that the interaction of the central monomer of the triplet (in this case the A monomer) with a C monomer is influenced by its bonded neighbors. In this scheme it is necessary to specify one independent pair probability, say f_{AB}, the probability of an AB pair. The interaction parameter for the blend then becomes[4]

$$\chi_{blend} = \chi_{comp} + \chi_{dist}$$

where χ_{comp} depends only on the composition of the copolymer and χ_{dist} depends both on composition and f_{AB}. What has been found is that there are optimal sequential arrangements of the A and B monomers for miscibility. The effect of sequence distribution on miscibility becomes particularly important for binary blends of AB copolymers.[5]

References

1. ten Brinke, G.; Karasz, F. E.; MacKnight, W. J. Macromolecules 1983, 16, 1827.
2. Kambour, R. P.; Bendler, J. T.; Bopp, R. C. Macromolecules 1983, 16, 753.
3. Paul D. R.; Barlow, J. W. Polymer 1984, 25, 487.
4. Balazs, A. C.; Sanchez, I. C.; Epstein, I. R.; Karasz, F. E.; MacKnight, W. J. Macromolecules 1985, 18, 2188.
5. Balazs, A. C.; Karasz, F. E.; MacKnight, W. J.; Ueda, H.; Sanchez, I. C. Macromolecules 1985, 18, 2784.

FLOW-INDUCED MIXING AND DEMIXING IN POLYMER BLENDS

James D. Katsaros, Michael F. Malone, and H. Henning Winter (speaker)
University of Massachusetts, Department of Chemical Engineering
Amherst, MA 01003, USA

Introduction: The miscibility of polymer blends depends on a delicate balance of entropic and enthalpic interactions. This balance may be easily disturbed by the application of external fields. Shear or extensional deformations (or combinations of these) are unavoidable in most processing operations. For example, a quiescent blend that is miscible in calorimetric, scattering, or microscopy studies may demix upon deformation and could be unsuitable for processing even at conventional rates. On the other hand, deformation may enhance miscibility and it may be possible to obtain some unique nonequilibrium properties by suitable processing, although this has not been confirmed experimentally. The few studies on polymer-polymer blends show that the shear or extensional deformation can induce miscibility already at modest deformation rates. Pressure seems to increase miscibility, although there is evidence that this effect reverses in endothermic systems. We will present recently obtained results which show that flow may, depending on temperature and composition, induce demixing in a polymer blend.

Background: There are relatively few studies of the effects of flow on polymer-polymer blend miscibility. Mazich and Carr (1983) used a cone plate apparatus to study the behavior of a polystrene/poly(vinyl methyle ether) blend (PS/PVME). They inferred an increase of the Lower Critical Solution Temperature (LCST) of 2 to 7 K at shear rates of 0.1 to 20 s^{-1} from a change in the slope of a viscosity-temperature plot. Katsaros, Malone and Winter (1986) studied a similar blend in planar stagnation flow, showing that an extensional field induces miscibility (transition from opaque to optical clarity) at deformation rates of approximately $1s^{-1}$ and above. The effect is sensitive to the composition and is greatly diminished above 65 weight% polystryene. Lyngaae-Jorgensen and Sondergaard (1987) found a homogeneous structure in a sheared blend of SAN and PMMA above the LCST. However, their shear rates were extremely high (10^3 s^{-1}). These experiments indicate that some unique mechanical properties can be achieved if the interconnected microstructure that is found in the early stages of spinodal decomposition above the LCST can be preserved in the quenched sample.

The effect of pressure is especially important for polymer processing which often requires high pressure levels. Maeda, Karasz and MacKnight (1986) showed that an increase in pressure from 1 to 200 MPa raised the coexistence temperature of a copolymer/homopolymer blend where the LCST remained independent of pressure. Walsh and Rostani (1985) found similar effects in a blend of ethylene-vinyl acetate copolymer with chlorinated polyethylenes. However, Rostani and Walsh (1987) also showed that certain oligomeric mixtures display either enhanced or diminished miscibility with increased pressure, depending on the sign of the enthalpy of mixing.

Most published work is not concerned with polymer blends but with solutions. Silberberg and Kuhn (1952) showed that the application of shear can induce miscibility in a ternary solution of polystyrene and ethyl cellulose in bezene. Since then, several studies of polymer solutions near the Upper Critical Solution Temperature (UCST) have been made, e.g., Ver Strate and Phillipoff (1974), Koningsveld and Kleintjens (1977), Wolf and Kramer (1980), and Wolf (1984). Usually, the deformation was found to cause demixing, i.e., to raise the coexistence temperature. However, there are also several observations to the contrary. Rangle-Nafaile, Metzner and Wissbrun (1984) reported an increase in the coexistence temperature of up to 30K for sheared solutions of polystyrene in dioctylphthalate.

Recent Experiments: Initial experiments showed that an extensional flow can raise the coexistence temperature by as much as 10K. In more recent studies, we have found that an extensional flow can also induce demixing in a PS/PVME blend at lower temperature and extension rates of 2 to 3 s^{-1}, see figure. The closeness of the glass transition causes problems in obtaining information over a wide temperature range. It is considered impossible to achieve thermodynamic phase equilibrium below the glass transition temperature of the mixture. We will show the location of the onset of phase separation for four PS/PVME compositions. The values for flow-induced phase separation at each composition correspond to a pressure of approximately 300 bar, measured at the capillary wall. The flow induced phase separation observed in our experiments is assumed to be due to the applied deformation and not due to pressure. We hypothesize that the flow raises the Upper Critical Solution Temperature above the glass transition temperatures of the blend. It is conceivable that at higher deformations of UCST may intersect the LCST curve and create an hourglass shaped phase diagram.

References: Katsaros, J.D., M.F. Malone, and H.H. Winter, Polym. Bull., 16, 83 (1986). Koningsveld, R., and L.A. Kleintjens, J. Polym. Sci., Polym. Symp., 61, 22 (1977). Lyngaae-Jorgenson, J., and K. Sondergaard, Polym. Eng. Sci. 27, 344 and 351 (1987). Maeda, Y., F.E. Karasz, and W.J. MacKnight, J. Apply. Polym. Sci., 32, 4423, (1986). Mazich, K.A. and S.H. Carr, J. Appl. Phys., 54, 551 (1983). Rangel-Nafaile, C., A.B. Metzner, and K.F. Wissbrun, Macromol., 17, 1187 (1984). Reich, S., and J.M. Gordon, J.Polym. Sci., Polym. Phys. Ed. 17, 371 (1979). Rostani, S., and D. J.Walsh, Polym. Eng. Sci. 27, 315, (1987). Silberberg, A., and W. Kuhn, Nature, 170, 450, (1952). Ver Strate, G., and W. Phillipoff, J. Polym. Phys., 24, 723 (1986). Walsh, D.J., and R. Rostami, Macromol., 18, 216 (1985). Wolf, B.A., and H. Kramer, J. Polym. Sci. Polym. Lett. 18, 789 (1980). Wolf, B.A., Macromol., 17, 615 (1984).

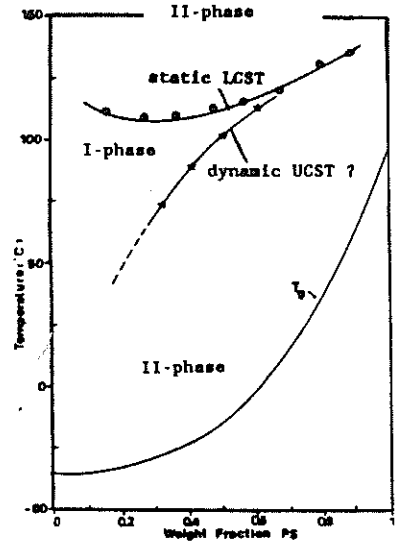


Fig.: Measured dynamic phase diagram of PS/PVME in extensional flow.

9/3

TOUGHNESS ENHANCEMENT IN PC/PMMA BLENDS VIA POLYMER PHASE SEPARATION

Thein Kyu, Jeanne M. Saldanha and Mark J. Kiesel
Center for Polymer Engineering, The University of Akron,
Akron, OHIO 44325.

Miscibility studies on polycarbonate/polymethyl methacrylate blends have been undertaken using time-resolved light scattering technique. It was found that the PC\PMMA blend exhibits miscible character with a miscibility window, reminiscent of a lower critical solution temperature[1]. Interconnected domain structures were observed when the blend was heated above the LCST temperature. A scattering halo also developed in the small-angle light scattering study, characteristic of spinodal decomposition. The time evolution of scattering peak was followed as a function of temperature jump for the 70/30 PC/PMMA blend. At low temperature jumps, the linearized Cahn-Hilliard theory[2,3] appears operative, however, deviations were seen at large temperature jumps or late stages of spinodal decomposition. This suggests that the general trend of phase separation in this PC/PMMA blend is prevailed by the non-linear behavior. The time evolution of the maximum intensity (I_m) and the corresponding wavenumber (q_m) obeys the power-law scheme with exponents of 3 and -1, respectively. These exponents are exactly the values predicted by Siggia[4] for the late stages of spinodal decomposition, which is identified to be a coarsening process driven by surface tension.

Melt mixing at biphase regime invariably resulted in phase separation, however, the domain size may be controllable depending on the time and temperature and the type of mixer used. A number of mechanical properties, notably Young's modulus, yield strength, plateau modulus and toughness were found to increase in the melt blended 70/30 PC/PMMA over that of pure PC, which is in good accord with the observation by Koo and coworkers.[5] This toughness enhancement may be attributed to good particle dispersion, particle size and good adhesion between the brittle PMMA and PC matrix. The compression molded 70/30 PC/PMMA in single phase regime, i.e. 40°C above the Tg of the blend, showed good transparency, but the mechanical properties were inferior to those of immiscible counter parts.

REFERENCES
1) T Kyu and J.M. Saldanha, J. Polym. Sci., Polym. Lett. Ed., 1987, in press.
2) J.W. Cahn, J. Chem. Phys. 42, 93; Metall. Soc. AIME 242, 166 (1966).
3) J.E. Hilliard in "Phase Transformations" ASME, p497, Oct. 1968.
4) E.D. Siggia, Phys. Rev. A, 20, 595 (1979).
5) K.K. Koo, T. Inoue and K. Miyasaka, Polym. Eng. Sci. 27, 741, (1985).

ACKNOWLEDGEMENT

The support of the Edison Polymer Innovation Corporation is greatfully acknowledged.

9/4

PHYSICOCHEMICAL INVESTIGATION OF THE COMPATIBILIZATION OF POLYAMIDE/POLYOLEFIN BLENDS: MORPHOLOGY, SPECIFIC INTERACTIONS AND THERMAL ANALYSIS

J.M. Willis, V. Caldas and B.D. Favis
Industrial Materials Research Institute, National Research Council Canada
75 De Mortagne Blvd., Boucherville, Que., Canada, J4B 6Y4

In previous work [1], the morphology of compatibilized polyamide/polyolefin blends prepared in a Brabender mixing chamber was studied quantitatively. The dimensions of the dispersed phase were significantly dependent upon the concentration of an ionomer compatibilizer (Surlyn, a terpolymer of polyethylene, methacrylic acid and isobutylacrylate) in the blends. The phase size decreased by as much as three to four times with the addition of as little as 0.5% Surlyn by weight in the blend.

The morphology of binary blends of Surlyn with polypropylene and polyethylene displays a two phase structure, as shown in Figure 1. There is, however, evidence of adhesion between the two phases in these blends. In contrast, binary blends of Surlyn with nylon appear homogeneous. No dispersed phase is observed in these blends with the exception of the 50%/50% (by weight) blend, where domains smaller than 0.1μm were observed. This can be seen in Figure 1, at high magnification (20000x). From a morphological standpoint, it appears that the nylon/Surlyn binary blend is significantly more compatible than the polyolefin/Surlyn binary blend, possibly as a result of greater interfacial interactions. Moreover, the extent of these interactions is dependent upon the methacrylate content of the Surlyn ionomer. When this quantity is reduced, a two phase structure is observed for the nylon/Surlyn binary blend at all blend compositions. Macknight et al. [2] have observed a similar dependence of the dispersed phase size on the methacrylic acid content of ethylene-methacrylic acid copolymers.

Physicochemical studies of these binary blends were undertaken in order to arrive at a better understanding of the effectiveness of Surlyn as an interfacial agent. Infrared results indicate that a specific interaction occurs between Surlyn carbonyl groups and polyamide amine groups. This interaction is absent between the polyolefins and Surlyn. Density measurements performed on the polyolefin/Surlyn binary blends display negative deviations from additivity. In contrast, the densities of the nylon/Surlyn binary blends display a positive deviation. Similar observations were made for the torque values measured during melt mixing of these blends in the Brabender mixing chamber.

Non-isothermal crystallization studies were performed using Differential Scanning Calorimetry. Crystallization rates were dependent upon the blend composition. More than one nucleation mechanism was observed, which alludes to differences in the physical interactions between the polymers in the binary blends.

The spectrometric, calorimetric and physical data obtained for the binary blends of Surlyn with polyamide, polypropylene and polyethylene concur with the morphological observations. This evidence suggests that there are much stronger interactions between Surlyn and nylon than between Surlyn and the polyolefins.

REFERENCES

1. J.M. Willis, V. Caldas and B.D. Favis, NRCC/IMRI Symposium "Polyblends-'88", Montreal, Canada, April 1988.

2. W.J. Macknight, R.W. Lenz, P.V. Musto and R.J. Somani, Polym. Eng. Sci., 25(18): 1124 (1985).

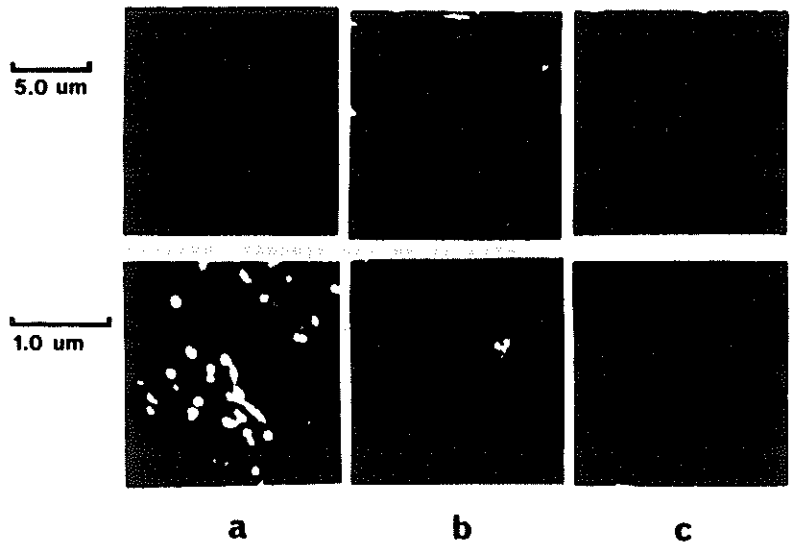


Fig. 1 Fracture surfaces of: a) 50% nylon/50% Surlyn; b) 50% polypropylene/50% Surlyn; c) 50% polyethylene/50% Surlyn.

ORIENTATION AND MECHANICAL PROPERTIES OF PC/LLDPE BLENDS

A. Ajji and R.E. Prud'homme

Centre de Recherche en Sciences et Ingénierie des Macromolécules, Chemistry and Chemical Engineering Departments, Université Laval, Québec, P.Q., Canada, G1K 7P4.

Blends of polycarbonate (PC) and linear low density polyethylene (LLDPE) were prepared by compounding the dry samples, followed by sheet extrusion. Specimens for the mechanical testing were cut from sheets of composition 0, 25, 50, 75 and 100 weight % of PC.

Mechanical properties (modulus, tensile strength and elongation at break) were measured for unoriented samples; the values obtained are typical of those of immiscible blends, i.e., modulus values are slightly below the line joining those of the homopolymers, whereas tensile strength and elongation at break values exhibit a minimum as a function of composition, as shown in Figures 1 and 2 for tensile strengh and elongation at break, respectively.

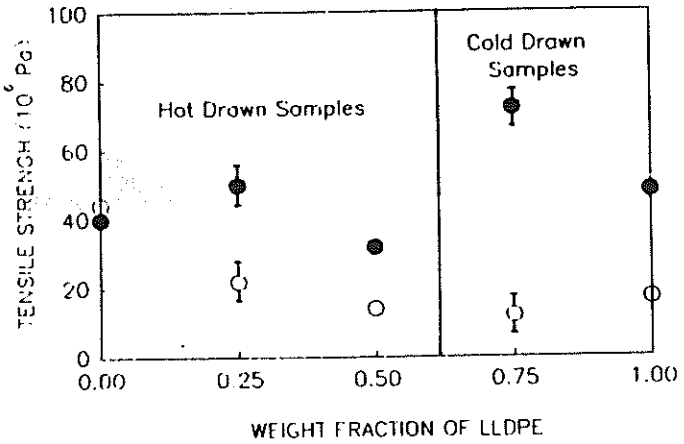


Figure 1.: Tensile strength of PC/LLDPE blends as a function of composition. Open circles: undrawn blends, filled circles: blends drawn to a draw ratio of 2.5.

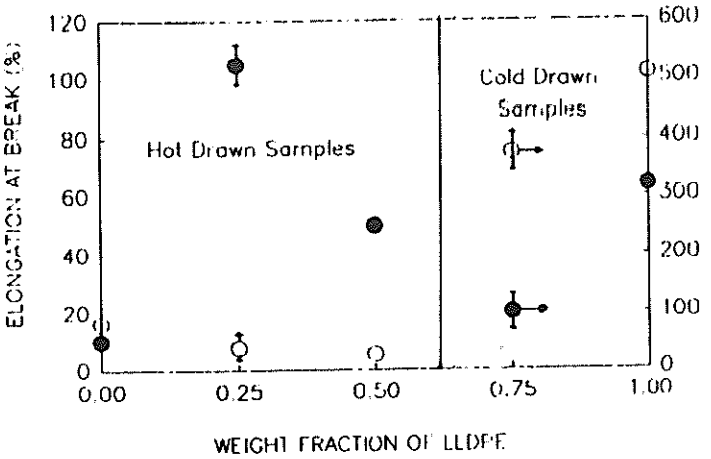


Figure 2.: Elongation at break of PC/LLDPE blends as a function of composition; symbols are as in Figure 1.

The specimens were then oriented to different draw ratios up to 5 at 165°C for the 50/50, 75/25 and 100/0 PC/LLDPE samples, and at room temperature for pure LLDPE and the 25/75 PC/LLDPE blend. For the hot drawn blends (50/50 and 75/25 PC/LLDPE), a significant increase in tensile strength and elongation at break is observed, as shown in Figures 1 and 2 for a natural draw ratio of 2.5. For the room temperature drawn samples (LLDPE and 25/75 PC/LLDPE), modulus and tensile strength values increase whereas elongation at break decreases (Figures 1 and 2).

This behavior is interpreted in terms of domain elongation under hot drawing and molecular orientation at room temperature. It agrees with similar results obtained for PS/PE blends [1]. The orientation of the samples was determined by birefringence and Raman spectroscopy. The degree of orientation of the homopolymers and blends at different draw ratios is compared.

[1] J.R. Stell, D.R. Paul and J.W. Barlow, Polym. Eng. Sci., Vol. 16 (7), 496 (1976).

9/6

THE EFFECT OF PROCESSING PARAMETERS ON THE FORMATION OF THE DISPERSED PHASE IN AN IMMISCIBLE BINARY BLEND

B.D. Favis and J.P. Chalifoux,
Industrial Materials Research Institute, National Research Council Canada
75 De Mortagne Blvd., Boucherville, Que., Canada, J4B 6Y4

Immiscible blends have distinct potential advantages from the physical properties standpoint. They form a multiphase system with a deformable minor phase and under the appropriate conditions morphological structures such as spheres, ellipsoids, fibres, plates and ribbons can be produced. In certain cases co-continuous phases may also be formed. The morphological structures mentioned above are generated in-situ while processing and these systems offer the potential to modify the dispersed phase through a wide range of size and shape. Control of these parameters however can be a very complex task. During processing of polymer blends several factors are especially important in determining the final size and shape of the minor phase: composition, interfacial tension, time of mixing, shear rate/shear stress, elasticity of the components and the viscosity ratio (ratio of viscosity of dispersed phase to that of the matrix). In previous papers [1, 2] we have studied the influence of composition and viscosity ratio. The goal of the present work is to gain insight into the influence of processing parameters on the morphology of the minor phase.

In this study an immiscible blend of polypropylene (PP) and polycarbonate (PC) was examined. Experiments were carried out in an internal mixer and the objective was to examine the influence of: the time of mixing, time under quiescent conditions and the speed of rotation of the rotors on the size and size distribution of the minor phase. The morphology was studied by light and electron microscopy and the photographs were quantitatively analyzed by semi-automatic image analysis.

The effect of the time of mixing was studied for up to 20 minutes at three viscosity ratios for polycarbonate dispersed in polypropylene. The viscosity ratios were 2.1, 6.9, and 12.8. The most significant particle size deformation and disintegration processes take place within the first two minutes of mixing. After two minutes very little reduction in the size of the minor phase is observed up to 20 minutes mixing time, although some phase size/time dependence was observed at intermediate viscosity ratio. These results illustrate two basic concepts from Taylor's work [3,4] on Newtonian fluids in shear flow, specifically that it is difficult to deform a dispersed phase of high viscosity and that it is difficult to deform small droplets.

The effect of time at 250°C under quiescent conditions was studied at 7% and 23% composition (volume fraction) for PP dispersed in PC and also for PC in PP. Coalescence coarsening was observed only for 30% PC in PP where the particle size was found to increase by 60% after approximately 90 minutes at temperature. The particle size distribution under the same condition broadens significantly with time as well. These results are discussed in terms of the matrix viscosity at low frequency of deformation.

The influence of rotor speed was studied for PP in PC and also for PC in PP at 7% vol. fraction. The results indicate that this blend is insensitive to changes in the speed of rotation of the rotor over a three to four fold range. These results are consistant whether or not PP (viscosity ratio $>$ 1) or PC (viscosity ratio $<$ 1) is the matrix. These blends appear therefore to not be highly dependent on shear stress/shear rate. The viscosity ratio/RPM relationship is also considered in light of the above results.

References

1. B.D. Favis, J.P. Chalifoux and P. Van Gheluwe, 45th Annual Technical Conference, Society of Plastics Engineers Inc., (ANTEC), Los Angeles, May 4-7, 1987; S.P.E. Technical Papers, 33, 1343 (1987).

2. B.D. Favis and J.P. Chalifoux, Proceedings of Industrial Materials Research Institute Symposium "Polyblends-'87", Boucherville, Que., Canada, April 28-29, 12/1-12/35 (1987); submitted to Polym. Eng. Sci.

3. G.I. Taylor, Proc. Royal Soc., A146, 501 (1934).

4. G.I. Taylor, Proc. Royal Soc., A138, 41 (1932).

9/7

Modification of the crystallization behaviour of thermoplastic polyesters by blending with amorphous nylon

V.M.Nadkarni,V.L.Shingankuli, J.P.Jog,
National Chemical Laboratory, Pune-411 008,India

ABSTRACT

Blending of thermoplastic polyesters with nylon has been a subject of interest because of the modification of physical properties and ester-amide block copolymer formation. It has been observed in case of blends of polyethylene terephthalate(PET) and nylon 6 that the blends show brittle failure in both tensile and impact tests because of the poor interphase properties resulting from the crystalline nature of the component polymers. Hence it was felt that the use of amorphous and aromatic nylon for blending may lead to better interphase properties.

The present work reports the thermal and crystallization behaviour of blends of three thermoplastic polyesters, namely, polybutylene terephthalate (PBT), polyethylene terephthalate(PET) and a co-polyester of 1-4 cyclohexane dimethanol, ethylene glycol and terephthalic acid (PETG) with an amorphous nylon based on terephthalic acid. All the three polyesters are semicrystalline. However, they differ considerably in their inherent crystallizing ability because of the differences in their chemical structure. Thus the effect of the inherent crystallizability of the polyester on the extent of modification in its crystallization behaviour by blending can be elucidated.

The thermal and crystallization behaviour of these blends was studied using differential scanning calorimetry. All the blends exhibitted a single glass transition temperature intermediate between those of the component polymers,indicating miscibility in the amorphous phase at the composition studied. The blending resulted in a higher degree of crystallinity in case of PET, whereas no significant changes were observed in case of PBT. The non-isothermal crystallization from melt indicated that the blends crystallized at a higher temperature and over a narrower temperature range compared to the base polyesters, suggesting enhanced nucleation and acceleration of the overall crystallization rate. However, the extent of the acceleration was different for the three polyesters.

The isothermal crystallization studies from melt revealed that the crystallization process of all the three polyesters is accelerated as a result of blending. The crystallization time versus temperature curves were shifted to higher temperatures and lower crystallization times. The crystallization of the blends at higher temperatures suggests enhanced nucleation process. This was confirmed by the shift of the induction time versus temperature curves for the blends to shorter times compared to the base polyesters. These observations are consistent with the non-isothermal crystallization results.

The observed effects may be attributed to specific interactions between the aromatic polyesters and the aromatic nylon molecules. The similarity in their chemical structure (terephthalic acid moiety) and the possibility of formation of hydrogen bonding would facilitate close molecular packing and the formation of ordered structures in the super-cooled molten phase. This may lead to enhanced nucleation of the polyesters.

9/8

PROCESSING OF STARCH BASED BIODEGRADABLE PLASTICS

R. P. Wool, Department of Materials Science and Engineering, University of Illinois at Urbana-Champaign, 1304 W. Green St., Urbana, IL 61801

Starch based blends of polyethylene are of interest for their biodegradable properties. In this paper we discuss the processing and compounding of cornstarch-based blends of polyethylene and other compatibilizing agents. The resulting properties of materials processed by injection molding and film blowing are detailed. Mechanisms of biodegradation in these starch based plastics are described. In particular criteria for biodegradation based on the percolative nature of microbial degradation are discussed. For continuous microbial degradation to occur the volume fraction of starch in the material must exceed the percolation threshold. Methods for determining the percolation threshold are presented. The effects of cornstarch loading in the range of 50-80% on the processability of these polymers are discussed. The kinetics of biodegradation are determined and the resulting effects of biodegradation on mechanical properties are presented. [1]

[1] Richard P. Wool and Michael A. Cole, "Microbial Degradation of Polymers," submitted for publication in "Engineering Materials Handbook, Vol. 2: Engineering Plastics," Plenum Press.



Simulation of invasion by fungi at percolation threshold.

STUDY ON NAPHTHALENE-RING-CONTAINNING THERMOTROPIC COPOLYESTER AND ITS BLEND WITH POLYETHYLENE TEREPHTHALATE

Zhenglong Zhou, Xiuge Wu and Muhuo Yu,
China Textile University, Shanghai, P.R.
of China

A series of thermotropic liquid crystalline copolyester based on p-acetoxybenzoic acid,2,7-diacetoxynaphthalene,terephthalic acid and polyethylene 2,6-naphthalate were prepared via melt transesterification. The resulting copolyesters were characterized by PGC and MS analysis.

The crystallizability of copolyesters C_1-C_7 are revealed by X-ray diffraction method. The X-ray diffraction curves for copolyester samples C_3,C_4,C_5 exhibit very weak crystalline reflection,which indicate that the five components in copolyesters may be distributed randomly on the macromolecular chains.

The melting temperatures of copolyester samples were measured by means of TOT and DSC methods and the relationship between the melting temperature of the copolyesters and the content of the 2,7-naphthalene diol unit was plotted in Fig.1. It has been shown that there exist the lowest melting temperature and after that the melting temperature increases again with the concentration of 2,7-dioxynaphthalene unit.

The blend sample of 40wt% copolyester C_4 and 60wt% polyethylene terephthalate shows the phase-separated optical pattern on a polarizing microscope and two glass transition temperatures are detected by dynamic mechanical measurements.

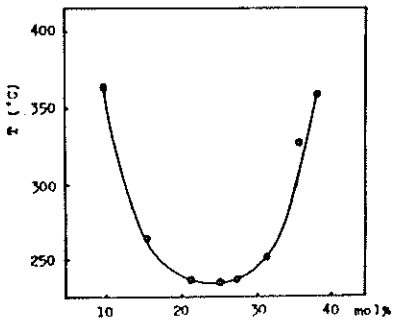


Fig.5 Relation between the melting temperature and the amount of 2,7-dioxynaphthalene unit.

An interesting feature of the as-spun fiber of the blend is shown in Fig.2. The as-spun fiber was chemically corroded by a conventional 50/50 phenol/tetrachloroethane mixture solvent and the SEM micrographs of the corroded fiber samples reveal the fibrillar microstructure of the blend,suggesting that the liquid crystalline copolyester macromolecules and the fibril alignment are highly oriented along the fiber axis and the mesomorphic copolyester phase and the PET phase are apparently separated in the blend as-spun fiber sample.



Magnification: 230
Fig.2 SEM micrograph of blend as-spun fiber (corroded by tetrachloroethane/phenol solvent).

References

1) M.Prasadarao, E.M.Pearce and C.D.Han, J.Appl.Polym.Sci., 27,1343(1982)
2) W.J.Jackson, Macromolecules, 16(7),1027(1983)

9/10

PERMANENCE OF PVC BASED POLYMER BLENDS INTENDED FOR BIOMEDICAL APPLICATIONS

S.N. PAL*, A.V. RAMANI* and N. SUBRAMANIAN**

*SREE CHITRA TIRUNAL INSTITUTE FOR MEDICAL SCIENCES AND TECHNOLOGY, POOJAPURA, TRIVANDRUM - 695 012.

**DEPARTMENT OF CHEMICAL ENGINEERING, IIT, MADRAS - 600 036.

The most widely used polymer in medical applications is Polyvinyl chloride. This is because (a) PVC is amenable to wide spread property modification and (b) it offers significant cost advantage over other speciality polymers. Some of the important medical applications of plasticised PVC are collection, storage and transportation of blood or blood products, containers for drug/fluid infusion, urine collection bags, catheters used in various parts of body, tracheostomy tube etc.

Since flexible PVC contain large amounts of low molecular wt. plasticizers, the plasticizers do migrate from PVC medical devices and enter into human body through different routes. Though there are differences in opinion regarding the possible effect of plasticizers on human, everybody would agree that it is desirable to avoid these plasticizers in PVC or at least reduce it to the barest minimum. One more problem that is usually faced is that plasticizer migration changes the mechanical properties of the PVC medical devices. For these reasons, for medical applications, it is desirable to 'flexibilize' PVC with nonmonomeric modifiers which is expected to result in eliminating/reducing the migration of monomeric plasticizers and improvements in permanence It is with these objectives that the present investigation was undertaken.

PVC-NBR blends have been tried in many industrial applications, but it does not seem to have been evaluated for medical applications in mind. In this study, plasticized PVC-NBR blends having non-resineous matter 4-36.5% (W) and plasticized PVC and NBR containing 20-40% and 0% non-resineous matter respectively were used. The blends were prepared as 'dry blends' in high speed mixer and then fused and made into sheet form in a heated roll mill. Refined vegetable oil which simulates the lipid component of blood and is used extensively for biological evaluation of biomaterials were used for migration experiments. The changes in tensile properties of the blend formulations when in contact with physiologically simulated media were also studied.

It was observed that amount of nonresinous matter extracted in vegetable oil was higher for plasticized PVC-NBR blends compared to plasticized PVC containing the same amount of non resineous matter. Presence of NBR stimulates migration. Therefore the expected advantage of plasticized PVC-NBR blend namely, use of lesser quantity of plasticizer for flexible medical applications can be realised only if a formulation is selected such that the contribution of NBR towards additional migration of non resineous substances is insignificant compared to the reduction in migration achieved by drastically reducing the initial amount of plasticizer in the blend.

Data on tensile properties of pre and post extraction samples indicate that plasticized PVC-NBR blend imparts relatively more permanence particularly in elongation compared to traditionally used plasticized PVC and this is desirable for flexible medical applications.

9/11

RHEOLOGY OF LIQUID CRYSTALLINE POLYMERIC BLENDS

T.H. Malik, P. Carreau, M. Chapleau and M. Grmela,

ordered structure. On the other hand, the increase in deformation

rate results in relatively low viscosities. An abrupt

RHEOLOGY OF LIQUID CRYSTALLINE POLYMERIC BLENDS

T.M. Malik, P. Carreau, N. Chapleau and M. Grmela.
Groupe de Recherche en Ingénierie des Polymères,
Department of Chemical Engineering,
Ecole Polytechnique,
Montréal, Qué., CANADA, H3C 3A7

One of the most dynamic area of development in polymer science and engineering has been the characterisation and applications of polymer liquid crystalline state. Thermotropic liquid crystal polymers form densly packed fibrous polymer chains in the molten form. The chain acts as self reinforcement for polymer structure, leading to exceptional retention of strenght and other properties over a wide range of temperature. However, the behavior of these polymeric systems blended with other polymers have been studied insuficiently.

In the present study, we have investigated the mechanical and rheological behavior of blends of thermotropic liquid crystalline polyesters with polycarbonate, nylon and polystyrene. The blends were prepared by melt blending at 280ºC. Mechanical measurements revealed that the blends containing 10 percent liquid crystalline polymer possess outstanding hardness and toughness shoving great potential as the plastic designed to carry structural loads. Constant stress rheometer, Rheometrics RSR was used to characterize rheological properties. During flow, blends exhibit yield stresses, suggesting the existence of ordered structure. On the other hand, the increase in deformation rate results in relatively low viscosities. An attempt is made to formulate an appropriate mathematical model of liquid crystalline polymeric mixtures.

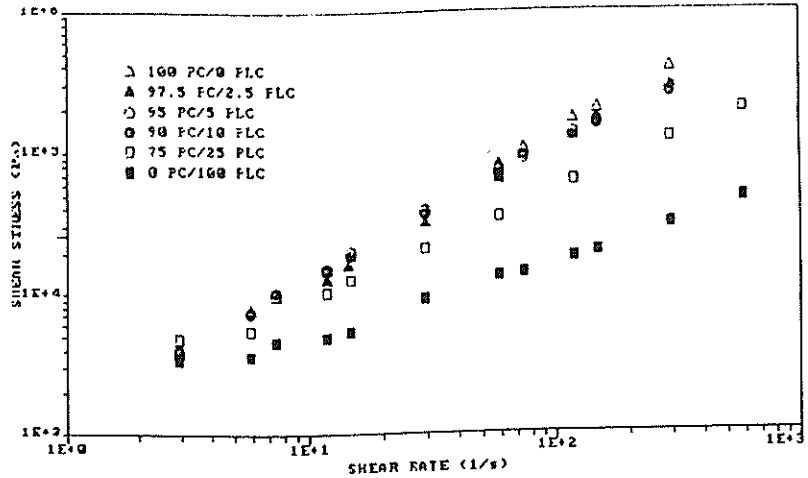


Fig.1: Shear stress vs shear rate for the liquid crystal Polyester (VECTRA)/Polycarbonate blends at 280ºC.

9/12

STRUCTURE FORMATION IN CRYSTALLIZING BLENDS

A. J. McHugh, D. A. Tree, Department of Chemical Engineering, University of Illinois, Urbana, Illinois, 61801.

Knowledge of the dynamics of structure formation and crystallization during processing of two-phase blend systems is important for the design and control of morphologies exhibiting desirable properties. In our work we have been concerned with the conditions under which fine dispersion of one phase occurs under flow leading to the formation of elongated, crystalline fibers. For the most part we have concentrated on blends of high density polyethylene or polypropylene in a linear low density polyethylene (LLDPE) carrier phase.

Table I shows a listing of the systems whose fibrillation characteristics have been studied.

Table I. POLYMERS USED AS MINOR PHASES

Materials	Melt Index	Mn	Melting Point °C
Marlex 6001 HDPE (Phillips Petroleum)	0.5	2.84×10^4	136
5520 PP (Shell Chemical)	5	-	164
1900 UHMWPE (Hercules)	-	2.9×10^6	144
E60-06 HWMPE (Celanese)	-	6×10^5	138
E60-600 HWMPE (Celanese)	-	1.6×10^5	142

The carrier phase is a LLDPE (Union Carbide, MI = 1.0, T_m = 125°C). Complete rheological data on the pure materials and their dilute (~ 1 wt %) blends have been obtained over a wide range of conditions using cone and plate, slit die, and capillary die flow devices. Fibrillation has been studied in several extrusion geometries including a converging channel film die (1), a slit die with a large converging channel entrance region (2), and a standard capillary (3). Dies are outfitted with optical windows to allow in-situ observation of the droplet deformation dynamics and subsequent crystallinity development (through birefringence measurement). In shearing flow, under our high Weber number conditions (i.e. low surface tension), the transient flow in the growing tail of a bursting drop will be extensional in nature and is well described by the following expressions:

$$\dot{\gamma} = \left(\frac{\lambda-1}{\lambda+1}\right)\frac{1}{t} = \left(\frac{\lambda-1}{\lambda+1}\right)\frac{a_o\dot{\gamma}_s}{\ell} \qquad (1)$$

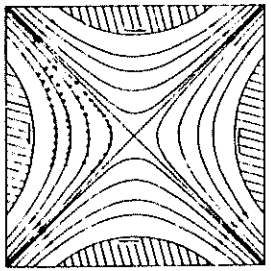
$$\ell = a_o\dot{\gamma}_s\left(\frac{\lambda+1}{\lambda-1}\right)t \qquad (2)$$

For a droplet undergoing bursting in a simple extensional flow in a medium such that $\lambda = O(1)$, the internal kinematics are determined by the outer flow. Thus one has:

$$\frac{d\ell}{dt} = \dot{\gamma}_E\ell \qquad (3)$$

All three expressions have been shown to compare well to droplet deformation data obtained under inhomogeneous flow conditions. Surprisingly, the superposed crystallization kinetics do not appear to affect the data fit.

In this work we will also report on observations being made using a 4-roll mill device. Figure 1 is an example of the carrier phase flow kinematics illustrating the planar extensional flow characteristic of this geometry. Observation of the droplet deformation dynamics and subsequent crystallinity development will be given.



Acknowledgements

This work has been supported under a grant from the National Science Foundation administered through the Materials Research Laboratory at the University of Illinois. Grant DMR 86-12860.

Nomenclature

- a_o = droplet radius at point of tail emission
- t = time
- ℓ = tail length (at time t)
- $\dot{\gamma}$ = extension rate in droplet tail
- $\dot{\gamma}_E$ = extension rate in carrier phase
- $\dot{\gamma}_S$ = shear rate in carrier phase
- λ = ratio of dispersed to carrier phase viscosity

References

1. S. L. Sakellarides and A. J. McHugh, Rheol. Acta, 26, 64 (1987).
2. S. L. Sakellarides and A. J. McHugh, Polym. Eng. Sci., to appear.
3. D. A. Tree and A. J. McHugh, Int. Polym. Proc., to appear.

9/13

FUTURE OF POLYMER BLENDS; EXPECTATIONS BASED ON TECHNICAL AND PATENT LITERATURE

L.A. Utracki, National Research Council Canada, Industrial Materials Research Institute, 75 de Mortagne, Boucherville, Que., Canada, J4B 6Y4

The plastics industry is young and growing with expected saturation of demand sometime in the 21st century. In North America, the increase of polymer production over the next 10 years is expected to be 1.140 tons/y, i.e. decreasing from 5% in 1986 to 3.6% in 1995. The world consumption of polymer alloys and blends, which in 1986 amounted to 12% of all plastics (16% in USA), is expected to grow at an annual rate of 9-10% to 19% (22% in the USA) by 1996 [1]. About 24% of all polymer alloys and blends, PAB, will be consumed by the automobile industry, with lesser amounts in business machine, electrical/electronics, and other industries. Consequently, the main impact of PAB will be in the area of metal replacement, as well as high temperature (continuous use temperature, $T \geq 150°C$) and high mechanical performance [2].

Every year 4,500 new PAB patents are published. A third of these deals with the high performance materials. It is useful to note the relative "popularity" of blends, grouping them according to the major component: 1. 26% polycarbonate (PC); 2. 23% thermoplastic polyesters (TPE); 3. 18% speciality polymers; 4. 15% polyamides (PA); 5. 14% polyphenylene-ethers (PPE);6. 4% polyoxymethylene (POM).

The above statistics are based on US and European patents and are therefore biased in favor of PC. The importance of PC vis-a-vis POM in North America is disproportionate; the consumption ratio of PC to that of POM in the USA is 2.67, in Europe 1.39, in Japan 0.68 and overall in the world 1.24.

There are about 200 commercial PAB on the market, each offered in a variety of grades. Annually, in the USA over 2,000 new thermoplastics grades are introduced; a majority originated from compounding and blending. Not only are grades offered for specific forming processes and/or applications but even to optimize a given part production of a single transformer. This "tailorability" is intrinsic to the PAB technology and in turn it reinforces demands for these materials.

Historically, PAB were designed either to improve some property of a major component or to improve the profit margin such as extension of performance of expensive resin [2]. Next, there has been a strong tendency to formulate multipurpose PAB, the materials which will simultaneously show good mechanical, thermal and chemical characteristics, for example: Xenoy, a multicomponent material based on polycarbonate/thermoplastic polyester blend with excellent mechanical properties and good solvent resistance.

As the PAB technology diversifies it is becoming difficult to identify one single trend as a standard-bearer of the future. However, the unification of polymer blends and composites technologies is a sign of things to come; an example: the Technopolymer structures of nonwoven glass mat with Xenoy [3]. This tendency is not new; it was mentioned in the technical and patent literature a long time ago [4, 5]. What is new is the growing commercialization.

In most cases the property-composition dependence is monotonic. Deviations can frequently be controlled by modification of compatibility. The linearity combined with a change of the fracture mechanism on addition of an immiscible ingredient gives a recipe for impact modification of engineering resins, e.g. polyamides [6-9]. Polyamide blends also provide an example of a tendency to control finished product properties via morphology of the dispersed phase [10].

The use of plastics in automobiles will increase from 102 in 1986 to 124 kg/vehicle in 1996 [11] resulting annually in about 6 million tons of polymer scrapped with the automobiles. Note that the recycling efficiency of aluminium is about 29%, that of polymers 1% [12]! There is growing concern about polymeric scrap, particularly in the automobile industry. Recycling via PAB technology is an attractive possiblity.

REFERENCES

1. R.M. Kossoff & Assoc. Inc., "The Future for Polymer Alloys III", study, 1987; Business Communications Co. market study for alloys and blends of plastics, 1987.
2. L.A. Utracki, DST-UNDP seminar "Recent Trends in Polymers and Their Composites", New Delhi, 18-21 Dec., 1986; J. Polym. Process., 2, 3(1987).
3. G.E. Co. News Release, July 8, 1987.
4. P. Teyssié, private communication.
5. W.T. Freed, U.S. Pat. No. 3,920,602 of 18 Nov., 1987 assigned to Celanese.
6. J.C. Woodberry and M.V. Moncur, U.S. Pat. No. 4,320,213.
7. P.W. Flood, C.D. Mason and S.R. Schulze, U.S. Pat. No. 4,335,223 of 15 July 1982, assigned to Allied Corp.
8. M.J. Roura, U.S. Pat. No. 4,346,194 of 24 Aug. 1982, assigned to E.I. DuPont de Nemours and Co.; Europ. Pat. Appl. No. 0,034,704.
9. W. Nielinger, B. Brassat, R. Binsack and D. Neuray, U.S. Pat. No. 4,381,371 of 26 Apr. 1983, assigned to Bayer A.G.
10. R.A.I. Eidwan, "Coex '85", 10 Oct. 1985.
11. "Plastics in Automotive Industry: A Worldwide Perspective 1986-1991 and Beyond", the Springborn/Harborside Research Study, 1987.
12. Franklin Associates Ltd., 1987.

9/14

RHEOLOGICAL ASPECTS OF PHASE SEPARATION KINETICS IN PS/PVME BLENDS.

A. Ajji, L. Choplin and R.E. Prud'homme

Centre de recherche en sciences et ingénierie des macromolécules, Departments of chemistry and chemical engineering, Université Laval, Québec, QC., G1K 7P4, Canada

PS/PVME blends are known to exhibit a phase separation behaviour as the temperature is increased. These blends are also known to have a transition region from the homogeneous blend (miscible), passing through a metastable region (immiscible) with dispersed domains of the minor phase in the matrix, to a spinodal region with interpenetrating domains.

In this study, emphasis is put on the rheological behavior in the dynamic mode of the blend compositions of 40/60, 50/50, 60/40 and 80/20 PS/PVME prepared from solutions in benzene, with molecular weights (Mw) of about 50,000 for both polymers (with some results for a PS of 100,000 in Mw). This choice in Mw is dictated by the need to have a nearly symmetric binodal and spinodal curves with respect to the 50/50 composition as illustrated in Figure 1.

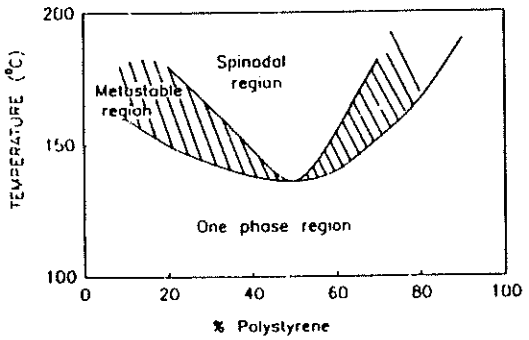


Figure 1.: Illustration of the phase diagram of PS/PVME blends having nearly the same molecular weights.

The rheological properties are studied for temperatures below the phase transition temperature as a function of time and of thermal conditions in order to follow their evolution and to study the kinetics of phase separation. An example of this condition-dependent evolution is shown in Figure 2., where the evolution of the loss tangent on the temperature for different heating rates show the dependence of the phase transition temperature on heating conditions.

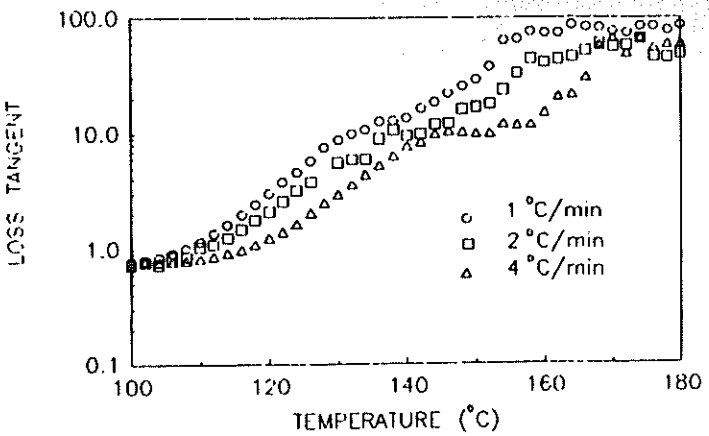


Figure 2.: Evolution of the loss tangent as a function of temperature for different heating rates for the 80/20 PS/PVME blend (PS of 100,000 Mw).

Also, a thermorheological analysis of the rheological properties in the phase transition region is performed. It is shown that the rheological properties are sensitive to the morphological changes in the blends and an apparent yield stress is observed after the phase separation occurred. Both data on homogeneous and phase separated systems are compared and related to the phase separation process in the blend.

9/15

MELT RHEOLOGY OF LLDPE/PP BLENDS: DYNAMIC BEHAVIOUR

For both systems the relationship between viscosity

MELT RHEOLOGY OF LLDPE/PP BLENDS: DYNAMIC BEHAVIOUR

M.M. Dumoulin — DuPont Canada Research Centre, Kingston, Ontario, Canada K7L 5A5

L.A. Utracki — Industrial Materials Research Institute, National Research Council of Canada, Boucherville, Canada J4B 6Y4

P.J. Carreau — Ecole Polytechnique, Montreal, Canada H3C 2A7

Research papers on LLDPE/PP blends are scarce. Yeh and Birley [1] have investigated blends containing 5 and 10 % of LLDPE in PP. They found that LLDPE imparted enough impact improvement to PP without detrimental effects on the yield stress to warrant commercial applications. A previous work in our laboratories [2] has shown that for a blend made of equal amounts of components of similar viscosities, the mechanical properties and shear viscosity were very close to the algebraic average of properties of the pure resins. The present work aims at examining the melt properties of the LLDPE/PP blends in the full range of concentration. Since the effect of the molecular weight of one component was to be evaluated, three polymers were selected so that the two blend systems prepared have very different ratios of shear viscosities.

The properties of the three commercial resins used in this study are given in Table 1. Two different systems were prepared by blending each of the LLDPE resins with PP on a Werner Pfleiderer twin-screw extruder with a temperature profile along the barrel from 190 °C at the entrance to 245 at the die. Seven compositions of 0, 5, 25, 50 ,75, 95 and 100 % were successively extruded, quenched and granulated. Finally, shear moduli: storage, G', and loss, G", were measured as a function of the frequency for all materials on a Rheometrics Mechanical Spectrometer, Model 605.

The G' vs frequency curves for blends containing 25 and 50% of PP show upwards deviations in the low frequency region. This increase in elasticity is characteristic of a yield stress phenomenon, already observed for filled polymer melts [3]. Treatment of the data using a modified Casson equation [4] allows the calculation of apparent yield stress values of 58 Pa for the blend LLDPE-1:50/PP:50 and 5 Pa for the blend LLDPE-2:50/PP:50. A microscopic examination of the dispersion in the blends shows two co-continuous phases at this concentration. This morphological feature could explain the larger elasticity of the material.

For both systems the relationship between viscosity and composition is far from linear. This is especially true for the LLDPE-2/PP blends for which negative deviations are observed at both ends of the concentration range. Both systems behave similarly in the sense that in each case the addition of a more viscous component induces a decrease in the viscosity of the resulting blend. For both systems, the 50:50 composition has a viscosity close to that predicted by the additivity rule. This is consistent with the previous observation that in this concentration range the blend is made of two co-continuous phases.

REFERENCES

1. P-L. Yeh and A.W. Birley; Plast. Rubber Proc. Appl., 5, 249 (1985)

2. M.M. Dumoulin, C. Farha and L.A. Utracki; Polym. Eng. Sci., 24, 1319 (1984)

3. L.A. Utracki and B. Fisa; Polym. Compos., 3, 193 (1982)

4. S. Onogi and T. Matsumoto; Polym. Eng. Rev., 1, 45 (1981)

TABLE 1 : PROPERTIES OF COMMERCIAL RESINS

Material	PP	LLDPE-1	LLDPE-2
Manufacturer	Hercules	Esso	Dow
Designation	6701	LPX-24	Dowlex 2517
Melt index (dg/min)	0.8	0.3	25
Density (23 °C) (kg/m3)	900	951	917

9/16

RHEOLOGICAL BEHAVIOR AND IMPACT STRENGTH OF POLY(VINYL CHLORIDE) BLENDS WITH POLY(ETHYLENE-CO-VINYL ACETATE)

Xi Xu Huilin Li Qi Wang Shaoyun Guo

(Polymer Research Institute, Chengdu University of Science and Technology, China)

ABSTRACT

The experimental results show that the impact strength of PVC/EVA blend strongly depends on EVA content, blending temperature and blending time, it reaches the maximum at 10 parts of EVA per 100 parts of PVC, and will be further increased when PE is added in. TEM observation confirms that the formation of EVA continuous network in PVC/EVA is responsible for the high impact strength of the blend. The plasticizing and rheological behavior of the blends were studied throuth a Brabender Plasticorder and a capillary rheolometer. EVA could promote the gelation of PVC, while PE could reduce the apparent viscosity of the blend and has the delayed action on gelation of PVC. The melt viscosity of the blend is smaller than that of PVC in case its EVA content is more than 7.5 parts, and decreased with increase of the shear stress. The temperature has a great influence on the viscosity of the blend, the effect is weakened as EVA content increased. By means of binary linear regression a series of mathematic models that could directly correlate the melt viscosity of the blend with both shear stress and temperature was established. The flow activation energy of PVC/EVA decreases with increase of EVA content. The addition of EVA reduces the non-Newtonian flow index, indicating the increased dependence of the melt viscosity of the blend on the shear stress (Table 1).

Table 1 E_η, n and A Value of PVC/EVA Blends

Sample	E_η(cal/mol)	n	A
PVC/EVA(100/0)	13876	0.3912	1.936×10^{-2}
PVC/EVA(100/3)	16130	0.3023	1.951×10^{-3}
PVC/EVA(100/5)	13719	0.2913	2.530×10^{-2}
PVC/EVA(100/7.5)	11736	0.2813	1.863×10^{-1}
PVC/EVA(100/10)	11316	0.2933	2.808×10^{-1}
PVC/EVA(100/15)	9414	0.3408	1.4082

Birefringence in Injection-Molded Disk of Two-Component Polymer Systems : PC/PS Blend , PC-PS Graft Copolymer, and PPE/PS Blend

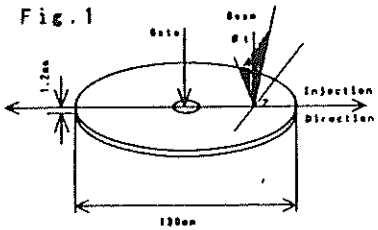
Y.Kijima*,T.Kawaki* and T.Inoue**
* Tokyo Central Research Laboratory,
Mitsubishi Gas Chemical Company, Inc
(Niijuku,Katsushika-ku,Tokyo 125,Japan)
** Department of Organic & Polymeric Materils
Tokyo Institute of Technology
(Ookayama,Meguro-ku,Tokyo 152,Japan)

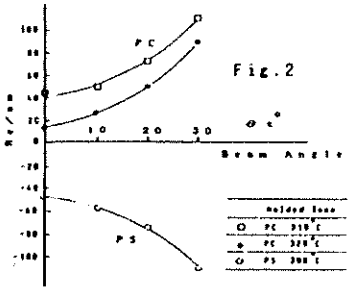
Polymer processing operations, such as injection-molding and extrusion, usually induce residual birefringence owing to frozen-in molecular orientation. Birefringence in an optical disk causes a high noise in the recording and reproducing systems (1,2,3). It is observed that the birefringence is reduced by combination of two polymers having opposite optical anisotoropies (4,5). We investigate the birefringence of injection-molded disk of the two -component polymer systems : polycarbonate(PC)/polystyrene(PS) blends, PC-PS graft copolymers, and poly(phenylene ether) (PPE)/PS blends.

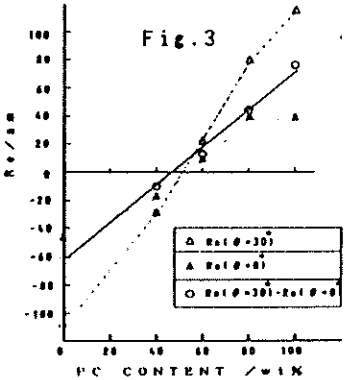
Fig.1 shows an illustration of an optical disk and a focussed beam. The birefringence of disk is generated for oblique incident beam as well as vertical incident beam. The birefringence versus incident beam angle in disks of PC and PS is shown in Fig.2.
PC and PS have opposite signs in the birefringence.
The birefringence of PC molded at different temperatures shows the similar angular dependence but different magnitude.

Birefringence of PC/PS blends (immiscible two-phase system) is measured by vertical(θt=0°) and oblique(θt=30°)incident beams (Fig.3). The observed birefringence depends on composition, molecular weight of PS, and injection temperature.
Linear relationship is seen between ΔRe:Re(θt=30°)-Re(θt=0°) and composition. Similar behavior is also observed in PC-PS graft copolymers (micro-phase separated system) and PPE/PS blends (single phase system) in Fig.4. Zero ΔRe is obtained at 60/40 - 50/50 and 30/70 in PC/PS and PPE/PS systems,respectively.

Disk substrates should have high transparency and optical homogeneity with small birefringence. PC/PS blend has low transparency since its domain size is about a few μm. Single-phase PPE/PS has no problem in the optical homogeneity but it is unstable for the processing at high temperatures. PC/PS graft copolymer is a phase-separated system but its domain size is quite small (Fig.5), so it really has high optical homogeneity. PC-PS graft copolymer seems to be the best candidate for the optical disk substrate.







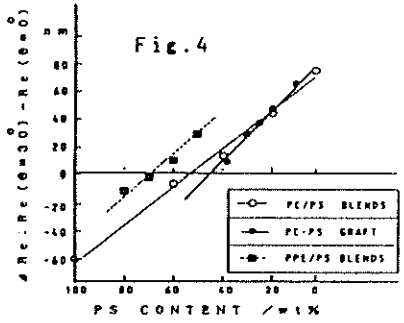


FIG 5



Fig.1 Disk and Optical alignment.
Disk has 130 mm diameter and 1.2 mm thick. The birefringence is measured at a position 43mm from the center of the disk by ellipsometer. An angle θt for an oblique incident beam is in a tangential direction for injection direction.

Fig.2 Angular dependence of birefringence.
PC : Iupiron H-4000, Mv=16000, PS:Mw=220000.

Fig.3 Re versus composition of PC/PS.
Cylinder temperatures : 300-320 °C.

Fig.4 ΔRe versus composition.

Fig.5 TEM of injection-molded PC-PS graft copolymer.
PC/PS weight ratio is 60/40.

References
(1) H.Yoshioka,Plastics,38,14(1987)
(2) S.Asano,Optical Memory Symposium '86,173(1986)
(3) A.Yoshizawa,Kougaku,15(5),414(1986)
(4) H.Saito and T.Inoue,J.Polym.Sci.,25,1629(1987)
(5) M.Pietrilla,Prog.Colloid.Polym.Sci.,71,125(1985)

EPOXY-LIGNIN POLYBLENDS

Dorel Feldmam, Marwan Khoury, Centre for Building Studies, Concordia University, 1455 De Maisonneuve Blvd. W., Montréal, Qué., Canada H3G 1M8

Polyblending is increasingly becoming a commercially important and inexpensive method of modifying the properties of polymeric materials at a reduced cost. In the case of epoxy polymers, a number of polymers have been used in epoxy polyblends and include polyamides, elastomers, poly(vinyl formal), poly(vinyl butyral), polyethylene, poly(vinyl chloride) poly(vinyl acetate), polyurethane and phenoplastes. In most cases, these polymers have functional groups capable of reacting with the epoxy.

The utilization of lignin as a macromolecular compound in material systems is relatively small and includes uses as component in thermosetting resins, as antioxidant, as reinforcement and as component in polyblends. In this study, the polyblend obtained, at room temperature, was a physical mixture between an epoxy polymer and lignin.

In a previous paper, the curing kinetics of epoxy-lignin polyblends were reported. In this study, mechanical properties of the polyblends and the unmodified epoxy system are discussed. These include the adhesive tensile and shear strengths, weatheribility, and the effect of post curing and elevated temperatures on the adhesive strength in shear.

The polyblends are prepared by manually stirring together the epoxy polymer system and Kraft lignin for five minutes at room temperature. The amounts of lignin used were 5, 10, 15 and 20 percent by weight. The gel time for the epoxy system and the polyblends varied between 21 and 25 minutes. All samples were cured for 24 hours at room temperature.

After this curing period, the specimens were subjected to the following conditions: 3 days curing (series A), laboratory conditions (Series L), natural weathering (Series NW), accelerated weathering (Series AW).

Results of shear testing of the four series are summarized in Fig. 1. Mean values are determined from 5 to 10 successful tests. In all the tests failure was in adhesion.

Besides the bulk strength of the adhesive, the strength of adhesive joints depends on the interfacial state of adhesion. With post curing, this state is improved due to the following factors:

1) The decrease in viscosity of the adhesive at higher temperatures, leading to better interfacial contact.

2) The dissolution or displacement of remaining contaminants on the adherent, which might have been insoluble in the adhesive at lower temperatures.

3) The relaxation of interfacial stress that might have existed upon initial curing.

Besides other findings of this study, under the conditions described, two major findings are:

- Polyblending with Kraft lignin (10-20% by weight) improves the adhesive tensile strength of the epoxy polymer system.

- The adhesive shear strength (by tension loading) of the epoxy system is not affected by polyblending with lignin.

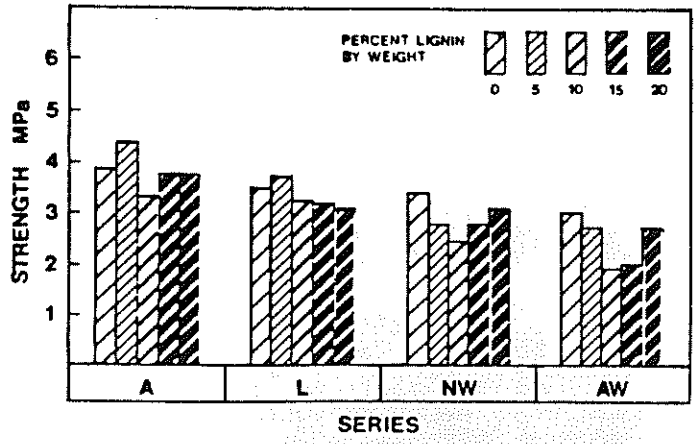


Fig. 1 Adhesive strength in shear by tension loading.
Series A: 3-days curing at room temperature.
Series L: 115 days at lab conditions, 23°C, 35-50% R.H.
Series NW: 115 days of natural weathering, Feb. 14-June 9
Series Aw: 108 days of accelerated weathering, 366 cycles

9/19

FORMATION OF MICROSTRUCTURE IN POLYBLENDS DURING FLOW.

D. Heikens

Eindhoven Technological University, Eindhoven, The Netherlands

BLENDING In most blending operations a shearing action is applied to a melt consisting of two or more polymers. If for a binary system the two polymers are able to form a molecular dispersion, the thin layers of each polymer formed in the last stage of the mixing operation by the shearing action, can only be converted to one molecular solution through diffusion of the two polymers from layer to layer. So a test after the possibility of this interdiffusion should contain the production of very thin layers of the two polymers. These layers can be produced by a static mixer and can be kept for a reasonable time in the molten state. If no change in the layers or at the interfaces is observed, the two polymers are not suitable to be dispersed in the molecular state at the temperature of the test. The thickness of the layers necessary for a test can be derived from diffusion coefficients from the literature. In general it can be expected that these layers should be in the order of micrometers, in order to obtain reasonable diffusion times of minutes. From polyethylene it is known that diffusion times are reciprocally proportional to the square of molecular weight, so preliminary experiments may be carried out with polymers of somewhat lower molecular weight. If a molecular dispersion is possible, this molecular blend can be prepared in an industrial apparatus, if the necessary small dimensions of microphases and adequate diffusion times in that apparatus at wanted diffusion times can be attained. In case of partial miscibility, which often means nearly no miscibility at all, in most mixing apparatus, laminar flow is the last and most important stage of the process. Studying the contents of an extruder producing a blend of low density polyethylene (LDPE) and polystyrene (PS), shows the very thin layers of both polymers. With a special type of extruder in which after the screw a torpedo with 8 holes was present, the resulting thread of polymer had a cross-section in which the pattern of the torpedo could clearly be observed. The thread was cut and extruded again. The cross-section still showed a torpedo pattern, proving that the extruder partially has selectional effects: it separates PS from LDPE, during melting of the pellets. A thread made from a blend of the two polymers mentioned, with the aid of a normal, single screw extruder has often a cross-section showing a spiral pattern. This pattern could be traced back and the number of turns could be calculated from apparatus dimensions and screw speed. Length sections of material drawn from the end of the extruder have a peculiar pattern, which can be understood by analyzing the flow pattern of the blend in the extruder.

PARTICLE FORMATION Due to the instability of thin layers or threads of a polymer phase in a matrix of a second polymer, spheres of the dispersed phase will be formed. Long ago Barentsen (1,2) showed that compression moulded samples of PS/LDPE blends (made on a two roll mill) contained particles of the polymer present in minority, dispersed in the matrix of the polymer in excess. For low concentrations of LDPE in PS, the particles of LDPE were larger than the particles of PS in the matrix of the, in this case, excess polymer LDPE. This could be expected as the viscosity of the LDPE matrix was higher than that of the PS matrix. In case of higher concentrations however, this kind of viscosity effects on particle dimensions are to be combined with coalescence effects. At about 20% of PS in LDPE and of LDPE in PS the particles of PS and LDPE have the same but much larger dimensions than in the cases mentioned above. Results from a very thorough research of Elmendorp (3) indicate also that for concentrations over 1% coalescence becomes very important. He also discussed coalescence of particles with mobile and immobile interfaces. Immobile interfaces lead to huge coalsescence times and were not found by PS dispersed in PE. The presence of block-copolymers will in general reduce the interfacial tension (1,2,3) and decrease the dimensions of the particles of the corresponding homo-polymers. Another effect of the block copolymer mentioned already by Barentsen (1,2) and particularly stressed by Elmendorp is the formation of immobile interfaces.This kind of interfaces as a kinetic phenomena will retard the condensation of small particles, already formed, to larger particles. The block copolymer works in about the same way as insoluble inorganic matter is preventing the adhesion of polymerparticles in suspension- polymerisation.

REACTION BETWEEN IMMISCIBLE POLYMERS IN A TWO PHASE SYSTEM. It is clear that reaction between the two phases will lead to the formation of block- or graft- copolymers. So, after a certain reaction-time the interfaces will be immobilised and, depending on the magnitude of the shearfield a certain minimum size of microphases will be attained and coalescence will be strongly counteracted. If microphases of about 10 micrometer are present and it is assumed that the thickness-contribution of the copolymer to the interphase-layer is not more than 5 nanometer, then for a volumefraction of about 50% of the polymers the total amount of block-copolymer will be only some tens of a percent, relative to the amount of total polymer. So very small conversion is needed for the interfacial effect wanted. The reaction rate at the interphases can be calculated , if a volume is assumed in which both polymers are interpenetrating and the reaction rate constants for the type of reaction wanted can be estimated from homogeneous reaction known from literature. As a first estimate of the thickness of this reaction volume 5 nanometer may be assumed.

1. D. Heikens and W. Barentsen, Polymer 18 (1977) 69. 2. D. Heikens, N. Hoen, W. Barentsen, P. Piet and H. Ladan, J.Pol.Scie., Pol. Symp. 62 (1978) 309.
3. J. J. Elmendorp, A study on polymer blending, Microrheology, Thesis, Technological University Delft, 1986 (in English)

10/1

MICROWAVE PROCESSING OF POLYMERS

T. C. Ward, J. D. Graybeal, J. P. Wolfe, J. E. McGrath, G. L. Wilkes and D. A. Lewis, Chemistry Dept. and Polymer Materials and Interfaces Laboratories, Virginia Polytechnic Institute and State University, Blacksburg, VA 24061, USA

Microwave processing of polymers, using tuned cavities, is a relatively new technology and offers a number of advantages over conventional thermal processing due to the mechanism of energy absorption. Microwave radiation of the type in this paper is not energetic enough to cause either ionization or bond scission directly but is postulated to accelerate the rate of "thermal" reactions. Energy is absorbed from the electric field by groups containing dipole moments, such as hydroxyl and amino groups, and, thus, can be preferentially deposited within the sample in contrast to thermal treatments. This can result in more efficient energy transfer with a corresponding reduction in production costs. Importantly, there is the possibility of reducing strong temperature gradients within the sample, particularly for composites, resulting in materials with enhanced mechanical properties.

We have shown[1] that the use of microwave radiation significantly accelerates the rate of cure for epoxy resins, thus providing shorter production cycles. Furthermore, we have demonstrated that the mechanical properties (fracture toughness and flexural modulus) are the same as after a four-hour conventional curing cycle. Thus, microwave processing can produce similar mechanical properties as does the slow and inefficient usual methods, but with an 8-10 fold reduction in the time required to obtain complete cure of the resin.

The polyimides have a wide range of applications from microelectronics to use as thermal blankets for satellites. A principal difficulty lies in processing this material and the long curing cycles required. Solubility of selected polyimides can be increased, resulting in easier forming, using solution imidization[2] rather than the traditional thermal treatment. However, very long imidization times (approx. 12 hours) are required. The use of microwave radiation to enhance this imidization reaction, therefore, has wide appeal and has been investigated.

Poly(amic acids) can be completely imidized using microwave radiation at 175°C in 15 minutes. One should contrast this with 12 hours for solution imidization at the same temperature. The kinetic details of this reaction may aid in interpretation of the actual mechanism of the acceleration in the reaction rate in both the epoxy resins and the imidization reaction.

Maleimide terminated poly(ether ketones) can provide lightly crosslinked high performance materials after curing. Below the glass transition temperature of 150°C, a crosslinking of the terminal functionalities increases the strength, fracture toughness and resistance to solvents while above the glass transition temperature, a high temperature elastomer is produced. Normally, a three-hour curing cycle is required, however, this is reduced to 10 minutes in the microwave system.

In this paper we will investigate the curing kinetics and mechanical properties of microwave processed polyimides and maleimide terminated poly(ether ketones).

References

1. D. A. Lewis, J. C. Hedrick, J. E. McGrath and T. C. Ward, Polymer Preprints, 28(2), 330(1987).

2. R. H. Bott, J. D. Summers, C. A. Arnold, C. P. Blankenship, Jr., L. T. Taylor, T. C. Ward and J. E. McGrath, SAMPE Journal, (in press).

RADIO-FREQUENCY HEATING OF REINFORCED UHMWPE

R. Gauvin, C. Ouellet, Ecole Polytechnique de Montréal
P.O. Box 6079, Station A, Montreal, Que., Canada

Ultra high molecular weight polyethylene (UHMWPE) has many outstanding properties such as high impact strength, even at low temperature and excellent abrasion and chemical resistance. With a typical molecular weight in excess of 3.10^6 g/mole, viscosity of molten UHMWPE is so high that it cannot be processed by forming techniques relying on the flow of molten polymer. Typically, it requires compression molding, ram extrusion, and sintering techniques. It machines well and many components are produced that way. However, all these techniques are time consuming and increase the cost. Recent years have seen the emergence of others methods to process UHMWPE. Among them, the use of high speed kinetic energy mixer, forging and modified injection molding have shown promising results.

In this work another approach to processing of UHMWPE is described. It involves the use of radio frequency radiations. UHMWPE has a non polar molecule and does not respond to dielectric heating. It is said to be "transparent" to high frequencies such as radio frequencies in the range of 50-150 MHz or microwaves. However, the dielectric behavior of carbon black polymer systems is subjected to interfacial polarization also known as Maxwell-Wagner effect. Interfacial polarization occurs in heterogeneous systems when one component has a much higher electrical conductivity than the other. For UHMWPE and carbon black, this interfacial polarization effect occurs for less than 1% by weight of carbon black, making the compound sensitive to RF excitation. The carbon black is then called a "sensitizer".

The size of primary particles of carbon black is several orders of magnitude less than that of the UHMWPE. With a proper blending method each polymer particle can be uniformly coated with carbon black. When subjected to RF excitation the heat softens the surface of UHMWPE particles and the material can be easily consolidated using adequate pressure. Large parts can then be molded in a few minutes.

The energy delivered to a material by an RF field is a function of field frequency, the square power of the field strength, the dielectric loss tangent and the dielectric constant of the material. The last two parameters are related to the percentage of carbon black. This is illustrated in Fig. 1 which shows the rate of heating of a carbon black UHMWPE blend as a function of the carbon black percentage. The UHMWPE used is the GUR-413 from Hoechst. These results were obtained using a flat platen electrodes type RF oven, having a power of 5 Kw and a fixed frequency of 55 MHz. As can be seen from the results, the percentage of carbon black is critical and must be very small. If the amount of carbon black is high, the compound is too conductive and sparks will occur resulting in polymer degradation.

In this work, 0.5% by weight of carbon black was used as sensitizer and dry blended with UHMWPE. The effect on heating rate of reinforcements such as glass fibers, glass spheres, glass flakes, mica and calcium carbonate was investigated. Tensile and impact properties of these composites are also reported.

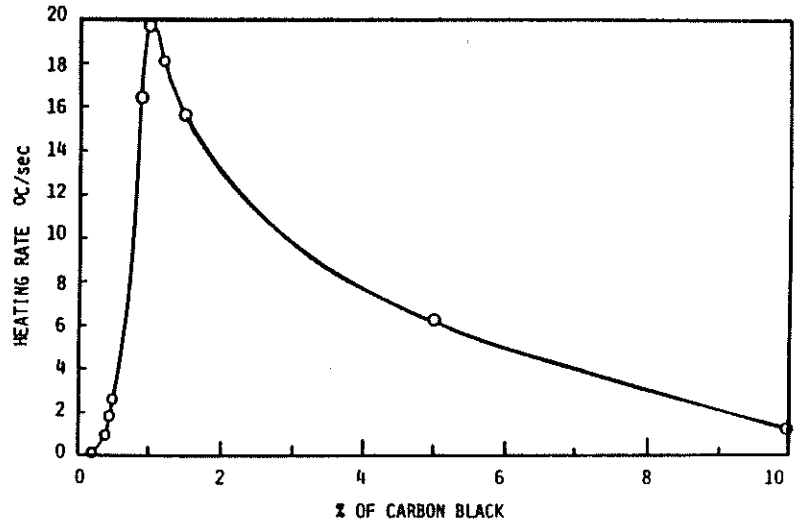


Figure 1 - Heating rate in an RF oven of a UHMWPE - carbon black dry blend as a function of the carbon black percentage.

10/3

VIBRO-THERMOFORMING OF THERMOPLASTIC SHEETS BASED ON REPEATED DEFORMATION

H. Yokoi*, H. Arakawa** and N. Kobayashi***
* Inst. of Industrial Science, Univ. of Tokyo, 7-22-1 Roppongi, Minato-ku, Tokyo 106 / ** Nachi-Fujikoshi Corp. Hydraulic Eng. Div., 20 Ishigane, Toyama 930 / *** Shin-etsu Polymer Co., Ltd. Products Development Center, 1-406-1 Yoshino-cho, Ohmiya 330, Japan

If plastics are repeatedly deformed in a short time during a precess similar to cold metal forming, the mechanical energy input will be transformed into thermal energy and accumulated in the deformation zone owing to the low thermal conductivity of plastics. This softened region has high formability and may be used for local thermoforming of thermoplastic sheets at room temperature.

Vibro-Thermoforming is based on the idea of making use of the high formability thus obtained for local precise forming. While the procedures are the same as for cold forming, the forming process itself is a thermoforming one. In this sense, we can say that Vibro-Thermoforming is a new forming process resulting from a combination of cold forming and thermoforming, which overcomes the deficiencies of these two processes.

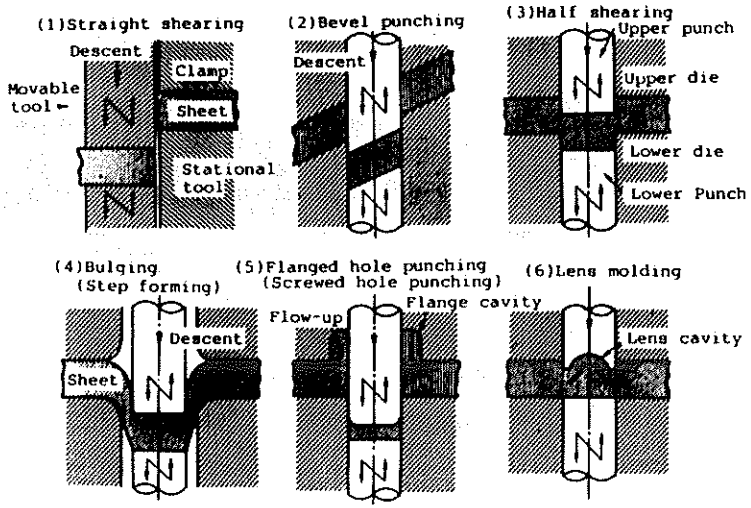


Fig. 1 Defferent types of Vibro-Thermoforming processes

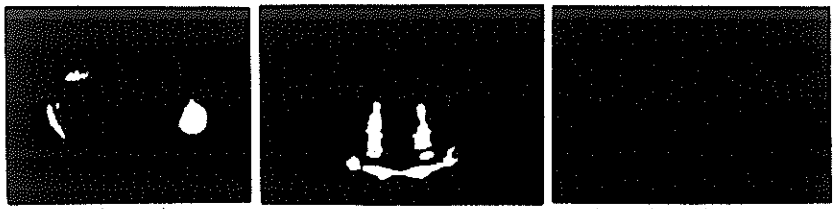
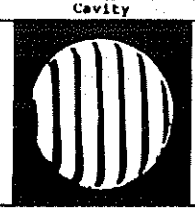
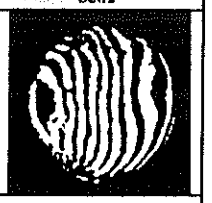


Fig.2 Appearances of the Vibro-Thermoformed samples

Fig.3 Comparison between the mold and the lens produced ►
(Olympus Optical Co., Ltd.)

	Cavity	Lens
Interference fringe		
Roughness of lens surface	Rmax less than 0.04μm	Rmax 0.152μm
Curvature radius	R9.991mm	R9.931mm

Several types of Vibro-Thermoforming processes as illustrated in Fig.1 have been proposed and examined already. They can be classified into 3 groups from the view point of the pattern of utilization of the heat-softened zone: (1) shear forming (straight, bevel and half shearing processes), (2) stretch forming (bulging and step forming processes), and (3) flow forming (flanged and screwed hole punching and lens molding). Vibro-Punching (1,2,3), which originated the Vibro-Thermoforming and has been already put into practice, is thought to belong to the simplest case of group (1).

The products processed by Vibro-Thermoforming (Fig. 2) present a high dimensional accuracy and stability as compared to cold-press-formed products. Moreover, the former process does not cause any cracking or crazing on the products. Lens molding is thus a promising method for the mass production of medium precision lenses (Fig. 3). However, along the boundary between the initial solid phase and the re-solidified phase there remains some residual stresses which we should try to reduce and minimize in the future.

References

(1) T.Nakagawa & H.Yokoi, Proc. of NAMRC-IX, pp.207(1981).
(2) H.Yokoi & T Nakagawa, Annals of CIRP, 32/1, pp.173(1983).

10/4

VIBRO-PUNCHING OF PLASTIC COMPOSITES AND THERMOPLASTIC SHEETS WITH POOR PUNCHABILITY

H. Yokoi and T. Nakagawa
Institute of Industrial Science, University of Tokyo
7-22-1 Roppongi, Minato-ku, Tokyo 106, Japan

Vibro-Punching (1-3) is a newly developed precision shearing process for plastic composites and thermoplastic sheets with poor punchability which can not be sheared precisely by any of the currently used precision shearing processes. The schematic process of Vibro-Punching is shown in Fig. 1. The sheet is clamped firmly between the upper and lower punches, which start vibrating synchronously in stage (1). After a certain number of vibration cycles, the neutral vibrating point shift down from the initial position to that shown in stage (2). After the punch has penetrated the hole, the vibration is stopped.

The finishing process is summarized as follows; (1) temperature rise in the shearing zone (and completely cutting of fibers in composites) by local material deformation, (2) shearing separation of the blank along the heat-softened region and burnishing of the sheared surface by the side surface of the vibrating punches, (3) copying of punch and die side surfaces onto the heat-softened sheared surfaces of the workpiece by the end.

The outstanding features of this method are summarized as follows: (1) sheared faces smoother than machined ones are obtained in a short time irrespective of the type of the polymer or reinforcement, (2) easy

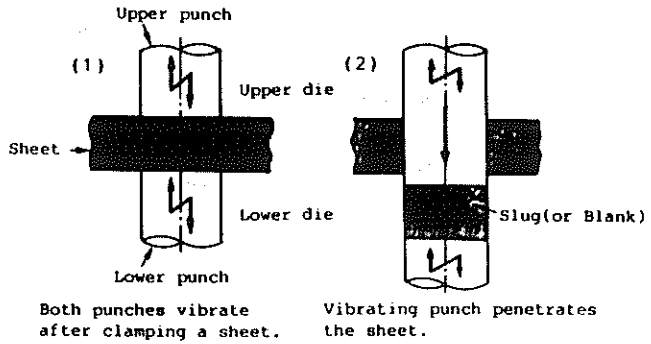
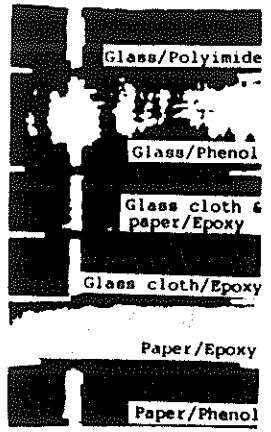


Fig. 1 Scheme of Vibro-Punching process



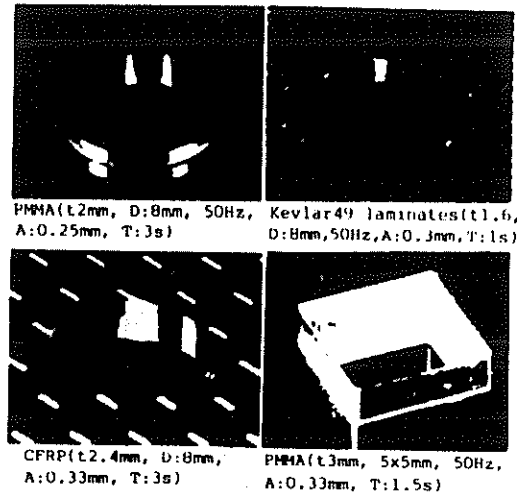


Fig. 2 Appearances of Vibro-Punched blanks and holes (D:tool diameter, A:amplitude, T:vibrating time)

manufacturing of non-circular blanks and holes, (3) applicability to either punching or blanking, (4) dimensional accuracy equivalent to that of metal shearing irrespective of the size of blanks and holes, (5) precise shearing of plastic composites and PMMA with poor punchability.

A frequency of 30-60 Hz and an amplitude per side of 10-20 percent of the sheet thickness are recomended in Vibro-Punching. This provides enough quality to punched products in 0.5-5.0 seconds in general. The appearance of the Vibro-Punched holes obtained is shown in Fig. 2. All the sheared edges on these samples have bright finished or transparent faces with Rmax 2-7 um.

Vibro-Punching has already been put into practice in Japanese industries, primarily for the punching and blanking of FRP sheets. The fundamental idea of repeated deformation processing can be extended also to Vibro-Thermoforming and to Vibro-Thermojoining.

References

(1) T.Nakagawa & H.Yokoi, Proc. of NAMRC-IX, pp.207(1981).
(2) H.Yokoi & T.Nakagawa, Proc. of ICCM-IV, pp.1625(1982).
(3) H.Yokoi & T.Nakagawa, Advanced Technology of Plasticity (Proc. of 1st ICTP), 2, pp.821(1984).

10/5

NEW PROCESS FOR ULTRADRAWN STRUCTURES

W.J. Tchir (Dow Chemical Canada, Highway 15,
Fort Saskatchewan, Alberta T8L 2P4),
H.P. Schreiber (Ecole Polytechnique, Chemical Engineering Dept.,
CP 6079, Succ. A. Montreal, Quebec H3C 3A7),
A. Rudin (University of Waterloo, Chemistry Dept.,
Waterloo, Ontario N2L 3G1),
R.J. Collacott, Dow Chemical Canada,
P.O. Box 3030, Sarnia, Ontario N7T 7M1)

Polyethylene filaments with moduli greater than 100 GPa can be made by a process in which the polyolefin is blended with paraffin wax to produce mixtures that contain 30 weight per cent or more polyethylene. These blends are shear modified and then extruded and stretched. Wax is removed from the resulting filaments by extraction with solvents like hexane. The extracted products are given a multiple stretch at controlled temperatures.

The wax apparently functions as a diluent that facilitates disentanglement of polymer chains during the extrusion step that is used for shear modification (1). An obvious process improvement can be realized by combining the filament extrusion and shear modification steps. Wax blends were made in our work by compounding the ingredients in a twin-screw extruder. Fluoroelastomer processing aids are advantageous, to reduce surface defects that may be encountered during melt processing of high molecular weight polymers.

In our experiments, filaments were extruded with a single screw extruder and then stretched in an air oven. Wax was removed from the drawn products by extraction with hexane at 60°C. The resulting fibres were restretched. Data in the attached tables show the molecular weight characteristics of two of the high density polyethylenes that were studied, along with representative values of fiber properties.

The technique described appears to be novel. It can be extended to other products, as well as filaments, and to other polymers.

References

(1) A. Rudin and H.P. Schreiber, Polym. Eng. Sci., 23, 422 (1983).

Table 1

Polymer Molecular Weights

HDPE	$\bar{M}n$	$\bar{M}w$	$\bar{M}z$
A	173,000	302,000	685,000
B	21,000	171,000	332,000

Table 2

Filament Production Conditions and Filament Properties

Material	Extrusion Temp. (°C)	Draw Temp.(°C)			Draw Ratio				Tensile Strength GPa	Tensile Modulus GPa
		1st	2nd	3rd stage	1st	2nd	3rd	Total		
HDPE A/wax 30/70	182	116	147	--	16.1	2.7	--	32	1.9	53
	195	116	147	145	12.5	2.4	2.0	61	2.1	106
HDPE A/wax 40/60	190	114	130	130				61	1.4	114
HDPE B/wax 40/60	190	114	100	--				21	1.0	85
		114	90	--				20	1.1	100
		114	74	--				26	1.5	111
		114	70	--				29	2.5	137

10/6

PREPARATION AND RHEOLOGICAL BEHAVIOR OF POLYIMIDE/SILICONE INTERPENETRATING POLYMER NETWORKS

Xi Xu Ming Hao

(Polymer Research Institute, Chengdu University of Science and Technology, China)

ABSTRACT

A series of polyimide/silicone interpenetrating polymer networks (IPN) was prepared from maleic anhydride (MA), 4,4'-diaminodiphenylmethane (MDA) or hexamethylenediamine (HMDA), and methyl vinyl silicone elastomer (MVSE) or polydimethylsiloxane elastomer (DMSE) for the purpose of making an improvement on performance and processability of polyimide. The prepolymer could be made by the following techniques:

1. Heterogeneous Solution Polymerization Dissolve silicone and MA in benzene and then add diamine stepwise at about 80°C. The pale yellow precipitate produced is repolymerized at 110°C for a period of 40 minutes, then vacuum-dried.

2. Homogeneous Solution Polymerization Same as that of the heterogeneous technique except toluene-dimethylformamide mixture and lukewarm water are used as solvent and precipitating agent respectively.

3. Melt Polymerization Add silicone pieces to diamine-MA melt at 110°C, then mix well.

4. Mixing Technique Mix silicone, MA and diamine with a twin roller at 110°C.

In the above techniques, the mole ratio of MA to diamine is 0.7—1.9 and the weight percents of silicone are 20%, 40%, 60% and 80% respectively. The IPN is made by thermal crosslinking the prepolymer in a mold. Table 1 gives the homogeneity (H) of IPN prepared by different technique. H is defined as:

$$H = \left(\frac{1}{5}\sum_{i=1}^{5}\frac{|a-b_i|}{a}\right)\times 100$$

where a is the weight percent of silicone added, b is that of silicone calculated by solvent-extraction process.

Table 1 Homogeneity of IPN Prepared

IPN	H			
	Technique 1	Technique 2	Technique 3	Technique 4
MA-HMDA(80)/DMSE(20)	5.5	—	8.6	6.2
MA-MDA(80)/MVSE(20)	5.3	6.1	8.4	6.5
MA-MDA(20)/DMSE(80)	5.4	6.3	8.5	5.9
MA-MDA(40)/DMSE(60)	5.1	6.9	8.2	6.6
MA-MDA(60)/DMSE(40)	5.1	6.9	8.2	6.6
MA-MDA(80)/DMSE(20)	5.0	6.0	7.8	6.9

The effects of the silicone content in the IPN and conditions of the heterogeneous solution polymerization on rheological behavior of the IPN were studied. The results show that the IPN is pseudo-plastic or plastic. Its apparent viscosity decreases with the increase of the silicone content in the IPN, while increases with the increased amount of benzene used for dissolving silicone.

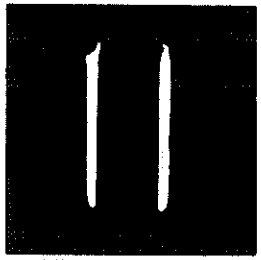
10/7

Nuclear Magnetic Resonance Imaging of Dynamic Polymer-Solvent Systems

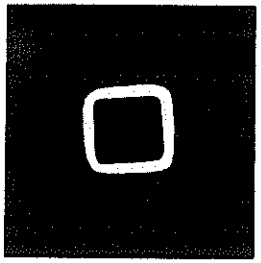
Thomas H. Mareci, Michael D. Cockman and Attilio Rigamonti

Departments of Radiology, Chemistry and Physics
University of Florida, Gainesville, Florida
and
Dipartimento di Fisica "A. Volta"
Universita di Pavia, Pavia, Italy

Nuclear magnetic resonance imaging has matured to the point where it has become a routine diagnostic procedure in medicine. We have been exploring applications of NMR imaging to problems in the chemistry and physics of materials. This talk will present our NMR study of the process of polymer swelling and dynamics of polymer chains in solution in real-time. In particular, a Fourier imaging sequence with T1 and T2 contrast was used to provide information on the phenomenology of the swelling process in the metastable states. The following images illustrate the information available during the swelling process. These images were taken during the swelling of polymethylmethacrylate in normal and deuterated chloroform as solvents.



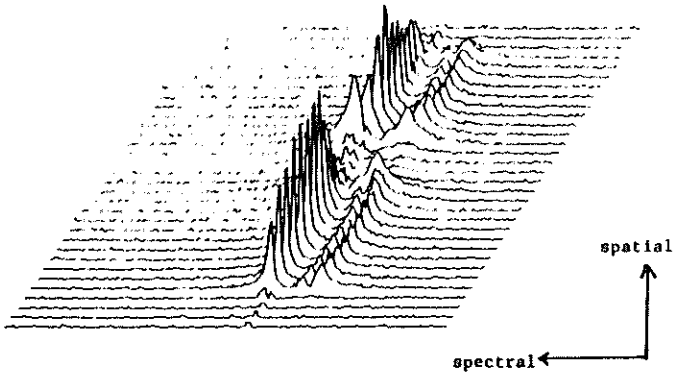
Swelling time, 2.5 hours



Swelling time, 3.5 hours

At the same time, T1 was measured in the high-resolution spectra of the region of the polymer being swollen to investigate local polymer chain dynamics while the concentration was changing by progressive swelling.

In addition, it is possible to combine spatial and chemical information with a single imaging technique. Many methods designed to combine spatial and spectral information have been proposed in the field of magnetic resonance imaging but their application to "real-world" systems has not been extensive. We present the application of a well-known, two-dimensional chemical-shift NMR imaging technique to the observation of a the same solid polymer, polymethylmethacrylate, dissolving in chloroform, acetone and their deuterated analogs. The spectra arising from different points in the polymer-solvent system are shown to change with time for a controlled concentration of polymer. An example is shown below.



The imaging technique permits the observation of spectra from the solid-liquid interface as well as the observation of the diffusion of the solvent into the polymer. Frequency shifts of the resonance peaks of the systems as functions of spatial position are partially explained by a simple magnetic susceptibility model.

VIBRO-THERMOJOINING OF PLASTICS BASED ON REPEATED DEFORMATION

H. Yokoi* and H. Arakawa**
* Institute of Industrial Science, University of Tokyo
7-22-1 Roppongi, Minato-ku, Tokyo 106, Japan
** Nachi-Fujikoshi Corp., Hydraulic Engineering Div.
20 Ishigane, Toyoma 930, Japan

Plastics with low thermal conductivity and low melting points can be easily heat-softened by a repeated deformation process in a short time. The heat-softened material is highly adhesive, which suggested the possibility of joining or welding plastics by a deformation process. The aim of this study is to examine typical Vibro-Thermojoining processes based on this idea and to confirm their feasibility through practical experiments.

Vibro-Thermojoining processes proposed hitherto can be classified into 2 groups according to shearing and material flow operations. All of them can be easily applied to the high-strength joining of different kinds of plastics, which constitutes a good feature of this method as compared to the existing ones.

The Vibro-Thermojoining based on shearing ((1)-(3) in Fig.1) makes use

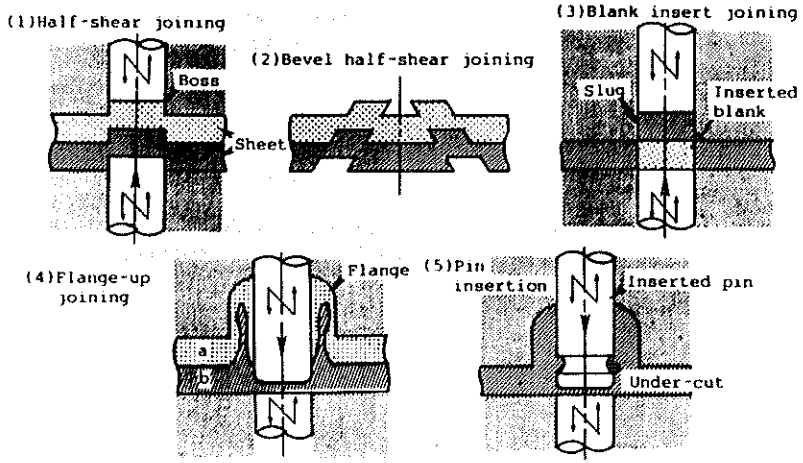


Fig. 1 Defferent types of Vibro-Thermojoinig processes

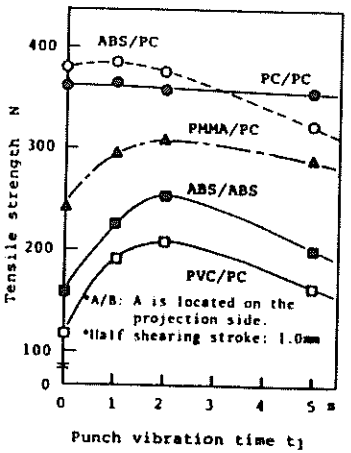


Fig. 2 Relations between punch vibration time t1 and tensile strength of the half-sheared lap joints (20Hz, amplitude: 0.7mm, diam.:8mm, t2.0mm)

Table 1 Joining strength of the samples produced by flange-up joining

a / b	PC	PMMA	PVC	PP
PC	1600/800	400/510	250/630	270/240
PMMA	670/470	420/720	700/630	190/250
PVC	580/640	330/630	470/540	230/270
PP	330/270	50/180	250/340	790/420

Fs/Ft, Fs: Shear strength(N)
Ft: Tensile strength(N)
Thickness:2mm, Joining time: 3s
Diameter : 8mm, a & b: see Fig.1-(4)

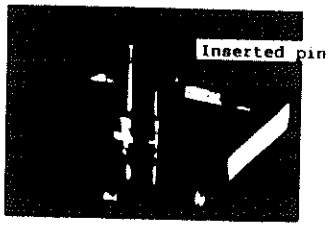


Fig. 3 Pin inserted sample(PVC, t3.0mm)

of the direct contact of each half-sheared face and the blending of the molten material along the shearing line. Half-shear joining (1) with sharp shapes of embossing is a coventional joining method whereby the joining strength reaches a considerably high level even in the combination of different kinds of materials (Fig. 2). Bevel half-shear joining (2), adding an anchor effect to the half-shear joining, has shown a 30-50 % increase in the joinig strength as compared to the normal half-shear joining. Blank insert joining (3) provides a unique product like two color molding with high sealing performance (for instance, endurance pressure of over 10 MPa in the case of a PMMA/PC sample with a thickness of 2mm).

The Vibro-Thermojoining based on material flow ((4) and (5) in Fig. 1) makes use of the mixing of molten polymers during material flow and of the mechanical joining by the anchor effect at under-cut portions. Flange-up joining (4) can provide a high-strength joint (Table 1) regardless of the existing oil at the joined portion. It is also possible to insert a pin on a specified portion without the need to make a previous hole. The pull-out strength of the pin is quite high -- a strength of 1.5 kN was obtained in the sample of Fig.3 (PVC:t3.0mm, pin diameter:8mm).

Interrelationship/Synergy Of The Different Forms Of Intellectual Property.

John H. Faro, Esq.
Faro and Associates
Boca Raton, Florida

Most individuals have some appreciation of the various forms of intellectual property that can be obtained; and, an appreciation, to a greater or lesser degree, of the rights which are conferred upon the individual possessing such property. What is not fully appreciated is the manner in which such intellectual property rights can complement one another and the extent to which the election to pursue certain rights may work a forfeiture of others.

The basic forms of patent protection include both the so called "utility" patent and the "design" patent. Each of these patents address different interests and the scope of protection accorded by each is distinct. The utility patent typically involves the claiming of the functional attributes of the elements of an invention whereas the design patent is directed to the ornamental features of an invention. It is possible to have both design and patent protection for a single product. In addition, the inventions which are defined by the claims of utility

patents may also be covered by copyright, for example, computer oriented inventions and process control oriented inventions. In addition, structural features of certain products may lend themselves to what is referred to as "trade dress" type of protection, (a type of protection which is analogous to trademark protection). The interrelationship of the utility patent, design patent and trade dress protection are at best misunderstood. This presentation will delve into the relationships of these rights to one another, the differences and the consequences of pursuing one form of protection over another.

ROLES OF INTERFACE AND MORPHOLOGY IN THE FRACTURE PERFORMANCE OF GLASS FLAKES REINFORCED POLYPROPYLENE COMPOSITES

J. Denault and T. Vu-Khanh, National Research Council Canada, Industrial Materials Research Institute, 75 De Mortagne, Boucherville, PQ, Canada J4B 6Y4

The effects of silane coupling agent and matrix morphology on the fracture performance of glass flakes reinforced polypropylene composites were investigated. Previous work (1) has shown that the addition of coupling agent to this thermoplastic composite can alter the matrix morphology at the interface by inducing specific nucleation at the filler/matrix interface (Figure 1). The nucleating ability of the silane coupling agent was attributed to the physisorbed layer of silane on the filler. It was also found (1) that the effect of coupling agent on the fracture performance, analyzed by the post yield fracture mechanics approach, depends on the concentration of the filler (Figure 2). Silane treatment has a detrimental effect at low concentrations of filler and a beneficial effect at higher concentrations. This fracture behavior has been qualitatively explained in terms of the competition between the contribution of the matrix/filler interface and the contribution of the matrix to the fracture energy of the composites. However, the fracture mechanism of these thermoplastic composites may also be dependent upon the morphology of the matrix itself. This is the subject of the present investigation.

The effect of matrix morphology on the fracture performance was investigated by testing samples of different levels of crystallinity. These materials were obtained by cooling the compression molded samples at different cooling rates. Rapid cooling results in a composite of low crystallinity and slow cooling gives composite of high level of crystallinity. Modification of matrix crystallinity in pure polypropylene and glass flakes polypropylene composites affects the fracture performance. The increase in the level of crystallinity of these materials gives rise to a reduction in the maximum crack growth resistance. Higher ductility of the matrix was demonstrated by scanning electron microscopy for samples of lower crystallinity. The low ductility of a more crystalline matrix results in a reduction of the energy dissipated in the plastic deformation of the matrix. There is, therefore, a concomitant decrease in the fracture energy.

Although the effect of matrix morphology seems to be very important in the case of pure polypropylene and untreated glass flakes polypropylene composites, this effect is negligible for the silane treated composites. Nevertheless, microscopic observations of the fracture surfaces of silane treated composites reveal an important reduction in the ductility of the matrix of the highly crystalline samples. The effect of thermal history on the fracture performance of pure polypropylene, untreated and silane treated glass flakes polypropylene composite is shown in Figure 3. It can be seen that an improvement in the matrix/filler interface inhibits the effect of matrix morphology on the fracture behavior of glass flakes polypropylene composites. The effect of morphological change on the fracture behavior of untreated and silane treated glass flakes polypropylene composites can be explained in terms of the competition between the contribution of the matrix/filler interface and the contribution of the matrix which one is a function of the level of crystallinity of the composite.

REFERENCE

1) J. Denault and T. Vu-Khanh, NRCC/IMRI Symposium "Composites '87", Montréal, Canada, 5-6 novembre 1987, p.19.1-19.22.

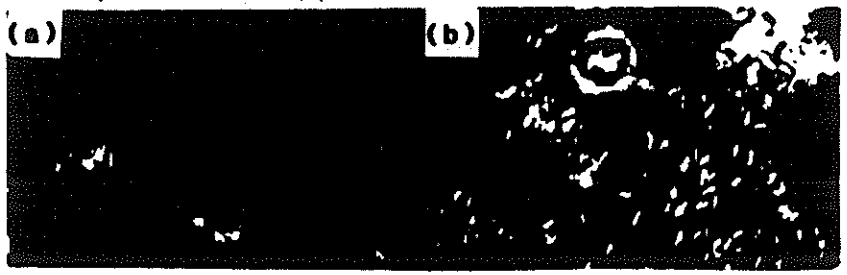


Figure 1 - Optical microscopic observations of the onset of crystallization of polypropylene in the presence of a) untreated glass flakes and b) silane treated glass flakes.

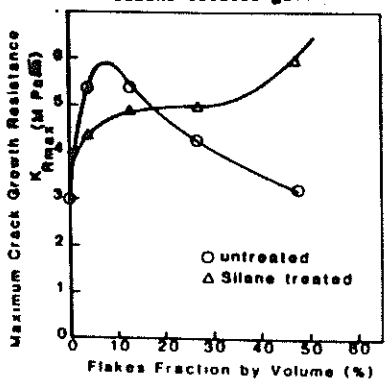


Figure 2 - K_{Rmax} as a function of filler concentration for untreated and silane treated glass flakes reinforced polypropylene.

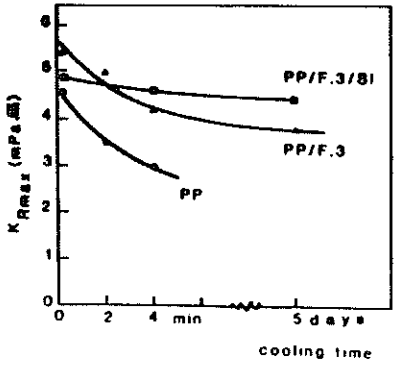


Figure 3 - K_{Rmax} as a function of thermal treatment for pure polypropylene, untreated and silane treated glass flakes polypropylene composites.

10/11

H. Jadamus and K.P. Richter
Huels AG, D-4370 Marl, West Germany

Plastics - Rubber Composites

Elastomers function in machines and appliances in many ways including as vibration and sound dampeners and in gas and liquid lines as seals or to transfer pressure from one medium to another. In order to reduce the stress on vibration dampeners, springs, seals or membranes or to facilitate installation, the elastomers are bonded to elements which are made from hard, stiff materials.

Metals and, in increasing quantities, plastics serve as the raw material for the stiffening elements. An advantage for plastic over metal is seen in its ease of forming and in its easier bondability to the elastomer. However, the bond between plastic and rubber is only accomplished through the use of adhesive agents that contain noxious solvents and whose application does not fit in with the rest of the production process.

A plastic, that would replace the normal combinations of plastic and adhesive agents, must

- be thermoplastically processable;
- be dimensionally stable at vulcanization temperatures;
- be bound inseparably with the rubber during the vulcanization step;
- have a property profile that corresponds with that of the rubber.

These properties are possessed by the new resins developed by HÜls and based upon PPE (VESTORAN(R)). In contrast to the usual PPE-Resins the bondable VESTORAN types do not contain a large portion of polystyrol or plasticizer as these would lower the softening temperature of the VESTORAN too much.

The most important constituent is polyoctenamer which raises significantly the impact resistance of the brittle base polymer.

The new VESTORAN products withstand, unchanged, working temperatures up to ca. 190°C. Temperatures such as one finds in paint annealing, soldering or vulcanization. The most important use for these products has been found in the bonding with rubber.

In this use the VESTORAN products are in competition with the semi crystalline nylon 6 and 66's - which require the use of adhesive agents for such combinations. While in competition with the nylon 6 and 66's, the VESTORAN products have different production and usage properties. Their mold shrinkage is lower, hence they do not warp even as glass fiber reinforced resins. They absorb little water and therefore are dimensionally very stable. They are, like the rubber, stable to hydrolysis, to acids as well as to alkalis. However, like the rubbers, they are not stable to organic solvents.

For the elastomeric part of the combination not all rubbers are equally suitable. Preferentially, one employs SBR rubber; blends of SBR and nature rubbers; and butadiene rubbers all with a sulfur cross-linking agent and ethylene-polypropylene rubbers with a peroxide cross-linking agent. The rubber contains the normal additives and is bonded with the Vestoran surface during the normal vulcanization process.

The bonded parts can be produced in a two-step process in which the plastic part is first molded and then subsequently inserted into the rubber mold or in a one-step process in which one uses a machine which injects the plastic and the rubber into the same mold.

Both processes can be fully automated which is not possible with the normal process which employs adhesion agents. Therefore a more uniform production quality is obtained.

Parts made with VESTORAN and rubber composites are, for example, axle bearings, springs, pads, bumpers, seals, electrical plug connectors, etc.

10/12

RAPID CURING OF EPOXY/GLASS BRAID COMPOSITES VIA DIELECTRIC HEATING

D. Wingard and C.L. Beatty, Univ. of Florida, Gainesville, FL

Introduction. Dielectric curing of epoxy/glass fiber composites with radio frequency is much more rapid than conventional thermal curing because the dielectric heating oscillates dipoles in the polymer matrix. This work involves the curing of both flat and cylindrical epoxy/glass braid composites by dielectric heating as well as thermal heating. The cylindrical composites were a prototype of a hand-held rocket launcher used by the military, and were subjected to a hydraulic burst test after cure. Burst pressure was correlated with dielectric cure time, glass content, void content and glass transition temperature (T_g) of the composites. The optimum dielectric cure time was also determined as a function of T_g.

Experimental. The epoxy system used was a low viscosity DGEBA-type resin with a cycloaliphatic amine curing agent in stoichiometric proportions. The filler used was Dow-Corning S-2 glass fibers woven in a triaxially braided structure. Composite samples were cured by dielectric heating using a Thermall Model LE-550 Dielectric Heater. For the cylindrical composites, a two-ply layer of glass braid was woven over a base sheet of Mylar on an aluminum mandrel. After the resin was applied by hand layup, the mandrel was wrapped in Teflon release film and the composite was cured on the dielectric heater with the aid of a horizontal rotator.

Results and Discussion. For the cylindrical composites, the T_g (measured by dynamic mechanical spectroscopy) increased with increasing dielectric cure time, becoming invariant after about 15 minutes of cure (Fig. 1). In fact, practically the same T_g was obtained for a composite sample cured dielectrically for 15 minutes as for a sample cured thermally for 2.75 hours. Figure 1 also shows a plot of surface temperature of a rotating composite as a function of dielectric curing time. This plot was obtained for a distance of 1/2" between the sample and the plate electrode of the dielectric heater.

Surprisingly, the burst pressure was fairly independent of the dielectric cure time. This is perhaps due to the ductility of the resin at short cure times. Burst pressure was also fairly independent of glass content, void content and the T_g of the composites. Glass content was determined by burning off the resin at 1200°F and observing the change in sample weight. Void content was calculated from the glass content and the density of the composite. The burst pressure of the RF-cured composites averaged 5,700 psi, which was very comparable to that of thermally cured composites.

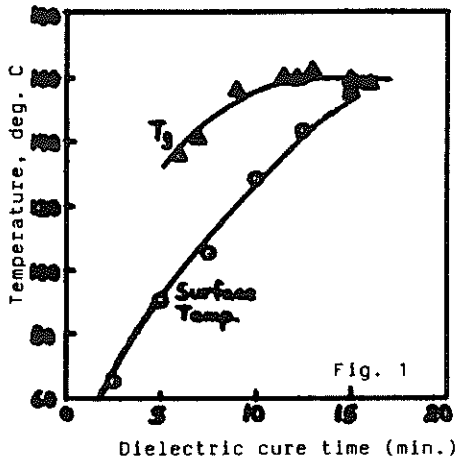


Fig. 1

II/1

THE RHEOMETRICAL BEHAVIOUR OF POLYMER MELTS

K Walters, D M Binding and T Al-Hadithi (Department of Mathematics, University College of Wales, Aberystwyth, U.K.)

The paper includes a review of current knowledge concerning the rheometrical behaviour of polymer melts, with particular emphasis being paid to steady simple, shear flow, oscillatory shear flow and extensional. The former yields the viscosity η and first normal stress N_1 as functions of shear rate $\dot{\gamma}$. The oscillatory shear experiments yield the dynamic viscosity η' and dynamic rigidity G' as functions of frequency ω. The extensional flow experiments yield the uniaxial extensional viscosity η_E as a function of strain rate $\dot{\epsilon}$. In determining the 'Trouton ratio' η_E/η, a proposal made by Jones, Walters and Williams (1987) is employed to estimate the effect of viscosity.

Well known empirical relationships like the Cox-Merz rule between the rheometrical functions are discussed and it is shown how it is possible to relate empirically the first normal stress difference N_1 to the dynamic data. This is a useful empiricism which permits normal stress determination at shear rates in excess of 300 sec^{-1} from oscillatory shear experiments carried out on a Weissenberg Rheogoniometer.

After a review of current knowledge concerning the behaviour of polymer melts in *extensional* flow, new results are presented from one of the first generation of extensional viscometers designed by Cogswell. This is a constant-stress device, which is limited to temperatures below 200°C.

The results from the constant-stress rheometer are compared with data obtained from a contraction-flow device which forms an integral part of a melt capillary rheometer. The so-called 'entry pressure losses' are interpreted using a new theory due to Binding (1988).

The extensional viscosity data from the constant-stress device and the contraction-flow experiment are shown to be in satisfactory agreement.

The whole question of extensional viscosity determination for polymer melts and solutions is discussed, with particular attention being paid to the difficulties involved. In the case of stiff systems like polymer melts, the main problem is the need to reach very high strains to ensure that the data is relevant to *steady state* extension at constant strain rate. In the case of mobile polymer solutions the problems are more accute. Here, the difficulties are associated with the whole question of generating flows which are equivalent to steady simple extension. It is argued that the best way to proceed is to concentrate on flows which have a high extensional component and for which a simple interpretation of the data can lead to extensional-viscosity *levels* and the correct trend with strain rate.

The usefulness of rheometrical data in the prediction of polymer-melt behaviour in more complex flows is discussed with particular reference to computational fluid dynamics.

It is argued that there is no obvious candidate for general use in numerical simulation studies and that the particular model to be employed should have regard to the application in mind. For example, in 'spinning' problems, it is clearly more important that the constitutive model employed is able to simulate the extensional flow properties than it is for the model to match normal stress behaviour.

References

1) D.M. Binding (1988), To appear in J. non-Newtonian Fluid Mechanics.
2) D.M. Jones, K. Walters and P.R. Williams (1987), Rheologica Acta 26, 20-30.

II/2

THE EFFECT OF PARTICLE SIZE AND CONCENTRATION ON THE MELT RHEOLOGY OF POLYSTYRENE-$CaCO_3$ COMPOSITES

J.D. Small, Jr. and A.L. Frioke
University of Florida, Gainesville, FL 32611
G.A. Campbell
Clarkson University, Potsdam, NY 13676

Knowledge of the rheological properties of polymer composite melts is critical in efficient engineering design, operation, and control of process equipment. This investigation was initiated to determine the effect of filler concentration and particle size on the melt rheological properties of well characterized polymer composites.

For this study, several polystyrene-$CaCO_3$ composites were compounded using a Banbury mixer and a twin screw extruder. The weight average molecular weight of the commercially available polystyrene resin was 220,000 molecular weight units, and the average particle sizes of the calcium carbonate fillers were 0.8, 2.0, and 20 microns. Each of these size fillers was compounded with the PS resin at filler loadings ranging from 2.5 to 25% by volume.

Rheological testing of the composites was accomplished using a Rheometrics RMS-800/RDS II Mechanical Spectrometer over a temperature range of 210-260°C in a nitrogen environment and in both dynamic oscillatory and steady shear modes. Steady shear viscosities were found to be comparable to the complex viscosities at shear rates or frequencies less than 10 S^{-1} or 10 rad/s. Complex viscosities and viscoelastic properties were measured over a range of frequency from 0.1 to 100 rad/s, and experimental results indicated that a nitrogen atmosphere was required to avoid oxidative degradation of the samples during the normal time scale of the experiments.

The complex viscosity, the storage modulus, and the loss modulus of the various composites were all found to be strongly dependent on filler concentration, filler particle size, frequency, and temperature. Correlations developed relating these properties and results of the various rheological models tested will be presented.

11/3

PREDICTION OF THE NON-NEWTONIAN VISCOSITY AND SHEAR STABILITY OF POLYMERIC LIQUIDS

W.-M. Kulicke, M. Bouldin

Institut für Technische und Makromolekulare Chemie, Universität, Bundesstraße 45, 2000 Hamburg 13, West Germany

The viscosity level in the range of the NEWTONian viscosity η_0, as well as in the non-NEWTONian range of the flow curve can be determined on the bases of a molecular modeling. Prerequisite is the information about the molecular parameters of the individual chains, which in many cases can be taken from hand books. In addition a shear stability criteria will be presented which predicts the boundary between a stable and a degraded polymer solution. By taking the actual state of solution into consideration these statements can also be extended to concentrated polymer solutions and polymer melts.

Very distinguished theoretical approaches have been derived for polymer melts and concentrated solutions. With the so-called 'entanglement-concept', BUECHE[1] postulated that above a critical molecular weight $M_W^{\ddagger}$ the observed interrelationship $\eta_0 \sim M_W^{3.4}$ is caused by intermolecular couplings, whereas for $M_W^{\ddagger} > M_W$ η is directly proportional to M_W. This model has also been extended to finite rates of deformation especially by GRAESSLEY[2] and STRATTON[3]. They were able to show that above $\dot{\gamma}_{cr}$ $(1/\tau)$ the couplings are loosened which leads to a reduction in the viscosity. Proceeding from this notion they were able to estimate the slope $(\partial \log\eta/\partial \log\dot{\gamma})$ in the linear region of the flow curve as well as the terminal relaxation time τ. These findings have enabled the prediction of $\eta(\dot{\gamma})$ as a function of M_W, c and $\dot{\gamma}$.

However in the case of less concentrated solutions the classical 'entanglement concept' does not lead to satisfactory results. Moreover a viscosity standardization is only obtained by plotting η_0 against the overlap parameter $c\cdot[\eta]$. As could be shown η_0 can be expressed by application of a simple power-series[4]. From these results it can be deduced that for semi-dilute polymer solutions the flow drag is also determined by entanglement density and that the degree of coil overlapping is strongly influenced by the nature of the polymer-solvent-interactions[5].

Plotting of the reduced viscosity against the reduced shear rate leads to no master curve in the case of semi-dilute polymer solutions. The reasons for this are that the terminal relaxation time is not described by BUECHE's approach and that the slope in the linear region of the flow curve is not constant and depends on the degree of coil overlapping. By introducing τ_{semi} and carrying out a slope correction one also obtains a perfect master curve for this concentration range as shown in fig. (1).

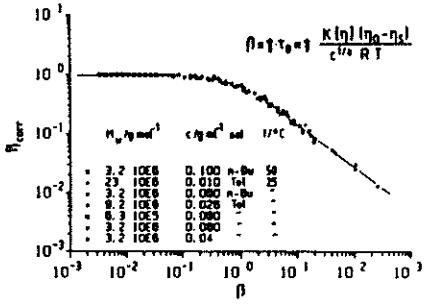


fig. 1 The slope corrected reduced viscosity as a function of the reduced shear rate $(\beta = \dot{\gamma}\cdot\tau_{semi})$ for narrowly distributed polystyrene

For technical application it is furthermore of some importance to know at which critical velocity shear induced degradation occurs. Simple considerations lead to the assumption that when all coupling points are loosened and the discrete chains are subjected to the velocity field and the degradation occurs. This is the case when $\eta_{sp}(\dot{\gamma})$ is equal to $c\cdot[\eta]$[6]. Further enhancement of the rate of deformation leads to chain scission. These results can also be extended to concentrated polymer solutions and melts.

References
1) Bueche,F.: J.Chem.Phys. 20, 1959 (1952)
2) Graessely, W.: Adv.Polym.Sci. 16, 1 (1974)
3) Stratton,R.A.: J.Coll.Interf.Sci. 22, 517 (1972)
4) Kulicke,W.-M., Kniewske,R.: Rheol.Acta 23, 75 (1984)
5) Kulicke,W.-M., Bouldin,M., Kehler,H. submitted for publication
6) Bouldin,M. Kulicke,W.-M., Kniewske,R. submitted for publication

LDV MEASUREMENTS OF FLOW OF VISCOELASTIC FLUID THROUGH ABRUPT CONTRACTIONS

R.C. Armstrong, W.P. Raiford, L.M. Quinzani and R.A. Brown
Department of Chemical Engineering
Massachusetts Institute of Technology
Cambridge, Massachusetts 02139 USA

This study examined the flow of a viscoelastic fluid through an axisymmetric sudden contraction geometry. A 4-beam, 2-color laser Doppler velocimetry (LDV) system was used to measure velocity components within the flow field. The test fluid was a solution of 5% polyisobutylene dissolved in tetradecane (PIB/C14). This is a shear-thinning solution, with a zero-shear-rate viscosity and relaxation time of η_0 = 1.3 Pa·s and λ_0 = 0.065 s. Results indicate that near the contraction plane, the radius of the small downstream tube, R_2, and the average velocity in the small tube, $\langle v_2 \rangle$, are the proper scalings for the flow. The elastic nature of the flow is measured with a shear-rate-dependent Deborah number based on a characteristic shear rate, $\dot{\gamma} = \langle v_2 \rangle / R_2$, and is defined as $De(\dot{\gamma}) = \lambda(\dot{\gamma})\dot{\gamma}$. The Reynolds number of the flow is analogously defined as $Re(\dot{\gamma}) = 2\rho\langle v_2 \rangle R_2/\eta(\dot{\gamma})$.

Experiments were performed with contraction ratios of 2:1, 4:1, and 8:1 and at high flow rates, where both elastic and inertial forces influenced the flow. Cable and Boger [1,2,3] have photographed high Reynolds number flow of polyacrylamide/water solutions, and provide some quantitative results concerning the growth of large upstream vortices and diverging streamlines. LDV data taken in the 4:1 geometry at a value of $\dot{\gamma}$ = 270 s^{-1}, $Re(\dot{\gamma})$ = 14.7, and $De(\dot{\gamma})$ = 1.0 show a weak corner recirculation region, as indicated by negative axial velocities near the outer wall. At higher flow rates, with $\dot{\gamma}$ = 900 s^{-1}, $Re(\dot{\gamma})$ = 85.9, and $De(\dot{\gamma})$ = 1.5, inertial forces have compressed the fluid toward the contraction plane. The corner vortex seen at lower flow rates has been eliminated, contrary to the observations of Cable and Boger; the elastic vortex growth is suppressed by the strong inertial forces. Cross-sectional scans of the axial velocity near the contraction plane, as shown in Fig. 1, indicate that a central core region is accelerating ahead of the outer region of the flow. The velocity profiles appear to be a superposition of two parabolic profiles.

[1,2,3] Cable, P.J. and D.V. Boger, AIChE J., 24 (5), 1978; AIChE J., 24 (6), 1978; AIChE J., 25 (1), 1979;

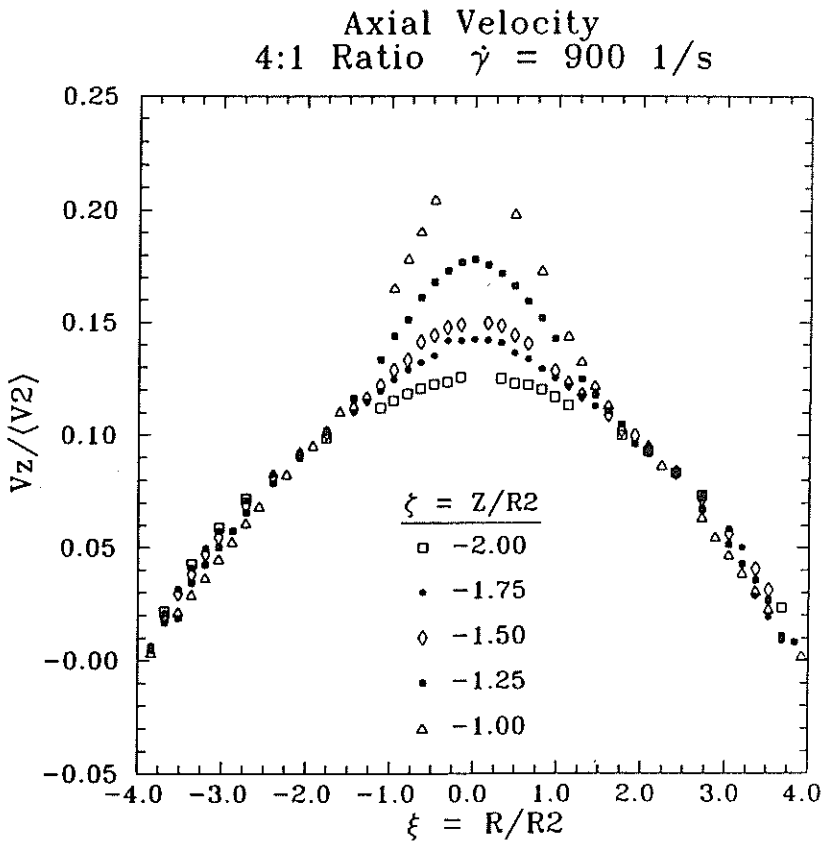


Figure 1. Axial velocity profiles of a 5% PIB/C14 solution at several locations near the contraction plane in a 4:1 axisymmetric sudden contraction. The value of $\dot{\gamma}$ = 900 1/s, $Re(\dot{\gamma})$ = 85.9, and $De(\dot{\gamma})$ = 1.5. The fluid within a central core region has accelerated, whereas the outer region of the fluid has retained its parabolic profile.

RHEOLOGICAL MEASUREMENT OF SOLVENT EFFECTS ON VISCOELASTIC PROPERTIES IN THE SEMIDILUTE REGIME

W. J. Shuely and B. S. Ince
Chemical R&D Center, APG, MD 21010-5423

It has been previously established that the complex processing behavior of a liquid can be controlled by varying the concentration and molecular weight of a polymer additive. This processing behavior can often be predicted by evaluating rheological data on the polymer solution of interest. Rheological instrumentation and methods are currently being developed to obtain basic data on those polymer solution properties which influence processing behavior.

The scope herein is limited to describing measurements and evaluating data on the influence of individual monomer-solvent interactions on the rheological behavior of polymer solutions in the semidilute regime. Also presented are preliminary data on the rheological detection of the transitions from the semidilute to the concentrated or dilute regimes.

The polymer under study is a high MW acrylic terpolymer employed commercially as a viscoelastic additive and also employed in rheological research. The solvents were selected because their solvent power extends over the theta-to-moderate-to-good range for solutions with the terpolymer.

Other polymers used in this study were homopolymers of the terpolymer: poly(methyl methacrylate) (PMMA), poly(ethyl acrylate) (PEA) and poly(butyl acrylate) (PBA). Rheological measurements were performed using the Rheometrics Fluids Rheometer (RFR) Model 7800 with cone and plate geometry. A number of preliminary conclusions are given below.

Relative Ranges: The coil expansion range estimated by the limiting viscosity number (LVN) was 4.08 to 1.27 dL/g or a factor of 3.2. This range covered polymer liquid interactions from near theta conditions to enhanced coil expansion due to specific hydrogen bonding by polymer-acceptor to liquid-donor. An example of a corresponding first normal stress difference (FNSD) range was 8000 to 370 dynes/sq. cm. for a factor of 22; the range applies to the specific set of experimental conditions that were held constant (shear rate, concentration, temperature).

An apparent viscosity range of 18. to 4.5 poise was obtained for a factor of 4.0 (at experimental conditions). In summary, the range factors for LVN, FNSD and apparent viscosity were 3.2, 22 and 4.0, respectively.

Rheological Examination: All polymer solutions reported were rheologically well-behaved and demonstrated normal pseudoplastic behavior without hysteresis. This included near-theta solvents and solvents that were shown to be only soluble with 18% of the polymer comonomer content (i.e., soluble only with the ethyl acrylate and butyl acrylate monomers).

Apparent Viscosity: For the coil density function [LVN x C] product of 6-15, the apparent viscosity was already independent of LVN for a shear rate of 10/sec and a moderate variance.

FNSD: For the semi-dilute regime coil density function defined by a [LVN x C] product of 6-15, the FNSD increased with decreasing LVN; a statistically significant relationship exists for ln FNSD versus linear LVN. Liquids that are preferentially soluble with low comonomer content are excluded.

Preferential Solvation: Given the three monomers (MMA, EA, BA) and the two states (soluble, insoluble), 8 unique classes of polymer-liquid interactions exist for the terpolymer. The classification of a liquids interaction as soluble/insoluble was determined by independent experimentation with the homopolymer.

The classifications ranged from "soluble" with all 3 monomers, to "insoluble" in all three (not applicable), to combinations of specific solubility with each comonomer. The results with the ca. 20 liquids studied to date required collapsing the 8 nominal classes into two: (1) soluble in 94-100% of the comonomers (MMA/EA or MMA/EA/BA) and (2) soluble in only 18% of the comonomers (EA/BA).

Considering the FNSD vs. LVN correlation with respect to both classes leads to the tentative conclusion that (1) either the "preferentially soluble with low comonomer content" liquids are anomalously high in FNSD and are forming a separate and distinct relationship, or (2) this preferentially soluble liquid set indicates an extremely rapid increase in FNSD as theta conditions are approached and/or when liquids are insoluble with a large fraction of the comonomers in a terpolymer (or copolymer). The interpretation is complex because co-correlation exists among theta conditions, low LVN, and preferential solubility (in a small fraction of the copolymer) and these conditions occur over a small LVN range. Identification of new liquids that fall within specific preferential solubility classes is underway to clarify the correlation.

II/3

PREDICTION OF THE NON-NEWTONIAN VISCOSITY AND SHEAR STABILITY OF POLYMERIC LIQUIDS

W.-M. Kulicke, M. Bouldin

Institut für Technische und Makromolekulare Chemie, Universität, Bundesstraße 45, 2000 Hamburg 13, West Germany

The viscosity level in the range of the NEWTONian viscosity η_0, as well as in the non-NEWTONian range of the flow curve can be determined on the bases of a molecular modeling. Prerequisite is the information about the molecular parameters of the individual chains, which in many cases can be taken from hand books. In addition a shear stability criteria will be presented which predicts the boundary between a stable and a degraded polymer solution. By taking the actual state of solution into consideration these statements can also be extended to concentrated polymer solutions and polymer melts.

Very distinguished theoretical approaches have been derived for polymer melts and concentrated solutions. With the so-called 'entanglement-concept', BUECHE[1] postulated that above a critical molecular weight M_W^s the observed interrelationship $\eta_0 \propto M_W^{3.4}$ is caused by intermolecular couplings, whereas for $M_W^s > M_W$ η is directly proportional to M_W. This model has also been extended to finite rates of deformation especially by GRAESSLEY[2] and STRATTON[3]. They were able to show that above $\dot{\gamma}_{CF}$ $(1/\tau)$ the couplings are loosened which leads to a reduction in the viscosity. Proceeding from this notion they were able to estimate the slope $(\partial \log\eta/\partial \log\dot{\gamma})$ in the linear region of the flow curve as well as the terminal relaxation time τ. These findings have enabled the prediction of $\eta(\dot{\gamma})$ as a function of M_W, c and $\dot{\gamma}$.

However in the case of less concentrated solutions the classical 'entanglement concept' does not lead to satisfactory results. Moreover a viscosity standardization is only obtained by plotting η_0 against the overlap parameter $c\cdot[\eta]$. As could be shown η_0 can be expressed by application of a simple power-series[4]. From these results it can be deduced that for semi-dilute polymer solutions the flow drag is also determined by entanglement density and that the degree of coil overlapping is strongly influenced by the nature of the polymer-solvent-interactions[5].

Plotting of the reduced viscosity against the reduced shear rate leads to no master curve in the case of semi-dilute polymer solutions. The reasons for this are that the terminal relaxation time is not described by BUECHE's approach and that the slope in the linear region of the flow curve is not constant and depends on the degree of coil overlapping. By introducing τ_{semi} and carrying out a slope correction one also obtains a perfect master curve for this concentration range as shown in fig. (1).

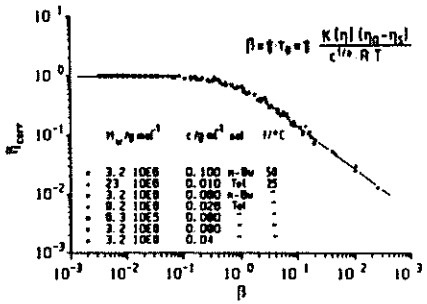


fig. 1 The slope corrected reduced viscosity as a function of the reduced shear rate ($\beta = \dot{\gamma}\cdot\tau_{semi}$) for narrowly distributed polystyrene

For technical application it is furthermore of some importance to know at which critical velocity shear induced degradation occurs. Simple considerations lead to the assumption that when all coupling points are loosened and the discrete chains are subjected to the velocity field and the degradation occurs. This is the case when $\eta_{sp}(\dot{\gamma})$ is equal to $c\cdot[\eta]$[6]. Further enhancement of the rate of deformation leads to chain scission. These results can also be extended to concentrated polymer solutions and melts.

References
1) Bueche,F.: J.Chem.Phys. 20, 1959 (1952)
2) Graessely, W.: Adv.Polym.Sci. 16, 1 (1974)
3) Stratton,R.A.: J.Coll.Interf.Sci. 22, 517 (1972)
4) Kulicke,W.-M., Kniewske,R.: Rheol.Acta 23, 75 (1984)
5) Kulicke,W.-M., Bouldin,M., Kehler,H. submitted for publication
6) Bouldin,M. Kulicke,W.-M., Kniewske,R. submitted for publication

II/7

RHEOLOGICAL PROPERTIES OF POLYCARBONATE / LIQUID CRYSTALLINE POLYESTER BLENDS

D.Acierno (University of Salerno, Salerno, Italy)
E.Amendola, C.Carfagna, L.Nicolais, R.Nobile (University of Naples, Naples, Italy)

The aim of the work has been to verify the possibility of employing a liquid crystalline polymer in blend with a typical engineering thermoplastic either to improve the processability or to enhance some mechanical properties.

The system chosen for the experiments has been the one made by the classical polyethyleneterephtalate-co-p-oxybenzoate produced by Tennessee Eastman Co. and a bisphenol-A polycarbonate by General Electric.

The materials, vacuum dried at 100 °C for 4 hrs, have been blended by making use of a single screw extruder at 240 °C. Blends have been prepared with compositions ranging from 5 to 50 w/w percent of LCP in PC.

Rheological measurements in shear flow have been carried out in the high shear rate region with the aid of a capillary viscometer (Rheoscope 1000 by CEAST). Flat entry capillaries with D = 1 mm and L/D = 5, 10, 20, 40 have been used, in order to evaluate the end effects in the way first outlined by Bagley. The Rabinowitch correction on the shear rate has been also performed.

In the low shear rate region a Rheometrics Mechanical Spectrometer (RDS-II) with a cone of 1.25 cm radius and 0.1 radian angle has been used.

All the measurements have been performed at the temperatures of 240 °C and 260 °C; additionally a few measurements have been performed also at 220 °C.

Typically the polycarbonate exhibits a Newtonian behaviour at low shear rates while shows a tendency to shear thin when subjected to high shear rates.

Similar flow characteristics are exhibited by the PC/LCP5 and PC/LCP10 blends. Moreover, in the whole shear rate range, the viscosity values of such blends are in between those of the pure polymers.

The PC/LCP50 blend is characterized by a Newtonian behaviour only in the very low shear rate region;a continuous shear thinning follows with a crossover of the PC flow curve at a low $\dot{\gamma}$ value at T = 240 °C. This resembles the behaviour of the pure LCP which also crossovers the PC, showing viscosity values higher than those of the PC at low shear rate values and viceversa viscosity values lower at high shear rate values. At T = 260 °C both the viscosity of the pure LCP and of the PC/LCP50 blend result lower than the viscosity of the PC in the whole shear rate region.

Thus, with respect to the objectives of the work, from the rheological data one may say that:

i) the LCP can be usefully employed as an aid processing agent giving a decrease in viscosity, when blended with PC, of the order of 30% already at 5% composition, in the shear rate region of interest in processing;
ii) the LCP seems to give a well oriented structure at higher compositions, as seen by a large drop in the viscosity and directly confirmed by SEM data, and then possibly to an enhancement of modulus.

II/8

*RHEOLOGY AND ENTRY FLOW OF SHORT GLASS FIBRE SUSPENSIONS

D V Boger and D U Hur
Department of Chemical Engineering
University of Melbourne
Parkville, Victoria, 3052
AUSTRALIA

The bulk rheology in terms of the steady and dynamic shear properties for short glass fibres suspended in inelastic Newtonian and model elastic (Boger) fluids is reported. Streakline photographic techniques are used to observe the secondary flow vortex present for these semi-dilute suspensions in tubular entry flow. The entry flow observations are interpreted in terms of flow properties of the various suspensions and are compared to finite element prediction carried out by Libscomb and Denn at the University of California, Berkeley (Fig. 1).

For fibres suspended in Newtonian fluids significant enhancement of the recirculating corner vortex is observed in tubular entry flows, even at volume fractions of glass fibres as low as 0.02%. The vortex enhancement relative to the Newtonian medium is flow rate independent for Reynolds numbers less than 0.1, but is strongly dependent on fibre concentration, fibre aspects ratio, the viscosity of the suspending medium and on the entry flow geometry itself (contraction ratio). The experimental results clearly show that the flow of dilute and semidilute suspensions of large aspect ratio fibres in entry flow is quantatively very different from that of the Newtonian suspending fluid. Thus a numerical simulation which neglects the effect of the fibres on the kinetics will fail to predict the fibre orientation in tubular entry flows. Excellent agreement between the observations in the tubular entry flow and predictions is however obtained using continuum theory for dilute suspensions which incorporates the statistical orientation distribution function in the constitutive equation.

The paper concludes with a discussion on the kinematics observed for glass fibres suspended in constant viscosity elastic liquids. Here the elasticity of the suspending fluid is the additional variable and the combined effect of the fibres and the suspending fluid elasticity is examined relative to known Newtonian and elastic liquid behaviour.

* Research in non-Newtonian fluid mechanics in Chemical Engineering at the University of Melbourne is supported by the Australian Research Grants Scheme.

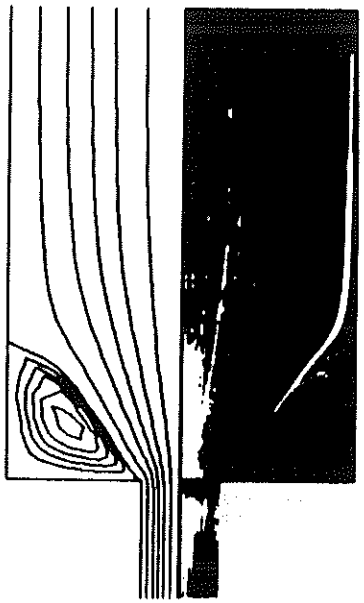


Fig. 1 Comparison between computed and experimentally observed streamlines in a 4.5:1 contraction, 0.045 $^{V}/_{V}$% 3 mm glass fibres in MCY4IN.

MOLECULAR ORIENTATION PROCESS IN PLASTICS INJECTION MOLDING

Mitsuyoshi Fujiyama, Polymer Development Laboratory, Tokuyama Soda Co., Ltd., Tokuyama-shi, Yamaguchi-ken 745, Japan

INTRODUCTION The orientation of molecular chains in injection-molded articles significantly affects the product properties, such as mechanical and optical properties, and is an important engineering problem. Interest in the molecular orientation process in injection molding has continued since quite early times and qualitative explanation has recently progressed to the stage of quantitative treatment. This paper reports an analysis of molecular orientation process in injection molding of polypropylenes(PP) and particulate-filled PPs from the viewpoint of growth of melt orientation at the gate and its relaxation in the cavity.

THEORY In this analysis, recoverable shear strain, γ_e is used as a measure of melt orientation. The recoverable shear strain having grown during passage through the gate, γ_{e0}, undergoes Maxwell-type relaxation with relaxation time, λ_1, while flowing through the cavity and becomes γ_{e1}. At this time, cooling is ignored until the flow front reaches a certain position x_1 in the flow direction of the cavity, and resin temperature is regarded identical to injected resin temperature, T_{melt}. It is, therefore, regarded that, meantime, relaxation occurs with relaxation time $\lambda_1(T_{melt})$. Then, the resin at position x_1 is cooled by the mold at temperature, T_{mold} and its temperature becomes T(t). The recoverable shear strain γ_{e1} undergoes temperature-dependent Maxwell-type relaxation with relaxation time $\lambda_2(T(t))$ and becomes residual recoverable shear strain γ_{er} when the resin temperature reaches the crystallization temperature T_c. γ_{er} is presumed to be proportional to the degree of orientation of an injection-molded article.

With V(cm^3/sec) for the injection rate, B(cm) for the width of the cavity and 2H(cm) for the thickness of the cavity, γ_{e1} is expressed as follows:

$$\gamma_{e1} = \gamma_{e0} \exp\left\{\frac{-2BHx_1}{V\lambda_1(T_{melt})}\right\} \qquad (1)$$

If Carslaw-Jaeger's equation for one dimensional nonsteady-state thermal conduction of infinite solid is applied, ignoring the latent heat of crystallization, time change of resin temperature, T(t), at y($0 \leq y \leq H$) from the center of the thickness direction is expressed as follows:

$$\frac{T-T_{mold}}{T_{melt}-T_{mold}} = 2\sum_{n=0}^{\infty}\frac{(-1)^n}{\pi(n+1/2)}\cos\left\{(n+1/2)\frac{\pi y}{H}\right\}\exp\left\{-(n+1/2)^2\pi^2\frac{\alpha t}{H^2}\right\} \qquad (2)$$

where α is thermal diffusivity. If equation (2) is written as t = f(T), residual recoverable shear strain γ_{er} is calculated by the following equation:

$$\ln\frac{\gamma_{er}}{\gamma_{e1}} = -\int_{T_{melt}}^{T_c}\frac{1}{\lambda_2(T)}\frac{df(T)}{dT}dT \qquad (3)$$

A half of cavity thickness, H, is divided into 10 equal parts, residual recoverable shear strain at the center of each division, $\gamma_{er,i}$ is calculated by equation (3) using computer, and mean residual recoverable shear strain γ_{er} is calculated by:

$$\gamma_{er} = \frac{1}{10}\sum_{i=1}^{10}\gamma_{er,i} \qquad (4)$$

EXPERIMENTAL Flexural test specimens(ASTM D790) were injection-molded from PPs with various molecular weight and PPs filled with talc and calcium carbonate at various contents by changing the cylinder temperature. Mechanical properties, such as flexural modulus, flexural strength and mold shrinkage and degree of molecular orientation, such as the thickness of skin layer, crystal orientation functions and orientation fraction(OF) were measured on the molded specimens. Recoverable shear strain γ_{e0} was obtained from the end correction coefficient measured by a capillary rheometer. Relaxation time λ_0 was obtained from complex viscosity $\eta^*(\omega)$ measured by a concentric cylinder rheometer following the Graessley's method. Crystallization temperature T_c was measured by DSC. Thermal diffusivity α was calculated from document data.

RESULTS Variation of calculated relative residual recoverable shear strain γ_{er}/γ_{e1} with thickness direction agreed well with those of measured c-axis orientation function f_c and OF. Variation of calculated mean residual recoverable shear strain γ_{er} with flow direction agreed well with those of f_c, OF and the thickness of skin layer. Fig.2 shows the relation between the thickness of skin layer and calculated γ_{er} of PP specimens molded at various cylinder temperatures. Similar results were obtained for particulate-filled PPs.

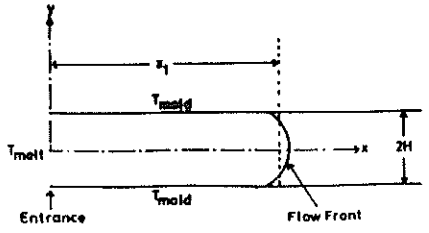


Fig. 1

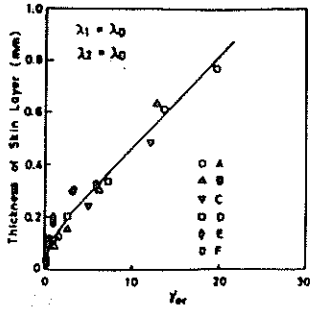


Fig. 2

11/10

THE IMPORTANCE OF EXTENSIONAL VISCOSITY TO THE EXTRUSION OF POLYMER MELTS

D.G. Baird, D.S. Done and R. Ramanathan (Polymer Materials & Interfaces Laboratory and Department of Chemical Engineering, Virginia Polytechnic Institute & State University) Blacksburg, VA 24061-6496

The entry flow behavior of polymer melts is of practical significance because of the onset of flow instabilities. Branched polymers such as low density polyethylene (LDPE) exhibit intense vortices in both planar and axisymmetric entry flow. Linear polymers such as polystyrene exhibit only small nearly indistinguishable vortices in planar entry flow but much larger ones in axisymmetric flow. Linear polymers such as L-LDPE and HDPE also tend to exhibit vortices in planar flow but in axisymmetric flow a weak vortex may be observed. The purpose of the present work has been to determine the origin of vortices in contraction flow.

A slit die was designed with glass windows in the die entry. The die entry geometry could be altered by the means of inserts to give different contraction ratios and entry angles. A particle tracer technique was used to depict the streamlines while flow birefringence was used to determine the stress field. Vortex growth was determined for LDPE as a function of wall shear rate and fluid elasticity as determined by the ratio of the primary normal stress difference (N_1) to twice the shear stress, (τ_{12}). This ratio, $N_1/2\tau_{12}$, is referred to as the Weissenberg number (We). There was no vortex growth for polystyrene as a function of We. Furthermore there was no correlation between vortex size and We as the elasticity of the two fluids could be changed merely by changing temperature. The one significant difference between these two polymers was that LDPE exhibits a strain hardening extensional viscosity while PS exhibits a strain softening extensional viscosity. However, birefringence measurements showed that the absolute magnitude of the stress in the contraction was the same for both polymers. Hence, the extensional viscosity by itself is not sufficient to account for the differences in vortex formation. When the extensional stresses were normalized to the downstream wall shear stress, a significant difference was observed. The extensional normal stresses along the die center line rose to a factor of two or three times higher than the wall shear stress (τ_w) for LDPE while for PS they only reached the same level.

It is proposed that the origin of the vortices rests in both the extensional and shear flow properties. In particular the strain hardening extensional viscosity leads to the formation of streamlines which detach from the wall forming a natural converging flow region. The curved streamlines lead to large dead regions in the corners. If the fluid shear thins at low shear rates then momentum can be transferred to the fluid leading vortices.

Numerical simulation of planar entry flow was carried out using finite element methods and the Phan Thien-Tanner model. The model has the capability of being able to change the extensional flow predictions without significantly affecting the shear flow predictions. The simulation predicted vortices for LDPE but not for PS which is in agreement with experimental observations. The only difference in the computations was the parameters used in the constitutive equation as determined from the extensional and shear flow properties.

RHEOLOGY AND MORPHOLOGY OF PC/LLDPE BLENDS

D.Acierno, V.Romano (University of Salerno, Salerno, Italy)
G.Demma, E.Martuscelli (C.N.R. I.T.P.R. Arco Felice (Na) Italy)
F.P.La Mantia, A.Valenza (University of Palermo, Palermo, Italy)

In the framework of an interlaboratory research project on polymer Blends (VAMAS) rheological properties of blends made out by a polycarbonate (Lexan, General Electric) and a linear low density polyethylene (Escorene, Esso Chemical) have been evaluated.

Shear flow tests have been performed at 245 °C on samples carefully dried (4h at 100 °C under vacuum) by means of a commercial capillary rheometer (Rheoscope 1000, CEAST).

Capillaries, 1mm in diameter and 10,20 and 40 mm in length, have been employed, both with a flat entry and with a 90° conical entry.

The explored range of shear rates has been $5\text{-}10^{3}$ sec^{-1}, in terms of true values, i.e. after performing the Rabinowitch correction.

The end effects have been considered in order to evaluate the shear stress, in the classic form suggested by Bagley.

The extruded samples have been fractured in liquid nitrogen and the fracture surfaces have been examined by means of a Scanning Electron Microscope (Philips SEM 501), both in the longitudinal and transverse direction.

The microscopical observations have put in evidence both the influence of the length of the capillary and the entry type on the morphology of the extrudates. More particularly for blends containing 25% of PC a larger orientation of the dispersed phase (PC) is obtained with the flat entry short capillary; for 50% PC blend only differences in the domain dimension can be observed, especially because of the large orientation always shown; for the 75% PC blend minor effects seem due to the length while the conical entry seems to favour orientation.

On the macroscopic side, i.e. as far as the flow tests results are concerned, the above effects appear less important. Namely the differences due to the different entry conditions are within the reproducibility range.

Thus from the Bagley plots single straight lines can be drawn through the Δp values coming out from different experiments and different entry conditions. All together one notices that the Bagley correction is negligible.

As for the viscosity results, it appears that, within the experimental error, there is no difference in the viscosity in the whole shear rate range among the LLDPE and the blends up to 50%. The 75% blend very slightly takes into account the presence of the PC, showing thus a smaller viscosity at low shear rate and a higher viscosity at higher shear rate as compared with LLDPE. This appears all together in line with the microscopical observation that even at high PC composition the matrix of the blend is the LLDPE.

11/12

PREDICTION OF FIBER ORIENTATION DISTRIBUTION AND RHEOLOGICAL PROPERTIES OF FIBER REINFORCED MELTS IN SIMPLE FLOWS

A.T. Mutel and M.R. Kamal, Department of Chemical Engineering
McGill University, Montreal, Canada, H3A 2A7

Fiber filled polymer melts exhibit highly non-linear rheological properties which are associated with very long time scales compared to the corresponding unfilled melts. Large stress overshoots, both in shear stress and first normal stress differences, were observed in simple shear at shear rates where no overshoots occurred for unfilled melts. Steady shear viscosities for filled melts showed a strong shear dependence, especially at such low shear rates where the unfilled polymer viscosity was independent of shear rate. Fiber orientation distributions measured under the same flow conditions indicate a strong correlation between these distributions and the observed rheological properties. Step shear experiments also indicate that structural changes associated with flow behavior are irreversible.

In light of the above observations, a theoretical model has been sought to describe the interdependence between the structural parameters and bulk rheological properties. A kinetic model has been developed, in which the particle interactions are modelled as a randomizing Markovian process. Fiber configuration in orientation space is then described by the Fokker-Planck equation. Once the fiber orientation distribution is known, rheological properties associated with the fiber structure are calculated from averages over orientation probability using Batchelor's equation (1). However, no analytical solution is possible for the Fokker-Planck equation for all Pe numbers (ratio of the time scales associated with the flow and diffusion processes). Analytical solutions are available only at asymptotic Pe numbers or for near spherical particles. In this study, the Fokker-Planck equation was solved numerically in orientation space using a finite-difference scheme which accommodates a periodic boundary condition. The effects of non-Newtonian flow properties are incorporated using Leal's analysis (2) for weak but accumulative viscoelastic effects instead of Jeffrey's equations. Non-Newtonian effects, in this way, are only incorporated through their effect on the orientation distribution.

Numerical results predict low- and high-shear rate plateaus with shear thinning behavior in the intermediate shear rate range. Large stress overshoots, followed by a smaller undershoot, are predicted in transient shear flow. Non-Newtonian behavior of the suspending fluid was found to cause a decrease in the steady stress contribution of fibers and to suppress the undershoots. Any type of initial orientation distribution can be assumed and the irreversibility in the structure is incorporated through an orientation distribution dependent diffusion constant. The experimental observations for the relative viscosity of fiber filled melts are in qualitative agreement with the predictions.

References

1) G.K. Batchelor, J. Fluid Mechanics, 41:3, 545 (1970).
2) L.G. Leal, J. Fluid Mechanics, 69:2, 305 (1975).

11/13

Mechanical and Physical Properties of Pearlite Filled. Styrene-Butadiene Rubber

T.Tincer and N.Ulkem

Department of Chemistry, Middle East Technical University

Ankara, TURKEY

The most important and well known reinforcement filler for rubbers is carbon black.Calcium sulphate, calcium carbonate, and clay are also widely used as filler together with carbon black.

In this study, expanded and micron -size pearlite (~ 5 μm) is used as filler for styrene-butadiene rubber.

Pearlite is a volcanic nature rock and is composed of mainly SiO_2 (71-75%), Al_2O_3 (8-12.5%),Na_2O-K_2O (2-8%) and other metal oxides.At elevated temperatures (800-1200°C) depending on its water content (2-7%) it expands from 4 to 20 times of its original size.The micron size pearlite is supplied from Etibank-Izmir Plant.

The blend composites of pearlite-SBR were prepared in the mixing head of Brabender.The mixing temperature (oil bath) was adjusted to 100°C and the mixing rate was varied from 10 to 60 phr with increasing 10 phr at each step. The sulfur content was changed from 0.5 to 2.5 with 0.5 phr ranges. The other additives were kept constant. The same type of recipes were prepared for carbon black composites for comparison. All blends were Vulcanized at 175°C and 15 atm pressure for 20 min. The test were carried out on the 2 mm thick sheets vulcanized rubber specimens.

The increase in temperature during blending in Brabender mixer is less in pearlite-SBR batch than carbon black SBR. At high carbon black concentrations, the mixing temperature is found to increase to 140°C while in all pearlite-SBR composites the temperature is never higher than 132°C. The mechanical tests shows that in pearlite-SBR compositions the elongation is improved and the samples are broken in longer strains than carbon black. On the other hand, the carbon black rubber has higher stress at break volues than that of pearlite (30-70% by volume) are appeared that the swelling in pearlite SBR composite is less.

Our prelimenary results illustrates that pearlite way be one of the future reinforcing material for rubbers in some certain applications.

RHEOLOGICAL CHARACTERISTICS OF SHORT CELLULOSE FIBER FILLED ELASTOMER

Zhou Yanhao
(Dept. of Polym. Sci., Beijing Inst. of Chem. Techn., Beijing, China)
White J.L., Nakajima N., Min K., Weissert F.C.
(Cent. for Polym. Eng., The Univ. of Akron, Akron, OH 44325, U.S.A.)

The investigation on the rheological behavior of rubber compounds filled with short fiber is not nearly enough. Only a few experimental studies have appeared(1-4).

In this paper the results of systematic studies on shear flow and elongational flow of SBR-1500 compounds prepared in Brabender plastocorder filled with short cellulose fiber Santoweb Dx (the volume fraction of Dx, i.e. ϕ, 0-0.20) are reported.

The rheological measurements of shear flow were carried out by the Monsanto Processability Tester (MPT) at 85°C-150°C, Multispeed Pressurized Mooney Viscometer (MPMV) at 100°C and Sandwich Rheometer (SR) at 100°C.

The rheological measurements of uniaxial elongational flow of rubber compounds at room temperature were carried out by the Monsanto Tensometer-500 with dumbbell samples at 12 constant tensile velocities 2×10^{-3}-2×10^{-1} mm/sec separately. The method is different from those reported by Cotten(5) and others.

The relationships between applied force (F), elongation ratio (λ) and time (t) were recorded simultaneously.

The elongational rate ($\dot{\varepsilon}$), elongational stress (σ_E) and transient elongational viscosity (η_e) are calculated from:

$$\dot{\varepsilon}=\frac{\partial V_1}{\partial x_1}=\frac{V}{L_0+Vt} \quad \cdots\cdots(1); \qquad \sigma_E=\frac{F(t)}{A(t)} \quad \cdots\cdots(2); \qquad \eta_e=\frac{\sigma_E}{\dot{\varepsilon}} \quad \cdots\cdots(3)$$

where V is tensile velocity, L_0 the original length of sample, F(t) the applied force as a function of time. A(t) is $1/\lambda$ times of original cross-section area (A_0).

The tension times at some elected can be determined from equation (1). By that time the F(t) and A(t) may be determined according to the relationship between (F) and (t), and the relationship between (λ) and (t). So that it is possible to calculate the (η_e) at certain time.

It is found that the viscosity-shear rate function is independent of instrument for MPT, MPMV and SR investigation (Fig.1), but it should be noticed that if the Mooney torque was corrected according to Nakajima's paper(6) then the torque and viscosity would decrease. It may be that the torque contribution from Section III defined in the paper(6) is not so big for these compounds exhibiting extremely nonlinear behavior. In addition, the temperature sensitivity of the compounds is small and the effect fiber loading level ($\phi \leq 0.20$) on the shear viscosity is more pronounced at lower shear rate ($< 10\ sec^{-1}$).

The transient elongational viscosity of rubber compounds can be measured by the constrant velocity tension method. There are no steady-state behavior in elongational flow for both SBR/Dx and SBR/N330/Dx even though $\dot{\varepsilon}$ is as low as 1.2×10^{-3} sec^{-1}. The η_e for all systems studied increase with increase in elongational rate and loading level (Fig.2, Fig.3) because of orientation.

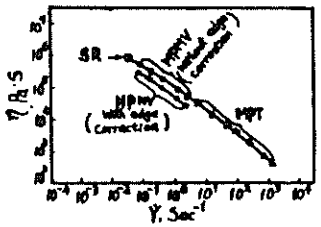


Fig.1 shear viscosity as a function of shear rate for SBR compounds filled with Santoweb (ϕ =0,15) at 100°C

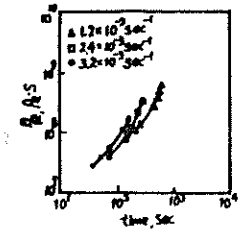


Fig.2 transient elongational viscosity as a function of time at room temperature(ϕ =0.05)

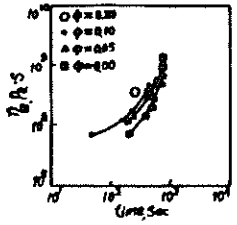


Fig.3 comparision of transient elongational viscosity of the different SBR/fiber compounds at $\dot{\varepsilon}=1.2\times10^{-3}$ sec^{-1} at room temperature

REFERENCES

(1) Lutskii, M.S., et al., Kauch. i Rezina, (1) 10 (1978)
(2) Goettler, L.A., et al., Rubb. Chem. Tech., 24, 277 (1981)
(3) Murty, V.M., et al., Plast. Rubb. Proc. Appl., 5, (4) 307 (1985)
(4) Setua, D.K., Int. J. Polym. Mater., 11,(1) 67 (1985)
(5) Cotten, G.R., et al., Rubb. Chem. Tech., 21, 749 (1979)
(6) Nakajima, N., et al., Rubb. Chem. Tech., 52, (5) 962 (1979)

SIMULATION OF THE AUTOCLAVE CURING PROCESS FOR CONTINUOUS FIBER/THERMOSETTING RESIN COMPOSITES

J. L. Kardos, M. P. Dudukovic (Materials Research Laboratory, Washington University, St. Louis, MO)

R. Dave (Michigan Molecular Institute, Midland, MI)

Severely detrimental voids and gradients in final resin concentration are two critical problems which arise during the production of thick, continuous fiber/thermosetting resin, structural laminates. We have developed void (1) and resin flow (2,3) submodels which, when combined with heat transfer (4,5), kinetics (6), and viscosity submodels (6), yield a master simulation model capable of selecting and optimizing processing cycles.

Void growth arises because of the temperature effect on the vapor pressure of volatile components dissolved in the resin (usually water). In the case of a graphite/epoxy prepreg equilibrated at room temperature with moisture at relative humidity $(RH)_o$, we have shown (1) that void growth during the cure cycle can be eliminated if the resin pressure at any point satisfies the following inequality,

$$P_{min} \geq 4.962 \times 10^3 \exp\left[\frac{-4892}{T}\right] (RH)_o$$

where T is °K and the constants are determined for a typical DDS-cured TGMDA epoxy system such as Hercules 3501-6. Thus, to prevent voids from forming, the autoclave and vacuum bag pressures must be adjusted to follow the temperature-time profile in such a way that the resin pressure at every point in the laminate must be greater than P_{min}. Resin flow will of course be dictated by the pressure profile, which means that the resin flow and void models are coupled through the resin pressure.

Our resin flow model (2) is based on the concept that when a bed of resin-saturated fibers is compressed during processing, the resulting flow and consolidation is analogous to the situation when a water-saturated soil is compressed (7). In both cases the network of solids is capable of supporting part of the pressure load, thus reducing the liquid hydrostatic pressure at any point. Utilizing Darcy's Law, the resin pressure and velocity profiles can be determined for 3-dimensional flow and one-dimensional consolidation.

Resin pressure and velocity profiles can be generated as a function of curing cycle. The resin pressure profile and the minimum resin pressure (P_{min}) required to prevent void growth are compared throughout the curing cycle in order to identify the level and duration of autoclave pressure required to suppress voids and at the same time create sufficient consolidation. After analyzing a number of different curing cycles, the following basic guidelines for autoclave and laminate boundary pressure selection have emerged. For any given time-temperature profile, a laminate boundary pressure cycle is chosen such that the boundary pressure at any time during the cure is greater than P_{min}, the minimum resin pressure needed to prevent void growth by moisture diffusion. Furthermore the autoclave pressure is maintained above the boundary pressure by a positive amount throughout the cure cycle in order to prevent resin backflow. These guidelines have been utilized to simulate the case of "free bleeding" (no dams and negligible bleeder cloth resistance).

The above guidelines have also been verified experimentally for commercial processes (8). Laminates made from prepreg with a 35% initial relative humidity exposure, using a standard cure cycle, were void-free; those made from prepreg with an 85% initial relative humidity exposure, using the same cure cycle, were full of voids. For the 85% laminate, the measured resin pressure within the laminate fell below P_{min} prior to gelation, resulting in void growth. On the other hand, the void-free 35% laminate exhibited no such resin pressure drop below P_{min}.

Acknowledgment

We are grateful to Mr. Flake Campbell, Mr. Drew Mallow, and Mr. Francis Muncaster of McDonnell Aircraft Company for many helpful discussions and for the experimental data.

References

1. J. L. Kardos, M. P. Dudukovic, and R. Dave, Advances in Polymer Science-Epoxy Resins and Composites, Vol. 80, Springer-Verlag, 1986, p. 101.
2. R. Dave, J. L. Kardos, and M. P. Dudukovic, Polymer Composites, 8, 29 (1987).
3. R. Dave, J. L. Kardos, and M. P. Dudukovic, Polymer Composites, 8, 123 (1987).
4. A. C. Loos and G. S. Springer, J. Comp. Mater., 17, 135 (1983).
5. F. C. Campbell, A. R. Mallow, and K. C. Ameudo, "Computer-Aided Curing of Composites," McDonnell Aircraft Company, 4th Interim Report, 1/1/85-3/31/85, Contract No. F33615-83-C-5088, AFWAL/MLBC, Wright Patterson AFB, OH 45433.
6. A. C. Loos and G. S. Springer, J. Comp. Mater., 17, 135 (1983).
7. T. W. Lambe and R. V. Whitman, Soil Mechanics, Wiley, NY, 1969.
8. F. C. Campbell, A. R. Mallow, and K. C. Ameudo, "Computer-Aided Curing of Composites," McDonnell Aircraft Company, 7th Interim Report, 10/1/85-12/31/85, Contract No. F33615-83-C-5088, AFWAL/MLBC, Wright Patterson AFB, OH 45433.

12/2

AN EXPERT SYSTEM FOR AUTOCLAVE CURE

F. L. Abrams, AFWAL/MLBC, Wright Patterson AFB, OH 45433
C. W. Lee, University of Dayton, Dayton, OH 45469

Autoclave curing is a complex process involving heat transfer, fluid flow and diffusion as well as, for thermosetting composites, chemical reactions. These are not steady state processes and the complex process variable interactions result in a control problem that is challenging, to say the least.

The current method of processing is to follow a standard recipe for manufacture of each part. Another strategy for controlling the process is to try to manipulate the processing conditions in such a way as to achieve the goals of the process. This paper presents a strategy for automation of the autoclave cure of composites by the latter strategy of manipulating the temperature and pressure of an autoclave to develop the desired properties in a composite material, and a means of implementing that strategy.

The goal of autoclave curing of composites is to produce, within the constraints of the material, the processing equipment and the cost, composite parts that are consistent and adequate in quality as defined by the desired physical and mechanical properties for the application at hand. This needs to be done in spite of some variability in the materials and processing vessel used. It must be done for parts and tools which vary in property and geometry. These requirements are difficult to meet with standard recipes.

Factors which determine the quality of composites include the degree of cure of the matrix and the degree of compaction of the part. It is advantageous, from a cost standpoint to accomplish these as quickly as possible. Rapid cures imply high reaction rates and, in turn, high temperatures. The process control strategy was to attempt to heat up the matrix as rapidly as possible, within the temperature constraints of autoclave, matrix and supporting material while acting to avoid undesirable situations such as runaway exotherms and large temperature gradients.

To implement the strategy it was necessary to have a means of detecting both the progress towards the desired goal and the onset of conditions leading to the situations we wished to avoid. The controller then had to have the intelligence to manipulate the autoclave temperature and pressure as required. A micro-dielectric sensor was used to determine the progress towards the goal of curing the matrix resin and compaction of the part. Thermocouples were used to detect the onset of exothermic conditions and large temperature gradients as well as keep the bag and autoclave temperatures within constraints. These data were interpreted by an expert system and compared to a symbolic model of the process represented by *process instances* such as CURE, EXOTHERM and LARGE-TEMPERATURE-GRADIENT. Once it was determined which of those instances were active, a second expert system determined the proper control actions to alter the process trajectory towards the goal or away from a problem. The adjustment was then passed to the autoclave controls. The hardware and software used to implement this strategy is described in Ref. 1.

This expert system controller possesses knowledge of the underlying principles of the curing process and make control decisions based on these principles rather than following a predetermined path. Therefore it was possible to use the same knowledge base to control the curing of parts of different thicknesses (Figure 1) and parts of different matrix material (Figure 2) and developed different paths in response to the processing conditions.

These cure cycles developed by the expert system controller differ drastically from the conventional cure cycles. Physical and mechanical testing of the parts has not indicated any ill effect of a shortened processing cycle, although more testing is needed. All test panels cured by this method were of satisfactory quality.

Reference

1) LeClair, S.R., Abrams, F.L., Lagnese, T.J., Lee, C.W., and Park, J.B., Qualitative Process Automation for Autoclave Cure of Composite Parts: AFWAL-TR-87-4083, AFWAL/MLTC, Wright-Patterson AFB, OH, Dec 1987.

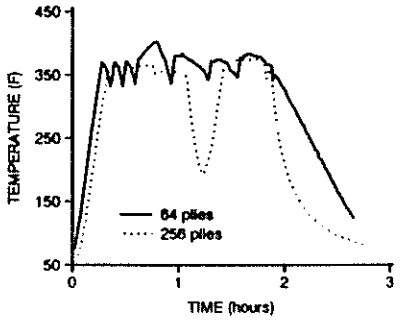


FIGURE 1: Cycles for 3501-6 Panels of Different Thicknesses.

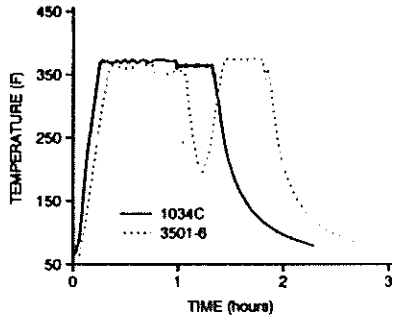


FIGURE 2: Cycles for 256-ply 3501-6 and Aged 1034C Panels

12/3

MECHANICAL PROPERTIES OF EPOXY/GLASS BRAID COMPOSITES

D. Wingard and C.L. Beatty, Univ. of Florida,
Gainesville, FL

Introduction. Epoxy resins are often used for the matrix resin of composites because of their temperature resistance, high modulus and high strength to weight ratio. This work involves measuring several mechanical properties of epoxy/glass braid composites cured thermally as well as with radio frequency by dielectric heating. Mechanical property tests performed included impact, lap shear and stress-strain, and comparisons were made between the mechanical properties of the rapidly cured composites and those of the thermally cured composites.

Experimental. The epoxy system used was a low viscosity DGEBA-type resin with a cycloaliphatic amine curing agent in stoichiometric proportions. The filler used was Dow-Corning S-2 glass fibers woven in a triaxially braided structure. The epoxy composite samples were prepared by "doctor blading" the resin with a tongue blade on both sides of two 6"x 6" layers of glass braid, then simply pressing the layers together. For samples cured by dielectric heating, the prepared composite was placed between two sheets of Airtech Teflon release film (.002" thick). The composite sample was compressed between the ground plate electrode and the sample platform with the aid of two 25-pound weights hanging from the outside of the hood of the dielectric heater. The quality of the sample was enhanced by using a layer of 1/8" thick PE foam sheet, two layers of 0.8 mm thick Teflon sheet, or a layer of polyimide foam sheet.

Thermally cured samples were prepared in much the same manner as the RF-cured samples, but the thermal curing time was much longer: B-stage cure for 45 min. at 250-275°F, and C-stage cure for 2 hrs. at 300°F.

Impact measurements were made using a Tinius Olsen modified Izod-type device. Lap shear measurements were made from samples cured by overlapping two 6"x 6" sheets of glass braid that were offset by two sheets of 0.8 mm thick Teflon sheet. After curing, the Teflon sheets were removed, leaving the layers of glass braid bonded together by a 1/2" wide strip of neat resin. The strength of the bond between the resin and the glass braid was measured with an Instron tensile tester. Stress-strain measurements were made on samples that were cut from the cured composite sheet and were routed into the typical "hourglass" shape used for tensile testing.

Results and Discussion. For impact testing, specimens were cut from both parallel and perpendicular to the longitudinal (warp) direction of the glass braid. Some samples were thermally B-stage and C-stage cured, while others were dielectrically cured for 15 and 20 minutes. It was found that a 15 minute dielectric cure time was a nearly optimum cure time beyond which the glass transition temperature of the composite was invariant. For the perpendicular braid direction, the impact energy was almost twice that of the parallel direction. Also, the impact energy of the dielectrically cured samples was about the same as that of the thermally cured samples.

For lap shear measurements, test specimens were cut only from the direction parallel to the longitudinal braid direction because of the large specimen size required by the ASTM procedure. It was found that the lap shear strength of samples cured dielectrically for 15 minutes was only about half that of the thermally cured samples.

For stress-strain measurements, the fracture stress in the perpendicular direction was at least twice that of the parallel direction. The tensile modulus in the perpendicular direction was more than twice that of the parallel direction. The fracture stress of the RF-cured samples was almost equal to that of the thermally cured samples in the parallel direction, but was considerably less than that of the thermally cured samples in the perpendicular direction.

12/4

INNOVATIVE FIBER AND FABRIC REINFORCEMENTS FOR ADVANCED COMPOSITES

J.M. Margolis
Margolis Marketing & Research Company
New York, New York

Conventional reinforced plastics are characterized by short glass fiber reinforcements, never more than one-inch long, and typically 1/4- or 1/8-inch chopped fiber. These fibers were considered a great advance over wood filler, which was one of the earliest reinforcements.

New applications require innovative fiber types and fabric configurations. Resin matrices contribute toughness, light weight, processibility, etc. New reinforcements provide higher specific strength/modulus, and other benefits especially for metals replacement. Principal fiber types and fabrics are:

Fibers
Aramids
Carbon/graphite
Thermoplastic polymers (PET, nylon)
Glass
Metal
Ceramics
Boron

Fabrics

Unidirectional
Woven
Knitted
Nonwoven
"3-Dimensional"

These essential fibers and fabrics provide a baseline for sophisticated reinforcements that add powerful performances to advanced composites.

Weave patterns such as plain, twill, satin and variations (e.g., 4-harness, 8-harness satin), rovings and braids; fabric weight and finish; stitch patterns represented by chain, lock tricot; and weft/warp, biaxial/triaxial and bias knitted fabrics can be designed for specific application requirements.

Vibration damping, ballistics, conductivity, magneticability, improved print through, as well as strength properties can be tailored for any given application. Reinforcements can accommodate (and often determine) the fabrication process.

Innovative fiber/fabrics are being developed for defense/aerospace products such as missile and rocket nozzles and casings; airframe structures; road vehicle driveshafts and suspension springs (coil as well as leaf); recreational boats; sporting goods from golf clubs and shafts to fishing rods to skis and ski poles; and medical implants such as orthotic devices (e.g., joints), other prosthetics and implants. Looking ahead, new reinforcements can be expected to be used in building/construction load bearing products such as beams, and bridge trusses.

Fiber/fabric systems can be designed for dry processes with prepregs and preforms, usually tape layup, compression molding/sheet forming, filament winding and pultrusion; or for wet processes, which includes resin transfer molding. specific reinforcement systems are produced with reduced catenary, for example, for pultrusion.

New reinforcement systems will be related to applications and processes in this paper.

AN ACCURATE AND CONVENIENT MODEL FOR THE DIE ENTRY FLOW OF POLYMER MELTS

S.P. CORSCADDEN, A.G. GIBSON and A.N. McCLELLAND♦

Department of Materials Science and Engineering,
University of Liverpool,
P.O. Box 147,
Liverpool L69 3BX,
U.K.

♦ Now at ICI, Chemicals and Plastics Division, Oil Works,
P.O. Box 1,Billingham, Cleveland TS23 1LB, U.K.

ABSTRACT

Because of the increasing volume of reinforced polymers, both thermoplastic and thermoset, being processed by injection moulding there is a need for a more quantitive understanding of the flow behaviour of these materials under processing conditions. There have been marked advances recently in computational techniques for predicting mould flow, but these have yet to be matched by parallel improvements in our understanding of the rheology of these materials.

In regimes dominated by shear, the flowing polymer may be modelled solely in terms of its shear flow behaviour, using a single power law model to relate shear stress to shear rate. However, when the flow involves a substantial extensional component, as is the case with long fibre reinforced materials, this procedure fails to describe the behaviour accurately. Extensional or convergent flow occurs at a number of points in injection moulding: the nozzle, the gate where the material enters the mould and in certain parts of the mould cavity itself. With many polymers, particularly those containing fibres, the pressure drop at these convergent regions is considerably higher than that predicted by the simple theory mentioned above. This is true, for instance, with DMC reinforced polypropylene and both short and long fibre reinforced nylon.

The processor needs to be able to calculate these pressure drops for two reasons: to reduce fibre degradation by minimising them and in order to make more accurate mould flow predictions. For example, it is sometimes necessary to balance flows into different cavities or different parts of a cavity by adjusting gate geometry.

The most appropriate technique for characterising the flow of injection moulding materials is capillary rheometry, where the material is forced to flow through a convergent die into a capillary of known geometry. Measurements can be performed, either in the laboratory, or with an instrumented injection moulding machine, equipped with pressure transducers and dies of the appropriate geometry. The latter method, which has found favour recently, has the advantages that the material flows through channels of realistic dimensions and undergoes the same thermal history as in moulding.

The overall pressure drop in capillary flow can be resolved into two components, due to:

(i) shear flow in the capillary, and
(ii) losses at the die entry and exit.

These can be separated by performing experiments with capillaries of different length, but the same diameter and entry geometry. A plot of total pressure against the capillary length to radius ratio (Bagley plot) is made, and extrapolation to zero L/R ratio gives the sum of the die entry and exit pressure losses. The exit loss is generally fairly small compared to the entry loss, so it will be neglected here.

The entry pressure value, given by the Bagley plot intercept, contains valuable information about extensional behaviour. Although polymer texts often give the impression that the entry pressure is a small proportion of the total pressure drop, representing a correction term which which may often be ignored, this is untrue with most polymers, especially reinforced ones. Under injection moulding conditions, the pressure drop in regions of convergence is very significant and may sometimes represent the largest pressure loss in the flow path. Attention to flow in convergent regions is critical to effective injection processing of reinforced polymers.

There has been some debate about the origins of the large die entry pressure drop observed with polymers. Originally it was attributed mainly to melt elasticity. However it is now accepted as being due to flow-induced molecular orientation, which considerably increases the resistance to extensional deformation. Elastic effects undoubtedly do exist, but it is unnecessary to know what proportion of the extensional strain in the flowing material is elastic if the behaviour is described solely in terms of the relation between stress and strain rate.

Extensional viscosities for fibre reinforced melts can be particularly large, since fibre orientation occurs as well as polymer molecular orientation.

F. N. Cogswell derived a theory for flow in converging dies where extensional and shear components were treated separately. The theory presented here, uses a similar approach and allows for the effect of the fluid anisotropy which results from flow orientation. By using a different coordinate system from that of Cogswell the entry flow behaviour can be modelled over the complete range of possible convergence angles. Only four constants are required to describe the behaviour of a particular material, and these are readily obtainable from capillary flow experiments.

A set of data on long fibre reinforced polypropylene moulding materials will be used to illustrate the applicability of this approach. Experimental values of the flow constants will also be given for other commercially important moulding compounds. Finally, use of the model for calculating the pressure drop due to flow in mould gates or convergences of arbitrary geometry will be outlined.

12/6

REFRACTION EFFECTS AND METAMORPHOSIS IN HARD ELASTIC POLYPROPYLENE (HEPP) DURING STRETCHING

R. Hosemann and I. Schulze

Gruppe Parakristallforschung, Bundesanstalt für Materialforschung und -prüfung, Unter den Eichen 87, 1000 Berlin 45, F.R.G.

Small angle X-ray diffraction from hard elastic polypropylene 5M-45B (HEPP) of Celanese shows a sharp long streak along the equator indicating total reflection and refraction effects equivalent to ~ 2000 Å long cylindrical parts within the fibre. This phenomenon was observed recently on fibres of HEPP, SiO_2-glass, Pt and Cu and could be calculated quantitatively [1]. The well known amorphous phase therefore does not exist in high modulus fibres similar to 11-times stretched samples of PE with fully extended chains [2]. A new mthod is described which explains the observed scattering by means of shape functions. One term depends on the lamellae, the other one on the fibrils, whilst the third takes care of the correlations between terms 1 and 2. The latter does not interfere with the calculation because it is simply another well separated component of the equatorial scattering analysis previously described by A. Guinier. Fibrils exist between the lamellae for extensions greater than ε_δ = 40 %. Below this value the diffuse equator scattering is explained by 100 Å long gaps between the chain molecules; from 5 vol.% packing density of the gaps at ε_δ = 0 % they increase to about 50 vol.% at ε_δ = 40 %. Here the gaps change their functions to become the surroundings of the fibrils. This thermodynamically-induced metamorphosis explains the metastable nature of the lamellae, the gaps and the fibrils, observed at ε_δ = 40 %. Here the long period doubles its length after 580 h. The pseudo-Hook domain disappears gradually during iterated strain-relaxation operations after 100 cycles. The stress-strain curve is similar, then, to that of a sulphur vulcanized natural rubber except that the E-modulus is now 100 times larger. The small angle scattering changes according to these phenomena: The number of lamellae becomes smaller and their mean distance increases to 2000 Å or more along the chain direction.

---

1) M.P. Hentschel, R. Hosemann, A. Lange und B. Uther, R. Brückner, Acta Cryst. (1987) A43, 506-513.

2) G. Capaccio and I.M. Ward, Nature, Phys. Sci. 293, 1143 (1973)

CONTINUOUS FIBRE REINFORCED THERMOPLASTICS

G Cuff & R H Turner
ICI Wilton Materials Centre,
England

Just 20 years ago, the field of fibre reinforced plastics could be split into two main divisions:-

1) high loadings of long fibres in thermosetting resins, which recognised that highest mechanical properties were achieved from the highest loading of the longest fibre, and

2) low loadings of short fibre in thermoplastic resins, because thermoplastics offered greater versatility in processing (particularly by injection moulding).

A brief examination of consumption of fibre reinforced composites in Europe shows that more than three quarters of products by weight are based on thermosets which reflects the comparative ease of impregnation with low viscosity resins as well as cost of feedstocks.

This situation is changing, however, so that both thermoplastic and thermoset composites are expected to increase sales in Europe by some 100,000 te by 1990.

In ICI the area of thermoplastics impregnation has advanced dramatically, in the following 2 areas:-

1) APC products in which continuous carbon fibre is impregnated with matrices such as polyetheretherketone, and

2) Verton products in which less expensive feedstocks have been brought together to extend the length of fibre retained after injection moulding or extrusion.

The increased awareness of the potential of continuous fibre reinforced thermoplastics is causing increasing numbers of companies to consider their strategy for the future. Continously impregnated tape materials are already being considered for application in aircraft structures and several other industries are starting to wonder whether they can benefit from such materials. The answer, almost certainly, is that they will benefit as long as the systems can be developed at the right quality and the right price.

ICI has exploited its APC impregnation technology to combine various reinforcing fibres eg glass, aramid and carbon with a wide range of thermoplastic resins to provide a range of widely differing mechanical and physical properties for amorphous or semi-crystalline products.

This work reviews the composite mechanical property data obtained from polypropylene, PET, polyethersulphone, polymethylmethacrylate, polycarbonate, polyurethene, polyamide (nylon 6:6) and polyetheretherketone with glass or carbon fibre.

The efficiency of fibre wetting with viscous polymer melts and its reflection in excellent fibre properties is indicated. Interfacial and matrix dominated properties are considered and the need to optimise fibre/matrix adhesion is discussed.

Most recent work at ICI is concentrating on two vital aspects which are required to open up large tonnage market opportunities:-

1) reduce the cost of impregnation, and

2) demonstrate reliable, low cost fabrication techniques to exploit design potential.

Some aspects of fibre orientation/placement will be discussed, and comments will be made on work aimed at application areas other than aircraft structures.

Heat Transfer Analysis of Thermoplastic Carbon Fiber Composite

M. Adams and G.A. Campbell
Clarkson University, Potsdam, New York 13676

In a effort to obtain higher use temperatures, the aerospace and the automotive industries are evaluating high glass transition temperature thermoplastics as an alternative for epoxys in glass fiber and carbon fiber composites. It might be expected that the processing conditions which would optimize the composites physical properties would be substantially different than those currently used on thermosets. In this presentation, we will discuss some of the processing parameters that can be altered in producing thermoplastic carbon fiber or glass fiber composites and the influence of some of these processing parameters on the physical properties of the composites that have been produced. Although a number of parameters are available for manipulation within the processing system, this paper will deal in the main with the effect of temperature and temperature transients on the fiber matrix adhesion.

During this investigation we have observed the influence of dissolved water and dissolved air on the quality of the composite. It was found that polystyrene must be thoroughly dried under vacuum prior to processing, in order to minimize degradation due to absorbed water. We have also investigated the effect of the molding temperature and the cooling rate on the morphology of the fiber and matrix of parts molded in a compression press. The mold used was designed to allow us to cool the part either homogeneously or nonhomogeneously due to the placement of the cooling water lines in the metal dye. The composite fiber matrix systems were tested using the methods normally used in metallurgy to determine the morphology in the area close to the fiber matrix interface. Such techniques as DSC and microscopy will be used on the polymer. Our results indicate that in thermoplastic composites great care must be taken to provide process parameters which minimize the effects of the very high glass transition temperature on the processes which are occurring deep within a thick composite. We will present both preliminary theoretical and experimental analysis on the heat transfer in the mold and a part of very simple geometry. The results of this analysis will be compared to the results obtained from the Drzal test for fiber-matrix adhesion.

12/9

LONG FIBER REINFORCED THERMOPLASTIC MATRIX COMPOSITES BY SLURRY DEPOSITION

D. F. Hiscock, D. H. Bigg
BATTELLE COLUMBUS DIVISION
505 King Avenue
Columbus, Ohio 43201

One of the principal reasons that thermoplastic matrix composites have not achieved widespread use is that the prepreg forming processes are much more complex than those used to prepreg most thermosetting matrix composites. Thermoplastic polymers must be processed at elevated temperatures (>200 C), and require high pressures (>7 MPa) to pump the high viscosity molten polymer into the reinforcing fibers. This implies the use of automated process equipment, which is economically justified only for high volume applications.

A process for producing long fiber reinforced thermoplastic matrix composites has been developed based on paper making technology. This process consists of depositing a mixture of a polymeric powder and reinforcing fibers from an aqueous slurry. The degree of homogeneity of the mixture and the subsequent ability to handle the dried sheet has been significantly improved by the addition of less than 0.2 percent pulp fibers, based on solids concentration, to the slurry. The maximum fiber concentration depended on the initial aspect ratio of the reinforcing fibers, with 20 volume percent easily obtainable with fibers having an aspect ratio of 1600:1.

The dried mat is then consolidated into a composite sheet with a continuous matrix phase by the application of heat and then pressure. The sequence of heating and applying pressure was varied to determine the most effective method of forming void free composite sheets. It was found that the highest quality sheets were produced when the mat was preheated prior to the application of pressure.

The wet forming process takes advantage of the low cost, high productivity characteristics of the basic paper making process to produce thermoplastic matrix composite prepreg sheets. This type of process offers significant potential for producing large volumes of high performance prepreg composites sheets at a competitive cost.

Tensile properties and the degree of reinforcement efficiency of composites produced by this process were found to be comparable to those produced by melt impregnation techniques. A polypropylene composite containing 20 volume percent glass fibers was produced that had a tensile strength of 120 MPa and a tensile modulus of 6.3 GPa.

12/10

FIBRE ORIENTATION MECHANISMS IN LONG FIBRE REINFORCED INJECTION MOULDINGS

B Rzepka and R S Bailey

Advanced Materials, ICI Wilton, Cleveland, UK.

Long fibre reinforced injection mouldable materials have recently been introduced and are already demonstrating appreciable property benefits (1). This property dividend is in part due to the greater fibre lengths attached with these materials (2), but can only be fully realised by having some knowledge of the fibre orientation mechanisms operative during injection moulding. Gibson et al (3) has shown that the granule geometry and hence fibre packing difference between long fibre compounds and those associated with conventional extrusion compounded formulations give rise to major rheological changes during flow. This in turn influences the mould filling process and hence the final moulded-in fibre orientation structure.

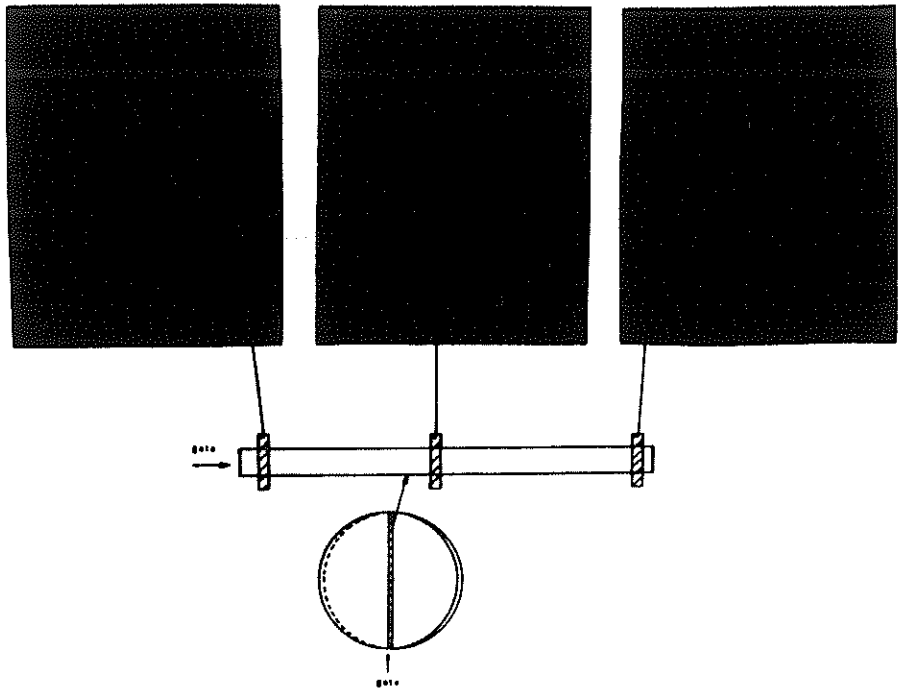
Skin-core microstructures have been reported widely in the literature as being characteristic of the fibre orientations in injection moulded composites. These effects are due to the fountain-flow mechanism proposed by Tadmor (4) and have been shown in this work to be operative for long fibre compounds.

In this study the mould filling process has been studied. There is a significant difference in final structure along the flow path of the mouldings produced and mechanisms controlling these effects are proposed (see fig 1). The injection moulding process parameters have also been varied over a wide range in order to characterise the influence of the melting stage and the injection stroke aspects upon the microstructure. These studies have been performed using a disc and parallel sided square plaque mouldings.

A wide range of microstructures was produced. It was possible to create a large core component or to completely eliminate it by changing the processing parameters. The shear applied by the plasticisation unit was used to generate radically different fibre length materials; it was noted that as the fibre length was reduced, so the core dimension became smaller. This observation highlighted the necessity to understand the mould filling and fibre orientation mechanisms if as long fibres as possible were to be aligned in the final mouldings. By altering the injection speeds, pressures, temperatures and the holding pressure cycle it was found that a microstructure could be produced which had a minimal core component.

This was achieved by using a low injection speed (giving rise to a more Newtonian fluid velocity profile and hence aligning fibres by a more uniform shear profile) and long holding pressure times. It was concluded from the work that a wide range of properties may be attained from controlling the injection moulding process parameters. This microstructural control may provide an opportunity to produce a degree of anisotropy according to the requirements of a moulding in service. This range of anisotropy is significantly wider than for short fibre materials and may be used as a useful tool in future.

FIGURE 1 THE EFFECT OF FLOW PATH AND POSITON IN A MOULDED DISC



REFERENCES

(1) R Bailey, M Davies and D R Moore
Processing-Property characteristics for long glass fibre reinforced polyamides. (In publication)

(2) R Bailey and H Kraft
A study of fibre attrition in the processing of long fibre reinforced thermoplastics.
Int Poly Processing 2 (1987) p94

(3) A G Gibson and A N McClelland
Rheology and packing effects in the injection moulding of long fibre reinforced composites
6th Conf ICCM (London 1987) VM1, p131

(4) Z Tadmor
Molecular Orientation in injection moulding
J Appl Poly Sin 18, S(1974) p 1753

RSB/ABSTRACT/JW
7 December 1987

12/11

THE EFFECT OF FIBER LENGTH ON THE MECHANICAL PROPERTY PERFORMANCE OF REINFORCED THERMOPLASTIC COMPOSITES

S. Ward, J. Crosby, and P. Mokay
LNP Engineering Plastics
Malvern, PA

Two different compounding techniques are typically used to produce discontinuous fiber reinforced composites: extrusion and pultrusion. In extrusion the matrix resin and 1/4" chopped fibers are melt mixed in an extruder, stranded and pelletized. This high shear process leads to significant fiber breakage. In pultrusion, continuous fiber strands are impregnated with matrix resin, formed as a rod or tape, and then chopped into pellets.

ICI's Verton pultrusion technique which separates the fiber bundles, allows for a high degree of fiber collimation. Due to the low shear involved in this process, relatively little fiber damage is sustained. The fiber length in the pultruded product is determined by the length of the pellet.

Parts injection molded from a half inch chopped pultruded pellet exhibit 10 times the average fiber length observed in short fiber extrusion compounded materials. This longer fiber length translates into improved mechanical properties.

Fiber length retention however is not solely responsible for the mechanical properties of a composite. The properties of these heterogeneous materials is also determined by fiber dispersion and orientation and by fiber-matrix adhesion. In some long fiber products it was found that optimum properties were obtained when parts were molded under high shear conditions. In these cases, fiber dispersion and orientation were dominant effects.

A detailed investigation that quantifies the effect of fiber length on the mechanical properties of long fiber reinforced thermoplastic composites will be presented. Mechanical properties of both compression and injection molded composites with various fiber lengths will be compared. This study will include data on nylon 6/6 reinforced with three very different fibers: glass, aramid and PAN carbon.

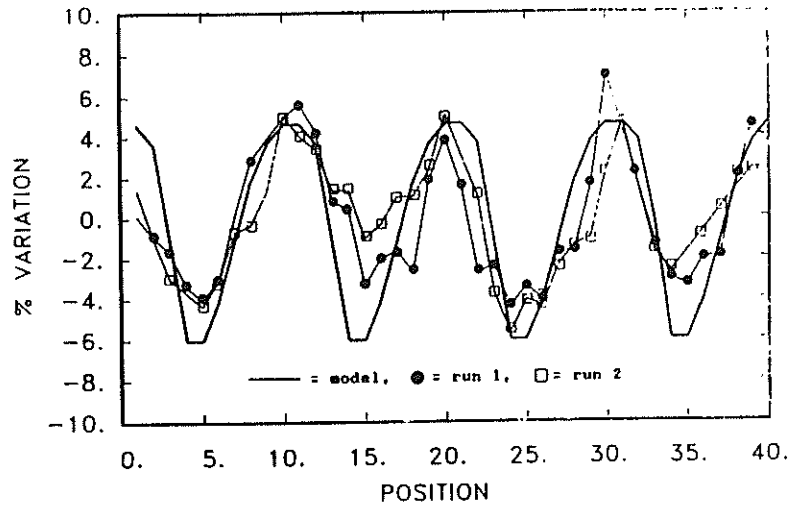


Figure 1. Model prediction vs two experimental runs

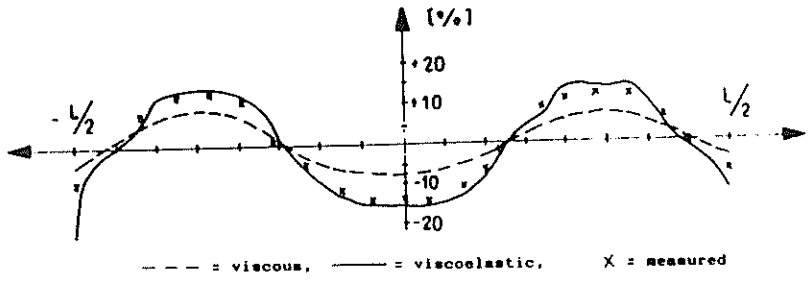


Figure 2. Model predictions vs experimental data

The Influence of Machine and Tool Parameters on Glass-Fibre Reinforced Polyamide

M Akay and D Barkley
Department of Mechanical and Industrial Engineering
University of Ulster
Shore Road, Newtownabbey
Co Antrim, N Ireland BT37 0QB

The advantages offered to polymeric matrices through fibre reinforcement are well established, however in the case of injection moulding of discontinuous fibre reinforced thermoplastics a realistic assessment of the reinforcement can only be made in the light of processing and tooling variables. This approach is required because of the strong and inextricable interactions between processing and material parameters e.g. melt flow and fibre orientation. Accordingly this paper will examine injection moulded short-glass fibre reinforced polyamide ("Maranyl") and long-glass fibre reinforced polyamide ("Verton") and aim to interrelate process variables, material structure and mechanical properties.

Mouldings were prepared in the form of plaques of 3.6mm x 73mm x 150mm and 2mm x 120mm x 120mm and dumbell tensile bars of 3mm x 13mm x 160mm using a Stubbe SKM51 injection moulding machine, rated at 500kN clamp force and 70ml shot volume. The mouldings were produced at 13MPa injection pressure, barrel temperature profile of 270, 280, 290, 300°C and cooling time of 30s. The rest of the machine settings i.e. screws rotational and ram speed, back-pressure and mould temperature were varied in order to effect variations in mould filling, fibre orientation and fibre degradation.

In order to assess the influence of certain tool - parameters on the flow and fibre distribution the moulds described below were designed and manufactured.

(a) a rectangular mould with triple pin-edge gates placed on the same side to facilitate a single melt flow-front or multi flow-fronts advancing adjacently.

(b) a multiple pin-edge gated mould to facilitate controlled multi-directional flow-advance. The mould incorporates additional flexibility to enable different gate sizes.

(c) a mould for producing dumbell tensile bars; where mould filling was conducted either through a single or double-gate arrangement and by adopting runners of different length. These possibilities were achieved by appropriately blocking off the runners.

Mouldings were evaluated for fibre length distribution, fibre orientation, tensile and flexural properties and impact fracture toughness.

Jetting (very rapid mould filling) was found to be a function of the ratio of the gate depth to mould-cavity depth, fibre length, fibre volume content, injection ram speed and mould release. Contrary to the expectation jetting occurred less frequently as the injection ram speed was increased. Jetting became a source of mechanical weakness but more significantly produced a poor surface appearance.

Weld-lines where the flows merged and joined together had no significant effect with unfilled polyamide however assumed significant with fibre reinforcement generating a source of mechanical weakness. At the weld-line there is a discontinuity in fibre orientation profile - fibres aligned themselves along the weld-line preventing reintegration of the flows.

Certain flow anomalies occurred at high fibre concentrations ($\geq$ 40% weight concentration), due to obstruction to the advancing flow by fibres interlocking across the flow direction and occurrence of a localised slip along the high sheer boundary layers where fibres are aligned predominantly with the flow. These phenomena caused an acceleration in flow along the sides resulting in the generation of multiple flow fronts.

The magnitude of the well-known surface-fore effect in fibre orientation, i.e. in the surface the fibres are predominantly aligned in the flow direction and in the core normal to this direction, was found to be affected by mould temperature and the runner length.

Flattening of the fibre orientation profile near the far end of the mould cavity manifested itself as a variation in the tensile properties of the representative test-pieces.

Mechanical fibre degradation under severe processing conditions, particularly of increased back-pressure, caused greater deterioration in mechanical properties with short-fibre reinforcement. The mechanical degradation of fibres in short-fibre reinforced polyamide resulted in a very narrow fibre length distribution whereas the distribution remained wide in long-fibre reinforced polyamide.

Fracture toughness properties, Gc and Kc, determined by impact loading of notched test bars had improved considerably, as did the static tensile and flexural properties, with fibre reinforcement although there was a great sensitivity to fibre orientation and to flaws, in the form of dislodged fibre ends, generated during test-piece machining.

NEW RESULTS FOR INJECTION MOULDING OF LONG FIBRE POLYAMIDE

Dr. E. Döring, Deutsche ICI GmbH, 6000 Frankfurt/M.-71
West Germany

Introduction

It is very known that the best mechanical properties of reinforeced plastics are achieved with long fibres like in the composites area. But the processing is difficult and composites are normally expensive.

On the other hand short-fibre reinforced pastics are used since many years as they can be processed via the injection moulding process. The final fibre length of 0.2 to 0.4 mm in the part leads to the consequence that the mechanical properties are not ideal. Long-fibre reinforced products with starting fibre length of 10 mm combine the good processability in the injection moulding process with good mechanical properties which are many times better than with conventional short-fibre products.

The greater final fibre length is guaranteed through the production process, as the fibres are impregnated in a special process, therefore the material can be processed like short-fibre material without large fibre damage.

Pultrusion Technology

The long-fibre products are not produced in the compounding process but in a special ICI Pultrusion Process. The final moulding stays in the original shape even when the polymer is ashed away at high temperatures. The long fibres keep the form of a skeleton whereas the short fibre form only a dust after ashing -

The fibre length distribution shows a typical 3 maxima behavious. The first maximum is created by shear forces in the cylinder and in the tool. The second maximum is in the region where most of the fibres stay. This is the region of fibre length which is responsible for the good mechanical properties. The third maximum is the original fibre length, this gives indication that there was no fibre damange.

The comparison between a short-fibre product and the long-fibre product indicates clearly the higher maximum of fibre length.
With long-fibre products not the modulus is increased but also the toughness. With conventional materials this can only be achieved by the addition of elastomer which decreases automatically the stiffness.
The higher modulus values in comparison to short-fibre products stay also in a wider temperature range.

The notched impact properties are improved in comparison to short fibres. The improvement is even higher with higher fibre content.

The creep properties are much better compared with short-fibre products, this is also true for higher temperature.

Concerning flow properties the spiral test at 300°C shows only minor drop in flow length for the long-fibre product. This effect has been proven also in many applications.

Influence of the processing conditions for the final fibre length:
Only with little fibre damage the expected properties can be achieved, therefore it is essential that the most suitable processing conditions are used. Most influence is created by the melt temperature, the back pressure, the injection speed and the size of the gate. Experiments have shown that a good reproducability can be achieved with optimum processing conditions.

Long fibre products are now processed by many injection moulders. Most of them use conventional screws but high melt temperatures (300°C), very low back pressure and low injection speed.

There are now special screw designs available for the long-fibre products, typically the design comparison of a long metering zone with low compression ratio, to melt the material with lowest possible friction and to keep the fibre length at a maximum.

New product development has lead to other matrix materials like polypropylene, polycarbonate, PPS, acetals, polyester-elastomers and PBT. All these materials have in common that the properties in comparison to their short-fibre products are improved.

Also other fibres have been used like aramid, carbon and steelfibres. Specifically the aramid fibres lead to exceptional low wear characteristics. Lubricated versions ith PTFE, silicone, MoS_2 and graphite are also available for special applications. Also flame-retardent systems are under development.

Conclusion:

The long-fibre injection moulding product based on different polymers and fibres offer a wide spectrum of new properties for the most versatile applications.

12/14

POSITION OF NEUTRAL PLANE DURING HOLLOW DISK COMPRESSION MOLDING OF LONG FIBRE-REINFORCED THERMOPLASTICS

H. Hojo, E. G. Kim, T. Onodera
H. Yaguchi, S. H. Kim and M. Koshimoto

Department of Mechanical Engineering II
Tohoku University, Sendai 980, Japan

1. Introduction It is important to grasp the flow state during molding of long fibre-reinforced thermoplastics, and to obtain the flow characteristics we should clarify the friction condition on the interface between the material and the mold. However, with no slip boundary condition many investigators studied models for processing of reinforced polymers by compression molding.[1] In case of metal, compression test on circular hollow disk has been used to investigate the friction condition.[2] In this paper, the composites is assumed to be fluid, and the circular hollow disk is compressed to derive the position of the neutral plane which explains the interfacial friction condition. By comparing the theory with the experimental results, the friction can be well explained. To obtain the neutral plane may be useful for the determination of charge pattern and charge position during molding.

2. Theory Circular hollow disk is compressed axially with road F between flat parallel rigid platens as shown in Fig.1. In this figure, r_i, r_o and r_n are inner, outer and neutral radii respectively. The total power E for compression is

$$E = E_i + E_f \qquad (1)$$

where E_i is the internal power of deformation and E_f indicates the friction losses between the composites and the mold. The value r_n is found by differentiating E with respect to r_n.[3]

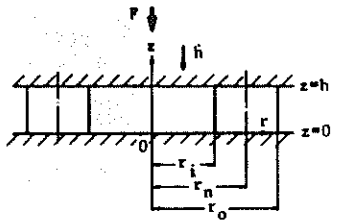


Fig.1 Compression of circular hollow disk

The internal power of deformation becomes

$$E_i = \int_v 2\mu \dot{\epsilon}_{ij} \dot{\epsilon}_{ij} \, dv \qquad (2)$$

where μ is the viscosity of the material and $\dot{\epsilon}_{ij}$ is the strain rate. During molding of the material, the neutral plane devides the regions of inward and outward flow: inward and outward flows become to be contraction and expansion viscosities μ_1, μ_2 respectively. Hence, E_i can be obtained by integrating Eq.(2) with the viscosities and the strain rates:

$$E_i = \pi\mu_2 \frac{\dot{h}^2}{h} \{ 2r_n^2(\xi - 1) + 3(r_o^2 - \xi r_i^2) + r_n^4(\xi/r_i^2 - 1/r_o^2) \} \qquad (3)$$

where $\dot{h}$, h are the closure speed and gap height respectively, and $\xi = \mu_1 / \mu_2$.

The power for friction losses is

$$E_f = \int_s \tau v_r \, ds \qquad (4)$$

In the above equation, the shear stress τ on the interface may be expressed as follows:

$$\tau = k_H v_r \qquad (5)$$

where k_H is the hydrodynamic friction coefficient and v_r indicates the radial velocity.

E_f, using Eqs.(4) and (5), is given by

$$E_f = k_H \pi \frac{\dot{h}^2}{h^2} \{ (r_o^4 - r_i^4)/4 - r_n^2(r_o^2 - r_i^2) + r_n^4 \ln(r_o/r_i) \} \qquad (6)$$

The neutral radius r_n can be obtained by manipulating Eqs.(1), (3) and (6):

$$\zeta^2 = \{ (\lambda^2 - 1) + 2\alpha(\xi - 1) \} / \{ 2\ln\lambda + 2\alpha(1 - \xi/\lambda^2) \} \qquad (7)$$

where $\zeta = r_n/r_o$, $\lambda = r_i/r_o$ and $\alpha = h\mu_2 / k_H r_o^2$.

3. Experiment, Results and Discussion The material used in the experiment was a stampable polypropylene composite sheet (matrix: polypropylene, reinforcement: long glass fibre mat, fibre content by weight: 40 wt%, thickness: 3.8mm, r_o: 50mm, r_i: 15, 25, 35mm). The mold consisted of two horizontal steel platens, and the temperature of mold was controlled by thermocouple and circulating oil. Molding temperature was 180°C and closure speed was 10, 50, 200mm/min.

Fig.2 shows the relationship between r_i/r_o and r_n/r_o (showing effect of α) for the viscosity ratio $\xi = 1.0$. The chain line is obtained with no slip boundary condition using the F.E.M.[1] on the assumption that the composites is Newtonian fluid, and solid lines are the values calculated from Eq.(7). If α becomes zero in Eq.(7), it means no slip on the interface, and the value obtained from F.E.M. analysis is equal to one for $\alpha = 0$. The dashed line is the value calculated from the Kudo's theory[2] in case of no slip on the interface for metal forming. Fig.3 indicates the experimental results. The points are the values obtained from the experiment and the equation derived by Avitzur[3] and the lines are the theoretical ones. From the figure, it is clear that the experimental results are in good agreement with the theory in case of $\alpha = 0.2$, and there is slip on the interface.

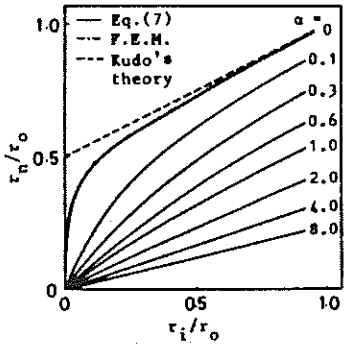


Fig.2 Relationship between r_i/r_o and r_n/r_o

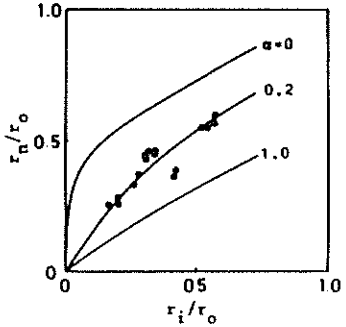


Fig.3 Comparison of theory with experimental results

4. Conclusion The interfacial friction condition is investigated from hollow disk compression molding. It can be seen that there is slip on the interface between the composites and the mold. The hydrodynamic friction coefficient can be measured from Eq.(7) and experiment.

Reference

(1) Lee, C. C., Folgar, F., Tucker, C. L., ASME. J. Eng. Ind. 106, 114(1984)
(2) Kudo, H. :Proc. of the 5th Japan National Congress for App. Mech., 75(1955)
(3) Avitzur, B. :Metal Forming :Processes and Analysis. McGraw-Hill, New York, Chapt.7 (1968)

12/15

FRACTURE BEHAVIOR OF LONGER GLASS FIBER REINFORCED POLYPROPYLENE

D. E. Spahr*', K. Friedrich*, R. S. Bailey#, J. M. Schultz', G. Nutting#

*Polymer & Composites Group, Technical University Hamburg-Harburg, 2100 Hamburg 90, West Germany

'Dept. of Chemical Engineering, University of Delaware, Newark De. 19716, USA

#Advanced Materials Group, Imperial Chemicals Industries, Wilton Centre, Cleveland TS6 8JE, U.K.

ABSTRACT

The toughness of injection molded, longer glass fiber reinforced Polypropylene (aspect ratio ≈200) was measured by fracture mechanics methods (K_C), instrumented Izod impact tests, instrumented falling weight tests. Microstructural features such as fiber orientation, and fiber distribution through the thickness were also measured. The toughness and microstructural features were compared to those of short fiber (aspect ratio ≈20) reinforced Polypropylene.

The fiber microstructure of 10-40 wt% long fiber and 40 wt% short fiber material was studied by optical and scanning electron microscopy. All materials had three layers, two surface layers where the fibers were oriented more or less parallel to the mold filling direction, and a core region where the fiber were oriented more or less perpendicular to the mold filling direction. The core region was relatively thin, never exceeding 23% of the total thickness. A variation in fiber distribution through the thickness was found, with the core of the long fiber material containing up to 40 w/v% more fibers than the surface layers. The short fiber material had a thinner core region and a more uniform fiber distibution than the long fiber material.

Compact tension specimens were cut from the injection molded plaques in two directions, L and T. In the T direction, the notch of the CT specimen was perpendicular to the mold filling direction, while in the L direction it was parallel to the MFD. The long fiber material was found to be virtually isotropic (K_{CT} - 5.3 $MPaM^{1/2}$ vs K_{CL} 5.6 $MPaM^{1/2}$) while the short fiber material was found to be highly anisotropic (K_{CT} 5.4 $MPaM^{1/2}$ vs K_{CL} - 3.5 $MPaM^{1/2}$). This was shown to be due to microstructural differences in the materials.

The instrumented impact tests measured both fracture energy and impact strength. In all tests it was found that the long fiber material had significantly greater fracture energies than the short fiber material, even though its impact strength was only slightly greater than that of the short fiber material. For example, in the Izod test, the 40 wt% long fiber material had a fracture energy of 9.7 KJ/M^2 and an impact strength of 14.2 MPa in the T direction, while, in the same direction, the short fiber material had a fracture energy of only 5.2 KJ/M^2 though its impact strength was 11.4 MPa.

Paper submitted for presentation at the 4th Annual International Polymer Processing Society Meeting, May 8-11, 1988, Orlando, Florida, USA

12/16

THE INFLUENCE OF INJECTION MOULDING PARAMETERS ON THE FRACTURE STRENGTH OF LONG GLASS FIBRE REINFORCED POLYAMIDE

M DAVIES, R S BAILEY & D R MOORE

ICI ADVANCED MATERIALS, PO BOX 90, WILTON, MIDDLESBROUGH, CLEVELAND, UK

ABSTRACT

The influence of injection moulding parameters on fracture strength (K_{Ic}) has been investigated using room temperature single edge notched three point bend fracture mechanics tests. Specimens were machined from parallel faced plates injection moulded with 50% (by weight) 'long' and 'short' glass fibre reinforced polyamide 66 using a gating system specially designed to ensure as far as possible a uniform filling of the mould. The advantage of using such a system being the high degree of microstructural uniformity throughout the resulting component. In this way the effect of varying parameters such as injection speed, back pressure, holding pressure, holding pressure time and barrel temperature have been investigated.

Unlike the results from many tests such as instrumented falling weight impact, the fracture strength values obtained for crack initiation both parallel to and perpendicular to the mould fill direction were found to be sensitive to the processing conditions used to prepare the plate mouldings. Microstructural investigations (both fibre length distribution and fibre orientation distribution) show a correlation between high fracture strength values and favourable microsctructural details i.e. many long fibres orthogonally oriented to the plane of crack propagation. As a consequence of this it is argued that a useful means of objectively evaluating the influence of injection moulding conditions on strength has been established.

The fracture strength values are analysed using a simple model based on the assumption of a three layer structure, namely two skin layers both of thickness h_s and a core layer thickness h_c. It is argued that the fracture strength appropriate to crack initiation at 0 and 90 degrees to the mould fill direction may respectively be expressed as

$$K_{Ic}^{0} = \frac{2h_s}{(2h_s + h_c)} \frac{V_f^s}{V_f} \eta_s^0 K_{\parallel} + \frac{h_c}{(2h_s + h_c)} \frac{V_f^c}{V_f} \eta_c^0 K_{\perp}$$

$$K_{Ic}^{90} = \frac{2h_s}{(2h_s + h_c)} \frac{V_f^s}{V_f} \eta_s^{90} K_{\perp} + \frac{h_c}{(2h_s + h_c)} \frac{V_f^c}{V_f} \eta_c^{90} K_{\parallel}$$

where V_f is the volume fraction of fibre reinforcement averaged throughout the moulding and V_f^c and V_f^s are the fibre volume fractions characteristic of the core and skin regions respectively. $K_{\parallel}$ and $K_{\perp}$ are fracture strengths for crack initiation parallel to and perpendicular to the fibre alignment direction in a uniaxial continuous fibre reinforced system with volume fraction of reinforcement V_f and η_s and η_c are respectively factors present to account both for the discontinuous nature of the reinforcement and its not uniaxial alignment. Using a number of simplifying assumptions and the results of measurements made during the examinations of the moulding microstructure, it is shown to be possible to quantify η_s^0 and η_c^0. A plot of η_s^{90} versus η_c^0 provides a useful means of assessing the effectiveness of the fibre reinforcement network at preventing crack initiation and it also provides a clear demonstration of the advantages of 'long' fibre reinforcement over 'short' fibre reinforcement.

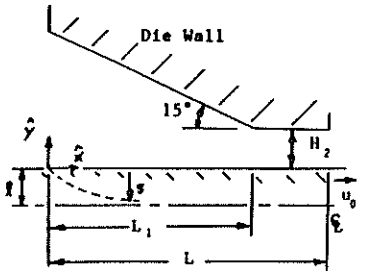
12/17

A THEORETICAL STUDY OF HOT MELT IMPREGNATION OF FIBER BUNDLES

C. Chmielewski, K. Jayaraman, and C.A. Petty
Department of Chemical Engineering
Michigan State University
East Lansing, MI 48824

Complex composite structures are often manufactured from simpler prepreg tapes containing unidirectional fibers surrounded by a continuous polymer matrix. Hot melt impregnation of resin into fiber bundles is often employed because of its simplicity and flexibility. However, in order to use this unit operation more effectively a better understanding of the underlying physical factors controlling the rate of formation of the prepreg product and its final composition is needed. Here the extent of impregnation of a viscous polymeric melt into a porous substrate being pulled through a wedge shaped die is studied theoretically.

Figure 1 illustrates the physical problem analyzed. Within the converging section of the die, the fluid pressure increases to a maximum just before the nip region. While this increase in pressure causes the hot melt to flow into the porous substrate according to Darcy's law, it hinders the flow of melt into the converging die. This subtle relationship between the flow within the die and the degree of impregnation into the substrate has been quantified by using a lubrication approximation for the pressure field and standard material balances. The prototype model, which comprises a set of three nonlinear ordinary differential equations, is used to predict the flow capacity of the die, the pressure distribution, and the extent of impregnation.



u_0, tow speed
μ, viscosity
k_T, permeability
ϵ, porosity

$\hat{P}(\hat{x})$, local fluid pressure relative to entry pressure
$\hat{s}(\hat{x})$, local penetration distance
$\hat{Q}(\hat{x})$, local volumetric flow rate per unit width

Figure 1. Die Geometry and Definition of Physical Parameters.

Figure 2 portrays the results predicted for a continuous prepreg process. The fiber bundle is dry at the entrance of the die. For the conditions shown, the moving tow controls the flow into the entry region of the converging section and in the exit region of the nip. Consequently, impregnation into the porous substrate occurs mainly in the neighborhood of the peak pressure. The nip region of the die, although important for overall flow control, plays a relatively passive role in the impregnation process.

For a fixed die geometry, Figure 3 shows that significant impregnation using this concept occurs for fiber bundles having permeabilities over a limited range. Conversly, an 'optimal' die geometry is predicted for a porous material with a specific porosity, permeability, and thickness. Figure 3 also shows the interesting feature that the onset of impregnation into the porous substrate is accompanied by a large decrease in the predicted peak pressure.

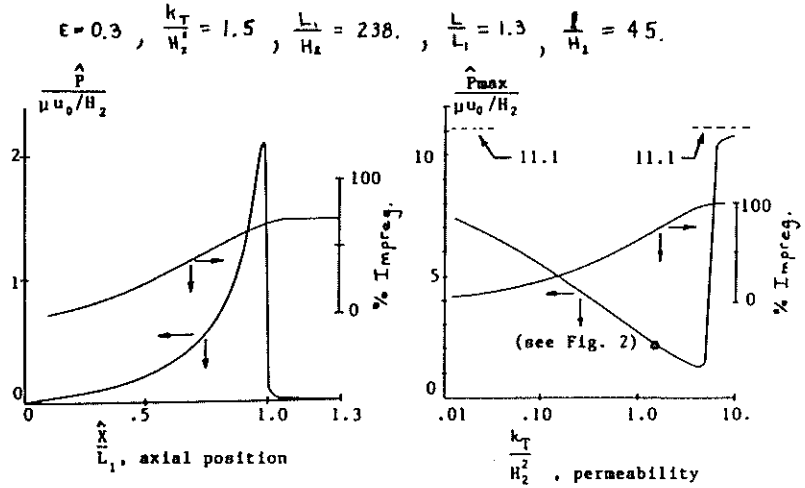


Figure 2. Pressure Distribution and Percent Impregnation for $\hat{P}(0) = \hat{P}(L) = 0$ and $\hat{S}(0) = 0$.

Figure 3. The Effect of Permeability on the Peak Pressure and Percent Impregnation.

A novel process for hot melt impregnation of thermoplastic resins into porous fibrous material based on the Weissenberg phenomenon will be presented. The new contacting device uses a rotating die to induce a large normal stress on the external surface of a cylindrical fibrous tow. Experimental impregnation rates of model viscoelastic fluids using this concept will be summarized.

References

1. Cattanach, J.B., G. Gulf, and F.N. Cogswell, "The Processing of Thermoplastics Containing High Loadings of Long and Continuous Reinforcing Fibers," J. Polymer Eng., 6, 345 (1986).

2. Cogswell, F.N., Hezzell, D.J. and Williams, P.J., "Fibre Reinforced Composites and Methods for Producing Such Composites," U.S. Patent 4559 262, December 17 (1985).

3. Peak, S.L., "Process for the Preparation of Reinforced Thermoplastic Composites," U.S. Patent 4563 232, January 07 (1986).

4. Chung, J., Furst, H., Gurion, Z., McMahon, P.E., Orwoll, R.D. and Palangio, D., "Process for Preparing Tapes from Thermoplastic Polymers and Carbon Fibers," U.S. Patent 4 588 538, May 13 (1986).

5. Bird, R.B., R.C. Armstrong and O. Hassager, Dynamics of Polymeric Liquids, Vol. 1, Wiley-Interscience (1981).

6. Metzner, A.B., W.T. Houghton, R.E. Hurd, and C.C. Wolfe, "Dynamics o f Fluid Jets: Measurement of Normal Stresses at High Shear Rates," Proc. Int'l. Symposium on Second-Order Effects in Elasticity, Plasticity, and Fluid Dynamics, Haifa, April 21-29, p. 650 (1962).

A CENTRIPETAL PUMP FOR HOT MELT IMPREGNATION OF FIBER BUNDLES WITH VISCOELASTIC FLUIDS

Nancy Losure, K. Jayaraman, C.A. Petty
Department of Chemical Engineering
Michigan State University
East Lansing, MI 48824

This paper explores the feasibility of making thermoplastic, fiber-reinforced composite prepregs by a novel modification of the hot-melt impregnation process already developed for thermoset composites. The conventional approach of manufacturing thermoplastic composites is the so-called film stacking process [1]. This method, which squeezes layers of fibrous material and polymeric films together for several hours at a high temperature, is a costly batch operation. Recently, ICI [2] patented a continuous hot-melt process based on calendering technology for relatively low molecular weight thermoplastic resins. Other alternatives are actively being investigated and include: improved solution processing techniques [3]; in situ polymerization; melt coating of individual fiber filaments [4]; powder and suspension impregnation using fluidized bed technology; and, fiber hybridization. It is noteworthy that none of the foregoing strategies for preparing thermoplastic composites exploits the unique rheological properties of viscoelastic fluids.

Because high molecular weight polymeric melts are viscoelastic fluids, they have some unusual and surprising properties [5]. For instance, the shear viscosity of the fluid decreases as the shear rate increases (shear thinning) and the primary normal stress difference is always positive. For some viscoelastic fluids, the primary normal stress difference may even be an order of magnitude larger than the shear stress [6]. This feature, which relates directly to the elastic nature of the fluid, accounts for the familiar extrudate swell phenomenon and the so-called Weissenberg effect. It also provides the underlying physical basis for the centripetal pump.

Although thermoplastic melt viscosities are significantly larger than either uncured thermoset melts (10 Pa-s) or water at room temperature (0.001 Pa-s), continuous hot melt impregnation of very small fiber tows may still be practical. One of the basic problems is to develop a method of creating a modest pressure drop across the fiber tow as it passes through the hot melt without breaking the individual fibers. If the available contact time for resin impregnation is 300s, then the pressure difference needed to completely wet a 200 micron tow containing 30 volume % fiber filaments (diameter 10 microns) by a fluid with a shear viscosity of 2,000 Pa-s is about 40,000 Pa (5.8 psi). This estimate assumes that the effective permeability of the tow is 3×10^{-8} cm^2. Such a modest pressure difference can easily be attained by utilizing the large normal stress effects characteristic of swirling viscoelastic fluids.

13/1

Isolation of Polymers from Liquid Solutions*

J. Thomas Lindt
Department of Materials Science and Engineering
University of Pittsburgh
Pittsburgh, PA 15261, U.S.A.

ABSTRACT

Separation techniques used to isolate polymers from liquid-phase solvent or monomer solutions play an important role in solution polymerization technology as well as in reactive processing. The objective of this paper is to classify the mass transfer mechanisms occurring during continuous devolatilization of superheated polymer solutions, in general, and to analyze these phenomena in an environment of a non-intermeshing counter-rotating twin-screw extruder, in particular.

Depending on the magnitude of the thermodynamic driving force for the diffusion processes utilized in devolatilization, the polymer extraction process is carried out in the presence or absence of aggressively growing foam i.e. in the high- or low-mass transfer rate regimes, respectively.

At sufficiently high mass transfer rates, the flow environment is dominated by explosive bubble growth. This mass transfer driven transport pattern will be analyzed using a novel approach based on a combination of equilibrium calculations, residence time distribution functions and kinetics of bubble growth. The new theoretical results will be compared to our experimental data obtained on solutions of amorphous polymers.

In the low-mass transfer rate regime, the transport environment is controlled by drag-driven flows. In contradistinction to the above high-mass transfer regime, attempts to analyze the mass transfer efficiency have been numerous dating from the early 1960's. Using this conventional, penetration theory based, approach the working of the low-mass transfer zone of the extruder will be interpreted using new experimental and theoretical evidence.

Applications of the above concepts to process design will be discussed.

---

* Abstract of a keynote paper to be given at the 4th Annual International Meeting of the Polymer Processing Society, May 8-11, 1988, Orlando, Florida

13/2

MODELLING OF POLYMER MELT DEVOLATILIZATION ENHANCED BY FOAMING

John R. Brie
Polymer Science and Engineering Department

and

Robert L. Laurence
Chemical Engineering Department

University of Massachusetts
Amherst, Massachusetts

Devolatilization is the process by which low molecular weight diluents are removed from polymer/diluent solutions. This is effected by subjecting the solution to low vacuum and high temperature in a devolatilizer, thereby flashing off the more volatile diluent. At these conditions, foaming of the solution occurs: bubbles nucleate in the supersaturated solution, grow, and rupture at the surface. Foaming is the dominant vehicle for mass transfer. An accurate model of foam-enhanced devolatilization must include processes which affect the foaming; these include bubble nucleation, growth, surface rupture, coalescence, breakage and stretching. The objective of this work is to develop such models.

Models of devolatilization developed to date are inadequate; either bubbles have not been accounted for[1], or unrealistic descriptions of the foaming process have been incorporated[2-4]. These include restricting all the bubbles to be of the same size (a distribution of bubble sizes is observed in experiments) and requiring that all bubbles nucleate at the entrance and rupture at the exit of the devolatilizer (both processes occur continuously throughout the devolatilizer).

A population balance approach to modelling foam-enhanced devolatilization has been developed which describes the bubble phase as a distribution over bubble sizes. The evolution of the diluent concentration and bubble distribution through the devolatilizer is governed by a mass balance on the diluent concentration coupled to a population balance on the bubble distribution. This approach is novel to devolatilization modelling and is the first to allow incorporation of realistic descriptions of the bubble phase dynamics.

To demonstrate this modelling approach, a model of a single screw devolatilizer was developed which accounts for bubble nucleation, growth and surface rupture. The model was evaluated by its ability to correlate existing experimental data. This model correlates the data well, significantly better than the model of Latinen[1], which is the most frequently used model of devolatilization. Also, a simplified model based on the quasi-steady state assumption (the number of bubbles is assumed to change slowly through the devolatilizer) was developed which gives good approximation to the Full Model and reduces significantly the model's complexity, as well as the computation time required for its numerical solution.

For the model to be used in devolatilizer design, two empirical model parameters which quantify the rate of bubble nucleation in the polymer/solvent solution must be determined. A scheme for measuring these two parameters is proposed. A bench scale experiment on a rolling drum apparatus (developed by Biesenberger and Lee[5]), which simulates the operation of a single screw devolatilizer, can be used to measure the extent of devolatilization of the solution. Using the model developed in this investigation, these two empirical model parameters may be inferred from the experimental data. In this way, the performance of a single screw devolatilizer may be predicted without any direct measurements on the full scale devolatilizer. This is essential if the model is to be used for devolatilizer design.

References

1. Latinen, G.: "Devolatilization of Viscous Polymer Systems", ACS Adv. Chem. Series, 34, 245 (1962)

2. Newman, R. E. and R. H. M. Simon;"A Mathematical Model of Devolatilization Promoted by Bubble Formation", 73'rd Annual AIChE Meeting, Chicago, Ill. (1980)

3. Powell K. G. and C. D. Denson; "A Model for the Devolatilization of Polymeric Solutions Containing Entrained Bubbles", 75'th Annual AIChE Meeting, Washington, D.C. (1983)

4. Yoo, H. J. and C. D. Han; "Development of a Mathematical Model of Foam Devolatilization", Pol. Proc. Eng., 2, 129 (1984)

5. Biesenberger J. A. and S. T. Lee; "A Fundamental Study of Polymer Melt Devolatilization", Soc. Plast. Eng. Natl. Meeting, 2 (1985)

13/3

STRUCTURE-PROPERTY RELATIONSHIPS IN INJECTION MOULDED THERMOSET AND THERMOPLASTICS STRUCTURAL FOAMS

A. Ahmadi, M.J. Brenner and P.R. Hornsby
Department of Materials Technology
Brunel University
Uxbridge
Middlesex UB8 3PH
England

Injection moulded plastics structural foams are characterised by a low density cellular core bounded by solid integral skins, which generally exhibit a higher stiffness to weight ratio with freedom from sinking in thick section parts, when compared with their solid counterparts. Their mechanical properties are potentially influenced by the structural form of the material, particularly the apparent density and density profile across the foam, the skin to core thickness ratio and the cell size and cell uniformity of the foamed core. In addition, surface defects arising from ruptured cells, introduced during fabrication of a structural form artefact may also limit the material toughness under impact loads. Further complications may arise with fibre-reinforced and semi-crystalline thermoplastics variants, since the degree of fibre alignment and nature of the crystalline microstructure may significantly influence ultimate mechanical performance.

The designer of such materials should also be aware that resulting structure of the component and consequently mechanical properties, strongly depend on the moulding technique employed (since many variants to the injection moulding procedure exist), and the processing conditions adopted.

From this complex array of variables, there is thus a need for greater understanding of the interrelationship between these parameters.

In this paper particular emphasis will be placed on elucidating the interdependence between structure and properties for a well-characterised polypropylene structural foam, (with and without short glass fibre reinforcement) made by a low pressure short-shot injection moulding technique, employing a chemical expansion system. Attention will be focused on establishing the significance of the structural parameters outlined above on selected physical properties, including flexural stiffness, impact strength and moulding distortion (in fibre reinforced grades). Models for estimating both flexural stiffness and impact strength will also be considered in relation to experimental findings.

Attention will also be given to discussing structure-property relationships in novel thermoset forms of structural foam made by recently developed techniques utilizing direct screw-transfer injection moulding. Results presented for dough moulding compound (DMC) and short-fibre reinforced grades of phenolic resin will demonstrate the wide range of structural variants and mechanical properties achievable with these materials and indicate their potential for use in high performance applications.

13/4

INTERPRETATION of POLYMER SWELLING/DRYING on a MOLECULAR BASIS

L. A. Errede, 3M Co. Corporate Research Laboratories
3M Center, Bldg. 201-2N-22, St. Paul, Minnesota 55144

Our studies[1,2] of swelling of poly(styrene-co-divinylbenzene) particles enmeshed permanently in a microporous network of PTFE microfibers have shown that the number, G, of sorbed molecules per repeat unit of polymer in thermodynamic equilibrium with excess test liquid is given by:

$$G = \alpha_s(\bar{\lambda}^{1/3} - \bar{\lambda}_o^{1/3}) \qquad \text{Equation 1}$$

where α_s is the number of adsorbed molecules per repeat unit of polymer, which is characteristic of the swelling power of the liquid, $\bar{\lambda}$ is the average number of atoms in the backbone of the polymer segments between cross-link junctions, and $1/\bar{\lambda}_o$ is the critical cross-link density above which G is not measurable. The α_s observed for liquids in homologous series of the type $A(CH_2)_nH$ and $A(CH_2)_nA$, where A is Ph, Cl, Br, I, CN, CO_2R, COR, OR or H, and n is 0 to 12, show that the major factor that affects α_s is the affinity of A for the functional group in the repeat unit of polymer (in this case the phenyl group). The number of methylene groups, n, in the rest of the sorbate molecule is a mitigating factor that affects α_s negatively, presumably because of steric hindrance to association of A with phenyl groups in the polymer. The results observed in these studies correlate well with the corresponding Hildebrand Solubility Parameters when appropriate entropy factors owing to molecular association are taken into consideration.

Our studies[3] of drying liquid saturated poly(Sty-co-DVB) particles enmeshed in a network of PTFE fibers have shown that it is possible to distinguish kinetically between two types of sorbed molecules; those that are sorbed-but-not-adsorbed to the polymer molecules that support the gel, and those that are adsorbed thereto. The former are eliminated first and the kinetics follow zero-order, i.e. :

$$\alpha_t = \alpha_o - rt, \qquad \text{Equation 2}$$

where α_o is the number of sorbed molecules per repeat unit at zero time, and r is the specific zero-order rate constant. The latter are eliminated therefter and follow first-order kinetics that reflect desorption from n populations of adsorption sites so that α_t is given by a linear combination of n exponential decay functions:

$$\alpha_t = \alpha_s' \sum_{i=1}^{n} f_i e^{-k_i t}, \qquad \text{Equation 3}$$

where α_s' is the residual number of sorbed molecules per repeat unit after elimination of the non-adsorbed molecules, f_i is the fraction of α_s' in the ith population, k_i is the decay rate of that population, and i is the identification number beginning at i=1 for the population with the fastest decay rate and ending with i=n for the population with slowest decay rate.

Since the polymer segments in the gel-state have considerable freedom of movement between cross-link junctions, the adsorption sites are equivalent, i.e. $f_1=1$ and $f_{i>1}=0$. Consequently α_t in the gel-state is given by:

$$\alpha_t = \alpha_s' e^{-k_1 t},$$

where $k_1=k_{gel}$ is the first-order rate constant for desorption from poly(Sty-co-DVB) in the gel-state. When the polymer begins to undergo transition from the gel-state to the glass-state at $\alpha_t=\alpha_g'$, the mobility of the segments decrease accordingly; the number of adsorbed molecules "trapped" by association with two or more repeat units increases at the expense of the population of molecules that are associated with only one repeat unit. This shift in populations distribution continues until transition from the pure gel-state ($\alpha_t=>\alpha_g'$) to the pure glass-state ($\alpha_t=<\alpha_g'$) is complete, causing the rate of elimination of sorbed molecules to decrease sharply. Thereafter each of the n populations created during this transition decrease independently in accordance with their respective decay rates as indicated in Equation 3.

In every case the logarithm of the rate constants, k_i, for desorption of volatile absorbate from polymer in the glass-state proved to be a linear function of i. The relationships noted for desorption of toluene, chloroform and acetone constitute a set of almost parallel lines given by:

$$\text{Log } k_i = \text{Log } k_0 - mi, \qquad \text{Equation 4}$$

where the slope $m=0.77\pm0.04$ is characteristic of the sorbent polymer, and intercept Log k_0 at i=0 is characteristic of the volatile sorbate molecule. The physical significance of these relationships will be discussed.

References

1) L. A. Errede, Macromolecules, 19, 654 (1986).
2) L. A. Errede, Macromolecules, 19, 1525 (1986).
3) L. A. Errede, M. J. Kueker, J. W. C. Van Bogart, Abstracts of the 1987 Summer National Meeting of the American Institute of Chemical Engineers. Paper No. 18b.

13/5

RHEOLOGICAL MEASUREMENT OF THE RIGID FOAM EXTRUSION OF POLYVINYLCHLORIDE

Kwang Ung Kim, Byoung Chul Kim, Soon Man Hong,
and Seong Keun Park

Polymer Processing Laboratory in
Korea Advanced Institute of Science and Technology
Seoul, Korea

It is prerequisite for the improvement of mechanical performance of foamed products to comprehend the flow properties of foaming system. Up to now, however, most of the practical fabrications of polyvinylchloride (PVC) have remained more of an art than a science because a serious thermal decomposition makes it difficult to measure the rheological properties.

A super-mixer (Kawada Seisakushyo, Japan) was used to compound PVC resin with various additives. To assess the processability of foam extrusion, the rheological properties of various unexpanded and expandable PVC formulations were measured with a capillary/slit die rheometer.

The unexpanded PVC formulation exhibited large entrance pressure drop; at 160°C, 29 MPa at 400 s^{-1} and 22 MPa at 113 s^{-1} Further, the viscosity of unexpanded formulation showed very strong shear rate dependence over the temperature range tested. That is, the power-law index of unexpanded PVC formulation (including 100 phr PVC (DP=800±50), 2 phr TM-700R (tin-mercaptide stabilizer), and 0.5 phr stearic acid) was extremely small; 0.061 at 170°C, 0.110 at 180°C, and 0.178 at 190°C. On the whole, it was increased with increasing the usage level of dioctylphthalate (DOP), a plasticizer (below the usage level 9 phr), and Acryloid K-125, a processing aid based on polymethylmethacrylate (PMMA) (below the usage level 15 phr). DOP normally reduced viscosity and first normal stress difference ($\tau_{11} - \tau_{22}$). On the other hand, Acryloid K-125 noticeably increased them. Both DOP and Acryloid K-125 decreased the activation energy of flow. In addition, the activation energy of flow was decreased as the shear rate increased.

With the expandable PVC formulations, the power-law index was not invariant even at the same temperature but was increased as the content of blowing agent increased. Further, it was increased as the temperature increased. At the same content, azodicarbonamide (ADCA), whose decomposition is sensitive to temperature, gave higher power-law index than sodium bicarbonate (SBC), whose decomposition mode is pressure-dependent. In the pressure profile, the deviation from straight pressure profile, particularly in the vicinity of die exit, was more pronounced with ADCA than with SBC. Inclusion of a chemical blowing agent generally gave a substantial viscosity reduction. The extent of the viscosity reduction was decreased with increasing shear rate. All the viscosity data of the expandable formulations appeared to fall on the single viscosity curve of the unexpanded formulation above the shear rate of around 100 s^{-1} within the processing temperature tested (160-170°C).

Incorporation of DOP and impact-modifiers based on butadiene rubber reduced both the initial bubble growth rate and the foaming efficiency of a chemical blowing agent probably due to the decrease of melt elasticity. This finds a use for manufacturing a rigid PVC structural foam by a single extrusion.

13/6

LIQUID TRANSPORT IN ANELASTICALLY DEFORMED GLASSY POLYMERS

J. P. Harmon
Eastman Kodak, Rochester, N. Y.
S. Lee
National Tsing Hua University, Hsinchu, Taiwan, R. O. C.
J. C. M. Li
University of Rochester, Rochester, N. Y.

Amorphous polymers can be deformed well beyond the yield point in compression without inducing failure. Upon load removal, an anelastic strain persists. This deformation is recoverable. Dimensional recovery is induced by heating specimens to above the glass transition temperature, or by sorption of penetrants which depress the glass transition temperature. This study characterizes sorption induced recovery and transport kinetics in a deformed, glassy matrix (1,2,3,).

Cross-linked poly(methyl methacrylate) discs were compressed in an Instron and a strain rate of 7 X 10^{-4}/sec. Displacement was varied, the largest displacement compressing the samples to 40% of their original height. Control samples were left undeformed.

Sorption studies were conducted over a range of temperatures using methanol (MEOH), ethanol (ETOH) and dimethylformamide (DMF). Penetration was followed by gravimetric measurements and by observation of the penetrant boundary with a light microscope. These penetrants swell the PMMA and transport is therefore characterized by both diffusion and relaxation parameters. An equation encompassing both parameters is presented in one and two dimensions. Transport may vary from pure diffusion control, (Case I Transport), to pure relaxation control (Case II Transport).

The following topics were investigated:

1. Sorption cycling (sorption, desorption and resorption).
2. The effect of % strain on transport.
3. The effect of aging on transport.
4. Deformational induced anisotropy.

Deformed samples absorbed MEOH at fast rates, and kinetics approached those of Fickian diffusion. Shape recovery accompanied swelling. Samples were desorbed in cyclohexanol. Resorption kinetics for both deformed and undeformed samples matched those of absorption for deformed samples. Thus, swelling and desorption induced rearrangements similar to those induced by deformation. ETOH sorption cycling followed the same trend, although, all kinetics shifted more toward relaxation control than in the case of methanol absorption.

DMF swelled the matrix extensively. Samples absorbed as much as 90% DMF. Kinetics for deformed samples indicated pure relaxation control. Undeformed samples sorbed at much slower rates. Extensive cracking was noted. Absorption in undeformed samples accelerated with time. This phenomenon is known as Super Case II transport and is associated with microstructural damage due to swelling.

23-34% strain persisted after deformation. The percent strain had no effect on methanol absorption kinetics. Since resorption kinetics in dimensionally recovered specimens match kinetics of absorption in deformed samples, the microstructural rearrangement associated with deformation and sorption cycling is not quantitatively related to strain.

A set of deformed samples was aged at 60°C for 12 hours. Absorption of MEOH at 50°C was monitored. Aging had no effect on transport kinetics in this system where transport was controlled mainly by the diffusion process.

Light microscopy revealed that transport of methanol in deformed samples was anisotropic. For thin slabs cut parallel to the deformation axis, a sharp front swept across the sample and extended much deeper than the sample thickness. In slabs cut perpendicular to the axis, a faint penetration front was observed and disappeared early. Control samples showed no anisotropy. Transport along the direction of compression was faster than that in the perpendicular direction. The relaxation parameter was 2-3 times higher. The diffusivity increased by a factor of 10. The relaxation velocity in the slow direction was still 2-5 times faster than that of control samples. Concentration profile analysis revealed that the concentration of methanol at the observed front was constant, irrespective of temperature. Differential scanning calorimetry on samples equilibrated at different methanol concentrations indicated that the sharp front observed was not due to the glass-rubber transition. The methanol concentration was varied from 25-100% by dilution with cyclohexanol. When equilibrium solubilities decreased from 20 to 10% and lower, sorption tapered off after an initial rapid stage. These solubilities are near the levels observed at the fronts for 100% methanol.

Microstructural rearrangements due to anelastic deformation are evidenced in transport properties. Anelastic strain does not necessarily define the microstructural state.

References:

1. J. P. Harmon, S. Lee, and J. C. M. Li, "Anisotropic Methanol Transport in PMMA after Deformation", Accepted for publication in Polymer.

2. J. P. Harmon, S. Lee, and J. C. M. Li, "Methanol Transport in PMMA: The Effect of Mechanical Deformation", J. Polymer Sci., Vol. 25, (1987) 3215-3229.

3. J. P. Harmon, "Penetrant Transport In Deformed PMMA", Ph.D. Thesis, University of Rochester, Rochester, N. Y., (1982).

RECENT DEVELOPMENTS IN EXTRUSION STABILITY OF POLYMERS

R. Ramanathan, R. Moynihan and D.G. Baird (Polymer Materials and Interfaces Laboratory and Department of Chemical Engineering) Virginia Polytechnic Institute and State University, Blacksburg, VA 24061-6496.

The major constraint on reducing processing costs of polymeric materials has been that imposed by instabilities introduced when shear stress levels in the die are raised above 0.1 MPa as a result of increasing rates of throughput. Interest in this area has been recently revived by Ramamurthy (1) and Kalika et.al. (2). They associate the instability, particularly in LLDPE, with failure of adhesion at the melt/metal interface, in the types of fracture known as sharkskin and stick-slip. Experiments conducted at our labs with low, linear low and high density polyethylenes as well as plasticized PVC sheds further light on the subject as discussed in the following paragraphs.

In experiments with capillaries (dia: 0.686 mm, L/D: 21,37,75) it was found that the onset of surface melt fracture (sharkskin) occurred at approximately 0.2 MPa for LLDPE and 0.13 MPa for HDPE whereas plasticized PVC exhibited no surface fracture. The onset of stick-slip failure occurred at about 0.35 MPa for LLDPE and at 0.30 MPa for HDPE. Again no such failure mode was observed for plasticized PVC. However gross distortion of the extrudate of the order one diameter was observed for all the polymers tested. Gross distortion was seen at wall shearstresses greater than 0.45 MPa for LLDPE, 0.32 for HDPE and 0.22 MPa for plasticized PVC. Moreover the degree of gross distortion seemed to decrease with increase in capillary length in the case of HDPE and plasticized PVC suggesting the influence of the entry region on the instability. Some influence of capillary length on the instability was also found for LLDPE, though to a lesser extent. Additionally, the degree of surface instability increased with increase in capillary length for HDPE and LLDPE which was an indication of the influence of the land region on the instability.

Complementary experiments with a 4:1 contraction planar entry flow die and an exit die, both fitted with quartz windows enabled optical techniques to be used in studying the onset of instability in these polymers. Flow birefringence experiments with circularly polarized light showed oscillation of the fringes at the entry, corresponding to the frequency of extrudate distortion in the case of PVC. Very low frequency oscillation of fringes were also observed for HDPE and LLDPE at the onset of surface imperfections in the extrudates. However the fringes stabilized in the die land region for HDPE and LLDPE whereas they did not stabilize for PVC. Preliminary flow visualization experiments with opaque particles showed a large dead space for PVC in the corners of the converging flow region with no recirculating vortex. However a small vortex appeared at moderate flow rates for LLDPE while HDPE completely filled the available space in the die entry region.

Hence the preliminary indications of this experimental investigation are that in general surface melt fracture and gross melt fracture may be initiated in the die entry region with little contribution from the die land, whereas stick-slip fracture may be a manifestation of both melt/metal adhesion failure in the land as well as instability initiated in the die entry.

References:

1. A.V. Ramamurthy, J. of Rheology, 30(2) 337-357 (1986).
2. D.S. Kalaika and M.M. Denn, J. of Rheology, 31(8) 815-834 (1987).

DIE DESIGN FOR DUAL WIRE INSULATION

E. Mitsoulis and F.L. Heng
Department of Chemical Engineering
University of Ottawa
Ottawa, Ontario, K1N 9B4, Canada

The wire-coating process is an industrially important process that deals with the coating of bare wires by some polymer resin for insulating purposes. In the coextrusion wire-coating technique two different polymers are concentrically coated on the moving wire in a single step. The advantages of dual insulation are in material savings and special characteristics, such as electrical properties, chemical resistance, color, etc. Since the parameters influencing the process are at least double from single-layer wire coating, numerical simulation is a favorite way for the analysis and design of the process.

Two die designs have been used in the literature for pressure-type dies. In one type, the two melts meet in an annular channel and travel together up to the point where they contact the moving wire. In another type, one melt moves on the wire under the influence of combined drag and pressure-driven flow until it reaches the tip of the torpedo where it meets the upper fluid flowing in an annulus under the influence of pressure-driven flow. From then on the two fluids travel together to the exit.

The mathematical analysis of the process is carried out using both the Lubrication Approximation Theory (LAT) and the Finite Element Method (FEM). The LAT provides quick approximate solutions for such quantities as pressure drop vs. flowrate and flowrate ratios (hence thickness ratios) and the stresses along the die walls and the wire. It also gives a good approximation for the interface location. It is mainly used to examine fast a variety of die designs and configurations for combinations of shear-thinning fluids (power-law or other viscosity curves). It can easily show the feasibility of operating conditions (e.g. negative pressures can be obtained if the wrong combination is used). It can also show if a die design is inappropriate in the case where wall shear stresses exhibit undesirable "jumps" due to abrupt changes in geometry.

For typical polymer melts (LDPE, HDPE, PS), the LAT has been used to study their flow in a variety of die designs. The results are then used to modify the design in order to give smooth stresses on the die wall that do not change sign, thus indicating a smooth streamlined flow.

Once a design has met the criteria from the LAT analysis, the FEM is then used for a more thorough study, incorporating nonisothermal effects and the full two-dimensional conservation equations. In particular, the unknown a priori free surface of the insulation after the die exit and the interface after contact of the two melts are solved for iteratively by constructing streamlines.

The energy equation is solved using a Streamline-Upwind/Petrov-Galerkin (SU/PG) FEM and bilinear quadrilateral elements that successfully suppress spurious oscillations in the temperature field, present when a standard Galerkin/FEM is used. SU/PG guarantees accurate and oscillation-free results for any value of the Peclet and Nahme numbers (highly convective flows with strong momentum-energy coupling due to a temperature-dependent shear viscosity).

The FEM analysis corroborates the findings from LAT that a die design is appropriate by satisfying the following criteria: (a) lack of recirculation, (b) a level interface running almost parallel to the wire, (c) smooth stresses on the die wall. The nonisothermal studies show that temperature-dependence of melt properties basically corrects the absolute values for pressure and stresses but it does not affect very much their distributions. Especially it is found that the interface location is not much influenced by thermal conditions but by the individual flowrates (hence flowrate ratios) for a given total coating thickness.

IMPROVED DESIGN OF A FISHTAIL SHEET DIE: 1-D AND 2-D THEORETICAL APPROACHES

J.-M. Charrier and R.V. Ciplijauskas
McGill University, Montreal, Quebec H3A 2A7, Canada

B. Vergnes and J.F. Agassant
Ecole des Mines de Paris, 06560 Valbonne Cedex, France

To demonstrate a novel process for making thermoformable short fiber-reinforced thermoplastic sheets, a special sheet die had to be designed and built ([1] and figure 1). A simple theoretical analysis, referred to here as the 1-D approach, was used to generate analytically the geometric characteristics of a contoured channel [2]. A numerical, finite difference-based program [3] has now been used to model the flow in the die channel. The results of this 2-D approach indicate that the flow, although reasonably uniform across the exit width, is slightly over-compensated away from the centerline (figure 2). Experimental results with a high density polyethylene resin of high melt index qualitatively confirm these results (figure 3). A numerical, finite element-based program [4] is now being assessed for its ability to make even more realistic predictions. The early "1-D" approach, the "2-D" approach and the current status of the latest approach will be described and discussed.

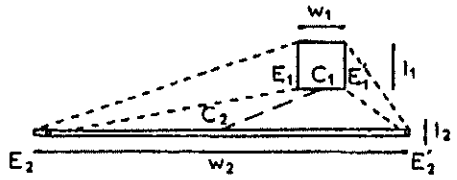


Figure 1 Special sheet die geometry

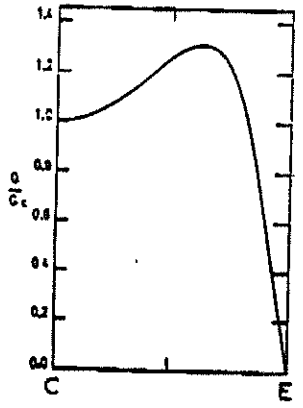


Figure 2 Numerical results (C: center E: edge)

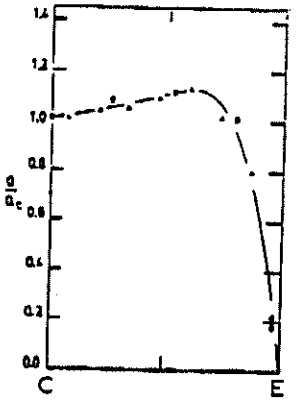


Figure 3 Experimental results (C: center E: edge)

References

[1] Charrier J.-M., Ciplijauskas R.V., Doshi S.R., Hamel F.H., "Fabrication and Thermoforming of Coextruded Short Fiber-Reinforced Thermoplastic Sheets", 44th ANTEC Technical Paper, Boston, 93 (1986).

[2] Charrier J.-M., Ciplijauskas R.V., Doshi S.R., Catani A., de Grandpre C., "A Special Sheet Design To Promote Random Planar Fiber Orientation", 45th ANTEC Technical Paper, Los Angeles (1987).

[3] Vergnes B., Agassant J.F., "Die Flow Computations: A Method to Solve Industrial Problems in Polymer Processing", Advances in Polymer Technology, 6, 4, 441-445 (1986).

[4] Crochet M.J., Davies A.R., Walters K., Numerical Simulation of Non-Newtonian Flow, Elsevier, Amsterdam (1984).

14/4

3-D EFFECTS IN CO-EXTRUSION

A. Karagiannis, A.N. Hrymak and J. Vlachopoulos
Department of Chemical Engineering, McMaster University
Hamilton, Ontario, Canada L8S 4L7

The interface shape in stratified flows of Newtonian fluids in long dies was investigated[1] with a Finite Element/ Generalized Reduced Gradient algorithm making use of the minimum viscous dissipation principle. The next step is the investigation of the fully three dimensional problem of the interface shape in stratified flows.

We first develop a Galerkin Finite Element u,v,w,p,h formulation to predict the shape of three dimensional Newtonian creeping jets. An innovative grid generation scheme involving the simultaneous use of two different types of three dimensional elements, brick and triangular prismatic elements, allowed for the simple and efficient parametrization of geometries of high complexity.

The existence of an unknown a priori free surface renders the problem non-linear and full Newton-Raphson iteration scheme with analytical derivatives of the Finite Element equations is employed. The numerical method involves the solution of large systems of the order of 8000-17000 equations.

The extrudate shape and swelling of Newtonian creeping jets emerging out of dies with rectangular, triangular, bow-tie and key-hole shaped geometries are investigated.

Generally, the extrudate shape does not follow the shape of the die. In certain cases sharp corners may swell less than flat regions (Fig.1,3). More complex geometries have very uneven swelling and depending on the geometry sharp corners may even contract as shown in Fig. 2 and 4. In the problems investigated (Newtonian) the calculated swelling ratios range from -7% to 50% and depend strongly on the die geometry. Rearrangement of the fluid takes place in the extrudate, the magnitude and extend of the phenomena depending on the die geometry.

Stratified flows are expected to exhibit different swelling behavior with respect to the die geometry and the viscosity and flow-rate ratio of the different phases. Results on stratified bicomponent extrusion of Newtonian fluids with a viscosity mismatch will be reported.

References

1) A. Karagiannis, H. Mavridis, A.N. Hrymak and J. Vlachopoulos, to appear in Pol. Eng. Sci. (1988)

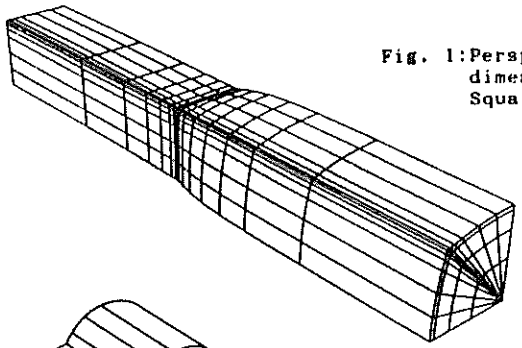


Fig. 1: Perspective view of three dimensional extrudate swell Square die

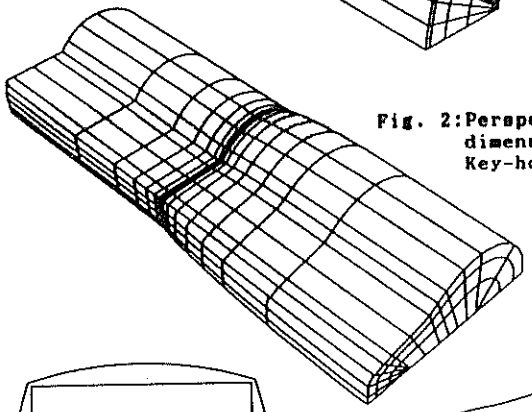


Fig. 2: Perspective view of three dimensional extrudate swell Key-hole shaped die

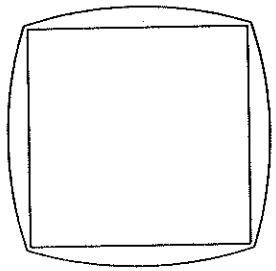


Fig. 3: Superposed die shape and final shape of the extrudate. Square die

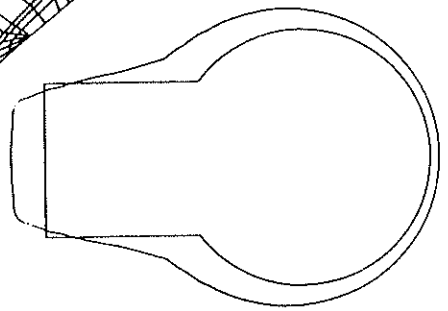


Fig. 4: Superposed die shape and final shape of the extrudate. Key-hole die

14/5

DIMENSIONAL VARIATION IN EXTRUSION OF POLYMERS: EXPERIMENT AND THEORY

S.E. Bechtel, K.J. Lin and J.D. Chang, Department of Engineering Mechanics, The Ohio State University, Columbus, Ohio 43210

In the extrusion of polymer melts from *nonaxisymmetric* profile dies, it is observed that the extrudate in general not only swells but also distorts, *in the sense that the extrudate cross section differs from the die aperture not only in size but also in shape*. We have conducted experimental and analytical studies to document and predict this distortion.

In the experimental study, polymer melts have been extruded from dies with elliptical and rectangular cross section (within these two families of shapes we have dies of various aspects ratios, length to mean diameter ratios and entry angles). For our purposes we define swell as change of cross-sectional area and distortion as change of cross-sectional aspect ratio. From measurements of the extrudate cross-sectional semiaxes as functions of distance from the die exit plane, we calculate swell (change of the product of the semiaxes) and distortion (change of the ratio of the semiaxes) for extrudates of polystyrene, low density polyethylene, high density polyethylene, linear low density polyethylene and polypropylene in several extruding conditions. Qualitatively, we observe that some samples swell with little distortion, others swell and distort, and yet a third set distorts with little swelling. Quantitatively, we measure the effect of extruding conditions (temperature, load) and die geometry (aspect and length to diameter ratios, entry angle) on the extrudate swell and distortion. The initiation portion of this experimental study (extensive measurements from a single 2:1 elliptical die) is documented in [1].

In addition to the experimental study we are developing analysis capable of modeling the swell *and distortion* of highly elastic, *nonaxisymmetric*, extrudates. Presently we have a one spatial dimension model for extrudates with arbitrary elliptical cross section. The theory is comprehensive, in that it is derived from the full 3-D free surface boundary value problem, with the following physical effects incorporated: viscoelasticity (viscosity, relaxation and retardation effects), shear stresses, time dependence, gravity, inertia, surface tension, and properties of the ambient fluid as they appear in the free surface interfacial conditions. In any particular industrial process only some of these physical effects are important. An advantage of our model is that, within one comprehensive theory, we are able to suppress or heighten any or all of the physical effects. We call the choice of relative importance of the effect the *regime* of extrudate behavior.

In the analysis of our model, we have found regimes which predict all three of the qualitatively different types of extrudate behavior observed in our experimental study. Behavior of the first type, characterized by swell with little distortion, and of the second type, characterized by swell and distortion, is exhibited in regimes in which elasticity is a leading order effect, but redistribution of momentum between directions in a material cross section is not allowed to leading order. Behavior of the third type, characterized by distortion without swell, is exhibited in regimes in which both elasticity and momentum redistribution within the extrudate cross section are leading order effects. Details of the derivation of our nonaxisymmetric extrudate theory, and analysis of the model can be found in [2-4].

1. S.E. Bechtel, K.J. Lin and J.D. Chang, Dimensional Variation in Extrusion of Polymers: Experiment and Theory, NSF Engineering Research Center for Net Shape Manufacturing, The Ohio State University, Report No. ERC/NSM-87-8 (1987).

2. S.E. Bechtel, M.G. Forest and K.J. Lin, On the Behavior of Viscoelastic Free Jets With Elliptical Cross Section, *J. Non-Newtonian Fluid Mech.*, to appear.

3. S.E. Bechtel, M.G. Forest and K.J. Lin, Effective Stress Rates of Viscoelastic Free Jets, *J. Non-Newtonian Fluid Mech.*, to appear.

4. S.E. Bechtel, K.J. Lin, M.G. Forest and D.D. Holm, 1-D Closure Models for 3-D Incompressible Free Jets: von Kármán Flow Geometry and Elliptical Cross Section, submitted to *J. Fluid Mech.*

ANALYSIS OF DIE DESIGN STRATEGIES BY SIMULATION AND EXPERIMENT

C.-C. Lee and J.F. Stevenson, GenCorp Research,
2990 Gilchrist Rd., Akron, OH 44305 USA

An optimized strategy for extrusion die design reduces iterations in die manufacture and provides an extruded product closer to specification. Finite element codes are a new and powerful tool to search for optimum design strategies but require experimental verification to be used with confidence.

The conventional criterion for die design, intended to minimize buckling and tearing, is a uniform gapwise-average velocity at the die exit. Because of the nonlinear relation between flow rate and channel thickness, the internal geometry of the die must be contoured to give a uniform exit velocity. Two contours were investigated here: (a) Straight-channel in which the die face profile was cut straight through the die, (Fig. 1 (bottom)) and (b) Back-relieved in which an additional diagonal cut was made to reduce flow resistance in thin sections of the die (Fig. 1 (top)). The die opening was asymmetric and similar in shape to a tire sidewall.

The experiment was performed on a 120-mm Troester cold feed pin-barrel extruder with a white sidewall compound. After leaving the screw, rubber flowed through the transition channel, preform, and die as shown in Fig. 2.

Comparisons between experiment and simulation were based on the gapwise average velocity at the die exit. Measurements of this velocity relative to line speed were obtained by applying a mass balance locally between the downstream extrudate dimensions and the corresponding die dimensions. Extrudate dimensions were obtained with a profilometer; locations on the extrudate were related to corresponding locations at the die exit by means of small notches in the die face which marked the extrudate (•in Figs. 3 and 4).

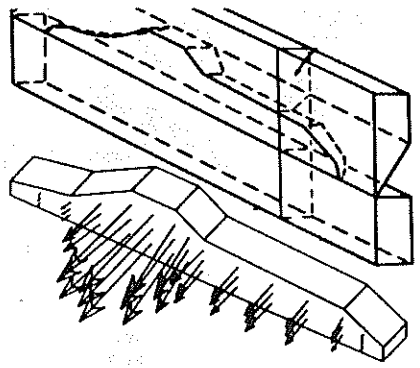


Fig. 1. (top) Back-relieved die plate, (bottom) Velocity vectors for power-law fluid in straight-channel die.

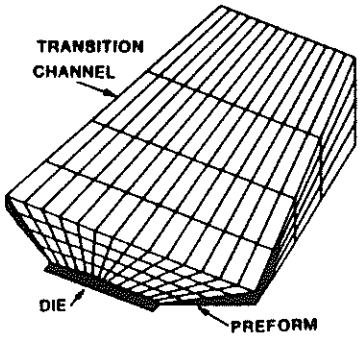


Fig. 2. Finite-element mesh for flow geometry.

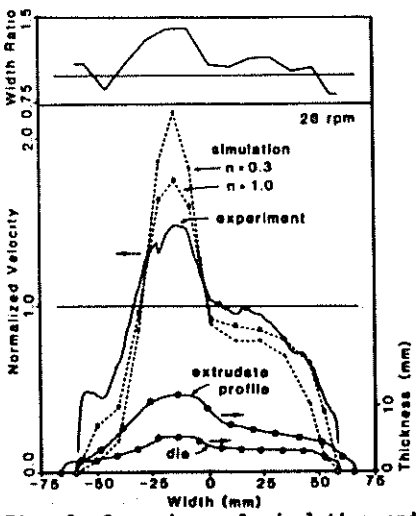


Fig. 3. Comparison of simulation and experiment for straight-channel die.

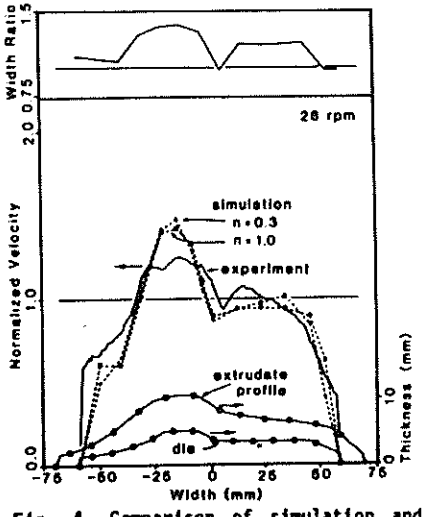


Fig. 4. Comparison of simulation and experiment for back-relieved die.

The local width ratio is the extrudate width between die marks divided by the corresponding distance between notches in the die face. Thirteen width ratios for each extrudate are plotted in Figs. 3 and 4. The higher resolution (130 points) plots of the gapwise average velocity in these figures were obtained using the interpolated width ratio data and ratios of the local extrudate thickness to the corresponding height of the die opening.

The simulations were carried out with a commercial finite element code 3DFLOW developed by Crochet. The equations of continuity and motion were solved using the penalty formulation for the mesh with eight-node elements shown in Fig. 2. An incompatibility resulting from the zero-surface-traction boundary condition at the flat die exit plane caused some oscillations in the flow field near the exit, but these did not significantly affect the results.

A calculated velocity field for the power-law model (n=0.3) is shown in Fig. 1 (bottom) for the straight-channel die. The gapwise average velocities for the Newtonian and power-law models are compared with experiment in Figs. 3 and 4. Both simulation and experiment show the back-relieved die gives a more uniform velocity profile. Other experimental data, also consistent with the simulation, show the measured velocity profiles are very similar at screw speeds of 10 and 26 rpm.

Differences between simulation and experiment may be due to slip at solid surfaces, streamlining of the finite element mesh, and the power-law model which cannot predict elongational flow and the zero-shear viscosity.

Optimal Design of Profile Extrusion Dies: A Full Three Dimensional Finite Element Solution Technique

Ronald R. Rakos, Arash Kiani, and Donald H. Sebastian
Department of Chemistry and Chemical Engineering, Stevens Institute of Technology
Castle Point Station, Hoboken, NJ 07030

Computer aided design techniques have become routinely used to enhance productivity in the injection molding industry. Use of computational aids is not so widespread for other important polymer processing operations. Flow through extrusion dies would seem to be a natural extension of mold filling analyses. However, several features of die flow mandate a fresh approach to this modeling problem. Profile die flow possesses all such features. Most injection mold filling models rely on the ability to represent flow in the mold cavity as predominantly planar. Velocity components normal to the cavity surface are legitimately neglected, reducing the analysis to a two dimension problem. Profile dies, on the other hand, may have significant secondary flows as the die cross section changes from a circular entry to the exit profile shape. In addition, the exit shapes generally lack any degree of symmetry necessitating a full three dimensional flow solution if the essence of the melt history is to be captured by the model. Creation of a simulation design tool requires several innovations not previously available: (1) development of a solution algorithm which can accommodate sufficient three dimensional detail, fit on conventional computing equipment, and be solved in a reasonable number of computing cycles, (2) implementation of an effective particle tracking algorithm to provide streamline information for flow balancing algorithms, and element deformation histories for elastic computations.(3) creation of a robust 3-D mesh generation scheme capable of fitting the progression of shapes from die entry to exit, and capable of automatically adapting to new flow field geometries generated by the flow balancing algorithm. This work presents original contributions in each of these problem areas.

A novel solution algorithm has been developed for the design equations which result from a finite element analysis of melt flow. The procedure is capable of solving the three dimensional flow problem without resorting to supercomputer resources. Once the solution of the flow equations is found one can calculate associated performance information such as residence time distribution, and fluid element streamlines. Knowledge of the streamlines can be used to modify the shape of the die to eliminate dead spots in the flow path. This procedure should lead to improved product quality, and decreased die pressures. The streamline information has been coupled with a custom mesh mapping technique which allows dynamic mesh modification. The profile die can be graphically cut open in any direction to view the velocity profile, residence time distributions and the exact shape of the mesh.

One of the major obstacles in applying the finite element technique to the solution of three dimensional flow problems is the solving of a large sparse symmetric matrix. The method that was found to be the fastest and most memory efficient was an incomplete Choleski Conjugate Gradient Method combined with a Ujawa algorithm for pressure updating. Using this technique one can solve a non-Newtonian simulation on a mesh consisting of 6000 eight noded linear elements (21,000 equations) in under 10 cpu hours on a VAX GPX II laboratory micro-computer with 16 MB of memory.

The three dimensional profile die mesh is constructed using a combination of isoparametric mesh generation preceded by transfinite bilinear interpolation. This technique generates a continuous mesh beginning with a circular extruder exit to a complex shape such as an "L" profile. An example of the mesh for such a die is presented in Figure 1. Note that hidden line removal has been implemented to block display of internal mesh lines. The momentum balance equations are solved to determine the pressure and velocity fields within the die. Figure 2 is an example of the velocity profile at the "L"-shaped die exit. Particle streamlines can be obtained by either by streamline tracking, or by solving the material coordinate equation using a galerkin finite element approach which gives the origin of every node in the finite element mesh. The latter,provides a rapid determination of complete element flow histories using the same solution grid as employed for the determination of velocity. Once the origin of all the points in the die are known, the streamlines can be constructed directly without having to trace each point as in the tracking method. Using a similar approach one can solve for the residence times of all the nodes in the profile mesh. An interactive "CAD" interface has been created to facilitate interpretation of the results. The die mesh can be graphically cut along any axis to show the streamline and residence time field. Knowing the dead zones and the streamlines, a new mesh is constructed dynamically to resolve design problems. The three dimensional equations of motion are then solved for the new geometry, producing new streamline and residence time information. The cycle is repeated until the profile die is streamlined and the dead zones are removed.

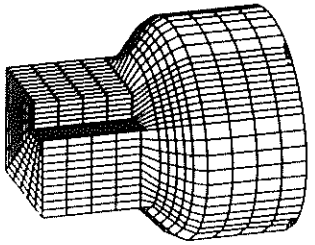


Figure 1. 3-D Mesh for L Profile

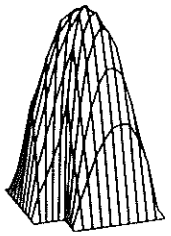


Figure 2. Exit Velocity Profile

FLOW OF POLYMERS THROUGH DIE WITH OSCILLATING BOUNDARY: MODELLING AND EXPERIMENTATION

A. I. Isayev, V. M. Wong and X. Zeng

Polymer Engineering Center
The University of Akron
Akron, OH 44325

Abstract

Extrusion of several thermoplastics has been carried out through an annular die having internal surface oscillating in the sound frequency range at different amplitudes. Oscillating shear flow has been imposed orthogonal to the main pressure flow, and die characteristics have been measured with and without imposition of oscillations. Modelling of orthogonal superposition of oscillations upon pressure flow has been performed using viscoelastic constitutive equation. The analysis includes a contribution to the die characteristics, due to interaction between nonlinear effects arising from the superposition of oscillatory and shear flows and due to vibrational heating of a polymer. Results of modelling are compared with the experimental data.

POLYMERS IN MICROELECTRONICS: AN OVERVIEW

David S. Soane and Zoya Martynenko
Department of Chemical Engineering
University of California
Berkeley, Ca. 94720

Major processes in integrated circuit fabrication are briefly examined in order to identify critical roles served by polymers in achieving the state-of-the-art in microelectronics (1). Three areas of polymer applications will be discussed in depth: lithography, intermetallic dielectrics, and encapsulation and packaging. Material and process requirements will be the main focus of discussion. Significant advances made in recent years as well as current and future research challenges will be specially emphasized. This review thus serves to enhance the awareness of the polymer community of major problems in polymer usage in the microelectronics industry.

During integrated circuit fabrication, photolithography, the science (and art) of transferring an image from a mask into a photosensitive film by irradiation, must be used at each level to create the pattern of conducting and insulating areas. This is the first instance where polymers make an invaluable contribution as photoresists. For a typical process, resist is applied onto a wafer to form a thin uniform film. With a glass plate or "mask" coated with an opaque material (usually chrome) bearing an array of circuit design patterns, selected areas of the photoresists are irradiated. Each layer of the circuit requires a unique pattern. The modified or exposed regions of the polymer exhibit a different rate of removal or development, in certain chemical reagents, resulting in the formation for a relief image of the mask. The pattern formed delineates the area for the subsequent modification of the underlying substrate in the unprotected regions. Through either chemical or physical processes, the substrate is altered while the remaining resist provides protection of the areas where no change is intended. Depending on the chemical nature of photoresists, either a positive or negative relief image of the original mask emerges in the substrate. Resists which produce negative images generally undergo cross-linking upon irradiation, rendering them insoluble in the developer solvent. Positive resists experience molecular changes which enhance their solubility in developer solutions such that the exposed regions are removed at a faster rate. Photoresist bakes which promote adhesion, relieve polymer stress, and drive off spincoating or developer solvents intersperse the process sequence. As the last step, the resist is stripped by wet or plasma methods. This photolithography sequence is repeated for every patterned circuit layer on the semiconductor device. Each time the mask is precisely aligned to the previous pattern on the wafer.

In recent years advances in photolithographic materials and equipment along with computer-aided design have enabled the production of integrated circuits of significantly increased density and complexity. To meet the demands, the metal lines have decreased in width (but not height to maintain low line resistance), thereby decreasing the pitch from tens of microns to feature sizes just over one micron. The resulting high aspect ratio is preferred for conductors to control electromigration by lowering current density. These factors combine to create the need for more than one interconnecting layer of metal separated by an inert dielectric.

Materials used as dielectrics in the multilayer interconnect technology must meet a number of stringent requirements for successful performance. These include, for instance, low defect density, high dielectric strength (low dielectric constant), high resistivity, thermal stability, excellent mechanical properties, good adhesion, and compatibility with existing IC materials. One active area of research is in the replacement of inorganic dielectrics with polymeric material, notably polyimides. The high resistance and breakdown voltages offer improved integrity, whereas low dielectric constants result in short media propagation times, low signal coupling and high characteristic impedance lines. However, the primary rationale for the adoption of polymers is topography planarization. Polyimide, in particular, has been selected also because of high thermal stability (up to 400°C) which is required for subsequent processing steps (e.g., metal sintering, bonding operations, etc.).

Polymers find the largest volume usage in IC fabrication during packaging and assembly as adhesives, encapsulants, and printed circuit board materials. During this operation, chips containing thousands of elements are first broken off the finished wafer. Each chip (or die) must then be interconnected with other components to allow communication with the outside world. Using wire bonding or flip chip technology, qualified chips may be mounted on substrates (dual-in-line packages (DIPs), chip carriers, etc.), which contain embedded conduction lines to provide electrical interconnection among the chips and perhaps other electrical elements. Substrates loaded with chips are then sealed or encapsulated to minimize moisture penetration. An alternative is to use tape automated bonding (TAB) to attach the chips to their substrates. The flip chip and TAB approaches are generally reserved for high-end products with large numbers of inputs/outputs, whereas plastic encapsulation of wire bonded chips in a molding operation suits low-end products with relatively few external interconnections. Hermeticity of the final package affects long term reliability. In the next level of interconnection, the packaged chips or hybrid modules are mounted on Printed Circuit Boards (PCBs).

(1) D.S. Soane and Z. Martynenko, "Polymers in Microelectronics; Fundamentals and Applications," Elsevier, Amsterdam and New York, 1988.

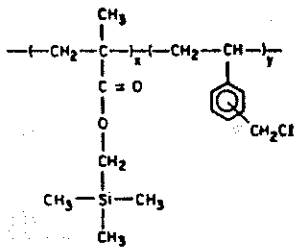
LITHOGRAPHIC PERFORMANCE OF SELECTED SILICON-CONTAINING RESISTS

M. J. Jurek, A. E. Novembre, R. G. Tarascon, I. P. Heyward, A. Shugard and E. Reichmanis, AT&T Bell Laboratories, Murray Hill, NJ

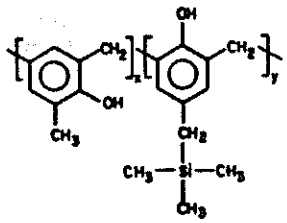
A trilevel lithographic scheme, consisting of a thick planarizing layer, a dry etching resistant layer, and an imaging layer, can be simplified to a bilevel approach with the advent of a variety of highly sensitive, O_2 reactive ion etching resistant silicon-containing resists.[1,2] We will discuss results obtained on two such bilevel organosilicon resists that are sensitive to both excimer laser (248 nm) and electron beam irradiation.

The first is a negative-acting copolymer comprised of trimethylsilylmethyl methacrylate (SI) and mixed m,p-chloromethylstyrene (CMS) isomers. The second is a positive resist consisting of a silylated novolac resin plus a sensitizer. The structures of both polymers are shown below.

P(SI-CMS)



SI - NOVOLAC



Copolymers of SI and CMS were prepared using standard free radical solution polymerization methods. For the material containing 90 mole % SI (14.5 wt% Si) and $<M_w> = 7x10^4$, the sensitivity ($D_g^{0.5}$) at 248 nm is 40 mJ/cm^2. The $D_g^{0.5}$ resulting from electron beam exposure is 5.1 μC/cm^2 at 20kV with a contrast of 2.5. The ratio of reactive ion etching rates of a planarizing layer HPR-204 to this material is 12 to 1 in O_2.[3] Swelling of the resist images during development was minimized through identification of a single component developer/rinse system. Resist geometrics in the 0.4 to 0.6 μm region have been delineated and transferred via reactive ion etching into 1.5μm of the planarizing layer.

The silylated novolac resist was prepared by the copolymerization of o-cresol and p-trimethylsilylmethyl phenol with formaldehyde. This low molecular weight polymer functions as a positive deep UV resist when mixed with a photoactive diazoquinone dissolution inhibitor. The sensitivity is 120 mJ/cm^2 and coded 0.8 μm line/space patterns have been resolved. An O_2 RIE resistance of 10.1 versus HPR-204 was obtained with samples containing 9.7 wt% Si.[4] To effect electron beam sensitivity, the silylated novolac is mixed with poly(2-methyl-1-pentene sulfone), (PMPS) which functions as a dissolution inhibitor. During irradiation PMPS undergoes spontaneous depolymerization and is vaporized, leaving the remaining film soluble in aqueous developer. This resist displays a sensitivity of 8 μC/cm^2, and a contrast of 1.6. Using this dose, coded 0.5 μm line/space patterns were resolved.

References

1. Y. Ohnishi, M. Suzuki, K. Saigo, Y. Saotome and H. Gokan, Proc. SPIE, 539, 62 (1985).
2. H. Gokan, Y. Saotome, K. Saigo, F. Watanabe and Y. Ohnishi, ACS. Symp. Ser. 346, 358 (1987).
3. A. E. Novembre, E. Reichmanis and M. Davis, Proc. SPIE, 631, 14 (1986).
4. R. G. Tarascon, A. Shugard and E. Reichmanis, Mat. Res. Soc. Symp. Proc. 76, 347 (1987).

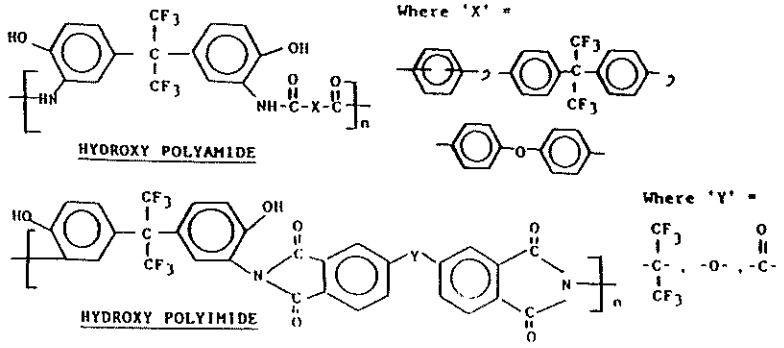
NEW HIGH TEMPERATURE STABLE PHOTORESISTS BASED ON SOLUBLE POLYIMIDES AND POLYAMIDES CONTAINING THE HEXAFLUOROISOPROPYLIDENE LINKING GROUP

W. H. Mueller, D. N. Khanna, Hoechst Celanese Corporation, SPG-Central Research, 500 Washington Street, Coventry, Rhode Island 02816

There has been a rising interest in the use of polyimides for microelectronic applications, such as; fabrication aids, passivation layers and interlayer dielectrics.[1-3] In order to reduce the number of processing steps when applying such coatings, several photoimageable systems[4-9] have been developed. However, their use has been limited due to shelf-life problems, long exposure time, image shrinkage, inconsistent photospeed and resolution.

The available positive acting photoresists are mostly novolak based and also have disadvantages. One major deficiency is their poor thermal behavior (Tg~70-120°C) which limits these resists to low temperature applications only. Ahne et al.[10] of Siemens AG reported heat resistant positive photoresists utilizing oligomeric or polymeric precursor stages of polybenzoxazoles.

In this paper we report a new family of high-temperature stable photoresists based on soluble polyimides and polyamides containing the hexafluoroisopropylidene linking group. Their chemical structures are outlined as follows:



A low temperature solution condensation method[11] was used for the synthesis of hydroxy polyamides. Hydroxy polyimides were synthesized by a high temperature solution condensation method[12]. The obtained polymers were characterized by solution viscosity, GPC, UV, IR, NMR, TGA and DSC. Tg's of these polymers range from 250-350°C. Both polyamides and polyimides are soluble in a variety of solvents commonly utilized for photoresist applications.

When formulated with diazoquinone sensitizers these polymers provide improved high-temperature resistant, base developable positive resist systems with good photospeed, high contrast and excellent resolution (~1 µm). Polyamide based resists when thermally annealed >250°C, provide heat resistant polybenzoxazole relief structures without thermal deformation with good adhesion and solvent resistance. Also, these photoresist formulations have no shelf-life problems and can be processed like known photoresists using broad band UV radiation sources.

The potential of these materials looks promising, and a thorough lithographic evaluation is in progress.

References

1) W.R. Iversen, Electronics, 11, 41-42 (Sept. 1980)
2) R. Iscoff, Semiconductor International, 116-119, (Oct. 1984)
3) K. Mukai, A. Saiki, K. Yamanaka, S. Harada and S. Shoji, IEEE J. Solid State Circuits, 13, 462 (1978)
4) R.E. Kerwin and H.R. Goldrick, Polymer Eng. Sci., 11, 426 (1971)
5) H. Ahne, H. Krüger, E. Pammer and R. Rubner, "Polyimides, Synthesis, Characterization, and Applications", Vol. 2, Plenum Press, 905-918 (1984)
6) H. Merrem, R. Klug and H. Härtner, "Polyimides, Synthesis, Characterization, and Applications", Vol. 2, Plenum Press, 919-931 (1984)
7) F. Kataoka, F. Shoji, I. Takemoto, I. Obara, M. Kojima, H. Yokono, T. Isogai, "Polyimides, Synthesis, Characterization, and Applications, Vol. 2, Plenum Press, 933-945 (1984)
8) O. Rohde, H. Riediker, A. Schaffner, J. Bateman, "Advances in Resist Technology and Processing II", Proceedings SPIE, Vol. 539, 175-180 (1985)
9) N. Yoda et al., J. Macromol. Sci. Chem., A-21 (13+14), 1641 (1984)
10) H. Ahne, E. Kühn and R. Rubner, U. S. Patent 4,339,521 (1982)
11) T. Kubota and R. Nakanishi, Polymer Lett., 2, 655-659 (1964)
12) A. Berger and R. Vora, Eur. Patent Appl., 0163518 (1985)

15/4

REACTIVE ION ETCHING OF POLYMER FILMS

B.C. Dems, F. Rodriguez, C.M. Solbrig, Y.M.N. Namasta, and S.K. Obendorf
School of Chemical Engineering, Olin Hall
Cornell University, Ithaca, NY 14853

The major role of polymer films during plasma treatment in the production of integrated circuits is to protect the substrate in selected areas. Thus the ability of the polymer to resist etching is of paramount importance. Unfortunately, all the other properties such as sensitivity, adhesion, reliability, and resolution all must be maintained in order for the lithographic process to proceed.

Anisotropic etching is used with plasmas based on fluorocarbons when a silicon oxide layer is being treated. Many studies have been reported on the relationship of structure and etch resistance for organic polymers. Typical of the results is that of Anderson (PhD Thesis, Cornell, 1985) who found that the etch rate was almost a linear function of phenyl content in a polymer film (Fig. 1). This finding seems independent of the location of the phenyl group since results for phenyl attached to the chain as in poly-(alphamethylstyrene) seem similar to those when the phenyl group is removed as in an amide or ester derivative of an itaconic acid copolymer.

Etching by an oxygen plasma can be used to cut through an underlying "planarizing" layer of an organic polymer. In this case, the top layer should act as a barrier, but the lower layer should etch as rapidly as possible. Inorganic materials which form resistant oxides are favored for the barrier layer. For example, some of our recent results (Figure 2) show that the etch rate of a polymer/tin compound mixture is quite sensitive to the tin content.

By far the most popular route to achieve oxygen etch resistance has been the inclusion of organosilicon moieties. These oxidize to form silicon oxide. However, the level of silicon needed to get a low rate often constrains the polymer film composition in such a way as to sacrifice other properties.

Experimental Conditions (Reactive Ion Etching of Coated Silicon Wafers)

	Figure 1	Figure 2
Gas:	CF_4 + 8%O_2	Oxygen
Pressure:	30 mTorr	35 mTorr
Power:	0.2W/cm^2	0.25 W/cm^2
Flow rate:	19 Std. cm^3/minute	20 Std. cm^3/minute

Figure 1.

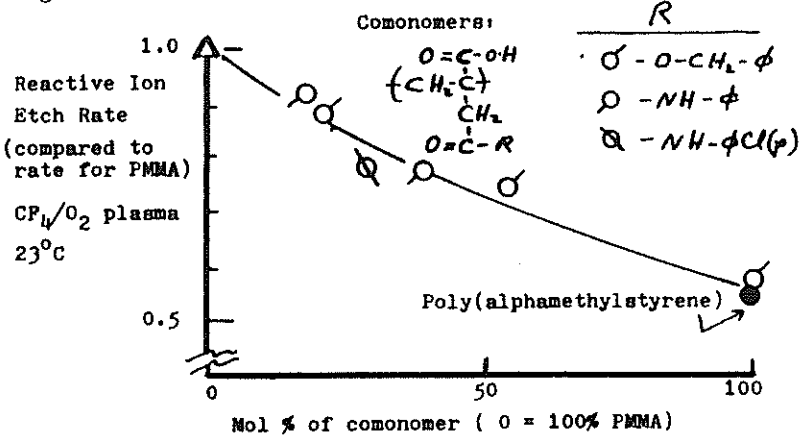
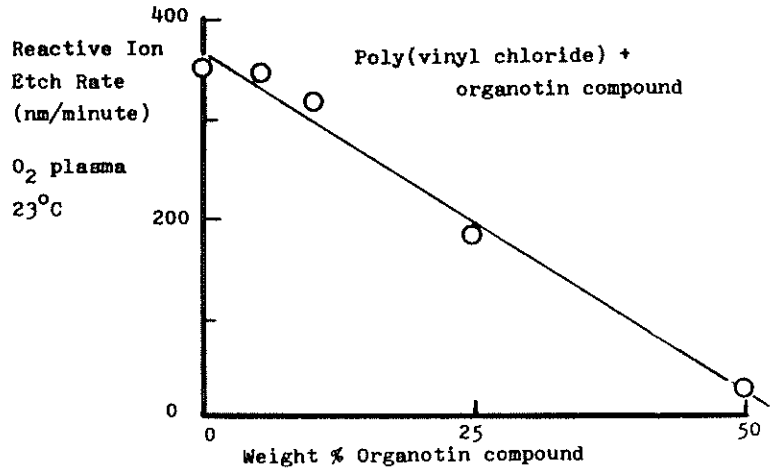


Figure 2.



Processing Ultrathin Polymer Films

by

Jerome B. Lando and Scott E. Rickert

We have continued our investigation of the optimal processing conditions for Langmuir Blodgett monolayer and multilayer films and the effect of these conditions on the performance properties of these films in electronic devices. In the case of our studies of phthalocyanine oligomer amphiphiles, not only have we adjusted the usual dipping variables for depositing a monolayer from the gas water interface (surface pressure, temperature, retention time, nature of the water substrate, dipping speed etc.). We have also designed the chemical structure of the amphiphile to allow the optimal morphology and structure in the resulting films. Application of these multilayer films in barrier films, as gas sensors and in metal-insulator-metal capacitors will be discussed.

We have found that our phthalocyanine amphiphiles, when properly configures can act as rapid gas detectors through changes in electrical conduction (Figure 1) and will distinguish between different gases. These phthalocyanine amphiphiles also act as good protective barriers and as excellent capacitor films in aluminum-phthalocyanine-aluminum structures (Figure 2).

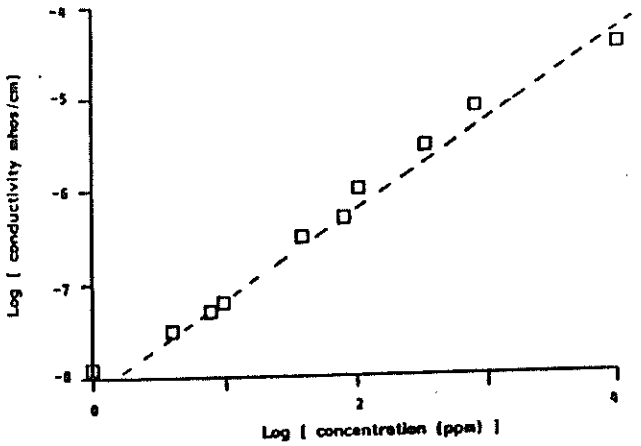


Figure 1. Conductivity vs. concentration for NO_2/N_2 gas at 17°C.

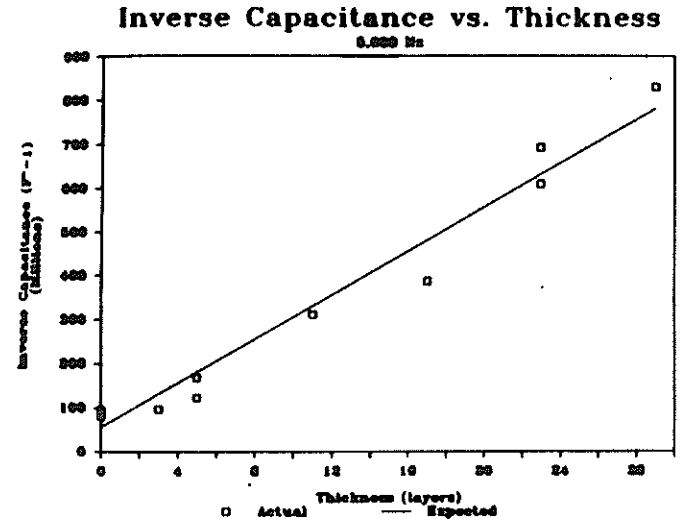


Figure 2. Inverse Capacitance vs. Thickness at 5KHz

15/6

FUNDAMENTAL STUDIES IN PLASTIC PACKAGING OF MICROELECTRONIC DEVICES

L. T. Manzione
AT&T Bell Laboratories
Murray Hill, NJ 07974

Plastic packaging is used to provide electrical, mechanical and environmental protection for more than 80% of the integrated circuit devices (ICs) produced in the world. Transfer molding is the process method for essentially all plastic packaging of ICs. Although the process itself is mature, it has not had the same level of fundamental engineering analysis as injection molding, or even the more recent reaction injection molding process. For this reason, mold design, process optimization and the development of new molding materials have largely been conducted through trial and error. This paper summarizes fundamental studies of the transfer molding process as it is used for the packaging of microelectronic devices. The objective of these studies is the reduction of flow induced stresses.

The molding compound rheology is required for subsequent experimental and numerical studies of flow induced stress. The shear rates encountered during the flow in a multi-cavity mold were computed and found to range from 15 sec^{-1} in the cavities to 5000 sec^{-1} through the gates. Several different techniques were developed to determine the rheology of this highly filled material over this wide range of shear rates. Cone and plate viscometry was used for shear rates below 20 sec^{-1} and temperatures from 120° to 145°C. A capillary rheometer built within a transfer mold (1) was used for shear rates of 500 to 1500 sec^{-1}. Pressure drop measurements through actual gate geometries (2) were used to obtain the high shear rate behavior. Data for several of the IC grade molding compounds were obtained and fit to a power law model. The materials are moderately non-Newtonian with power law indices of 0.35 to 0.70. The viscosity increase due to polymerization was included through the chemical kinetics, obtained through a combination of gel time and calorimetry data.

The flow and heating of the molding compound in the transfer pot were elucidated through flow visualization studies and a numerical model (3). The flow field was found to be a stagnation point flow against the bottom of the cylindrical pot. The extrudate temperatures were found to be approximately 105°C, compared to an initial or preheat temperature of 90°C, and fairly insensitive to transfer speed and cylinder diameter. The numerical model extended these results to predict chemical conversion and viscosity.

The transfer pot study established the initial conditions for flow of the molding compound through the runner system. Runner lengths can be up to 30 cm, and significant heating will occur over that distance in the narrow runners with a mold temperature of 170°C. Therefore, the length of the runner will to a large extent determine the temperature, viscosity and flow induced stress when the molding compound contacts the chips. Once again, experimental measurements were combined with semi-empirical correlations to obtain the temperature and viscosity of the molding compound during flow in a runner (2).

The flow induced stresses on the chips depend on the product of the velocity and viscosity. It has been shown that molding compound selection, material temperature, and runner length can be used to minimize the viscosity. The material velocity can be changed by the transfer speed and the mold filling profile. Molding is often conducted at the longest transfer speed allowable prior to substantial viscosity increase due to polymerization. Longer fill times may actually increase flow induced stresses by increasing the viscosity. Balanced filling, however, can reduce molding compound velocity while maintaining the same fill time since most IC packaging molds fill non-uniformly. A mathematical model for predicting the filling profile of multi-cavity packaging molds for different runner and gate geometries was developed (2). This model uses actual pressure drop measurements in a one dimensional network flow scheme to predict the filling of all cavities in the mold.

REFERENCES

1. L.L. Blyler,et.al.,Polym Eng Sci, 26(20),1399 (1986)
2. L.T. Manzione,et.al., SPE ANTEC Papers, 1988
3. L.T. Manzione,et.al.,Accepted for pub. in Polym Eng Sci.

STABLE BROMINATED EPOXIES FOR MICROELECTRONIC ENCAPSULATION

C.S. Wang, D.B. Fritz, A. Mendoza,
The Dow Chemical Company, Freeport, TX 77541

One of the most frequent failures encountered in encapsulated micro devices is the so-called open circuit which results from a break of the bonding wire between the circuitry. The breakage is primarily due to corrosion. This is initiated by the impurities in epoxy resins, such as halogens, which upon exposure to heat and moisture generate a corrosive acid.

Since the introduction of the low chloride epoxy resins, the wire bond failure due to the chloride impurities in the resin has become much less prominent than that due to the bromine from the fire retardant in the encapsulation formulation. Water extracts of molding compounds after high temperature storage were found to contain bromide ion levels directly proportional to the bromine content in the molding compounds. A direct relationship between failure rate and bromine content in the molding compound has also been established(1).

Meta-halogenated phenols are generally known to be more chemically and thermally stable than their ortho- or para-halogenated counterparts(2). The instability of ortho- or para-brominated phenols is due to the formation of an unstable cyclohexadienone structure via keto-enol tautomerization. Upon heating, this unstable cyclohexadienone structure generates free radicals ($Br^{\cdot}$) which in turn abstract protons from a neighboring molecule to form HBr.

Epoxy derivatives of novolacs containing stable brominated phenolics have been synthesized and incorporated in molding compounds for use in microelectronic encapsulation. The stable brominated cresol epoxy novolac contributes the expected improvements in thermal and hydrolytic stability to the molding formulation while providing fire retardancy properties. The key contribution, however, is an extension of device reliability when encapsulated micro devices are subjected to the Bias Pressure Cooker Device Test (BPC). BPC data under 1 atmospheric steam and 250°F with bias revealed that stable brominated cresol epoxy novolac out performs standard high purity resins.

References

(1)K. Tanaka, et. al., MEPPE (1986)
(2)A. Factor, J. of Polymer Science, II, 1691 (1973)

STRESS CHARACTERIZATION OF EPOXY MOLDING COMPOUNDS

W. F. van den Bogert, M. Molter and D. J. Belton
Philips Research Lab. Sunnyvale, Signetics Corp.
811 E. Arques Avenue, Sunnyvale, CA, 94086

In integrated circuit manufacturing, packaging is a crucial final step to ensure integrity of the part. Plastic packaging is popular because of cost considerations but introduces special reliability concerns.

In conventional processing of epoxy molding compounds, encapsulation of integrated circuits takes place at a relatively high temperature (180 C) and under sufficient pressure (about 6.9 MPa) to achieve a transfer time of approximately 20 sec. After quenching in air, molded parts are subjected to a heat treatment (frequently 4 h at 175 C) resulting in structural relaxations in the polymer network with only a slight increase in degree of cure. The thermal expansion mismatch between the silicon die, the leadframe and the molding compound results in large thermal stresses. To evaluate the reliability of plastic packaged integrated circuits thermal stress testing is often used. In

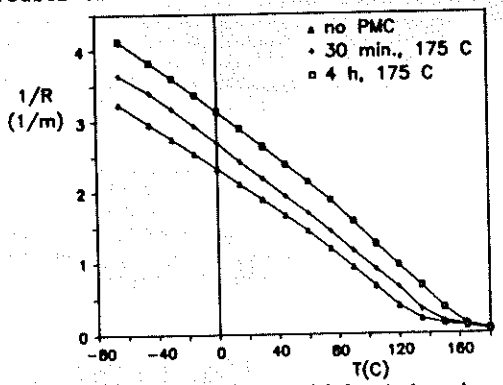


Figure 1: Influence of post mold heat treatment on stress.

thermal shock testing packaged parts are subjected to temperature shocks from -65 C to 150 C (liquid to liquid, 5 min. dwell time, 6 sec. transfer time). Such thermal stress testing can result in top to bottom metal shorts, passivation cracking or plastic cracking.

The generation of thermal stress has been the subject of a recent study [1] in our laboratory. Thermal stress generation is governed by the thermomechanical properties of the materials involved. Suitable experiments allow the determination of the temperature dependent coefficient of thermal expansion (TMA) and the temperature and frequency dependent mechanical properties (DMA). For a simple bilayer structure, it is possible to calculate thermal stresses and express the result in terms of the curvature 1/R of the structure as function of temperature. In this paper stress characterization of molding compounds as a result of the combined effect of post mold cure and thermal shock testing will be discussed.

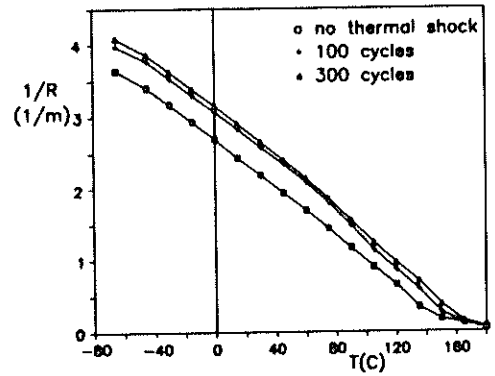


Figure 2: Influence of thermal shock testing on stress.

In fig. 1 calculated 1/R values for different post mold heat treatments are given. We have observed that heat treatments longer than 4 h at 175 C do not change the 1/R values any further. In fig. 2 calculated 1/R values for the same molding compound with a heat treatment at 175 C for 30 min. after zero, 100 and 300 thermal shock cycles are given. The 1/R values found after 300 thermal shock cycles (post heat treatment 175 C, 30 min) and those found after a heat treatment at 175 C for 4 h are approximately the same. Post mold treatments therefore lead to a stable polymer network that generates a relatively high, but constant, thermal stress at each temperature.

References:

[1]: W. van den Bogert et. al., Proc. IEEE/CHMT IEMTS, Anaheim, CA, 1987, p. 170; IEEE Trans. CHMT, (in press)

15/9

THE BIREFRINGENCE PROBLEM IN OPTICAL DISK SUBSTRATES: A MODELING APPROACH

J. Greener, Diversified Technologies Group Research
Laboratories, Eastman Kodak Company, Rochester, New York 14650

One of the challenges for polymer processors in the emerging optical storage technology is producing an optically flat, dimensionally stable plastic substrate with zero or very low levels of birefringence. The minimization of birefringence is especially critical in the case of magneto-optical (eraseable) systems where the storage mechanism is based on the Kerr effect. In these systems retardation levels in excess of 20-30 nm can have a detrimental effect on the carrier-to-noise ratio and other performance measures of the storage device. In general, low birefringence can be attained either through the use of materials with low intrinsic optical anisotropy or through judicious manipulation of the injection molding process--the most widely used process for producing plastic substrates. To date, the latter option appears to be more viable since very few materials with low intrinsic anisotropy have so far been developed for this application on a commercial scale.

In this study we attempted to model the birefringence buildup problem in a center-gated disk during the injection molding process in order to develop rational, physically-based strategies for reducing birefringence in molded substrates. The model computes the hydrodynamic stresses in the molding cavity during the injection phase of the process which are then allowed to relax non-isothermally. The inhomogeneous stress relaxation process after the cessation of flow is described by the non-linear viscoelastic constitutive equation due to Wagner. Temperature changes during the post-filling phase, as estimated from one-dimensional conductive heat transfer analysis, are coupled to the stress relaxation problem following the Matsui-Bogue approach. The residual stresses are then converted to birefringence profiles via the stress-optical law. Some results of the model will be compared to experimental data and, based on the analysis, general strategies for controlling birefringence in molded substrates will be outlined. The limitations of the model, particularly its inability to account for the effects of cooling stress, packing and coining will be discussed and general ad-hoc approaches to incorporate these effects in the model will be described.

THERMOPLASTICS WITH NOVEL PROPERTIES AND THEIR IMPACT ON ELECTRONICS

H. Münstedt, BASF Aktiengesellschaft, Ludwigshafen am Rhein, Federal Republic of Germany

High temperature resistant thermoplastic polymers (HT-polymers) are gaining more and more importance. Polysulfone, polyethersulfone, polyetherimide, polyphenylenesulfide, polyetherketone, and liquid crystalline polymers, for example, are available from several companies. New grades are under development.

Continuous use temperatures up to 250 °C open applications for these polymers which have been the domain of duromers, ceramics, and metals. From a comparison of the viscosity functions and the stability in the molten state with the corresponding properties of commodity plastics it becomes obvious that well established processing operations like extrusion and injection molding can successfully be applied to high temperature resistant polymers. The presentation of other distinguished properties like flame resistance without additives, low smoke density, and stability with respect to various solvents and detergents demonstrates that HT-polymers are promising materials for innovations in many fields.

Of particular interest are these polymers for new developments in electronics. The potential of different HT-polymers for injection molded printed circuit boards (PCB) will be assessed and the advantages this technique offers will be discussed with special emphasis on the three-dimensionality which opens up new functions to the PCB. On the other hand, problems like dimensional stability under the heat treatment due to different soldering processes and adhesion of the copper circuits to the substrate materials will be stressed.

Another impact of HT-polymers on innovations in electronics can be seen in the field of packaging of electronic components. By an assessment of the unique properties of liquid crystalline polymers (LCP) with respect to the requirements for a packaging material for electronic devices the high application potential of LCP will be demonstrated. In addition to the pronounced resistance to heat, low viscosities, small thermal expansion coefficients, low permeability with respect to water vapor, extreme purity, and a high filling potential for inorganic materials of good thermal condutivity make LCP a promising candidate to compete with heat curable polymers which are widely used today in packaging of electronic parts. Besides that, the injection molding technique applicable to the thermoplastic liquid crystalline polymers offers some advantages compared with the transfer-molding process in use for duromers.

Furthermore, the innovation potential of LCP for glass fibre optics will be discussed. Fibre coatings, extruded strength members, and coupling elements are applications for which LCP are particularly well suited due to unique properties like adjustable thermal expansion coefficient and high modulus in flow direction of the melt.

15/11

New Materials For Multilayer Microelectronic Applications: Polymerization and Properties of Bisbenzocyclobutene Based Polymers

S.F. Hahn, P.H. Townsend, J.A. Gilpin, D.C. Burdeaux
M.E. Pruitt Research Center, Dow Chemical U.S.A.
1712 Building, Midland, MI 48674

Organic polymers are finding increased usage as insulators in the construction of microelectronic interconnection structures, where these materials may offer significant improvements in circuit density and signal speed due to their unique dielectric properties. Novel bisbenzocyclobutene polymers are being developed for this purpose, and the polymerization chemistry and physical and electrical properties of these materials is described in this paper.

It has been found that prepolymerization (B-staging) of the bisbenzocyclobutene monomer to provide an oligomeric mixture is advantageous in the fabrication of insulative layers. Films are formed via spin or spray coating solutions of these oligomers, followed by complete cure to polymer. Techniques for prepolymerization and film formation will be discussed.

The physical properties of the cured polymers will be reported. Of special interest are the dielectric constant and dissipation factor, measured at ca. 2.7 and 0.0001 (at 1 KHz), respectively, for a 30 micron bisbenzocyclobutene polymer film. This polymer also features low water absorption (0.2 percent by weight, 24 hour water boil) and relatively good thermal stability. Determination of polymer mechanical and dimensional properties over a wide temperature range have also been examined.

15/12

SPIN-ON-GLASS AS A PLANARIZING INTERLAYER DIELECTRIC FOR VLSI

T. Rucker, H.Y. Lin, P.L. Pai and C.H. Ting
Components Research, Intel Corp., 3601 Juliette Lane, Santa Clara, CA 95051

Multi-levels of conductor patterns are required to provide the necessary interconnection for VLSI chips. One of the most serious problems encountered is the severe surface topography generated by repeated deposition and etching cycles. A variety of processes are under investigation to planarize or smooth the chip surface. A spin-on dielectric film is probably the simplest way to partially planarize the surface for multi-level interconnections.

We have studied a variety of spin-on glass (SOG) materials such as silicates, siloxanes, and other silicon-oxygen polymers for interlayer dielectric applications as an alternative to polyimide materials. The material properties were characterized as a function of curing conditions by Infrared Spectroscopy (IR), and by stress and electrical measurements. The process compatibility issues such as wet and dry etch rates, outgassing properties, and chemical resistance were also studied. An evaluation procedure has been developed which will allow us to determine a materials compatibility in the IC manufacturing process.

We found that an SOG that has a lower hydroxide or water content exhibited a lower dielectric constant and better processing capabilities. The hydroxide content for siloxane materials was found to be sensitive to annealing conditions and resist stripping method and varied greatly for the different SOG samples evaluated. Figure 1 compares the Si-OH peak located at 940 cm^{-1} of the IR transmission spectra of siloxane annealed under O_2 and N_2 ambient. It is clear that high temperature annealing in O_2 creates a significant increase in the hydroxyl group concentration in the siloxane films. Outgassing experiments show that the siloxane material, before processing, has no appreciable water adsorption, whereas after processing IR shows a significant increase in water content. A high water content also degrades SOG interlayer dielectric qualities. We have also used Secondary Ion Mass Spectrometry (SIMS) to characterize model SOG systems after each processing step and to monitor surface changes which affect subsequent processing steps.

Another major concern in SOG processing is crack formation over severe surface topography. Initial results have shown that this problem is not only affected by the material properties and processing conditions but also by time. The SOG materials, which immediately after annealing have no cracks, exhibit cracking after one day exposure to the ambient.

Finally, test structures using a combined CVD/SOG dielectric layer were fabricated and tested. Figure 2 show the planarizing effect of a 0.4μm SOG film coated over 1.0μm Al topography. The SOG properties and the processing sequence needed to incorporate these dielectric films into VLSI devices will be described.

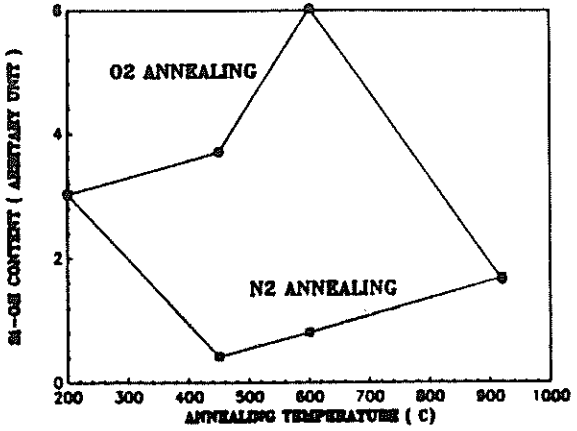


Figure 1: Infrared transmission spectra of SOG sample after O_2, and N_2 anneal. O_2 annealing increases the hydroxyl group concentration in the SOG film.

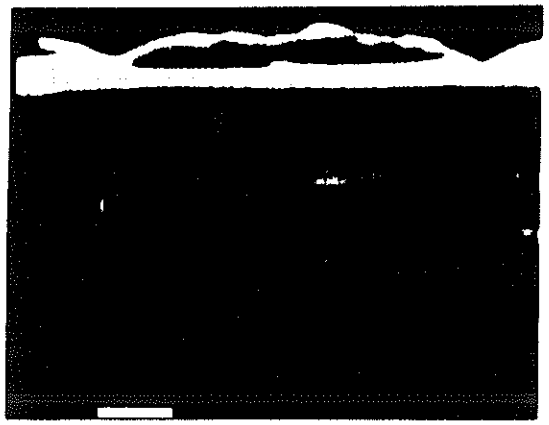


Figure 2: A wafer is planarized over a 1 μm Al line by a combination of SOG (.4μm, dark band) and CVD.

15/13

NEW EPOXY ENCAPSULANTS WITH CONTROLLED THERMAL EXPANSION COEFFICIENTS FOR PACKAGING

Noriyuki Kinjo and Masatsugu Ogata, Hitachi Research Laboratory, Hitachi Ltd.
4026 Kuji-cho, Hitachi-shi, Ibaraki-ken, 319-12, Japan

Epoxy molding compounds for microelectronic devices have been and will continue to be the main stay of encapsulation materials in view of their cost and productivity advantages. On the other hand,as chip sizes become larger due to increased integration of devices, compacter packages are in demand to realize the higher integration. Advances in surface mounting technologies demand also encapsulation materials which have extremely low thermal stress and excellent stability at the elevated temperratures used in reflow soldering.

Most of the low thermal stress molding compounds now on the market are based on epoxy resins having rubber particles dispersed as flexibilizers to lower the elastic modulus in the cured state. Although this method has been successful so far, it will not to lead any further lowering of the thermal stress, a requirement which is becoming greater and more important in VLSI applications. Further effort to prepare molding compounds with their inherent thermal stress remarkably decreased is being made by matching thermal expansion coefficients(TECs) between molding compounds and inserts. The purpose of this paper is to discuss the dominant factors determining the TECs of epoxy molding compounds for LSIs.

Increasing the amount of fillers to be added is very effective for lowering thermal expansion coefficient, but it consequently degrades resin moldability because viscosity is increased. To deal with such problems, development of fillers that cause no viscosity rise in resins, or addition of flexibilizers must be considered. Mooney's viscosity equation(1), explains the influences of filler shape and content on the viscosity of the compounds.

$$\ln \eta r = \frac{Ke}{1-\phi/\phi m} \qquad (1)$$

where ηr: relative viscosity; Ke: Einstein coefficient(depending on shapes and aggregation of grains); ϕ: volume fraction of fillers; ϕm: the maximum volume fraction allowed for fillers(depending on particle size distribution, shapes or aggregation of grains). In compliance with the above formula, spherical fillers have used by expanding and controlling the grain size distribution in order to prevent increased viscosity of the resin compounds when the quantity of added filler is increased.

Fig.1 relates viscosity of epoxy molding compounds and filler content. The particle size distribution is varied over a wide range, which is represented by the n value of the Rosin-Rammler equation. The decrease in the n value, which means a broader distribution of particle sizes, results in a decreased viscosity of the molding compounds. As a results of this, it became possible to control the TECs of the epoxy molding compounds in the range from 0.8 to 2 X 10^{-5} K^{-1}.

The thermal expansion behavior of base epoxy resins should be discussed, even though the TEC of the base resins is not so dominant decreasing the TEC of the compounds when compared with the effect of filler content.

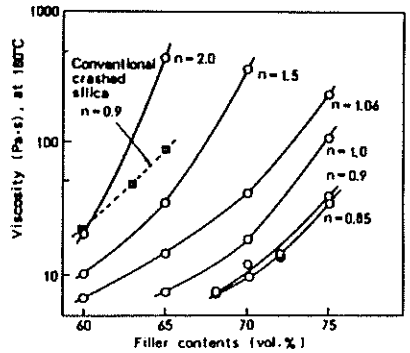


Fig.1. Effect of the grain size distribution of the spherical fillers on the viscosity of the epoxy molding compounds.

PREDICTION OF PARISON SWELL IN THE BLOW MOLDING PROCESS

- Comparison between Calculated and Measured Values -

HARALD KAISER, Institut für Kunststofftechnologie,
Universität Stuttgart, Böblinger Straße 70,
7000 Stuttgart 1, West Germany

Various calculation models for prediction of the swell behavior of polymers have been developed in the past. These models can only be used to describe very simple die geometries and are usually limited to very long dies of constant geometry ignoring entrance effects. The flow conditions before the die exit and its influence on the velocity and temperature profiles is not considered.

The normal stresses are very important in describing the swell behavior of polymers in a conical section. The development of such normal stresses was experimentally demonstrated by Kaioni, Schümmer in the past. On account of the equation of state used in these studies, these normal stresses resulting from the extensional deformations were not taken into consideration in their model.

In this study, an integral-type equation of state, derived by Lodge and modified according to Wagner and Laun was used as rheological equation of state for the material behavior. It describes both the elastic and viscous behavior of a melt.

$$\underline{\sigma}(t) = -p(t)\cdot\underline{E} + \int_{-\infty}^{t} m(t,t')\cdot\underline{C}_t^{-1}(t')\cdot dt'$$

where
- $\underline{\sigma}(t)$: stress tensor at an observation time-instant t,
- $p(t)$: isotropic pressure of the melt
- $\underline{E}$: unit tensor,
- $m(t,t')$: memory functional,
- $\underline{C}_t^{-1}(t')$: Finger deformation tensor at the time-interval (t,t')

In order to calculate the swell behavior, a discreet relaxation spectrum is needed. This relaxation spectrum is determined from measurements the storage and loss modulus (G', G'') carried out using an oscillatory rheometer system. The velocity and stress distribution in the die can then be calculated using the equation of motion and the equation of state.

The parison shape can be calculated with reference to the stress distribution at the die exit and the influence of the gravitational force. The swell ratio can be described as a function of the melt throughput, the temperature, the geometry and the type of material. To verify the mathematical model, calculated values were compared with experimental data, measured using an image processing system.

PROCESSING CHARACTERISTICS OF PET IN THE THERMOELASTIC REGION: APPLICATION TO BLOW MOULDED AND THERMOFORMED CONTAINERS

Barry Haworth, Fred H. Axtell & Adebayo O. Ola
Institute of Polymer Technology & Materials Engineering
University of Technology, Loughborough, Leicestershire LE11 3TU, UK.

The stimulus for the recently increased commercial importance of plastics based upon Polyethylene Terephthalate (PET) has been the ease with which PET can be fabricated into lightweight containers offering exceptional toughness, permeation resistance and consumer appeal, by Injection Stretch Blow Moulding (ISBM) and by Thermoforming. Successful processing is critically dependent upon the ability of amorphous PET to be shaped and crystallised under the influence of strain in the temperature range above the glass transition. The research in this paper details some attempts to characterise the flow and deformation characteristics of PET in the thermoelastic range; results from a series of commercial practical trials are also selected to support the simulative studies.

PROCESS SIMULATION

The Rutherford Elongational Rheometer, initially specified according to the principles of a similar instrument (1), was developed further in our laboratories to analyse the uniaxial flow characteristics of high elongational viscosity materials such as polymer melts and rubber-like systems. Based upon input measurements of force, displacement and time, servo-control of end-separation velocity was used to yield a constant strain-rate mode of uniaxial deformation. PET sheet of 1.45 mm gauge (ex-ICI Chemicals & Polymers Group, Wilton, UK; quoted IV of 0.73 dl/g) was used in our test programme: the chill-roll cast-sheet was optically isotropic and clear, with no evidence of pre-crystallisation.

Figure 1 illustrates the typical response of amorphous PET at 100 °C. Constant strain-rate data show departures from a common locus at positions which vary according to deformation rate. Increasing resistance to further deformation with time, in processes involving free-surface flows, represents a desirable response which is likely to promote even thickness distributions in containers. Also, the rate-dependent departure from the time-baseline indicates a critical magnitude of strain (in the engineering strain range 2-4, according to temperature) at which significant chain-stiffening occurs. The stress growth rate after the transition is extremely high for PET, in comparison to olefinic and vinyl polymers; stress-induced crystallisation is responsible for this effect. Raw data of the type shown in Figure 1 may be reprocessed to yield conventional true stress-true strain curves: with respect to crystallinity development, temperature effects appear to dominate changes attributable to strain rate. It is also feasible to study viscoelastic characteristics on the Rutherford rheometer: stress relaxation and recovery data have supported the hypothesis of Meissner (2), that the transition reported above is a non-linear effect, as opposed to an inelastic response.

High-temperature, uniaxial tensile tests have been used to generate data for PET, which has been analysed according to a power law deformation model previously proposed for thermoformable plastics (3,4). For PET, the overall validity of the model is limited due to the onset of strain-induced crystallisation. We propose that low-strain behaviour be separated from the post-crystallised response, of which a high 'Strain-Crystallisation Index' (n') reflects the propensity to form crystalline order; n' decreases with increasing sheet temperature, and varies from 7.7 to 3.1 over the range 80-110 °C.

PRACTICAL PROCESSING STUDIES

Practical ISBM studies were carried out on a Sidel machine producing 2-litre containers from 47g preforms. Commensurate with the predicted data from the extensional rheometer, the major effects of increasing inflation rates were to enhance various mechanical properties in the hoop direction, and significantly, to increase the thickness distribution uniformity, thereby promoting increased column buckling stability.

An extensive series of Thermoforming experiments showed the dependence of part thickness uniformity upon sheet, mould and plug temperatures and the effect of the draw depth (strain magnitude). For draw ratios exceeding 2:1, the thickness distribution parameter illustrated in Figure 2 is primarily determined by sheet temperature; for shallow draws, thickness distribution is generally inferior, and is a more complex function of processing conditions.

REFERENCES

(1) Munstedt, H; J. Rheol. 23, 421-436, 1979.
(2) Meissner, J; Trans. Soc. Rheol. 16, 405-420, 1972.
(3) Lai, M.O. & Holt, D.L; J.Appl.Polym.Sci. 19, 1209-1220, 1975.
(4) Lai, M.O. & Holt, D.L; J.Appl.Polym.Sci. 19, 1805-1814, 1975.

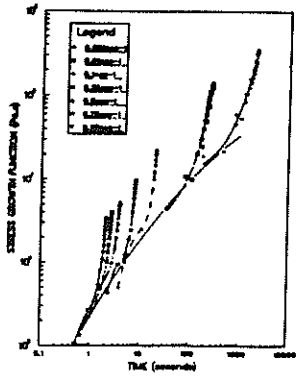


FIGURE 1 PET DEFORMATION DATA AT 100 °C

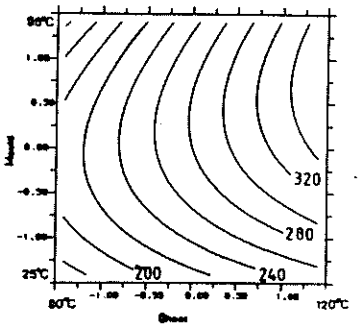


FIGURE 2 THICKNESS DISTRIBUTIONS IN THERMOFORMED PET CONTAINERS

16/3

FINITE ELEMENT SIMULATION OF INJECTION MOLDING

M.J. Crochet, F. Dupret

Unité de Mécanique Appliquée
Université Catholique de Louvain
Place du Levant, 2
1348 Louvain-la-Neuve, Belgium.

A program developed in our department is devoted to the numerical simulation of injection molding. The non-isothermal filling of thin flat molds of arbitrary shape is predicted for power-law fluids, using the Hele-Shaw approximation (which allows neglect of the pressure variation in the gap direction).

In view of the time-dependent flow region during filling and the transient heat exchanges occurring within the polymer, the problem is transient and the computational domain is changing with time. Even with thin cavities, the problem is also three-dimensional because the temperature gradient in the gap direction is important compared to its counterpart in the mid-surface directions.

We obtain an accurate description of the pressure, velocity and temperature fields, and also the moving melt fronts, by solving the set of partial differential equations describing the physics of the flow. More precisely, the mass equation provides an elliptic equation on the pressure field, whilst the energy equation provides a 3D transient parabolic equation on the temperature field. The shape of the moving front is calculated as a function of time from the gap average velocity at the front (the latter being proportional to the front pressure gradient).

An important difficulty lies in generating after every time increment an appropriate finite element mesh covering the filled part of the mid-surface. Our approach is to select at the outset a fixed mesh which covers the whole flow domain. During filling, the front moves through the fixed mesh, while the program generates a temporary mesh using as many elements as possible from the original one. The remaining elements are generated in order to obtain a well-behaved temporary mesh.

Pressure discretization is performed at the successive time steps using classical Lagrangian quadratic or biquadratic shape functions. As the problem is non-linear because of the dependence of viscosity upon shear rate, we resort to Newton's method for obtaining the solution.

A second difficulty lies in calculating the temperature field. Thermal exchanges have an influence on the velocity profile and may affect the front motion, since the polymer viscosity is temperature dependent and since partial solidification generally occurs near the cold walls of the cavity. We discretize the temperature field by using Lagrangian finite element interpolants in the mid-surface directions, while Chebyshev polynomials constitute the approximation in the gapwise direction. Discrete equations are obtained by use of the Galerkin method combined with a collocation procedure. Time integration is performed by means of a third order mixed explicit-implicit scheme, in order to ensure stability and precision.

Special attention is focused on the influence of the fountain flow (occurring at the front) on the temperature field. As non-negligible heat advection in the gap direction is observed in the front region of the flow, a suitable front thermal boundary condition must be introduced, in order to avoid undue heat losses at the front.

Several examples have shown the performance of the program. More recent investigations deal with the simulation of partial solidification during filling and with the filling of box-like thin objects.

References

[1] Williams & Lord, Polym. Eng. Sci. 15(8), 553-582 (1975).
[2] Hieber & Shen, J. Non-Newt. Fluid Mech. 7(1), 1-32 (1980).
[3] Couniot & Crochet, NUMIFORM Conf., 165-170 (1986).
[4] Vanderschuren & Dupret, NUMIFORM Conf., 199-204 (1986).

Mechanical stability of gas/liquid foams

H. Mainecke and M.H. Pahl
Mechanische Verfahrenstechnik, Universität(GH) Paderborn, West Germany

Foam is characterized as a disperse system consisting of liquid or solid substance with a high gas hold up. Foams result from a mechanic gas entry with mixing apparatures or by expansion of physical or chemical propellants. Solid plastic foams can be characterized in such way that the liquid structure consolidates after the formation of foams. The formation of the foam structure from liquid plastic is critical. To describe the stability of the fuam in this phase more exactly, tests have been made with soap foams.

If you look at the foam as a micro system, a differentation of the foam structure by the gas hold up 'φ' is possible. Such foam system are called:

$\varphi > 0{,}74$ as 'Polyederschaum'
$0{,}52 \leq \varphi \leq 0{,}74$ as 'Kugelschaum'
$\varphi < 0{,}52$ as gas dispersion

The real geometry of the 'polyederschaum' can be described except 3 vol % where the lamella form a pentagonal polyeder with two surfaces. The Lamella strike together with an angle of 120 degree and form the triangular plateau border. As a result of the radius of curvature a capillary pressure is caused which effects a drainage of the lamella liquid in the plateau border. By this the lamella consistency decreases up to a critical value, where the lamella burst (cell bursting). Equations for the realization of the connections between the lamella consistency, radius at the plateau border, bubble diameter and liquid hold up are given.

The stability of the foam bubbles is defined by the drainage behavior of the liquid, the interactions in the lamella, the capillary pressure as well as the system pressure resp. hydrostatic pressure and the gravity.

The drainage of the lamella is described with the model for squeeze flows from parallel plates and the drainage from the plateau border as a chanal flow.

The interpretation of the flow and deformation processes in the foam system during the expansion results from high speed films at a flow channel. These proceedings can be described with a two-dimensional modal. 'Kugelschäume' with a gas hold up $\varphi \leq 0{,}74$ and gas dispersions show rheological behavior analogous to suspensions rheological. The 'Polyederschaum' that is poor of liqid ($\varphi > 0{,}74$) shows peculiar mechanism.

The flow behaviour e. g. in the flow channel separates into a wall stick/slip effect and a slip between the cells. For the characterization of the foam stability with mechanical strain yield boundary, foam viscosity and foam elasticity have been determined by volume strain in a defined shear distance. The deformation of the foam system e. g. during the expansion procedure results in a burst of single lamella, where the degree of dispersion in the foam changes and the elastic characteristics of the lamella become effective.

For the explanation of this burst mechanism high speed films were made with circular single lamella. For the mechanical strain, drops from true to type liquid were put onto the lamella with different speed. The burst of the lamella is a based on a critical expansion speed for the used stuff system and lamella density where the lamella are not stabilized by liquid movements as a result of the Gibbs and Marangoni effect.

16/5

NUMERICALLY STABLE FINITE ELEMENT TECHNIQUES FOR VISCOELASTIC CALCULATIONS IN SMOOTH AND SINGULAR GEOMETRIES, Robert C. King, Minas R. Apelian, Robert A. Brown, and Robert C. Armstrong, Department of Chemical Engineering, Massachusetts Institute of Technology, Cambridge, MA 02139, USA.

Finite element calculations of viscoelastic flows are reported that use a restructured form of the momentum equation for an Upper-Convected Maxwell (UCM) model which makes explicit the elliptic character of this equation. Sets of mixed-order approximations for velocity, stress and a modified pressure are used to test the algorithm for the flow between eccentric rotating cylinders and the stick-slip problem. Calculations using Galerkin's method to discretize both the Explicitly Elliptic Momentum Equation (EEME) and the constitutive equation yield solutions which converge with mesh refinement for the flow between eccentric rotating cylinders. Calculations for the stick-slip problem are reported for a Modified Upper-Convected Maxwell (MUCM) model for which the stress field shows Newtonian growth near the singularity; the results with the EEME formulation converge with mesh refinement. Both sets of calculations are limited at high values of the Deborah number by the formation of elastic boundary layers that are identified in the momentum equation by the growth of low-order derivative terms that involve velocity gradients and the local divergence of the stress. Similar convergence is seen in calculations which use either bilinear or biquadratic Lagrangian approximations to the components of stress, although computations with the biquadratic basis are very sensitive to the weighted residual method used for the constitutive equation in the eccentric cylinder problem. Streamline-Upwind Petrov-Galerkin (SUPG), and artificial diffusivity (AD) formulations of the constitutive equation are tested for solution of both problems by calculations of the stress fields with fixed kinematics and by solution of the coupled problem. The SUPG method improves the performance of the calculations with the QQL basis set for the eccentric cylinder problem by removing a mode for spatial oscillations at high De. For calculations with the UCM model, adding artificial diffusion to the constitutive equation in the stick-slip problem changes the dominant balance for the stress field near the singularity, making it appear as an integrable stress approximation for fixed mesh. The Newtonian-like growth of the stress near this point for the MUCM model is recovered with the AD method and calculations converge to moderate De.

TGMOLD: A Computational Approach For Modelling The Non-Isothermal Flow During Injection Molding

S.Subbiah and S. I. Güçeri
Center for Composite Materials,
Department of Mechanical Engineering,
University of Delaware, Newark, Delaware 19716.

A numerical grid generation scheme is used for modelling the non-isothermal, non-Newtonian flow of polymer melts in thin-walled mold cavities of arbitrary shapes. The Hele-Shaw approximations are used to simplify the general flow equations to 2-dimensional planar flow. The non-isothermal nature of the flow is modelled using a temperature and shear-rate dependent viscosity model. The temperature distribution in the flow field is calculated using a three-dimensional, transient approach while a psuedo steady-state approach is used to predict the free surface locations.

The arbitrary shapes of the fluid as it flows through the mold cavity are analyzed exactly (without interpolation) by generating a mesh that envelopes the current fluid domain completely at every timestep. The curvilinear mesh is generated numerically by mapping the irregular flow domain to a more regular shape in a computational domain. The governing equations are transformed and solved in the computational domain using well-developed finite-difference methods. The point-wise solutions obtained are then mapped back to the flow domain.

Elliptic, Poisson-type equations are used to generate the mesh due to their inherent 'smoothness' and ability to handle boundary discontinuities. This scheme requires only the specification of the boundaries of the mold cavity and all the necessary meshes are self-generated to follow the fluid as it fills the cavity. Such a mapping uses the free surface itself as one of the boundaries, thus obviating the need for local interpolation here. At each time step, the previous mesh is used as the initial guess for generating the new mesh, and this facilitates rapid mesh generation.

For the temperature field, convection is considered to be the dominant heat transfer mechanism in the mold plane, while conduction is considered dominant through the gapwidth. The fountain flow occurring at the free surface is partially accounted for by setting the temperature of the free surface to be equal to the temperature of the fluid element at the mid-plane immediately behind the melt front. The Carreau equation is used to model the non-Newtonian behavior of the polymer melt and an Arrhenius term is used to model the temperature dependance of the viscosity.

The point-wise velocities obtained from this simulation were used in conjunction with **FIBOR**, a program that integrates Jefferey's equation along the streamlines to predict the fiber orientations in dilute suspensions of short fiber reinforced melts.

The results were compared with analytical solutions and experimental observations, indicating good accuracy. The method described here has been developed into a code **TGMOLD** that is available from the University of Delaware.

Ref: "Non-Isothermal flow of polymers into two-dimensional, thin cavity molds: A numerical grid generation approach", S. Subbiah, D. L. Trafford and S. I. Güçeri, to be published in the Journal of Heat and Mass Transfer.

P1

DIRECT OBSERVATION OF MOLD FLOW UNDER HIGH INJECTION PRESSURE AND SPEED

H. Yokoi, T. Hayashi and Y. Murata
Institute of Industrial Science, University of Tokyo
7-22-1 Roppongi, Minato-ku, Tokyo 106, Japan

A real-time observation of the processes taking place inside an injection mold is thought to be a quite effective method to concretely investigate these processes. In this study we developed a testing mold for the direct observation of the behavior of molten plastics flowing inside a cavity. The proposal testing mold has the advantage of being practical and easily usable on a conventional injection machine.

The original system developed for direct observation under high injection pressures and high speed conditions consists of a glass-inserted metal mold and a CCD camera with syncronous stroboscopic units. The glass-inserted metal mold was constructed from standard mold parts, can be set on a usual injection machine, and works under usual injection pressures.

As shown in Fig.1, a glass prism is inserted into a hole in a metal mold to work as the core. One face of the prism meets a cavity and another face

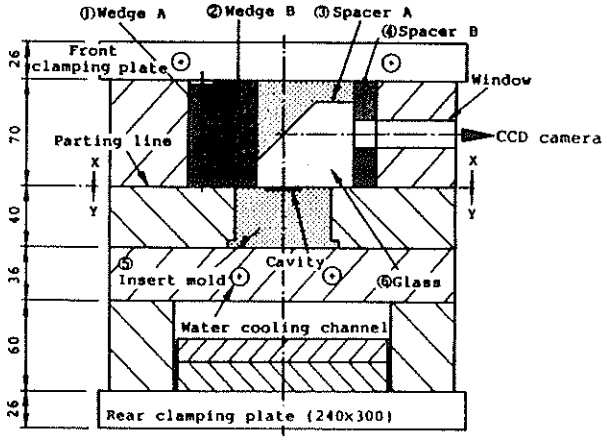
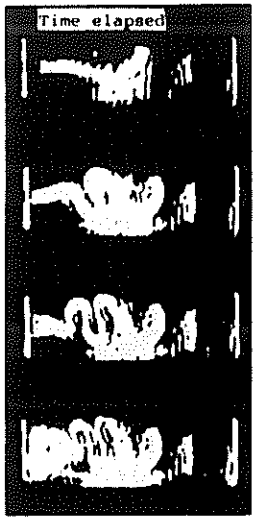


Fig. 1 Fundamental structure of the glass-inserted metal mold



◀Fig. 2 Observation of jetting phenomena(POM)

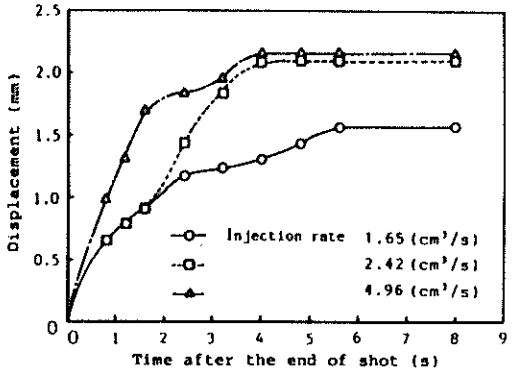


Fig. 3 Flow front behavior during cooling process (POM, cavity:25x65x2mm, side gate)

meets a window in the side wall of the mold, so that images from inside are reflected at the oblique face and picked out from the window parallelly to the parting face of the mold. The prismatic block is fixed by two sets of wedges under a certain pre-compression force. The hydrostatic stresses generated during the injection process prevent the brittle glass block from breakage. This device permits the observation of the filling of the mold cavity by the molten material coming from the gate and also the obervation of the cooling process.

Using this device we succeeded in observing jetting phenomena (Fig. 2); the generation of weld lines under high pressure (polymer pressure is 30-80 MPa inside the cylinder) and an injection time of less than 0.5s; and the gradual progress of the flow fronts of short shots during the cooling process in the mold (only in the case of crystalline polymers, Fig. 3). These results show the potentiality of this device as a readily available and practical testing mold for the analysis of injection molding defects, for the evaluation of machine performance or for the verification of numerical simulation results.

P2

TWO-LAYER FLEXIBLE PRINTED CIRCUITS USING LOW THERMAL EXPANSION POLYIMIDES

J.Imaizumi*, K.Nagao*, H.Nomura*, E.Satoh*, M.Katoh*,
S.Numata**, and N.Kinjo**
*:Goshomiya Works, Hitachi Chemical Co., Ltd.,
1150 Goshomiya, Shimodate-shi, 308 Japan
**:Hitachi Research Laboratory, Hitachi, Ltd.,
4026 Kuji-cho, Hitachi-shi, 319-12 Japan

An epoch making metal clad film (MCF) for flexible printed circuits (FPCs) have been cooperatively developed by Hitachi Chemical Co., Ltd. and Hitachi, Ltd. It consists of only two layer, a low thermal expansion polyimide and copper without an adhesive, and it can be simply manufactured, by a direct coating method.

This new type MCF(MCF-5000I) has desirable properties of high heat resistance, high folding endurance, high dimensional stability, nonflammability and excellent stabilities for its mechanical and electrical properties.

In general, organic polymers including polyimides have high thermal expansion coefficients ($> 3 \times 10^{-5} K^{-1}$) compared with inorganic materials ($< 2 \times 10^{-5} K^{-1}$). So, thermal stress due to the difference in their thermal expansion coefficients produces many problems when organic polymers are combined with inorganic materials. In an investigation of the relationship between chemical structure and thermal expansion coefficient for various polyimides, several low thermal expansion polyimides were discovered. Their thermal expansion coefficients were almost the same as inorganic materials.

The MCF (MCF-5000I) is one useful application of the low thermal expansion polyimides. Its advantages are as follows:

1) The manufacturing process can be simplified.

The MCF (MCF-5000I) is manufactured by a direct coating method of coating polyamic acid (precursor of polyimide) solution onto copper foil, followed by drying and heating to complete the imidization reaction. The problems of warping in MCF due to thermal stress can be solved, because the thermal expansion coefficient of polyimide can be controlled easily to match that of copper foil. Therefore, the number of manufacturing steps can be decreased from six to three.

2) High performance MCF and FPCs are obtained.

Conventional MCF has been obtained by lamination of polyimide film and copper foil with adhesive, so the properties are significantly affected by the adhesive which causes the deterioration of the properties. On the contrary, when the low thermal expansion polyimide is used, the new type MCF without the adhesive layer can be obtained. Table 1 shows the comparison of the conventional MCF and newly developed MCF.

Table 1 General properties of new type MCF (MCF-5000I) and conventional one

Items		MCF-5000I	Conventional type
Thermal			
Soldering stability		400°C/1min.	260°C/1min.
Glass transition temp.	°C	420*	390
Thermal index(UL-746)	°C	105*	105
Flammability (UL-94)	-	V-0	-
Dimensional stability			
Thermal (300°C/30min)	%	0.17	0.36
Humidity	$\times 10^{-5}$ RH%	1	2.3
Mechanical			
Tensile strength	MPa	250	165
Tensile elongation	%	30	70
Modulus	GPa	5.9	3.5
Folding endurance	Times	120	70
Peel strength at RT	kg/cm	2.5	1.5
at 200°C	kg/cm	1.6	0.1
Electrical			
Insulation resistance		10^{13}	10^{13}
Dielectric constant		3.2	3.5
Dissipation factor		0.035	0.04

*:Provisional recognition (Target recognition : 180°C)

P3

PROPERTIES OF WELD LINE IN INJECTION MOLDING PARTS

Hiroyuki HAMADA* Zenichiro MAEKAWA* and Kiyotaka TOMARI**
* Faculty of Textile Science, Kyoto Institute of Technology
Matsugasaki, Sakyo-ku, Kyoto, Japan 606
** Osaka Municipal Technical Research Institute
Morinomiya, Joto-ku, Osaka, Japan 536

INTRODUCTION

Weld line or knit line must be generated in complicated injection molded parts. It reduced the mechanical properties and the other properties of the moldings because it changed the morphological structure. Our previous reports show that the strength of fiber reinforced polycarbonate molding is reduced more than 50%. It is well known that the strength reduction due to weld line is often caused by the V-notch effect on the surface of the molded parts. And for transparent polymers such as polystyrene (PS) weld line looks like a crack, that is a serious problem when it is used for an exterior part. In this study, the influence of molding conditions on the tensile strength of PS samples with weld line is examined. The quantitative method to measure the size of the V-notch can be established. Further, the effective methods to improve the mechanical weakness and the defects of external appearance of weld line are discussed.

EXPERIMENTS

Two types of experiments are carried out in this investigation.

(EXPERIMENT 1) Dumbbell type tensile test specimens either with or without weld line are molded under several molding conditions. The injection pressure is controlled in two step. The filling pressure (Pf) is altered to the holding pressure (Ph) when two melt fronts meet together. Pf and Ph are based on the minimum filling pressure (M.F.P.). Cylinder temperature is 180°C and mold temperature is 40°C. The variation of the strength with cutting the surface of the molding and removing weld line by a milling machine is measured.

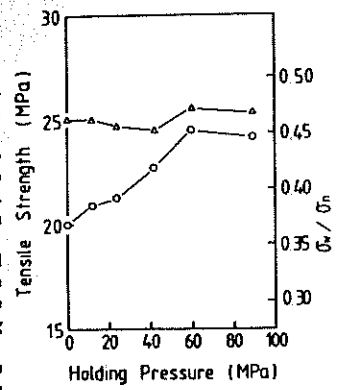


Fig. 1
Relationship between tensile strength and holding pressure, Filling pressure ○:41.9MPa, △ :59.8MPa.

(EXPERIMENT 2) The samples molded in this experiment are thin rectangular plates (200*100*3mm) with weld line at the center. The ceramic heater is buried in the middle of the cavity. The weld line region is rapidly heated and cooled by the heater during injection molding and then the width of weld line is measured by using microscope. The voltage supplied to the heater is 0, 20, 40, 60, 80, 100v. Cylinder temperature is 200°C and mold temperature is 40°C. The injection pressure is 125.5MPa.

RESULTS AND DISCUSSIONS

EXPERIMENTS 1 shows the results as follows.

1) Weld line strength and molding conditions

Fig. 1 shows the relationship between weld line strength and injection pressure. Weld line strength is independent on the holding pressure when the filling pressure is 59.8MPa. The ratio of the strength of the sample with weld line to the one without weld line is about 45%. When the filling pressure is 41.9MPa, the strength is the minimum at Ph=0 and increases linearly with increasing the holding pressure. More than about 58.8MPa it becomes constant value, which is equal to the one at Pf=59.8MPa. The strength is getting higher with rising the filling pressure. The reason is considered to be that melt fronts can fuse sufficiently as the flow rate increased at high pressure.

2) Measurement of the "Depth of weld line"

Fig. 2 shows the relationship between the depth of cut (Dc) and the tensile strength. The strength increases with increasing the depth of cut (max. about 50%). The V-notch is perfectly removed with cutting more than certain amount and the strength can not rise any more. The saturation point is defined as the "Depth of weld line". The improvement of the strength, however, is limited only by removing the V-notch. The relation between injection pressure and the depth of weld line is indicated in Fig. 3. The depth is constantly about 0.2mm at the higher filling pressure (59.8MPa). On the other hand, at the lower filling pressure (41.9MPa), it changes from about 0.3mm to 0.2mm with increasing the holding pressure. That tendency corresponds to the relationship between the injection pressure and weld line strength.

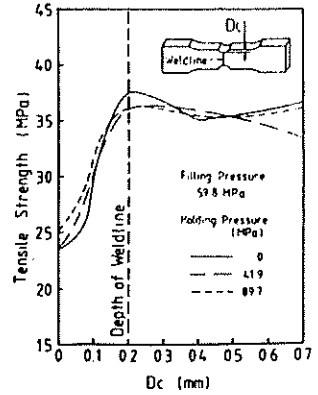


Fig. 2
Relationship between tensile strength and depth of cut(Dc), Filling pressure : 59.8MPa.

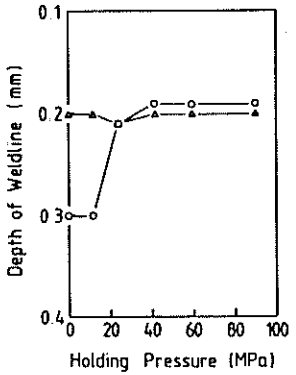


Fig. 3
Relationship between holding pressure and depth of weld line, Filling pressure ○:41.9MPa, △ :59.8MPa.

EXPERIMENTS 2 shows the result as follow.

3) Elimination of weld line

The width of weld line decreases linearly when the voltage increase 0 to 60v and weld line is eliminated perfectly over 60v. The eliminated line is about 25mm long and it is equivalent to the heat generating zone of the heater. This indicates that weld line disappears instantaneously only at the heat generating zone.

P4

STUDIES ON FIBRE DEGRADATION DURING COMPOUNDING AND INJECTION MOULDING OF CARBON, METAL AND GLASS FIBRE FILLED THERMOPLASTICS

B. Franzén, C. Klason, J. Kubát, Polymeric Materials Dept., Chalmers University of Technology, S-412 96 Gothenburg, Sweden.

The mechanical parameters of parts manufactured from short-fibre reinforced thermoplastic composites are determined by the length distribution of the fibres. Since the fibres suffer severe damage during the compounding steps their ultimate length in the finished part is usually only a fraction of the initial value. This investigation reports on the fibre degradation process in two types of compounding machinery (Buss CoKneader, ZSK twin-screw extruder), and during subsequent injection moulding in a conventional machine. The bulk of the results relates to low-density polyethylene (LDPE) containing metal fibres (aluminium and brass, AF and BF). In some additional experiments, polymers reinforced with carbon fibres (CF) and glass fibres (GF, 10 mm) were used.

Pronounced fibre degradation was observed in the melting zone of the compounding extruders. In fact, the passage of the compound along the rest of the compounding screw and the subsequent injection moulding operation resulted in relatively minor additional fibre length reduction. CF suffered more severe degradation than the other two fibre types, the average lengths in the injection moulded test bars being 0.2, 0.8, and 0.6 mm for CF, AF, and BF, respectively.

When the fibre component is added to the melt, fibre breakdown takes place directly in the melt, and some further damage occurs during passage to the die and in the die.

The fibre length distribution was characterized by the ratio L_w/L_n, where L_w and L_n denote the weight and number averages, respectively. In spite of the difference in properties between the metal (diameter 90 μm, initial length 2-4 mm) and carbon fibres (diameter 7 μm, initial length 2-5 mm), the ultimate L_w/L_n ratio was found to be 1.3 ± 0.2 regardless of the processing conditions. A value of 1.4 has been reported earlier for distributions resulting from length reduction processes where the fracture occurs in the middle of the fibres (1). This may be associated with buckling in the flow field proposed by Forgacs and Mason as a possible fracture mechanism (2-4). For the metal fibres, however, the buckling stresses are too high; they cannot be related to the shear field acting upon the fibres.

A certain degree of phase separation during mould filling was reflected in a fibre concentration gradient along the length of the test bars. The variation in fibre content could amount to several percent.

With regard to the mechanical parameters of the moulded test bars, the modulus showed the expected increase with fibre content. The modulus values were compared with the predictions of the Tsai-Halpin formula. For the metal fibres agreement was good, while the rigidity of the CF/LDPE material was significantly above the theoretical value. An increase in the orientation of the matrix due to the high viscosity of the filled melt appears to provide a plausible explanation for this difference. The creep behaviour of the filled systems has also been studied.

References

1) R. Meyer et al., Brit J Appl Phys, 17, 409 (1966)
2) O. Forgacs et al., J Colloid Sci 14, 457 (1959)
3) L. Czarnecki et al., J Appl Polym Sci, 25, 1217 (1980)
4) A. Salinas et al., Polym Eng Sci, 21, 23 (1981)

P5

PLASTICS MACHINERY CONTROL SYSTEM PMC-1000

Axel Seidensticker, Philips GmbH, Kassel, West Germany
Pyrometer Instrument Company
Northvale, NJ

The PMC-1000 was developed by the Industrial Automation Division of Philips in 1982-84 in cooperation with two major German OEM's and the Philips Plastics Processing Division. You may already know that Philips is also one of the worlds largest Plastic Processors with over 1000 plastic machines used to manufacture a wide variety of plastics parts from the miniature laser pick-up lens for Compact Disc Players to large housings for television sets. The PMC-1000 was developed solely for Plastics Machinery control--Injection Molding, Blow Molding and Extrusion, based on the years of experience in this field by both the electronics and plastics processing specialists at Philips.

Some of the attractive features of this system are:

- Sensitive profiling (in 64 steps) of hose thickness on continuous or storage-head blow molders with partial (non symetric) wall-thickness control (complex blow molded parts--e.g. fuel tanks). With continuous extrusion, for example, the T-Profile Card ensures a time-dependent profile with high resolution. Other functions provided by this card are pre-set zero shift, profile synchronizing, and "interrupts" at selectable points of the profile.
  For blow molders with discontinuous (accumulator head) parison extrusion, the S-Profile Card provides a time-dependent profile with very fine graduation and high resolution. For this, the annular slit is adjusted as a function of the piston position. Piston speed is controlled exactly and can also be profiled.
  By means of preselected set-value profile for special deforming cylinders, very precise variations in the partial wall-thickness of the parison are possible. This enables optimum wall-thicknesses to be achieved with a minimum of material; even with very unsymmetrical moldings.
  Similarly, preselected set-value profiles are possible for the mandrel cylinder. Profile synchronization can be triggered by various operating modes, e.g. with parison pre-forming or direct-starting. The "interrupt" points along the profile are freely selectable.
- Absolute position measurement with ultrasonic sensors and high resolution of 0.1mm (0.0039"). Because the system is based on absolute measurement, there is no need for re-calibration after a power failure; the sensor "always knows where it is". Furthermore, uncritical mounting tolerances between ring magnet and measurement tube allow simple installation in any position.
- Precise closed loop speed control of mold, ejector piston in accumulator head, blowing and stretching mandrels.
- Autonomous closed loop controls for acceleration and braking of various movements for optimized time and/or energy requirements.
- Process temperature control (DPID behavior) with multi-loop micro-processors.
- Self-diagnosis of function modules, plausibility checks and individual alarms in clear text.
- Four channel full graphics.

P6

EFFECT OF AGING CONDITIONS ON THE MECHANICAL PROPERTIES OF WOOD FIBERS FILLED POLYSTYRENE COMPOSITES

P. Maiga, M.Sc., and A. Cole, University of Quebec in Three Rivers, C.P. 500, Three Rivers, Quebec, Canada, G9A 5H7

The wood-based fillers are potentially attractive reinforcements, because they are cheap, light, flexible, strong and renewable source. Unfortunately, the polar nature of these fillers affects adversely the adhesion to the nonpolar thermoplastic matrix. Among the various methods to improve the compatibility between cellulose and pastic matrices are the treatment with coupling agents (e.g. isocyanate) and pre-coating or grafting of the fibers with coupling agent and/or corresponding polymer.

The mechanical properties and dimensional stabilities of non-treated and treated (e.g. 3% poly (methylene (polyphenyl isocyanate)) (PMPPIC); fibers coated with 10% polymer + 8% PMPPIC or grafted with 89,1% add-on of polystyrene) composites of high impact polystyrene (PS 525) and chemithermomechanical pulp (CTMP; hardwood aspen) were evaluated under various aging conditions : a) testing at different temperatures varied from +25 °C to -40 °C; b) testing after immersion in boiling water for different times varied from 3 hours to 24 hours and c) testing after exposure to heat at 105 °C for different duration varied from 1 day to 5 days.

Both the stress and modulus rise linearly with the decrease of testing tempure but elongation and energy follow the reverse trend. The mechanical properties except modulus increase only when composites are immersed under hot water for shorter duration of time (say, 3 hours). On the other hand, all the properties are deteriorated due to the longer period of immersion. The water uptale value as well as cross section area increase linearly associated with immersion time. But, the treated composites show better dimensional stability compared to non-treated fiber-filled composites.

Likewise, when attention was paid to the effect of heat exposure, it is observed that the mechanical properties particularly for treated composites are enhanced compared to values at ordinary condition. Dimensional stability under this condition also supports this observation. Table 1 illustrates the comparative mechanical properties of treated and PMPPIC treated composites under all the aging conditions.

Table 1. Variation of Mechanical Properties under Different Aging Conditions

Treatment	Change % with respect to properties at room temperature								
(Aging Conditions)	Testing temperature (° C)			Immersion in water (hrs)			Heat Exposure at 105 °C (days)		
	0	-20	-40	3	12	24	1	2	5
				STRESS					
Polystyrene	+41,1	+73,2	+106,0	+0,6	-0,6	+0,6	-7,7	-10,7	-12,5
Non-treated	+53,4	+54,7	+44,0	-40,8	-45,8	-45,8	-3,0	-2,2	-7,2
3% PMPPIC	+45,4	+81,2	+86,3	+4,1	-6,0	-15,6	+6,0	+11,9	+6,9
				ELONGATION					
Polystyrene	+26,7	+40,0	+200,0	+6,7	+13,3	+13,3	+20,0	+26,7	+20,0
Non-treated	+111,8	+58,8	+41,2	+52,9	+41,2	+47,1	+47,1	+52,9	+35,3
3% PMPPIC	+14,7	-3,0	-26,5	+11,8	+17,7	+41,2	+14,7	+11,8	+8,8
				MODULUS					
Polystyrene	-2,1	-7,1	-9,9	-4,9	-8,5	-9,2	-5,6	-9,9	-12,0
Non-treated	+6,6	+12,7	+24,4	-34,0	-38,6	-41,6	+3,6	-13,2	-13,7
3% PMPPIC	+2,9	+10,9	+38,3	-13,7	-22,9	-30,9	+1,1	+10,3	+2,9

The more resistance of the treated wood fibers-filled composites under different aging conditions suggests the formation of an efficient interfacial area between the fiber and the polymer matrices.

P7

Orientation Effects on the Dynamic Mechanical Properties of Polyurethane Thermoplastic Elastomers

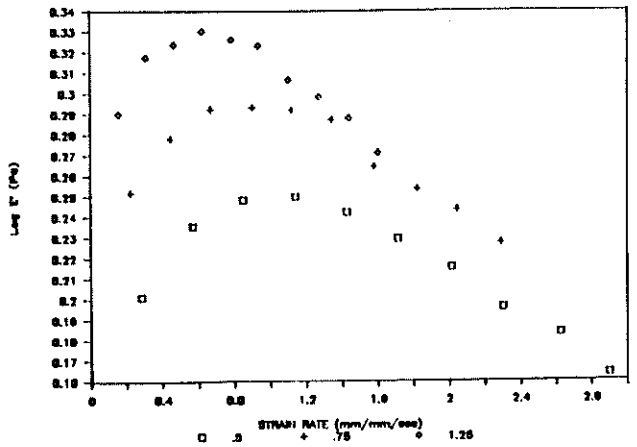
D. Bennett and C.L. Beatty, Univ. of Fl., Gainesville, Fl.

Introduction: The stress-strain behavior of polymers are known to be rate sensitive. This rate sensitivity is the basis for time-temperature superposition and the ability to create master stress-strain curves from short duration tests and appropriate shift factors. There is, however, a range of strain rates outside of which the time-temperature superposition does not hold. An upper bound exists where increased strain rate no longer results in increasing modulus but rather results in decreasing modulus with increasing strain rate. Recently Liu and Harrison showed that there is a critical draw rate for a polymer after which the time-temperature superposition principle no longer holds (1). Their results showed that with increasing draw rate beyond this limiting draw rate their is decreasing Young's modulus and yield stress.
It would therefore be expected that there exists a functional dependence of this limiting draw rate, viz strain rate, on the initial conditions of the specimen (offset strain and ambient temperature). In particular, results of this study found that there was an inverse relationship between the limiting strain rate for time-temperature superposition and both offset strain and temperature.

Experimental: The polymers used were polyurethane based elastomers, Pellathane 2103-55DE and 2103-80AE, both manufactured by Dow Chemical Company. The test samples were compression molded following the manufacturers specifications. Modulus vs. strain rate data were generated on a MER 1000 (Instrumentors) by subjecting the sample to a sinusoidal tension-tension displacement while varying the offset strain and ambient temperature.

Results and Discussion: A comparison of the modulus versus strain rate curves for different offset strains revealed that with increasing offset strain (extension ratio) there was a corresponding decrease in the limiting strain rate (Fig 1). The transition between the regions of linear viscoelastic behavior (low strain rates) and non-linear behavior (high strain rates) could be identified by the maximum in the modulus versus strain rate curve. This transition appeared gradual suggesting that the internal heating which is responsible for the strain rate limit for linear behavior also affects the behavior of the material at lower strain rates although to a lesser degree. A similar inverse relationship was found to exist between the strain rate limit and increasing temperature.

Conclusion: For the polyurethane system studied there exists a limiting strain rate above which the effects of internal heating of the material control the shape of the modulus vs. strain rate curve. This internal heating is in accordance with the thermodynamics of rubber elasticity and represents an important aspect which must be considered in the application of rubbery systems. Thus, this limiting strain rate, below which the time-temperature superposition and the linear viscoelasticity hold more precisely, could be used by the designer as a valuable guideline.



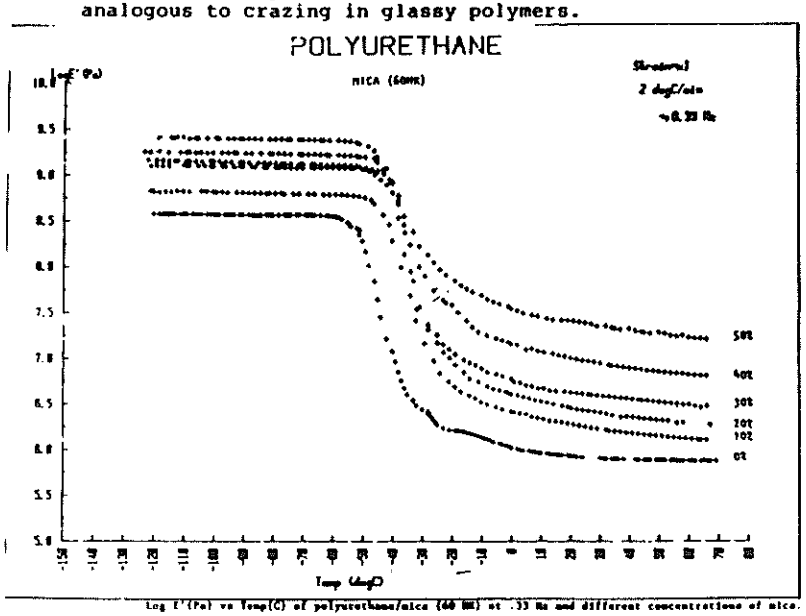
Figureb 1 Modulus Strain rate sensitivity as a function of extension ratio, .

Reference
1. Liu, T. and Harrison, I.R., Polymer, Vol. 29, 233

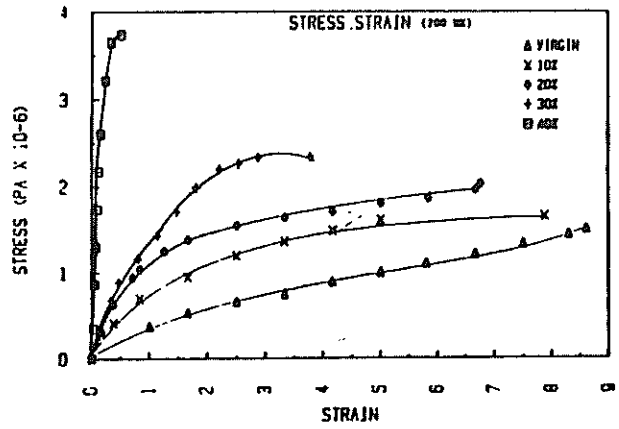
P8

Dynamic Mechanical Properties and Stress-Strain Behavior of Polyurethane Mica Composites.
K. Chehab, and C.L. Beatty, University of Florida, Gainesville, Fl. 32611.

A series of compression molded polyurethane composites were prepared with 60 and 200HK mesh mica. Filler concentration ranged from 10 to 50 wt%. The influence of mica flake sizes, concentration, surface area and orientation on dynamic mechanical and tensile stress-strain properties was investigated using a Polymer Laboratories Dynamic Mechanical Thermal Analyzer (DMTA), and an Instron Deformation System model 1125. The flexural and tensile modulus increases for the small size particles and decreases for the large size particles even at low concentrations of mica, where as the percent elongation decreases for both mica sizes with increasing mica content. table 1. Molecular weight between entanglements varied from 1.531 to 1.828 Kg/mole for the small size particles (200hk) and from 1.201 to .121 Kg/mole for the large size particles (60HK). Glass transition temperatures of the soft segment increased from -42 degree celsius for the unfilled to -27 and -26 for 50 wt% small and large size mica flakes respectively. Careful observations of tensile deformation of the samples clearly shows that large mica filler samples exhibit delamination and whitening analogous to crazing in glassy polymers.



Log E'(Pa) vs Temp(C) of polyurethane/mica (60 HK) at .33 Hz and different concentrations of mica.



Tensile stress-strain graphs of polyurethane/mica flakes of 200 HK grade at different concentrations.

MICA

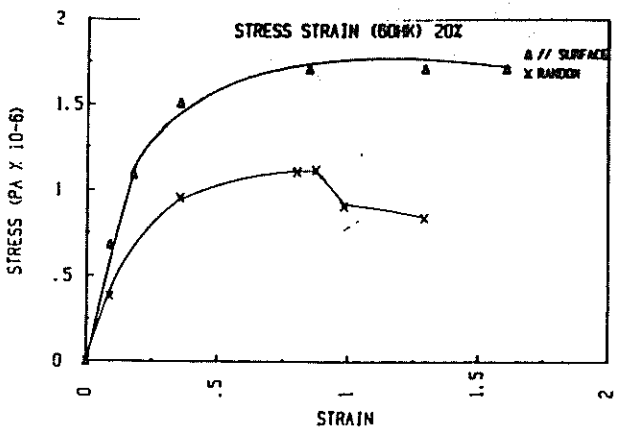
Designation Code	Average Flake Diameter	% mica	Tensile E(Pa) at 25°C	Flexural E(Pa) at 25°C	Parallel Tensile E(Pa) at 25°C	Random Tensile E(Pa) at 25°C	Random Flexural E(Pa) at 25°C
200HK	74 micron	virgin	$.374\times10^6$	0.5×10^5	---	---	---
		10	1.09×10^6	1.75×10^6	---	---	---
		20	1.89×10^6	2.63×10^6	3.0×10^6	2.89×10^6	2.2×10^6
		30	2.06×10^6	4.63×10^6	---	---	---
		40	10.5×10^6	6.77×10^6	---	---	---
		50	---	8.54×10^6	---	---	---
60HK	250 micron	10	1.08×10^6	2.28×10^6	---	---	---
		20	3.9×10^6	3.61×10^6	7.01×10^6	4.33×10^6	1.75×10^6
		30	16.4×10^6	5.30×10^6	---	---	---
		40	7.18×10^6	1.2×10^7	---	---	---
		50	---	3.01×10^7	---	---	---

P9

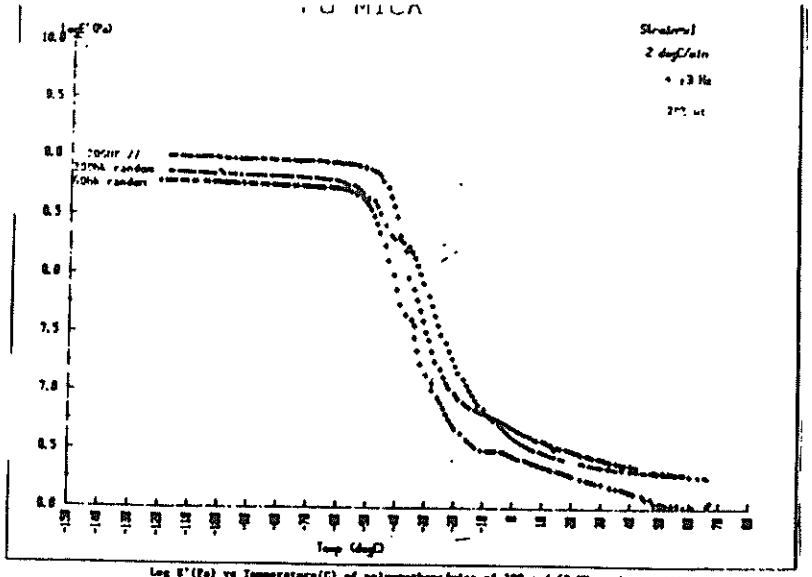
Mica Flake Orientation Effects on Dynamic Mechanical Properties of Polyurethane Mica Composites.

A. Hoelzer, K. Chehab, S. R. Bates and C.L. Beatty, Univ. of Fl., Gainesville, Fl.

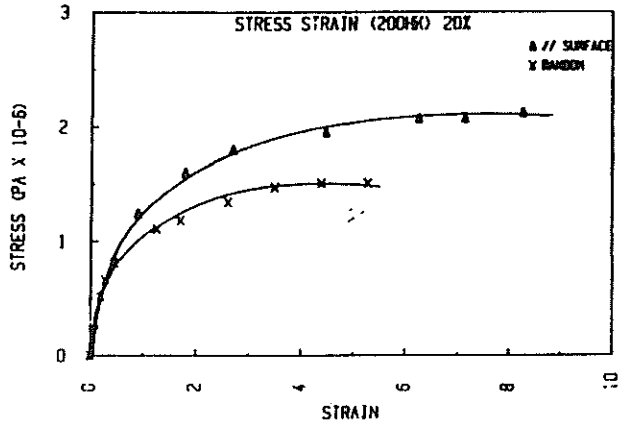
Polyurethane-Mica composites exhibited anisotropic properties due to the preferential orientation of mica flakes parallel to the surface. The flake orientation was examined by wide angle X-Ray diffraction for 20 wt% mica samples of 200 and 60HK mesh flake sizes. It is clear from the X-Ray data that samples of polyurethane-mica taken from the surface of a 6 inch thick composite show a planar orientation of the flakes, where as samples taken from the center of the composite show a random or ellipsoidal orientation. Variation in mica orientation for different mica mesh sizes influence Dynamic Mechanical and Tensile stress-strain properties of polyurethane mica composites. A decrease of 8 degree Celsius in the glass transition temperature was reported and a flexural modulus decrease of approximately half a decade due to the random orientation of large size mica flakes. However, a minimal decrease in flexural modulus is reported with a 2 degree Celsius increase in glass transition temperature for random orientation of the small size flakes. Random orientation of the mica flakes effects, for both particle sizes on the stress-strain properties of the polyurethane mica composites are shown in figure 1 & 2. A decrease in tensile modulus, % elongation and failure stress is recorded in both cases for the randomly oriented flakes. A drop in stress for the large size particles in random orientation is noted earlier at 30 and 40 wt% filler with planar orientation of mica flakes, which was attributed to the particle failure of the composite due to agglomeration of filler particles and shown by other researchers (Xavier and Sharma) as a flake pullout process.



Tensile stress-strain of polyurethane/mica (60 HK) at 20%wt. with random and parallel orientation of mica to the surface.



Log E'(Pa) vs Temperature(C) of polyurethane/mica of 200 and 60 HK grades at 20%wt. concentration and 3 Hz with random and parallel orientation of mica flakes to the surface.



Stress vs strain of polyurethane/mica (200 HK) at 20%wt. concentration with random and parallel orientation to the surface.

P10

IMPACT STRENGTH AND PHASE SEPARATION IN PC/PBT ALLOYS

H. Bertilsson, B. Franzén, J. Kubát, Department of Polymeric Materials, Chalmers University of Technology, S-41296 Gothenburg, Sweden.

The embrittlement of commercial polycarbonate/polybutylene terephthalate (PC/PBT) alloys (Xenoy CL 100 and Makroblend PR 52) has been investigated and quantified in terms of the strain energy, G_{Ic}, since the materials were found to follow linear elastic fracture mechanics.

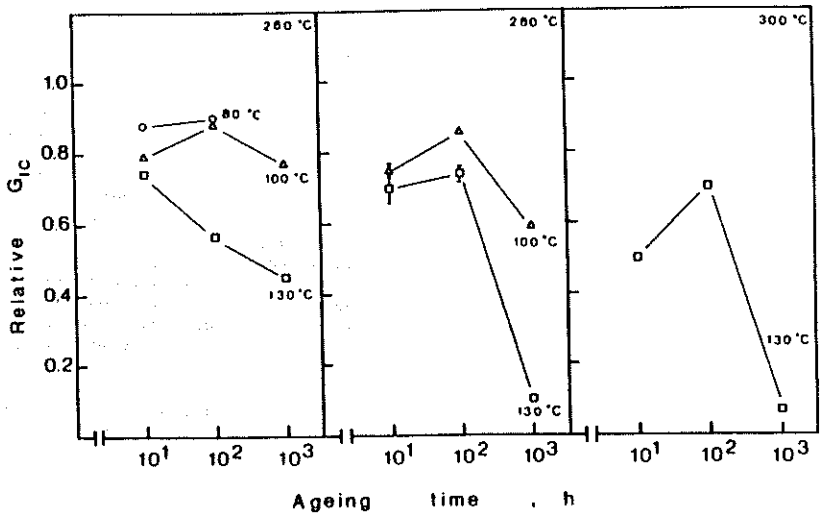


Fig. 1. The fracture energy (G_{Ic}), normalized with respect to unaged material, versus ageing time at 80°C, 100°C and 130°C. Xenoy samples injection moulded at 260°C, 280°C and 300°C. Test temperature -20°C.

Processing temperature was found to increase the embrittlement, as well as ageing, as shown in Fig. 1. In Fig. 1 G_{Ic} is normalized with respect to unaged samples injection moulded at 260°C, 280°C and 300°C.

Injection moulding was found to create a coarse layered morphology which became thinner upon ageing. However, dynamic mechanical tests indicated a phase separation. After ageing at 130°C for 1000 hours the tan δ maximum appeared at 150°C compared to 133°C for unaged samples. For pure PC the peak was at 154°C at the test frequency. Ageing as well as overheating the melt during processing resulted in decreased T_m for the PBT but increased crystallinity. We conclude that no substantial transesterification takes place in either case, but rather substantial chain scission occurs. The higher and more perfect crystallinity found in heat of fusion data has been confirmed with WAXS experiments, and the chain scission with GPC.

For specimens moulded at 260°C and aged at 130°C for 2000 hours the density increased from 1222 kg/m^3 to 1248 kg/m^3. A minor part of this increase was due to secondary crystallization during ageing. This was determined in DSC tests. The rest is thus a densification of the amorphous phases. This very high densification, caused primarily by phase separation and secondary crystallization, increases the yield stress more than commonly found during physical ageing in pure amorphous polymers after injection moulding. It is our opinion that this process is the main reason for the substantial embrittlement found during ageing at elevated temperatures.

P11

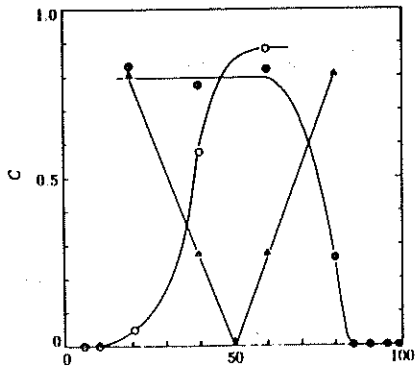
"BLENDS OF POLYCARBONATE AND POLY(HEXAMETHYLENE SEBACATE): II. RELATIONSHIP OF BLEND COMPATIBILITY TO SOLUTION BEHAVIOR"

by

K. Fujioka, Y. Baba, A. Kazemoto, N. Malone and C.L. Beatty*
Department of Chemistry, Osaka Institute of Technology
Osaka, Japan
*Materials Science and Engineering, University of Florida
Gainesville, Florida

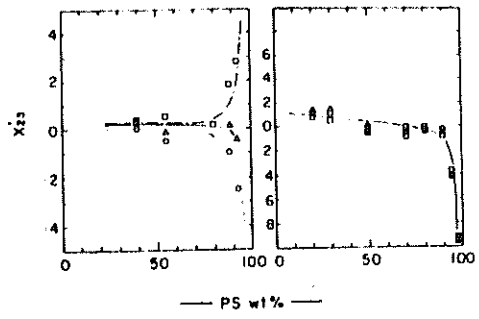
The compatibility between polymers, especially poly(styrene) poly(n-butyl methacrylate), and poly(styrene-co-n-butyl methacrylate) was studied by using visible spectroscopy, differential scanning calorimetry, inverse gas chromatography and dielectric relaxation spectroscopy. The results showed that the compatibility between these polymers depends not only upon the composition of the copolymer and homopolymer with which it is blended, but also upon the percentage of copolymer chains in the blend. Each experimental technique provides slightly different results concerning the degree and the range of compatibility. These results suggest that a variety of experimental techniques aid in the elucidation of the extent and nature of the compatibility of mixed polymers. The dielectric relaxation data indicate that the compositional regions deemed compatible by other techniques and high frequency dielectric measurements appear to be phase separated when examined at low frequencies. Thus, the compatibility of polymers may not be limited to strictly compatible or incompatible behavior, but may also include intermediate behavior such as partially mixed regions that coexist with phase-separated domains.

Figure 1



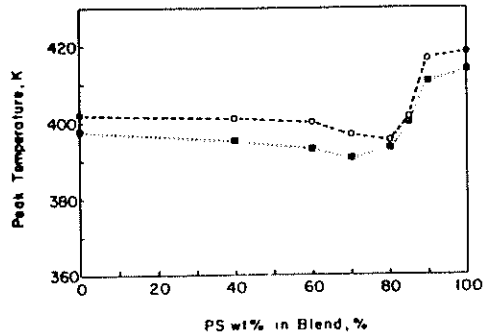
Dependence of extent or degree of compatibility, C, on PS wt % for three blend systems. Key: ●, PS/P(S-nBMA) system; ○, P(nBMA)/P(S-nBMA) system, and Δ, P(S-nBMA)/P(S-nBMA) system.

Figure 2



Free energy interaction parameter χ_{23} between polymers for (left) PS-60/40 P(S/nBMA) and (right) PS-80/20 P(S/nBMA) blend systems. Key: ○, 393 K; Δ, 413 K; and □, 443 K.

Figure 3



Dependence of transition temperature on PS wt % in blend at high dielectric relaxation measurement frequencies. Key: ○, 100 kHz; and ■, 40 kHz.

P 12

SYNTHESIS,CHARACTERIZATION AND PROPERTIES OF NYLON-G-POLY(ETHYLENE GLYCOL)COPOLYMERS

Chang Sik Ha,Nam Gyun Yun and Won Jei Cho
Department of Polymer Science and Engineering,
Pusan National University,Pusan 607,KOREA

The miscibility of Nylon 6 with other polymers has been known to be very poor because of the strong hydrogen bonding within the molecule and several attempts have been made to modify nylon 6 including the newly designed block and graft copolymers.As a first step of the successive studies to investigate the miscibility of Nylon6-containing polyblends with any other polymers, Nylon6-g-poly(ethylene glycol) graft copolymers were synthesized and characterized in this study.

The graft copolymers were produced by two step reactions;poly(ethylene glycol)(PEG) was chlorinated with thionyl chloride($SOCl_2$) in carbon tetrachloride and the chlorinated PEG was then grafted onto Nylon 6 with tin chloride in O-chlorophenol.The chlorination of PEG and grafting were characterized by titration and Infrared Spectrum. The molecular weight was measured by gel permeation chromatography (GPC). The inherent viscosities of the graft copolymers were ranged from 0.41 to 0.72 dl/g in 85 % formic acid at 30°C, and the polydispersities of the graft copolymers were ranged from 2.5 to 3. The characterization of the graft copolymers is summarized in Table 1.

In this study,the effects of the molecular weight and mole ratios of PEG and reaction times were discussed.The thermal properties and crystalline structure of the Nylon6-g-PEG graft copolymers were also investigated using Differential Scanning Calorimetry(DSC) and X-ray diffractometer.

From the DSC experiments,the melting temperature of Nylon 6 was decreased whereas the melting temperature of PEG increased with increasing molecular weight of PEG,reacton time of grafting and mole ratio of Nylon 6/PEG.
It was found in X-ray diffraction studies that the grafting of PEG onto Nylon 6 changed the crystal structure of Nylon 6,where the proportion of α-crystal to γ-crystal reduced for all the graft copolymers regardless of the molecular weight of PEG or mole ratio of Nylon6/PEG.

Table. 1. Characterization of the Nylon6-g-PEG graft copolymers.

Samples[a]	η_{inh}[b]	$Mw\times10^{-5}$	$Mn\times10^{-5}$	Mw/Mn	wt% of PEG
Nylon 6	0.381	0.3452	0.1732	2.00	0
N-g-P1	0.615	0.8472	0.3362	2.52	38.70
N-g-P2	0.629	0.8971	0.3632	2.47	43.32
N-g-P4	0.715	0.8342	0.3184	2.62	36.85
N-g-P6	0.615	0.8527	0.3267	2.61	36.60
N-g-P2(0.5)	0.430	0.5173	0.1815	2.85	5.41
N-g-P2(1)	0.478	0.8296	0.2851	2.91	18.51
N-g-P2(2)	0.509	0.7844	0.2960	2.65	20.19
N-g-P2(5)	0.629	0.8971	0.3632	2.47	43.32
N-g-P2(8)	0.486	0.9242	0.3851	2.40	48.12
N-g-P2(10)	0.431	0.8777	0.3901	2.25	50.75
N-g-P2(1/5)	0.553	0.8125	0.3250	2.50	29.88
N-g-P2(1/10)	0.629	0.8971	0.3632	2.47	43.32
N-g-P2(1/15)	0.481	0.8714	0.3740	2.33	49.12
N-g-P2(1/20)	0.418	0.9084	0.3951	2.29	52.35

a) N-g-P1 ;Nylon6-g-PEG1000
N-g-P2(0.5) ;PEG mol. wt.-2000, grafting reaction time-0.5 hr
N-g-P2(1/5) ;PEG mol. wt.-2000, mole ratio of Nylon6/PEG2000=1/5

b) η_{inh} ; dl/g in 85% Formic acid at 30°C

REFERENCES

1.I.Sakurada,S. Yasuyoshi and S.Yasui,Polymer,78,37(1964).
2.M.H.El-Rafie,M.I.Khalil and A.Hebéishi,J.Appl.Polym.Sci.,19,1677(1975).
3.M.I.Khalil,S.H.Abdel-Fattah and A.Kantouch,J.Appl.Polym.Sci.,19, 2699 (1975).
4.F.Candau,F.A. Taromi and P.Rempp, olymer,18,1253 (1977).
5.Y.S.Hur,C.S.Ha and W.J.Cho,Polymer(Korea),10,4,293(1986).
6.K.Mitsuishi,S.Kodama and H.Kawasaki,J.Appl.Polym.Sci.,32,4229(1986).

P13

EFFECT OF BLENDING POLYOLEFINES ON THE RHEOLOGY AND PROPERTIES OF NYLON -6

Y P Singh, B V Ankleshwaria, M D Daxini & M H Mehta
Research Centre, Gujarat State Fertilizers Co. Ltd.
PO : Fertilizernagar 391 750 Dist : Vadodara, INDIA

INTRODUCTION:

In polymer alloying technology, existing materials are engineered to obtain new polymer systems with properties beyond those of the indivisual components. Inspite of having an unique combination of properties like toughness at higher temperature, chemical and wear resistance etc., versatility of Nylon 6 as engineering plastic becomes limited because of its poor impact strength at lower temperature, moisture senstivity and poor processibility. Present studies have, therefore, been undertaken for modifying Nylon 6 for improving impact resistance, moisture resistance and processability in order to exploit its full potential.

Experimental:

Nylon-6 alloys of various compositions were prepared by melt mixing in the single screw extruder. Post extrusion conditions were varied for DSC measurements. Torque-time relationship various alloys was measured on Rheomix-600 of Torque Rheometer. DSC measurement were carried out using DSC-4 of Perkin Elmer.

Results & Discussion:

Incoporation of HDPE alongwith the third component, i.e. Zn salt of ethylene methacrylic acid copolymer improves impact strength of Nylon-6 by three fold indicating the preferential location of the third component at the interface between dispersed particle surface and matrix resin producing an encapsulant phase between them. The processibility of Nylon-6 is improved as fusion torque for Nylon alloys is reduced considerably while terminal torque indicating melt strength of the material is increased (Fig.1). Moisture resistance of the alloys has been improved. It is anticipated that $^{-}$NHCO bridge responsible for higher moisture sensitivity is distrubed by inclusion of HDPE and ethylene graft copolymer, as Zn salt of methacrylic acid component of ethylene copolymer is expected to have greater interaction/reaction with $^{-}$NHCO group of Nylon 6.

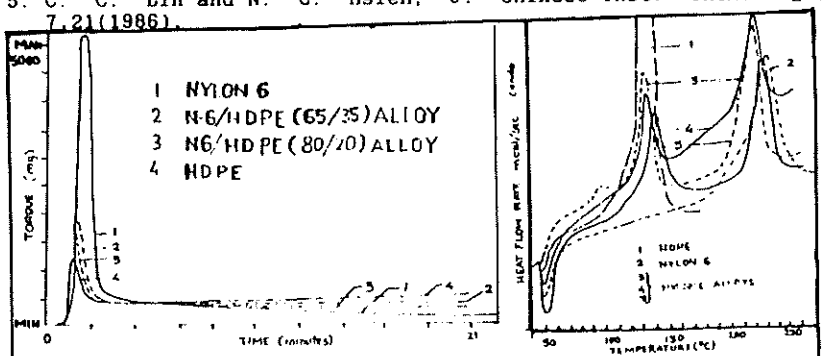
Crystallinity of the component polymer is one of the major limiting factor in the compatibility of Nylon 6/HDPE alloys. Indivisual components crystallize at different temperature and impart incompatibility to the system eventhough the component may be compatible in melt. DSC Thermogram for same Nylon 6/HDPE (80/20) are differing when material is put to different cooling treatment indicating the extent of homogenity in favour of the material cooled faster (no.3). Visual observastion of the extrudate confirm the behaviour as the material cooled immediately (no.3) is far more transparent. Morphological and fracture studies are in progress to reinforce the present observation.

Acknowledgement:

Technical help rendered by Mr. D P Shah is acknowledged with thanks.

Reference:

1. Y P Singh, B V Ankleshwaria and M H Mehta, Int. Sem. Performance Plastics, Bombay, 14-15 February, 1986.
2. Y P Singh, B V Ankleshwaria and M H Mehta, GSFC Research Report, 1986.
3. S. Cimmino, L.D. Orazio et.al.; Polym. Eng.Sci.,24(1), 49(1984).
4. Y P Singh, "Ph.D Thesis", IIT Kharagpur (1983).
5. C. C. Lin and N. C. Hsieh, J. Chinese Inst. Chem. Eng., 7,2)(1986).



Torque Time Relationship for Nylon 6 and its Alloys Fig: DSC Thermogram of Nylon-6 & its Alloys

P14

PLASMA POLYMERIZATION AS COATING PROCESS FOR PLASTIC AND METALLIC PARTS

P. Plein, G. Menges, Institut für Kunststoffverarbeitung, Pontstraße 49,
D-5100 Aachen, West Germany

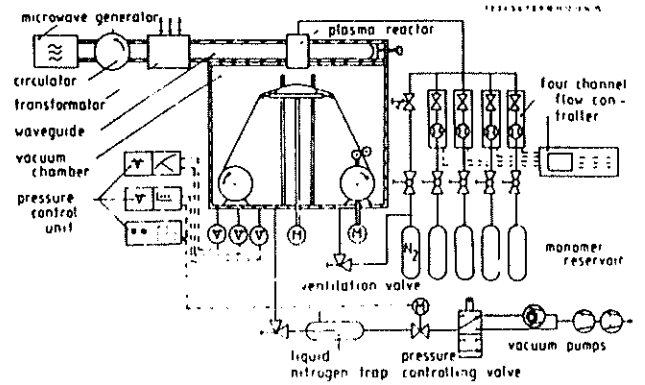
Low pressure plasma polymerization has been investigated for more than twenty years. However, efforts to use this process as an economical coating process on an industrial scale have failed up to now due to the low coating rates. During the last few years the application of microwave generated plasmas has made it possible to obtain technically significant coating rates.

In this paper a microwave plasma polymerization unit will be presented on which coating rates of about two micrometers per minute which fits the challenge of practical applications can be realized (fig. 1). Coatings have been realized using different monomers. The results will be presented; coating rates, film structure and film properties will be shown regard to the different process parameters. Generally one can find the following typical properties of plasma polymerized films:

- high degree of three-dimensional crosslinking,
- high density (about two times higher than conventionel polymers),
- high thermal stability (decomposition temperature greater than 390 °C),
- high chemical stability (the films are not soluble in solvents),
- high scratch resistance
- good diffusion barrier effects

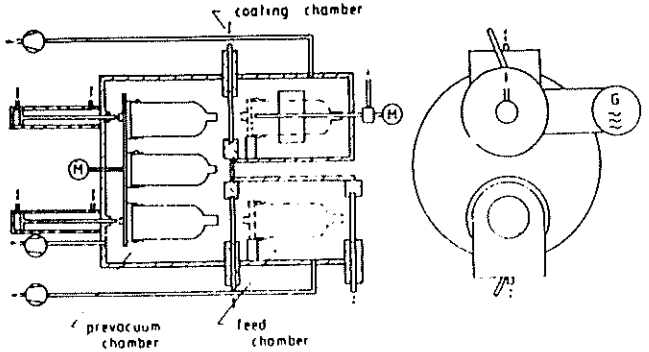
Parts with complicated geometries, for example blow moulded bottles can be coated on the inside by plasma polymerization especially for avoiding the diffusion of organic fluids through the walls.

A second plasma polymerization unit designed especially for this applicaton will be presented (Fig. 2). First results of inside coating experiments will be shown. Moreover other imaginable ranges of application of the plasma polymerization process will be discussed.



Plasmapolymerization equipement

Fig 1



Plasmapolymerization equipement

Fig 2

P15

QUATITATIVE CHARACTERIZATION OF IMPACT FRACTURE OF POLYMERS

T. Vu-Khanh, National Research Council Canada, Industrial Material Research Institute, 75 De Mortagne, Boucherville, PQ, Canada, J4B 6Y4

The quantitative characterization of impact fracture of plastics is still a subject of great interest. The most common tests used in impact are the Charpy and Izod types. In these tests, analysis methods based on fracture mechanics have been developed with the objective of providing a quantitative description of the impact fracture process.

Under impact, polymers can break in very distinct manners. Several modes of fracture have been identified depending on the amount of plastic deformation at the crack tip and the stability of crack propagation. For each mode, an appropriate analysis must be used to determine the impact fracture energy of the material.

Brittle fracture occurs when the strain energy stored in the sample up to the point of fracture is much larger than the energy dissipated in the creation of the two fracture surfaces. In this case the crack grows in an unstable manner. The energy absorbed by the specimen to fracture is that which is elastically stored in the sample. A method has been proposed for this mode of fracture to determine the fracture energy at crack initiation (1).

The development of copolymers and polymer blends has resulted in materials exhibiting more and more ductile behavior in impact. When the polymer is semi-ductile, stable crack propagation occurs before unstable fracture. For this semi-ductile fracture mode, a method using two material parameters has been proposed (2) to characterize the impact resistance of the polymer. The method allows the determination of an average value of the fracture energy in the stable crack propagation stage and the fracture energy at instability (Fig. 1).

When the material is ductile, unstable fracture does not occur. The crack propagation is generally completely stable. For this mode of fracture the measurement of fracture energy is still controversial. The present method is based on the assumption of constant fracture energy during the fracture process. The energy absorbed by the sample is considered as proportional to the fracture surface. For many ductile plastics, this method often gives abnormally high values of impact fracture energy. Furthermore, an inconsistent negative intercept of the absorbed energy versus fracture surface plot is generally observed.

The inconsistencies of the current method have been shown to be related to a variation of fracture energy with crack propagation (3). A new method is proposed for the characterization of impact fracture. This method is based on a constant rate of increase in crack growth resistance with crack extension. Two material parameters can therefore be determined from the proposed model; a fracture energy at crack initiation and an equivalent tearing modulus. The model describes closely the variation of the energy absorbed by the specimen to fracture with the fracture surface (Fig. 2). It demonstrates the cause of the abnormally high value of fracture energy and explains the inconsistent negative intercept of the current method.

Although the tearing modulus is only defined for small amounts of crack extension, the results showed that the concept could be successfully extended to the case of large magnitudes of crack propagation.

REFERENCES

(1) Plati E. and Williams J.G., Polym. Eng. Sci., 15, 470 (1975).

(2) Vu-Khanh T. and de Charentenay F.X., Polym. Eng. Sci., 25, 841 (1985).

(3) Vu-Khanh T., "Determination of the Impact Fracture Parameters in Ductile Polymers", 7th International Conference on Deformation, Yield and Fracture of Polymers, Cambridge, England, April 11-14, 1988.

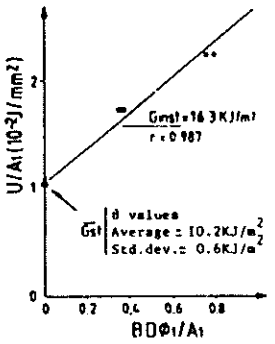


Fig. 1: Determination of impact fracture energies in semi-ductile polymers (PA 11, Ref. 2).

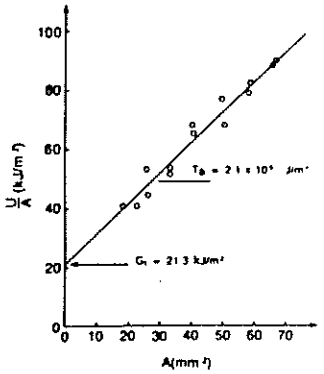


Fig. 2: Determination of impact fracture parameters in ductile polymers (toughened PA 66, Ref. 3).

DYNAMIC MECHANICAL PROPERTIES OF PVC PLASTISOLS: THE EFFECTS OF CURE CONDITIONS AND PLASTICIZER MIGRATION

W. Daher, C. Garrett, J. P. Harmon and C. L. Beatty
University of Florida, Gainesville, Florida

Dynamic mechanical spectroscopy is an efficient method for monitoring plasticizer-polymer matrix interactions. This study is concerned specifically with poly(vinyl chloride)-di-octyl phthalate plastisols. The topics encompassed are:

1. The effect and efficiency of oven versus RF cure.
2. The effect of cure time.
3. Plasticizer migration in cured plastisols after storage at different temperatures.
4. The effect of per cent plasticizer in relation to the variables listed above.

Suspension polymerized poly(vinyl chloride) (PVC)(Geon from BF Goodrich) was mixed with di-octyl phthalate (DOP) plasticizer in a Hobart Mixer. Samples contained 40,50,60 and 70 weight per cent DOP. Samples were degassed under vacuum and cured under the appropriate conditions.

A Dynamic Mechanical Thermal Analyzer (DMTA) from Polymer Laboratories was used to monitor loss and storage moduli, tangent delta and the breadth of the transition. Samples were tested in flexure at frequencies from 3-30 Hz at temperatures from -150 to 200°C.

The extent of cure was monitored as a function of time for oven and RF treated samples. Intermediate stages of cure are easily noted on modulus versus temperature plots. A typical example is shown in figure I. Here, a 40% DOP sample was cured for 5 minutes at 180°C in a vacuum oven. Two glass transitions are evidenced in the plot. Samples cured at times over 15 minutes at 180°C exhibit only a single transition.

Dynamic mechanical thermal analysis evidenced plasticizer migration in the matrix when fully cured samples were stored at different temperatures, -15°C, 25°C and 80°C. Tangent delta versus temperature plots clearly depict changes in the primary transition. In 50,60 and 70 % DOP aged samples,the breadth of the transition increased and the maximum in tangent delta was displaced to higher temperatures. The magnitude of the shift decreased with decreasing plasticizer content. In the 40 % samples, the glass transition temperature remained constant. A 40% sample was post cured at 195°C for 20 minutes. The glass transition of this sample was depressed by 4°C due to the heat treatment. The breadth of the transition also decreased. Activation energies for the primary transition increased with storage under different temperatures. The storage induced increase in activation energy and increase in the glass transition temperature indicates that migration of the plasticizer within or out of the samples decreases the plasticizing action of the DOP.

It is shown here that dynamic mechanical spectroscopy is an effective method for monitoring cure efficiency and plasticizer migration in plastisols.

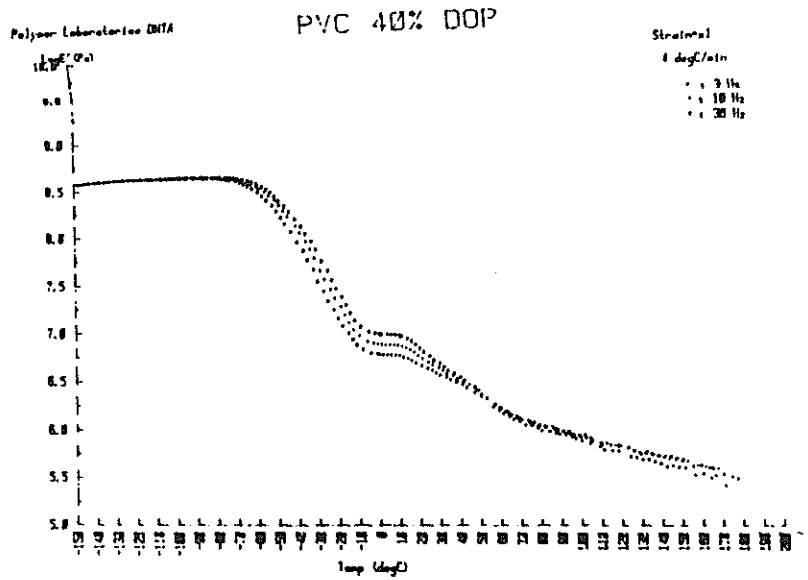


Figure I.

Modulus versus temperature plot for 40% DOP in PVC cured at 180 C for 5 minutes.

P17

FATIGUE RESISTANT ANTI-CORROSION COATINGS

J. P. Harmon
S. Singleton
C.L. Beatty
University of Florida
Gainesville, Florida

The evaluation of coatings for use in corrosive environments requires optimum adhesion and coating strength and impermeability. The inability of unfilled polymers to meet these requirements has led to the formulation of complex primer/coating systems. Plasma polymerized coatings may offer an alternative to this technology. This study focuses on the superiority of plasma coatings in a corrosive environment (0.1 M $FeCl_3$, pH 1).

The substrate, type 302 Steel, was sensitized at 800°C for 2 hours to precipitate chromium carbide along the grain boundaries. This results in a substrate that is labile to intergranular corrosion. Polycarbonate (PC), polystyrene (PS) and poly(methyl methacrylate) (PMMA) were applied to the steel by dip coating from solutions in chloroform. Polyurethane, PU, was applied with a brush and crosslinked at 80°C for 16 hours. Methy methacrylate monomer was polymerized on the surface of the steel using a RF plasma reactor at 75 watts power. The monomer pressure was 50-300 microns.

Fatigue resistance of uncoated samples was determined by a Tinius Olsen Folding Endurance Tester. This instrument imposes a tensile stress on double fold bending stresses. Cycles to failure were recorded for varying tensile loads. Coated samples were fatigued to 25, 50 and 75% of the fatigue limit for each tensile load. Plasma coatings and PU coatings showed no delamination or adhesive failure. Dip coated samples failed by cracking and delamination.

A microhardness diamond pyramid indentor was used to apply varying loads to the surface of the coatings. The diagonal of the delamination area versus load curve characterized adhesion. No delamination occurred in the PU or the plasma coatings.

When samples were placed in the corrosion bath for 24 hours, dip coated samples showed extensive corrosion in the area of the fold. The polyurethane samples were permeable to the corrosive liquid. Extensive pitting was noted. Importantly, plasma coatings showed no evidence of corrosion within the time period studied.

Additional studies are being conducted with a variety of plasma monomers and substrates.

P18

Microwave Processing and Measurement of Properties for Various Fiber/Epoxy Ratios

Martin C. Hawley, Jinder Jow, Cheryl Schwalm, Steve Singer, and John DeLong

Department of Chemical Engineering
Michigan State University
East Lansing, Michigan 48824-1226

ABSTRACT

Microwave curing of polymer matrix/fiber composite materials is more time and energy efficient than conventional thermal curing. In order to achieve optimum processing conditions for microwave curing, a throrough understanding of the effects of microwave radiation on the cure kinetics, mechanisms, and thermal properties of the the composite material is necessary. The processing history of the composite in turn affects it mechanical properties.

Two fundamental features of using microwave heating are: 1) fast and direct heating, and 2) selective heating which is dependent on the dielectric loss of the materials. In the case of an epoxy/ graphite fiber composite, the fiber, which is a highly dielectric loss material, is heated first. Heat is conducted from the fiber outward to the matrix and cure reaction is initiated at thte interface between the fiber and the matrix. A comparison between microwave heating and thermal heating in an epoxy/carbon fiber composite is shown in Figure 1. The arrows in Figure 1 indicate the direction of heat flux. Fibers serve here as the heating, reinforcing, and interacting element during microwave processing. The end-use properties of microwave-cured composites may be significantly affected by the density of the heating element (various fiber/epoxy ratio) when compared to thermally cured samples.

In an effort to gain a better understanding of the nature of the matrix/fiber interface and the surrounding interphase region, the effects of microwave and thermal processing of a diaminodiphenyl sulfone (DDS)-cured diglycidyl ether of bisphenol A (DGEBA)-type epoxy containing various carbon fiber volume fractions have been studied. The results have been analyzed in the context of the following:

1. Bonding at the fiber-matrix interface. The degree of interfacial bonding has been characterized using differential scanning calorimetry (DSC) to measure the reaction exotherm and glass transition temperature (Tg) in epoxy matrices containing either surface treated or untreated carbon fibers of various fiber volume fractions. Changes in the exotherm and Tg have been interpreted in terms of the bonding at the fiber/matrix interface.

2. Extent of cure in the bulk matrix and in the interphase region. The extent of cure in the two regions has been measured using Fourier transform infrared spectroscopy (FTIR) for samples cured either thermally or with microwaves. Differences in extent in the respective regions are possibly due to the effects of interfacial bonding and/or adsorption of the curing agent onto fiber surfaces. Further, faster curing near the interface in microwave-processed composites reflects the concentration of energy in the highly conductive carbon fibers and results in better matrix/fiber adhesion under controlled processing conditions.

3. Temperature profiles in the curing composite. Uneven heating resulting from both thermal processing (increasing temperature from sample boundary to center) and microwave processing (increasing temperature from sample center to boundary) have been reduced using a combined thermal-microwave processing technique. This reduction in temperature gradient has been achieved using either convective or conductive thermal heating.

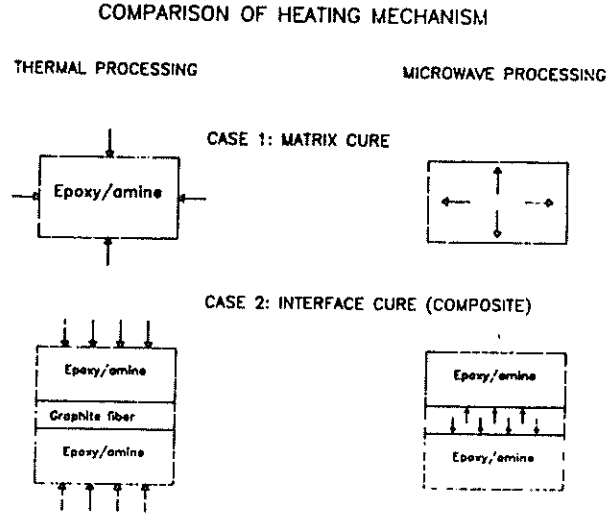


Figure 1. Comparison of microwave and thermal heating mechanism

P19

POLYMERS IN CERAMICS PROCESSING

Krishna Venkateswamy, Ceramics Program Systems, 840 Memorial Drive, Cambridge, MA 02139 (Present address: Monsanto Chemical Company, 260 Springside Drive, Akron, OH 44313)

Synthetic organic polymers play a vital part in processing of ceramics[1]. Polymers act as a vehicle to process ceramic powders, in which the reinforceability of polymers is made use of in processing the fillers themselves. The general processing steps of ceramics with polymers is schematically shown in Figure 1. The ceramic particles are dispersed in a polymer solution (concentrated) in the case of a solution process (tape casting or solution dry spinning of ceramic fibers) or in a melt (as in the case of injection molding). The solidification (forming) to near net shape can be by drying or cooling depending on the process. The polymer (with the additive package) acts as a binder for ceramic particles at this stage, imparts green strength (the part is referred to as green body), and facilitates easy handling of part including machining if needed. The green ceramic body is a very highly filled polymer system (80 to 90 wt% filler). The organic binder (polymer with the additive package) is removed by thermal degradation, and the final ceramic product is obtained by higher temperature fusion of particles. The polymer binder technology has facilitated the growth of continuous production of ceramic parts to near net shape (tape casting of films, injection molding of parts, etc.).

The use of natural polymers, such as gum, waxes, etc., has been prevalent for a number of years to make ceramic parts.[2] With the growing need of applications of ceramics in high technology, such as substrates, packages, specialized engine components, etc., the selection of polymers for specific application is a demanding task. The selection of polymer binders is based on their chemistry (affinity with the ceramic particles), dispersability of ceramic particles, and clean (facile) binder burnout characteristics.

Some of the common polymer systems used are thermoplastics such as polyvinylbutyral, polyvinyl alcohol and thermosets such as urea and formaldehyde[1]. More recent work done in our laboratory have led into the development of novel polymerizable binders[3,4] which offer significant advantage of dispersability of ceramic particles over conventional binder systems. In this paper, polymers used in ceramics processing will be discussed in general. Particular emphasis will be given on their criteria for selection with some specific examples.

References

1) L. Hench and G. Onoda Ed., "Ceramic Processing Before Firing", John Wiley & Sons, N.Y. 411, (1978).

2) C.C. Michel and E.W. Emrich, J. American Ceramic Society, 29(5), (1946).

3) K. Venkateswamy and R. Waack, U.S. Patents pending (1987).

4) K. Venkateswamy and R. Waack, Proceedings of RETEC on Engineering Polymers and Composites, SPE, Rosemont, IL, p. 296, September (1987).

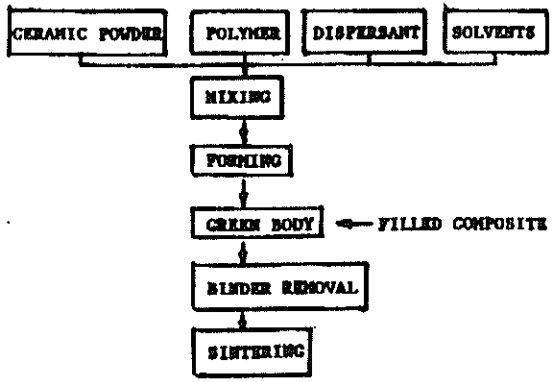


Figure 1 Schematic representation of ceramics processing using polymers. Solvents are used in the solution process.

P20

STRESS-STRAIN BEHAVIOR OF POLYOLEFINE FILLED WITH PLASMA TREATED MICA

Xiaoyi Gong Xi Xu
(Polymer Research Institute, Chengdu University of Science and Technology, China)

Xueshu Liu
(Changchun Institute of Applied Chemistry, Academia Sinica)

ABSTRACT

The stress-strain behavior of mica filled polyolefine was studied through an Instron tensile tester, the surface of mica used has been treated by ethylene plasma of radio frequency. The results show that the elastic modulus E of the filled polyolefine changes with volume fraction of the filler V_f according to the modified simple mixing rule:

$$E = E_m \cdot (1 - V_f) + A \cdot E_f \cdot V_f$$

where A manifests effect of the plasma treatment, the subscripts m and f stand for matrix and filler of the filled polymers respectively. For HDPE filled with virgin mica, A = 0.240; with treated mica, A = 0.487 (radio frequency output 60 w), 0.451 (100 w), 0.315 (160 w). For LDPE filled with virgin mica, A = 4.26×10^{-2}; with treated mica, A = 8.66×10^{-2}(60 w), 8.15×10^{-2} (100 w), and 9.18×10^{-2}(160 w). For mica filled PS, A is enhanced by the treatment from 0.495 to 0.600 (100 w). The relation between E of the filled HDPE and treating time t can be formulated by:

$$E = E_o + (E_\infty - E_o)\ (1 - e^{-t/\tau})$$

In case mica content is 25 % (wt), output is 60 w and 100 w, E_∞ is 510 MPa and 240 MPa; τ is 5.2 and 4.4 min respectively.

An equation describing the relationship between the breaking strength σ and V_f of filled LDPE and PS is proposed. It is:

$$\sigma = \sigma_\infty + (\sigma_m - \sigma_\infty) e^{-aV_f}$$

where σ_∞ is a parameter characterizing the effect of plasma treatment. For virgin mica filled LDPE, σ_∞ = 8.60 MPa, a = 50.6; for treated mica filled ones, σ_∞ = 10.3 MPa, a = 120 irrespective of the treating conditions. For treated mica filled PS, the strength is higher than that of the untreated one, it changes with V_f according to:

$$\sigma = 39.0 + 5.3\ e^{-96.2\ V_f} \qquad (\text{MPa})$$

in case the output is 100 w and treating time is 8 min. The dependence of σ of filled HDPE on V_f agrees with the generalized Nielsen's equation. No improvement of the strength made by the plasma treatment is observed.

The breaking elongation of the filled PS is enhanced by plasma treatment of mica. When filler content is 10 % (wt), the increase is 40 %. No evidence indicating the effect of the treatment on the elongation of filled HDPE or LDPE is obtained.

P21

DYNAMIC MECHANICAL PROPERTIES OF GLASS PARTICLE REINFORCED IONIC POLYURETHANE

by
W. Williams and C.L. Beatty

Ionic polyurethane and composites composed of 10, 38 and 150μ unsized fumed silica were fabricated and dried. Flexural dynamic mechanical spectroscopy measurements were made with a Polymer Laboratory DMTA. Addition of filler resulted in an increase in modulus and measures the glass transition temperature as the concentration of glass filler is increased. This suggests that the glass is reinforcing and that increased surface area results in more bonding and thus, immobilization of the polyurethane matrix. Reducing the glass reinforcing particle size results in a more rapid initial increase in the glass transition temperature as the weight of filler is increased. At a 10 wt% loading, the activation energy for the glass transition process is nearly invariant as the filler particle size is decreased except for the 150μ filler sample, which suggests that the relaxation process is basically the same for all but the 150μ filled sample.

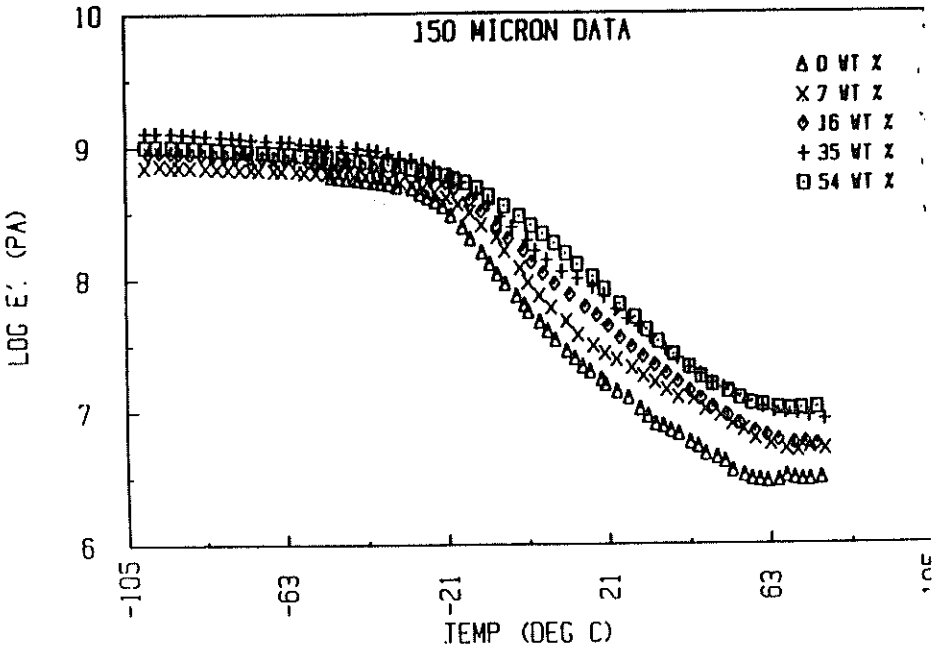


Figure 1. Storage modulus vs. temperature at 0, 7, 16, 35 and 54 wt. % filler for 150 micron spheres.

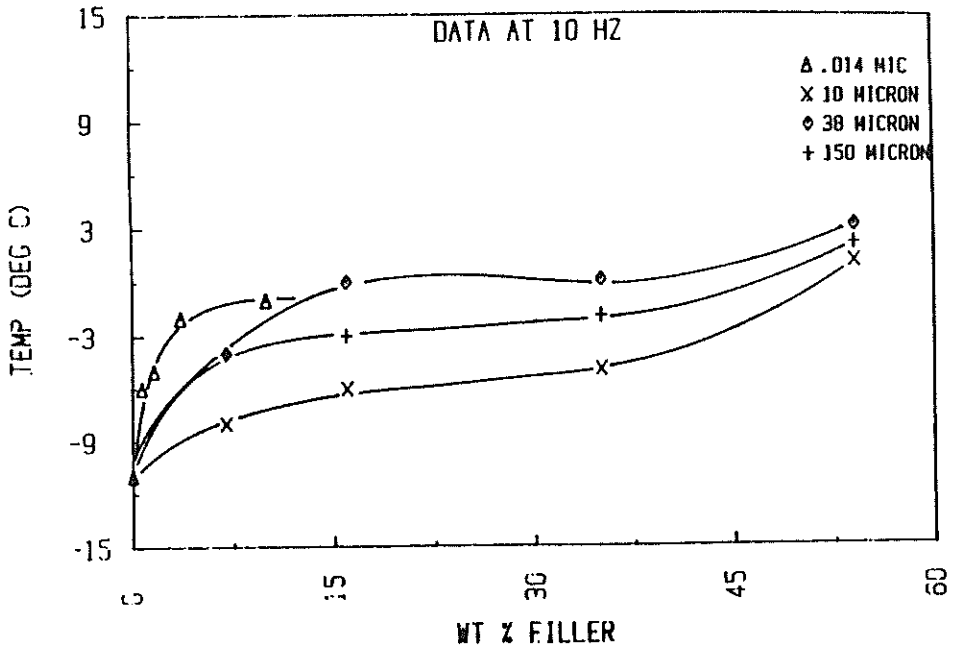


Figure 2. Glass transition temperature vs. filler at 10 Hz.

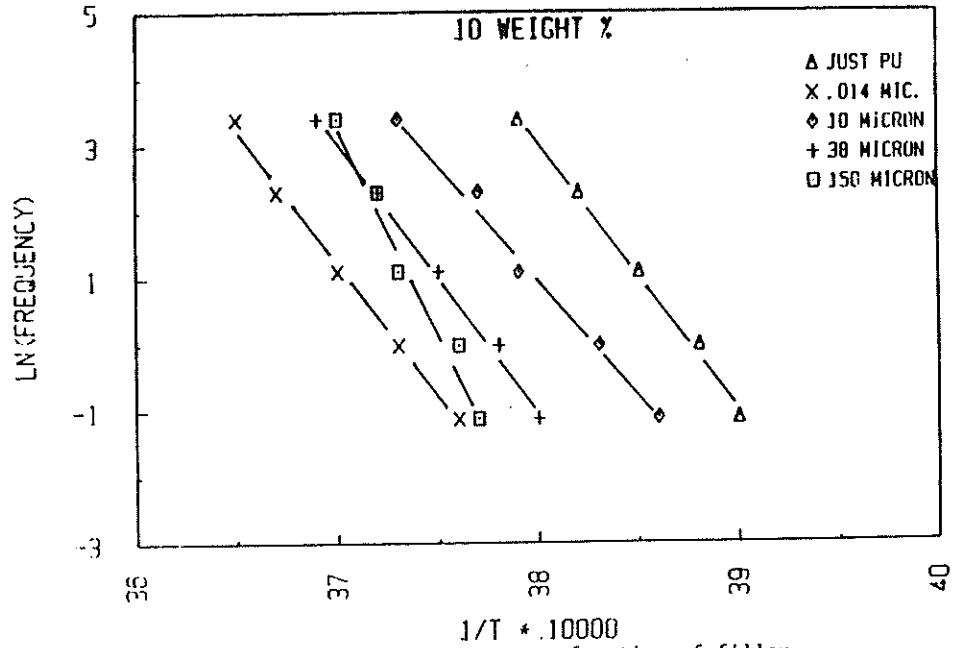


Figure 3. Activation energy as a function of filler

P22

STRESS-STRAIN BEHAVIOR OF GLASS REINFORCED DRY IONIC POLYURETHANE

by
W. Williams and C.L. Beatty

An ionic polyurethane was utilized as the matrix polymer with 10, 38 and 150μ sieved portions of glass beads. A 0.014μ unsized fumed SiO_2 was also used as a filler in this study. Tensile stress-strain measurements were made on composites fabricated from these materials. Data was analyzed and compared to the predictions of linear, inverse and logarithmic rules of mixtures as well as the following models: Guth and Smallwood, Nielsen, Eilers and van Dyck, Mooney, generalized Kerner and modified Kerner. The surface area of the reinforcing particles was determined and cross-checked via micropycnometry, scanning electron miscroscopy coupled with Zeiss digital image analysis. The tensile stress-strain data was reanalyzed in terms of reinforcement surface area. Large particles appear to result in higher modulus composites at equivalent filler surface areas for filled composites.

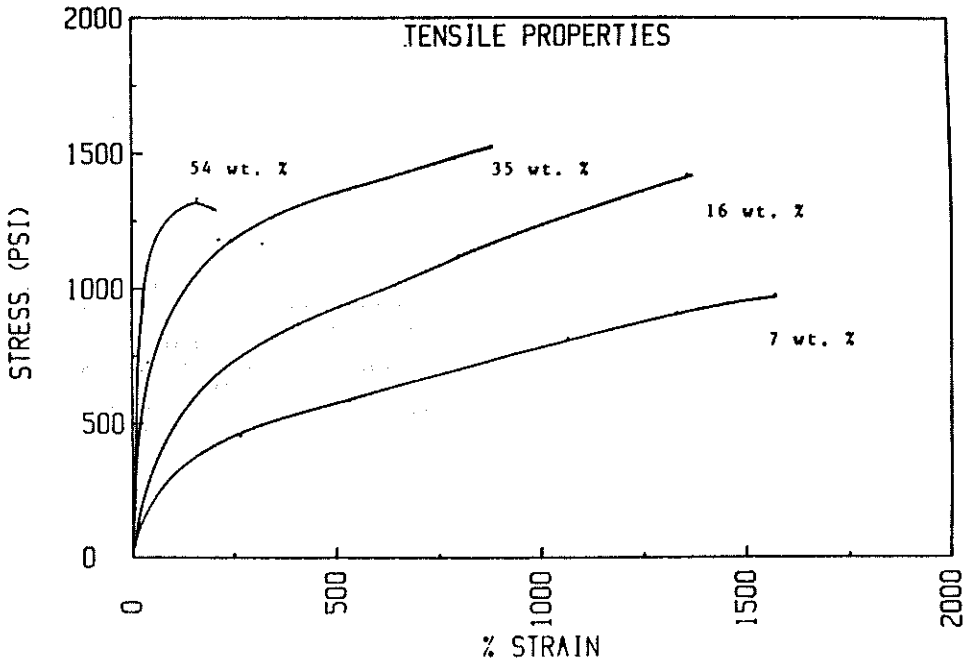


Figure 1. Stress vs. strain for 10 micron samples at 7, 16, 35 and 54 wt. % filler.

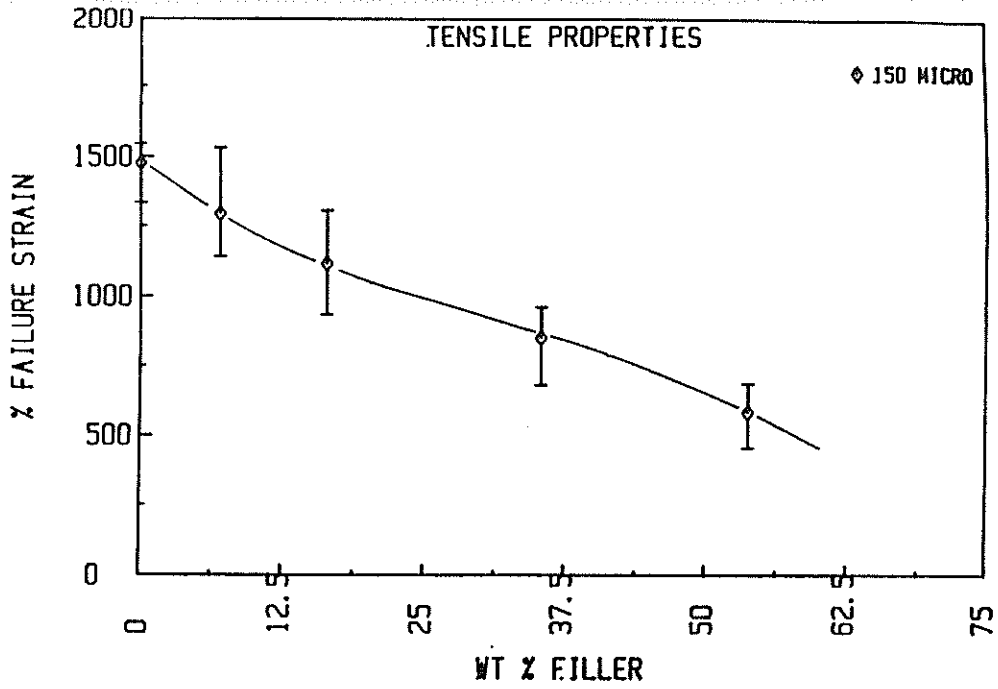
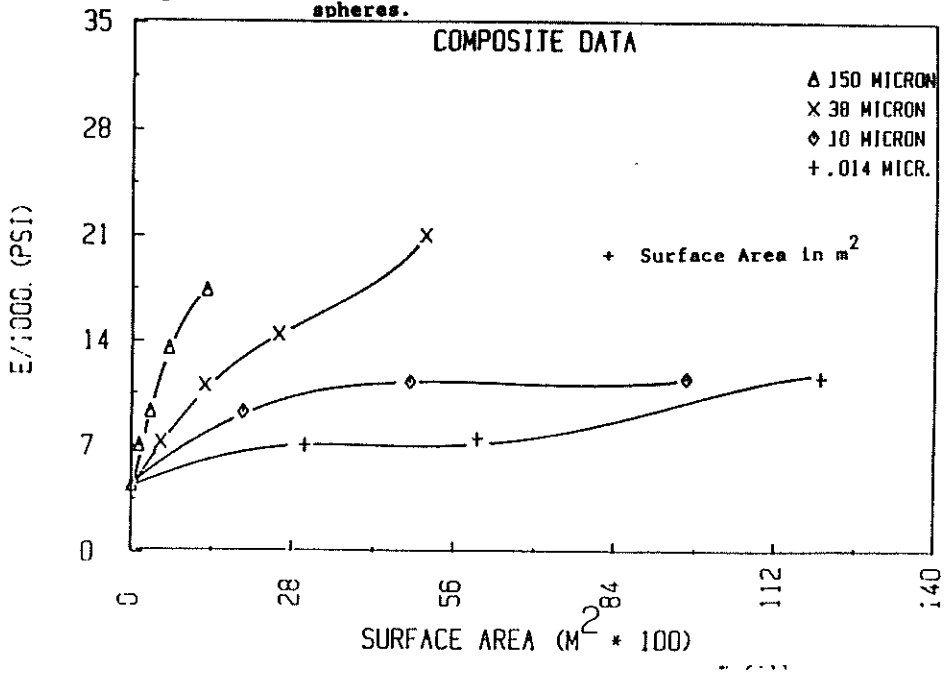


Figure 2. Failure strain vs. wt. % filler for 150 micron spheres.



P23

EFFECT OF COUPLING AGENTS ON LAP SHEAR STRENGTH OF GLASS IONIC POLYURETHANE JOINTS

by
W. Williams and C.L. Beatty

Glass microscope slides were carefully cleaned and treated with either a silane or a titanate coupling agent utilizing techniques recommended by the coupling agent supplier. Prosil 221 manufactured by PCR Company of Gainesville, Florida, was the gamma-aminopropyltriethoxy silane used and KR-TTS was the organo-titanate agent supplied by Kenrich Petro Chemicals, Inc. Both were recommended for polyurethanes by the suppliers. The coupling agent was confirmed to be on the glass surface via FTIR. The concentration of coupling agent was determined gravimetrically. As can be seen from the figures, the silane coupling agent increased the ionic polyurethane/glass by shear strength from ~ 17 psi to ~ 100 psi for the silane treated glass. The titanate treated glass exhibits an increase in lap shear strength to ~ 45 psi at the nearly coupling agent coverage (6-9 g.lm)

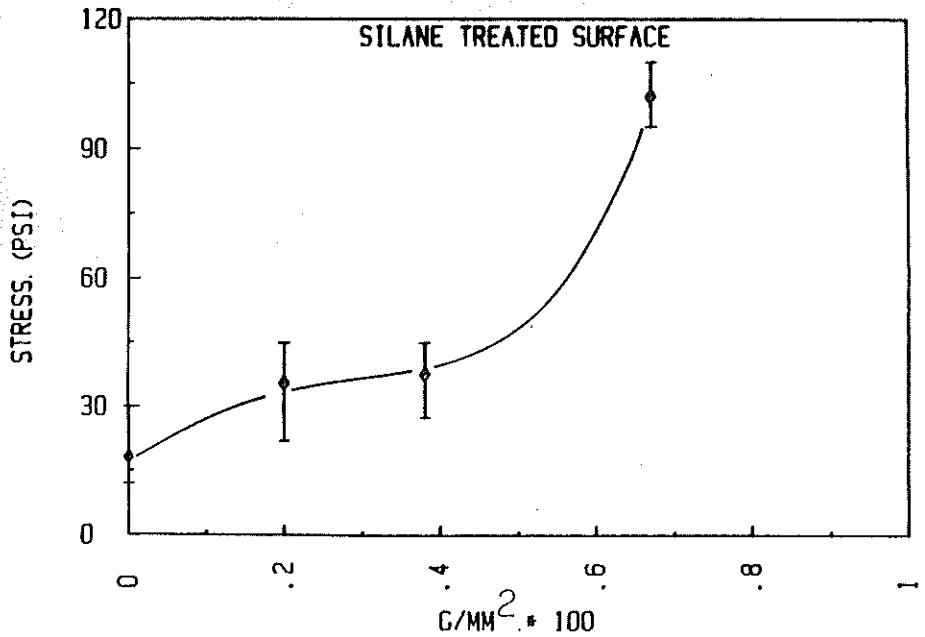


Figure 1. Lap shear strength results for silane treated surface.

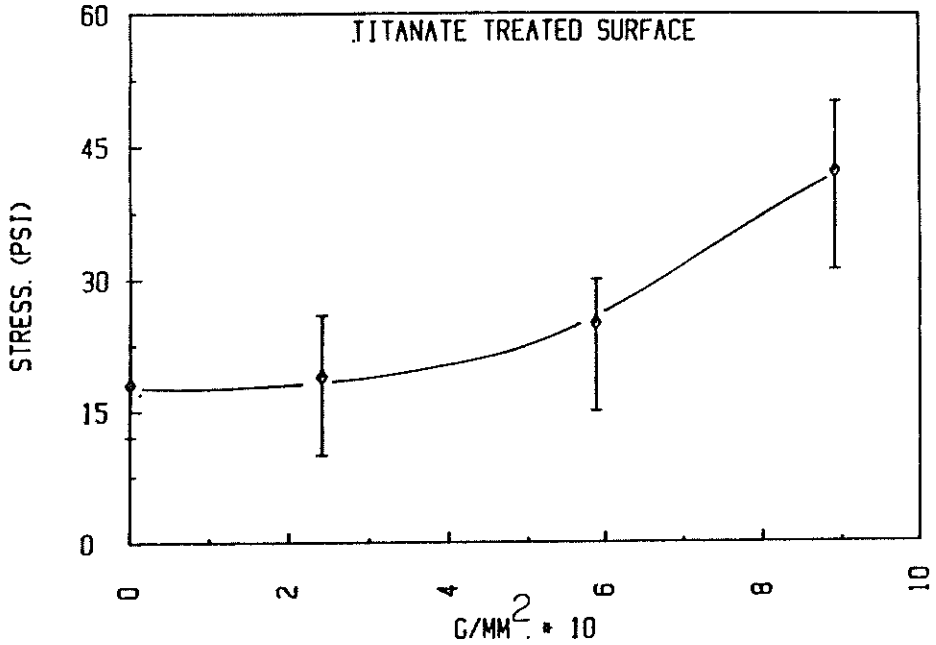


Figure 2. Lap shear strength results for titanate treated surface.

P24

THE STUDY OF EXTENDED CHAIN CRYSTALS OF GEL SPUN PE FIBRES

Zongquan Wu*, Anqiu Zhang, Kequan Chen, Pin Lu, Baojun Qian

Man-made Fibre Research Institute
CHINA TEXTILE UNIVERSITY

Abstract

Ultra high strength and modulus PE fibre's manufacturing are now rapidly increasing in Netherland, United States,and Japan, because of its unique strangth, low in specific gravity, outstanding durability, and especially its low cost .

There are two problems remained unsolved, ie, is there extended chain crystals in UHMWPE fibre produced through gel spinning? and what is the unit cell structure in extended chain crystals of PE under non-equilibrated state possessing high internal stress after ultra high streching?

We studied the supermolecular structure of ultra drawing PE fibres systematically with the help of WAXD,density gradient measurement, DSC and TEM, and drew the following conclusions:

1. Crystallinity and orientation of PE fibres increase with the increase of the draw ratio, which affects the mechnical properties of fibres markedly, if the draw ratio lies below 40 . As the draw ratio increases, for example higher than 40,the crystallinity and orientation approach saturation. The further improvement in mechanical properties of fibres attributes to the transformation of folded chain crystals into extended chain or secondary crystal by ultra high drawing.

2. When the draw ratio is over 10 , two endothermic melting peaks can be shown in DSC graph , the corresponding temperature being 136.7-145.3 °C and 151.2-153.2 °C the latter is the melting temperature of secondary crystal. The content(%) Of secondary crystals can be calculated by overlapping melting peak separation . The reason for other authors failure to discover the melting temperature of secondary crystal must be their failure to extracting trace amount of the solvent from the testing samples.

3. The unit cell remains orthorhombic even if the draw ratio increases to 50 . As the draw ratio increases , the length in a and b axes shrink while that in c axis changes quite insignificantly. Extrapolating the content of secondary crystal to 100%, unit cell parameters of secondary cryatal can be calculated as:
a=7.26 A b=4.84 A c=2.54 A
(the corresponding crystal density is d_c=1.042 g/cm^2)
which differs not only with the unit cell parameters of folded chain crystal but with extended chain cryatal in hexagonal under the equilibrated state obtained from heat setting at ultra high pressure ,

4. TEM study on the residue of these etched PE fibres offer a reply whether the secondary crystal is extended chain crystal or just the folded chain crystal holded tightly by amorphous but oriented PE macromolecules.

---

* address : Man-made Fibre Research Institute
CHINA TEXTILE UNIVERSITY
1882 West Yan-an Road
Shanghai,P>R>China

P25

ANIONIC POLYMERIZATION AND COPOLYMERIZATION OF PHENYL VINYL SULFOXIDE AND THERMAL DEGRADATION STUDIES OF POLY(PHENYLVINYLSULFOXIDES), Rustom Kanga, Mark Buese and T. E. Hogen-Esch, Department of Chemistry, University of Florida, Gainesville, FL 32611

The polymerization of phenylvinylsulfoxide was carried out in THF at -78 °C using various anionic initiators. It was found that delocalized carbanion initiators such as triphenylmethyllithium are effective initiators as are methyllithium and 1-lithio-1-(phenylsulfinyl)ethane. The block copolymerization of phenylvinylsulfoxide and styrene was also carried out. The molecular weight distributions in most cases were found to be quite narrow (< 1.3). TGA and pyrolysis mass spectrometry was used to characterize the elimination step. TGA of poly(phenylvinylsulfoxide) shows two stages of decomposition, the first stage at 190-200 °C corresponding to the elimination of phenylsulfenic acid and the second stage at a higher temperature (450 °C) typical of polyacetylene decomposition. Pyrolsis-mass spectrometry at low temperature (~ 190 °C) shows mainly the decomposition products of phenylsulfenic acid whereas the one at higher temperatures (~ 400 °C) shows formation of various alkyl aromatics typical of polyacetylene.



Fig. 1. 200 MHz ^{1}H NMR of styrene-PVS copolymer.

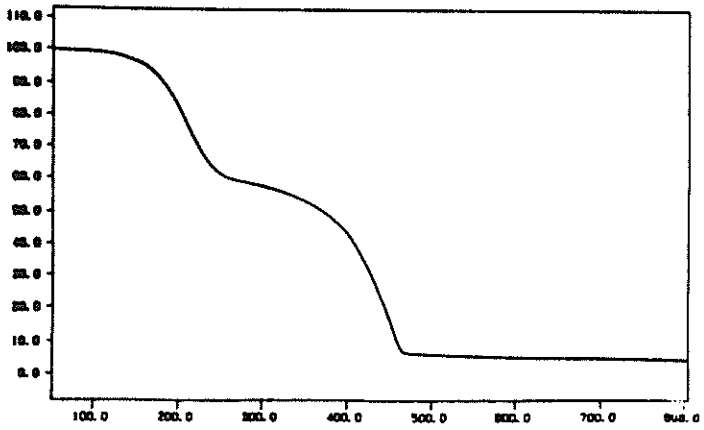


Fig. 2. Weight % vs. temperature (TGA) curve of styrene-PVS copolymer.

P26

RELAXATIONAL PROPERTIES OF PET FIBERS

H. Hristov and J. M. Schultz, University of Delaware, Newark, DE 19711, USA

The structural relaxation of polymeric fibers subjected to various external fields (mainly temperature and tension) is of major importance with regard to their industrial applications. The thermal shrinkage of PET fibers melt-spun at different spinning speeds has been intensively studied[1-3], while differential thermal analysis data appear episodically in the literature[3,4]. In the present work, we have investigated the relaxational behavior of commercial PET fibers (Rhone-Poulenc Company) melt-spun at 3, 4, 5 and 6 km/min by means of DSC, WAXS and fiber shrinkage. The DSC runs were made at heating rates from 2 to 30 deg/min in three degrees of constraint:: samples with free ends, fixed ends and under stress. As a reference sample amorphous PET ribbon of very low orientation, obtained by rapid quenching from melt was used. In figure 1 are shown the thermograms of fibers melt-spun at 3 km/min: free ends (1), fixed ends

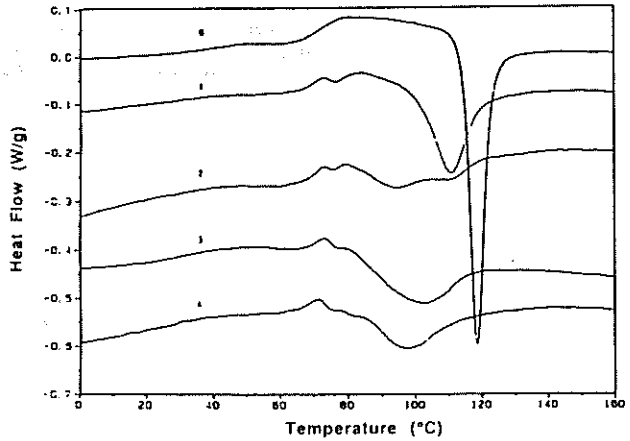


Fig. 1. DSC curves of PET fibers

(2), under stress (3), 4 km/min free ends (4), and the amorphous ribbon (0) at heating rate 8 deg/min. The results show that the relaxational process in fibers which are free to contract is complicated, with several stages. The multi-stage relaxation is confirmed in isothermal shrinkage measurements, where relaxational times ranging from 10ms to more than 10s are observed at elevated temperatures. Fixing the ends (curve 2) leads to considerable inhibition of the high temperature relaxation endotherm and a clearly expressed second (low temperature) crystallization exotherm. The first relaxational endotherm remains intact even after the application of external stress (curves 1-3). The above-described behavior of these low crystalline, low oriented fibres can be consistently explained if it is assumed that the amorphous material is found in two types of domains: oriented domains which bear the stress and practically unoriented domains with soft relaxational modes. X-ray results show that after heating to 77°C, the amorphous phase undergoes a structural change characterized by an increase of the local order but without threedimensional crystallinity. It is suggested that this reorganization occurs in the oriented domains. The amorphous phase of the highly crystalline highly oriented fibres (5 and 6 km/min) appears to be more homogeneous and the relaxational process less complex.

References

1) G. Perez, in High-Speed Fiber Spinning, A. Ziabicki and H. Kawai, Eds. (Wiley, New York, 1985), p. 333.

2) H. Heuvel and R. Huisman, J. Appl. Polym. Sci. 22, 2229 (1978).

3) P. Peszkin, J. M. Schultz and J. S. Lin, J. Polym. Sci., Polym. Phys. Ed., 24, 2591 (1986).

4) H. Heuvel and R. Huisman, in High-Speed Fiber Spinning, A. Ziabicki and H. Kawai, Eds. (Wiley, New York, 1985), p. 295.

P27

Computer Aided Design of Single Screw Extruders

Pierre G. Lafleur and Karim Amellal
Groupe de Recherche en Ingénierie des Polymères
Department of Chemical Engineering
Ecole Polytechnique
Montréal, Québec, CANADA, H3C 3A7.

Extrusion is one of the most important operation in the polymer processing industries. In today's competitive world, plastic product manufacturers deal with demands for high quality levels, short production lead times and small-lot delivery schedules. In order to improve their productivity, they rely on computer-aided design, engineering, and manufacturing (CAD/CAE/CAM).

The performance of an extruder is governed by its capacity to convey, melt and pump the polymeric material. The development of mathematical models for the simulation of single screw plasticating extruders has been covered extensively in the literature. Despite these developments, the perfect model that will help the practicing polymer engineer to design extruder screws using only the properties of the polymer, does not exist.

A comprehensive model has been developed for steady-state computer simulation of a single screw plasticating extruder in order to predict the performance of the extruder, the optimum screw design and the operating conditions. In order to achieve these objectives the model takes into account the three zones of the extruder: the solid conveying section, the plasticating section and the metering section.

For the analysis of the solid conveying zone, a combination of Darnell and Mol (1) solid-solid friction model and of the viscous drag model developed by Chung (2) is employed. As suggested by Lindt (3), for the analysis of the plasticating zone, a rigid solid bed combined with cross-channel circulation is used. In the metering section, a finite-difference technique is used to solve the momentum, continuity and energy equations coupled with appropriate boundary conditions. Curvature effects and leakage flow are taken into consideration. The predictions of the model are compared to experimental results obtained with two screw designs under different operating conditions.

Experimental data were obtained on a 45 mm single screw extruder with a L/D of 24:1. The extruder was equipped with six pressure transducers located at various positions along the barrel. A BELL torque sensor was installed on the screw shaft to measure the torque generated by the polymer during extrusion. Two screw geometries were tested, each equipped with an inside water cooling system:

1) A standard square pitch screw with a compression ratio of 3:1 and a 10 turns feed section, a 7 turns transition section and a 7 turns metering section.

2) A 2.5:1 compression ratio screw with a tapered root diameter over the full length.

(1) Darnell, W.H., and E.A.J. Mol, SPE J., vol. 12, p. 20 (1956)

(2) Chung, C.I., SPE J., vol. 26, p. 32 (1970).

(3) Lindt, J.T., Polym. Eng. Sci., vol. 25, p. 585 (1985).

P28

DSC ANALYSIS OF REACTION RATE KINETICS OF A DGEBA/MIXED AMINE EPOXY

M. Stoy, A. Fricke, D. Wingard* and C.L. Beatty*, Dept. of Chem. Eng. and Matl. Sci. and Eng.*, Univ. of Florida, Gainesville, FL

Introduction. Differential Scanning Calorimetry was used to follow the curing reactions of a diglycidyl ether of bisphenol-A (DGEBA) epoxy resin and a mixed aromatic curing agent. Of particular interest was the effect of stoichiometric ratio on the curing kinetics for this system. The data were interpreted in terms of several rate expressions from the literature. In addition, the time to gelation of the epoxy system, determined by dynamic mechanical analysis, was used to determine the conversion at the gel point.

Experimental. The curing system used in this work was a DGEBA epoxy resin (Shell Epon 828) and a mixed aromatic amine curing agent consisting primarily of equal amounts of m-phenylenediamine (m-PDA) and methylenedianiline (MDA). Several amine/epoxy ratios (A/E) were prepared: 0.81, 1.2 and 2.0.

A Perkin-Elmer DSC-7 was used in this study. Isothermal experiments were conducted in the temperature range 80-140°C. Transient heat liberated during instrument start-up was corrected for by making a second scan on the cured sample. The cumulative heat generated during cure, ΔH_t, was obtained as a function of time by numerically integrating the rate data. The ultimate heat of cure, ΔH_{ult}, was determined from dynamic experiments at heating rates of 2.5-20°C/min. The conversion α was calculated from $\alpha = \Delta H_t / \Delta H_{ult}$.

Results and Discussion. It was found that several kinetic models from the literature did not fit the experimental data well for this epoxy/amine system. The models began to deviate significantly from the data at conversions less than 20%. This is shown in Fig. 1 in a plot of the difference between the calculated and experimental rate, $\Delta\dot{\alpha}$, vs. conversion, α, at 100°C and an amine/epoxy ratio of 1.2. This deviation in α occurs much earlier than the gel point determined by dynamic mechanical analysis, suggesting that diffusional limitations are not responsible for the poor agreement between the data and the models.

We suggest that the models may fail because they do not take into account the different reactivities of the amino hydrogens for the two amines. Also, experiments should be done with each amine individually to try and separate the effect of multiple reactions.

References.

1. M.E. Ryan and A. Dutta, Polymer, 20, 203 (1979).
2. G.L. Hagnauer, B.R. LaLiberte and D.A. Dunn, "Epoxy Resin Chemistry II," R.S. Bauer, Ed., ACS Symp. Ser. No. 221, American Chemical Society, Washington, D.C., 1983, p. 229.
3. J. Mijovic, J. Kim and J. Slaby, J. Appl. Polym. Sci., 29, 1449 (1984).
4. A. Moroni, J. Mijovic, E.M. Pearce and C.C. Foun, J. Appl. Polym. Sci., 32, 3761 (1986).
5. M.A. Golub, N.R. Lerner and M.S. Hsu, J. Appl. Polym. Sci., 32, 5215 (1986).
6. C.C. Riccardi, H.E. Adabbo and R.J.J. Williams, J. Appl. Polym. Sci., 29, 2481 (1984).
7. S. Sourour and M.R. Kamal, Thermochimica Acta, 14, 41 (1976).

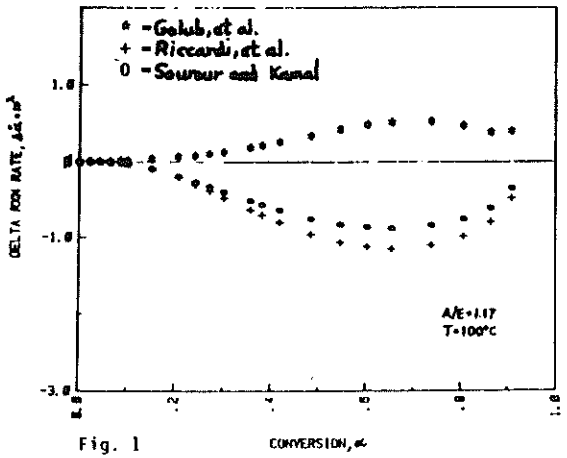


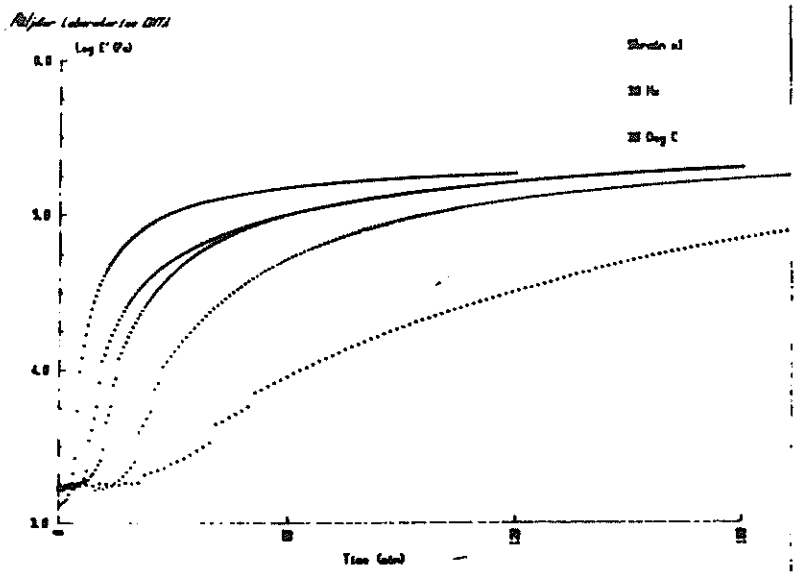
Fig. 1

P29

Use of Dynamic Mechanical Spectroscopy for Polyurethane Reaction Rate Studies.

by
K. Chehab, G. Campell* and C.L. Beatty
Dept. of Mat. Sci. & Eng., Univ. of Fl.,
Gainesville, Fl; and *Dept. of Chem. Eng,
Clarkson University, Potsdam, NY.

Dynamic mechanical shear measurements are reported on crosslinked polyurethane liquid castable systems as a function of reaction time, temperature and shear rate. Dynamic shear modulus is related to the reaction kinetics of the system. With these relations overall activation energies and reaction rate constants of modulus are interpreted from the data. Rates of reaction moduli were found to increase with curing temperature and frequency or shear rate. table 1. Apparent activation energies were higher than overall activation energies of moduli which indicates two different reaction mechanisms before and after gelation. Cured samples were scanned in temperature from -100C to 250C in shear to determine the effect of curing conditions on the final morphology and structure of the cured systems. Activation energies, glass transition temperatures of the soft and hard segments, shear moduli and the degree of hydrogen bonding between the soft and hard segments and the hard segments combined were interpreted with respect to the degree of phase separation. A lower degree of phase separation was obtained at high curing shear rates which resulted in a higher glass transition temperature of the soft segment and a lower one for the hard segments. At low curing shear rates the transitions shifted outwards resulting in a lower and a higher transition temperatures for the soft and hard segments respectively. Activation energies and transition temperatures of scanning are reported in table 2.



Cured at 3 Hz.

Curing Temp(C)	Gelation Time(min)	Rate Constant liters/mole.sec	Apparent Ea. Kj/mole	Overall Ea. Kj/mole
100	5.5	3.4127E-04	43.197	31.44
80	9.99	1.7241E-04		
70	15.8	1.52 1E-04		
50	33.79	.84246E-04		
30	142	.29744E-04		

Cured at 30 Hz.

Curing Temp(C)	Gelation Time(min)	Rate Constant liters/mole.sec	Apparent Ea. Kj/mole	Overall Ea. Kj/mole
100	4.15	11.865E-04	29.76	26.347
80	8.33	8.1634E-04		
70	12.49	7.0402E-04		
50	24.13	3.2184E-04		
30	37.8	2.0696E-04		

TABLE 1.

Samples cured at 30 Hz.

Temp(C)	Freq(Hz)	Tg1(C) soft seg.	Tg2(C) hard seg.	Ea1 Kj/mole	Ea2 Kj/mole	Mwe Kg/mole.	Mwc Kg/mole.
100	3	-15	176	249	305	13.5	1712
	10	-12	181				
	30	-10	189				
80	3	-13	180	237	336	13.5	1712
	10	-10	186				
	30	-9	192				
70	3	-12	183	190	541	22.8	1712
	10	-8	185				
	30	-5	190				
30	3	-12	186	168	913	91.9	2012

Samples cured at 3 Hz.

Temp(C)	Freq(Hz)	Tg1(C) soft seg.	Tg2(C) hard seg.	Ea1 Kj/mole	Ea2 Kj/mole	Mwe Kg/mole.	Mwc Kg/mole.
100	3	-18	190	157	948	14.3	1008
	10	-13	191				
	30	-10	194				
80	3	-16	183	151	432	22.1	1008
	10	-10	186				
	30	-8	192				
70	3	-20	186	137	691	29.1	1008
	10	-15	189				
	30	-10	192				
50	3	-18	173	125	548	27.8	1345
	10	-14	176				
	30	-8	190				
30	3	–	178	–	484	–	1345
	10	–	181				
	30	–	186				

Table 2: Dynamic Mechanical Properties (DMTA) of Polyurethane samples scanned from -100 to 250 C at 3 frequencies and 0.01% mm dynamic displacement. Samples cured at 3 and 30 Hz.

P30

EFFECT OF MIXING ON BEAD SIZE AND SEQUENCE DISTRIBUTION IN STYRENE/N-BUTYL METHACRYLATE COPOLYMERS

by

S. Canova, T. Anderson and C.L. Beatty

The quality of mixing during the suspension copolymerization of styrene and n-butylmethacrylate was shown to affect the sequential microstructure of the copolymer. the sequential microstructure of sequence distribution as it is often called is related to the degree of randomness of the monomer units in the copolymer chain.

A relative measure of this degree of randomness was provided by fluorescence spectrophotometry in which the excimer-to-monomer intensity ratio from the fluorescence spectrum was the basis for comparison. Fluorescence spectra of a number of copolymer samples and from their various bead size fractions were obtained.

In addition to these fluorescence measurements, differential scanning calorimetry provided glass transition temperatures (Tg) for the same samples. The glass transition temperature also gives insight into the nature of the polymer microstructure. For the styrene/n-butylmethacrylate system, the glass transition temperature for the copolymer (60.4°C) was less than that calculated by a bulk additive method (66.4°C). This indicates that neighboring dissimilar units in this copolymer rare repulsive and that an increase in the degree of randomness would decrease the glass transition further.

In combination, differential scanning calorimetry and fluorescence spectrophotometry measurements are supportive of each other. It was shown that the excimer-to-monomer intensity ratio and Tg both decreased as bead size increased in a slowly agitated batch, but as the beads neared their maximum diameter, the excimer-to-monomer intensity ratio and Tg began to increase. These trends were not so pronounced as agitation speeds were increased. These affects are explained by the bead velocity in relation to the external and internal heat transfer resistance of the beads.

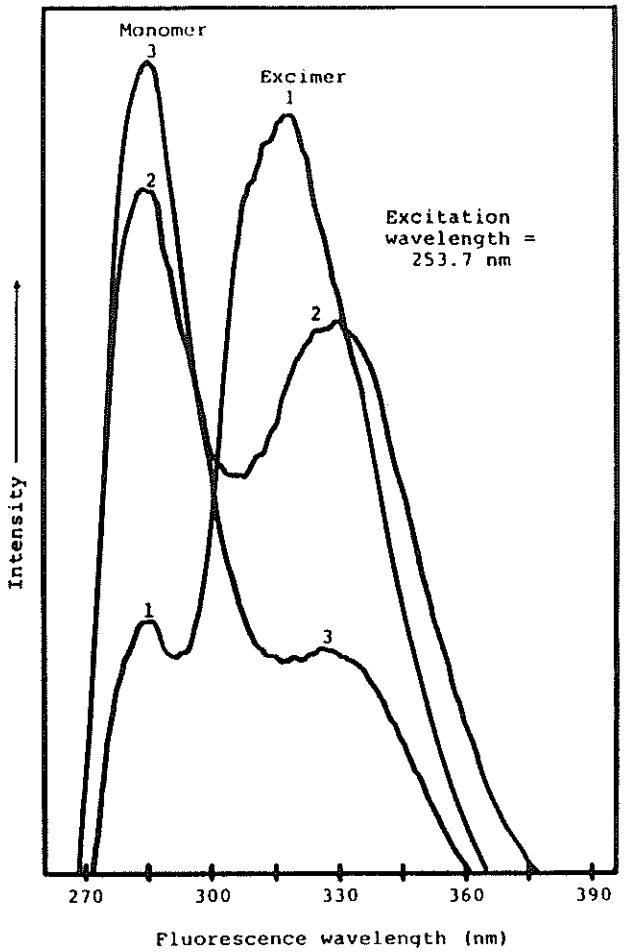


Figure 1. Fluorescence spectrum of 3 copolymer samples. Curve 1 = P-15558-15 (72.2 mole % styrene), 2 = 84.5 mole % styrene standard, and 3 = >2000 micron fraction for the 330 rpm batch (69 mole % styrene).

P31

FLEXURAL ENDURANCE OF BIAXIALLY ORIENTED POLYCARBONATE FILM AS A FUNCTION OF ORIENTATION AND TENSILE STRESS

J. Pujol, L. Rivera, and C. L. Beatty
University of Florida, Gainesville, FL

Introduction

The effects of orientation and stress intensity on the flexural fatigue lifetime of a biaxially oriented polycarbonate film were investigated. The film was tested in three directions relative to roll (i.e. parallel(0°), 45°, perpendicular (90°)) in the applied stress range 360 psi to 5390 psi.

Material

The polymer tested was a 4.9 ± 0.1 mil biaxially oriented polycarbonate film made by General Electric Company.

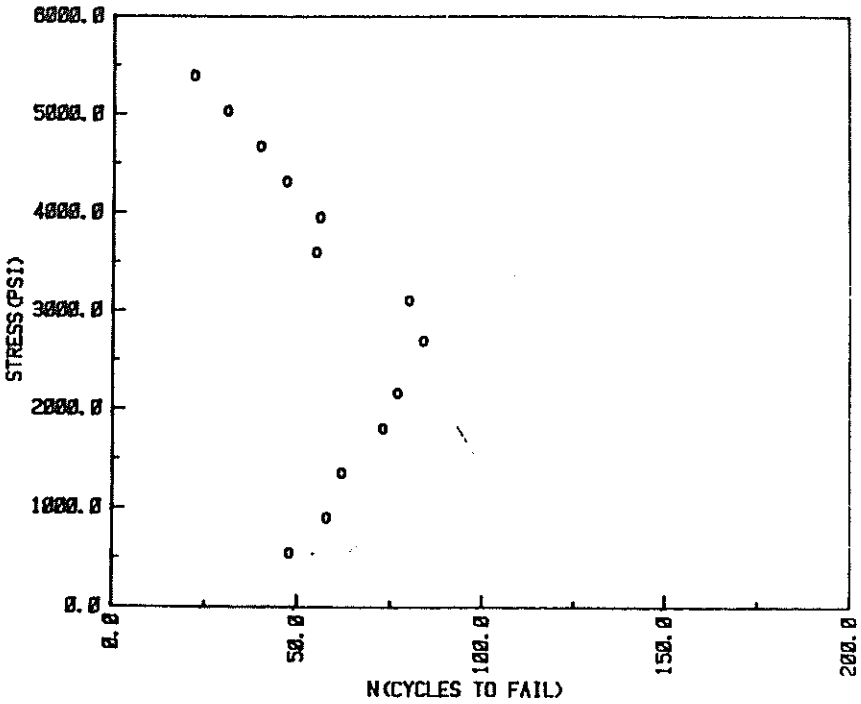
Equipment

The instrument used was a Tinius Olsen Folding Endurance Tester with a flexing frequency of 2.88 cycles/sec.

Results

The flexural fatigue life of the polycarbonate film was found to be independent of flexing direction. In addition it was found that the fatigue life increased with increasing applied stress in the lower stress region but decreased with increasing stress in the higher stress region. In other words a fatigue lifetime inversion was observed. This latter observation can be explained in terms of a transition from craze-dominated to shear-dominated crack growth at greater applied stresses as outlined in "Shear and Craze Competition in Sub-Critical Fatigue Crack Growth," by M. T. Takemori and D. S. Matsumoto of General Electric Company. The accompanying graph is indicative of the results.

References: M. T. Takemori and D. S. Matsumoto, "Shear and craze Competition in Sub-Critical Fatigue Crack Growth," Polym. Prepr. (Am. Chem. Soc. Div. Polym. Chem.) 1985, 26 (2).



Polycarbonate (GE): Flexural Fatigue data; perpendicular to roll.

P32

POLYOLEFIN-WOOD FIBER COMPOSITES

R.G. Raj , B.V. Kokta and C.Daneault, Centre for research in pulp and paper, University of Quebec at Three-Rivieres, Three-Rivieres, Quebec - G9A 5H7, Canada

Wood fibers show intresting potential as fillers for thermoplastics. These fibers offer number of advantages such as low cost, higher specific strength and modulus, renewable nature and under goes little damage during processing. The main problem encountered during the fabrication of these composites are lack of adhesion at the polymer-fiber interface and poor dispersion of the filler in the polymer matrix. By using suitable additivies/coupling agents the bonding at the interface can be improved.

In the present study, a number of common thermoplastics Polyethylene (high density, HDPE), Polypropylene (PP) and Polyvinyl chloride (PVC) were reinforced with Chemithermomechanical pulp (CTMP, average aspect ratio 11.9). Different coupling agents/bonding agents used were:

a) Silane A-172 Vinyltri (2-Methoxy Ethoxy) Silane

b) Silane A-1100 Gamma-Amino Propyl Triethoxy Silane

c) Polymethylene Polyphenyl isocyanate (PMPPIC)

The compounding of polymer and fiber was done in an extruder and the samples were compression molded at 150-165°C. From Table 1 it can be seen that the stress generally decreased in untreated fiber composites. After isocyanate treatment in HDPE-CTMP aspen fiber composites the stress reached a maximum value of 38.0 MPa at 30.0% fiber level compared to 24.7 MPa of polymer. The silane A-172 and PMPPIC treatment was not effective in PP-CTMP aspen fiber composites. However, the stress increased marginally after isocyante treatment in PVC-wood fiber composites. The modulus remained relatively unaffected by fiber treatment.

Table.1 Tensile properties of different thermoplastics-wood fiber composites

Composite (treatment)	Ultimate stress (MPa)			Elongation at break (%)			Elastic modulus (MPa)		
(fiber wt %)	10.0	20.0	30.0	10.0	20.0	30.0	10.0	20.0	30.0
HDPE	24.7			861.9			966		
a)Untreated	23.3	20.5	20.1	16.2	9.8	5.2	978	1085	1529
b)PMPPIC	27.8	31.7	38.1	15.2	10.2	9.1	1013	1143	1634
PP	32.2			12.8			1053		
a)Untreated	23.6	22.9	22.1	4.8	4.1	3.5	1093	1206	1653
b)Si A-172	27.1	24.6	23.6	4.2	3.7	3.4	1473	1670	1712
c)PMPPIC	24.2	22.8	20.8	5.0	3.9	3.4	1184	1250	1669
PVC	24.4			149.8			368		
a)Untreated	18.2	17.8	17.2	64.1	18.5	9.4	586	669	679
b)Si A-1100	16.8	16.1	16.0	102.5	28.4	11.0	388	503	605
c)PMPPIC	21.4	25.9	27.3	65.4	31.2	19.8	389	733	812

CRYSTALLIZATION IN POLYMER PROCESSING

K. Katayama, H. Tsuji, S. Murakami and K.J. Ihn
Institute for Chemical Research, Kyoto Univ.,
Uji, Kyoto-fu 611, Japan

In high-speed melt-spinning of poly(ethylene terephthalate) [PET], thinning of a filament is greatly accelerated at a certain point from the spinneret showing neck formation,[1] and it was pointed out that rapid crystallization takes place simultaneously with the neck formation.[2,3] What causes this neck formation? There are two explanations. One is a drop of the extentional viscosity of the polymer melt for some reasons. The other is a premonitory change in the structure[4,5] (rod-like regions with some regularity are generated in the amorphous medium), and this two-phase system shows stress-softening which is often observed in composite materials. The structure change in melt spinning, however, is too rapid to ascertain the real cause for the neck formation. Thus, the crystallization of oriented amorphous PET was investigated in the temperature range where the crystallization rate is comparatively low, focusing our interest on the generation and development of structure.

As an oriented amorphous specimen, fibers spun at a spinning speed of 3000 m/min and then stretched 60% were used. The elongation of 60% roughly corresponds to the end point of the necking in the stress-strain curve of the fiber. As the first step, the changes in SAXS and WAXS profiles of the specimen were observed with a PSPC system during heating process at a rate of 0.34°C/min in a series of time span of 100 sec. Figure 1 shows profiles of SAXS along the meridian and WAXS along the equator. According to the DSC measurement, the crystallization starts at about 70°C and ends at 110°C. In this temperature range, however, broad WAXS peaks show rather low degree of perfection in the crystalline part, and very weak SAXS intensity indicates a quite small density difference between crystalline and amorphous parts. This is contrary to the fact that in the oriented crystallization of polyethylene, the crystalline peaks in WAXS are sharp even in the early stage of crystallization. Thus, the crystallization of oriented amorphous PET is considered to be a continuous series of transformation from the amorphous toward perfect crystalline state, rather than one-step transformation. To obtain more detailed information on structure formation and crystallization kinetics, isothermal crystallization must be studied at various temperatures. Furthermore, electron microscopic observation of the crystallization process of oriented thin films, using both dark-field and defocus contrast methods, will give us a deeper insight into the mechanism of oriented crystallization of polymers. These studies are now in progress.

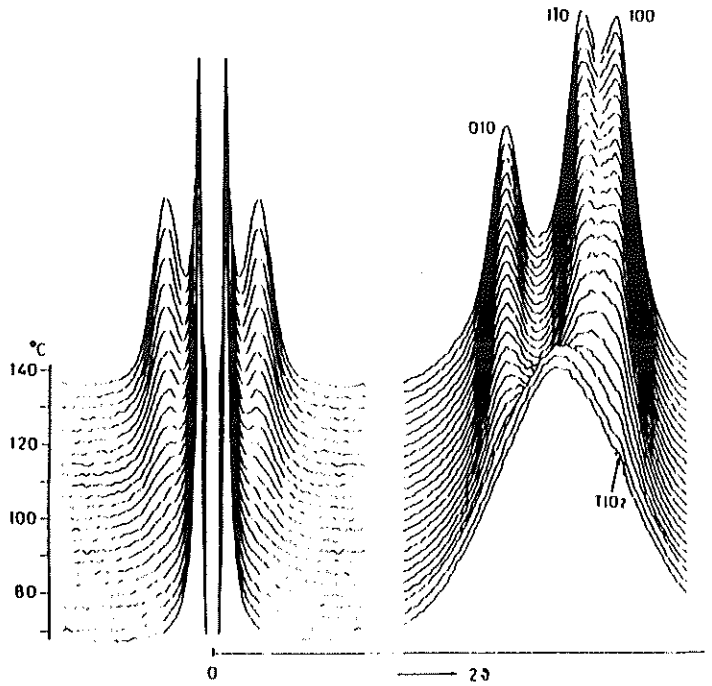


Fig.1 Change in profiles of SAXS along the meridian and WAXS along the equator during heating process.

References

1) G. Perez et al., Proc. 18-th Int. Man-Made Fibre Conf., Dornbirn, Austria (1979)
2) J. Shimizu, Sen-i Gakkaishi, 38, p-499 (1982)
3) M. Matsui, ibid., 34, p-508 (1982)
4) K. Katayama, ibid., 34, p-63 (1978)
5) K. Nogami et al., Bull. Inst. Chem. Res., Kyoto Univ., 55, 227 (1977); K. Nogami, Thesis, Kyoto Univ., (1983)

P 35

STUDY OF FILLER ORIENTATION IN INJECTION MOLDED PIECES BY MECHANICAL AND THERMOANALYTICAL METHODS

G.Bánhegyi, G.Naderi /Research Institute for Plastics, H-1950, Budapest, Hungary/

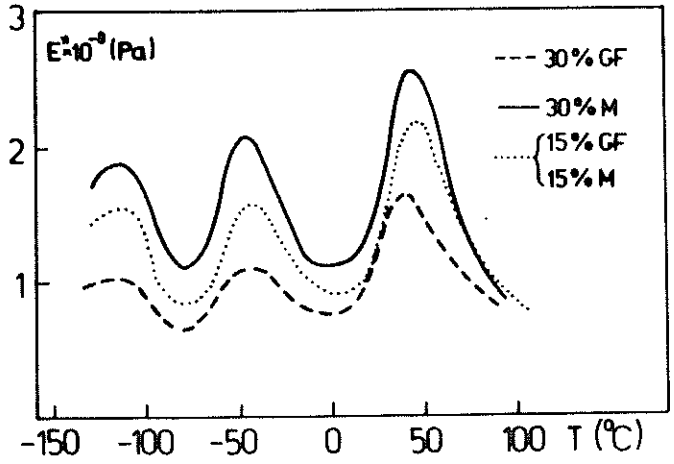
Mineral filled and glassfiber reinforced plastics become more and more important in various branches of industry. Fillers and reinforcements increase stiffness, reduce creep and warpage of the parts. Nonspherical fillers usually tend to orient during processing /as injection molding or extrusion/ which results is anisotropic part properties. This is an advantage if orientation can be controlled, but if intricate shapes are molded or if the gating is not designed properly, orientation can cause warpage or other undesirable effects.

In this study some mechanical and thermal properties of glassfiber /GF/ and Al_2O_3 mineral /M/ filled nylon-6 samples were studied. Samples were cut from injection molded 80x80x4 mm sheets parallel and perpendicularly to the flow direction. In some cases isotropic 1 mm thick pressed plates were used as well. All samples contained 30 wt% filler, but one 30 wt% glassfiber, the other one 30 wt% mineral and the last one 15 wt% GF and 15 wt% M. Measured properties are summarized in the Table. According to DSC and DMA studies /the latter is shown on Fig.1./ the presence of various fillers does not cause big differences in the matrix crystallinity and relaxation properties. The anisotropy can be well observed on flexural moduli and thermal expansion coefficient values of the GF and GF/M filled samples. Mineral filled specimenst are practically isotropic. The impact strengths are not sensitive to filler orientation.

Physical properties of glassfiber /GF/ and mineral /M/ filled nylon-6 samples. Total filler content is 30 wt%.

Property	GF 30	GF/M 15/15	M 30
Linear expansion coefficient $\times 10^{-5}$			
∥	2.9	4.9	14.9
⊥	11.5	11.2	16.0
Charpy notched impact strength, kJ/m^2, 23°C			
∥	6.6±0.7	8.0±1.5	7.4±2.3
⊥	7.7±1.7	7.5±1.3	8.0±1.8
Flexural modulus, N/mm^2			
∥	4600± 30	3100±130	2400± 60
⊥	3200±200	2700±260	2500±200
DSC crystallinity /%/			
	31.2	30.4	28.7

Figure 1. Mechanical losses of isotropic compression molded samples.



P 36

INCREMENTAL DRAWING OF POLYETHYLENE TEREPHTHALATE

A. Misra, B. Dutta and A. K. Mukhopadhyay
Centre for Materials Science & Technology,
Indian Institute of Technology, Delhi
New Delhi-110016, India

ABSTRACT

Polyethylene terephthalate (PET) fiber for textile use are produced by the process of melt spinning and subsequent drawing. It is possible to stretch polyester fibers which are melt spun in normal production to several times their original length. This produces an orientation of the macromolecules in the direction of fiber axis. This is accompanied by stress induced crystallisation and the crystallites so produced also orient themselves in the stretching direction (1). In the conventional drawing process (CDP), the stretching of the fiber takes place between two sets of rollers, with the take-up roller rotating at considerably higher speeds than the feed roller. As an alternative to this process is the drawing of melt spun fibers in a number of successive steps such that a small amount of drawing occurs at each step. In such a process, invented by Sussman(2), the fibers are drawn incrementally and is referred to as Incremental drawing process (IDP). A typical IDP set-up consists of two cones with approximately 40 micro-terraced steps. The steps are designed such that the fibers nest in them without slippage to the lower step. The cones rotate at equal speeds connected to a single motor. The drawing is simply the ratio of the diameter of take-up step to the diameter of feed step. The drawing of nylon-6 by IDP has been carried out successfully(3) to produce fibers of properties superior to those obtained by CDP. The improvements of properties were explained on the basis of stuctural analysis.

Drawing of PET by IDP has not yet been reported so far. This paper deals with exploring the potential of this technique for drawing of PET multifilament yarns. Different lines of thought have been considered for developing a suitable heating system for the incremental drawing set-up. Presently, a chamber type of heating system has been designed ensuring the maintenance of uniform temperature inside the chamber with a minimum loss of heat. The chamber is heated by a circulating hot air system and the drawing bodies (microterraced cones) are enclosed inside the chamber. The multifilament yarn is drawn along the surface of two corotating cones.

Multifilament PET-POY (polyethylene terephthalate-partially oriented yarn) has been successfully drawn at 80°C at speeds ranging from 100 m/min. to 300 m/min. The actual draw ratio and the denier of the drawn yarns was close to the calculated value. Results of PET-POY drawn by IDP have been compared with those from the same yarn drawn by CDP. Drawn fibers have been tested for tenacity, initial modulus and breaking extension. The structure of these fibers has been characterized by determining birefringence, f_o, f_c and % crystallinity.

It has been observed that mechanical properties of the IDP drawn yarn are considerably superior than those of CDP drawn yarn. In general the IDP drawn fibres show higher initial modulus and tenacity than fibers drawn to equivalent draw ratios by CDP. Mechanical properties have been correlated with the structure. The effect of temperature of drawing and the drawing speed on the mechanical properties as well as on the structure has been investigated. Lastly, fibers have been taken from several steps and analysed to study the development of structure upon drawing.

REFERENCES

1. Ludwig, H. "Polyester fibres - Chemistry & Technology" Wiley Interscience, N.Y., 1971.
2. M.V. Sussman, U.S. Pat. 3,978,192 (1976).
3. A. Misra, B. Dutta and V. Kaliprasad, Drawing of Nylon-6 by the Novel Incremental Drawing Process, J. of App. Poly. Sci., 31, 441-455 (1986).

P37

RECENT TECHNIQUES FOR YIELD STRESS MEASUREMENT

D. De Kee, Department of Chemical Engineering, University of Windsor, Windsor, Ontario, N9B 3P4, Canada.

This contribution reports on some recent techniques which have been developed to describe the yield stress.

There are two major methods for determining a yield stress: a) dynamic methods, b) static methods. A static method is preferable, since it does not rely on disturbing the three dimensional structure of the sample material prior to the measurement. The question then arises as to whether or not the different techniques for measuring the yield stress are actually determining the same quantity.

Dynamic methods include techniques such as analysis of torque decay curves, pressure decay curves, and the ubiquitous extrapolation of shear stress data. Results from extrapolation techniques, depend on the sensitivity of the apparatus and usually lead to unacceptable results.

Recently, two more reliable static techniques for yield stress measurement have been proposed; a) a method based on a vane test (1), which is applicable for regions of high solid concentration and b) a method based on modification of an automatic surface tension analyzer (2).

Figure 1 shows a schematic diagram of the vane apparatus. As the vane rotates, with the material between the blades moving along with the vane, the region of the concentrated suspension close to the edges of the vane blades deforms elastically, until "bond breakage" occurs. The maximum in the recorded torque-time response is then associated with the yield stress. The use of the vane method may become problematic at lower solid concentration, where the viscous stress might become significant in comparison with the "network" stress. Also, yielding may take place mostly in front of each blade instead of at the edges.

Figure 2 shows a schematic diagram of the modified surface tension analyzer. Here, a plate is immersed in the sample. The elevator platform is subsequently lowered, while the output from the transducer is recorded. A marked change in slope in the recorded force versus time plot allows one to calculate the yield stress.

The vane method was tested using highly concentrated bauxite residue suspensions. The plate method was tested with SBS triblock copolymer solutions. In this latter study, a comparison of yield stress values with extrapolated viscometric data at different temperatures revealed a crossing-over of some of the extrapolated straight lines (for different temperatures) at low shear rates. This resulted in unacceptable (yield stress increasing with temperature) yield stress predictions.

While both the vane and the plate method allow the quantitative study of structural recovery of thixotropic suspensions, the plate method should be able to perform better at lower solid concentration.

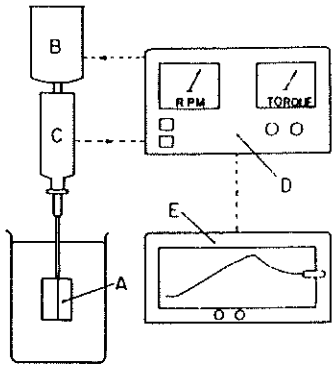


Figure 1: Schematic diagram of the vane apparatus for yield stress measurement.

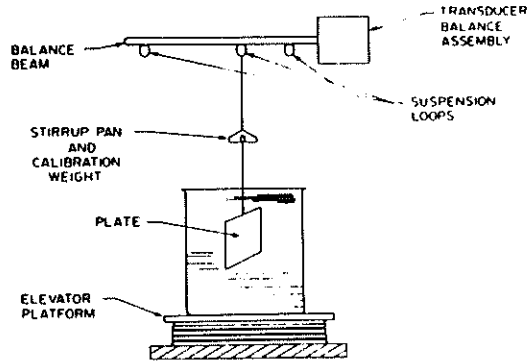


Figure 2: Schematic diagram of the plate apparatus for yield stress measurement.

References

1. N.Q. Dzuy and D.V. Boger, J. Rheol., 27(4) 321 (1983).
2. D. De Kee, P. Mohan and D.S. Soong, J. Macromol. Sci.-Phys., B25(1&2), 153 (1986).

P38

EFFECT OF SORBED WATER ON THE DYNAMIC MECHANICAL PROPERTIES OF AN IONIC POLYURETHANE

by

W. Williams and C.L. Beatty

An ionic polyurethane, obtained from Wilmington Chemical Corporation, has been studied as a function of water content. Significant changes in tensile stress-strain, dielectron relaxation spectroscopy and dynamic mechanical spectroscopy results were noted as the water content was varied. These effects are due to both water-ionic domain and water-polymer interactions. Tg and modulus varied in a none-linear fashion with water content consistent with sequential plasticization of the polymer and ionic domains.

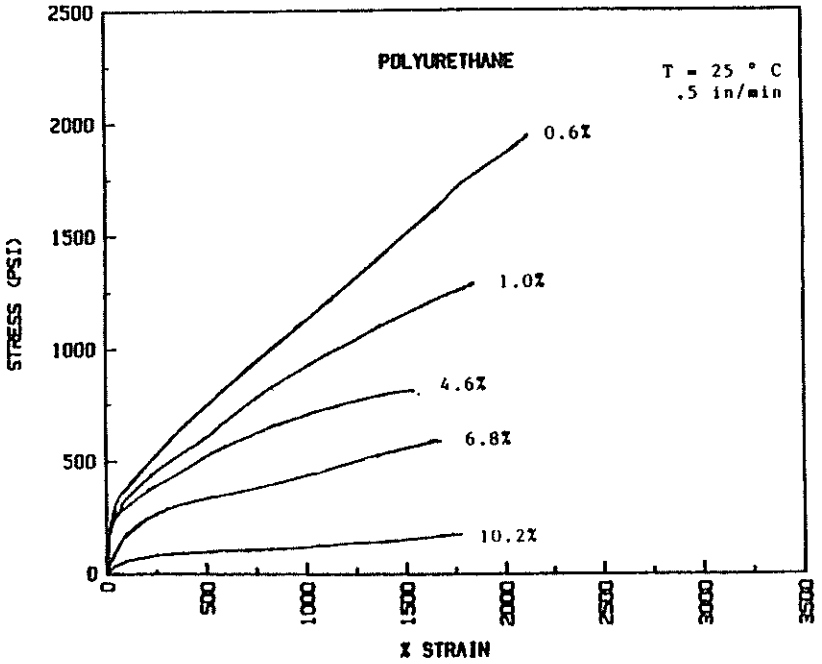


Figure 1. Stress vs. % strain of ionic polyurethane as a function of water content.

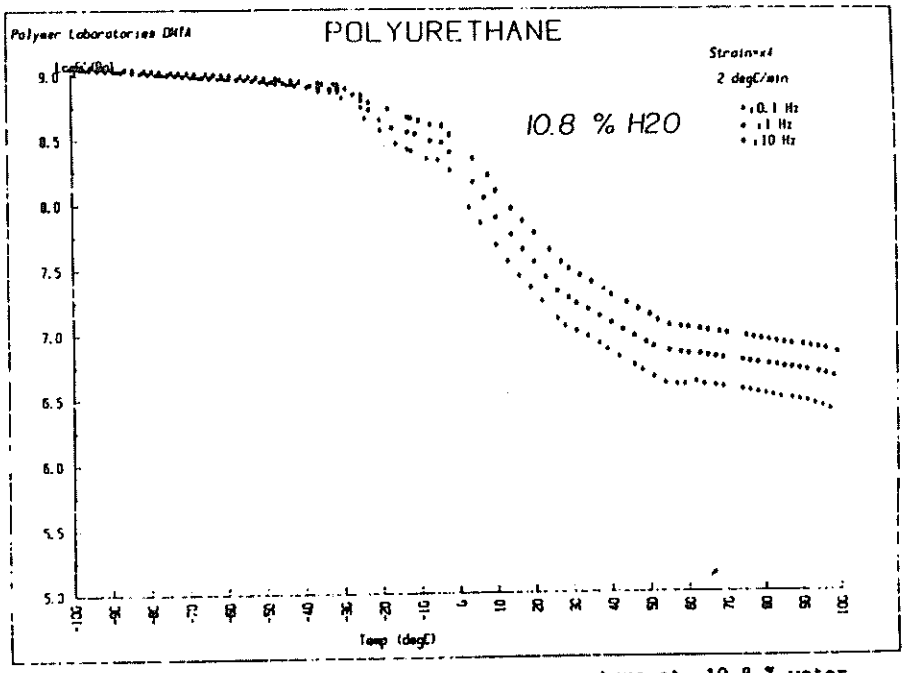


Figure 2. Storage modulus vs. temperature at 10.8 % water.

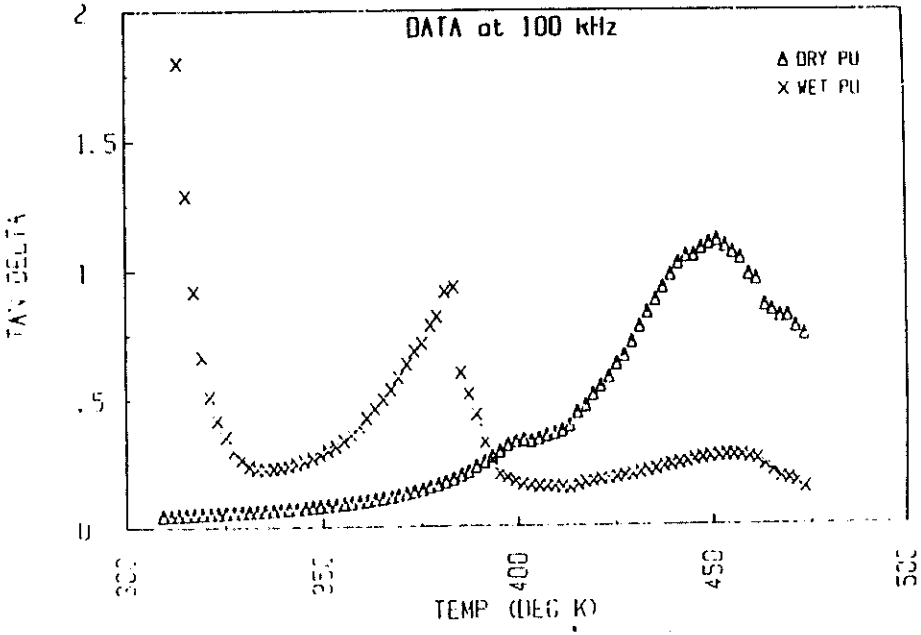


Figure 3. Wet and dry tan delta vs. temperature at 100 kHz.

P39

SORPTION OF LIQUIDS INTO FOAMS AND SUBSEQUENT CHANGES IN MECHANICAL PROPERTIES OF THE FOAMS

J. P. Harmon, D. Wingard, D. Bennett, J. Dixon, W. Williams, and C. L. Beatty.
University of Florida,
Gainesville, Florida

The effect of penetrant sorption on viscoelastic dynamic properties of closed cell foams has been determined. The foams characterized were a rigid polyurethane with a density of 10pcf and crosslinked polyethylenes with densities of 2 and 6 pcf. Samples were immersed in JP5 jet fuel, hydraulic fluid and 1,1,1-trichloroethane at selected temperatures. A significant equilibrium sorption was noted at elevated temperatures:

	% PENETRANT SORBED		
FOAM	1,1,1-TCE	HYDRAULIC FLUID	JP5 JET FUEL
6 pcf PE	90% (69°C)	64% (85°C)	93% (96°C)
2 pcf PE	95% "	79% "	95% "
PU	50% (69°C)	34% (164°C)	55% (187°C)

These samples, along with unswollen control samples were characterized with a Polymer Laboratories Dynamic Mechanical Thermal Analyzer. A single cantilever beam geometry was used. Samples were scanned at 3 Hz from -150°C up to temperatures where softening significantly reduced the support of stress.

In polyethylene control samples the damping peak for the glass transition appeared at -128 to -130°C. The glassy storage modulus, E', decreased by over a decade as the foam density decreased from 6 to 2 pcf. The storage moduli for sorbed samples at -128 to -130°C was higher than that of control samples and dependent on the penetrant:

JP5 > 1,1,1-TCE > Hydraulic Fluid > Control

This increase in stiffness is attributed to the fact that the penetrants are below their freezing points in this temperature range. At higher temperatures a sharp damping peak occurs at the penetrant melting point, -86°C for JP5, -34°C for 1,1,1-TCE and -60°C for JP5. Concurrently, there is a drop in modulus due to plasticization of the polyethylene matrix by the penetrant. Values for room temperature storage moduli follow the order:

Control > Hydraulic Fluid > 1,1,1-TCE > JP5

In polyurethane foam samples, the freezing point of the penetrants was below the glass transition of the polymer in sorbed samples. The glassy storage modulus at -100°C was slightly lowered by the penetrants. The damping peaks due to solvent melting were much broader in the rigid polyurethane matrix than those observed in rubbery polyethylene samples. As the glass transition was approached, the foams collapsed and loosened from the grips. The increase in tangent delta at the beginning of this region was monitored. The temperature at which tan delta reached a value of 0.2 was recorded:
Control (83°C)> Hydraulic Fluid (80°C)> JP5 (50°C)> 1,1,1-TCE (38°C)

Penetrants at temperatures below the melting point, but above the glass transition of the polymer impart rigidity. This may be due to penetrant trapped in the cells of the foam. Sharp melting transitions are evidenced by dynamic mechanical spectroscopy. When melting transitions are below the glass transition of the matrix, the damping peak broadens.

P 40

MODELING AND VISUALIZATION OF THE FLOW OF MISCIBLE AND IMMISCIBLE POLYETHYLENE BLENDS THROUGH CAPILLARIES AND SLITS

B. Tremblay and L.A. Utracki, National Research Council Canada, Industrial Materials Research Institute, 75 de Mortagne, Boucherville, Que., Canada, J4B 6Y4

Two series of linear low density polyethylene, LLDPE, were used; Series I (with low density polyethylene, LDPE) was immiscible, whereas Series II (with another type of LLDPE) was miscible. The molecular as well as the flow properties of neat resins and their blends were previously determined [1]. The most important finding of that study was the observed direct correlation between the strain hardening in uniaxial extension, SH, and processability on the film blowing line; larger SH better processability. In accord with the previous findings it was observed that LLDPE showed very little, if any, SH whereas in LDPE SH was very large, leading to increase of the uniaxial strain viscosity by a factor of four. In blends of Series I addition of even 10 wt% of LDPE to LLDPE was sufficient to generate SH.

The present work concentrates on two aspects of flow properties of these polymers: (i) flow visualization in capillaries and slits, and (ii) modeling of flow behavior with a special emphasis on the non-linear viscoelastic behavior of blends in uniaxial extension. The experimental set-up for flow visualization is basically a transparent capillary or slit attachment to an Instron Capillary Rheometer, ICR, illuminated on a meridian plane by a planar laser beam with a photographic camera as recording device. The streamlines above the dies at constant shear rate, $\dot{\gamma}$, were of prime interest. It was observed that as small changes as 1% in composition of Series I blends generate noticeable variation in vortex size, VS. As $\dot{\gamma}$ increases The VS increases as well; VS for LLDPE was found to be much smaller than for LDPE. However, detailed visualization study demonstrated that the entrance angle (defined in Figure 1) versus $\dot{\gamma}$ dependence passes through a minimum. This behavior is noticeable for melts with intermediate SH, such as 90/10, 80/20 or 50/50 LLDPE/LDPE blends. Similar relation was observed for polydimethylsiloxanes [2] with few branches (50 ppm). With yet further increase of $\dot{\gamma}$ vortex generated by the flow of the 90/10 LLDPE/LDPE blend would actually detach from the lip at the entrance to the capillary. This shifting of the vortex away from the die was even more stricking for the PDMS mentioned previously. The experiments with a series of LLDPE resins and miscible blends of Series II allowed to conclude that VS increases with an increase in the molecular weight distribution. The flow visualization also allowed studies of the elastic turbulence in the die entry region which lead to a distortion of the extrudate (melt fracture, MF). Plot of the critical values of $\dot{\gamma}$ for MF to occur vs. composition in Series I passed through a minimum at 50 to 80 wt% of LDPE. The effect of temperature on VS and MF was also studied. Observation of the extrudate revealed that sharkskin, characterized by distinct ridges was found for the following compositions: 100/0, 90/10, 80/20, whereas a surface roughness was observed without ridges at the compositions of 50/50 and 20/80.

The results of flow visualization were computer modeled using a commercially available finite element program with various constitutive equations (Phan-Thien Tanner, Oldroyd-B, etc.). The modeling allowed to develop a correlation between the magnitude of strain hardening and vorticity at the die entrance region.

REFERENCES

[1] B. Schlund and L.A. Utracki, Polym. Eng. Sci., 27, 359, 380, 0000 (1987); L.A. Utracki and B. Schlund, ibid., 27, 367, 0000 (1987).

[2] B. Tremblay, Ecoulement de polymères fondus dans les orifices: étude expérimentale des écoulements secondaires et de la stabilité, modélisation des effets viscoélastiques (in English), Thèse de Doctorat de INPG, Univeraité Scientifique et médicale de Grenoble (1986).

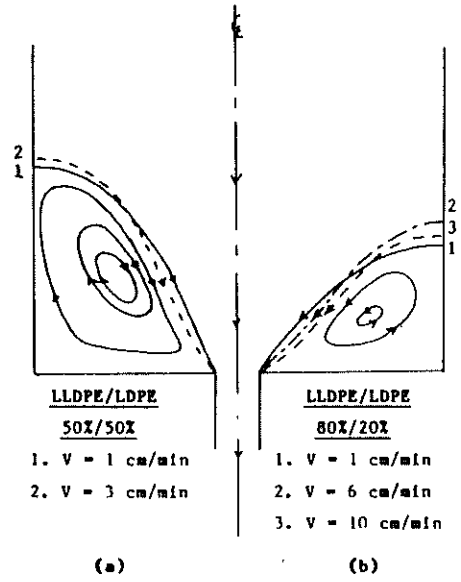


Figure 1

P 41

APPLICATION OF A LUMPED PARAMETER METHOD ON CONTROL VOLUMES FOR FLOW SIMULATION INSIDE EXTRUSION DIES

J.Vlcek[1], V.Kral[1], J.Perdikoulias[2], and J.Vlachopoulos[3]

1 Rubber and Plastic Research Institute, Gottwaldov, 764 22, Czechoslovakia
2 Brampton Engineering (1983) Inc., 8031 Dixie Rd. S., Brampton, Ontario, Canada
3 Department of Chemical Engineering, McMaster University, Hamilton, Ontario, Canada, L8S 4L7

The method of lumped parameters on control volumes is a numerical approximation technique that allows one to solve 3-D flow problems in polymer processing. The method assumes that there are only significant flows in 2 directions and that equations for poiseuille flow apply. Thus the solution is much faster than complete and rigorous 3-D solutions (finite element) and in many cases accurate enough for design purposes. The lumped parameter method has been used to describe flow, pressure and temperature fields in various types of extrusion equipment such as spiral mandrel dies, sheet and film dies and profile dies. The only condition is that the flow gap be much smaller than the other two dimensions.

The lumped parameter method was used to predict the volumetric flow distribution in an existing 100 mm spiral mandrel die with 4 spirals and no post spiral sections (chamber, lips restrictors). The percent variation in volumetric flow rate around the circumference of the die was compared to the percent variation in thickness of a tube produced from the same die. The results, shown in figure 1 , are in good agreement.

The lumped parameter method can also include viscoelastic behaviour in order to obtain even more accurate solutions as is demonstrated in the following example. The volumetric flow distribution in a 1600 mm wide flat die was simulated using the lumped parameter method. Figure 2 contains the results of the simulations along with the actual performance of the die. The dashed line represents the volumetric flow distribution as predicted using a purely viscous material. The solid line represents the same predictions using a viscoelastic fluid represented by a White-Metzner model. The results are again made dimensionless by plotting the percent variation from the mean. The measured percent thickness variation is indicated in figure 2 by the crosses (x). Figure 2 shows that the comparison between theory and experiment is improved when viscoelasticity is included.

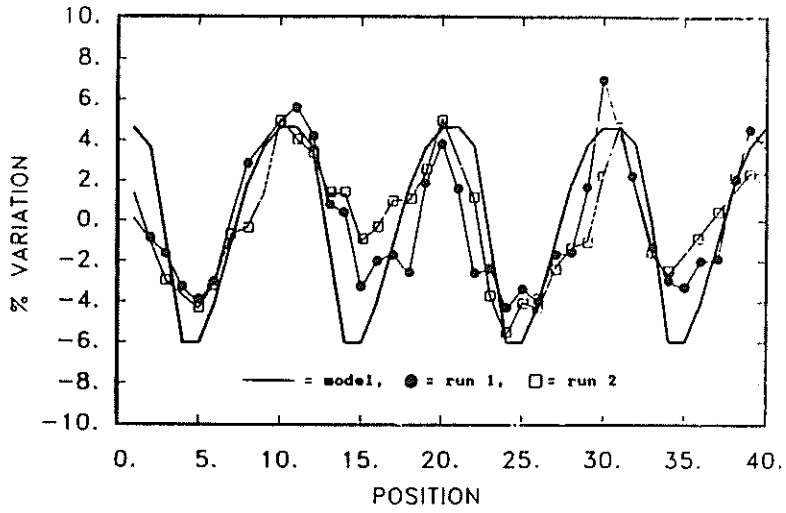


Figure 1. Model prediction vs two experimental runs

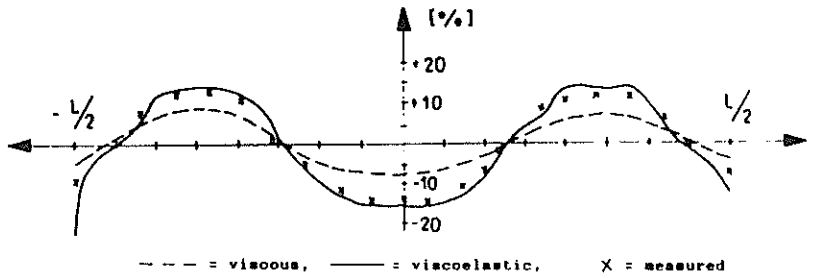


Figure 2. Model predictions vs experimental data

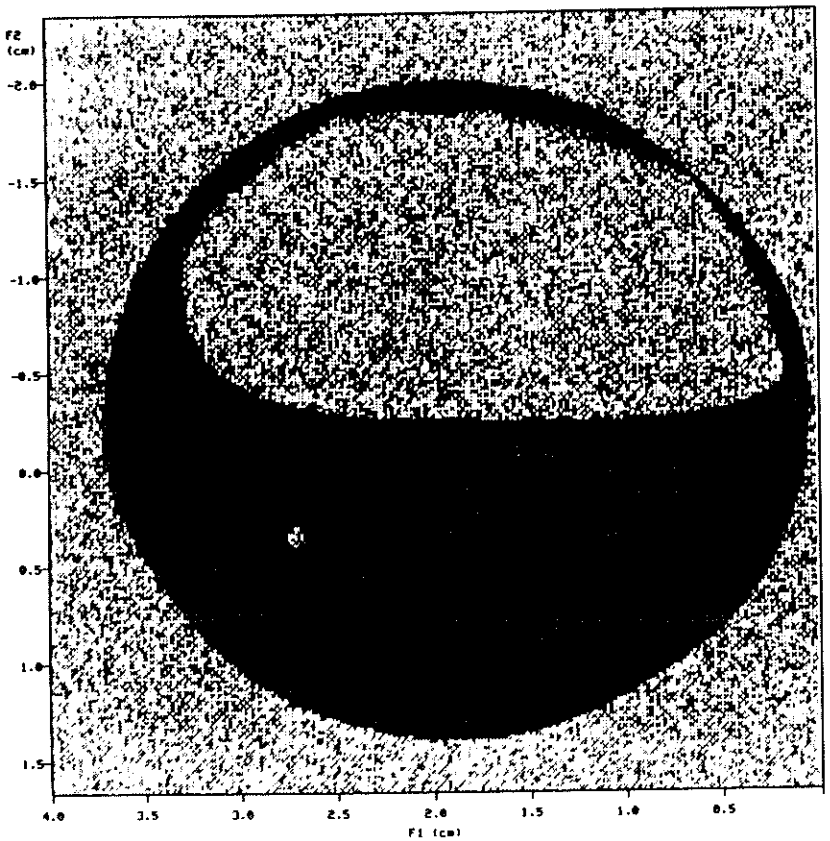
P42

Nuclear Magnetic Resonance Imaging of Flow During Polymer Extrusion

Thomas H. Mareci, Julie Harmon and Charles L. Beatty

Departments of Radiology, Physics, and Materials Science & Engineering
University of Florida, Gainesville, Florida

The technique of nuclear magnetic resonance imaging has matured to the point where it has become a routine diagnostic procedure in medicine. Recently we have been exploring the potential application of NMR imaging to materials science and engineering. This presentation will discuss our study using NMR imaging of the process of polymer flow during extrusion. In particular, a Fourier imaging sequence with T1 and T2 contrast was used to provide information on the phenomenology of the extrusion process. The following is an image of a water-soluble polymer gel containing small pieces of solid nylon line. This image illustrates the information available using this technique. The pieces of solid nylon line appear light against the dark background of the water resonance signal of the polymer gel.



This system was used as a test of the concept of using NMR imaging to visualize the flowing polymer. The above image represents a stop flow picture of the polymer flow. The image represents a 4.4 mm thick slice perpendicular to the axis of the bottle containing the gel with an in-plane resolution of 160 microns x 160 microns. The bottle was lying on its side so that the gel formed a meniscus at the top surface which is clearly visible in the image. The technique required 128 seconds to collect the image information. In this case, the gel flow was so slow that the imaging technique could be completed before any motion could be observed. Under more practical conditions, this type of imaging would be too slow to image flowing polymer. To overcome this problem, we have constructed a specialized gradient coil system so that we can applied the echo-planar imaging (1) technique to this problem. This technique can produce an image in approximately 200 msec and can be repeated any number of times to effectively produce a motion picture of the polymer flow.

1. P. Mansfield, J. Phys. C. 10, L55 (1977)

P43

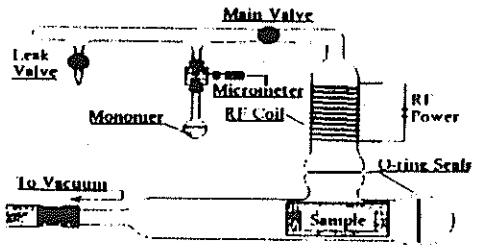
Patterned Ceramic Coatings by CO_2 Laser Pyrolysis

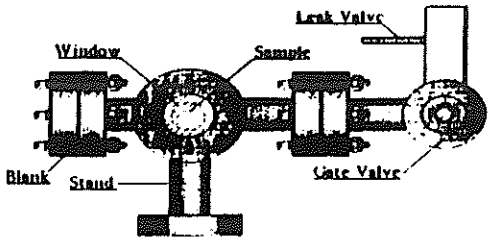
M. Johnson, C. Watson, J. Eyler and C.L. Beatty*, Department of Chemistry and *Department of Materials Science and Engineering, University of Florida, Gainesville, FL

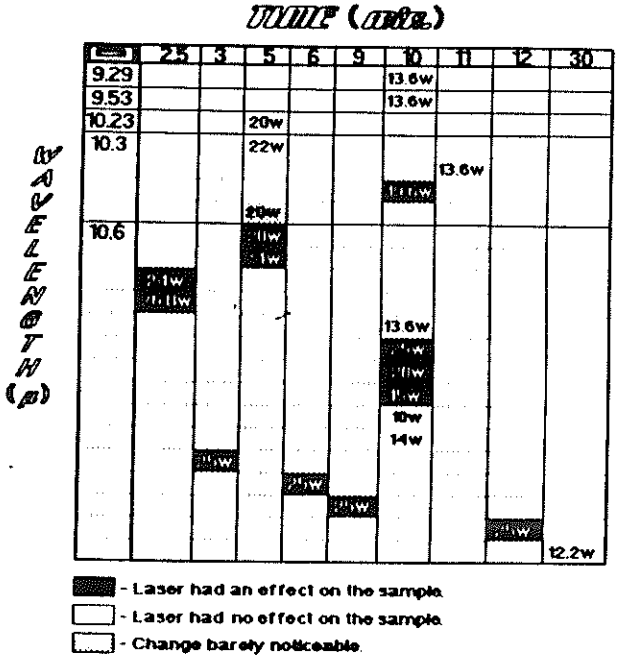
Polymeric precursors can be produced by R.F. plasma polymerization of organometallic small molecules which when thermally pyrolyzed can produce ceramic coating (1). A unique feature of the ceramic coatings produced by this technique is that they are well-adhered to the substrate even after pyrolysis. In addition, uniform thin (e.g., <1μ) coatings can be deposited over an irregular surface as the plasma polymerization process proceeds through the gas phase.

In this work a CO_2 laser has been utilized to selectively pyrolyze the crosslinked, R.F. plasma produced precursor. Variation of wavelength and power of the CO_2 laser has been studied to determine the laser operating range and time required for pyrolysis. It appears that a power in excess of 25 watts at a wavelength of 10.6 microns is desirable for rapid pyrolysis to ceramic. A strong acid wash has been developed to remove the unpyrolyzed R.F. plasma polymerized polymer coating.

The ceramic derived from R.F. plasma polymerization of tetramethylsilane followed by CO_2 laser pyrolysis results in a very light yellow to very light green color coating that suggests very low free carbon and other impurities. The brown color that results during thermal pyrolysis at 400° or 800°C suggests that the kinetics of pyrolysis is different for the CO_2 laser and thermal pyrolysis routes.







P44

DETERMINATION OF BULK PROPERTIES FROM MECHANICAL THERMAL ANALYSIS OF GLASS SUPPORTED PMMA

K. Wolking, T. Hogen-Esch, C.L. Beatty and M. Johnson
University of Florida
Gainesville, Florida

The determination of the bulk dynamic mechanical properties of amorphous polymers through the glass transition by a single analytical technique is difficult due to the large change in material stiffness with temperature. This problem may be overcome by supporting the material on a substrate. In this work, glass cloth was chosen as a support because of its low stiffness and constant properties over a wide range of temperatures. One major advantage of this method is the small weight of polymer required. All samples tested contained less than 0.1 grams of polymer.

A 10 bundle per centimeter square-weave glass cloth by Corning was soaked in chromic acid cleaning solution to remove sizing. Samples were cut to fit on a microscopy slide used to support the sample during preparation. A 5 or 10 weight per cent solution in chloroform of a commercial PMMA from Polysciences, Inc. was used to coat the samples. Each coat of the 5% solution added about 2.5% by weight of PMMA on an area basis. Samples were prepared by dip coating microscope slides. The samples were dried in a vacuum oven at 80 C for 24 hours to remove chloroform.

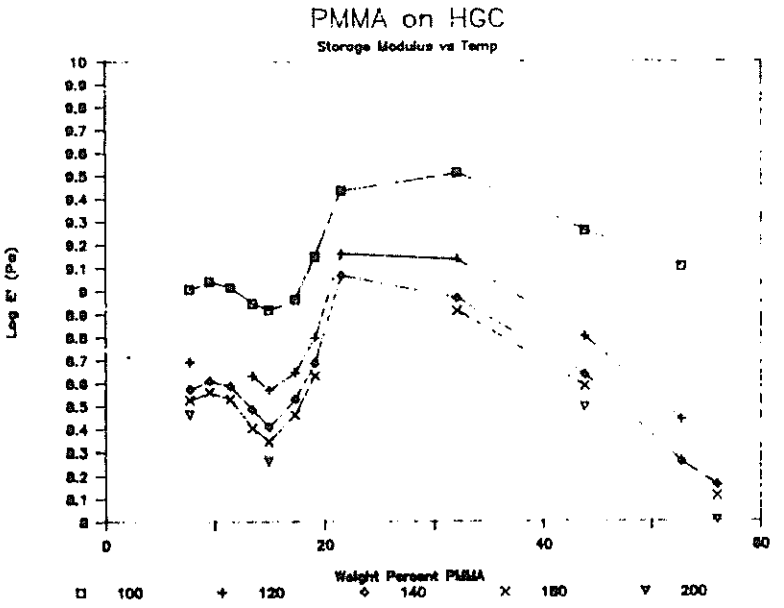
The samples were then cut approximately 18mm x 20mm to fit in the small clamping frame of a Polymer Laboratories Dynamic Mechanical Thermal Analyzer, to be run in single cantilever bending mode. Each sample, except for the bulk samples, was scanned at a temperature from -150 to 200 C, at frequencies from 0.33 to 30 Hz. The bulk samples were scanned at a temperature from -150 to 50 C. In addition, a sample of uncoated glass cloth was run from -150 to 200 C.

Storage and loss moduli plots were constructed for samples ranging from uncoated cloth to bulk PMMA. There were slight variations in the properties in the glass cloth sample. These are apparently due to absorbed water. As the PMMA loading increased, the magnitude of the change in loss modulus and loss tangent increased.

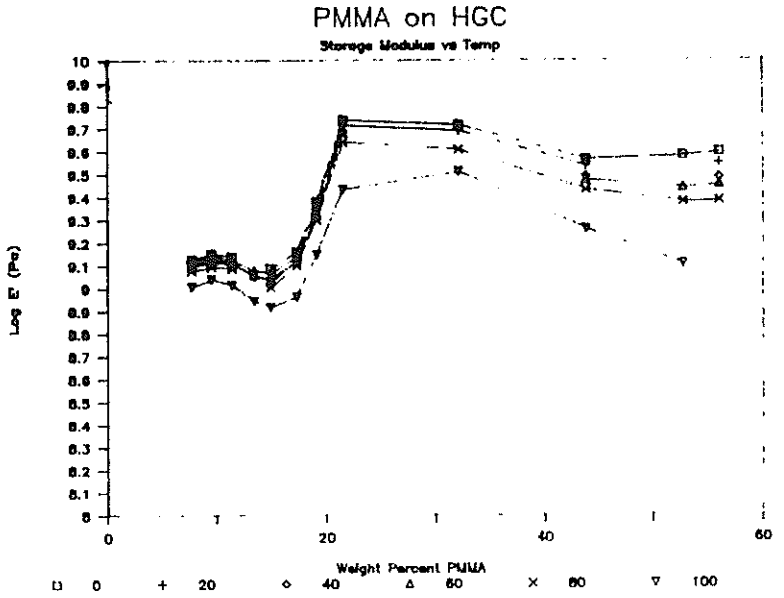
The storage moduli of all samples rose rapidly at small levels of loading. The modulus then levelled off near the bulk values in the glass region. Above the glass transition, the moduli of the samples decrease with increasing loading. At these temperatures, it is impossible to measure the bulk properties in flexure. Figures I and II are plots of storage modulus versus temperature for a representative set of data.

This technique is useful for approximating the bulk dynamic mechanical properties of polymers using very small samples. In the glassy region, extrapolation to bulk properties is reasonable. In the rubbery plateau region, additional research is being done to determine if a useful relationship exists. In particular, the location of the polymer within the cloth (i.e. in the bundles or on the surface) and surface effects need to be accounted for.

II



I



P 45

SCREW DESIGN IN INJECTION MOULDING

H.E.H. Meijer
Eindhoven University of Technology
Eindhoven, Netherlands

C.P.J.M. Verbraak
DSM-Research
Geleen, Netherlands

The performance of screws of advanced design in injection moulding has been investigated with respect to four different objectives:

1. improvement of distributive mixing;
2. improvement of dispersive mixing;
3. increase of plasticating capacity; and
4. reduction of inhomogeneity of melt temperature.

The screws used are three zone screws with different compression ratios, screws with pineapple or Maddock/Egan mixing elements, with one or two channel barrier sections, with static mixers mounted in the valve or in the nozzle, or with combinations of these different elements.

It has been shown that a constant melt temperature during injection moulding can best be achieved by the use of improved screw design. Especially with large shot weights, other measures, such as an increase of back pressure, are not as effective and imply an increase of cycle time. Optimum screws, in this respect, are multi-channel barrier screws with phase separation and maximum use of contact surface for heat exchange with the barrel. For application of these screws, which are known from continuous extrusion processes, in the injection moulding process, special attention should be paid to the transport capacity by drag flow in solid and melt channels, because of the limited pressure generating capacity caused by the varying effective length of the screw during plasticating. The benefits of these screws with respect to the effective residence time and residence time distribution in the melt may be important for temperature sensitive polymers. Obviously, for these polymers dead spots (residence time) and broad flights with narrow clearances (melt temperature) must be avoided as much as possible. If only prevention of the occurrence of unmolten pellets in the mouided part is aimed for, a simple ring with sliths acting like a sieve is sufficient. However, if barrier screws are used for this purpose, the extra flights not only stop the unmolten material but also considerably improve the mixing. With these screws the need for back pressure is absent. Distributive mixing is promoted by multi-channel sections like the Maddock type of mixer. A substantial decrease of the percentage of masterbatch without loss of color intensity in the part can easily be obtained with screws having such a section. Here also, optimizing the helix angle together with the number, depth and width of the inlet and outlet channels for minimum pressure drop is recommendable. The number of channel pairs strongly depends on the screw diameter and on the maximum allowable temperature rise, which is related to the viscosity of the polymer. Where the pressure drop can be estimated with a simple Newtonian model, non-isothermal power law calculations are necessary to determine the temperature rise.

Sufficient dispersive mixing can be achieved by direct blending, as shown with a PP-EPDM mixture on the most powerful setup (a barrier or a kneading section with a multi-channel mixing section combined with back pressure). With the rather difficult blend used (high molecular weight EPDM) the morphology and most of the properties are satisfactory, although too much degradation of the PP occurs.

This experimental study has clearly shown that, by modifying the screw design in the injection moulding process, the improvements in melt quality, which are a prerequisite for high quality moulding, can be achieved.

P46

USING MOLD OPENING TO RELATE THE MOLDING PROCESS TO THE MOLDED PRODUCT

Frederick J. Buja, P.E.
K-Technologies
A Kodak Company
Rochester, New York

Mold opening can define molding process and molded product "consistency." The extreme limits for a molding process is from short (non-filled) to flash (over-packed). A normal molding process will be somewhere between these limits to produce an acceptable product.

Both mechanical and thermal strains occur during two stages of the injection molding process. First, a mechanical strain is caused by the machine's packing pressure during final packing and then material shrinkage during cure.

A sensor to monitor and record mold parting-line movement can document consistency of the molding process. The changes in mold parting-line relate directly to the molded product's part weight and parting-line dimension. Response of a production 2-cavity mold parting-line to controlled changes in mold clamp tonnage and in-mod material pressure will be presented.

P47

"A PROCEDURE FOR MEASUREMENT OF MIXING IN COMPLEX GEOMETRIES FOR CREEPING FLOW: CASE STUDY : COUNTER-ROTATING TWIN SCREW EXTRUDER"

David Bigio

Saeid Zerafati

University of Maryland
College Park, MD 20742

Mixing is an important step operation in many manufacturing processes. In polymer processing, effective mixing is essential to many products and processes of technical and commercial significance. Different polymers are mixed to create products which combine the mechanical properties of several materials.

Line and area growth as a function of total average strain have long been accepted as measure of mixing in creeping flow. But, until now it has only been applied to very simple flow regimes [Spencer and Wiley, Erwin]. In these cases, determination of the orientation of the interface with respect to strain field was simplified because the velocity profile (or the strain field) was constant in the direction of flow. Applying this measurement to a very complicated flow like the flow in the nip region of a CRTSE, in which the velocity field changes with respect to x and y and also the orientation of the interface changes continuously with respect to velocity vector, seemed to be impractical and, did not give insight into mixing in the nip region. Furthermore, details about the effect of each part of the nip region on the mixing was needed. Therefore a measure of the mixing was needed which takes into account the spatially varying rate of strain tensor. In a previous study [Bigio, Zerafati], the rate of increase of the length of interface was used as a mixing measure showing the effect of the nip region. The need to confirm the results with the reorientation theory of interface leads to a new measurement of mixing which is more basic than the previous measure.

In this method, it is recognized that the direction of the interface relative to velocity field determines the orientation of the interface and, the orientation of the interface is considered to be the main factor of the mixing rate. The angle between interface and velocity vector at each point of the region can be considered as a new measure for mixing. This measure is one step more fundamental than the former measure because, in fact, this is the cause of the increase of the length of the interface and, this will be shown clearly in this paper. This angle is a direct measurement of the orientation and, reorientation is considered to be the main cause of the increase of mixing rate.

For demonstration of the use of this new measure, it was applied to a 2-D version of nip region of a CRTSE. A finite element code named FIDAP which was available on SDSC CRAY-X/mp was used to solve the creeping flow equations in the nip region. The output from FIDAP calculated the velocity and pressure field in the region. The output of FIDAP was then used as input to a programs which measures the orientation of an arbitrary interface with respect to local velocity vector field at each step and, compares the result with the rate of increase of the length of interface. The results show a direct relation between the rate of increase of the length of interface and the orientation of the interface with respect to local velocity vector field. This angle also represents the degree of reorientation of the interface as it proceeds in the nip region which is a substantial contribution towards the understanding of the role of different parts of the nip region on mixing.

1) Spencer & Wiley, J. of Colloid Sci., 6, 1951.
2) L. Erwin, PE & S, 18(9), 738, 1978.
3) Bigio & Zerafati, SPE, ANTEC, 1988.

P49

"EFFECTS OF SPACING FIBERS IN EPOXY COMPOSITE SYSTEMS USING COPPER OR TUNGSTEN WIRES"

J.M. YARBORO AND C.L. BEATTY
DEPT. OF MATERIALS SCIENCE AND ENGINEERING
UNIVERSITY OF FLORIDA
GAINESVILLE, FLORIDA 32611

INTRODUCTION

For the model composite system epon shell 828 with amine curing agent magnolia 360 is used as the matrix. For the fibers 100 micron diameter copper wire and 25 micron diameter tungsten wire are used.

ANALYSIS

The spacings of the wires were varied and tested on the Dynamic Mechanical Thermal Analyzer to find modulus, glass transition temperature, and calculated activation energies. The distance between wires range from 30 microns to 700 microns. Data was also collected by varying the angles of the unidirectional wires at 0, 45, and 90 degrees and their properties were compared. Also muti-layer samples will be tested and compared to the unidirectional wire models.

Also to be calculated are molecular weight of crosslinks, ratio of matrix to fiber, and amount of shrinkage of the model system. These will be compared to pure epoxy systems.

CONCLUSION

The results shown are that a decrease in wire spacing shows an increase in modulus and an increase in actvation energies. These values are much larger than pure epoxy values. Shown is a volume ratio matrix and fibers giving maximum modulus and activation energies.

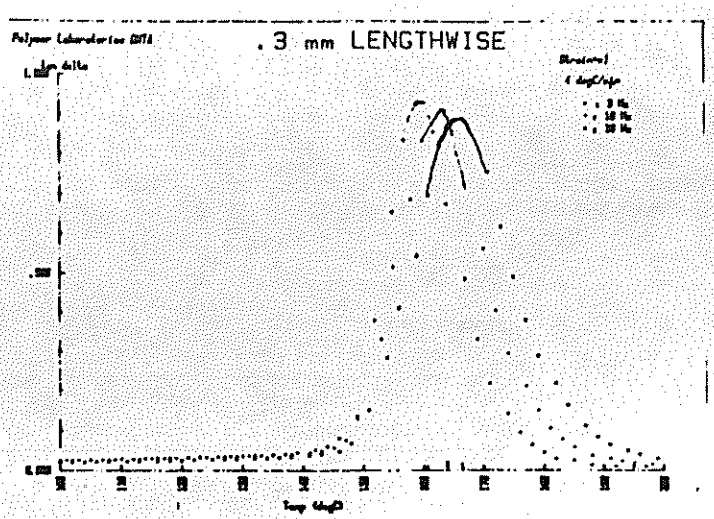


Figure 1. Copper wire - glass transition temperature.

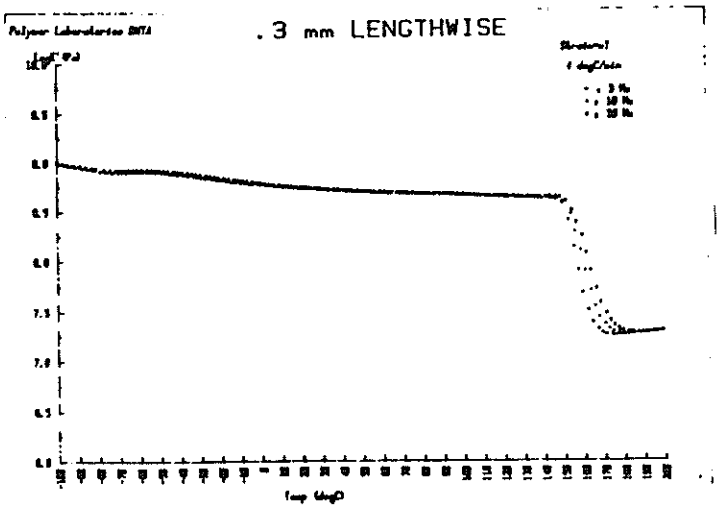


Figure 2. Copper wire - log modulus.

P 50

A STUDY ON DYNAMICALLY COVULCANIZED POLY(VINYL CHLORIDE)/NITRILE RUBBER 40 BLENDS

LUO NING
Department of Applied Chemistry
Northwest Institute of Light Industry
Xianyang, Shaanxi, China

ZHANG YINXI
Northwest China Rubber Mechanical Goods
Research Institute of MCI
Xianyang, Shaanxi, China

A series of blends of poly(vinyl chloride) (PVC)/nitrile rubber 40 (NBR-40) with different composition ratios were prepared by dynamic covulcanization in a Brabender Plasticorder. Some different curatives were used in this work.

The dynamically covulcanized blends have such properties as higher strength, lower tension set and fabricability as thermoplastics (Table 1).

TABLE 1
Properties of PVC/NBR-40 (50/50) blends.

Stock number	1	2	3	4	5
Hardness (Shore A)	52	58	56	58	52
Elongation at break (%)	590	500	560	570	370
Tensile strength (MPa)	4.6	12.8	10.8	13.4	6.6
Modulus at 100% (%)	1.5	2.1	2.0	1.9	1.7
Tension set (%)	47	13	20	17	10
Tear strength (Kg/cm)	27	35	36	37	22
X1	1	2.8	2.2	2.9	1.2
X2	1	0.3	0.4	0.4	0.2

X1 = Proportion of tensile strength.
X2 = Priportion of tension set.
Recipes: 1. uncured, 2. sulfur cured, 3. TCY cured, 4. TMTD cured, 5. PVC/Krynac-810 blend, uncured.

Figure 1 shows the best blends contained at least 60% insoluble gel. A important condition to prepare the PVC/NBR-40 thermoplastics blends seems that NBR is fully vulcanized and PVC is partially vulcanized.

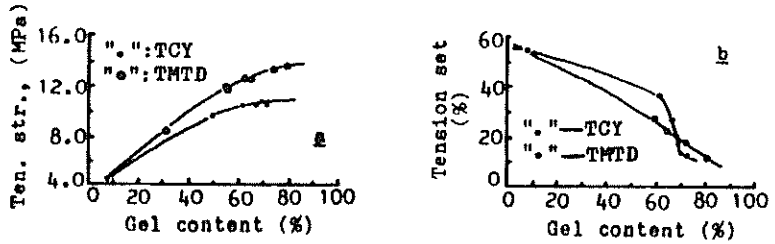


Figure 1. The effect of gel content on properties of PVC/NBR-40 (50/50) blends.

The SEM observations indicate that the dynamically covulcanized blends were homogenous.



a. PVC/NBR-40 = 80/20 uncured.

b. PVC/NBR-40 = 80/20 cured.

Figure 2. SEM observations of blends dynamically covulcanized by TCY curative.

A structure model of the semi-interpentrating polymer network (semi-IPN) material is suggested for explaining the features of the blends. A new way to prepare semi-IPN with fabricability as thermoplastics is presented in this paper.

REFERENCES

1. Nakamura, Y., Mori, Y., Takezawa, R. and Saito, M., co-crosslinking of PVC and NBR. Nippon Gomu Kyokaishi. 1979, 52, 584-91.

P 51

STRUCTURED BLENDS

H.E.H. Meijer, P.J. Lemstra and P.H.M. Elemans, Dept. of Polymer Technology, Eindhoven University of Technology, P.O. Box 513, 5600 MB Eindhoven, The Netherlands

Miscibility of polymers is an exception rather than a rule. As a consequence the final properties of a blend in general will depend on the morphology, resulting from the properties of the constituents and the processing routes and conditions. Amongst others the morphology is influenced by the volume fraction and viscosity ratio of the polymers, the interfacial tension and the mixing time and type of flow. In practice a specific morphology, realised during the compounding process and optimized for a desired property, may well be destroyed during subsequent processing, i.e. shaping the blend into a product, such as extrusion or injection moulding. For successful blending, knowledge of the mixing and extrusion processes is necessary as well as an exploration of different routes to control the structure and the morphology, like fixation via compatibilizers, reactive processing and crosslinking with peroxides or radiation treatment.

Different morphologies, for example droplets or fibres in a matrix stratified structures and cocontinuous structures, can be obtained as will be demonstrated with the model system HDPE/PS. Only a very few of these structures are intrinsically stable, most of them are intermediates. This can be understood from flow analysis in extruders, static mixers and continuous mixers like the corotating twin screw extruder and the Buss cokneader, provided that the modelling yields results not only for shear rate and shear stress, but also for the (limited) residence time and number of reorientations during shearing, depending on screw design and processing conditions. Examples will be given. On the other hand, knowledge of the distributive and especially the dispersive mixing process explains the time dependent, interfacial tension drive distortions of fibers (Rayleigh disturbances) and platelets in matrices and the deformation of droplets determined by the ratio of shear stress and interfacial tension and depending on the viscosity ratio of the dispersed and the continuous phase.

Despite all this, control of the different morphologies may be important for the desired product properties like impact modification (droplets in matrices), reinforcement (fibers) and barrier properties (stratified structures). Apart from the use of a compatibilizer that influences the interfacial tension, which can be measured a.o. via the growth rate of Rayleigh disturbances as will be shown, fixation of a specific structure via γ or EB radiation can be very successful, provided that the matrix is relatively insensitive for radiation treatment and that the dispersion, fibers or platelets crosslink easily. Examples of PA/LDPE, PA/EVOH and (PET)EVOH will be shown. In this way structured blends can be realised which can be optimized for specific properties in a careful designed compounding process, and fixate via EB treatment before subsequent shaping processes like extrusion, blowing and injection moulding.

LIST OF AUTHORS

- A -

T. Aalto, 8/9
F.L. Abrams, 12/2
D. Acierno, 11/7, 11/11
M. Adams, 12/8
S.G. Advani, 1/27
J.F. Agassant, 1/8, 1/19, 3/10
14/3, 4/19
A. Ahmadi, 13/3
A. Aiji, 9/5, 9/14
M. Akay, 12/12
P.S. Allan, 1/14
M.A. Alonzo, 8/2
E. Amendola, 11/7
M. Amon, 1/17
T. Anderson, P30
B.V. Ankleswaria, P13
M.R. Apelian, 16/5
H. Arakawa, 10/3, 10/8
R.C. Armstrong, 11/4, 16/5
F.H. Axtell, 16/2

- B -

F. Baba, 1/24
Y. Baba, P11
R. Bailey, 12/10, 12/16
D.G. Baird, 8/21, 11/10, 14/1
W. Baker, 5/11
S.T. Balke, 5/9
G. Banhegyi, P35
A. Barbe, 1/19
D. Barkley, 12/12
R.H. Barq, 3/10
S.R. Bates, P9
C.L. Beatty, 1/16, 3/25, 5/6, 10/12,
12/3, P7, P8, P9, P11, P16,
P17, P21, P22, P23, P27, P28,
P29, P30, P31, P38, P39, P42,
P43, P49
P. Beaufils, 4/19
J. Beautemps, 8/8
S.E. Bechtel, 14/5
D.J. Belton, 15/8
A. Beningfield, 3/25
D. Bennett, 1/16, P7
E.C. Bernhardt, 1/4
G. Bertacchi, 1/4
H. Bertilsson, P10
F.E. Bertrand, 4/2
M.J. Bevis, 1/14
D.M. Bigg, 12/9
D. Bigio, 4/6, 6/10, P47
D.M. Binding, 11/1
K.G. Blizard, 8/21
T.J. Blong, 4/17
D.V. Boger, 11/8
D.C. Bogue, 8/3
Y.M. Boluk, 6/3
M. Bouldin, 11/3
M.J. Brenner, 13/3
J.R. Bric, 13/2
H. Brody, 3/22
R.A. Brown, 11/4, 16/5
I. Bruker, 1/10
R. Brzoskowski, 7/4
M. Bucse, P25
F.J. Buja, P46
D.C. Burdeaux, 15/11

- C -

M. Cakmak, 3/3, 8/12, 8/13
V. Caldas, 9/4
G.A. Campbell, 12/8, 1/16, 3/1, P29
S. Canova, P30
C. Carfagna, 11/7
P. Carreau, 4/4, 9/11, 9/15,
B. Catoire, 3/21
J.P. Chalifous, 9/6
J.D. Chang, 14/5
J.P. Chang, 7/5
L.S. Chang, 2/4
N. Chapleau, 9/11
J.M. Charrier, 14/3
K. Chehab, P7, P8, P9, P29
G. Chen, 8/6
I. Chen, 1/3
K. Chen, P24
L. Chengxiang, 7/9
P. Cheung, 5/9
C. Chmielewski, 12/17
M. Cho, 2/5
W.J. Cho, P12
L. Choplin, 9/14
B. Chung, 7/5
T.S. Chung, 1/6
R.V. Ciplijauskas, 14/3
A. Co, 3/6
P.D. Coates, 5/12
M.D. Cockman, 10/7
A. Cohen, 8/5
C. Cohen, 5/4
J.S. Colton, 1/26
D. Cook, 4/13
R. Cooke, 4/13
S.P. Corscaden, 12/5
J.L. Cottalorda, 1/19
D.J. Coyle, 2/3
M.J. Crochet, 1/18, 16/3
J. Crosby, 12/11
J.A. Cuculo, 3/24, 8/6
G. Cuff, 12/7

- D -

W. Daher, P16
C. Daneault, P32
R. Dave, 12/1
M. Davies, 12/16
R.B. Davis, 1/27
M.D. Daxini, P13
D. DeKee, P37
J. DeLong, P18
G. Demma, 11/11
B.C. Dems, 15/4
J.L. den Otter, 5/5
J. Denault, 10/10
M. Denn, 3/15, 11/6
O. Denizart, 1/8
B.L. Deopura, 8/11, 8/18
M.G. Dibbs, 8/5
J. Dixon, P39
J.F. Dizor, 3/25
E. Doering, 12/13
D.S. Done, 11/10
L. Donghong, 7/9
M.P. Dudokovic, 12/1
M.M. Dumoulin, 9/15
F. Dupret, 16/3
B. Dutta, P36

- E -

W. Ehrfeld, 5/3
P.H.M. Elemens, P51
B. Ernst, 1/21
L.A. Errede, 13/4
S. Etoh, 1/24
J. Eyler, P43

- F -

W. Fagang, 7/9
J.D. Fan, 1/20
G.W. Farell, 8/20
J. Faro, 10/9
B.D. Favis, 9/4, 9/6
D.L. Feke, 6/2
D. Feldman, 9/18
J.F. Fellers, 8/20
P. Filz, 1/28
G. Fischer, 1/12
H.H. de Frahan, 1/18
B. Franzen, P4, P10
P.K. Freakley, 7/6
A.L. Fricke, 1/16, 11/2, P27
K. Friedrich, 12/15
D.B. Fritz, 15/7
M. Fujiyama, 11/9
A. Fukami, 1/24
K. Fukumori, 1/25
K. Fujioka, P11

- G -

M. Gadbois, 4/2
R. Gauvin, 10/2
E. Gemdjian, P5
A.G. Giacomin, 4/15
A.G. Gibson, 12/5
J.A. Gilpin, 15/11
L.A. Goettler, 7/1, P42
X. Gong, P20
J.D. Graybeal, 10/1
J. Greener, 15/9
H.D. Griffin, 7/11
M. Grmela, 9/11
E.G. Grulke, 6/14
S.I. Guceri, 16/6
C. Guerrero, 4/4
S. Guo, 9/16

- H -

C.S. Ha, P12
T. Habinak, 4/15
T.A. Hadithi, 11/1
R.S. Haldar, 8/11, 8/18
R. Hagege, 3/21
P. Hagmann, 5/3
S.F. Hahn, 15/11
D.C. Hall, 7/2
H. Hamada, 1/2, P3
A.E. Hamielec, 5/10
M. Hao, 10/6
J.P. Harmon, 13/6, P16, P17, P39, P44
T. Hashimoto, 8/17
J.M. Haudin, 3/5, 3/10
M.C. Hawley, P18
B. Haworth, 16/2
S. Hayashi, 3/13
T. Hayashi, P1
N.W. Hayman, 3/22
I.P. Hayward, 15/2
H. Hegele, 2/1
D. Heikens, 9/19
F.L. Heng, 14/2
F. Hensen, 3/13
C.A. Hieber, 1/1
D.F. Hiscock, 12/9
A. Hoelzer, P9
T.E. Hogen-Esch, P25, P44

H. Hojo, 12/14
P. Hold, 6/1
S.M. Hong, 13/5
H. Horibe, 1/24
P.R. Hornsby, 13/3
R. Hoseman, 12/6
B.C. Howard, 7/2
A.N. Hrymak, 1/13, 14/4
D.V. Hur, 11/8
K.S. Hyun, 4/10

- I -

R.J. Ihm, P34
H. Ikeuchi, 3/14
Y.J. Im, 1/20
J. Imaizumi, P2
B.S. Ince, 11/5
T. Inoue, 8/1, 9/17
K. Inubuse, 5/7
A.I. Isayev, 14/8
H. Ishihara, 3/14
M. Iso, 5/7
K. Iwakura, 8/13
I. Iwata, 5/7

- J -

P. Jaaskelainen, 8/9
S. Jabarin, 2/4
C.L. Jackson, 8/2
H. Jamadus, 10/11
M.S. James, 7/5
J. Jaw, P18
K. Jayaraman, 6/14, 12/17, 12/18
S.R. Jenkins, 4/10
L. Jianxiong, 5/13
J.P. Jog, 9/7
A.F. Johnson, 5/12
B.V. Johnson, 4/17
M. Johnson, P43
E. Jung, 3/16
B.J. Jungnickel, 3/2
M.J. Jurek, 15/2

- K -

A. Kagemoto, P11
H. Kaiser, 12/1
A. Kaito, 8/10
D.H. Kalyon, 2/2
M.R. Kamal, 1/7, 11/12
O. Kamigaito, 1/25
T. Kanai, 3/4, 1/9
A. Kaneda, 1/22
H.J. Kang, 3/3
A. Karagiannis, 14/4
J.L. Kardos, 12/1
S. Kase, 3/17
K. Katayama, P34
M. Kato, 8/10
M. Kato, P2
T. Kawako, 9/17
D.D. Kechajov, 5/14
D.N. Khanna, 15/3
M. Khoury, 9/18
A. Kiani, 14/7
M.J. Kiesel, 9/3
T. Kikutani, 3/19
B.C. Kim, 13/5
B.H. Kim, 1/11
E.G. Kim, 12/14
J. Kim, 1/20, 6/6
K.U. Kim, 13/5
M.H. Kim, 6/13
S.C. Kim, 5/2
S.H. Kim, 12/14
Y. Kimima, 9/17
R.C. King, 16/5
N. Kingo, 15/13
N. Kinjo, P2
K. Kirjavainen, 3/8
C. Klason, P4
I. Klein, 4/14
L. Kliner, 5/8
W.C. Ko, 8/3
N. Kobayashi, 10/3
M. Koch, 4/9
B.V. Kokta, P6, P32
R. Konga, P25
M. Koshimoto, 12/14
P. Kral, P41
J. Kubat, P4, P10
K. Kubota, 4/11
W.M. Kulicke, 11/3, 11/6
T. Kunugi, 3/7
T. Kurauchi, 1/25
A.P. Kuriakose, 7/10
C. Kwag, 6/6
T. Kyu, 9/3

- L -

B. Lagman, 6/4
F.P. La Mantia, 11/11
M. Lambla, P33
J.B. Lando, 15/5
D. Lang, 4/3
R.L. Laurence, 13/2
G. Le Bourvellec, 3/9, 8/8
C.C. Lee, 14/6
C.W. Lee, 12/2

H.S. Lee, 1/5
J. Lee, 6/6
K. Lee, 6/6
K.H. Lee, 5/2
L.J. Lee, 1/20, 5/1
S. Lee, 13/6
P.J. Lemstra, 3/11, P51
D.A. Lewis, 10/1
H. Li, 9/16
J.C.M. Li, 13/6
C.M. Lin, 3/6
C.Y. Lin, 8/6
H.Y. Lin, 15/12
J.S. Lin, 8/15
K.J. Lin, 14/5
P. Lin, P24
T. Lindt, 13/1
M.J. Liou, 8/4
X. Liu, P20
Z.J. Lobos, 7/6, 7/8
S. Lorek, P33
N. Losure, 12/18

- M -

Y. Maeda, 3/18
Z. Maekawa, P3
D. Maldas, P6
T.M. Malik, 9/11
M.F. Malone, 9/2
N. Malone, P11
I. Manas-Zloczower, 6/2
L.T. Mangione, 15/6
T.H. Mareci, 10/7, P42
J.M. Margolis, 12/4
R. Marin, 2/5
E. Martuscelli, 11/11
Z. Martynenko, 15/1
G. Mathew, 7/10
T. Matsuoka, 1/25
H. Mavridis, 1/13
A.N. McClelland, 12/5
J.E. McGrath, 10/1
M. McHugh, 9/12
M.H. Mehta, P13
H.E.H. Meijer, P45, P48, P51
H. Meinecke, 16/4
G. Menges, 1/28, P14
W.H. Meuller, 15/3
C. Miaw, 4/3
W. Michaeli, 4/1
P. Michel, 4/5, 6/8
J. Militky, 3/20
R.W. Miller, 3/25
K. Min, 6/13, 11/14
M. Mineo, 3/18
A. Misra, 8/11, 8/18, P36
E. Mitsoulis, 14/2
P. Mokay, 12/11
M. Molter, 15/8
S. Montes, 7/7
D.R. Moore, 12/16
R.A.F. Moore, 3/26
H. Morinaga, 3/19
R. Moynahan, 14/1
A.K. Mukhopadhyay, P36
M. Munstedt, 15/10
S. Murakami, P34
Y. Murata, P1
A.T. Mutel, 11/12

- N -

S. Naderi, P35
V.M. Nadkarni, 9/7
K. Nagao, P2
T. Nakagawa, 10/4
N. Nakajima, 7/3, 7/7, 11/14
K. Nakayama, 8/10
S. Nakayma, 8/10
N. Narazaki, 1/2
P. Navard, 1/21
S. Nawrot, P33
W. Neubauer, 2/7
K.L. Nichols, 6/14
L. Nicolais, 11/7
N. Ning, P50
R. Nobile, 11/7
H. Nomura, P2
J.W.M. Noordemeer, 6/7
A.E. Novembre, 15/2
S. Numate, P2
G. Nutting, 12/15

- O -

K.T. O'Brien, 1/23
M. Ogata, 14/13
C. Ogbonna, 1/14
H.Y. Oh, 1/11
H. Ohji, 4/11
T. Ohta, 1/25
K. Oka, 3/18
N. Okui, 8/14
A.O. Ola, 16/2
S. Omi, 5/7
P. O'Neill, 6/5
T. Onodera, 12/14
C. Ouellett, 10/2
Y. Oyanagi, 4/11

- P -

M.H. Pahl, 16/4
P.L. Pai, 15/12
S.N. Pal, 9/10
K. Palit, 1/3
S.K. Park, 13/5
G.C. Peischl, 1/10
C.A. Petty, 12/17, 12/18
P. Plein, P14
W. Potente, 4/5, 4/9, 6/8
R.E. Prud'homme, 9/5, 9/14
J. Pujol, P31, P44
S. Pyun, 6/6

- Q -

B. Qian, P24
L.M. Quizani, 11/4

- R -

R.R. Rahalkar, 7/12
W.P. Raiford, 11/4
R.J. Raj, P32
R.R. Rakos, 14/7
R. Ramanathan, 11/10, 14/1
A.V. Ramani, 9/10
C. Rauwendaal, 4/7
E. Reichmanis, 15/2
K.P. Richter, 10/11
S.E. Rickert, 15/5
A. Rigamonti, 10/7
L. Rivera, P31
F. Rodriguez, 15/4
V. Romano, 11/11
T. Rucker, 15/12
A. Rudin, 4/13
S. Ruetsch, 3/26
B. Rzepka, 12/10

- S -

M.R. Sadeghi, 7/3
J. Saeki, 1/21
K. Saijo, 8/17
D. Saint-Royre, 4/16
T. Sakai, 61/2, 8/14
J.M. Saldanka, 9/3
M. Saleem, 5/11
D.R. Salen, 3/26
R.J. Samuels, 8/16
I.C. Sanchez, 9/1
E. Satoh, P2
A. Savolainen, 3/8
G. Schenkel, Plenary
B. Schmid, 1/12
H.P. Schreiber, 4/18, 6/3, 10/5
S.M. Schultheis, 6/8
J.M. Schultz, 3/23, 12/15, P26
I. Schulze, 12/6
C. Schwalm, P18
P. Schwarz, 1/12
D.H. Sebastian, 14/7
Y. Sekiguchi, 8/10
S.R. Settlemire, 1/16
H. Shaojun, 5/13
M.T. Shaw, 8/2
S.F. Shen, 5/4
Y. Shi, 8/19
J. Shimizu, 3/19
K. Shimizu, 1/9
V.L. Shingankuli, 9/7
W.J. Shuely, 11/5
A. Shugard, 15/2
S. Singer, P18
Y.P. Singh, P13
S. Singleton, P17
J.D. Small, 1/16, 11/2
D.E. Spahr, 12/15
D.S. Soane, 15/1
C.M. Solbrig, 15/4
M. Sotton, 3/21
J.A. Southern, 3/25
H. Sristov, P26
J.F. Stevenson, 14/6
M. Stoy, P27
R.J. Streu, 4/10
W.L. Sturm, 2/6
S. Subbiah, 16/6
N.P. Suh, 8/4
Z. Suhe, 7/9
E. Suokas, 1/15
W. Szydlowski, 6/11

- T -

H. Takahashi, 1/25
S. Takahashi, 8/10
T. Takaheshi, 8/14
T. Takahiro, 8/14
A. Takaku, 3/19
H. Tang, 7/6, 7/8, 7/12
P.A. Tanguy, 4/2
R.G. Tarascan, 15/2
W.J. Tchir, 10/5
H. Thapar, 1/14
M.H. Theil, 3/24
T. Tincer, 11/13
C.H. Ting, 15/12
D.B. Todd, 6/9
K. Tomari, 1/2

P. Tormala, 1/15
P.H. Townsend, 15/11
D.A. Tree, 9/12
B. Tremblay, P40
M. Tsuji, P34
C.L. Tucker, 1/27
P.A. Tucker, 8/6
R.M. Turner, 12/7
C. Tzoganakis, 5/10

- U -

N. Ulkem, 11/13
Y. Uryu, 1/9
L.A. Utracki, 9/13, 9/15, P40

- V -

A. Valenza, 11/11
W.F. van den Bogert, 15/8
J. van der Kooi, 7/2
K. Venkataswamy, P19
S. Venkatraman, 5/8
C.P.J.M. Verbraak, P45, P48
B. Vergnes, 14/3, 4/19
W. Vidrine, 3/12
A. Vincellette, 4/4
M. Vincent, 1/8, 1/19
J. Vlachopoulos, 1/13, 5/10, 14/4
J. Vleck, P41
T. Vu-Khanh, 10/10, P15

- W -

K. Walters, 11/1
C.W. Wang, 15/7
H.P. Wang, 1/5
K. Wang, 1/1
Q. Wang, 9/16
Y.D. Wang, 8/13
S. Ward, 12/11
T.C. Ward, 10/1
C. Watson, P43
H.D. Weigmann, 3/26
F.C. Weissert, 11/14
J.L. White, 3/3, 6/11, 6/13, 7/4, 7/7, 8/9, 8/12, 11/14
G.L. Wilkes, 10/1
W. Williams, P21, P22, P23, P38, P39
J.M. Willis, 9/4
M. Wilms, 6/7
T.S. Wilson, 8/21
D. Wingard, 5/6, 10/12, 12/3, P27, P39
H.H. Winter, 9/2
H. Wobbe, 4/12
J.F. Wolfe, 10/1
K. Wolking, P44
V. Wong, 14/8
R.P. Wool, 9/8
J.W. Wu, 8/12
X. Wu, 9/9
Z. Wu, P24
J.L. Wybo, 1/19

- X -

X. Xu, 9/16, 10/7, P20

- Y -

Y. Yabushita, 7/4
H. Yaguchi, 12/14
K.S. Yang, 3/24
Y.S. Yang, 5/1
Z. Yanhao, 7/9, 11/14
J.M. Yarboro, P49
H. Yasuda, 3/14
Z. Yinxi, P50
H. Yokoi, 10/3, 10/4, 10/8, P1
D. Young, 3/15
M. Yu, 9/9
N.G. Yun, P11

- Z -

A.E. Zachairades, 8/7
X. Zeng, 14/8
S. Zerafati, 6/10, P47
A. Zhang, P24
Z. Zhou, 9/9